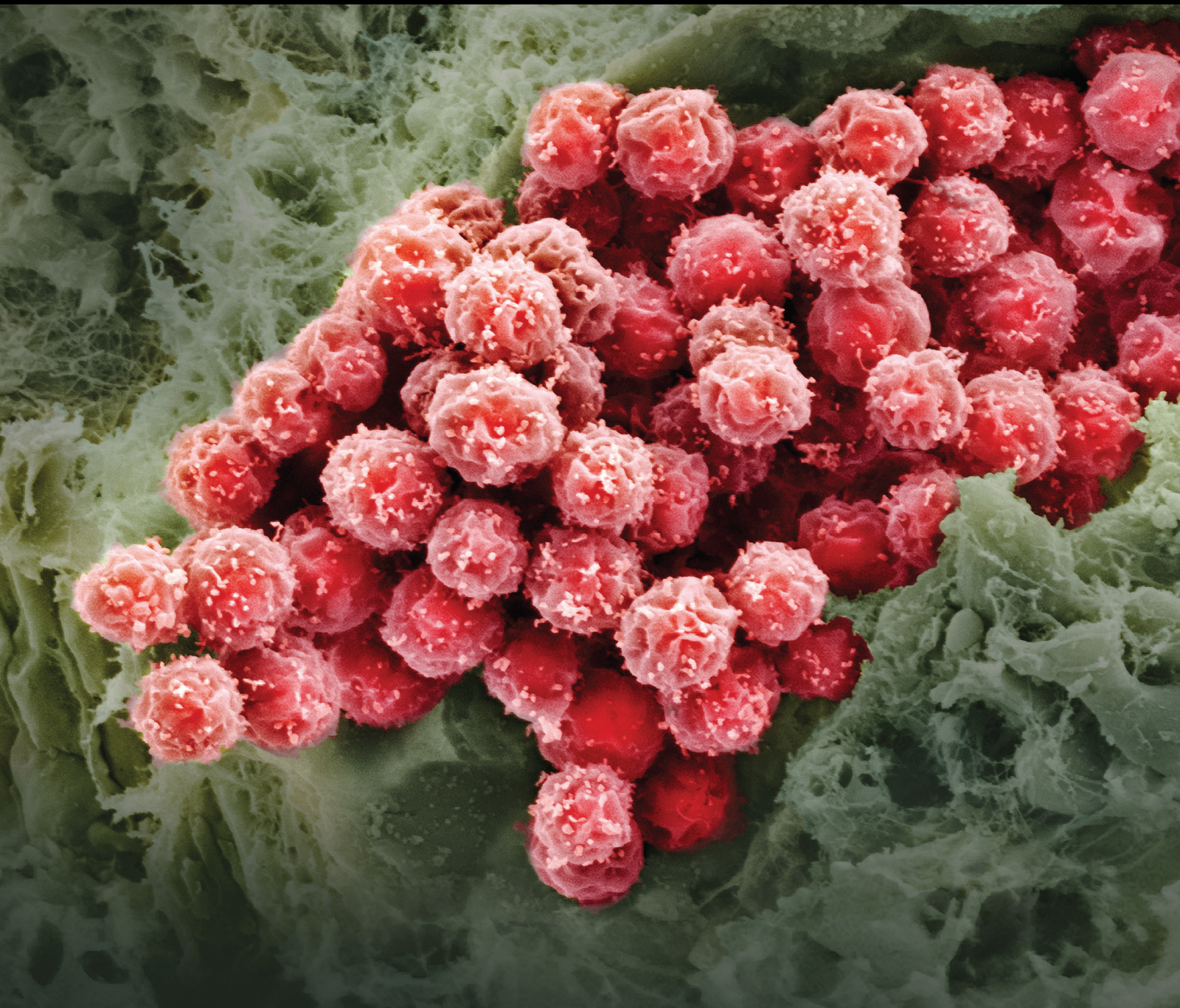


Stem Cells International

# Mesenchymal Stem Cells and Regenerative Medicine 2020

Lead Guest Editor: Huseyin Sumer

Guest Editors: Sangho Roh and Jun Liu



---



**Mesenchymal Stem Cells and Regenerative  
Medicine 2020**



Stem Cells International

---

## **Mesenchymal Stem Cells and Regenerative Medicine 2020**

Lead Guest Editor: Huseyin Sumer

Guest Editors: Sangho Roh and Jun Liu



---

Copyright © 2021 Hindawi Limited. All rights reserved.





This is a special issue published in “Stem Cells International.” All articles are open access articles distributed under the Creative Commons Attribution License, which permits unrestricted use, distribution, and reproduction in any medium, provided the original work is properly cited.







# Chief Editor

Renke Li , Canada

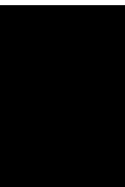
## Associate Editors

James Adjaye , Germany  
Andrzej Lange, Poland  
Tao-Sheng Li , Japan  
Heinrich Sauer , Germany  
Holm Zaehres , Germany




## Academic Editors

Cinzia Allegrucci , United Kingdom  
Eckhard U Alt, USA  
Francesco Angelini , Italy  
James A. Ankrum , USA  
Stefan Arnhold , Germany  
Marta Baiocchi, Italy  
Julie Bejoy , USA  
Philippe Bourin , France  
Benedetta Bussolati, Italy  
Leonora Buzanska , Poland  
Stefania Cantore , Italy  
Simona Ceccarelli , Italy  
Alain Chapel , France  
Sumanta Chatterjee, USA  
Isotta Chimenti , Italy  
Mahmood S. Choudhery , Pakistan  
Pier Paolo Claudio , USA  
Gerald A. Colvin , USA  
Joery De Kock, Belgium  
Valdo Jose Dias Da Silva , Brazil  
Leonard M. Eisenberg , USA  
Alessandro Faroni , United Kingdom  
Ji-Dong Fu , USA  
Marialucia Gallorini , Italy  
Jacob H. Hanna , Israel  
David A. Hart , Canada  
Zhao Huang , China  
Elena A. Jones , United Kingdom  
Oswaldo Keith Okamoto , Brazil  
Alexander Kleger , Germany  
Laura Lasagni , Italy  
Shinn-Zong Lin , Taiwan  
Zhao-Jun Liu , USA  
Valeria Lucchino, Italy  
Risheng Ma, USA  
Giuseppe Mandraffino , Italy

Katia Mareschi , Italy  
Pasquale Marrazzo , Italy  
Francesca Megiorni , Italy  
Susanna Miettinen , Finland  
Claudia Montero-Menei, France  
Christian Morszeck, Germany  
Patricia Murray , United Kingdom  
Federico Mussano , Italy  
Mustapha Najimi , Belgium  
Norimasa Nakamura , Japan  
Karim Nayernia, United Kingdom  
Toru Ogasawara , Japan  
Paulo J Palma Palma, Portugal  
Zhaoji Pan , China  
Gianpaolo Papaccio, Italy  
Kishore B. S. Pasumarthi , Canada  
Manash Paul , USA  
Yuriy Petrenko , Czech Republic  
Phuc Van Pham, Vietnam  
Alessandra Pisciotta , Italy  
Bruno P#ault, USA  
Liren Qian , China  
Md Shaifur Rahman, Bangladesh  
Pranela Rameshwar , USA  
Syed Shadab Raza Raza , India  
Alessandro Rosa , Italy  
Subhadeep Roy , India  
Antonio Salgado , Portugal  
Fermin Sanchez-Guijo , Spain  
Arif Siddiqui , Saudi Arabia  
Shimon Slavin, Israel  
Sieghart Sopper , Austria  
Valeria Sorrenti , Italy  
Ann Steele, USA  
Alexander Storch , Germany  
Hirotaka Suga , Japan  
Gareth Sullivan , Norway  
Masatoshi Suzuki , USA  
Daniele Torella , Italy  
H M Arif Ullah , USA  
Aijun Wang , USA  
Darius Widera , United Kingdom  
Wasco Wruck , Germany  
Takao Yasuhara, Japan  
Zhaohui Ye , USA



---

Shuiqiao Yuan , China  
Dunfang Zhang , China  
Ludovic Zimmerlin, USA  
Ewa K. Zuba-Surma , Poland




## Contents

### **Comparison of the Migration Potential through Microperforated Membranes of CD146+ GMSC Population versus Heterogeneous GMSC Population**

Mohamed Al Bahrawy 



Research Article (14 pages), Article ID 5583421, Volume 2021 (2021)

### **Gene Profiles in the Early Stage of Neuronal Differentiation of Mouse Bone Marrow Stromal Cells Induced by Basic Fibroblast Growth Factor**

Lili Yu, Wei Hong, Haijie Yang, Yin Yan Xia, and Zhiwei Feng 




Research Article (17 pages), Article ID 8857057, Volume 2020 (2020)

### **Mechanically Stretched Mesenchymal Stem Cells Can Reduce the Effects of LPS-Induced Injury on the Pulmonary Microvascular Endothelium Barrier**

Jin-ze Li, Shan-shan Meng, Xiu-Ping Xu, Yong-bo Huang, Pu Mao, Yi-min Li, Yi Yang, Hai-bo Qiu , and Chun Pan 



Research Article (12 pages), Article ID 8861407, Volume 2020 (2020)

### **Isolation and Characterization of Multipotent Canine Urine-Derived Stem Cells**

Yan Xu , Tao Zhang, Yang Chen, Qiang Shi, Muzhi Li, Tian Qin, Jianzhong Hu, Hongbin Lu , Jun Liu, and Can Chen 



Research Article (12 pages), Article ID 8894449, Volume 2020 (2020)

### **The Potential Use of Mesenchymal Stem Cells and Their Derived Exosomes as Immunomodulatory Agents for COVID-19 Patients**

Faisal A. Alzahrani , Islam M. Saadeldin , Abrar Ahmad , Dipak Kumar , Esam I. Azhar, Arif Jamal Siddiqui , Bassem Kurdi , Abdulrahim Sajini , Abdulmajeed F. Alrefaei , and Sadaf Jahan 



Review Article (11 pages), Article ID 8835986, Volume 2020 (2020)

### **Myocardin-Related Transcription Factor A (MRTF-A) Regulates the Balance between Adipogenesis and Osteogenesis of Human Adipose Stem Cells**

Laura Hyväri, Sari Vanhatupa, Heidi T. Halonen, Minna Kääriäinen , and Susanna Miettinen 

Research Article (17 pages), Article ID 8853541, Volume 2020 (2020)

### **Differentiation Potential of Early- and Late-Passage Adipose-Derived Mesenchymal Stem Cells Cultured under Hypoxia and Normoxia**

Ashley G. Zhao , Kiran Shah , Julien Freitag, Brett Cromer , and Huseyin Sumer 


Research Article (11 pages), Article ID 8898221, Volume 2020 (2020)

### **A Xeno-Free Strategy for Derivation of Human Umbilical Vein Endothelial Cells and Wharton's Jelly Derived Mesenchymal Stromal Cells: A Feasibility Study toward Personal Cell and Vascular Based Therapy**

Hataiwan Kunkanjanawan, Tanut Kunkanjanawan, Veerapol Khemarangsarn, Rungrueng Yodsheewan , Kasem Theerakittayakorn, and Rangsun Parnpai 


Research Article (8 pages), Article ID 8832052, Volume 2020 (2020)

### **Dental Tissue-Derived Human Mesenchymal Stem Cells and Their Potential in Therapeutic Application**

Lu Gan, Ying Liu, Dixin Cui, Yue Pan, Liwei Zheng, and Mian Wan 


Review Article (17 pages), Article ID 8864572, Volume 2020 (2020)

### **Peripheral Circulation and Astrocytes Contribute to the MSC-Mediated Increase in IGF-1 Levels in the Infarct Cortex in a dMCAO Rat Model**

Xiaobo Li, Wenxiu Yu, Yunqian Guan, Haiqiang Zou, Zhaohui Liang, Min Huang, Renchao Zhao, Chunsong Zhao, Zhenhua Ren, and Zhiguo Chen 





Research Article (13 pages), Article ID 8853444, Volume 2020 (2020)

### **Spatial Distributions, Characteristics, and Applications of Craniofacial Stem Cells**

Geru Zhang, Qiwen Li, Quan Yuan, and Shiwen Zhang 


Review Article (9 pages), Article ID 8868593, Volume 2020 (2020)

### **Mesenchymal Stem Cell-Derived Extracellular Vesicles and Their Therapeutic Potential**

Ashley G. Zhao , Kiran Shah , Brett Cromer , and Huseyin Sumer 


Review Article (10 pages), Article ID 8825771, Volume 2020 (2020)

### **Bone Marrow Concentrate in the Treatment of Aneurysmal Bone Cysts: A Case Series Study**

Lorenzo Andreani, Sheila Shytaj , Elisabetta Neri, Fabio Cosseddu, Antonio D'Arienzo, and Rodolfo Capanna



Research Article (4 pages), Article ID 8898145, Volume 2020 (2020)

### **Dental Pulp Mesenchymal Stem Cells as a Treatment for Periodontal Disease in Older Adults**

Beatriz Hernández-Monjaraz, Edelmiro Santiago-Osorio, Edgar Ledesma-Martínez, Itzen Aguiñiga-Sánchez, Norma Angélica Sosa-Hernández, and Víctor Manuel Mendoza-Núñez 


Research Article (12 pages), Article ID 8890873, Volume 2020 (2020)

### **IL-37 Gene Modification Enhances the Protective Effects of Mesenchymal Stromal Cells on Intestinal Ischemia Reperfusion Injury**

Dejun Kong , Yonghao Hu, Xiang Li, Dingding Yu, Hongyue Li, Yiming Zhao, Yafei Qin, Wang Jin, Baoren Zhang, Bo Wang, Hongda Wang, Guangming Li, and Hao Wang 


Research Article (12 pages), Article ID 8883636, Volume 2020 (2020)

### **Patient-Centered Outcomes of Microfragmented Adipose Tissue Treatments of Knee Osteoarthritis: An Observational, Intention-to-Treat Study at Twelve Months**

Nima Heidari , Ali Noorani, Mark Slevin, Angela Cullen, Laura Stark, Stefano Olgiati, Alberto Zerbi, and Adrian Wilson

Research Article (8 pages), Article ID 8881405, Volume 2020 (2020)

### **Functions of Circular RNAs in Regulating Adipogenesis of Mesenchymal Stem Cells**

Fanglin Wang, Xiang Li, Zhiyuan Li, Shoushuai Wang, and Jun Fan 

Review Article (12 pages), Article ID 3763069, Volume 2020 (2020)



## Contents

---

### **Immunomodulatory Properties of Stem Cells in Periodontitis: Current Status and Future Prospective**

Mengyuan Wang, Jiang Xie, Cong Wang, Dingping Zhong, Liang Xie , and Hongzhi Fang 

Review Article (14 pages), Article ID 9836518, Volume 2020 (2020)

### **Cerebrospinal Fluid Pulsation Stress Promotes the Angiogenesis of Tissue-Engineered Laminae**

Linli Li, Yiqun He, Han Tang, Wei Mao, Haofei Ni, Feizhou Lyu , and Youhai Dong 

Research Article (12 pages), Article ID 8026362, Volume 2020 (2020)

### **Retinoic Acid Signal Negatively Regulates Osteo/Odontogenic Differentiation of Dental Pulp Stem Cells**

Jiangyi Wang , Guoqing Li, Lei Hu, Fei Yan, Bin Zhao, Xiaoshan Wu, Chunmei Zhang, Jinsong Wang, Juan Du , and Songlin Wang 

Research Article (12 pages), Article ID 5891783, Volume 2020 (2020)

## Research Article

# Comparison of the Migration Potential through Microperforated Membranes of CD146+ GMSC Population versus Heterogeneous GMSC Population

Mohamed Al Bahrawy <sup>1,2</sup>

<sup>1</sup>Stony Brook University, NY, USA

<sup>2</sup>Oral Medicine and Periodontology Department, Faculty of Dentistry-Ain Shams University, Cairo, Egypt

Correspondence should be addressed to Mohamed Al Bahrawy; bahrawy@asfd.asu.edu.eg

Received 25 June 2020; Accepted 31 August 2020; Published 12 March 2021

Academic Editor: Sangho Roh

Copyright © 2021 Mohamed Al Bahrawy. This is an open access article distributed under the Creative Commons Attribution License, which permits unrestricted use, distribution, and reproduction in any medium, provided the original work is properly cited.

**Background.** Guided tissue regeneration (GTR) is a powerful modality for periodontal regeneration, but it blocks the periosteum and gingival stem cells (GMSCs), from supporting periodontal wound by the nutrients, growth factors, and regenerative cells. The microperforated membrane considered a rewarding solution for this major drawback; GMSCs can migrate through a GTR microperforated membrane toward a chemoattractant, with the blocking of other unfavorable epithelial cells and fibroblasts. In the absence of a sole marker for MSC, a homogeneous population of GMSC is difficult to isolate; using CD146 as confirmatory markers for MSC identification, testing the behaviour of such homogeneous population in migration dynamics was the question to answer in this study. **Materials and Methods.** GMSCs from healthy crown lengthening tissue was isolated ( $n = 3$ ), its stem cell nature was confirmed, CD146 and CD271 markers were confirmatory markers to confirm homogenous stem cell population, and magnetic sorting was used to isolate GMSC with CD146 markers. A homogenous CD146 population was compared to heterogeneous GMSCs of origin; the population doubling time and MTT test of the two populations were compared. Migration dynamics were examined in a transwell migration chamber through  $8 \mu\text{m}$  perforated polycarbonic acid membrane, and  $0.4 \mu\text{m}$  and  $3 \mu\text{m}$  perforated collagen-coated polytetrafluoroethylene membrane (PTFE) and 10% fetal bovine serum (FBS) were the chemoattractants used in the lower compartment to induce cell migration, were incubated in a humidified environment for 24 hours, then migrated the cell in the lower compartment examined by a light and electron microscope. **Results.** GMSCs fulfilled all the minimal criteria of stem cells and showed low signal 10% for CD146 on average and extremely low signal 2% for CD271 on average. Magnetic sorting optimized the signal of CD146 marker to 55%. GMSC CD146 population showed nonstatistically significant shorter population doubling time. CD146 homogeneous population migrated cell numbers were statistically significant compared to the heterogeneous population, through  $0.4 \mu\text{m}$  and  $3 \mu\text{m}$  perforated collagen membrane and  $8 \mu\text{m}$  perforated polycarbonate membrane. Scanning electron microscopy proved the migration of the cells. **Conclusions.** A subset of the isolated GMSC showed a CD146 marker, which is considered a dependable confirmatory marker for the stem cells. In terms of GMSC migration through the microperforated membrane, a homogeneous CD146 population migrates more statistically significant than a heterogeneous GMSC population.

## 1. Introduction

Periodontitis is a chronic inflammatory bacterial infection, where the oral flora organizes a biofilm subgingivally, which constitutes a continuous challenge to the host immune

system that responds by continuous inflammatory cytokine shower that affects the body homeostasis; with time, deregulated immune response eventually results, and a hyperresponsive immune reaction causes the destruction of the tooth-supporting apparatus, leading to tooth loss.



Periodontitis is considered an irreversible degenerative disease of the odontogenic supporting tissue; this throws light on the immune-mediated nature of periodontal disease [1].

A historical debate did exist about the periosteum's role in bone growth, repair, and regeneration. Two theories have been contrasting; one postulated that periosteum is an inert membrane covering the bone with no exact role [2]; the other considered the periosteum as a functioning membrane with osteogenic potentials, responsible for regeneration and bone growth. A number of classical experiments created strong evidence that leads to modern literature where the essential role of periosteum for bone healing was understood. A classical study when the periosteum surrounding fractures removed the result was the absence of callus in the fracture [3].

Guided tissue regeneration technique (GTR) was based on blocking the growth of unfavorable cells from invading the periodontal wound, namely, the gingival epithelium and connective tissue, but as collateral damage to this technique, were scalding the alveolar bone from its periosteum by elevating a full-thickness flap. Blocking the periodontal wound by a barrier membrane from the periosteum in fact excludes the wound area from a powerful regenerative source which is an essential source of blood and nutrient supply; besides that, the periosteum is a niche of biologic mediators and progenitor cells essential for the regeneration process [4].

Not only periosteum but GTR also deprive the periodontal wound from the gingival connective tissue, to block the rapidly proliferating fibroblasts which can invade the periodontal wound before the slowly proliferating periodontal ligament and bone cells, but regrettably, a well-recognized population of stem cells named the gingival mesenchymal stem cells (GMSC) is blocked from the wound [5, 6] if GMSCs allowed migrating to the periodontal defect and induced to differentiate; using the suitable biological factors into periodontal ligament cells and osteoblasts with a well-designed organized scaffold, biological factor release cascade, such as a system, would satisfy the real aim of GTR. Thus, the occlusive barrier membrane of the classical GTR is unfavorable for periodontal regeneration [4].

In comparison to bone marrow stem cells, the gold standard, the first stem cell described, and the most studied, GMSC was superior in nearly every aspect, besides its ease of harvesting with very low morbidity; no scaring; homogeneous population; high proliferation rate without the need for special growth factors; morphology stable within successive passages; reduced senility; and stable karyotype, maintains its telomerase activity to later passages, and shows very low tumorigenic potential [5]; this concluded that the gingiva is a very good source of stem cells compared to the bone marrow, with functionally competent MSCs, that can be used with a wide range of medical applications.

Gamal and Iacono's clinical study tested macroperforated GTR and posted improved clinical outcome, followed by a series of studies in 2014 and 2016; they hypothesized that GTR membrane perforation allowed bone morphogenic protein (BMP-2) and platelet-derived growth factor (PDGF-BB), besides vascular endothelial cell growth factor (VEGF) and other nutrients migrating freely through the membrane,

which was the reason for the improved clinical outcomes [7–9]. In 2018, Al Bahrawy et al.'s *in vitro* study concluded that macroperforation jeopardizes the GTR membrane occlusive function and its mechanical properties; this study postulated a new development of Gamal and Iacono's concept by a microperforated membrane, a concept was proved, GMSCs can migrate through the microperforation under chemoattractant influence, and the membrane was occlusive for cell migration in the absence of a chemoattractant; hence, the GTR membrane could be a selective occlusive barrier allowing the migration of the desired cells while blocking others, under the influence of the right chemoattractant [4].

A cell to be considered stem cell must be multipotent, can differentiate to other cell types than the tissue of origin, must be clonogenic, and has strong proliferation power. In fact, only a fraction of the plastic adherent cells showed these characteristics; this is explained by the heterogeneous population of the isolated cells and attributed to the nature of tissue of origin [10]. Another issue to consider is the absence of one specific marker that can identify stem cells from other mature cells; many surface markers, for example, CD73, CD90, CD105, CD146, or even neural crest markers; and intracytoplasmic markers like STRO-1, OCT-4, Nanog, Nestin, and Notch-1 that could be used to characterize stem cells [11, 12], taking into consideration that different stem cells from different tissue origins show a different set of markers, but as a minimal criterion, cells must show a high signal of CD73, CD90, and CD105 together. The main drawback with these three markers was that they are expressed by fibroblast, although in weak signal [13]; besides, fibroblast morphology was identical to MSCs; both did plastic adherence and fibroblast dipotency, can differentiate to at least two other cell lines, and made identification of fibroblast from MSC *in vitro* not an easy task; this urged the need for at least additional cell marker.

It was well described that MSC is located around blood vessels; in 2008, Covas and colleagues compared MSC from different tissue origins to fibroblasts and pericytes, and they concluded that 12 MSC populations were very similar to 4 fibroblasts and 2 pericyte populations phenotypically; the only difference was fibroblast weak signal of the CD146 surface marker compared to MSC and pericytes; both showed a strong signal of this marker in flow cytometry. Comparing the 3 cells genetically, they concluded that the gene expression pattern of MSC is similar to pericytes and stellate hepatic cells, not fibroblast which showed the gene expression pattern of myofibroblasts and smooth muscle cells [14].

Another evidence of the pericyte and MSC similarity was proved in other studies, where the 3 minimal markers of MSCs CD73, CD90, and CD105 have a vascular and perivascular distribution pattern *in vivo* [15, 16]; to confirm this assumption, other MSC-specific markers were examined, namely, CD146, NG2, Stro-1, and 3G5, which confirmed the previous results of the vascular and perivascular distributions of these markers [15, 17]. Connecting all of this data together, we can conclude the close nature of MSC and pericytes *in vivo* in contrast to fibroblast; this data built strong evidence that CD146 which is essentially a pericyte marker would be a good candidate to confirm MSC; besides

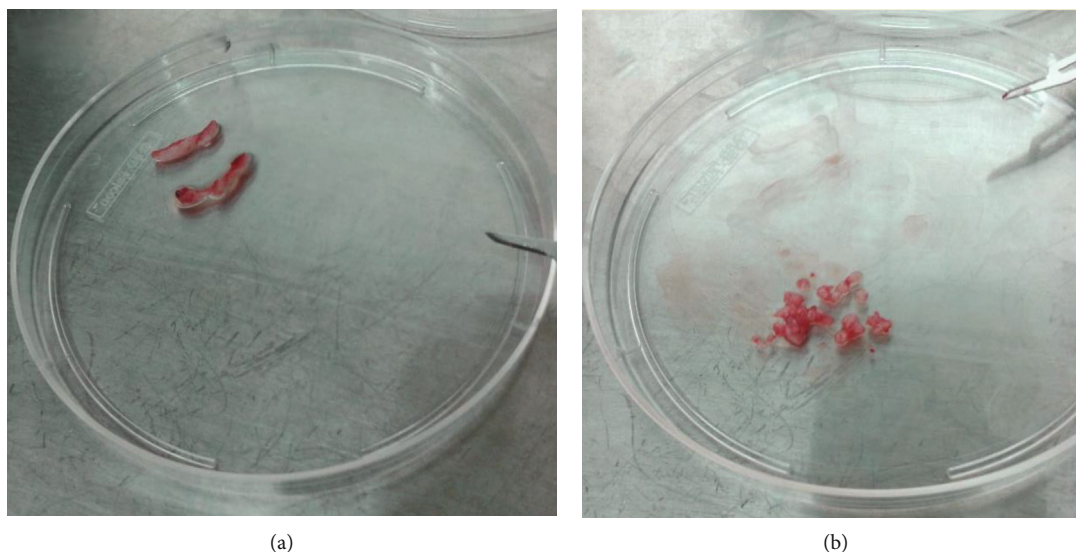


FIGURE 1: (a) Healthy gingival tissue specimen of discarded crown lengthening procedures. (b) Gingival connective tissue was meshed to 1 mm pieces using a surgical blade.

the other three fundamental markers, a cell population expressing them all with a high signal is a homogeneous MSC population.

From all of what was mentioned, we conclude that depriving the wound area from GMSC with its multipotent abilities was not a good idea because it is an important source of regeneration. It has undenied the breakthrough the GTR technique had achieved in the periodontal treatment in general and in the regeneration concept, in particular, but it is now clear the GTR by its traditional occlusive membrane is not the best practice for the regeneration procedure, and microperforation of this membrane is essential; besides, utilizing a full system of specific chemoattractant in the periodontal wound side of the membrane for GMSCs will let this powerful cells invade the wound area, to achieve the optimum outcome of GTR technique, with organized chronologically activated cell differentiation induction biological factors.

## 2. Materials and Methods

**2.1. Sample Selection.** Gingival specimens are healthy gingival tissue of discarded crown lengthening procedures of outpatients who attended at Stony Brook University dental care clinics Figure 1(a). A parallel case-control experimental study of two groups was designed. Four subjects accepted to participate in this study, all experiments were done in triplicate ( $n = 3$ ), and participants were informed about the nature of the experiment and verbally accepted the use of their discarded tissue in stem cell research. The ethical committee of scientific research at School of Dentistry Ain Shams University and Stony Brook University had approved this study (IRB 575741).

The gingival epithelium was carefully scalded from the specimen; the connective tissue was meshed to very small pieces using the surgical lancet Figure 1(b) then digested in 2 mg/ml Dispase II overnight at 4°C (Sigma-Aldrich, St.

Louis, USA) and then in Collagenase IV (Fisher Scientific, Massachusetts, USA) for 40 minutes at 4°C; the resulted cell suspension was strained in 40  $\mu$ m strain to remove the impurities, then centrifuged at 1200 rpm for 8 minutes. The resultant single-cell suspension was inoculated in 10 cm cell culture dish, in alpha-minimal essential medium (alpha-MEM 1 $\times$ , Gibco, Thermo Fisher Scientific, Massachusetts, USA), supplemented with 10% fetal bovine serum (FBS) (Hyclone, Thermo Fisher scientific, Massachusetts, USA) and 50 U/ml penicillin G with 50  $\mu$ g/ml streptomycin and 2.5  $\mu$ g/ml amphotericin B (Fungizone, Thermo Fisher scientific, Massachusetts, USA), at a concentration of 60 cells/cm<sup>2</sup>. The single-cell suspension plates were incubated in 37°C, 5% CO<sub>2</sub> humidified incubators. Cells reached confluence after approximately 28 days for the first passage, then subcultured in a P100 plate for the next passages, and reached confluence on average in 14 days.

**2.2. Colony-Forming Unit.** At passage five, cultured cells were detached using 0.05% trypsin/EDTA, cells were diluted in alpha-MEM (Gibco, Thermo Fisher Scientific, Massachusetts, USA) enriched with 10% FBS (Hyclone, Fisher Scientific, Massachusetts, USA) at a concentration of 10<sup>3</sup> cell/ml in P10 dishes, and media were changed every 3 days and examined under a microscope till typical fibroblast colonies of 100 cells formed.

**2.3. Population Doubling Assay.** Menicanin et al.'s protocol was followed; briefly, GMSCs were seeded in 24-well plate with a concentration of 5  $\times$  10<sup>3</sup> cells/cm<sup>2</sup>; when 90% confluence was reached, cells were detached using 0.05% trypsin/EDTA and then counted, cells were diluted and reseeded with the same concentration in another 24-well plate, and the same procedure was repeated for five passages. Cells were counted in each passage, and population doubling was calculated using this formula:  $\log^2$  final cell number/ $\log^2$  seeding cell number [18].

**2.4. Flow Cytometry Assay.** At the 5th passage, cell culture was washed twice by PBS, then detached using 0.05% trypsin/EDTA; detached cells were resuspended in 1% bovine serum albumin as a blocking buffer for half an hour. Cells were aliquoted with a concentration of  $1 \times 10^5$  cells in two test tubes, then  $2 \mu\text{g/ml}$  of CD73 and its isotype control fluorescein isothiocyanate- (FITC-) conjugated mouse monoclonal antibodies in each tube, and then incubated for 30 minutes in  $4^\circ\text{C}$  (BD Pharmingen, San Jose, California, United States). The same procedure was done with CD90 and its isotype using APC-conjugated mouse monoclonal antibodies (BD Pharmingen, San Jose, California, United States), for CD105 and its isotype using Alexa 555 goat anti-mouse monoclonal antibodies (Dako, Agilent, Santa Clara, USA) and finally, for CD146 and CD271 and their isotype PE-conjugated mouse monoclonal antibodies (BD Pharmingen, San Jose, California, United States). After incubation buffer was aspirated, cells were washed twice by resuspension in PBS and centrifugation at 1200 rpm for 8 minutes, and cells were then transferred to a flow cytometry facility for the analysis of stem cell marker expression. Regarding the hematopoietic markers, namely, CD14, CD34, and CD45, the same protocol was followed with no difference.

## 2.5. In Vitro Differentiation Assay

**2.5.1. Osteogenic Differentiation.** Cell suspension at passage 4 was seeded in six-well plates with a concentration of  $8 \times 10^3$  cells/cm<sup>2</sup> in a ready-made osteogenic induction medium (Gibco StemPro, Thermo Fisher Scientific, Massachusetts, USA), according to Gronthos et al.'s protocol; the medium was changed every 3 days for 28 days in humidified incubators ([19, 20]), the cell cultures were washed twice by PBS, fixed by 4% paraformaldehyde for 1 hour, washed again twice by distilled water, finally stained by 2% Alizarin Red for 45 minutes, finally washed 4 times by distilled water and 2 times by PBS, and checked under a microscope (Figure 2).

**2.5.2. Adipogenic Differentiation.** Cell suspension at passage 4 was seeded in six-well plates with a concentration of  $8 \times 10^3$  cells/cm<sup>2</sup> in a ready-made adipogenic induction medium (Gibco StemPro, Thermo Fisher Scientific, Massachusetts, USA) according to Pittenger et al.'s protocol; the medium was changed 2 times per week for 28 days [21]. After that time, the cell cultures were washed twice with PBS, fixed by 4% paraformaldehyde for 1 hour, and washed again twice by distilled water; the cell culture is washed by 60% isopropanol for 5 minutes, then stained for 5 minutes by Oil Red O in isopropanol (300 mg Oil Red in 100 ml isopropanol), washed by tap water, and finally stained by hematoxylin for 1 minute, again washed by tap water, and checked under a phase-contrast microscope (Figure 2).

**2.5.3. Chondrogenic Differentiation.** Cell suspension at passage 4 was seeded in six-well plates with a concentration of  $8 \times 10^3$  cells/cm<sup>2</sup> in a ready-made chondrogenic induction medium (Gibco StemPro Thermo Fisher Scientific, Massachusetts, USA); the medium was changed 2 times per week for 28 days. After that time, the cell cultures were washed twice by PBS, fixed by 4% paraformaldehyde for 1 hour,



FIGURE 2: Ready-made osteogenic, adipogenic, and chondrogenic stem cell differentiation media (Gibco StemPro, Thermo Fisher Scientific, Massachusetts, USA).

washed twice by distilled water, then stained in dark with Alcian blue (10 mg in 60 ml ethanol with 40 ml acetic acid) overnight; the next day, the cell culture was destained by 120 ml ethanol with 80 ml acetic acid for 20 minutes, finally washed 2 times by PBS, and then checked under a microscope (Figure 2).

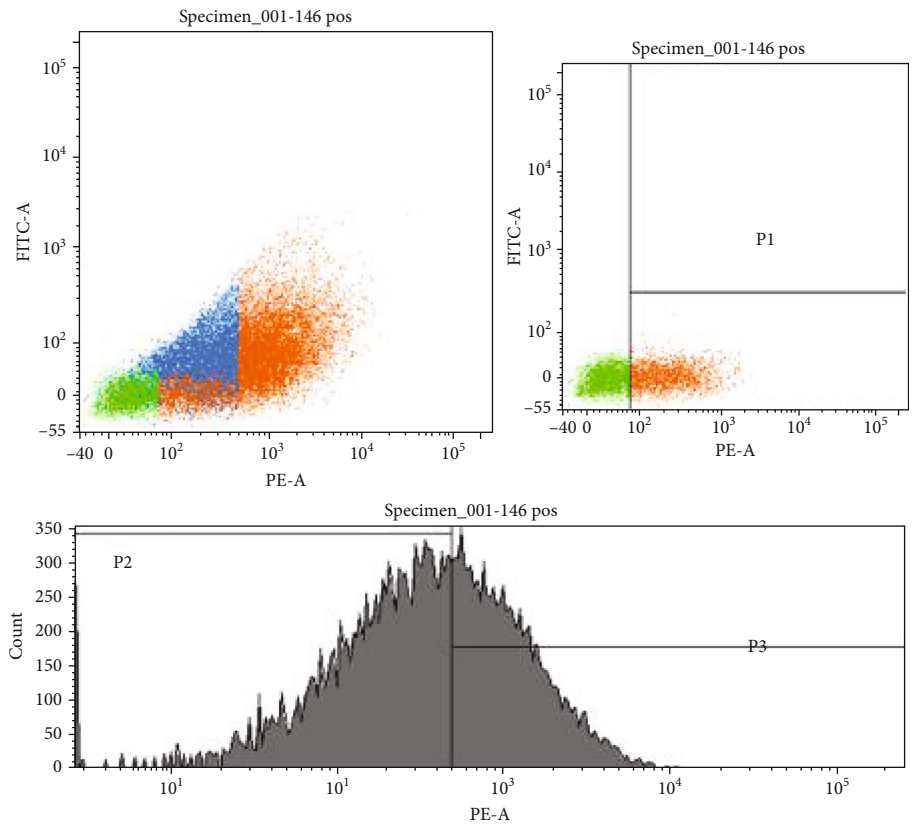
**2.5.4. MTT Assay.** Detached cell culture of the fourth passage was suspended in  $500 \mu\text{l}$  alpha-MEM (Gibco, Thermo Fisher Scientific, Massachusetts, USA) enriched with 10% FBS (Hyclone, Fisher Scientific, Massachusetts, USA), poured in spectrophotometer tube, and left in a humidified incubator ( $37^\circ\text{C}$ , 5%  $\text{CO}_2$ ); the negative control was a medium-enriched tube without cells, within the same incubator. The next day,  $100 \mu\text{l}$  of MTT stain was added, and tubes were incubated for another 4 hours; then, media were aspirated and  $1000 \mu\text{l}$  of dimethyl sulfoxide (DMSO) was added, and tubes were analysed by a spectrophotometer at a 595 nm wavelength.

## 2.6. Cell Sorting

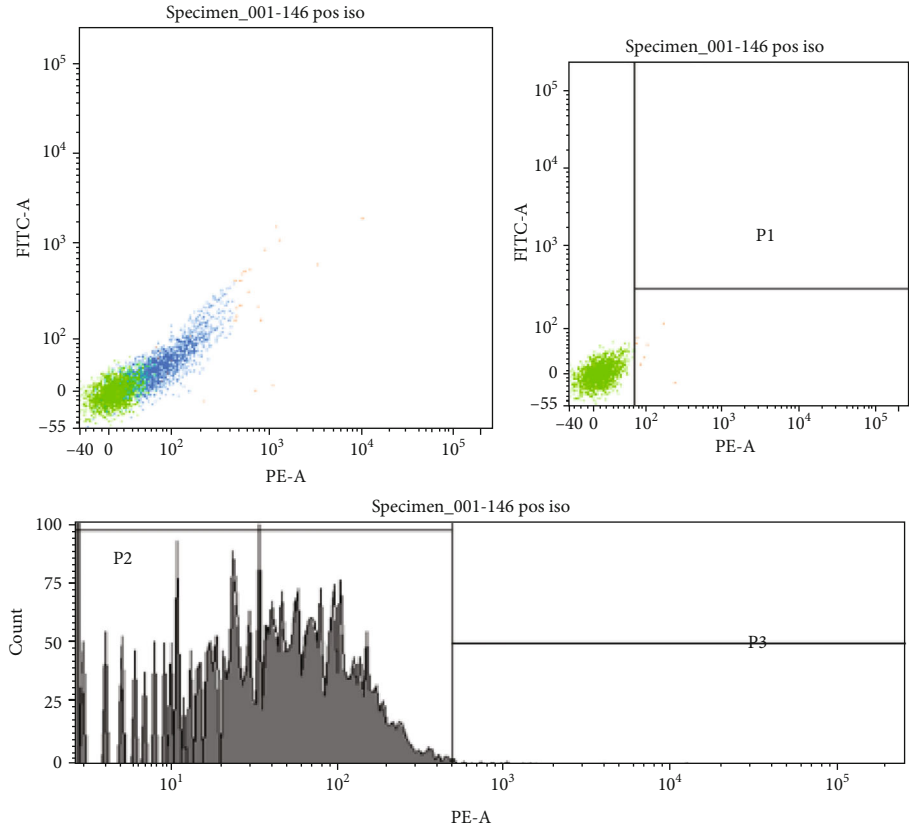
**2.6.1. Flow Cytometry Cell Sorting.** The same protocol of cell characterization was followed; the only difference was not to fix the cells; it has to be noted that the sorting procedure was done as soon as possible after cell detachment, as the cells were suspended in serum-free media; finally, after sorting by the machine, cells were collected in media enriched with 20% FBS.

**2.6.2. Magnetic Sorting.** After detaching, cells were counted and suspended in 1 ml of buffer of the cell sorting kit (MACS cell separation, Miltenyi Biotech, USA). Cells were





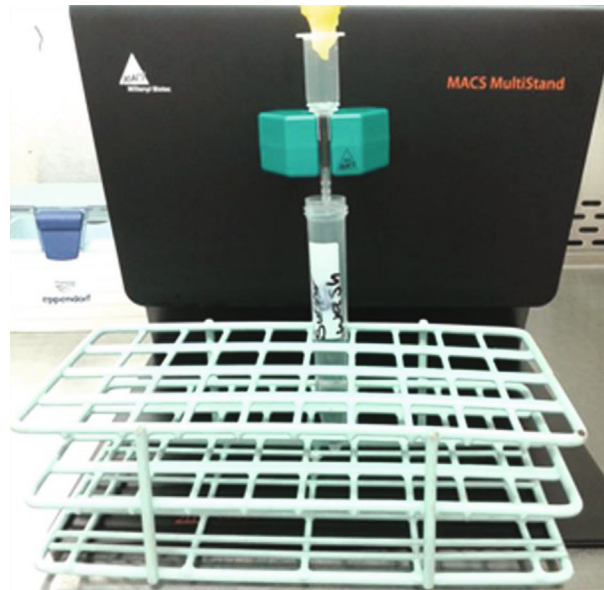
(a)



(b)

FIGURE 3: Continued.





(c)

FIGURE 3: (a) The confirmatory flow cytometry graph of the magnetic sorted GMSC homogeneous CD146-positive population, which optimized the signal to 55% purity. (b) The flow cytometry graphs of the negative control isotype, which showed no signal of the CD146 marker. (c) The magnetic sorting kit.

centrifuged at  $300 \times g$  for 10 minutes, the buffer was suctioned,  $20 \mu\text{l}$  Fc block was added, and  $20 \mu\text{l}$  CD146 marker was labelled with microbeads. Tubes were incubated in  $4^\circ\text{C}$  for 14 minutes, washed in 1 ml buffer, and centrifuged at  $300 \times g$  for 10 minutes. Cells were suspended in  $500 \mu\text{l}$  MAC buffer solution. The magnetic sorting column was primed by  $500 \mu\text{l}$  MAC buffer solution, the cell suspension was added in the sorting column, and the column was washed three times using  $500 \mu\text{l}$  MAC buffer solution in each. Finally, we plunged out the cells from the sorting column using serum-free alpha-MEM Figure 3.

## 2.7. Migration Assay

**2.7.1. Microscopic Perforated Membranes.** In the transwell chemotaxis migration chamber (Boyden chamber) was the test used to analyse the migration dynamics of GMSCs (Corning Life Sciences, New York, USA); 2 types were used, namely, 12 mm perforated collagen-coated polytetrafluoroethylene (PTFE) membrane with a pore size of  $0.4 \mu\text{m}$  and  $3 \mu\text{m}$  pores and a 6.5 mm perforated polycarbonate membrane with a pore size of  $8 \mu\text{m}$ . Cultured heterogeneous GMSCs were the positive control group, and the homogeneous CD146-positive sorted and expanded GMSCs were the experiment group. Cells were detached using 0.05% trypsin/EDTA, then suspended in serum-free alpha-MEM diluted to  $1 \times 10^4$  concentration and added to the upper compartment of the chemotaxis chamber inserts. For both groups, the lower compartment of the chemotaxis chamber received alpha-MEM with 10% fetal bovine serum as a chemoattractant (Hyclone, Fisher Scientific, Massachusetts, USA), The migration chamber plates were incubated for 24 hours in a humidified atmosphere ( $37^\circ\text{C}$ , 5%  $\text{CO}_2$ ).

The next day, the migration inserts were collected from the plates, and media in the upper compartment aspirated. The inserts were washed two times in PBS. Using a cotton swab, the upper side of the membrane was scraped thoroughly to remove all the cells still attached to the upper compartment. Cells on the lower side of the membrane were fixed by 4% paraformaldehyde for 2 minutes; inserts were washed 2 times in PBS; cells were then permeabilized by 100% methanol and stained by crystal violet (1% in 80% ethyl alcohol, Sigma Aldrich) and washed again two times in PBS; membrane was examined under the microscope at 40x magnification; migrated cells were counted in 5 different areas; and the average was counted.

**2.7.2. Scanning Electron Microscope.** Membranes were cut off the migration inserts, fixed by 4% paraformaldehyde for 2 minutes, and left to dry. Membranes were soaked in 50%, 70%, 80%, 90%, and 100% ethyl alcohol for 10 minutes each, finally frozen in minus  $80^\circ\text{C}$  overnight, then sent to an electron microscope facility, were coated by gold, and examined by the electron microscope.

**2.7.3. Statistical Evaluation.** All statistical analyses were done using SPSS v20 program, IBM; the descriptive analysis was used to determine the distribution of the data, and graphs were plotted; according to it, the Mann-Whitney  $U$  test was the test of choice according to the data distribution, the alpha significance of difference was set at  $p < 0.05$ , and all experiments were done in triplicate.

## 3. Results

**3.1. Colony-Forming Potential.** Seeded GMSCs in P10 dish showed typical distinctive fibroblast-like colonies of 50 to

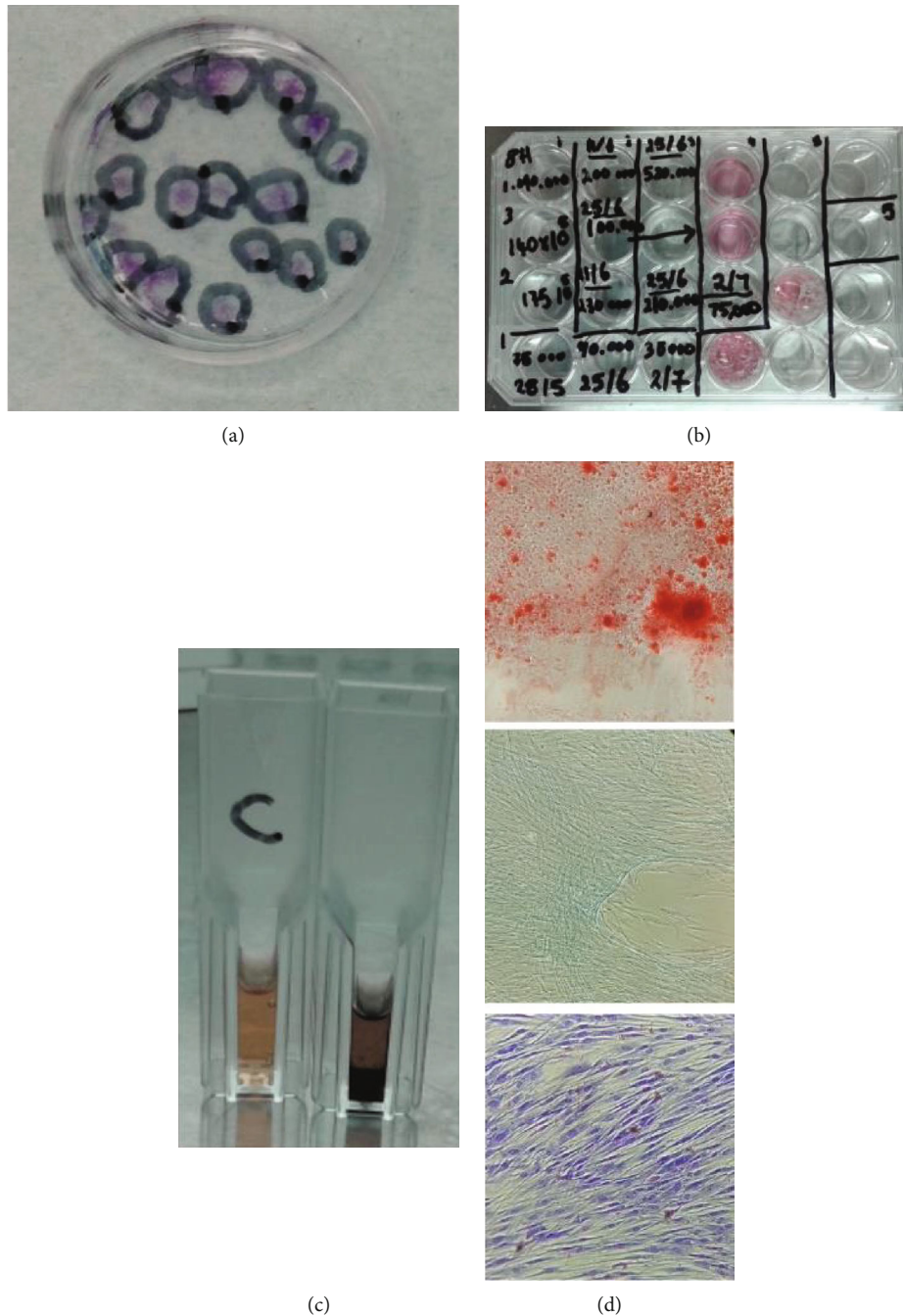
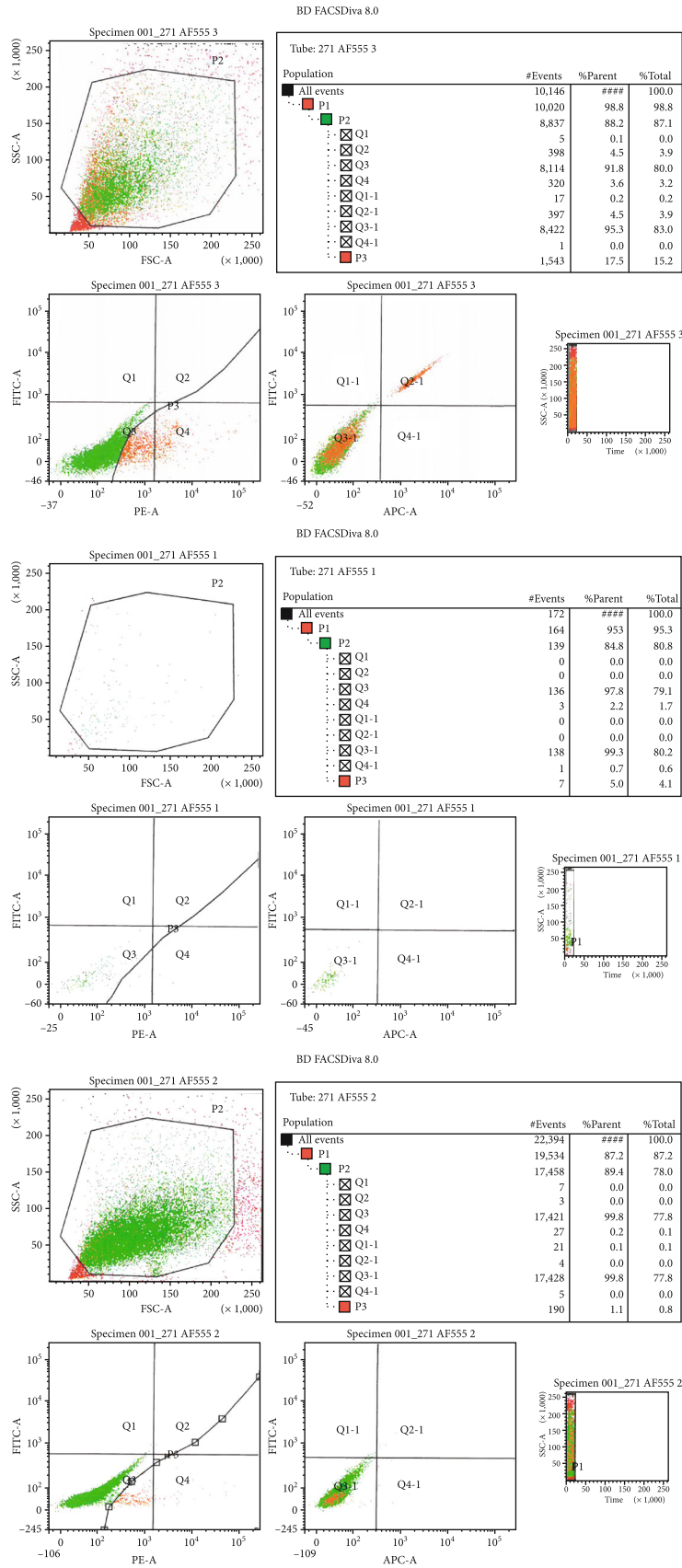


FIGURE 4: (a) Representative image of CFU experiment showing stem cell colony-forming potential. (b) Representative image showing the cell population doubling potential. (c) Representative image for the MTT assay showing black deposits in the experiment tube compared to the control group. (d) Representative image showing cell differentiation potential; calcium deposition (upper), cartilage glycoprotein deposition (middle), and fat droplet deposition (lower).

100 cells/colony after on average 14 days of culturing in vitro; all experiments were done in triplicate ( $n = 3$ ) for each group; no significant difference was noted between the heterogeneous GMSC group and CD146-positive homogeneous GMSCs in shape, form, or number of cells in colonies ( $p > 0.05$ ; Mann-Whitney  $U$  test); the only difference noted was that the homogeneous CD146-positive group reached 100 cell colonies 1 day earlier on average compared to the heterogeneous group (Figure 4(a)).

**3.2. Population Doubling Potential.** The two groups were similar in showing strong proliferation capability. The population doubling time was nonsignificantly less in the CD146-positive homogeneous group compared to the heterogeneous group ( $p > 0.05$ ; Mann-Whitney  $U$  test) (Figure 4(b)).

**3.3. Cell Characterization.** Both groups lacked the expression of hematopoietic markers, namely, CD14, CD34, and CD45, and both groups could express the main MSC markers,



(a)

FIGURE 5: Continued.

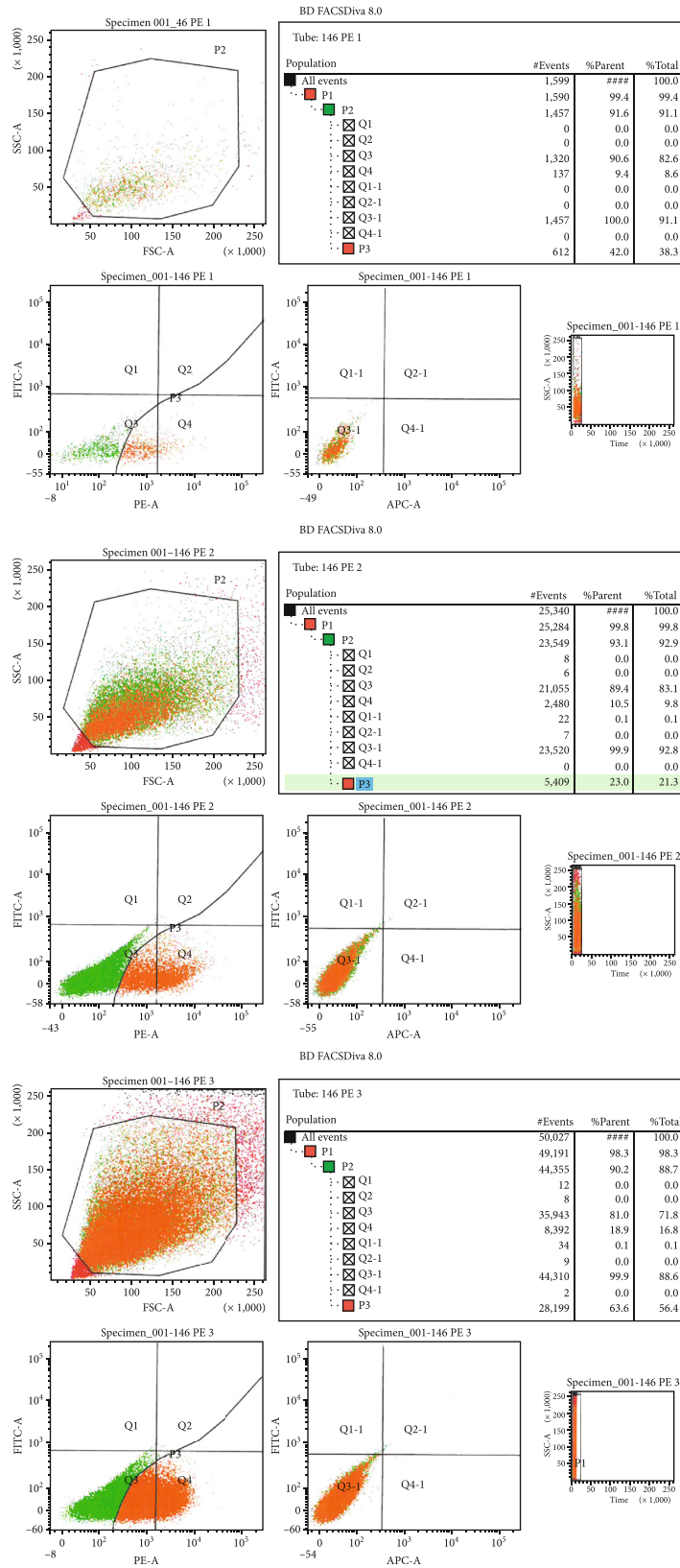


FIGURE 5: (a) The CD271 flow cytometry graphs of 3 cell lines of the heterogeneous GMSC population, signal percentage of cell line A: 2% (upper), cell line B: 1% (middle), and cell line C: 4% (lower). (b) The CD146 flow cytometry graphs of 3 cell lines of the heterogeneous GMSC population, signal percentage of cell line A: 10% (upper), cell line B: 11% (middle), and cell line C: 17% (lower).



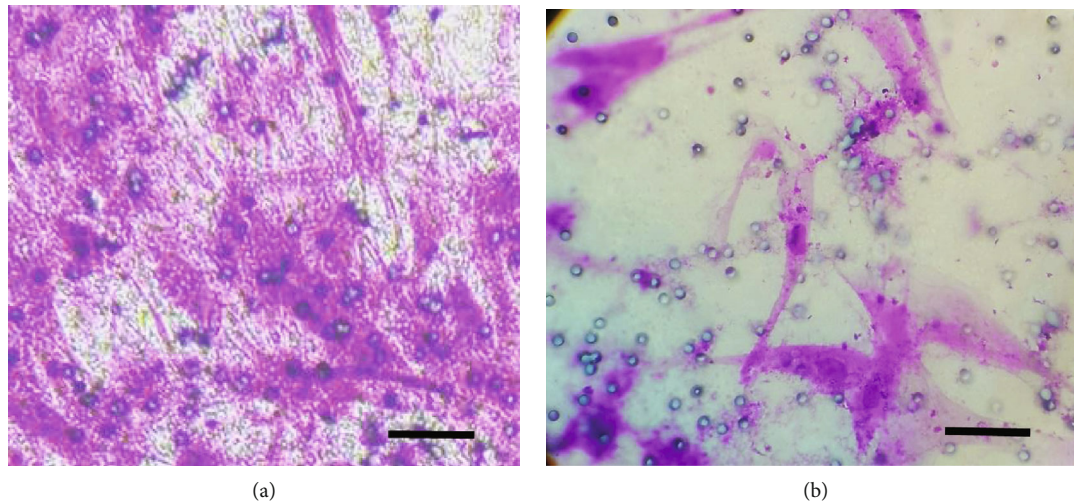


FIGURE 6: (a) Migrated CD146-positive homogeneous GMSC in the lower compartment of 8  $\mu\text{m}$  perforated polycarbonate membrane toward fetal bovine serum as a chemoattractant; cells stained with crystal violet; 10,000 cells seeded in the upper compartment. (b) Migrated heterogeneous GMSC in the lower compartment of 8  $\mu\text{m}$  perforated polycarbonate membrane toward fetal bovine serum as a chemoattractant; cells stained with crystal violet; 10,000 cells seeded in the upper compartment (40x magnification).

namely, CD73, CD90, and CD105 with a strong signal for the three; another 2 markers tested the CD146 which showed a weak signal of 11% on average Figure 5(b) and CD271 which showed a very weak signal of 2% on an average Figure 5(a); this was another reason to choose the CD146 as a confirmatory marker for the gingival connective tissue stem cells, where CD271-positive GMSCs were very rare in the gingival isolated stem cells.

**3.4. Flow Cytometry Cell Sorting.** Using flow cytometry cell sorting module, the cells expressing the CD146 marker were isolated successfully, and the isolated cells were attached to plastic and started to show a fibroblast-like shape the next day. Unfortunately, after 3 days, all the isolated cell dishes showed bacterial contamination, in all the plates; the experiment was repeated three times with the same tragedy; this forced us to resort to magnetic sorting.

**3.5. Magnetic Cell Sorting.** Using a magnetic sorting method for cell isolation, CD146 homogeneous cell population was isolated successfully, cells showed plastic adherence after a longer time than expected, and cells did not show fibroblast-like morphology except after two to three days on average; an explanation might be that the magnetic sorting antibodies hinder the MSC attachment to the plastic; after that, cells behaved normally and showed a colony-forming unit after 12 to 13 days on average; another confirmatory flow cytometry assay was done to ensure the homogeneity of the CD146 cell population, which showed 55% signal (Figures 3(a)–3(c)).

**3.6. Cell Metabolic Activity.** This MTT test examined the metabolic activity of the cultured cells and hence its vitality. Both the experiment and the heterogeneous cell groups showed no significant difference between them regarding its metabolic activity ( $p > 0.05$ ; Mann–Whitney  $U$  test) (Figure 4(c)).

**3.7. Multilineage Differentiation Potential.** GMSCs of both groups cultured in osteogenic induction media for 28 days showed osteogenic differentiation capacity, which was proved by calcification stained by Alizarin Red stain. Cells of both groups cultured in chondrogenic induction media for 28 days showed chondrogenic differentiation capacity proved by cartilage glycoprotein deposits stained by Alcian blue stain. Finally, cells of both groups cultured in adipogenic induction media for 28 days showed lipid deposits proved by lipid droplets stained by Oil Red stain. Control GMSCs cultured in alpha-MEM media with 10% FBS for 28 days did not stain any deposits with three mentioned stains (Figure 4(d)).

### 3.8. Transwell Migration Potential

**3.8.1. Migration through Polycarbonate Membrane 8  $\mu\text{m}$  Pore Size.** A significantly higher number of CD146-positive homogeneous GMSCs migrated through the membrane compared to the heterogeneous GMSC population toward the 10% FBS chemoattractant, (the  $z$ -score is 2.50672. The  $p$  value is 0.01208. The result is significant at  $p < 0.05$ ) (Figures 6(a) and 6(b), Table 1).

**3.8.2. Migration through Collagen-Coated PTFE Membrane 0.4 and 3  $\mu\text{m}$  Pore Size.** A significantly higher number of CD146-positive homogeneous GMSCs migrated through the 0.4 (the  $z$ -score is 2.08893. The  $p$  value is 0.03662. The result is significant at  $p < 0.05$ ) and 3  $\mu\text{m}$  pores (the  $z$ -score is 2.50672. The  $p$  value is 0.01208. The result is significant at  $p < 0.05$ ) compared to the heterogeneous GMSCs toward 10% FBS in the lower compartment of the transwell migration chamber as a chemoattractant (Table 1); to be noted, the migration of cells of both groups through 0.4  $\mu\text{m}$  was nonsignificantly less than the migration through 3  $\mu\text{m}$  pores; both were statistically significantly less than migrated cells through the 8  $\mu\text{m}$  pores.

TABLE 1: The average number of migrated cells counted in five, random fields at 40x light microscope magnification. For 8 microns, the  $z$ -score was 2.50672. The  $p$  value was 0.01208. The result was significant at  $p < 0.05$ . For 3 microns, the  $z$ -score was 2.50672. The  $p$  value was 0.01208. The result was significant at  $p < 0.05$ . For 0.4 microns, the  $z$ -score was 2.08893. The  $p$  value was 0.03662. The result was significant at  $p < 0.05$ .

Experiment	8 microns		3 microns		0.4 microns	
	CD146+	Heterogeneous	CD146+	Heterogeneous	CD146+	Heterogeneous
1	202*	90	41*	25	3*	2
2	149*	50	40*	22	3*	2
3	229*	45	33*	26	2*	1
4	223*	60	30*	24	3*	2

\*A statistically significant difference of GMSC CD146 homogeneous population compared to the heterogeneous GMSC population.

3.9. *Scanning Electron Microscope*. No morphological difference was noticed in the cell shape or form or migration pattern through the micropores between the two groups. Both groups' cells looked to be flatter and spread over a larger area over the polycarbonate membrane compared to the collagen membrane. On collagen, the cells of both groups looked more bulbous and extend strands all over the collagen meshwork Figures 7(a)–7(d).

#### 4. Discussion

The principle of GTR is to block the migration of the gingival epithelium along the cementum wall of the pocket, creating a space for stabilization of the blood clot to allow the periodontal ligament (PDL) cells to invade the blood clot for the aim of periodontal tissue regeneration [22]. The GTR membrane is hence a physical barrier that has a biologic effect on the healing process of the PDL, affecting the differentiation and proliferation of the mesenchyme, and through clot protection during early stages of healing maintains space for the growing periodontal tissue, to repopulate the wound area with selective tissue populations. Hence, the GTR membrane is considered a biomechanical membrane.

In 2018, Al Bahrawy et al. [4] proved the concept that GMSCs can migrate through microperforated membranes of GTR in the presence of a suitable chemoattractant, while in the absence of the chemoattractant, the membranes were totally occlusive for cell migration; this can be a basis for a new generation of the GTR technique, where a selective barrier membrane was employed, which was occlusive for undesired cells in the gingival tissue, namely, the epithelium and connective tissue cells, and allowed the homing of GMSCs from the gingival tissue to the periodontal wound by utilizing a suitable chemoattractant in the wound area [4].

In the present study, the proliferation and the migration potential of homogeneous CD146-positive GMSC population were compared to a heterogeneous GMSC population of origin; the reason for choosing the CD146 marker to isolate the GMSC population was the unique characteristics of that marker, being not expressed by the fibroblasts and expressed by nearly all the MSC populations, which made it a very good candidate as a marker that insured the stemness of the cell population.

In this study, homogeneous CD146-positive cell population migrated significantly more than the heterogeneous

GMSC population, through 0.4  $\mu\text{m}$ , 3  $\mu\text{m}$ , and 8  $\mu\text{m}$  pores of microperforated membranes toward 10% FBS in alpha-MEM media as a chemoattractant; also, the homogeneous population showed nonsignificantly better proliferation capacity than the heterogeneous GMSC population; this could prove the hypothesis that the homogeneous CD146 population can show more proliferation potential and migration chemodynamics through microperforated membranes compared to the heterogeneous GMSC population; this might be explained by a better migration potential of the CD146-positive cells or the existence of a chemoattractant factor in the serum more specific for the CD146-positive cells; this result needs further investigation.

The isolated cells demonstrated all the criteria of the International Society of Cellular Therapy of stem cells, namely, plastic adherence; the ability of colony forming; expression of immunophenotype markers CD105, CD73, and CD90; lack the expression of hematopoietic markers CD45, CD34, and CD14; and finally multipotent differentiation potential [6, 21, 23]. In comparison to the heterogeneous GMSC population, CD146-positive homogeneous GMSCs were similar in every aspect, except for faster proliferation, and a significant number of cells migrated to the lower compartment of the migration chamber during 24-hour period.

In this study, 10% FBS was utilized as the chemoattractant for both the homogeneous and the heterogeneous GMSC populations to assess their migration potential through microperforated membranes. In both groups, cells were seeded in the upper compartment with a concentration of 10,000 cells; this concentration was chosen according to our previous study which proved that adding a greater number of cells in the upper compartment made cell identification and counting absolutely difficult in the lower compartment [4].

GMSCs actively migrated irrespective to the effect of gravitational forces or fluid diffusion forces. In both groups, the rate of cell migration in 24-hour intervals only varied according to the sizes of the pores, where the highest migration rate was through the 8  $\mu\text{m}$  pores and the least through the 0.4  $\mu\text{m}$  pores. GMSCs from both groups did not migrate with statistical significance through the 0.4  $\mu\text{m}$  and 3  $\mu\text{m}$  pores within the same group, but with statistically significant difference between groups in favor of the homogeneous population group; instead, there was a statistically significant difference in the rate of cell migration through the 8  $\mu\text{m}$



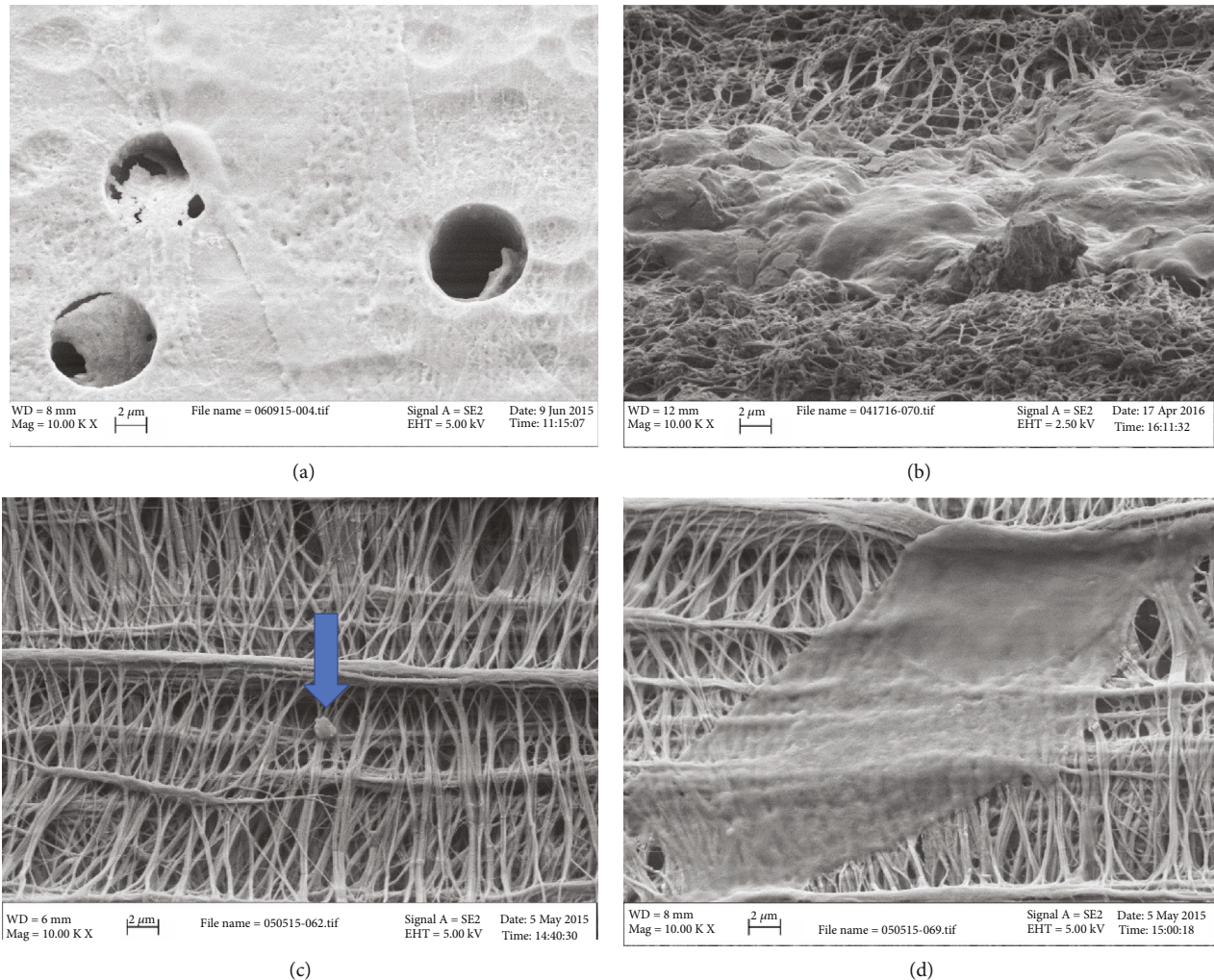


FIGURE 7: (a) Scanning electron microscope image of migrated GMSCs in the lower compartment of 8-micron pore perforated polycarbonate membrane. (b) Scanning electron microscope image of migrated GMSCs in the lower compartment of 3-micron pore perforated collagen-coated PTFE. (c) Scanning electron microscope image of 0.4-micron pore perforated collagen-coated PTFE showing a GMSC process extending between collagen strands. (d) Scanning electron microscope image of 0.4-micron pore perforated collagen-coated PTFE showing fully migrated GMSC.

compared to  $3\ \mu\text{m}$  and  $0.4\ \mu\text{m}$  within the same group and with a significant difference between the groups in favor of the homogeneous population group. This peculiar finding suggests that the  $8\ \mu\text{m}$  pore size might have a selective migratory effect on GMSCs according to its population homogeneity.

The SEM image analysis was indifferent in morphology between the heterogeneous and the homogeneous groups; both groups showed a fibroblast-like morphology. GMSCs from both groups showed a flatter shape with longer pseudopodia over the polycarbonate membrane, compared to GMSCs migrated through collagen membrane which looked rougher with many extensions to collagen strands; the difference can be explained by the difference in the membrane roughness, the rougher collagen membrane, and the flat polycarbonate membrane [24–26]; this was consistent with previous researches which proved the effect of different substrates on the shape and morphology of the attached cells [27, 28] and even specifically investigated the effect of polycar-

bonate and collagen substrates on the morphology of the attached cells in Rasmussen et al.'s study [28, 29].

## 5. Conclusion

Homogeneous CD146-positive GMSC populations were more dynamically active in the migration through microperforated membranes and have shorter proliferation time, where  $8\ \mu\text{m}$  perforation showed the highest number of migrated cells compared to  $0.4$  and  $3\ \mu\text{m}$  pores. This would throw light on the importance of chemotaxis on homogeneous GMSC migration through the microperforated membrane, using a specific chemoattractant for the homing of specific GMSC population which would migrate more rapidly and proliferate better compared to a nonspecific chemoattractant which would attract less homogeneous or heterogeneous GMSCs to the periodontal wound, a pivotal development in the guided tissue regeneration technique. Studying the effect of different chemotaxis factors on

different stem cell lines to choose the best chemoattractive factor is recommended, besides determining the best stem cell line within the GMSC heterogeneous population that can differentiate to multiple cells in the periodontal wound for optimum regeneration results.

## Data Availability

All the raw data of this study are available for whom is concerned.

## Conflicts of Interest

The author declares that there are no conflicts of interest.

## References

- [1] M. M. Al Bahrawy, K. K. A. Ghaffar, M. S. El-Mofty, and A. A. Rahman, "The mutual effect of hyperlipidemia and proinflammatory cytokine related to periodontal infection," *Egyptian Journal of Oral and Maxillofacial Surgery*, vol. 2, no. 2, pp. 87–95, 2011.
- [2] S. L. Haas, "The importance of the periosteum and the endosteum in the repair of transplanted bone," *Archives of Surgery*, vol. 8, no. 2, pp. 535–556, 1924.
- [3] B. K. Hall and H. N. Jacobson, "The repair of fractured membrane bones in the newly hatched chick," *Anatomical Record*, vol. 181, no. 1, pp. 55–69, 1975.
- [4] M. Al Bahrawy, A. Gamal, K. A. Ghaffar, and V. Iacono, "In vitro migration dynamics of gingival mesenchymal stem cells through micro perforated membranes," *International Journal of Dentistry and Oral Health*, vol. 4, no. 5, 2018.
- [5] G. B. Tomar, R. K. Srivastava, N. Gupta et al., "Human gingiva-derived mesenchymal stem cells are superior to bone marrow-derived mesenchymal stem cells for cell therapy in regenerative medicine," *Biochemical and Biophysical Research Communications*, vol. 393, no. 3, pp. 377–383, 2010.
- [6] Q. Zhang, S. Shi, Y. Liu et al., "Mesenchymal stem cells derived from human gingiva are capable of immunomodulatory functions and ameliorate inflammation-related tissue destruction in experimental colitis," *Journal of Immunology*, vol. 183, no. 12, pp. 7787–7798, 2009.
- [7] A. Y. Gamal and V. J. Iacono, "Enhancing guided tissue regeneration of periodontal defects by using a novel perforated barrier membrane," *Journal of Periodontology*, vol. 84, no. 7, pp. 905–913, 2013.
- [8] A. Y. Gamal, M. Aziz, M. H. Salama, and V. J. Iacono, "Gingival crevicular fluid bone morphogenetic protein-2 release profile following the use of modified perforated membrane barriers in localized intrabony defects: a randomized clinical trial," *Journal of the International Academy of Periodontology*, vol. 16, no. 2, pp. 55–63, 2014.
- [9] A. Y. Gamal, K. A. Abdel-Ghaffar, and V. J. Iacono, "Gingival crevicular fluid vascular endothelial cell growth factor and platelet-derived growth factor-BB release profile following the use of perforated barrier membranes during treatment of intrabony defects: a randomized clinical trial," *Journal of Periodontal Research*, vol. 51, no. 3, pp. 407–416, 2016.
- [10] K. C. Russell, D. G. Phinney, M. R. Lacey, B. L. Barrilleaux, K. E. Meyertholen, and K. C. O'Connor, "In vitro high-capacity assay to quantify the clonal heterogeneity in trilineage potential of mesenchymal stem cells reveals a complex hierarchy of lineage commitment," *Stem Cells*, vol. 28, no. 4, pp. 788–798, 2010.
- [11] F. Ferro, R. Spelat, A. P. Beltrami, D. Cesselli, and F. Curcio, "Isolation and characterization of human dental pulp derived stem cells by using media containing low human serum percentage as clinical grade substitutes for bovine serum," *PLoS One*, vol. 7, no. 11, article e48945, 2012.
- [12] C. Morsczeck, G. Schmalz, T. E. Reichert, F. Völlner, K. Galler, and O. Driemel, "Somatic stem cells for regenerative dentistry," *Clinical Oral Investigations*, vol. 12, no. 2, pp. 113–118, 2008.
- [13] K. E. Schwab, P. Hutchinson, and C. E. Gargett, "Identification of surface markers for prospective isolation of human endometrial stromal colony-forming cells," *Human Reproduction*, vol. 23, no. 4, pp. 934–943, 2008.
- [14] D. T. Covas, R. A. Panepucci, A. M. Fontes et al., "Multipotent mesenchymal stromal cells obtained from diverse human tissues share functional properties and gene-expression profile with CD146<sup>+</sup> perivascular cells and fibroblasts," *Experimental Hematology*, vol. 36, no. 5, pp. 642–654, 2008.
- [15] M. Crisan, S. Yap, L. Casteilla et al., "A perivascular origin for mesenchymal stem cells in multiple human organs," *Cell Stem Cell*, vol. 3, no. 3, pp. 301–313, 2008.
- [16] C. Vaculik, C. Schuster, W. Bauer et al., "Human dermis harbors distinct mesenchymal stromal cell subsets," *The Journal of Investigative Dermatology*, vol. 132, no. 3, pp. 563–574, 2012.
- [17] S. Shi and S. Gronthos, "Perivascular niche of postnatal mesenchymal stem cells in human bone marrow and dental pulp," *Journal of Bone and Mineral Research*, vol. 18, no. 4, pp. 696–704, 2003.
- [18] D. Menicanin, P. M. Bartold, A. C. W. Zannettino, and S. Gronthos, "Identification of a common gene expression signature associated with immature clonal mesenchymal cell populations derived from bone marrow and dental tissues," *Stem Cells and Development*, vol. 19, no. 10, pp. 1501–1510, 2010.
- [19] S. Gronthos, S. E. Graves, S. Ohta, and P. J. Simmons, "The STRO-1<sup>+</sup> fraction of adult human bone marrow contains the osteogenic precursors," *Blood*, vol. 84, no. 12, pp. 4164–4173, 1994.
- [20] S. Gronthos, A. C. W. Zannettino, S. J. Hay et al., "Molecular and cellular characterisation of highly purified stromal stem cells derived from human bone marrow," *Journal of Cell Science*, vol. 116, no. 9, pp. 1827–1835, 2003.
- [21] M. F. Pittenger, A. M. Mackay, S. C. Beck et al., "Multilineage potential of adult human mesenchymal stem cells," *Science*, vol. 284, no. 5411, pp. 143–147, 1999.
- [22] A. H. Melcher, "On the repair potential of periodontal tissues," *Journal of Periodontology*, vol. 47, no. 5, pp. 256–260, 1976.
- [23] D. J. Prockop, "Marrow stromal cells as stem cells for nonhematopoietic tissues," *Science*, vol. 276, no. 5309, pp. 71–74, 1997.
- [24] H. J. Ronold, S. P. Lyngstadaas, and J. E. Ellingsen, "Analysing the optimal value for titanium implant roughness in bone attachment using a tensile test," *Biomaterials*, vol. 24, no. 25, pp. 4559–4564, 2003.
- [25] P. M. Brett, J. Harle, V. Salih et al., "Roughness response genes in osteoblasts," *Bone*, vol. 35, no. 1, pp. 124–133, 2004.
- [26] L. Li, K. Crosby, M. Sawicki, L. L. Shaw, and Y. Wang, "Effects of surface roughness of hydroxyapatite on cell attachment and

- proliferation,” *Journal of Biotechnology & Biomaterials*, vol. 2, p. 150, 2012.
- [27] J. M. Payne, C. M. Cobb, J. W. Rapley, W. J. Killoy, and P. Spencer, “Migration of human gingival fibroblasts over guided tissue regeneration barrier materials,” *Journal of Periodontology*, vol. 67, pp. 236–244, 1996.
- [28] J. Zhao, L. Huang, R. Li et al., “Dynamic culture of a thermo-sensitive collagen hydrogel as an extracellular matrix improves the construction of tissue-engineered peripheral nerve,” *Neural Regeneration Research*, vol. 9, no. 14, pp. 1371–1378, 2014.
- [29] C. H. Rasmussen, D. R. Petersen, J. B. Moeller, M. Hansson, and M. Dufva, “Collagen type I improves the differentiation of human embryonic stem cells towards definitive endoderm,” *PLoS One*, vol. 10, article e0145389, 2015.

## Research Article

# Gene Profiles in the Early Stage of Neuronal Differentiation of Mouse Bone Marrow Stromal Cells Induced by Basic Fibroblast Growth Factor

Lili Yu,<sup>1,2</sup> Wei Hong,<sup>1,3</sup> Haijie Yang,<sup>4</sup> Yin Yan Xia,<sup>5</sup> and Zhiwei Feng<sup>1,2,5</sup> 

<sup>1</sup>School of Basic Medical Sciences, Xinxiang Medical University, Xinxiang, China

<sup>2</sup>Institute of Precision Medicine, Xinxiang Medical University, Xinxiang, China

<sup>3</sup>Sanquan College of Xinxiang Medical University, Xinxiang, China

<sup>4</sup>School of Life Science and Technology, Xinxiang Medical University, Xinxiang, China

<sup>5</sup>School of Biological Science, Nanyang Technological University, Singapore

Correspondence should be addressed to Zhiwei Feng; 123066@xxmu.edu.cn

Received 28 April 2020; Revised 30 November 2020; Accepted 8 December 2020; Published 24 December 2020

Academic Editor: Jun Liu

Copyright © 2020 Lili Yu et al. This is an open access article distributed under the Creative Commons Attribution License, which permits unrestricted use, distribution, and reproduction in any medium, provided the original work is properly cited.

A stably established population of mouse bone marrow stromal cells (BMSCs) with self-renewal and multilineage differentiation potential was expanded *in vitro* for more than 50 passages. These cells express high levels of mesenchymal stem cell markers and can be differentiated into adipogenic, chondrogenic, and osteogenic lineages *in vitro*. Subjected to basic fibroblast growth factor (bFGF) treatment, a typical neuronal phenotype was induced in these cells, as supported by neuronal morphology, induction of neuronal markers, and relevant electrophysiological excitability. To identify the genes regulating neuronal differentiation, cDNA microarray analysis was conducted using mRNAs isolated from cells differentiated for different time periods (0, 4, 24, and 72 h) after bFGF treatment. Various expression patterns of neuronal genes were stimulated by bFGF. These gene profiles were shown to be involved in developmental, functional, and structural integration of the nervous system. The expression of representative genes stimulated by bFGF in each group was verified by RT-PCR. Amongst proneural genes, the mammalian *achate-schute* homolog 1 (Mash-1), a basic helix-loop-helix transcriptional factor, was further demonstrated to be significantly upregulated. Overexpression of Mash-1 in mouse BMSCs was shown to induce the expression of neuronal specific enolase (NSE) and terminal neuronal morphology, suggesting that Mash-1 plays an important role in the induction of neuronal differentiation of mouse BMSCs.

## 1. Introduction

Bone marrow stromal cells (BMSCs) contain mesenchymal stem cells [1] which are capable of differentiating into various progenies of mesodermal origins, such as osteoblast, chondrocyte, and adipocyte [2]. Studies have demonstrated that BMSCs can also exhibit neural phenotypes after transplantation and ameliorate the deficiency of different neuronal disorders [3–6]. BMSCs can be differentiated into various neural cells by adopting various protocols *in vitro* [7, 8], demonstrating the multipotent differentiation capacities and promising therapeutic values of BMSCs. However, the differentiation notion has been strongly debated recently as

a stress response to the use of some chemicals adopted in neuronal differentiation protocols [9, 10]. It has also been suggested that BMSCs-derived neuronal cells only obtain partial neuronal features as assessed by the examination of a set of neuronal genes, compared to that obtained from neural stem cells [11]. Thus, further determination of neuronal traits of differentiated BMSCs with an appropriate differentiation strategy would be required for better illustration of this phenomenon albeit the presence of *in vivo* transplantation studies documenting the physiological properties of neuronal differentiated BMSCs.

Currently, most neuronal genes as examined in differentiated BMSCs were primarily used as benchmark markers for



neuronal differentiation but seldom use for elucidating the mechanisms of initiating and/or regulating neuronal differentiation. Recent studies revealed that gene silencing to suppress the discordant phenotypes in BMSCs was also important for neuronal differentiation [12], suggesting that dynamic gene regulation was involved in neuronal differentiation of BMSCs. Moreover, it is rather difficult to determine the neuronal phenotypes of BMSCs based on the availability of a very limited pool of neuronal genes identified [11]. cDNA microarray analysis is a powerful tool for gene profiling analysis and has been widely used in gene expression kinetics determination. Two studies have applied this method to unravel the neuronal gene regulation profile in mouse BMSCs. For instance, Mori studied the neuronal differentiation of immortalized human BMSCs [13] and found that the genes analyzed were from late phase of one-week neuronal differentiation process, rather than from earlier initiating stage. This revelation would reflect the neural features of dominant genes in differentiated BMSCs. Yamaguchi, whom further studied the neuronal gene expression profile in DMSO induced neuronal differentiation of BMSCs [14], fell directly into the previous debate of BMSC differentiation as a direct result of the addition of certain compound which triggered an acute nonphysiological stress response thus rendering it unreliable. To study the neuronal differentiation under proper physiological condition, we have established a model of basic fibroblast growth factor (bFGF) induced mouse BMSC neuronal differentiation [15]. In this report, we intend to further examine the gene expression profile at early stages of neuronal differentiation as induced by bFGF with microarray analysis in our attempt to further clarify the mechanisms underlying neuronal differentiation of BMSCs.

bFGF, a 154-amino acid peptide, is the first growth factor employed in pilot study examining the neuronal differentiation capacity of BMSCs [16, 17]. Besides its wide range of biological activities on cell growth, differentiation, and survival, FGF evoked signaling pathway has also been shown to be the prerequisite factor for neural induction in chick embryo [18] and inducer of posterior neuronal precursors in the neural tube [19]. In the nervous system, members of the FGF affect the differentiation and migration of neurons, the formation and maturation of synapses, and the repair of neuronal circuits following insults [20]. Basic fibroblast growth factor increases the transplantation-mediated therapeutic effect of bone mesenchymal stem cells following traumatic brain injury [21]. In *in vitro* studies, bFGF could induce neurotube formation from ES cells [22], and transdifferentiation of the pigmented epithelial cell into retinal neurons [23] has also been reported. Dual delivery of bFGF and NGF-binding coacervate confers neuroprotection by promoting neuronal proliferation [24]. All these findings singled out bFGF as a potent proneural factor with wide range capabilities. However, the mechanisms underlying, especially that of neuronal transdifferentiation, are poorly understood. BMSCs transfected with the intracellular domain of the Notch was found to be more effectively induced into neuron-like cells in the presence of bFGF [9]. The Notch signaling pathway has been demonstrated to play a pivotal role

in neurogenesis of *Drosophila* [25]. Deregulation of Notch signaling is involved in many neurodegenerative diseases and brain disorders [26, 27]. Several groups of molecules, including the bHLH family, are directly regulated by Notch pathway, which conventionally regulate neural determination and differentiation [28, 29]. Furthermore, all genes of the Notch pathway are found to be preserved in vertebrates [30]. A clear example would be Mash-1, a bHLH family member gene, which is obviously affected in mouse by the mutation of Notch signaling pathway and in which contributed to neurogenesis [31]. However, it remains unclear how Notch signaling is involved in regulating the neuronal differentiation of BMSCs.

In our attempt to better understand the genes involved in the neuronal differentiation of BMSCs, we adopted the cDNA microarray strategy to sequentially analyze bFGF-activated neural genes at various time points. We observed that bFGF-activated neural genes exhibit distinct expression kinetics and most importantly are involved in various neural activities. We further demonstrated that the mammalian proneural gene, Mash-1, was induced at an early stage of differentiation, and BMSCs can be driven into neuronal cells by the overexpression of Mash-1. Our work provides an insight of the molecular mechanisms of neuronal differentiation of BMSCs by bFGF.

## 2. Material and Methods

**2.1. Isolation and Culture of Mouse BMSCs.** Bone marrow stromal cells (BMSCs) of 8-week-old male Swiss mice were initially cultivated in Dulbecco's Modified Eagle Medium (DMEM; Invitrogen) supplemented with 10% fetal bovine serum (FBS; Invitrogen), 10% newborn calf serum (NCF; Invitrogen), 100 U/ml penicillin, and 100 mg/ml streptomycin (Invitrogen). The cells were incubated at 37°C in 5% CO<sub>2</sub> in 100 mm tissue culture dishes for 2-3 days, and nonadherent cells were removed by medium replacement. Adherent cells were further cultured for 7-10 days to reach 90% confluence and defined as the first passage. After detachment with 0.25% Trypsin/0.5 mM EDTA, around 25% of the cells were transferred to a new culture flask. A fairly homogeneous cell population was achieved after 4-5 passages, and these cells could be continuously cultured for up to 50 passages without obvious growth retardation.

**2.2. Fluorescence Activated Cell Sorting (FACS) Analysis.** Samples containing  $1 \times 10^6$  cells were resuspended in 300  $\mu$ l of FACS buffer (PBS + 2%FBS) and incubated for 20 minutes at 4°C with 3  $\mu$ l of fluorescein isothiocyanate-(FITC-), phycoerythrin- (PE-), allophycocyanin- (APC-), and peridinin chlorophyll protein- (Per-CP-) conjugated antibodies, respectively, against surface markers CD34, CD44, CD45, CD90.1, CD117, CD105, and Sca-1. All antibodies were from Pharmingen (BD Pharmingen). After addition of 6 ml FACS buffer, cells were pelleted by 5 min centrifugation at  $260 \times g$  at 4°C. The labelled cells were resuspended in 500  $\mu$ l FACS buffer and analyzed by BD FACS Aria flow cytometer.

**2.3. Adipogenic Differentiation.** Flat BMSCs were plated onto 6-well tissue culture plates at a density of  $5 \times 10^4$  cells per well and incubated for 24 hours before treatment with adipogenic differentiation medium (500 nM Dexamethasone, 250  $\mu$ M isobutyl-methylxanthine (IBMX), 100  $\mu$ M indomethacine, and 5  $\mu$ M insulin in basal DMEM supplemented with 10% FBS, 10% FCS, and 1% penicillin-streptomycin). The media was changed every 3 days, and adipogenic differentiation was assessed by Sudan Black staining 10 days postinitial adipogenic induction.

**2.4. Sudan Black Staining.** Cells were rinsed with PBS and fixed with Baker's Solution for 10 minutes, followed by 3 minutes exposure to 100% propylene glycol. The cells were then stained with Sudan Black for 2 hours followed by 3 washes with water. This was followed by another 2 minutes of exposure to 85% propylene glycol and a final 3 washes with water. Positive Sudan Black stained cells appear blue black under light microscopy.

**2.5. Chondrogenic Differentiation.** Chondrogenic differentiation was induced using the high-density micromass culture technique [32]. A 10  $\mu$ l drop of a concentrated cell suspension ( $1 \times 10^6$  cells/ml) was placed onto the centre of the well (of a 24-wells tissue culture plate) and allowed to attach and aggregate for 2 hours at 37°C with 5% CO<sub>2</sub>. Chondrogenic induction medium (50 nM ascorbic acid-2-phosphate, 6.25  $\mu$ g/ml insulin, and 10 ng/ml transforming growth factor  $\beta$ 1 in basal DMEM supplemented with 1% FBS and 1% penicillin-streptomycin) was then gently overlaid, avoiding disruption to the attached cells. The media was then changed every 3 days, and the chondrogenic phenotype was determined by Alcian Blue staining 3 weeks postinitial chondrogenic induction.

**2.6. Alcian Blue Staining.** Micromass cultures were rinsed with PBS and fixed in 2% paraformaldehyde for 15 minutes. They were then rinsed with 3% acetic acid for 5 minutes to bring down the pH to 2.6 followed by 20 minutes staining with 1% Alcian Blue (pH 2.6). Cells were then washed twice with water before being observed under light microscopy. The highly sulfated proteoglycans of cartilage matrices were positively stained blue.

**2.7. Osteogenic Differentiation.**  $1 \times 10^4$  cells were plated onto a 24-wells plate and cultured in an osteogenic differentiation medium (50  $\mu$ M ascorbic acid-2-phosphate, 10 mM  $\beta$ -glycerophosphate, and 100 nM dexamethasone in DMEM basal medium supplemented with 10% FBS and 1% penicillin-streptomycin) after 24 hours incubation. The media was changed every 3 days. Osteogenic differentiation was assessed by Alizarin Red S staining 3 weeks postinitial osteogenic induction.

**2.8. Alizarin Red S Staining.** Cells were rinsed twice with PBS and fixed in ice-cold 70% ethanol for an hour at -20°C. After a few rinses with deionised water, cells were incubated with 40 mM Alizarin Red S (pH 4.1) for 20 minutes at room temperature with gentle shaking. A further 4 washes with deionised water were carried out to clear away unspecific

staining on the cells. Secretion of calcified extracellular matrix was confirmed as red stains with Alizarin Red S Staining.

**2.9. Neurogenic Differentiation.** For neuronal differentiation, BMSC cells were isolated and split every other day. Neurogenic differentiation was induced by exposure to 10 ng/ml basic fibroblast growth factor. The neuronal differentiation medium (low glucose DMEM supplemented with 10% of FBS and 10 ng/ml bFGF) was added starting from passage 5. Neuronal differentiation was monitored by microscopic observation, and the expression of neuronal markers was analyzed by RT-PCR, western blotting, and immunohistochemistry.

**2.10. cDNA Microarray Analysis.** BMSCs were harvested at 4, 24, and 72 hours post-bFGF treatment, and total RNAs were extracted using Trizol reagent following the manufacturer's instructions (Invitrogen). cDNAs were synthesized and subjected to Agilent's Mouse Development Oligo Microarray (Agilent Technologies). The microarray experiment was repeated twice using RNA samples from independent experiments, and the result reported was based on the average of these two independent experiments. cDNAs which showed at least 2-fold difference were selected for further analysis. cDNA microarray experiment was blinded to investigator, and microarray data analysis was also assessed by three independent investigators who were blinded to the sample.

**2.11. Reverse Transcription Polymerase Chain Reaction Analysis.** The expression of ChAT, GAP43, Hes5, Mash1, NSE, Tau, SERT, MAP2, and  $\beta$ 3-tubulin was determined by reverse transcription polymerase chain reaction (RT-PCR). Total cellular RNA was isolated using Trizol reagent (Invitrogen) and reverse transcribed using Invitrogen's First Strand cDNA Synthesis Superscript III RT Kit. PCR amplification was performed using the following primers (shown in brackets in the following order: sense and antisense), ChAT (5'-TGTGAGGAGGTGCTGGACTTA-3', 5'-GCCAGGCGTTTGTAGATA-3'), GAP43 (5'-GCTAGCTTCCGTGGACACATA-3', 5'-AGGCACATCGGCTTGTTTA-3'), Hes5 (5'-ATGCTCAGTCCCAAGGAGAA-3', 5'-CGCTGGAAGTGGTAAAGCAG-3'), Mash1 (5'-GCTCTGGCAAGATGGAGAGT-3', 5'-CCAGGTTGACCAACTTGACC-3'), Tau (5'-CCCTGGAGGAGGAATAAGA-3', 5'-GCAGACACTTCATCGGCTAGT-3'), and NSE (5'-TGATCTTGTCGTCGGACTGTGT-3', 5'-CTTCGCCAGACGTTTCAGATCT-3'). All primer sequences were determined through established GenBank sequences. Duplicate PCRs were amplified using  $\beta$ -actin (5'-TGTTACCAACTGGGACGACA-3', 5'-TCTCAGCTGTGGTGGTGAAG-3', 392 bp) as a control for assessing PCR efficiency and subsequent analysis by agarose gel electrophoresis.

**2.12. Quantitative Real-Time PCR (qRT-PCR).** Total RNA was extracted using Trizol reagent in accordance with the manufacturer's instructions. After the treatment with RNase-free DNase I (Invitrogen) to remove genomic DNA



contamination, RNA (1  $\mu$ g) was reverse transcribed into cDNA using Moloney murine leukemia virus reverse transcriptase (Promega, Madison, USA). Real-time PCR was performed using Power SYBR Green PCR Master Mix (Applied Biosystems, Foster City, CA, USA) in an ABI PRISM 7500 real-time cycler (Applied Biosystems). The mRNA levels of the target gene were normalized to that of  $\beta$ -actin. Melting curves were constructed using the Dissociation Curves software to ensure that only a single product was amplified. According to the method of Livak and Schmittgen, the intensity of the relative expression was based on  $2^{-\Delta\Delta CT}$  equation. The sequences of primers for PCR are listed as follows: SERT (5'-TGCCTTTTATATCGCCTCCTAC-3', 5'-CAGTTGCCAGTGTCCAAGA-3'), MAP2 (5'-TCAGGAGACAGGGAGGAGAA-3', 5'-GTGTGGAGGTGCCA CTTTTT-3'),  $\beta$ 3-tubulin (5'-CATGGACAGTGTTCGG TCTG-3', 5'-CGCACGACATCTAGGACTGA-3'), SV2a (5'-GGTTCACGACACCAACATGC-3', 5'-ACTTTGGTT CGGGCTGCATA-3'), and SNAP-25 (5'-CGCAATGAG CTGGAGGAGAT-3', 5'-TCCCTTCTCAATGCGTTCC).

**2.13. Western Blot.** Cells were lysed with lysis buffer (50 mM Tris-Base, 100 mM NaCl, 5 mM EDTA, 1 mM EGTA, 5 mM MgCl<sub>2</sub>, 10% glycerol, 1% Triton X-100, and Roche's Complete Protease Inhibitor tablet) and were centrifuged at 14,000  $\times$  g for 20 minutes at 4°C. 50  $\mu$ g of proteins from the supernatants was separated by 8%-12% SDS-PAGE gel and transferred to a PVDF membrane. Immunoblotting was carried out with polyclonal antibodies to ChAT, GAP43, Hes5, Mash1, NSE, Tau, and  $\beta$ -actin, respectively. After incubation with peroxidase-conjugated secondary anti-immunoglobulin antibodies, the membranes were developed using Pierce's West Pico Chemiluminescence method.

**2.14. Electrophysiology.** For whole-cell current recording, cells were patched as previously described (37). The bath solution contained (in mM) NaCl 150, KCl 5, MgCl<sub>2</sub> 1, CaCl<sub>2</sub> 2.2, Hepes 10, and pH 7.3 with NaOH, and the osmolarity was adjusted to 310 mOSM with glucose. The pipette solution contained (in mM) aspartic acid potassium salt 120, MgCl<sub>2</sub> 5, EGTA 0.5, Hepes 10, ATP 2, GTP 0.3, and pH 7.3 with KOH, and the osmolarity was adjusted to 295 mOSM. Whole-cell current was obtained under voltage clamp with Axopatch 200B amplifier (Axon Instruments); the software used was pClamp 8.1 (Axon Instruments). The current was sampled at 10 kHz and filtered at 1 kHz. Leak was subtracted on-line using P/4 protocol. The pipette used was 1-2 m $\Omega$ , and the series resistance was typically <5 m $\Omega$  and compensated by 75%. The holding potential was set at -70 mV and depolarized to different voltages to evoke channel opening.

**2.15. Plasmid Construction.** The coding region of mouse Mash-1 was cloned into the pREP10 vector using convenient restriction sites. PCR product of Mash1 was digested with *Kpn* I and *Xho* I, purified and ligated to digested pREP10 expression vector. The bHLH domain of Mash-1 was then fused to the V5 epitope. All constructs generated by PCR

were verified by sequencing prior to use, and protein expression was confirmed by western blotting with antibodies to Mash-1 and epitope tag V5.

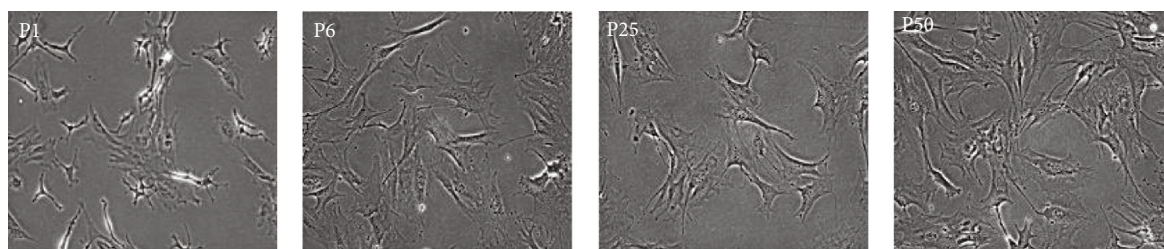
**2.16. Transfection.**  $5 \times 10^5$  cells were seeded to 100 mm tissue culture dishes and allowed to grow overnight prior to transfection. 30  $\mu$ g of plasmid DNA was mixed with 60  $\mu$ l of Lipofectamine 2000 Reagent to initiate the complex forming. Transfection was initiated by adding the mixture to the cells directly. Cells were extracted and assayed 3 days posttransfection.

**2.17. Immunofluorescence Staining.** For immunofluorescence staining, cells were seeded on Lab-Tek chamber slides and fixed with precold methanol at -20°C for 3 min. Then, the cells were permeabilized with 0.2% TritonX-100 in PBS for 15 min and blocked with 10% normal goat serum in PBS at room temperature for 30 min. The cells were incubated with the primary antibodies at 37°C for 1 h, washed with PBS twice, and then were incubated with the appropriate fluorescein isothiocyanate-conjugated secondary antibodies for 30 min. Finally, the cells were mounted with an antifluorescence quenching sealing liquid for observation under a fluorescence microscope.

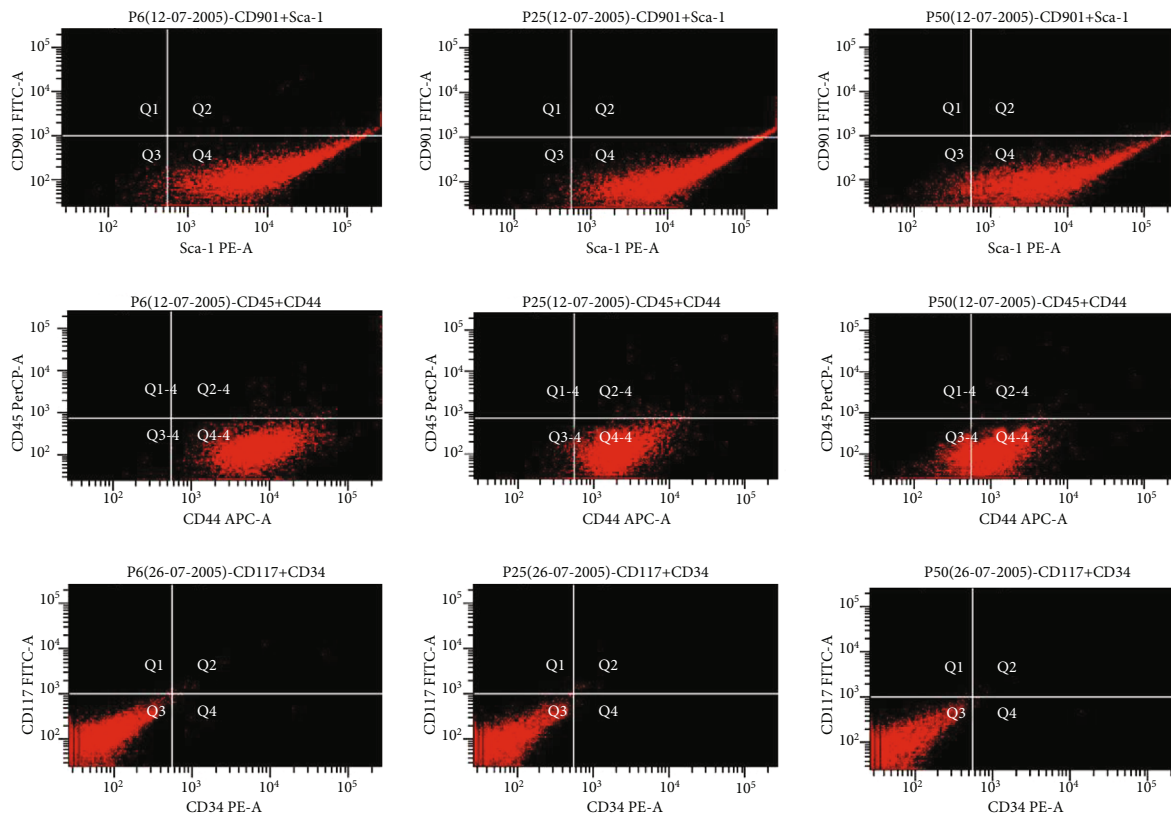
**2.18. Statistical Analysis.** All data are presented as mean  $\pm$  standard error of the mean (SEM). Student *t*-test was used to determine significance between individual comparisons. One-way ANOVA tests with Bonferroni's corrections were used for multiple comparisons. The calculations were performed using the SPSS version 11.0 statistic software. *P* values < 0.05 were considered statistically significant.

### 3. Results

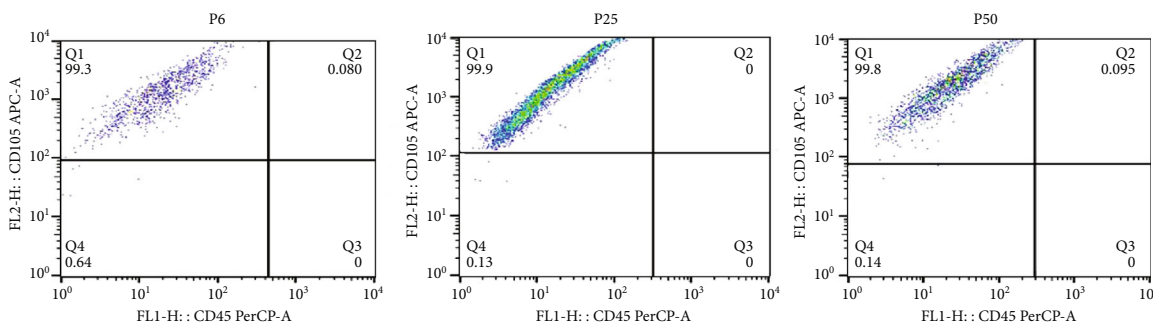
**3.1. Multipotency of BMSCs at Different Passages.** Mouse BMSCs were isolated from the femur bones of mice and cultured in DMEM supplemented with 10% FBS, 10% FCS, and 1% penicillin-streptomycin. A fibroblast-like cell population eventually was obtained after 4-5 passages, and this cell population can grow continuously for more than 50 passages under our experimental condition without losing much of its plasticity and appeared healthy. Cell growth rate was lower at early passages due to competition from other cell types, and a stable stage of homogenous cell population was reached after 4-5 passages. Cell morphology as tracked from passages 6 to 50 showed a consistent phenotype and level of homogeneity (Figure 1(a)). It has been reported that cell features and plasticity may vary for the long-term *in vitro* culture [33]. Thus, we examined several cell surface markers of BMSCs at different passages. The flow cytometry results showed that these cells exhibited high levels of Sca-1 [34], a stem cell marker, and CD44 [35], a mesenchymal marker across passages 6, 25, and 50 (Figure 1(b)). As suspected, all hematopoietic cell markers, CD90.1, CD45, CD34, and CD117, were undetectable or poorly expressed in BMSCs at all passages (Figure 1(b)). We also detected the other marker CD105 for identification of BMSCs at different passage, which was positive as suspected (Figure 1(c)). These data demonstrated that this highly homogeneous cell population



(a)



(b)



(c)

FIGURE 1: Characterization of BMSCs. (a) BMSCs from initial isolation to passage 50. Cell morphology became relatively homogeneous from passage 6 onwards and maintained the appearances till passage 50 or later. (b) Fluorescent-activated cell sorting (FACS) analysis for cell surface markers. Throughout the passages, markers for mesenchymal stem cells, Sca-1 and CD44, remained highly elevated and slightly decreased with passage number. The expressions for CD90.1, CD45, CD117, and CD34 were negligible throughout thus excluding contamination of hematopoietic stem cells from the isolated culture. (c) FACS analysis for CD105 and CD45. The expression of CD105 was positive, and CD45 was negligible.

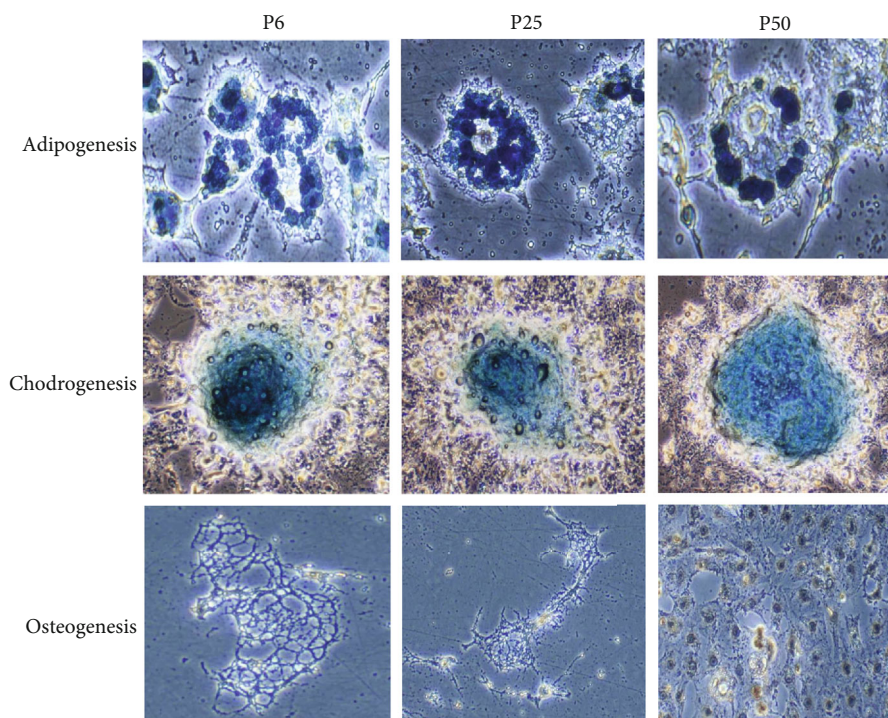


FIGURE 2: Developmental potential ability of BMSCs in vitro. BMSCs at passages 6, 25, and 50 were induced under adipogenic, chondrogenic, and osteogenic conditions. The presence of clusters of lipid containing adipocytes was detected by Sudan blue staining after adipogenic induction for 5 days. Cells show chondrocyte morphology and are positive for Alcian black stain after chondrogenic induction for 21 days. Cells show osteocyte morphology and are positive for Alizarin red stain after osteogenic induction for 21 days.

at indicated passages exhibit mesenchymal stem cell markers and is free from obvious hematopoietic cells contamination.

To determine the multilineage differentiation capacity of BMSCs, cells were subjected to a series of differentiation towards mesenchymal origins, namely, adipocytes, chondrocytes, and osteoblasts. As shown in Figure 2, cells at 6 and 25 passages could differentiate into adipocytes and chondrocytes as determined by biochemical tests, while cells at passage 50 could differentiate into all three cell types. These results are consistent with earlier observation that BMSCs with the capacity of adipocyte differentiation have high capacity of colony forming [36] and probably a longer life span and plasticity as well. Though the default commitment of BMSCs is to undergo osteogenic differentiation, this phenomenon is only observed at the early developmental stages of BMSCs.

**3.2. Neuronal Differentiation of BMSCs Induced by bFGF.** A model for mouse BMSC neuronal differentiation by bFGF [15] has been established to elucidate the molecular mechanism of neuronal differentiation of mouse BMSCs in physiological conditions. Mouse BMSCs treated with bFGF alone for 3 to 6 days exhibited typical neuronal morphology as evidenced by shrunken cell bodies and elongated cell processes (Figure 3(a)). Choline O-Acetyltransferase (ChAT) is the enzyme responsible for the biosynthesis of acetylcholine, which presently the most specific marker for identifying cholinergic neurons in the central and peripheral nervous systems. Growth associated protein (GAP) 43 is a polypeptide

that is induced in neurons when they grow axons. Neuron-specific enolase (NSE) is a dimeric isoform of the glycolytic enzyme enolase found mainly in neurons, which is relatively specific for neuronal cells. A Tau protein is a protein found in neurons, primarily in the central nervous system, which interacts with tubulin to strengthen the neural tubes in the axons of neurons. In order to gather more evidences on neuronal phenotypes, we examined these neuronal differentiation markers by RT-PCR. As shown in Figure 3(b), mRNA levels for ChAT, GAP-43, NSE, and Tau were significantly upregulated upon bFGF treatment. Similar expression patterns in protein levels were also observed for these genes (Figure 3(c)). Full unedited western blot images are supplied in Supplemental data 1. Consistently, after bFGF treatment, differentiated neuronal cells exhibited characteristic electrophysiological properties as determined by whole-cell patch clamp technique. As shown in Figure 3(d), the typical whole cell current trace was detected in 6-day neuronal differentiated cells. We also detected other related markers. Serotonin transporter (SERT) is a critical serotonin transporter in the function of serotonergic neurons, as a biomarker of serotonergic neurotransmission in the central nervous system. Microtubule-associated protein (MAP) 2 is thought to be involved in microtubule assembly, which is an essential step in neurogenesis.  $\beta$ 3-Tubulin is one of six  $\beta$ -tubulin isoforms, which is highly expressed during axon guidance and maturation and that is a great neuronal marker. To determine these markers, qRT-PCR method was employed, and a high level of SERT, MAP2, and  $\beta$ 3-tubulin expression was detected



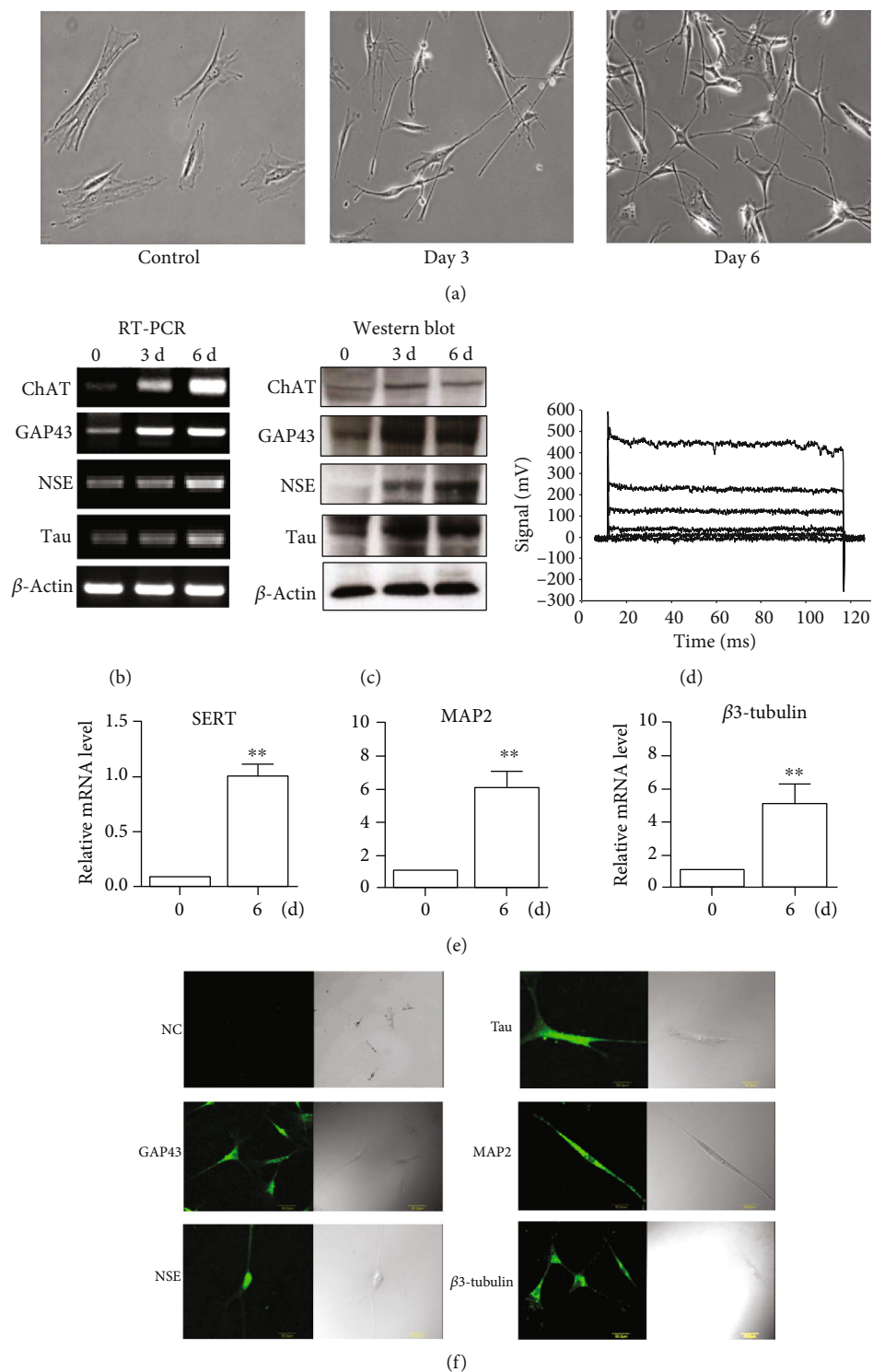


**FIGURE 3: Neuronal differentiation induced by bFGF.** (a) Morphological observation of BMSCs subjected to 10 ng/ml bFGF for 3 and 6 days. Typical signs of a developing neuron, such as cell body shrinkage, axonal elongation, and neurite outgrowth, were observed. The distinctive observation is heightened at day 6 postadministration. (b) RT-PCR representation of marked increase in genes regulating neuronal development and maturation as evidently shown by increase of ChAT, GAP43, NSE, and Tau. (c) Western blotting results supported the same observation of increased neuronal gene expression at protein levels which strengthened the deduction of a neuronal development and eventual maturation. (d) The electrophysiological properties of these differentiated cells were examined by patch clamping method at day 6 post-bFGF administration. (e) The expressions of SERT, MAP2, and  $\beta$ -tubulin were determined by qRT-PCR at day 6 post-bFGF administration. Data of qRT-PCR indicate the mean  $\pm$  SEM of three experiments. (f) Distribution of neuronal differentiation markers. Immunofluorescence staining using specific antibodies against GAP43, NSE, Tau, MAP2, and  $\beta$ -tubulin was performed in BMSCs with bFGF treatment for 3 days. NC: negative control. Images are representatives of at least three experiments.

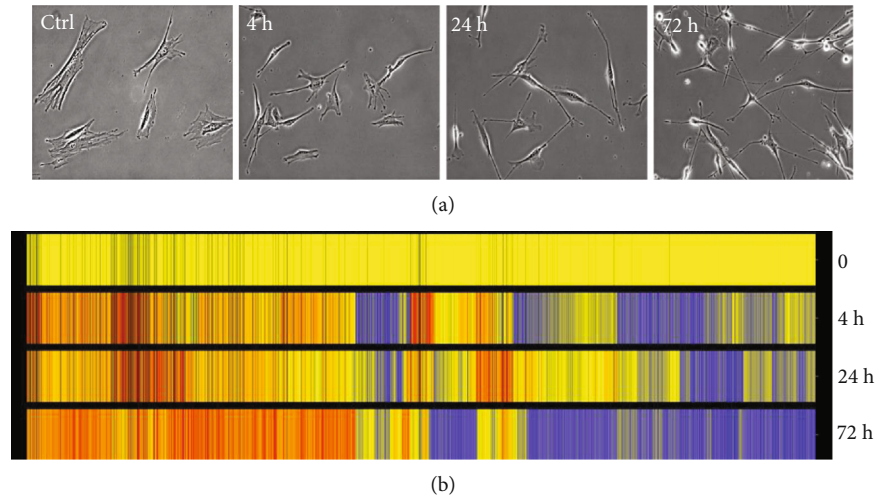


FIGURE 4: Cluster analysis of genes associated with neuronal differentiation. Colored bar representation of the cDNA microarray using total RNAs extracted from BMSCs at 4, 24, and 72 hours post-bFGF treatment. The yellow bars represent the levels of gene in the untreated cells, and the red ones are the upregulated genes, whereas the blue bars stand for the downregulated genes.

(Figure 3(e)). We also used immunofluorescence staining to test these proteins, and results showed that BMSCs treated with bFGF exhibited high expression of neurogenesis-related markers, including GAP43, NSE, Tau, MAP2, and  $\beta$ 3-tubulin (Figure 3(f)). As our data indicated in these figures, we found both ChAT and SERT were induced in bFGF-induced BMSCs, which showed these cells have a potential ability towards cholinergic and neurons serotonergic neuronal differentiation. All this data indicates after bFGF treatment, BMSCs differentiate towards at neuronal direction.

**3.3. Overview of bFGF-Induced Gene Expression Profiles in Mouse BMSCs.** The gene expression profiles of mouse BMSCs were analyzed by microarray analysis in attempt to gather a more complete picture of genes participating in neuronal differentiation and in determining the molecules responsible for converting BMSCs into neuronal cells. Since we have previously observed that neuronal phenotypes can be strongly induced 72 hours post-bFGF treatment [15], total RNAs were extracted from BMSCs after 0, 4, 24, and 72 hours treatment by bFGF, respectively, which was supposedly representing the neural initiation, differentiation, and maturation stages of these differentiated cell phenotype. Otherwise, the fibroblast-like BMSCs started to change its morphology to that resembling neuronal cell phenotype at around 24 hours posttreatment (Figure 4(a)), and these changes were tracked further to include observation of neurite-like structures outgrowth and even to a point of joining and connecting with adjacent differentiated cells at 72 hours, suggesting that the time points designed were suitable for detecting early expressed genes. Cross-talking of adjacent cells mimics the action of matured neurons in forming synapses for information transfer and having been able to observe such a connection in our differentiated neuronal cells do provide evidences with a glimpse of hope that these differentiated cells might eventually become functional neurons. After reverse-transcription into cDNA, samples were hybrid-

ized with DNA oligonucleotide chips representing around 21,000 genes (Agilent Technologies). To ensure the results, two independent neuronal differentiation experiments and microarray analysis were performed. From the even gene expression values at different time points, 1148 genes were identified whose expression levels were more than two-fold changes at one or more time points compared with that of untreated sample. These genes were grouped according to their expression pattern with hierarchical clustering and shown by colored bar representation (Figure 4(b)).

As stated above, mouse BMSCs started to exhibit neuronal morphology at 24 hours post-bFGF treatment, and we assume that the selected time points could reflect the neuronal induction, differentiation, and maturation of BMSCs at 0, 4, 24, and 72 hours of bFGF treatments, respectively. Several typical genes in each group were listed with the concrete expression ratio at different time point compared to untreated cells (Figure 5). Accordingly, changes in gene expression were grouped as early upregulated (Figure 5, Group A), middle upregulated (Figure 5, Group B), late upregulated (Figure 5, Group C), and constitutively upregulated (Figure 5, Group D) based on the folds of induction at these time points. Since the gene downregulation was also shown to be involved in the neuronal differentiation of BMSCs [12], two downregulated groups were also listed, the middle downregulated (Figure 5, Group E) and constitutively downregulated (Figure 5, Group F) gene expressions.

**3.4. Neuronal Gene Expression Profiles.** From the list of genes upregulated by bFGF, about 300 neural-related genes with at least 5-fold upregulation at one or more time point were identified. These genes can be classified into two groups, early upregulated neural genes and continuous upregulated neural genes (Table 1). There are mainly four genes in the first group, synaptic vesicle glycoprotein 2a (SV2a), chemokine (C-C motif) receptor 1 (CCR1), synaptosomal-associated protein 25 (SNAP-25), and gamma-aminobutyric acid (GABA) receptor. SV2a has been demonstrated to be

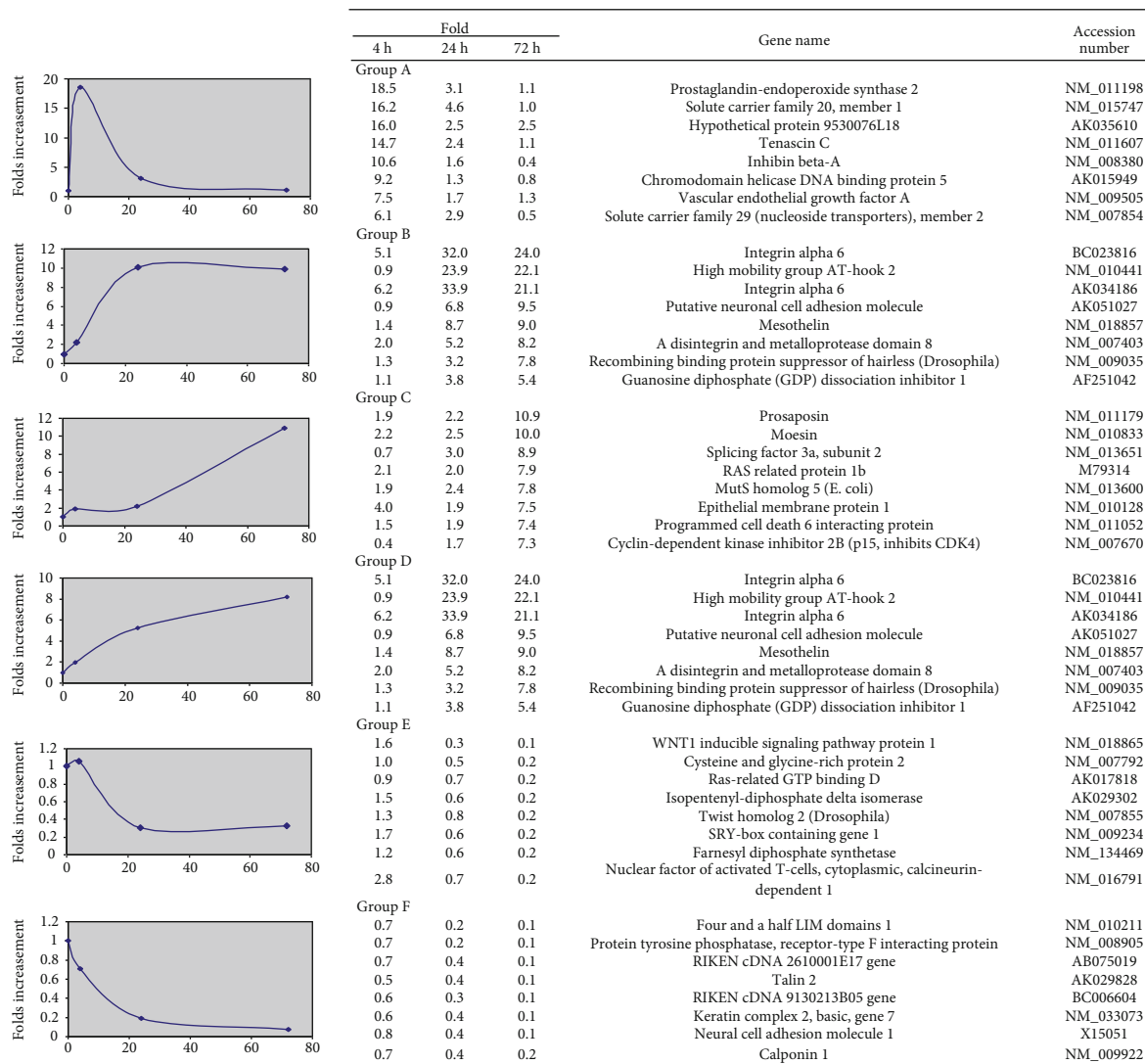


FIGURE 5: Classification of differentially expressed genes. Classification of top upregulated genes with reference to various neural stage activities analyzed by cDNA microarray analysis on bFGF-treated BMSCs for 4, 24, and 72 hours. The values at each time points were obtained by comparing with the level of the untreated. Several typical genes in neuronal developmental function at different six groups after bFGF treatment were listed.

involved in vesicle trafficking and exocytosis, processes crucial for neurotransmission, and plays a crucial role in modulating epileptogenesis [37]. CCR1-mediated signal transduction is critical for the recruitment of effector immune cells to cause neuroinflammation and is an early and specific marker of Alzheimer's disease [38]. SNAP-25 is one of the key proteins involved in the formation of neural soluble N-ethylmaleimide-sensitive factor attachment protein receptors (SNAREs), which are responsible for the calcium-dependent exocytosis of neurotransmitters, that is a major step in neurotransmission and normal functioning of brain [39]. GABA receptors are involved in inhibitory synapses within the central nervous system [40]. There are mainly four genes in the continuous upregulated neural genes group, including semaphorin 5A, P2-activated kinase 1, putative neuronal cell adhesion molecule, and semaphorin

6A. Semaphorin 5A is a bifunctional axon guidance cue for axial motoneurons [41]. Putative cell adhesion membrane molecule Vstm5 regulates neuronal morphology and migration in the central nervous system [42]. Nrf2 in ischemic neurons promotes retinal vascular regeneration through regulation of semaphorin 6A [43].

Similarly analyses as above, about 300 neural-related genes with at least 2-fold upregulation at one or more time point were also identified. These genes can be classified into several groups according to likelihood of neural functions involved (Table 2). The first group participates in neuronal development, and the representative genes are fibroblast growth factor receptor (FGFR), Nestin, Chordin, and the empty spiracles homolog 1. Nestin is a widely used marker for neuronal stem cell and expressed at early stage of neuronal differentiation [16, 44]. Chordin, a homolog of short-



TABLE 1

Fold			Gene name	Accession number
4 h	24 h	72 h		
Early upregulated neuronal genes				
9.6	4.0	3.0	Synaptic vesicle glycoprotein 2a	NM_022030
5.9	3.7	3.4	Chemokine (C-C motif) receptor 1	NM_009912
5.5	2.1	1.6	Synaptosomal-associated protein 25	NM_011428
5.3	1.1	1.0	Gamma-aminobutyric acid receptor	NM_008076
Continuous upregulated neuronal genes				
4.4	6.3	11.0	Semaphorin 5A	NM_009154
2.0	7.4	8.2	P2-activated kinase 1	NM_011035
0.9	4.7	7.5	Putative neuronal cell adhesion molecule	AK051027
3.7	5.2	6.1	Semaphorin 6A	NM_018744

gastrulation in *Drosophila*, has been shown to stimulate neural induction in *Xenopus* [45]. FGFR was demonstrated to play an important role in neurogenesis [46], and we also found that FGFR-1 is required for the neuronal differentiation of BMSCs induced by bFGF [15]. Genes in the second group are proneural transcription factors [47], such as achaete-scute complex homolog-like 1 (Mash-1), hairy and enhance of split 5 (Hes-5), neuronal PAS domain-2 and -3, and neuronal D4 (neurogenic differentiation 4). Mash-1, also known as achaete-scute family bHLH transcription factor 1 (ASCL1), is regulated by Notch signaling [29]. Mash-1 functions in controlling the generation of progenitors in central nervous system (CNS) and external sensory organs in the peripheral nervous system (PNS) [48, 49]. This gene encodes a member of the bHLH family of transcription factors. The protein activates transcription by binding to the E box (5'-CANNTG-3'). Dimerization with other bHLH proteins is required for efficient DNA binding. This protein plays a role in the neuronal commitment and differentiation and in the generation of olfactory and autonomic neurons [50]. Interestingly, Hes-5 gene was shown to suppress the function of Mash family and promote cell proliferation via the Notch signaling [51, 52]. Neuronal D4, a member of NeuroD family, plays a neuronal determination effect in neural development, and overexpression of Neurogenin1 can induce neuronal-like phenotype in human mesenchymal stem cells [53, 54]. Neuronal PAS domain proteins are shown to be involved in bFGF-stimulated adult neurogenesis [55]. In conclusion, gene upregulation from these two groups suggests that they may be involved in neurogenesis of BMSCs. The third group represents axonal, which includes genes such as Dynein-4 and -10, and Netrin-1 is involved in axonal genesis. Dynein family factors are the key motors of axon growth [56]. Netrin is a potent axon growth factor [57] and has been observed to be induced more than 20 folds in this study. Overall, these groups of

genes may contribute to the cell morphological changes as reported here.

Genes involving neural activities or functions can be grouped into either neurotransmitter molecules (the fourth group) or ion transport (the fifth group) or peptide signaling (Table 2). A typical molecule of neurotransmitters is Complexin-1, which is a cytosolic molecule and can bind to SNAP receptor to compete with SNAP [58]. Two syntaxin family members, Syntaxin 3 and 4A, were also upregulated in this study. Syntaxin family members are expressed only in the nervous system and implicated in docking of synaptic vesicles [59]. The highest expressed molecule in ion transport is Gamma-aminobutyric acid receptor alpha 6. Genes in this family play a very important role in depolarization of neuronal cells [60]. Several members of semaphorin were upregulated by bFGF in this study. Semaphorin is expressed on the cell membrane and has been demonstrated to regulate guidance of growth cones [61].

A group of receptor genes was also clearly upregulated, such as G-protein-coupled receptors (the sixth group) (Table 2). G-protein-coupled receptors were also demonstrated to have nonneuronal functions. GRP54, for instance, was involved in reproductive development [62] and GRP65 in signaling cascade [63]. Additionally, the opioid receptor is well known for mediating the morphine action [64].

**3.5. Mash-1 Promotes BMSCs Neuronal Differentiation.** Neuronal differentiation involves complicated gene regulation, in which the molecules related to signal transduction and gene transcription play a crucial role. We thus would like to suggest the following neuronal differentiation model complete with gene regulation networks after taking into consideration our findings on neuronal genes as induced by bFGF and the neuronal differentiation process. In determining the gene pool which plays a major role in turning BMSCs into neuronal cells, we decided to focus on genes from the first two classes, which are involved in neurogenesis and are also related to gene transcription. Amongst proneural genes, the mammalian achaete-scute homolog 1 (Mash-1), a basic helix-loop-helix transcriptional factor, was further demonstrated to be significantly upregulated. Mash-1 stood out as it was upregulated more than 4 folds at 4 hours and reached another 8 folds at 72 hours posttreatment, respectively (Table 2).

RT-PCR analysis for Mash-1 was carried out to assess the credibility of our microarray result at the mRNA level. This step is to ensure that the result obtained from cDNA microarray is not due to artifacts or unregulated signal amplification when processing the samples. As shown in Figure 6(a) (left panel), the transcription level of Mash-1 was increased in response to bFGF. The protein levels of Mash-1 were significantly emerging and increased after 24 h, which were observed as demonstrated by Western blot (Figure 6(a), right panel). Full unedited western blot images are supplied in Supplemental data 2. The expressions of neuronal-related genes, including GAP43 and Hes5, were also detected after bFGF treatment, which are also upregulated, but later than Mash-1 at mRNA levels (Figure 6(a)), indicating that Mash-1 may play an initiating role in driving neuronal differentiation of BMSCs. We also used immunofluorescence

TABLE 2

4 h	Fold 24 h	72 h	Gene name	Accession number
<b>Neural development</b>				
1.7	1.1	1.9	Syntrophin, acidic 1	NM_009228
2.1	3.0	0.8	Nestin	NM_016701
2.2	1.9	2.3	Empty spiracles homolog 1	X68881
0.9	2.4	5.8	Sema domain, immunoglobulin domain	NM_013657
2.3	1.5	4.5	Fibroblast growth factor receptor 1	NM_010206
1.6	1.5	2.2	Chordin	NM_009893
2.0	1.3	1.4	Sema domain, seven thrombospondin repeats	NM_013661
<b>Transcription factor</b>				
4.5	2.3	8.5	Achaete-scute complex homolog-like 1	NM_008553
4.4	1.9	9.9	Hairy and enhancer of split 5	NM_010419
1.4	1.5	3.2	Neuronal PAS domain protein 3	NM_013780
1.1	0.7	2.4	Neuronal PAS domain protein 2	NM_008719
3.1	2.1	1.4	Neurogenic differentiation 4	NM_007501
0.9	1.8	5.9	Ets variant gene 1	NM_007960
3.2	1.9	4.6	v-maf muculoaponeurotic fibroblast carcinoma oncogene	NM_010756
<b>Axonal</b>				
2.0	1.4	1.7	Kinesin family member 5C	NM_008449
2.0	2.2	2.2	Reticulon 4 receptor	NM_022982
1.2	1.6	2.7	Dynein, axonemal, light chain 4	NM_017470
2.1	1.8	0.5	Ephrin B1	NM_010110
1.4	1.1	2.1	Slit homolog 1	AF144627
3.1	3.3	2.8	Dynein, axonemal, heavy chain 10	Z83812
21.8	15.2	22.1	Netrin 1	NM_008744
<b>Neurotransmitter</b>				
0.1	3.6	5.1	Ral guanine nucleotide dissociation stimulator	NM_009058
1.0	2.3	0.8	Amyloid beta precursor protein-binding	AF020313
1.4	1.2	3.2	Syntaxin 4A	NM_009294
1.4	1.0	2.2	Syntaxin 3	D29797
3.0	1.3	5.3	Complexin 1	NM_007756
3.7	5.3	3.7	Suppressor of cytokine signaling 2	NM_007706
2.4	1.4	2.3	Solute carrier family 6 (neurotransmitter transporter)	AK036136
<b>Ion transporter</b>				
0.7	2.4	1.8	Gamma-aminobutyric acid receptor, alpha 4	AK013727
3.2	3.3	5.1	Gamma-aminobutyric acid receptor, alpha 6	NM_008068
1.8	1.2	1.9	Sema domain, transmembrane domain	NM_013662
2.0	1.3	1.4	Sema domain, seven thrombospondin repeats	NM_013661
2.8	4.0	3.7	Cholinergic receptor, nicotinic, alpha polypeptide 7	NM_007390
1.3	1.6	1.7	Cholinergic receptor, nicotinic, beta polypeptide 1	NM_009601
<b>G-protein</b>				
0.8	2.6	2.2	CD97 antigen	NM_011925
2.8	1.5	4.5	Opioid receptor, mu 1	NM_011013
0.6	2.2	1.0	G-protein-coupled receptor 56	NM_018882
2.9	1.1	1.6	Chemokine receptor 3	NM_009914
3.0	3.1	3.9	G-protein-coupled receptor 50	NM_010340
3.8	2.0	4.1	G-protein-coupled receptor 54	NM_053244

TABLE 2: Continued.

4 h	Fold 24 h	72 h	Gene name	Accession number
Others				
0.9	4.7	7.5	Putative neuronal cell adhesion molecule	AK051027
1.0	2.3	0.8	Amyloid beta precursor protein-binding	AF020313
2.3	1.7	1.7	EF hand calcium binding protein 2	NM_054095
1.4	1.0	2.7	Activity-dependent neuroprotective protein	NM_009628
2.7	2.1	4.7	Brain glycogen phosphorylase	NM_153781.1
1.7	2.4	3.2	Phospholipase C, epsilon 1	BC025027

staining to test Mash1. The results showed that BMSCs treated with bFGF after 72 h exhibited high expression of Mash1, and neurogenesis-related markers, including GAP43 and Hes5, were also expressed on these cells (Figure 6(b)). To determine the proneuronal effect of Mash-1 in BMSCs, we cloned and transfected Mash-1 into mouse BMSCs. After transfection, Mash-1-overexpressing BMSCs exhibited neuron-like morphology, which was evidenced by elongated neurites and cell body shrinkages (Figure 6(c)). Biochemical analysis revealed a higher expression of neuronal marker, NSE, in Mash-1-overexpressing BMSCs (Figure 6(d)). NSE has neurotrophic and neuroprotective properties on a broad spectrum in central nervous system neurons. We also detected the expression of synaptic-associated genes, including SV2a and SNAP-25 (Figure 6(e)). SV2a is an essential vesicle membrane protein expressed in virtually all synapses and could serve as a suitable target for synaptic density. SNAP-25 is one of the N-ethylmaleimide-sensitive fusion protein receptor, which involved in synaptic vesicle docking and subsequent fusion with the target membrane. The data show SV2a and SNAP-25 were highly induced in Mash-1-overexpressing BMSCs, indicated a potential synaptic capability in these cells. All these results combined with our earlier observation suggest that Mash-1 may be a crucial proneuronal differentiation factor upon bFGF treatment.

#### 4. Discussion

BMSCs were demonstrated to exhibit neural phenotypes both *in vivo* and *in vitro* under favourable conditions. Neural properties of BMSC generated cells, in most cases, were determined by measuring the expression of a few neural markers, which, in our opinion, would not reflect completely the phenotypes of neural traits [11] and leave the neuronal differentiation mechanisms much to our own imagination. In order to get a global pattern of gene expression changes in neuronal differentiation of BMSC, we investigated the kinetic changes of gene profiles of neuronal differentiated mouse BMSCs with the employment of cDNA microarray analysis. Our study revealed a strong inclination to upregulation of neural genes with various neural functions and properties. Interestingly, we further demonstrated that the Notch signaling molecule, Mash-1, plays an important role in driving BMSCs into adopting neuronal phenotype. These observations suggest that neuronal differentiation of BMSCs might

mimic or undertake certain conserved neuronal differentiation pathways.

The powerful analytical tool of microarray analysis has been used to determine the neural properties of bFGF differentiated BMSCs. Mori et al. reported the first neural gene profiles by using immortalized human BMSCs [13] which was adopted by Yamaguchi in further determining the neural gene expression [14]. However, both of them used RNAs extracted from cells differentiated for more than a week as their templates, and Yamaguchi had even been using a series of chemicals including DMSO and beta-mercaptoethanol, to differentiate BMSCs, which was strictly argued as being a stress-induced response [10, 65]. Moreover, they covered only a small pool of genes in their studies where most of the neural genes identified were neural markers or molecules expressed in the mature/differentiated cell. In our study, we used bFGF alone to induce mouse BMSC neuronal differentiation at around 2-3 days, and the differentiated cells acquired electrophysiological properties [15]. The obvious upregulations of wide range neural genes suggest that neuronal differentiated BMSCs can adopt many neural phenotypes under physiological condition and not merely on neural marker expressions [11].

Neuronal differentiation of BMSCs, especially induced with various chemicals, was challenged as being a direct stress-induced response [65], and the cellular neurite-like processes of neuronal differentiated BMSCs in most studies were demonstrated to be formed by cytoplasm shrinkage, rather than the growth of neurites [10]. However, in our study, many axonal growths related genes such as Netrin-1 and Dyncine were obviously upregulated from 4 hours treatment by bFGF onwards. The high levels of expression of these genes clearly indicate that the neurite-like cell processes as observed are that of being an active protrusion and not simply a cell shrinkage phenomena as argued. Moreover, a large number of genes, including ion transportation, neurotransmitters, and peptide signaling such as GABA receptor, complexin, and opioid receptor, were also upregulated. In agreement to our previous finding, neuronal cells from bFGF-treated BMSCs exhibit electrophysiological properties [15], completing with a wide range of expression of neural genes, and it is clear that this indicated BMSCs could acquire more complete neuronal traits under physiological stimulation.

Studies on the development of the nervous system of *Drosophila* demonstrated that Notch receptor initiated signaling pathways play a crucial role in neuroblast generations,

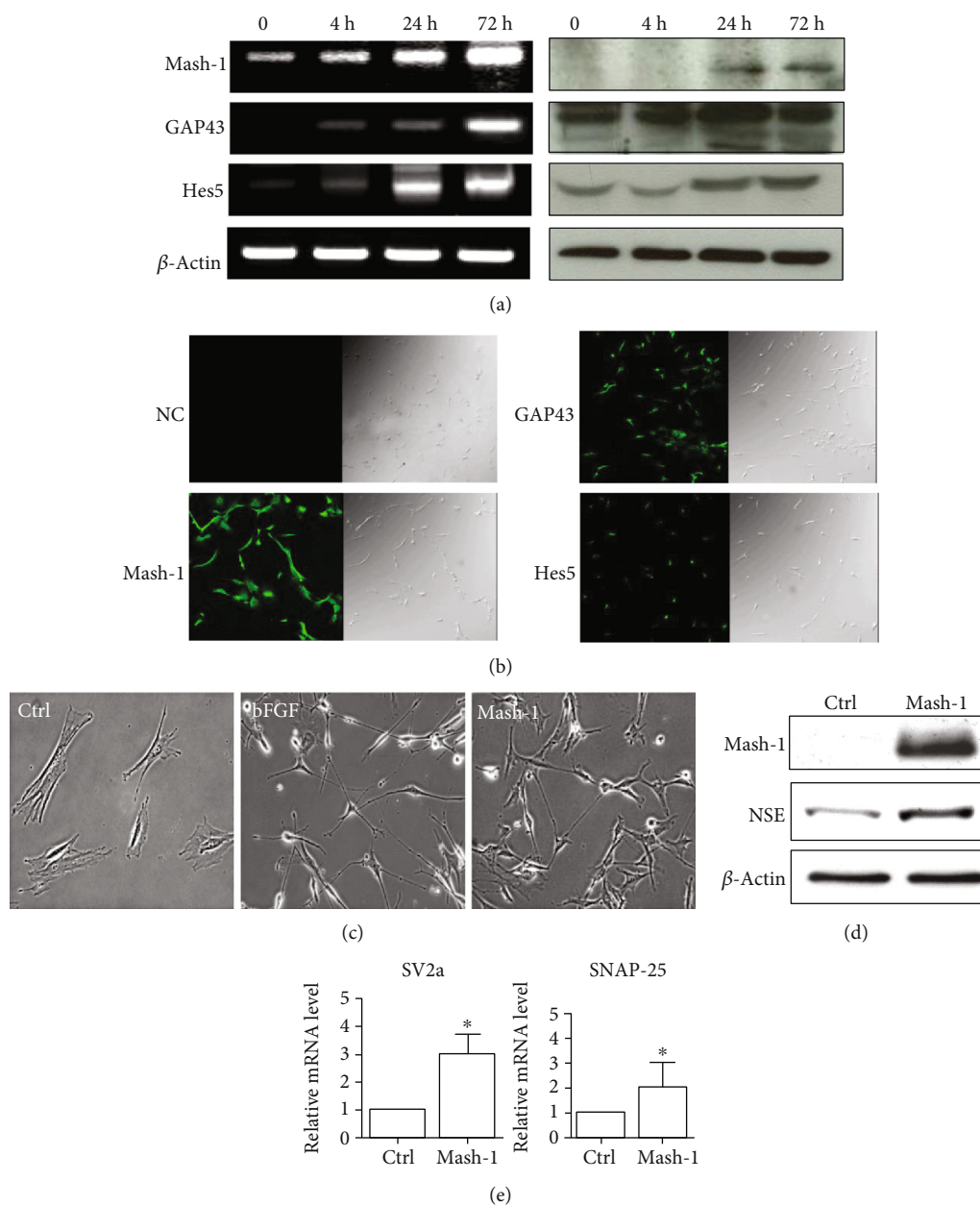


FIGURE 6: Overexpression of Mash-1 promotes neuronal differentiation of BMSCs. (a) RT-PCR (left) and western blot (right) representation of selected markers from cDNA microarray which showed consistencies with the data as analyzed. (b) Distribution of neuronal differentiation markers. Immunofluorescence staining using specific antibodies against GAP43, Mash-1, and Hes5 was performed in BMSCs with bFGF treatment for 24 hours. NC: negative control. Images are representatives of at least three experiments. (c) Mash-1 overexpressing BMSCs showed a typical neuronal morphology. (d) Western blotting analysis showed a significant increase of the NSE expression in Mash-1 overexpressing BMSCs compared to control cells. (e) The expression of SV2a and SNAP-25 were determined by qRT-PCR in Mash-1 overexpressing BMSCs. Data of RT-PCR indicate the mean  $\pm$  SEM of three experiments.

of which several groups of genes, including the bHLH family, are induced to regulate neural determination and differentiation [66]. In *Drosophila*, bFGF signaling pathway has been demonstrated to interact with the Notch signaling pathway in various cell types [67]. All the Notch pathway genes are preserved in vertebrates and expressed in nervous system and others [26]. The initiation and differentiation of BMSCs into neuronal cells by physiological factors were clearly involved in several neurogenesis pathways which are well

documented in the development of *Drosophila* and neural stem cell differentiation. Though a close comparison to the *Drosophila* model could be drawn, distinctions of BMSC neuronal differentiation from that observed in *Drosophila* should still be addressed.

In BMSCs, the intracellular domain of Notch (NICD) was shown recently to be capable of inducing BMSC neuronal differentiation. This function was further demonstrated to be coordinated with bFGF [9]. Interestingly, bFGF was



shown to promote the activity of Notch pathway in embryonic neuroepithelial precursor cells to inhibit differentiation [67]. The components of the Notch signaling pathways can be influenced by bFGF to affect the oligodendrocyte differentiation [68]. However, the mechanisms of the cross-talk between Notch and bFGF signaling pathways are need further identified. Adopting screening by microarray, we observed an astounding upregulation of Mash-1, the vertebrate homolog of bHLH transcription factor, which was also known as achaete-scute complex homolog-1 and shown to control the generation of progenitors for the central nervous system and external sensory organs in the peripheral nervous system [69, 70]. Previous study has delineated transcription factors Mash-1 and Prox-1 played a role in early steps during differentiation of neural stem cells in the developing central nervous system [48]. Mash1 has an important role in Notch signaling and the differentiation of neurons [71]. When we overexpressed Mash-1, BMSCs exhibited similar neuronal structures as differentiated by bFGF (Figure 6). These results suggested that Mash-1 could probably be the key factor to genes regulated by bFGF responsible for driving BMSC differentiation to neuronal cells. Similarly as our studies, Wang et al. show that under conditions of differentiation, Mash1-overexpressing BMSCs exhibit an increased expression of neuronal markers and a greater degree of neuronal morphology compared to control (non-Mash1-overexpressing cells) [72]. Xu et al. also indicated that overexpression of Mash-1 gene in promoting differentiation of mouse embryonic stem cells into neural cells [49]. Additionally studies showed Mash1-dependent Notch signaling pathway also regulates GABAergic neuron-like differentiation of BMSCs [50, 73].

Given so abundant investigations and reviews, various biomarkers of neuronal cells in characteristics were applied. Thus, it is necessary to apply multiple markers to the analysis cell type. In this work, we used these markers to identify the bFGF-induced neuronal differentiation of BMSCs. Gathering the analyzed data, we catch many markers were established in the development of bFGF-induced neurogenesis. While more neural markers may allow better reflection of neural traits, others believe that it is also true that science seeks to synthesize the identification of biological processes with fewer markers. However, it is difficult, using a single marker, to identify a single cell type exclusively. This work meets both ends, and Mash-1 is very useful gene for this purpose to identify the neuronal origin, which invokes to give a conceptual vision to the study of the stem cells and regenerative medicine.

In conclusion, our work reveals that the cross-talk is through the activation of downstream Notch components though the detail mechanisms of the activation of Mash-1 by bFGF. Concerns over the level of initiation, determination, and differentiation of BMSCs to proneuronal cells as induced by bFGF should be further analyzed. It is further noted that in this study, bFGF-induced neuronal differentiation of BMSCs opened a window of opportunity to studying the underlying mechanisms involved in the complex process of neuronal differentiation and maturation at physiological condition of BMSC neurogenesis. The genetic engineering of BMSCs will be a useful avenue for obtaining neuron-like donor cells for the treatment of neurological disorders.

## Data Availability

The data used to support the findings of this study are included within the article.

## Conflicts of Interest

The authors have declared that no competing interests exist.

## Acknowledgments

This work was supported by grants from the National Natural Science Foundation of China (Grant No. 81671226, No. 81500675, and No. 82070895).

## Supplementary Materials

Full unedited western blot images of Figures 3(c) and 6(a) data are supplied in Supplementary materials. (*Supplementary Materials*)

## References

- [1] D. J. Prockop, "Marrow stromal cells as stem cells for nonhematopoietic tissues," *Science*, vol. 276, no. 5309, pp. 71–74, 1997.
- [2] P. Bianco, M. Riminucci, S. Gronthos, and P. G. Robey, "Bone marrow stromal stem cells: nature, biology, and potential applications," *Stem Cells*, vol. 19, no. 3, pp. 180–192, 2001.
- [3] G. C. Kopen, D. J. Prockop, and D. G. Phinney, "Marrow stromal cells migrate throughout forebrain and cerebellum, and they differentiate into astrocytes after injection into neonatal mouse brains," *Proceedings of the National Academy of Sciences of the United States of America*, vol. 96, no. 19, pp. 10711–10716, 1999.
- [4] C. Ide, Y. Nakai, N. Nakano et al., "Bone marrow stromal cell transplantation for treatment of sub-acute spinal cord injury in the rat," *Brain Research*, vol. 1332, pp. 32–47, 2010.
- [5] M. Chopp, X. H. Zhang, Y. Li et al., "Spinal cord injury in rat: treatment with bone marrow stromal cell transplantation," *Neuroreport*, vol. 11, no. 13, pp. 3001–3005, 2000.
- [6] S. Corti, F. Locatelli, D. Papadimitriou, S. Strazzer, and G. P. Comi, "Somatic stem cell research for neural repair: current evidence and emerging perspectives," *Journal of Cellular and Molecular Medicine*, vol. 8, no. 3, pp. 329–337, 2004.
- [7] S. Corti, F. Locatelli, S. Strazzer, M. Guglieri, and G. P. Comi, "Neuronal generation from somatic stem cells: current knowledge and perspectives on the treatment of acquired and degenerative central nervous system disorders," *Current Gene Therapy*, vol. 3, no. 3, pp. 247–272, 2003.
- [8] J. R. Sanchez-Ramos, "Neural cells derived from adult bone marrow and umbilical cord blood," *Journal of Neuroscience Research*, vol. 69, no. 6, pp. 880–893, 2002.
- [9] M. Dezawa, "Specific induction of neurons and Schwann cells from bone marrow stromal cells and application to neurodegenerative diseases," *No Shinkei Geka*, vol. 33, no. 7, pp. 645–649, 2005.
- [10] B. Neuhuber, G. Gallo, L. Howard, L. Kostura, A. Mackay, and I. Fischer, "Reevaluation of in vitro differentiation protocols for bone marrow stromal cells: disruption of actin cytoskeleton induces rapid morphological changes and mimics neuronal



- phenotype," *Journal of Neuroscience Research*, vol. 77, no. 2, pp. 192–204, 2004.
- [11] R. Raedt, J. Pinxteren, A. van Dycke et al., "Differentiation assays of bone marrow-derived Multipotent Adult Progenitor Cell (MAPC)-like cells towards neural cells cannot depend on morphology and a limited set of neural markers," *Experimental Neurology*, vol. 203, no. 2, pp. 542–554, 2007.
- [12] H. Egusa, F. E. Schweizer, C. C. Wang, Y. Matsuka, and I. Nishimura, "Neuronal differentiation of bone marrow-derived stromal stem cells involves suppression of discordant phenotypes through gene silencing," *The Journal of Biological Chemistry*, vol. 280, no. 25, pp. 23691–23697, 2005.
- [13] T. Mori, T. Kiyono, H. Imabayashi et al., "Combination of hTERT and bmi-1, E6, or E7 induces prolongation of the life span of bone marrow stromal cells from an elderly donor without affecting their neurogenic potential," *Molecular and Cellular Biology*, vol. 25, no. 12, pp. 5183–5195, 2005.
- [14] S. Yamaguchi, S. Kuroda, H. Kobayashi et al., "The effects of neuronal induction on gene expression profile in bone marrow stromal cells (BMS)-a preliminary study using microarray analysis," *Brain Research*, vol. 1087, no. 1, pp. 15–27, 2006.
- [15] H. Yang, Y. Xia, S. Q. Lu, T. W. Soong, and Z. W. Feng, "Basic fibroblast growth factor-induced neuronal differentiation of mouse bone marrow stromal cells requires FGFR-1, MAPK/ERK, and transcription factor AP-1," *The Journal of Biological Chemistry*, vol. 283, no. 9, pp. 5287–5295, 2008.
- [16] D. Woodbury, E. J. Schwarz, D. J. Prockop, and I. B. Black, "Adult rat and human bone marrow stromal cells differentiate into neurons," *Journal of Neuroscience Research*, vol. 61, no. 4, pp. 364–370, 2000.
- [17] I. B. Black and D. Woodbury, "Adult rat and human bone marrow stromal stem cells differentiate into neurons," *Blood Cells, Molecules & Diseases*, vol. 27, no. 3, pp. 632–636, 2001.
- [18] S. I. Wilson, E. Graziano, R. Harland, T. M. Jessell, and T. Edlund, "An early requirement for FGF signalling in the acquisition of neural cell fate in the chick embryo," *Current Biology*, vol. 10, no. 8, pp. 421–429, 2000.
- [19] D. Henrique, D. Tyler, C. Kintner et al., "cash4, a novel achaete-scute homolog induced by Hensen's node during generation of the posterior nervous system," *Genes & Development*, vol. 11, no. 5, pp. 603–615, 1997.
- [20] T. Taetzsch, V. L. Brayman, and G. Valdez, "FGF binding proteins (FGFBPs): modulators of FGF signaling in the developing, adult, and stressed nervous system," *Biochimica et Biophysica Acta - Molecular Basis of Disease*, vol. 1864, no. 9 Part B, pp. 2983–2991, 2018.
- [21] Y. LIU, X. C. YI, G. GUO et al., "Basic fibroblast growth factor increases the transplantation-mediated therapeutic effect of bone mesenchymal stem cells following traumatic brain injury," *Molecular Medicine Reports*, vol. 9, no. 1, pp. 333–339, 2014.
- [22] S. Chiba, M. S. Kurokawa, H. Yoshikawa et al., "Noggin and basic FGF were implicated in forebrain fate and caudal fate, respectively, of the neural tube-like structures emerging in mouse ES cell culture," *Experimental Brain Research*, vol. 163, no. 1, pp. 86–99, 2005.
- [23] D. S. Sakaguchi, L. M. Janick, and T. A. Reh, "Basic fibroblast growth factor (FGF-2) induced transdifferentiation of retinal pigment epithelium: generation of retinal neurons and glia," *Developmental Dynamics*, vol. 209, no. 4, pp. 387–398, 1997.
- [24] Y. Wu, Z. Wang, P. Cai et al., "Dual delivery of bFGF- and NGF-binding coacervate confers neuroprotection by promoting neuronal proliferation," *Cellular Physiology and Biochemistry*, vol. 47, no. 3, pp. 948–956, 2018.
- [25] E. Knust and J. A. Campos-Ortega, "The molecular genetics of early neurogenesis in *Drosophila melanogaster*," *BioEssays*, vol. 11, no. 4, pp. 95–100, 1989.
- [26] R. Zhang, A. Engler, and V. Taylor, "Notch: an interactive player in neurogenesis and disease," *Cell and Tissue Research*, vol. 371, no. 1, pp. 73–89, 2018.
- [27] A. Engler, R. Zhang, and V. Taylor, "Notch and neurogenesis," *Advances in Experimental Medicine and Biology*, vol. 1066, pp. 223–234, 2018.
- [28] G. S. Richards and F. Rentzsch, "Regulation of *Nematostella* neural progenitors by SoxB, Notch and bHLH genes," *Development*, vol. 142, no. 19, pp. 3332–3342, 2015.
- [29] J. F. Brunet and A. Ghysen, "Deconstructing cell determination: proneural genes and neuronal identity," *BioEssays*, vol. 21, no. 4, pp. 313–318, 1999.
- [30] N. Gaiano and G. Fishell, "The role of notch in promoting glial and neural stem cell fates," *Annual Review of Neuroscience*, vol. 25, no. 1, pp. 471–490, 2002.
- [31] J. L. de la Pompa, A. Wakeham, K. M. Correia et al., "Conservation of the Notch signalling pathway in mammalian neurogenesis," *Development*, vol. 124, no. 6, pp. 1139–1148, 1997.
- [32] L. Zhang, P. Su, C. Xu, J. Yang, W. Yu, and D. Huang, "Chondrogenic differentiation of human mesenchymal stem cells: a comparison between micromass and pellet culture systems," *Biotechnology Letters*, vol. 32, no. 9, pp. 1339–1346, 2010.
- [33] A. Banfi, G. Bianchi, R. Notaro, L. Luzzatto, R. Cancedda, and R. Quarto, "Replicative aging and gene expression in long-term cultures of human bone marrow stromal cells," *Tissue Engineering*, vol. 8, no. 6, pp. 901–910, 2002.
- [34] C. Baustian, S. Hanley, and R. Ceredig, "Isolation, selection and culture methods to enhance clonogenicity of mouse bone marrow derived mesenchymal stromal cell precursors," *Stem Cell Research & Therapy*, vol. 6, no. 1, p. 151, 2015.
- [35] L. S. Meirelles and N. B. Nardi, "Murine marrow-derived mesenchymal stem cell: isolation, in vitro expansion, and characterization," *British Journal of Haematology*, vol. 123, no. 4, pp. 702–711, 2003.
- [36] I. Sekiya, B. L. Larson, J. R. Smith, R. Pochampally, J. & G. Cui, and D. J. Prockop, "Expansion of human adult stem cells from bone marrow stroma: conditions that maximize the yields of early progenitors and evaluate their quality," *Stem Cells*, vol. 20, no. 6, pp. 530–541, 2002.
- [37] W. Loscher, M. Gillard, Z. A. Sands, R. M. Kaminski, and H. Klitgaard, "Synaptic vesicle glycoprotein 2A ligands in the treatment of epilepsy and beyond," *CNS Drugs*, vol. 30, no. 11, pp. 1055–1077, 2016.
- [38] M. Halks-Miller, M. L. Schroeder, V. Haroutunian et al., "CCR1 is an early and specific marker of Alzheimer's disease," *Annals of Neurology*, vol. 54, no. 5, pp. 638–646, 2003.
- [39] A. Noor and S. Zahid, "A review of the role of synaptosomal-associated protein 25 (SNAP-25) in neurological disorders," *The International Journal of Neuroscience*, vol. 127, no. 9, pp. 805–811, 2016.
- [40] J. Brohan and B. G. Goudra, "The role of GABA receptor agonists in anesthesia and sedation," *CNS Drugs*, vol. 31, no. 10, pp. 845–856, 2017.

- [41] J. D. Hilario, L. R. Rodino-Klapac, C. Wang, and C. E. Beattie, "Semaphorin 5A is a bifunctional axon guidance cue for axial motoneurons in vivo," *Developmental Biology*, vol. 326, no. 1, pp. 190–200, 2009.
- [42] A. R. Lee, K. W. Ko, H. Lee, Y. S. Yoon, M. R. Song, and C. S. Park, "Putative cell adhesion membrane protein Vstm5 regulates neuronal morphology and migration in the central nervous system," *The Journal of Neuroscience*, vol. 36, no. 39, pp. 10181–10197, 2016.
- [43] Y. Wei, J. Gong, Z. Xu et al., "Nrf2 in ischemic neurons promotes retinal vascular regeneration through regulation of semaphorin 6A," *Proceedings of the National Academy of Sciences of the United States of America*, vol. 112, no. 50, pp. E6927–E6936, 2015.
- [44] U. Lendahl, L. B. Zimmerman, and R. D. G. McKay, "CNS stem cells express a new class of intermediate filament protein," *Cell*, vol. 60, no. 4, pp. 585–595, 1990.
- [45] Y. Sasai, B. Lu, H. Steinbeisser, and E. M. De Robertis, "Regulation of neural induction by the Chd and Bmp-4 antagonistic patterning signals in *Xenopus*," *Nature*, vol. 376, no. 6538, pp. 333–336, 1995.
- [46] R. Mayor, N. Guerrero, and C. Martinez, "Role of FGF and noggin in neural crest induction," *Developmental Biology*, vol. 189, no. 1, pp. 1–12, 1997.
- [47] N. Bertrand, D. S. Castro, and F. Guillemot, "Proneural genes and the specification of neural cell types," *Nature Reviews. Neuroscience*, vol. 3, no. 7, pp. 517–530, 2002.
- [48] Torii Ma, F. Matsuzaki, N. Osumi et al., "Transcription factors Mash-1 and Prox-1 delineate early steps in differentiation of neural stem cells in the developing central nervous system," *Development*, vol. 126, no. 3, pp. 443–456, 1999.
- [49] L. Xu, D. Ding, X. Li, Q. Shi, Y. Wang, and C. Zhou, "Over expression of Mash-1 gene in promoting differentiation of mouse embryonic stem cells into neural cells," *Zhongguo Xiu Fu Chong Jian Wai Ke Za Zhi*, vol. 29, no. 12, pp. 1553–1559, 2015.
- [50] Q. Long, Q. Luo, K. Wang, A. Bates, and A. K. Shetty, "Mash1-dependent Notch signaling pathway regulates GABAergic neuron-like differentiation from bone marrow-derived mesenchymal stem cells," *Aging and Disease*, vol. 8, no. 3, pp. 301–313, 2017.
- [51] Z. H. Liu, X. M. Dai, and B. Du, "Hes1: a key role in stemness, metastasis and multidrug resistance," *Cancer Biology & Therapy*, vol. 16, no. 3, pp. 353–359, 2015.
- [52] R. Kageyama and T. Ohtsuka, "The Notch-Hes pathway in mammalian neural development," *Cell Research*, vol. 9, no. 3, pp. 179–188, 1999.
- [53] L. Sommer, Q. Ma, and D. J. Anderson, "Neurogenins, a novel family of atonal-related bHLH transcription factors, are putative mammalian neuronal determination genes that reveal progenitor cell heterogeneity in the developing CNS and PNS," *Molecular and Cellular Neurosciences*, vol. 8, no. 4, pp. 221–241, 1996.
- [54] L. Schäck, S. Budde, T. Lenarz et al., "Induction of neuronal-like phenotype in human mesenchymal stem cells by overexpression of neurogenin1 and treatment with neurotrophins," *Tissue & Cell*, vol. 48, no. 5, pp. 524–532, 2016.
- [55] A. A. Pieper, X. Wu, T. W. Han et al., "The neuronal PAS domain protein 3 transcription factor controls FGF-mediated adult hippocampal neurogenesis in mice," *Proceedings of the National Academy of Sciences of the United States of America*, vol. 102, no. 39, pp. 14052–14057, 2005.
- [56] M. E. Porter, "Axonemal dyneins: assembly, organization, and regulation," *Current Opinion in Cell Biology*, vol. 8, no. 1, pp. 10–17, 1996.
- [57] T. Serafini, T. E. Kennedy, M. J. Gaiko, C. Mirzayan, T. M. Jessell, and M. Tessier-Lavigne, "The netrins define a family of axon outgrowth-promoting proteins homologous to *C. elegans* UNC-6," *Cell*, vol. 78, no. 3, pp. 409–424, 1994.
- [58] H. T. McMahon, M. Missler, C. Li, and T. C. Südhof, "Complexins: cytosolic proteins that regulate SNAP receptor function," *Cell*, vol. 83, no. 1, pp. 111–119, 1995.
- [59] M. K. Bennett, N. Calakos, and R. H. Scheller, "Syntaxin: a synaptic protein implicated in docking of synaptic vesicles at presynaptic active zones," *Science*, vol. 257, no. 5067, pp. 255–259, 1992.
- [60] M. Gassmann and B. Bettler, "Regulation of neuronal GABA(B) receptor functions by subunit composition," *Nature Reviews. Neuroscience*, vol. 13, no. 6, pp. 380–394, 2012.
- [61] R. J. Pasterkamp, "Getting neural circuits into shape with semaphorins," *Nature Reviews. Neuroscience*, vol. 13, no. 9, pp. 605–618, 2012.
- [62] A. S. Kauffman, J. H. Park, A. A. McPhie-Lalmansingh et al., "The kisspeptin receptor GPR54 is required for sexual differentiation of the brain and behavior," *The Journal of Neuroscience*, vol. 27, no. 33, pp. 8826–8835, 2007.
- [63] M. Liu, R. M. Parker, K. Darby et al., "GPR56, a novel secretin-like human G-protein-coupled receptor gene," *Genomics*, vol. 55, no. 3, pp. 296–305, 1999.
- [64] G. Rossi, Y. X. Pan, J. Cheng, and G. W. Pasternak, "Blockade of morphine analgesia by an antisense oligodeoxynucleotide against the mu receptor," *Life Sciences*, vol. 54, no. 21, pp. -PL375–PL379, 1994.
- [65] P. Lu, A. Blesch, and M. H. Tuszynski, "Induction of bone marrow stromal cells to neurons: differentiation, transdifferentiation, or artifact?," *Journal of Neuroscience Research*, vol. 77, no. 2, pp. 174–191, 2004.
- [66] B. P. San-Juan and A. Baonza, "The bHLH factor deadpan is a direct target of Notch signaling and regulates neuroblast self-renewal in *Drosophila*," *Developmental Biology*, vol. 352, no. 1, pp. 70–82, 2011.
- [67] C. H. Faux, A. M. Turnley, R. Epa, R. Cappai, and P. F. Bartlett, "Interactions between fibroblast growth factors and Notch regulate neuronal differentiation," *The Journal of Neuroscience*, vol. 21, no. 15, pp. 5587–5596, 2001.
- [68] Y. X. Zhou and R. C. Armstrong, "Interaction of fibroblast growth factor 2 (FGF2) and notch signaling components in inhibition of oligodendrocyte progenitor (OP) differentiation," *Neuroscience Letters*, vol. 421, no. 1, pp. 27–32, 2007.
- [69] J. Battiste, A. W. Helms, E. J. Kim et al., "Ascl1 defines sequentially generated lineage-restricted neuronal and oligodendrocyte precursor cells in the spinal cord," *Development*, vol. 134, no. 2, pp. 285–293, 2007.
- [70] M. Sugimori, M. Nagao, N. Bertrand, C. M. Parras, F. Guillemot, and M. Nakafuku, "Combinatorial actions of patterning and HLH transcription factors in the spatiotemporal control of neurogenesis and gliogenesis in the developing spinal cord," *Development*, vol. 134, no. 8, pp. 1617–1629, 2007.
- [71] A. Serre, E. Y. Snyder, J. Mallet, and D. Buchet, "Overexpression of basic helix-loop-helix transcription factors enhances neuronal differentiation of fetal human neural progenitor cells

in various ways,” *Stem Cells and Development*, vol. 21, no. 4, pp. 539–553, 2012.

- [72] K. Wang, Q. Long, C. Jia et al., “Over-expression of Mash1 improves the GABAergic differentiation of bone marrow mesenchymal stem cells in vitro,” *Brain Research Bulletin*, vol. 99, pp. 84–94, 2013.
- [73] K. Oishi, K. Watatani, Y. Itoh et al., “Selective induction of neocortical GABAergic neurons by the PDK1-Akt pathway through activation of Mash1,” *Proceedings of the National Academy of Sciences of the United States of America*, vol. 106, no. 31, pp. 13064–13069, 2009.

## Research Article

# Mechanically Stretched Mesenchymal Stem Cells Can Reduce the Effects of LPS-Induced Injury on the Pulmonary Microvascular Endothelium Barrier

Jin-ze Li,<sup>1</sup> Shan-shan Meng,<sup>1</sup> Xiu-Ping Xu,<sup>1</sup> Yong-bo Huang,<sup>2</sup> Pu Mao,<sup>2</sup> Yi-min Li,<sup>2</sup> Yi Yang,<sup>1</sup> Hai-bo Qiu ,<sup>1</sup> and Chun Pan <sup>1</sup>

<sup>1</sup>Jiangsu Provincial Key Laboratory of Critical Care Medicine, Department of Critical Care Medicine, Zhongda Hospital, School of Medicine, Southeast University, Nanjing 210009, China

<sup>2</sup>The State Key Laboratory of Respiratory Disease, Guangzhou Institute of Respiratory Disease, Department of Critical Care Medicine, The First Affiliated Hospital of Guangzhou Medical University, Guangzhou 510120, China

Correspondence should be addressed to Chun Pan; [panchun1982@gmail.com](mailto:panchun1982@gmail.com)

Received 30 June 2020; Revised 10 October 2020; Accepted 16 October 2020; Published 30 October 2020

Academic Editor: Huseyin Sumer

Copyright © 2020 Jin-ze Li et al. This is an open access article distributed under the Creative Commons Attribution License, which permits unrestricted use, distribution, and reproduction in any medium, provided the original work is properly cited.

Mesenchymal stem cells (MSCs) may improve the treatment of acute respiratory distress syndrome (ARDS). However, few studies have investigated the effects of mechanically stretched -MSCs (MS-MSCs) in *in vitro* models of ARDS. The aim of this study was to evaluate the potential therapeutic effects of MS-MSCs on pulmonary microvascular endothelium barrier injuries induced by LPS. We introduced a cocultured model of pulmonary microvascular endothelial cell (EC) and MSC medium obtained from MSCs with or without mechanical stretch. We found that Wright-Giemsa staining revealed that MSC morphology changed significantly and cell plasma shrank separately after mechanical stretch. Cell proliferation of the MS-MSC groups was much lower than the untreated MSC group; expression of cell surface markers did not change significantly. Compared to the medium from untreated MSCs, inflammatory factors elevated statistically in the medium from MS-MSCs. Moreover, the paracellular permeability of endothelial cells treated with LPS was restored with a medium from MS-MSCs, while LPS-induced EC apoptosis decreased. In addition, protective effects on the remodeling of intercellular junctions were observed when compared to LPS-treated endothelial cells. These data demonstrated that the MS-MSC groups had potential therapeutic effects on the LPS-treated ECs; these results might be useful in the treatment of ARDS.

## 1. Introduction

To date, the emerging virus SARS-CoV-2 is causing a worldwide public health emergency; 17% critically ill patients developed acute respiratory distress syndrome (ARDS) [1]. Despite numerous efforts towards reducing mortality in established ARDS, in hospital mortality still remains near 40% [2]. The main pathophysiology associated with ARDS in critically ill patients is the failure of pulmonary microvascular endothelium barrier integrity [3]. Therefore, maintaining the integrity of the endothelium barrier is critical for ARDS treatment.

Mesenchymal stem cell (MSC) therapy is a potential method to treat ARDS [4], and our previous studies [5, 6]

have shown concrete benefits both *in vitro* and *in vivo*. However, clinical trials of allogeneic MSC transplantation have provided conflicting evidences. In one trial, MSC treatment in patients with ARDS produced a short-term improvement in oxygenation [7]. Yet, another trial demonstrated no significant difference in the 28-day mortality between patients treated with MSCs and a control group (30% in the MSC group versus 15% in the placebo group) [8]. When injected intravenously, MSCs preferentially homed to the lungs and engrafted at sites of injury in the pulmonary microvascular endothelium layer [9]. The therapeutic function of MSCs presents from the beginning of their engraftment on the endothelium layer to their merger with the layer [10]. During this period, MSCs are not only affected by biochemical



factors but also by different kinds of mechanical stimulation coming from the microenvironment they have lived in [11]. Better integration of experimental and clinical data could provide further insight into the use of MSC-based therapy in this setting.

Mechanical stimulation on the lung tissue exists constantly in physiological and pathological states, such as ARDS [12, 13]. When utilized with mechanical ventilation to maintain essential oxygenation of ARDS patients, mechanical stimulation conducted through the lung tissue microenvironment varies from mild to severe levels and generates different degrees of lung compliance [14, 15]. Mechanical stretch may approximate the mechanical ventilation with low tidal volumes that are commonly used in the lung-protective mechanical ventilation required to treat ARDS previously [16] and nowadays [17]. When MSCs are introduced into the lung microenvironment to treat ARDS, they have to encounter different degrees of mechanical stimulation. Evidences have shown that mechanical stimulation can affect behavior of MSCs, such as morphology [18], adhesion [19], and differentiation [20, 21]. Therefore, mechanical stretch on MSCs could play an important role on the treatment of LPS-induced EC injuries.

The aim of this study was to present evidences of MS-MSC therapeutic effects on EC injuries treated by LPS. To test this hypothesis, we conducted a cocultured model of the EC and MSC medium obtained from MSCs with or without mechanical stretch. And, we evaluated the repair ability of the medium from MSCs or MS-MSCs on LPS-induced EC injuries.

## 2. Materials and Methods

**2.1. Mesenchymal Stem Cell Culture and Mechanical Stretch.** First passage human bone marrow mesenchymal stem cells (MSCs) were obtained from ScienCell Research Laboratories (San Diego, California, USA). The cells were characterized by the supplier. MSCs were maintained in the mesenchymal stem cell medium (MSCM; 5%FBS, 1% mesenchymal stem cell growth supplement, and 1% penicillin/streptomycin solution). The media were purchased from ScienCell Research Laboratories (San Diego, California, USA). Cells were cultured at 37°C in an incubator with an atmosphere of 5% CO<sub>2</sub> air. Every 3 to 5 days, cells were passaged when they reached 70-80% confluency and passages from 3 to 8 of the cells were used for all experiments.

MSCs were preconditioned by mechanical stretch (MS) *in vitro* with a BioFlex strain unit (BioFlex, Flexcell International Corporation, Hillsborough, NC, USA) as described previously [22]. MSCs were seeded onto a six-well plate containing flexible collagen type I-coated silicone rubber membranes at the bottom of each well and incubated at 37°C in 5% CO<sub>2</sub> atmosphere with 95% humidity (BioFlex, Flexcell International Corporation, Hillsborough, NC, USA). MSCs were cultured for 3 or 5 days to reach 70-80% confluency and subjected to mechanical stretch of 10% or 20% elongation for 24 h or 48 h using a computer-controlled vacuum stretch apparatus (FX-5000 Tension Plus System, Flexcell International Corporation, Hillsborough, NC, USA). The

untreated MSC group did not receive mechanical stretch and was incubated in the same incubator. MSCs and supernatant from all groups were collected at scheduled time points and prepared for use in this study. Supernatants from the stretched MSC and control groups were collected and centrifugated to remove dead cells and cell debris.

**2.2. Endothelial Cell and Dermal Fibroblast Culture.** First passage human pulmonary microvascular endothelial cells (ECs) and human dermal fibroblasts (HDF) were obtained from ScienCell Research Laboratories (San Diego, California, USA), and the cells were cultured in an endothelial cell medium (ECM; 5%FBS, 1% endothelial cell growth supplement, and 1% penicillin/streptomycin solution) and fibroblast medium (FM; 5%FBS, 1% fibroblast growth supplement, and 1% penicillin/streptomycin solution), respectively. All mediums were purchased from ScienCell Research Laboratories (San Diego, California, USA). Cells were cultured at 37°C in the incubator with an atmosphere of 5% CO<sub>2</sub> air. Every 3 to 5 days, cells were passaged when they reached 70-80% confluency.

**2.3. Endothelial Cell Intervention with LPS and Coculture System.** ECs at a density of 50,000 per well were seeded in the upper chambers (0.4 μm pore size polyester membrane from Corning, Inc.) and cultured for 2 to 3 days to produce a confluent monolayer, and MSCs were seeded in the lower chambers. Then, cells were treated with LPS (100 ng/mL, Sigma) for 6 hours before permeability was tested, as previously described [23]. After adding 10 μL 40 kDa fluorescein isothiocyanate- (FITC-) Dextran (Sigma-Aldrich) to each upper insert and incubating for 40 minutes in an incubator, 100 μL medium from the upper and lower chambers was withdrawn. Then, the medium was transferred to a 96-well plate and read using excitation and emission wavelengths of 490 nm and 530 nm, respectively.

**2.4. Morphology Assessment of Mesenchymal Stem Cells.** To observe cell morphology, cells were stained with Wright-Giemsa stain (Sigma Aldrich) according to the manufacturer's protocols as previously described [24]. After air drying the wells, MSCs were inspected under a light microscope (Olympus, Tokyo, Japan).

**2.5. Cell Proliferation Assay.** Untreated and mechanically stretched MSCs were seeded at 2000 cells per well onto 96-well plates and cultured in an incubator with a humidified atmosphere of 5% CO<sub>2</sub> at 37°C. 10 μL of Cell Counting Kit-8 (CCK-8) solution (Beyotime, China) was added per well, and cells were cultured for 1 hour at 37°C, before measuring absorbance at 450 nm with a microplate reader.

**2.6. Identification of MSCs by Flow Cytometry.** Untreated and mechanically stretched MSCs were identified by flow cytometry (BD Bioscience, San Diego, CA) as described previously [25]. Harvested MSCs were washed with PBS and resuspended to 1 × 10<sup>6</sup> cells/mL, and 100 μL of cell suspension was incubated with fluorescein-conjugated monoclonal antibodies against CD90, CD29, and CD45 (BD Pharmingen, San Diego, CA), respectively. Samples were mixed in the dark

for 20 minutes, then resuspended and centrifuged at 1000 rpm for 5 minutes at room temperature. Supernatants were removed, and cells were resuspended with PBS to 200  $\mu$ L for flow cytometry analysis.

**2.7. Enzyme-Linked Immunosorbent Assay.** The supernatants from all MSC groups were collected and centrifuged to remove cell fragments. Levels of tumor necrosis factor (TNF- $\alpha$ ), interleukin-6 (IL-6), and interleukin-10 (IL-10) in the culture medium were detected by ELISA (ExCellBio, Shanghai, China). All tests were performed according to the manufacturer's instructions. All samples were examined in duplicate.

**2.8. Endothelial Permeability Examination.** ECs were seeded in the upper chamber in 24-well culture plates (0.4  $\mu$ m pore size polyester membrane from Corning, Inc.) and cultured for 2 to 3 days to produce a confluent monolayer. Then, cells were treated with LPS (100 ng/mL, Sigma) for 6 hours before permeability was tested, as previously described [23]. After adding 10  $\mu$ L 40 kDa fluorescein isothiocyanate- (FITC-) Dextran (Sigma-Aldrich) to each upper insert and incubating for 40 minutes in an incubator, 100  $\mu$ L medium from the upper and lower chambers was withdrawn. Then, the medium was transferred to a 96-well plate and read using excitation and emission wavelengths of 490 nm and 530 nm, respectively.

**2.9. Apoptosis of Pulmonary Microvascular Endothelial Cells.** An Annexin V-FITC Assay Kit (Sigma-Aldrich) was used to assess the percentage of ECs undergoing apoptosis, according to the manufacturer's instructions. ECs were harvested and washed with PBS and suspended in 1x binding buffer at a cell concentration of  $1 \times 10^6$  cells/mL. Then, 10  $\mu$ L propidium iodide solution (PI) and 5  $\mu$ L annexin V-FITC conjugate (annexin V) were added to each sample and gently mixed. After 10 minutes incubation in the dark at room temperature, samples were analyzed using a flow cytometer (BD Biosciences, USA).

**2.10. Western Blotting Analysis.** Western blotting was used to detect the expression of VE-cadherin and Connexin-43 on ECs as previously described [26]. Total proteins from ECs after different treatments were extracted with RIPA lysis buffer (Beyotime Institute of Biotechnology, Shanghai, China) supplemented with 1 mmol/L phenylmethylsulfonyl fluoride (PMSF), and then separated with 10% sodium dodecyl sulphate-polyacrylamide gel electrophoresis and transferred onto polyvinylidene fluoride membranes (Beyotime, China). Afterwards, membranes were blocked in 3% BSA for 2 hours at room temperature and incubated at 4°C overnight with primary antibodies against VE-cadherin (Abcam) or Connexin-43 (Cell Signaling Technology). The next day, membranes were washed in TBS-T and incubated in HRP-conjugated secondary antibody (Boster biotechnology, Wuhan, China) for 1 hour at room temperature. Then, ECL (Beyotime, China) was applied to detect the bands with a chemiluminescence imaging system (ChemiQ 4800mini; Ouxiang, China).

**2.11. Immunofluorescence Staining.** In a transwell system, ECs were seeded on the upper inserts and cultured to form a confluent monolayer for 3 or 5 days. After treating with LPS for 6 hours, cells were then washed with cold PBS and fixed with 4% paraformaldehyde for 10 minutes. Samples were permeabilized with 0.25% Triton X-100 for 10 minutes, blocked with 1% bovine serum albumin (BSA), and incubated overnight with VE-cadherin primary antibody (AB) (1:200 rabbit polyclonal anti-VE-cadherin) (Abcam, ab18058, Ireland) at 4°C. After incubation for 6 hours, samples were incubated with a secondary FITC-conjugated goat anti-rabbit IgG (1:700 Alexa Fluor 488 IgG) (Biosciences, Ireland) and stained with (VWR, Ireland) for 1 h at room temperature. Cell nuclei were stained with DAPI (VWR, Ireland) for 1 min at room temperature, washed in PBS, and imaged using confocal microscopy (Leica SP8, Ireland).

**2.12. Statistical Analyses.** Statistical analyses were performed using the SPSS 20.0 software package (SPSS Inc., Chicago, IL, USA). Results were presented as the mean  $\pm$  standard deviation. Group comparison was analyzed by one-way analysis of variance, followed by Tukey's test.  $p < 0.05$  was considered statistically significant.

### 3. Results

**3.1. MSCs Improved Paracellular Permeability of LPS-Induced EC Injury.** To determine if MSCs protected ECs from LPS-induced injury, we used a transwell coculture system (Figure 1(a)) to assess paracellular permeability when MSCs were added at varying seeding concentrations, from  $1 \times 10^5$  cells per well to  $5 \times 10^5$  cell per well. Permeability significantly decreased when MSCs were plated at  $3 \times 10^5$  cell per well (Figure 1(b); \* $p < 0.05$ ) and decreased further as the density of MSCs increased. This suggested that the therapeutic effect of MSCs on endothelial cell permeability improved as the density of MSCs increased.

**3.2. Description of the Mechanical Stretch Method of MSCs.** MSCs were seeded on six-well mechanical stretch plates with collagen type I-coated flexible silicon rubber membranes placed at the bottom of each well and were preconditioned by mechanically stretching these plates during cell culture (Figures 2(a) and 2(b)). An example of a six-well mechanical stretch plate is presented in Figure 2(c). MSCs were plated on the silicon rubber membrane and stained with Wright-Giemsa stain. A schematic view of a well under mechanical stretch is presented in Figure 2(d). The first column shows the side view of two wells containing either untreated or mechanically stretched MSCs. The second column presents an illustration of untreated or mechanically stretched MSCs, respectively.

**3.3. Mechanical Stretch Affected Morphology and Proliferation of MSCs.** MSCs were seeded on the six-well plates and subjected to different categories of mechanical stretch (MS), including untreated, 10% MS for 24 hours (MS-10%-24 h), 10% MS for 48 hours (MS-10%-48 h), 20% MS for 24 hours (MS-24%-24 h), and 20% MS for 48 hours (MS-20%-48 h). Morphological differences were observed

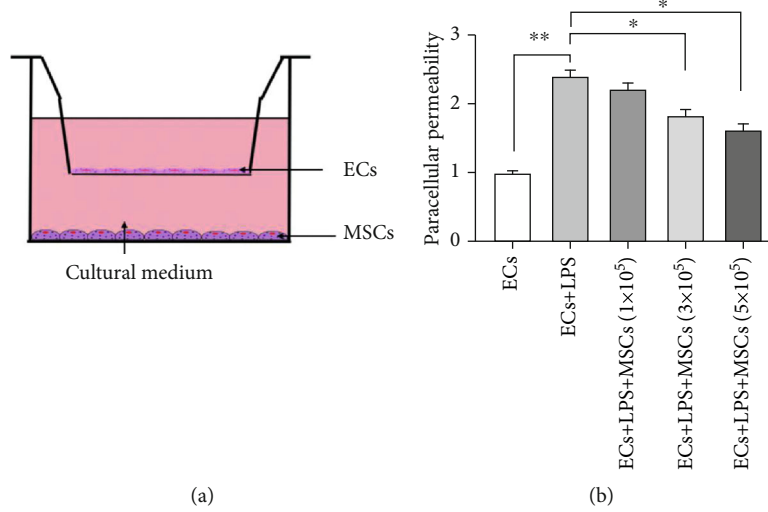


FIGURE 1: Paracellular permeability of ECs induced by LPS. (a) Schematic view of the transwell coculture system. (b) Effect of adding different numbers of MSCs on the paracellular permeability of ECs. Statistically significant differences were presented ( $n = 3$ ;  $*p < 0.05$ ,  $**p < 0.01$ ). ARDS: acute respiratory distress syndrome; MSCs: mesenchymal stem cells; ECs: endothelial cells; LPS: lipopolysaccharide.

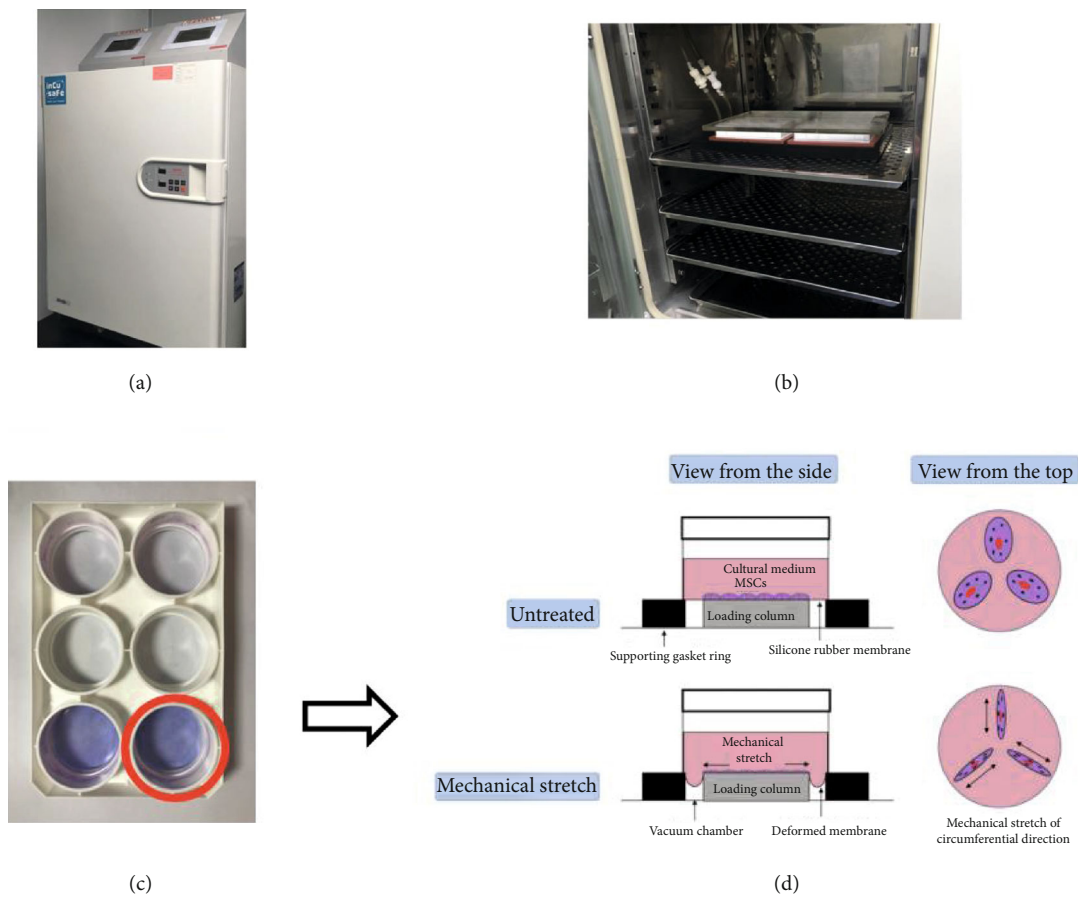


FIGURE 2: Illustration of method used to precondition MSCs by mechanical stretching. MSCs were seeded onto a six-well plate with collagen type I-coated flexible silicone rubber membranes at the bottom of each well in a mechanical stretch system. (a) Outside view of the mechanical stretch system. (b) Inside view of the mechanical stretch system. (c) Example of a six-well mechanical stretch plate. (d) Illustration of a well under mechanical stretch.

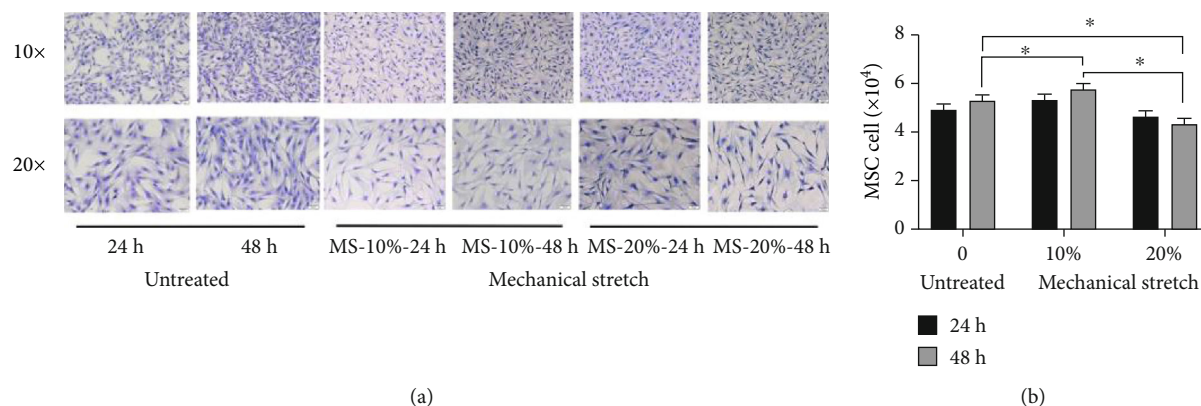


FIGURE 3: Effects of MS on MSC morphology and proliferation. (a) Changes to MSCs morphology with or without MS were presented in a time and magnitude dependent manner. (b) MSC cell number after MS. Statistically significant differences are presented ( $n = 3$ ;  $*p < 0.05$ ). MS: mechanical stretch.

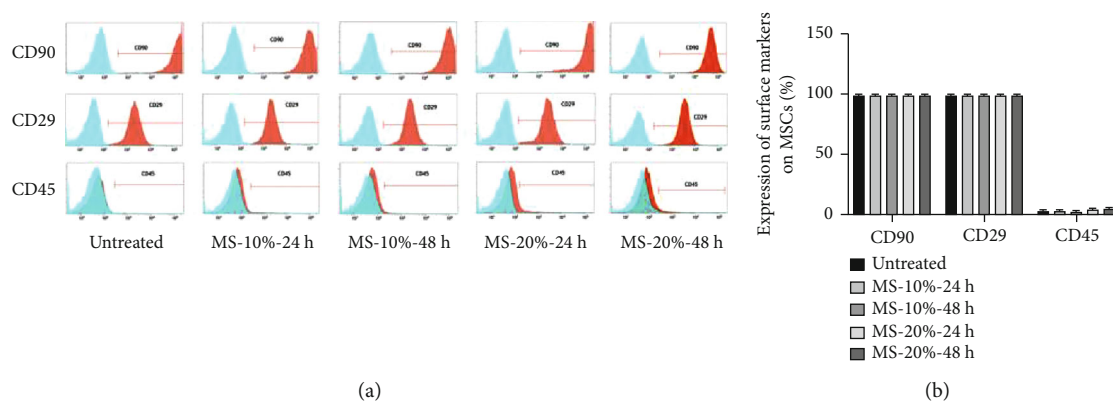


FIGURE 4: Identification of mesenchymal stem cells (MSCs). Immunophenotypic analysis of surface markers by flow cytometry. (a) Cyan peak: isotype control; red peak: sample. (b) Effects of mechanical stretching on the expression of MSC surface markers CD90, CD29, and CD45 as analyzed by flow cytometry.

following treatment (Figure 3(a)). Cells in all groups remained firmly adhered to the seeding surface. Compared to untreated MSCs, the MS-MSCs showed signs of atrophy, appearing thinner and flattened, and have increasingly shrunk in a time- and magnitude-dependent manner. Moreover, cell proliferation significantly increased in the MS-10% groups (Figure 3(b);  $*p < 0.05$ ) but decreased in the MS-20% groups ( $**p < 0.01$ ). Proliferation in the MS-20%-48 h group was significantly lesser than that in the MS-10%-48 h group ( $*p < 0.05$ ). These data suggest that MS affected the morphology and proliferation of MSCs significantly.

**3.4. Mechanical Stretch Did Not Alter Expression of Surface Markers on MSCs.** Surface markers on MSCs served as an index parameters for the identification of MSCs [25]. To determine if surface marker expression changed when MSCs were preconditioned to mechanical stretch, we used flow cytometry to analyze major surface markers of MSCs for identification, such as CD90, CD29, and CD45 (Figure 4). The results showed no statistical change in the expression with high levels of CD90 and CD29 expressions on nearly 99% of cells in all treatment groups and low levels of CD45

expression on fewer than 5% of cells for all treatment groups. The results suggest that MS did not alter the expression of surface markers.

**3.5. Mechanical Stretch Affected the Production of Inflammation Mediators in MSCs.** Studies have shown that MS can induce biological function change [27]. To evaluate the effects of MS on the inflammatory function of MSCs, we examined the inflammatory mediators TNF- $\alpha$ , IL-6, and IL-10 presented in the MSC supernatants by enzyme-linked immunosorbent assay. The results showed that TNF- $\alpha$  and IL-6 increased statistically as time and magnitude of mechanical stretch increased (Figures 5(a) and 5(b);  $*p < 0.05$ ), but the MS-10%-24 h group did not produce significant differences when compared to the untreated MSC group. However, IL-10 did not significantly change in all groups (Figure 5(c)). These results showed that MS could statistically increase the TNF- $\alpha$  and IL-6 levels.

**3.6. MS-MSCs Decreased Paracellular Permeability of Pulmonary Microvascular Endothelium Barrier Injured by LPS.** Evaluation of paracellular permeability is a critical step



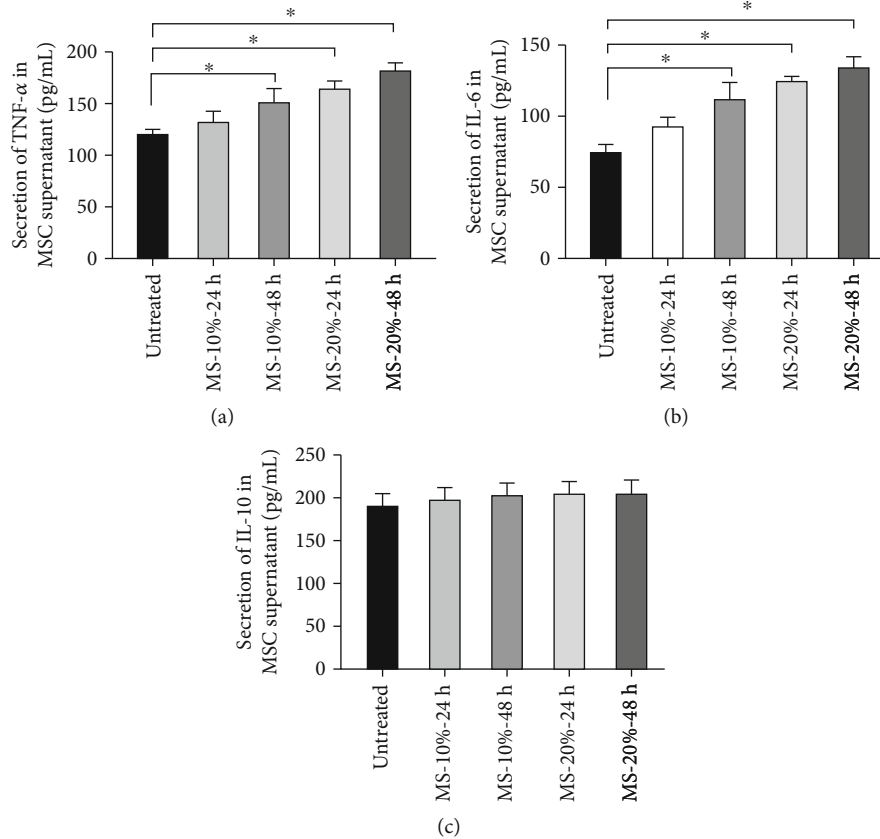


FIGURE 5: Effects of MS on inflammation mediators secreted by MSCs. ELISA was used to detect the concentrations of (a) TNF- $\alpha$ , (b) IL-6, and (c) IL-10 in the supernatant of the MSC groups ( $n = 3$ ;  $*p < 0.05$ ). ELISA: enzyme-linked immunosorbent assay; TNF- $\alpha$ : tumor necrosis factor- $\alpha$ ; IL-6: interleukin-6; IL-10: interleukin-10.

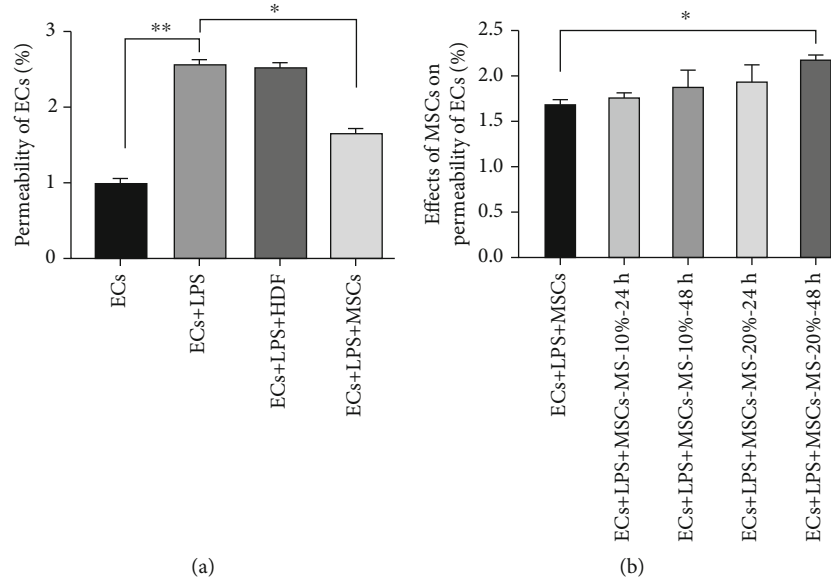
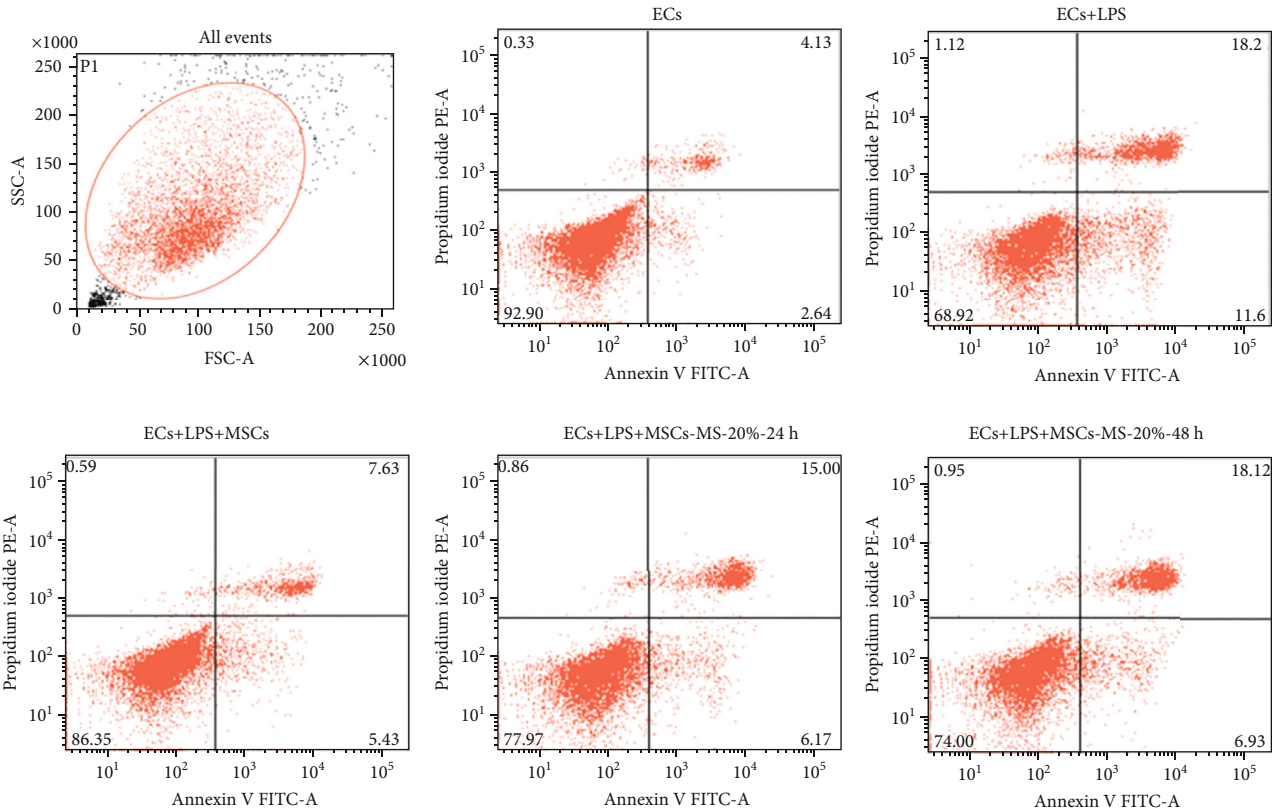
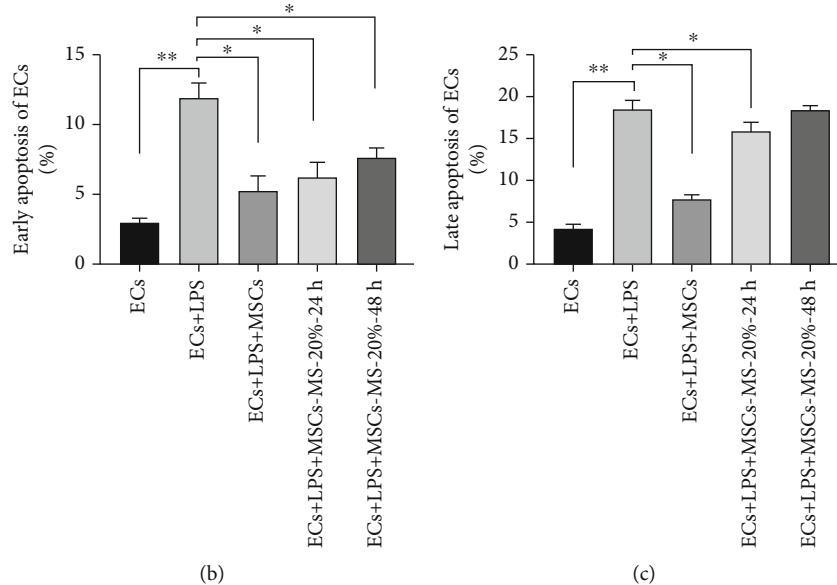


FIGURE 6: Effects of MS-MSCs on permeability of ECs treated with LPS. Permeability of ECs induced by LPS was detected using FITC-Dextran ( $n = 3$ ;  $*p < 0.05$ ,  $**p < 0.01$ ). HDF: human dermal fibroblasts; FITC: fluorescein isothiocyanate; ECs: endothelial cells; MS: mechanical stretch.



(a)



(b)

(c)

FIGURE 7: Effects of MS-MSCs on apoptosis of ECs. (a) Flow cytometric analysis of ECs was performed to assess apoptotic and necrotic cells. (b) Early apoptotic ECs stained only with annexin V were presented in the lower right quadrant. (c) Late apoptotic or necrotic ECs stained both with annexin V and PI were presented in the upper right quadrant ( $n = 3$ ;  $*p < 0.05$ ,  $**p < 0.01$ ). ECs: endothelial cells; PI: propidium iodide.

in assessing the integrity of the pulmonary microvascular endothelium barrier [28]. We introduced a transwell coculture system to evaluate the effects of MS-MSCs on the paracellular permeability of LPS-treated ECs. Treatment with LPS significantly increased the paracellular permeabil-

ity of the pulmonary microvascular endothelium barrier (Figure 6(a);  $**p < 0.01$ ). And MSCs significantly attenuated the increased paracellular permeability induced by LPS (Figure 6(a);  $*p < 0.05$ ), while HDF showed no effect on the increased permeability. These results suggested that

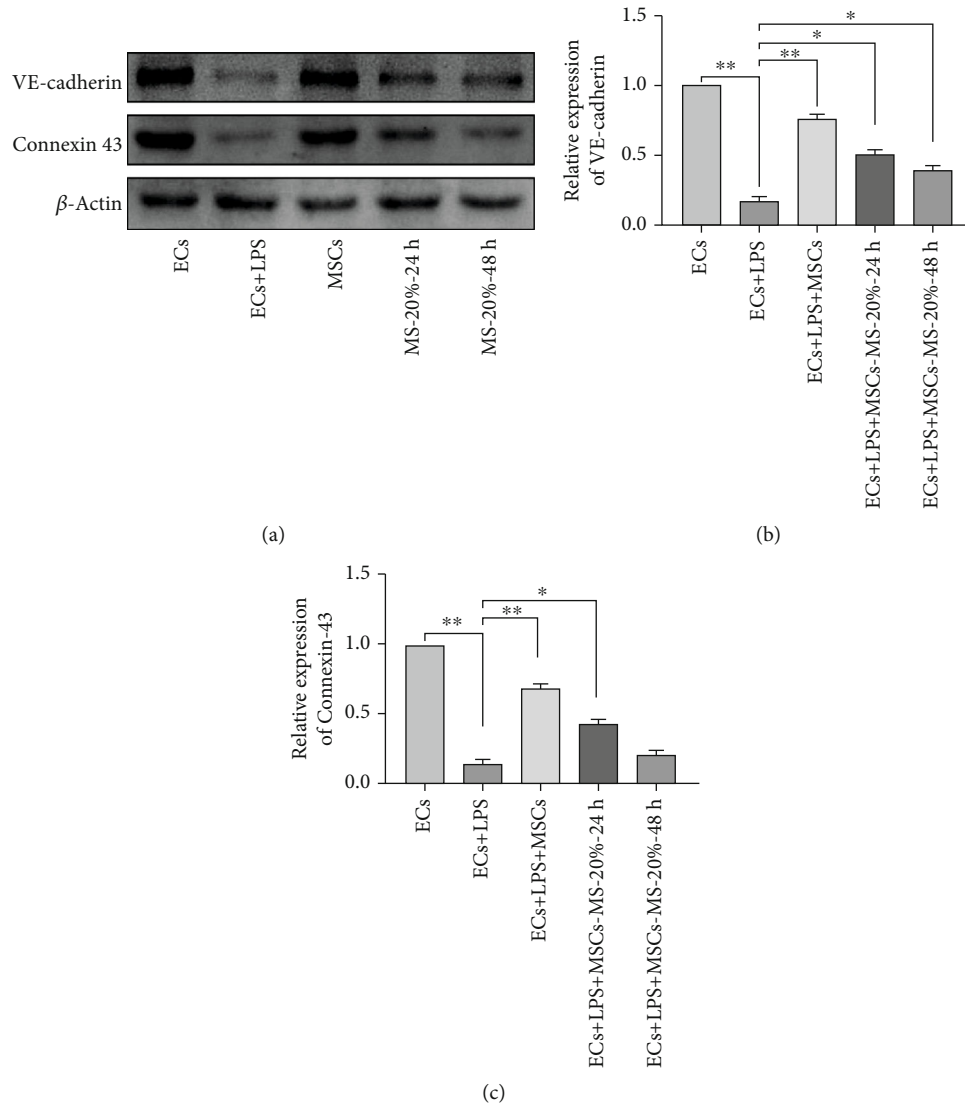


FIGURE 8: Effects of MS-MSCs on endothelial intercellular junction protein. Western blotting presented protein expression of VE-cadherin and Connexin-43 (a). Compared with the LPS-treated EC group, the MSC and MS-MSC groups increased VE-cadherin (b) and Connexin-43 (c) expressions ( $p < 0.01$ ). VE-cadherin: vascular endothelial cadherin.

MS-MSCs attenuated the increased permeability of LPS-treated ECs.

**3.7. MS-MSCs Attenuated Apoptosis of ECs Induced by LPS.** LPS is a useful agent to induce injury and apoptosis on pulmonary microvascular endothelial cells [29]. In this study, we applied the flow cytometry to evaluate the effect of MSCs on apoptosis of ECs treated with LPS (Figure 7(a)). LPS could significantly induce the apoptosis of ECs both in early and late states (Figures 7(b) and 7(c);  $**p < 0.01$ ), but MSCs decreased the apoptosis of LPS-treated ECs ( $*p < 0.05$ ). Furthermore, the MS-20%-24 h MSC group could significantly attenuate both early and late apoptosis of ECs ( $*p < 0.05$ ), similar to the untreated MSC group (Figure 7(b)). However, the MS-20%-48 h group significantly decreased early apoptosis ( $*p < 0.05$ ) but not late apoptosis of ECs, although it showed a trend towards attenuating apoptosis (Figure 7(c)).

**3.8. MS-MSCs Restored Intercellular Junction Proteins.** Intercellular junction proteins play an important role in maintaining the integrity of the pulmonary microvascular endothelium barrier. VE-cadherin [3] and Connexin-43 [30] present critical effects on regulating the permeability of the barrier. To investigate the effects of MS-MSCs on endothelium barrier integrity, we examined the expression of these two key proteins. Compared with the LPS-treated ECs, MSCs increased the expression of VE-cadherin and Connexin-43 (Figures 8(b) and 8(c);  $**p < 0.01$ ). We also applied immunofluorescent staining to detect the protein expression of ECs and observed the cells under confocal microscopy. The results showed that VE-cadherin located on the surface of ECs were destroyed after LPS treatment, thus leading to the loss of integrity of the pulmonary microvascular endothelium barrier (Figure 9). These data indicated that MS-MSCs restored the intercellular junction of LPS-treated ECs.

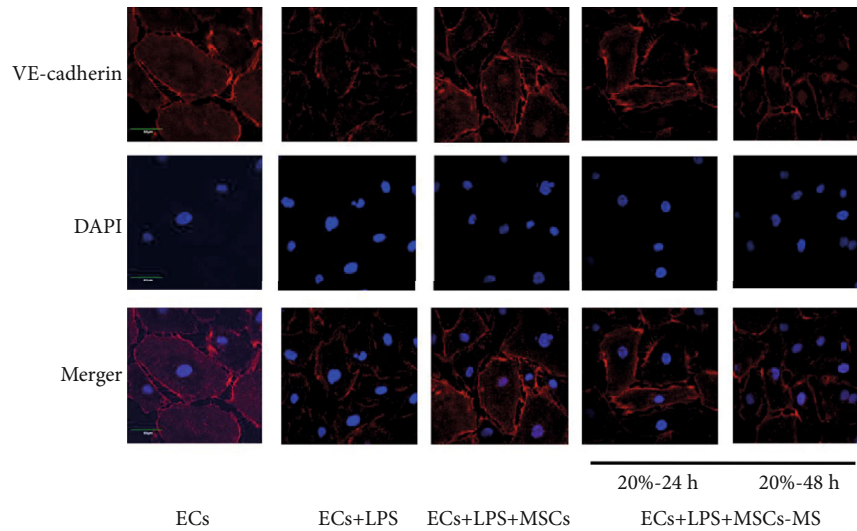


FIGURE 9: Effects of MS-MSCs on VE-cadherin. VE-cadherin was detected by immunofluorescent staining and observed by confocal microscopy. VE-cadherin: vascular endothelial cadherin; DAPI: 4',6-diamidino-2-phenylindole.

#### 4. Discussion

ARDS is the leading cause of mortality in ICU patients [31] and featured with acute diffuse lung injury, which results in severely injured lung compliance and increased pulmonary vascular permeability [3]. MSC is a promising method to restore endothelial function [32], but when engrafted on the alveolocapillary barrier, the efficacy of MSCs under mechanical stretch in the context of decreased lung compliance remains unproven. Our study tried to reveal the effect of mechanically stretched MSCs on restoring the injured alveolocapillary barrier. We applied a mechanical stretch system to simplify yet still mimic the mechanical microenvironments present within the lung in a simplified way. We demonstrated that mechanical stretch could impact MSC morphology and biological function in a time- and magnitude-dependent manner and that MS-MSCs could restore the increased permeability of endothelial cells induced by LPS.

The alveolocapillary barrier provides an essential function in regulating the diffusive exchange of molecules. Loss of barrier integrity could lead to excessive leakage of fluid and proteins from the vasculature to the alveoli, producing the pulmonary edema common in ARDS [33]. Sepsis plays a major role in extrapulmonary edema, and the endothelial barrier stands as the first line of defense in keeping LPS out of the vascular system [34]. Studies have demonstrated that endothelial injury is a more important consideration in extrapulmonary ARDS than pulmonary ARDS [35, 36]. As a major factor driving sepsis and lethal septic shock, LPS has been studied in *in vivo*, *in vitro*, and *ex vivo* settings [37, 38]. Hereby, we adopted LPS and a transwell coculture system to investigate the effects of MSCs on the permeability of the alveolocapillary barrier. We found that increased permeability by LPS was significantly decreased by MSCs as the cell density increased accordingly.

Manipulation of mesenchymal stem cell functions is important for tissue engineering and regenerative medicine. Heterogeneous mechanical properties of the alveolocapillary barrier in ARDS caused a complicated microenvironment for the engraftment of MSCs [36]. So, we used an apparatus to mimic and simplify the mechanical properties within the lung tissue in clinical field, as 10% mechanical stretch for physical stimulation and 20% for severe pathological status. Our previous research had applied this method and acquired positive therapeutic results of pulmonary fibrosis investigation [22]. In this study, we tried to discover evidences of mechanically stretched MSCs in restoring increased permeability of endothelial barrier induced by LPS. While MSCs injected via the bloodstream preferred to engraft on and merge into the injured sites of the pulmonary microvascular endothelial barrier [9]. Studies have proved that MSCs can coexist with endothelial cells and other kind of cells in the barrier for about 24 to 48 hours. [35, 39] Therefore, we investigated MSCs under these time durations of 10% and 20% mechanical stretch as used previously [22]. We demonstrated that mechanical stretch affects cell morphology and cell proliferation, suggesting that mechanical stretch is important for the maintenance of MSC functions.

The most attractive characteristics of MSCs are the stemness and self-renewal. These properties make them a promising therapeutic tool in many clinical field, such as the kidney [40], liver [41], and lung [42]. The stemness of MS-MSCs is analyzed by the expression of surface markers. When under the mechanical stretch modes in this study, whether MSCs could maintain their stemness is crucial for the LPS-treated EC therapy. The expression of CD90, CD29, and CD45 did not change with the intervention of different mechanical stretch patterns. All groups exhibit similar expression of the surface markers. The results indicate that, in 48 h with the maximum MS-20%, the MSCs could maintain the stemness.

Increased permeability resulted from the disruption of the pulmonary endothelial barrier [36]. EC apoptosis played



a vital role in EC barrier integrity [43]. We have been proved that MSCs without mechanical stretch could repair the injured EC barrier in a cell density-dependent manner. Nowadays, tissue engineering shows great impact on MSC therapy and achieved great advances [44]. Mechanical stretch, a method to mimic the mechanical properties of the lung tissue, played an important role in the microenvironment where MSCs engrafted. Novel strategies to isolate the mechanical factor could shed some light on MSC application. Our results indicated that LPS can induce both early and late apoptosis, and mechanically stretched MSCs decreased EC apoptosis but decreased slightly as the time and magnitude of MS increased. Thus, mechanical stretch may account for the restoring effect on the injured EC barrier through EC apoptosis.

Constant remodeling of intercellular junctions to regulate the transendothelial permeability is essential in maintaining endothelium barrier functions. Treatment with LPS can also alter the apoptotic status of endothelial barrier cells and badly damage the paracellular architecture of causing the endothelial barrier to function abnormally and producing pulmonary edema [43]. Of the intercellular junction proteins, VE-cadherin and Connexin-43 are vital for the barrier integrity and could act as index parameters to evaluate the disruption of barrier [45]. The results presented that endothelial barrier integrity was severely damaged by LPS, but MS-MSCs increased VE-cadherin and Connexin-43 expressions, which favored the integrity of the endothelial barrier. Therefore, MS-MSCs restored the increased permeability of the endothelial cell partially by remodeling of VE-cadherin and Connexin-43.

The following limitations to this research should be noted. The mechanical stretch system that we used in this study applies a vacuum to generate mechanical stretch, but as the culture medium is flowing between the MSCs, other categories of mechanical stimulations, including shear force and pressure force, are not absent and may influence cells in some level. These forces could also produce a biological response and may thus affect MSC function. However, by their nature, these three forces are often mixed together and are difficult to study separately. This could be addressed in future studies.

## 5. Conclusions

In conclusion, our experiments reveal that MS-MSCs statistically improved the increased permeability of the EC barrier induced by LPS, through decreasing the apoptosis of ECs and increasing the remodeling of intercellular junctions. These findings provide additional *in vitro* evidences for the therapeutic potential of MSCs and may be useful for the clinical utilization of MSCs.

## Abbreviations

ECs:	Endothelial cells
ARDS:	Acute respiratory distress syndrome
MSCs:	Mesenchymal stem cells
MS:	Mechanical stretch

LPS:	Lipopolysaccharide
ELISA:	Enzyme-linked immunosorbent assay
FITC:	Fluorescein isothiocyanate
TNF- $\alpha$ :	Tumor necrosis factor-alpha
IL:	Interleukin
VE-cadherin:	Vascular endothelial-cadherin.

## Data Availability

The data used to support the findings of this study are included within the article.

## Conflicts of Interest

The authors declare that they have no competing interests.

## Acknowledgments

The authors would like to thank Dr. Ruoyu Hu for his valuable support. The study was supported by the National Natural Science Foundation of China (Grant/Award Numbers: 81300043, 81571847), Jiangsu Province's Medical Key Discipline (laboratory) (Grant/Award Number: ZDXKA2016025), and Key Laboratory of Environmental Medicine Engineering (Grant/Award Number: 2020EME001).

## References




- [1] N. Chen, M. Zhou, X. Dong et al., "Epidemiological and clinical characteristics of 99 cases of 2019 novel coronavirus pneumonia in Wuhan, China: a descriptive study," *The Lancet*, vol. 395, no. 10223, pp. 507–513, 2020.
- [2] M. J. Cummings, M. R. Baldwin, D. Abrams et al., "Epidemiology, clinical course, and outcomes of critically ill adults with COVID-19 in New York City: a prospective cohort study," *The Lancet*, vol. 395, no. 10239, pp. 1763–1770, 2020.
- [3] M. Y. Radeva and J. Waschke, "Mind the gap: mechanisms regulating the endothelial barrier," *Acta Physiologica*, vol. 222, no. 1, 2018.
- [4] J. G. Laffey and M. A. Matthay, "Fifty years of research in ARDS. Cell-based therapy for acute respiratory distress syndrome. Biology and potential therapeutic value," *American Journal of Respiratory and Critical Care Medicine*, vol. 196, no. 3, pp. 266–273, 2017.
- [5] S. Hu, J. Li, X. Xu et al., "The hepatocyte growth factor-expressing character is required for mesenchymal stem cells to protect the lung injured by lipopolysaccharide *in vivo*," *Stem Cell Research & Therapy*, vol. 7, no. 1, p. 66, 2016.
- [6] S.-S. Meng, F. M. Guo, X. W. Zhang et al., "mTOR/STAT-3 pathway mediates mesenchymal stem cell-secreted hepatocyte growth factor protective effects against lipopolysaccharide-induced vascular endothelial barrier dysfunction and apoptosis," *Journal of Cellular Biochemistry*, vol. 120, no. 3, pp. 3637–3650, 2018.
- [7] G. Zheng, L. Huang, H. Tong et al., "Treatment of acute respiratory distress syndrome with allogeneic adipose-derived mesenchymal stem cells: a randomized, placebo-controlled pilot study," *Respiratory Research*, vol. 15, no. 1, p. 39, 2014.
- [8] M. A. Matthay, C. S. Calfee, H. Zhuo et al., "Treatment with allogeneic mesenchymal stromal cells for moderate to severe acute respiratory distress syndrome (START study): a

- randomised phase 2a safety trial,” *The Lancet Respiratory Medicine*, vol. 7, no. 2, pp. 154–162, 2019.
- [9] A. Sohni and C. M. Verfaillie, “Mesenchymal stem cells migration homing and tracking,” *Stem Cells International*, vol. 2013, Article ID 130763, 8 pages, 2013.
- [10] C. Steingen, F. Brenig, L. Baumgartner, J. Schmidt, A. Schmidt, and W. Bloch, “Characterization of key mechanisms in transmigration and invasion of mesenchymal stem cells,” *Journal of Molecular and Cellular Cardiology*, vol. 44, no. 6, pp. 1072–1084, 2008.
- [11] J. Grune, A. Tabuchi, and W. M. Kuebler, “Alveolar dynamics during mechanical ventilation in the healthy and injured lung,” *Intensive Care Medicine Experimental*, vol. 7, Supplement 1, p. 34, 2019.
- [12] L. Knudsen and M. Ochs, “The micromechanics of lung alveoli: structure and function of surfactant and tissue components,” *Histochemistry and Cell Biology*, vol. 150, no. 6, pp. 661–676, 2018.
- [13] R. Goetzke, A. Sechi, L. De Laporte, S. Neuss, and W. Wagner, “Why the impact of mechanical stimuli on stem cells remains a challenge,” *Cellular and Molecular Life Sciences*, vol. 75, no. 18, pp. 3297–3312, 2018.
- [14] A. L. Mora Carpio and J. I. Mora, *Ventilator Management*, StatPearls, Treasure Island, FL, USA, 2020.
- [15] The Acute Respiratory Distress Syndrome Network, “Ventilation with lower tidal volumes as compared with traditional tidal volumes for acute lung injury and the acute respiratory distress syndrome,” *The New England Journal of Medicine*, vol. 342, no. 18, pp. 1301–1308, 2000.
- [16] E. Spinelli, T. Mauri, J. R. Beitler, A. Pesenti, and D. Brodie, “Respiratory drive in the acute respiratory distress syndrome: pathophysiology, monitoring, and therapeutic interventions,” *Intensive Care Medicine*, vol. 46, no. 4, pp. 606–618, 2020.
- [17] W. Alhazzani, M. H. Møller, Y. M. Arabi et al., “Surviving sepsis campaign: guidelines on the management of critically ill adults with Coronavirus Disease 2019 (COVID-19),” *Intensive Care Medicine*, vol. 46, no. 5, pp. 854–887, 2020.
- [18] T. M. Maul, D. W. Chew, A. Nieponice, and D. A. Vorp, “Mechanical stimuli differentially control stem cell behavior: morphology, proliferation, and differentiation,” *Biomechanics and Modeling in Mechanobiology*, vol. 10, no. 6, pp. 939–953, 2011.
- [19] C. W. Li, Y. T. Lau, K. L. Lam, and B. P. Chan, “Mechanically induced formation and maturation of 3D-matrix adhesions (3DMAs) in human mesenchymal stem cells,” *Biomaterials*, vol. 258, article 120292, 2020.
- [20] E. D. O’Cearbhaill, M. A. Puchard, M. Murphy, F. P. Barry, P. E. McHugh, and V. Barron, “Response of mesenchymal stem cells to the biomechanical environment of the endothelium on a flexible tubular silicone substrate,” *Biomaterials*, vol. 29, no. 11, pp. 1610–1619, 2008.
- [21] A. Nieponice, T. M. Maul, J. M. Cumer, L. Soletti, and D. A. Vorp, “Mechanical stimulation induces morphological and phenotypic changes in bone marrow-derived progenitor cells within a three-dimensional fibrin matrix,” *Journal of Biomedical Materials Research Part A*, vol. 81A, no. 3, pp. 523–530, 2007.
- [22] R. Zhang, Y. Pan, V. Fanelli et al., “Mechanical stress and the induction of lung fibrosis via the midkine signaling pathway,” *American Journal of Respiratory and Critical Care Medicine*, vol. 192, no. 3, pp. 315–323, 2015.
- [23] S. M. Armstrong, V. Khajoe, C. Wang et al., “Co-regulation of transcellular and paracellular leak across microvascular endothelium by dynamin and Rac,” *The American Journal of Pathology*, vol. 180, no. 3, pp. 1308–1323, 2012.
- [24] F. Liu, J. Y. Lee, H. Wei et al., “FIP200 is required for the cell-autonomous maintenance of fetal hematopoietic stem cells,” *Blood*, vol. 116, no. 23, pp. 4806–4814, 2010.
- [25] M. Dominici, K. le Blanc, I. Mueller et al., “Minimal criteria for defining multipotent mesenchymal stromal cells. The International Society for Cellular Therapy position statement,” *Cytotherapy*, vol. 8, no. 4, pp. 315–317, 2006.
- [26] Q. H. Chen, A. R. Liu, H. B. Qiu, and Y. Yang, “Interaction between mesenchymal stem cells and endothelial cells restores endothelial permeability via paracrine hepatocyte growth factor in vitro,” *Stem Cell Research & Therapy*, vol. 6, no. 1, p. 44, 2015.
- [27] A. Saparov, V. Ogay, T. Nurgozhin, M. Jumabay, and W. C. W. Chen, “Preconditioning of human mesenchymal stem cells to enhance their regulation of the immune response,” *Stem Cells International*, vol. 2016, Article ID 3924858, 10 pages, 2016.
- [28] S. Pati, M. H. Gerber, T. D. Menge et al., “Bone marrow derived mesenchymal stem cells inhibit inflammation and preserve vascular endothelial integrity in the lungs after hemorrhagic shock,” *PLoS One*, vol. 6, no. 9, article e25171, 2011.
- [29] F. Meng, A. Meliton, N. Moldobaeva et al., “Asef mediates HGF protective effects against LPS-induced lung injury and endothelial barrier dysfunction,” *American Journal of Physiology-Lung Cellular and Molecular Physiology*, vol. 308, no. 5, pp. L452–L463, 2015.
- [30] K. Parthasarathi, “Endothelial connexin43 mediates acid-induced increases in pulmonary microvascular permeability,” *American Journal of Physiology-Lung Cellular and Molecular Physiology*, vol. 303, no. 1, pp. L33–L42, 2012.
- [31] G. Bellani, J. G. Laffey, T. Pham et al., “Epidemiology, patterns of care, and mortality for patients with acute respiratory distress syndrome in intensive care units in 50 countries,” *JAMA*, vol. 315, no. 8, pp. 788–800, 2016.
- [32] J. Walter, L. B. Ware, and M. A. Matthay, “Mesenchymal stem cells: mechanisms of potential therapeutic benefit in ARDS and sepsis,” *The Lancet Respiratory Medicine*, vol. 2, no. 12, pp. 1016–1026, 2014.
- [33] Y. Zayed and R. Askari, *Respiratory Distress Syndrome*, StatPearls, Treasure Island, FL, USA, 2019.
- [34] D. Brooks, L. C. Barr, S. Wiscombe, D. F. McAuley, A. J. Simpson, and A. J. Rostron, “Human lipopolysaccharide models provide mechanistic and therapeutic insights into systemic and pulmonary inflammation,” *European Respiratory Journal*, vol. 56, no. 1, article 1901298, 2020.
- [35] M. A. Matthay, P. Anversa, J. Bhattacharya et al., “Cell therapy for lung diseases. Report from an NIH-NHLBI workshop, November 13-14, 2012,” *American Journal of Respiratory and Critical Care Medicine*, vol. 188, no. 3, pp. 370–375, 2013.
- [36] M. Jozwiak, J. L. Teboul, and X. Monnet, “Extravascular lung water in critical care: recent advances and clinical applications,” *Annals of Intensive Care*, vol. 5, no. 1, p. 38, 2015.
- [37] D. C. Morrison and J. L. Ryan, “mechanisms,” *Annual Review of Medicine*, vol. 38, no. 1, pp. 417–432, 1987.
- [38] Z. Yang, D. Sun, Z. Yan et al., “Differential role for p120-catenin in regulation of TLR4 signaling in macrophages,” *Journal of Immunology*, vol. 193, no. 4, pp. 1931–1941, 2014.

- [39] A. L. Ryan, L. Ikonou, S. Atarod et al., “Stem cells, cell therapies, and bioengineering in lung biology and diseases 2017. An official American Thoracic Society workshop report,” *American Journal of Respiratory Cell and Molecular Biology*, vol. 61, no. 4, pp. 429–439, 2019.
- [40] A. J. Peired, A. Sisti, and P. Romagnani, “Mesenchymal stem cell-based therapy for kidney disease: a review of clinical evidence,” *Stem Cells International*, vol. 2016, Article ID 4798639, 22 pages, 2016.
- [41] C. Hu, L. Zhao, J. Duan, and L. Li, “Strategies to improve the efficiency of mesenchymal stem cell transplantation for reversal of liver fibrosis,” *Journal of Cellular and Molecular Medicine*, vol. 23, no. 3, pp. 1657–1670, 2019.
- [42] M. A. Matthay, “Treatment of acute lung injury: clinical and experimental studies,” *Proceedings of the American Thoracic Society*, vol. 5, no. 3, pp. 297–299, 2008.
- [43] E. Fan, D. Brodie, and A. S. Slutsky, “Acute respiratory distress syndrome: advances in diagnosis and treatment,” *JAMA*, vol. 319, no. 7, pp. 698–710, 2018.
- [44] S. W. Lane, D. A. Williams, and F. M. Watt, “Modulating the stem cell niche for tissue regeneration,” *Nature Biotechnology*, vol. 32, no. 8, pp. 795–803, 2014.
- [45] D. Mehta and A. B. Malik, “Signaling mechanisms regulating endothelial permeability,” *Physiological Reviews*, vol. 86, no. 1, pp. 279–367, 2006.

## Research Article

# Isolation and Characterization of Multipotent Canine Urine-Derived Stem Cells

Yan Xu <sup>1,2,3,4</sup>, Tao Zhang,<sup>1,2,3,4</sup> Yang Chen,<sup>1,2,3,4</sup> Qiang Shi,<sup>1,2,3,4</sup> Muzhi Li,<sup>1,2,3,4</sup> Tian Qin,<sup>1,2,3,5</sup> Jianzhong Hu,<sup>1,2,3,5</sup> Hongbin Lu <sup>1,2,3,4</sup>, Jun Liu,<sup>6</sup> and Can Chen <sup>1,2,3,7</sup>

<sup>1</sup>Key Laboratory of Organ Injury, Aging and Regenerative Medicine of Hunan Province, Changsha, China 410008

<sup>2</sup>Hunan Engineering Research Center of Sports and Health, Changsha, China 410008

<sup>3</sup>Xiangya Hospital-International Chinese Musculoskeletal Research Society Sports Medicine Research Centre, Changsha, China 410008

<sup>4</sup>Department of Sports Medicine, Xiangya Hospital, Central South University, Changsha, China 410008

<sup>5</sup>Department of Spine Surgery, Xiangya Hospital, Central South University, Changsha, Hunan, China 410008

<sup>6</sup>Department of Limbs (Foot and Hand) Microsurgery, Affiliated Chenzhou No.1 People's Hospital, Southern Medical University, Chenzhou, China 423000

<sup>7</sup>Department of Orthopedics, Xiangya Hospital, Central South University, Changsha, China 410008

Correspondence should be addressed to Hongbin Lu; hongbinlu@hotmail.com and Can Chen; chencanwow@foxmail.com

Yan Xu and Tao Zhang contributed equally to this work.

Received 15 June 2020; Revised 20 August 2020; Accepted 28 August 2020; Published 30 September 2020

Academic Editor: Sangho Roh

Copyright © 2020 Yan Xu et al. This is an open access article distributed under the Creative Commons Attribution License, which permits unrestricted use, distribution, and reproduction in any medium, provided the original work is properly cited.

Current cell-based therapies on musculoskeletal tissue regeneration were mostly determined in rodent models. However, a direct translation of those promising cell-based therapies to humans exists a significant hurdle. For solving this problem, canine has been developed as a new large animal model to bridge the gap from rodents to humans. In this study, we reported the isolation and characterization of urine-derived stem cells (USCs) from mature healthy beagle dogs. The isolated cells showed fibroblast-like morphology and had good clonogenicity and proliferation. Meanwhile, these cells positively expressed multiple markers of MSCs (CD29, CD44, CD90, and CD73), but negatively expressed for hematopoietic antigens (CD11b, CD34, and CD45). Additionally, after induction culturing, the isolated cells can be differentiated into osteogenic, adipogenic, chondrogenic, and tenogenic lineages. The successful isolation and verification of USCs from canine were useful for studying cell-based therapies and developing new treatments for musculoskeletal injuries using the preclinical canine model.

## 1. Introduction

Stem cells and tissue-derived stromal cells stimulate the repair of degenerated and injured tissues, motivating a growing number of cell-based therapies in the musculoskeletal field [1, 2]. Mesenchymal stem cells (MSCs) showed a good self-renew ability and were capable of differentiating into the progeny of several lineages, including osteoblasts, chondrocytes, adipocytes, fibroblasts, tenocytes, and myo-

blasts [3–7]. Thus, it was the most commonly used cell source in cell-based therapies. In recent years, preclinical and clinical studies have determined that the MSCs isolated from the bone marrow, peripheral blood, adipose tissue, synovium, and periosteum [3, 8, 9] have the therapeutic potential for the regeneration of injured musculoskeletal tissues, such as the bone, cartilage, tendon, enthesis, and intervertebral disc [10–14]. However, these types of MSCs are restricted by the invasive and painful harvesting procedures, which



may cause donor site morbidity and limit their use for autogenous approaches. Therefore, finding a stem cell harvested without invasive and painful procedures would help us escape from the dilemma of the current cell-based therapies.

Urine-derived stem cells (USCs) isolated from urine have received significant attention and been studied as a promising candidate for the development of new cell-based therapies owing to their multilineage potential (differentiation into osteocytes, chondrocytes, adipocytes, neurocyte, myocytes, and endothelial cells) and sufficient proliferation capacities [15, 16]. The advantages of USCs include noninvasive and low-expense harvesting as well as being considered ethical. Additionally, USCs have been isolated from autologous urine which do not induce immune responses or rejection [15, 16]. Therefore, USCs are considered as an attractive alternative source for cell-based therapies to enhance musculoskeletal tissue regeneration.

Currently, most of the cell-based therapies on musculoskeletal tissue regeneration were determined in rodent models. A direct translation of those promising cell-based therapies to humans exists a significant hurdle. For solving this problem, a number of large animal species have been used by researchers to bridge the gap from rodents to humans [17–21]. Among these large animal species, canine represents a compelling model for translational studies. Compared with the rodents, dogs are large, long-lived, genetically diverse, and share many physiological and biochemical similarities with humans. Until now, canine models have been successfully used to develop adult bone marrow transplantation, gene therapy, and allograft rejection protocols for use in humans [22–24]. In addition, dogs have good compliance and response to learned behaviors, such as treadmill exercise; it was used to evaluate new therapies for cardiovascular and orthopedic diseases [25, 26]. Based on these benefits, the preclinical canine models in osteoarthritis, anterior cruciate ligament reconstruction, rotator cuff repair, meniscal injury, and nonunion fracture have been developed and described in recent articles [27–33], which can be used to bridge the gap from rodents to humans. Although USCs have been successfully isolated in humans, no report has described the protocol of isolating USCs from canine (cUSCs). Therefore, it is imperative to isolate cUSCs to facilitate future studies on regenerative strategies for musculoskeletal tissue injuries.

In this study, we described the isolation and identification of cUSCs for the first time, and its morphology at different passages, surface markers, proliferation capacity, clonogenicity, and multilineage differentiation potential were investigated *in vitro*. The protocol developed for isolating cUSCs is an essential step to extrapolate USC-based therapy from a preclinical canine model for clinical management of tissue injuries.

## 2. Materials and Methods

**2.1. Ethics Statement.** The local animal ethics committee approved the experimental protocol for the use of beagle dogs in this study.

**2.2. Canine USC Isolation and Expansion.** The procedures of cUSC isolation and culture are depicted in Figure 1. Briefly, three healthy dogs were anesthetized with 3% pentobarbital sodium (0.15 mL/kg), and about 20 mL of urine sample was obtained from each dog with a sterile catheter. After centrifugation at  $400 \times g$  for 10 min, the supernatant was discarded, and about 1 mL of the remaining liquid in the tube was gently resuspended with 10 mL PBS containing 1% antibiotic-antimycotic (Gibco, USA). And then, the mixture was centrifuged at  $200 \times g$  for 10 min, and the supernatant was discarded. Three milliliters of primary medium (Table 1) was added into the remaining liquid, and the cell pellet was gently resuspended. The cell supernatant was averagely transferred into two wells of a 12-well plate. After the first 48 h, each well was added with 1 mL of primary medium. At the second 48 h, 1 mL of primary medium was replaced with 1 mL of fresh proliferation medium (Table 2). The whole medium was changed with a proliferation medium every 3 days. The cells were passaged when reaching 80–90% confluence. Passage 3 cells were used for further experiments.

**2.3. Colony-Forming Unit (CFU) Assay.** The CFU-F assay was performed to evaluate the clonogenicity of the isolated canine-derived cells. Briefly, canine USCs were plated on a 6-well plate in triplicate at 20 cells per well. After 10 days of cultivation, the cells were stained with 1% crystal violet (Solarbio, CHN), and the stained colonies bigger than 2 mm were counted. The CFU-F assay was performed independently in three dogs.

**2.4. Cell Proliferation.** The proliferation of isolated cells was evaluated at time points of 1, 3, 5, 7, and 9 days using the Cell Counting Kit-8 (CCK-8) (7seabio, China). Briefly, canine USCs were plated in a 96-well plate at  $2 \times 10^3$  cells per well and incubated at  $37^\circ\text{C}$  with 5%  $\text{CO}_2$ . At the desired time point, the cells in each well were incubated with 10  $\mu\text{L}$  of CCK-8 reagent and 100  $\mu\text{L}$  serum-free medium. After incubating the plate at  $37^\circ\text{C}$  with 5%  $\text{CO}_2$  for 2 h, the absorbance at 450 nm was recorded using a microplate reader (Varioskan LUX, Thermo, USA). Each experiment was performed in four replicates. The cell proliferation assay was performed independently in the three dogs.

**2.5. Surface Markers of Isolated Cells.** The surface markers of isolated cells were analyzed by flow cytometry analysis. Briefly, the isolated cells ( $1 \times 10^6$  cells, passage 3) from the three dogs were, respectively, suspended in 100  $\mu\text{L}$  phosphate-buffered saline (PBS) containing 10  $\mu\text{g}/\text{mL}$  antibodies for PE-conjugated CD29 (303003, BioLegend, USA), PE-conjugated CD44 (103024, BioLegend, USA), PE-conjugated CD90 (561970, BD Biosciences, USA), PE-conjugated CD105 (bs-0579R-PE, Bioss, CHN), FITC-conjugated CD73 (bs-23233R-FITC, Bioss, CHN), PE-conjugated CD34 (559369, BD Biosciences, USA), and FITC-conjugated CD45 (11-5450-42, eBioscience, USA). After incubation for 30 min at  $4^\circ\text{C}$ , the cells were washed with PBS and then resuspended in 500  $\mu\text{L}$  of PBS for analysis. As for CD11b, the isolated cells ( $1 \times 10^6$  cells,

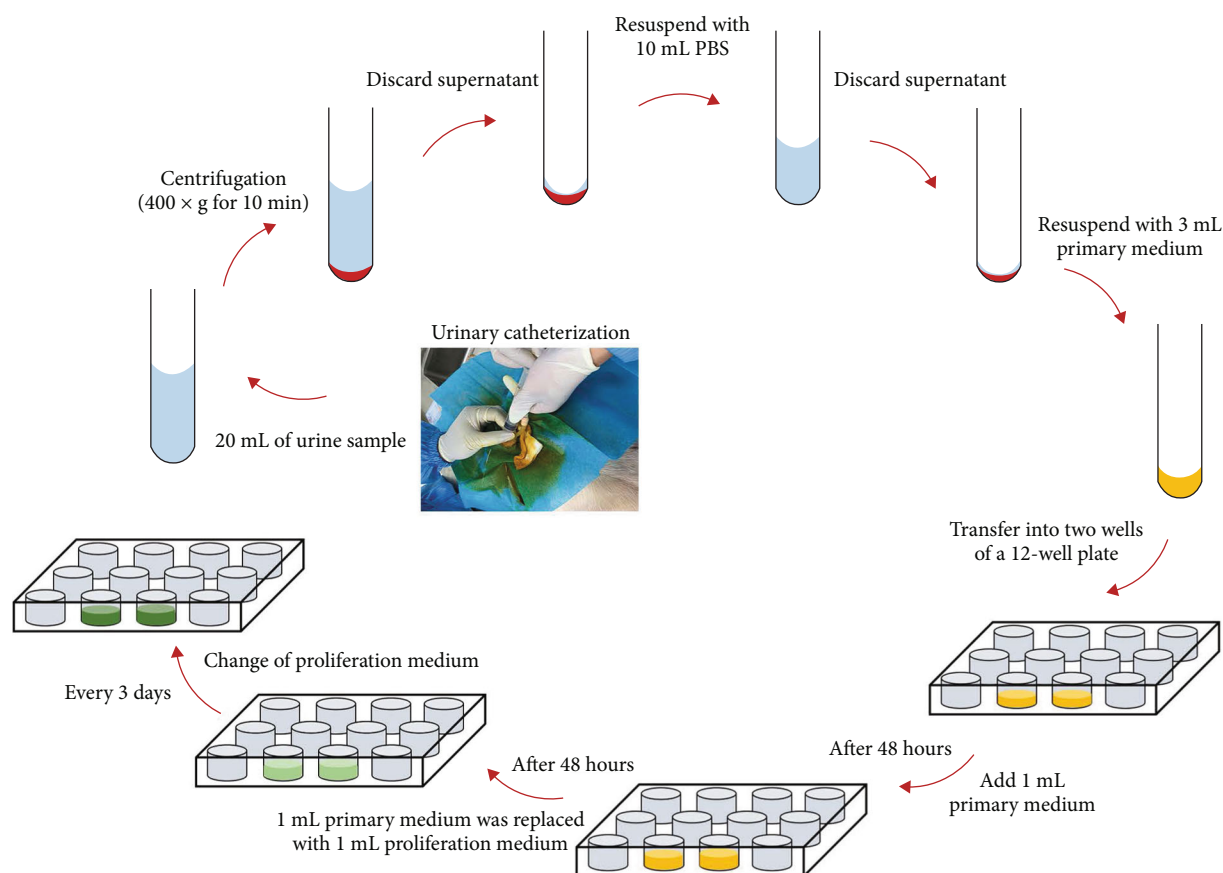


FIGURE 1: Schematic diagram showing the procedure of canine USC isolation and culture.

TABLE 1: Reagents and formula of the primary medium for canine USCs.

Reagents	Formula (mL)
REGM SingleQuot kit (Lonza, USA)	2.6 mL
DMEM/F-12 (Gibco, USA)	86.4 mL
Fetal bovine serum (Gibco, USA)	10.0 mL
Antibiotic-antimycotic (Gibco, USA)	1.0 mL

TABLE 2: Reagents and formula of proliferation medium for canine USCs.

Reagents	Formula (mL)
DMEM/F-12 (Gibco, USA)	43.5 mL
RE basal medium (Lonza, USA)	42.9 mL
REGM SingleQuot kit (Lonza, USA)	600.0 $\mu$ L
Fetal bovine serum (Gibco, USA)	10.0 mL
Antibiotic-antimycotic (Gibco, USA)	1.0 mL
GlutaMAX (Gibco, USA)	1.0 mL
MEM non-essential amino acids (Gibco, USA)	1.0 mL
bFGF (Peprotech, USA)	500 ng
PDGF-BB (Peprotech, USA)	500 ng
EGF (Peprotech, USA)	500 ng

passage 3) were suspended in 100  $\mu$ L phosphate-buffered saline (PBS) containing 10  $\mu$ g/mL CD11b (MA5-16604, eBioscience, USA). After incubation for 30 min at 4°C, the cells were washed with PBS and then labeled with goat anti-rabbit IgG (H+L) cross-adsorbed secondary antibody, FITC (F-2765, Invitrogen), at a dilution of 1:500 for 1 h at room temperature. Cell fluorescence was evaluated by flow cytometry using a DXP Athena™ flow cytometry system (Cytex) and analyzed with FlowJo 10 software (Tree Star, USA).

**2.6. Osteogenic Differentiation.** The isolated cells were cultured in complete medium at 5000 cells/cm<sup>2</sup> in 6-well plates. When the cultured cells reached 80%-90% confluence, three wells of cells were cultured with basal complete medium (as the control group), and the other three wells of cells were cultured with osteogenic differentiation medium (MUBMD-90021, Cyagen, CHN) (as the osteogenic group). The medium was changed every 3 days. After 7-day culture, quantitative real-time polymerase chain reaction analysis (qRT-PCR) was performed for evaluating the expression of osteogenic genes (Runx2, Spp1, Bglap) in the cells. The primer sequences were listed in Table 3. Meanwhile, Runx2 expression was evaluated by immunofluorescence assay using the anti-Runx2 antibody (ab76956, Abcam, USA). Additionally, Alizarin Red was used to stain the calcium nodules for assessing osteogenic differentiation of isolated cells

TABLE 3: Primer sequences used for qRT-PCR analysis.

Markers	Gene	Primer sequence (5'-3')
Osteogenic genes	Runx2	Forward CAGACCAGCAGCACTCCATA
		Reverse CAGCGTCAACACCATCATT
	Bglap	Forward CTGAATCCCACAAAGGTGGT
		Reverse CTCGTCACAGTTGGGGTTGA
	Spp1	Forward TAGCCAGGACTCCGTTGACT
		Reverse ACACTATCACCTCGGCCATC
Chondrogenic genes	Sox9	Forward GCTCGCAGTACGACTACACTGAC
		Reverse GTTCATGTAGGTGAAGGTGGAG
	Col2a1	Forward GAAACTCTGCCACCCTGAATG
		Reverse GCTCCACCAGTTCTTCTTGG
	Acan	Forward ATCAACAGTGCTTACCAAGACA
		Reverse ATAACCTCACAGCGATAGATCC
Adipogenic genes	PPAR $\gamma$	Forward primer TCACAGAGTACGCCAAAAGT
		Reverse primer ACTCCCTTGTCATGAATCCT
	FABP4	Forward ATCAGTGTAACGGGGATGTG
		Reverse GACTTTTCTGTCATCCGAGTA
	LPL	Forward ACACATTACAAGAGGGTCAC
		Reverse CTCTGCAATCACACGGATG
Tenogenic genes	Tnmd	Forward GATCCCATGCTGGATGAG
		Reverse TACAAGGCATGATGACACG
	Scx	Forward AAGCTCTCCAAGATCCGAGACACTG
		Reverse AAGAAGGGCCCAGAGTGGC
	Mkx	Forward AGACATGTCATGGCCACAAA
		Reverse TGATGATGAGGGAGACACCA
Housekeeping	GAPDH	Forward CCATCTTCCAGGAGCGAGAT Reverse TTCTCCATGGTGGTGAAGAC

after a 21-day culture. To conduct Alizarin Red assay, the cells were washed twice with PBS, followed by 10 min fixation in 70% ethanol and incubated in 0.5% Alizarin Red solution for 30 min, followed by PBS washing to remove the residual dye. The images of stained cells were obtained using a fluorescence microscope and a light microscope, respectively.

**2.7. Adipogenic Differentiation.** The isolated cells were cultured in complete medium at 5000 cells/cm<sup>2</sup> within 6-well plates. When the cultured cells reached 95-100% confluence, three wells of cells were cultured with basal complete medium (as the control group), and the other three wells of cells were cultured with adipogenic differentiation medium (MUBMD-90031, Cyagen, CHN) (as the adipogenic group). The medium was changed every 3 days. After 7-day culture, qRT-PCR was performed for evaluating the expression of adipogenic genes (PPAR $\gamma$ , FABP4, LPL) in the cells. Meanwhile, the PPAR $\gamma$  expression was evaluated by immunofluorescence assay using an anti-PPAR $\gamma$  antibody (ab45036, Abcam, USA). The primer sequences were also listed in Table 3. Additionally, Oil red O was used to stain the neutral lipid vacuoles within cells for assessing the adipogenic differentiation of isolated cells after a 21-day culture. The steps for Oil red O staining assay are described below: the cells were

washed twice with PBS and then fixed with 70% ethanol for 20 s. After that, they were incubated with filtered 0.3% Oil red O solution for 15 min, followed by thorough washing with PBS. The images of stained cells were viewed using a light microscope.

**2.8. Chondrogenic Differentiation.** The isolated cells were cultured in complete medium at 5000 cells/cm<sup>2</sup> within 6-well plates. When the cultured cells reached 80%-90% confluence, three wells of cells were cultured with a basal complete medium (as the control group), and the other three wells of cells were cultured with a chondrogenic differentiation medium (MUBMD-90041, Cyagen, CHN) (as the chondrogenic group). The medium was changed every 3 days. After 7-day culture, qRT-PCR was performed for evaluating the expression of chondrogenic genes (Sox9, Acan, Col2a1) in the cells. The primer sequences are listed in Table 3. Meanwhile, Sox9 expression was evaluated by immunofluorescence assay using the anti-Sox9 antibody (PA5-23383, Invitrogen, USA). Additionally, Alcian blue was used to stain the deposition of proteoglycan around the cells for assessing the chondrogenic differentiation of isolated cells after a 21-day culture. The Alcian blue staining assay was performed by the following steps: the cells were washed twice with PBS

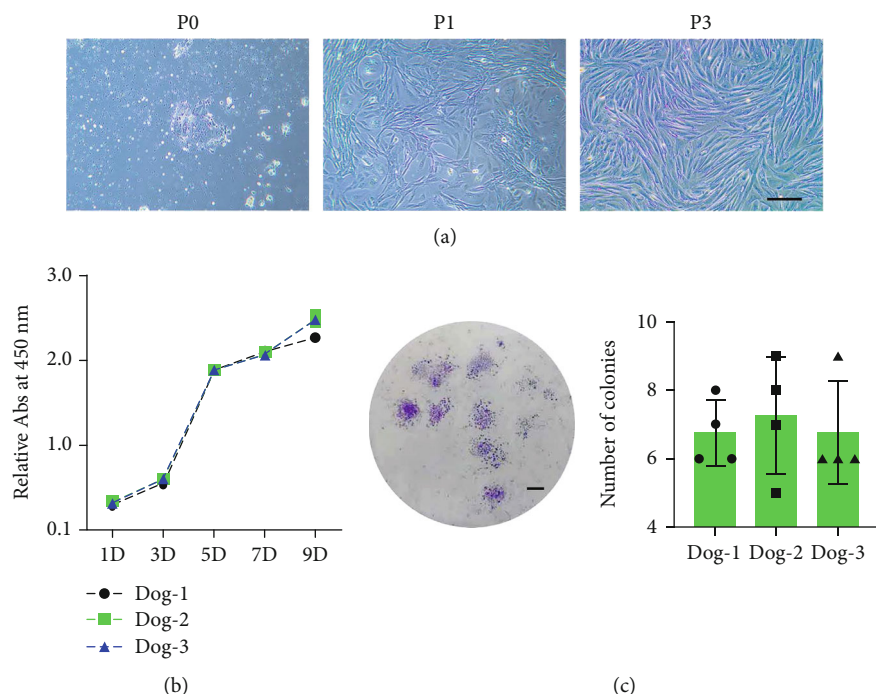


FIGURE 2: (a) Morphology of cells isolated from canine urine at different passages. At P0, spindle-shaped or round-shaped cells were observed. At P1, spindle-shape and fibroblast-like morphology cells were observed. Scale bars = 200  $\mu$ m. (b) The proliferation of urine-derived cells was determined by CCK-8 assay. Four samples were measured for each time point. The experiment was performed independently in the three dogs. (c) Colony-forming unit assay of the isolated cells after 10 days of culture. Scale bars = 2 mm.

and then fixed with 70% ethanol for 20 s. After that, they were incubated with Alcian blue solution for 30 min, followed by thorough washing with PBS. The images of stained cells were obtained using a fluorescence microscope and a light microscope, respectively.

**2.9. Tenogenic Differentiation.** The isolated cells were cultured in complete medium at 5000 cells/cm<sup>2</sup> within 6-well plates. When the cultured cells reached 80%-90% confluence, three wells of cells were cultured in basal medium alone (as the control group) or supplemented with 50 ng/ml BMP-12 (PeproTech) (as the tenogenic group). The medium was changed every 3 days. After 7-day culture, qRT-PCR was performed for evaluating the expression of tenogenic genes (Tnmd, Scx, and Mlx) in the cells. The primer sequences were listed in Table 3. Meanwhile, Tnmd expression was evaluated by immunofluorescence assay using the anti-Tnmd antibody (ab81328, Abcam, USA). The images of stained cells were obtained using a fluorescence microscope.

**2.10. Statistical Analysis.** All quantitative data are presented as mean  $\pm$  standard deviation. The comparison of the two groups was done using a two-tailed, unpaired Student's *t*-test, and the comparison of multiple groups was done using a one-way factorial analysis of variance (ANOVA) followed by the comparison of individual means with Tukey's test. The statistical analyses were performed using the SPSS 25.0 software (SPSS, USA).  $p < 0.05$  was regarded as statistically significant. All the experiments have been performed at least three biologically independent replicates.

### 3. Results

**3.1. Morphology and Proliferation of Urine-Derived Cells.** At days 5–7 after primary culture, adherent cells and colonies with spindle-shape or round-shape were observed, and lots of dead sperm were suspended in the medium (Figure 2(a)). In passage 1, most of the isolated cells exhibited a spindle-shape and fibroblast-like morphology, and few of them still displayed round-shape (Figure 2(a)). At passage 2 or 3, the canine urine-derived cells exhibited a homogeneous spindle-shaped morphology (Figure 2(a)). CCK-8 assay indicated that passage 3 of the isolated cells proliferated with a high rate within the first 5 days (Figure 2(b)).

**3.2. Clonogenicity of Urine-Derived Cells.** The clonogenicity of the isolated urine-derived cells was determined using the CFU assay. After 10 days of culture, cells isolated from urine formed adherent cell colonies (Figure 2(c)). Statistically, the isolated cells formed  $6.92 \pm 1.31$  colonies at a density of 40 cells per well (Figure 2(c)).

**3.3. Surface Marker of Urine-Derived Cells.** Flow cytometric analysis showed that passage 3 urine-derived cells positively expressed multiple markers of MSCs (CD29, CD44, CD90, and CD73), but negatively expressed for hematopoietic antigens (CD11b, CD34, and CD45) (Figure 3). These immunophenotypic profiles were in accordance with the criteria for defining MSCs proposed by the International Society for Cellular Therapy (ISCT) [34].

**3.4. Osteogenic Differentiation Potential.** After 7 days of culture, the cells in osteogenic induced medium showed a



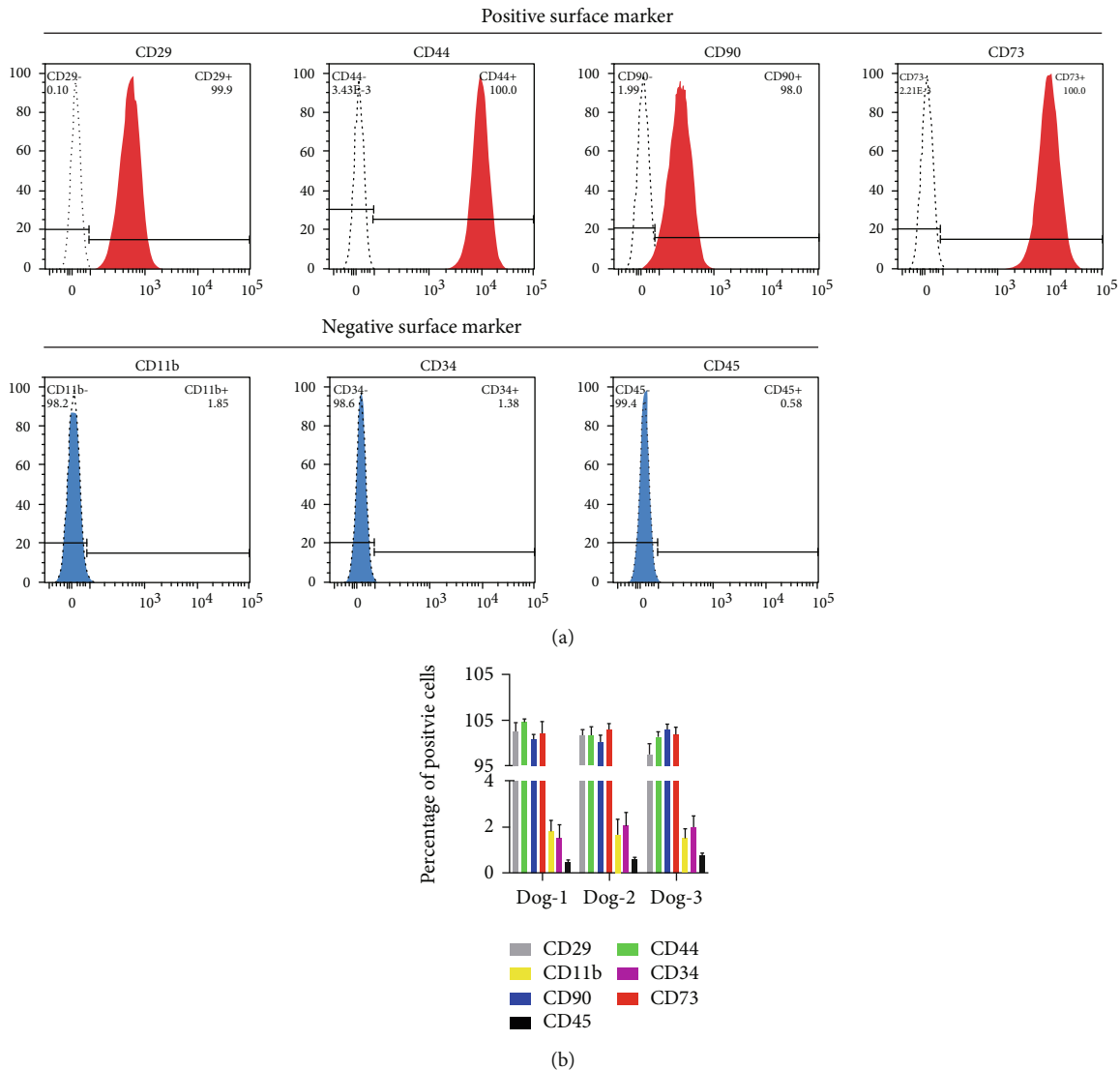


FIGURE 3: Flow cytometry for the isolated cells. (a) Representative histograms demonstrating positive and negative staining of urine-derived cells from a single dog. (b) Percentage of positive cells for the urine-derived cells isolated from three canine donors.

significantly higher mRNA expression level of *Runx2*, *Bglap*, and *Spp1* compared with the cells in basal medium ( $p < 0.05$  for all) (Figure 4(a)). Additionally, most of the cells cultured in osteogenic induced medium are positive for *Runx2* protein expression (Figure 4(b)). After 21 days of osteogenic induction, Alizarin Red assay showed that osteogenic induced cultures had calcium nodules, while the calcium nodules were absent in the basal cultures (Figure 4(c)).

**3.5. Adipogenic Differentiation Potential.** After 7 days of adipogenic induced medium, the mRNA expression level of *PPAR $\gamma$* , *FABP4*, and *LPL* were significantly upregulated in the cells under adipogenic induced medium when compared with the cells under basal medium. Qualitatively, there was a  $2.45 \pm 0.23$ ,  $4.79 \pm 0.24$  and  $3.62 \pm 0.21$ -fold increase for *PPAR $\gamma$* , *FABP4*, and *LPL* upon adipogenic induction compared to basal cultures, respectively ( $p < 0.05$  for all) (Figure 5(a)). Immunofluorescence assay showed that the

cells in the adipogenic group expressed the *PPAR $\gamma$*  obviously, while limited expression was showed in the cells under basal complete medium (Figure 5(b)). Under the influence of adipogenic induction, the isolated cells achieved an adipocytic phenotype by the end of the third week. The presence of intracytoplasmic lipid droplets was confirmed by Oil Red O staining only in induced cultures (Figure 5(c)), but not in basal cultures.

**3.6. Chondrogenic Differentiation Potential.** After 7 days of chondrogenic induction, the increased expression of chondrogenic-associated markers (*Sox9*, *Col2a1*, *Acan*) was found in the chondrogenic group with respect to the control group ( $p < 0.05$  for all) (Figure 6(a)). Moreover, immunofluorescence assay showed that the cells cultured in the chondrogenic differentiation medium were positive for *Sox9* expression, while no *Sox9* expression was found in the cell cultured on basal complete medium (Figure 6(b)). After 21

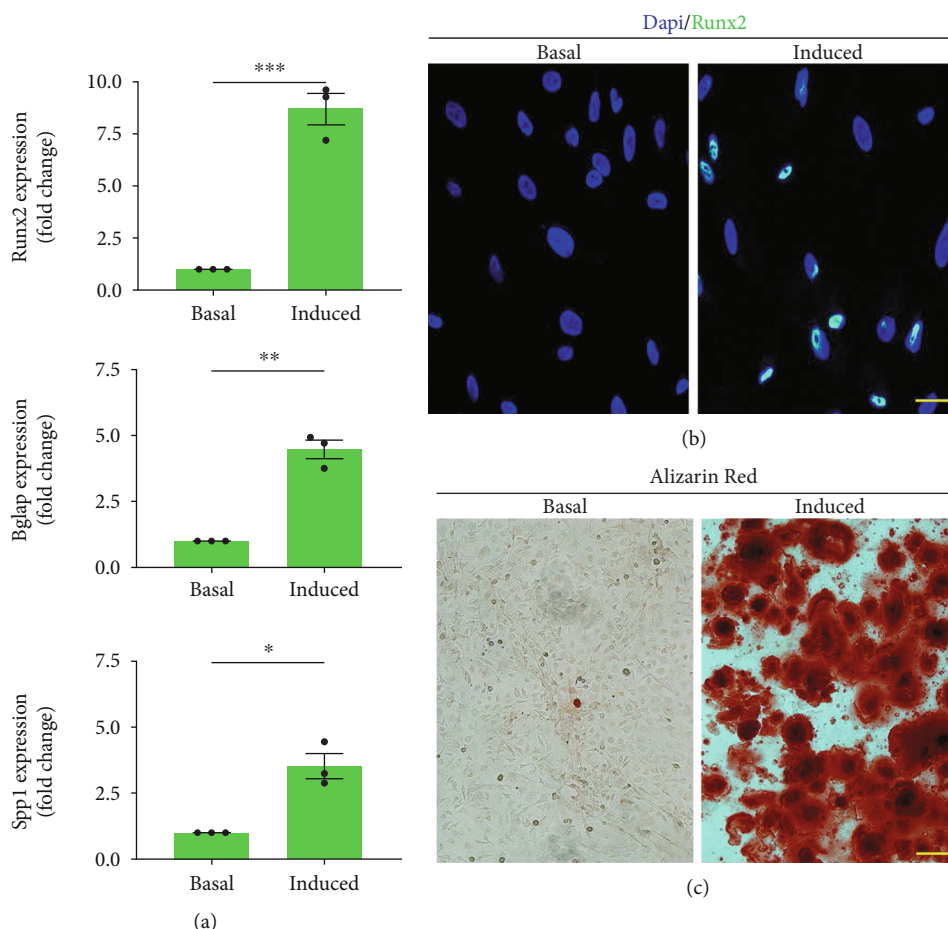


FIGURE 4: Osteogenic differentiation of urine-derived cells in vitro. (a) Osteogenic gene (Runx2, Bglap, SPP1) expression compared between osteogenic medium and its respective basal cultures.  $**p < 0.01$ ,  $***p < 0.001$ . Runx2: Runt-related transcription factor 2; Bglap, bone  $\gamma$ -carboxyglutamate protein; Spp1, secreted phosphoprotein. (b) The Runx2 protein expression of the urine-derived cells after 7 days of osteogenic induction. Scale bars =  $15 \mu\text{m}$ . (c) Alizarin Red staining of cells after 21 days in osteogenic or basal medium. Calcium nodules were seen in the osteogenic induced medium. Scale bars =  $20 \mu\text{m}$ .

days of chondrogenic induction, there was glycosaminoglycan deposition found around the cells by Alcian blue staining (Figure 6(c)).

**3.7. Tenogenic Differentiation Potential.** The isolated cells exposed to the tenogenic induced medium for 7 days showed a significant enhancement in the Tnmd, Scx, and Mxk expression with respect to the cells under basal cultures ( $p < 0.05$  for all) (Figure 7(a)). Immunofluorescence assay showed that the cells in the tenogenic induced medium obviously expressed the Tnmd protein, while limited expression was showed in the cells under basal medium (Figure 7(b)).

#### 4. Discussion

MSCs have been isolated from several canine sources, including the bone marrow, adipose tissue, synovium tissue, infrapatellar fat pad, umbilical cord vein, and ovarian tissue [8, 35–38]. In this study, we describe for the first time the isolation, characterization, and differentiation potential of MSCs obtained from canine urine samples, namely, cUSCs. The isolated cUSCs displayed spindle-shaped cells with rapid

proliferation potential and were able to self-renewal forming colonies from single cells and showed osteogenic, adipogenic, chondrogenic, and tenogenic differentiation. The protocol developed for isolating cUSCs will be convenient for extrapolating USC-based therapies from a preclinical canine model for clinical management of tissue injuries.

Plastic adherence is one of the most obvious characteristics of MSCs. Our study showed that the isolated cUSCs adhered to plastic and displayed a spindle-shaped morphology, similar to those reported from humans [15, 39]. Previous studies reported that USC derived from human urine (hUSCs) proliferated to 70–80% confluence no more than 3 days [16, 40], while the other two studies indicated that USC derived from humans proliferated to 70–80% confluence no more than 5 days [41, 42]. Similarly, our study showed that after 5 days, the cUSCs proliferated to 70–80% confluence.

Surface markers are another index to identify MSCs. A relative consensus currently exists regarding the surface markers detected with flow cytometry for human MSCs [34]. Unfortunately, a consensus regarding an acceptable flow cytometry profile remains to be determined for canine MSCs. Our study demonstrated that the isolated cell from

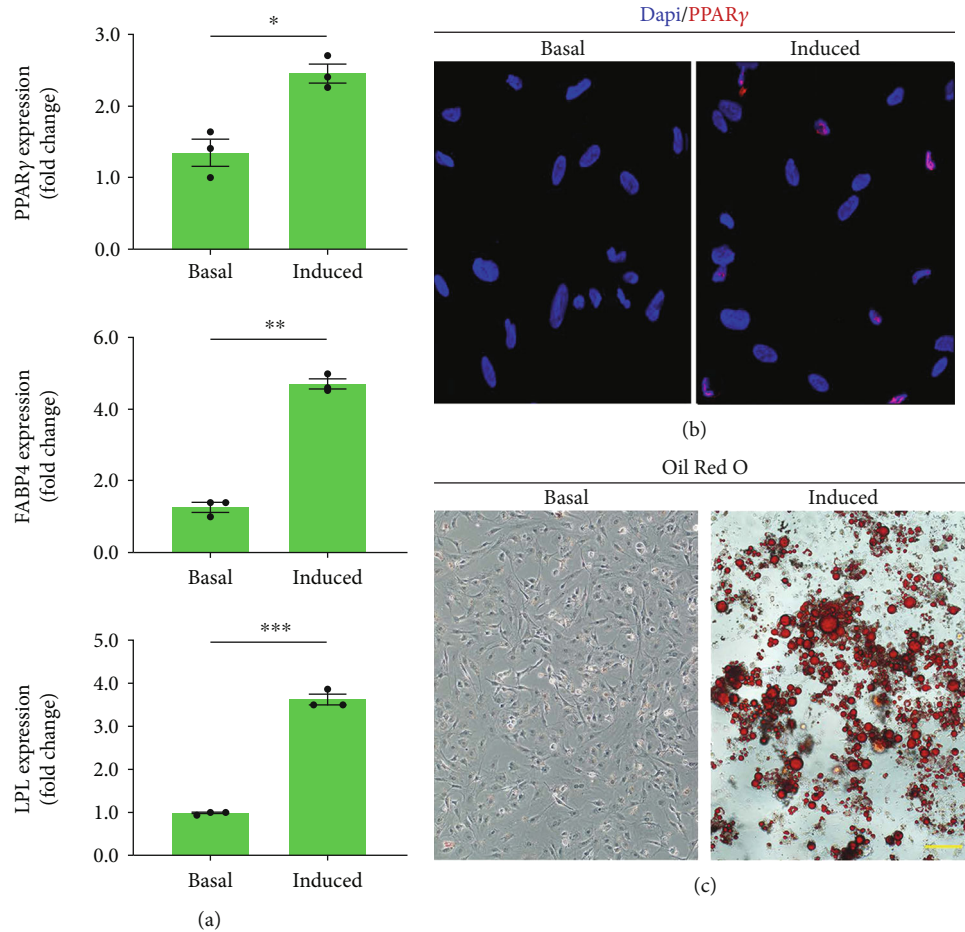


FIGURE 5: Adipogenic differentiation of urine-derived cells in vitro. (a) adipogenic gene (PPAR $\gamma$ , FABP4, and LPL) expression compared between adipogenic medium and its respective basal cultures. \* $p < 0.05$ , \*\*\* $p < 0.001$ . PPAR $\gamma$ : peroxisome proliferator-activated receptor  $\gamma$ ; FABP4: fatty acid-binding protein 4; LPL, lipoprotein lipase. (b) The PPAR $\gamma$  protein expression of the urine-derived cells after 7 days of adipogenic induction. Scale bars = 15  $\mu\text{m}$ . (c) Oil Red O staining of cells after 21 days in adipogenic or basal medium. Intracytoplasmic lipid droplets were seen in the adipogenic induced medium. Scale bars = 20  $\mu\text{m}$ .

canine urine was positive for CD29, CD44, CD90, and CD73, while lacking expression of CD45, CD11b, and CD34, which corresponds to the MSC surface markers specified by the International Society for Cellular Therapy (ISCT) [34]. The expressions of these surface markers were consistent with USCs from humans [39, 42].

During osteogenic differentiation of the isolated cUSCs, calcium phosphate deposition and osteogenic-specific gene expressions were tested. Runx2 and Spp1 are known to be upregulated during the osteogenic differentiation of human MSCs [43, 44]. Bglap is a bone-specific gene required for matrix mineralization [45]. In cUSCs with osteogenic induction, Runx2, Spp1, and Bglap were found to be significantly upregulated expressed at day 21, and lots of calcium nodules positive for Alizarin Red staining formed at the culture plate. These results were consistent with similar studies in hUSCs [39].

During the process of cUSC adipogenic differentiation, lipid droplet formation and adipocyte-specific gene (PPAR $\gamma$ , FABP4, and LPL) expression were detected. The cellular function of FABP4 is the coupling of fatty acids to several molecular targets as a fatty acids chaperone [46]. Via perox-

isome proliferator response elements, the transcription of FABP4 is directly coupled to PPAR $\gamma$  for enhancing the adipogenic differentiation of MSCs [47]. During the process of adipogenesis, the expression of FABP4 was found to be upregulated in cUSCs. In addition, PPAR $\gamma$  might play a critical role in adipogenesis by binding to the enhancer of adipocyte-specific genes, such as LPL, leptin, fatty acid-binding protein, and the adipocyte P2 gene (aP2) [48, 49]. Thus, the cUSCs under adipogenic induction presented significantly higher expression of PPAR $\gamma$  and LPL with respect to the untreated cUSCs.

As for the chondrogenic differentiation capacity of cUSCs, there exists a dispute. Pei et al. reported that USCs did not present the ability to differentiate into chondrocytes in a 5% O $_2$  and 5% CO $_2$  incubator up to 14 days [50], while some studies have determined that USCs could differentiate toward the chondrogenic lineages after chondrogenic induction for 28 days [51–53]. Meanwhile, some studies showed that USCs could differentiate into chondrocytes but presented relatively lower chondrogenic potential with respect to MSCs derived from adipose tissue (ASCs) or bone marrow (BMSCs) [40, 54]. But another study indicated that USCs

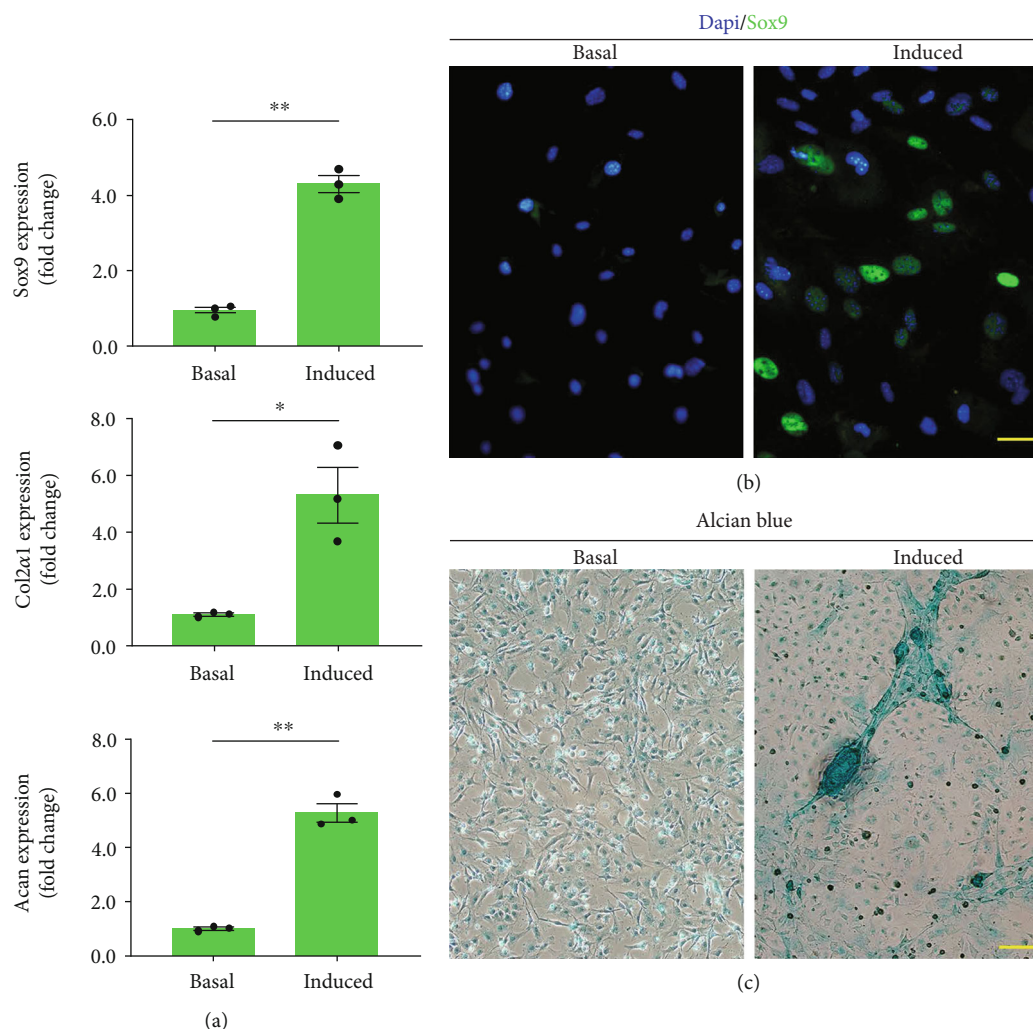


FIGURE 6: Chondrogenic differentiation of urine-derived cells in vitro. (a) Chondrogenic gene (Sox9, Col2a1, Acan) expression compared between the chondrogenic medium and its respective basal cultures. \* $p < 0.05$ , \*\* $p < 0.01$ . Sox9, sex-determining region Y-box 9; Col2a1, collagen type II; Acan, Aggrecan. (b) The Sox9 protein expression of the urine-derived cells after 7 days of chondrogenic induction. Scale bars = 15  $\mu\text{m}$ . (c) Alcian blue staining of cells after 21 days in chondrogenic or basal medium. Glycosaminoglycan deposition around the cells was seen in the chondrogenic induced medium. Scale bars = 20  $\mu\text{m}$ .

possessed a similar biological characteristic to ASCs and had multilineage differentiation ability [51]. Herein, the chondrogenic potential of cUSCs was shown by a synthesis of proteoglycans using Alcian blue staining. The expressions of Col2a1 and Acan (major cartilage extracellular matrix components) were upregulated in the cUSCs after chondrogenic induction in a 20%  $\text{O}_2$  and 5%  $\text{CO}_2$  incubator. This study indicated that the isolated cUSCs under chondrogenic induction could differentiate into chondrocytes.

BMP-12 is a critical growth factor involved in guiding MSC tenogenic differentiation [55, 56]. Thus, we added it into the culture medium of cUSCs and then determined the tenogenic differentiation potential of cUSCs by evaluating their tenogenic gene (Tnmd, Scx, and Mxk) expression and Tnmd protein expression. Stimulated by BMP-12 for 7 days, the expression level of Tnmd and Scx was significantly upregulated in cUSCs. Scx is critically involved in the development of tendon progenitors, and Mxk is a critical transcription fac-

tor for the subsequent tendon differentiation and maturation [57], while the gene expression of Tnmd, a well-known late-stage tenogenic marker [58], was also significantly overexpressed. The enhanced expression of tendon-related genes following BMP-12 treatment is in good agreement with other studies performed on MSCs from humans and rats [55, 56].

A limitation of this study is that the multilineage differentiation potentials of cUSCs were not evaluated in vivo. Previous literatures indicated that the hUSCs have the ability to differentiate into the bone, cartilage, and urinary tract tissue [16, 39, 41]. In future studies, we used the cUSCs combined with tissue-engineering scaffold for regenerating the bone, cartilage, tendon, and urinary tract tissue in the preclinical canine model.

In conclusion, for the first time, cUSC was successfully isolated from canine urine, which presented clonogenicity and high proliferation capacity. In addition, these cells express the specific-makers of MSCs and can differentiate



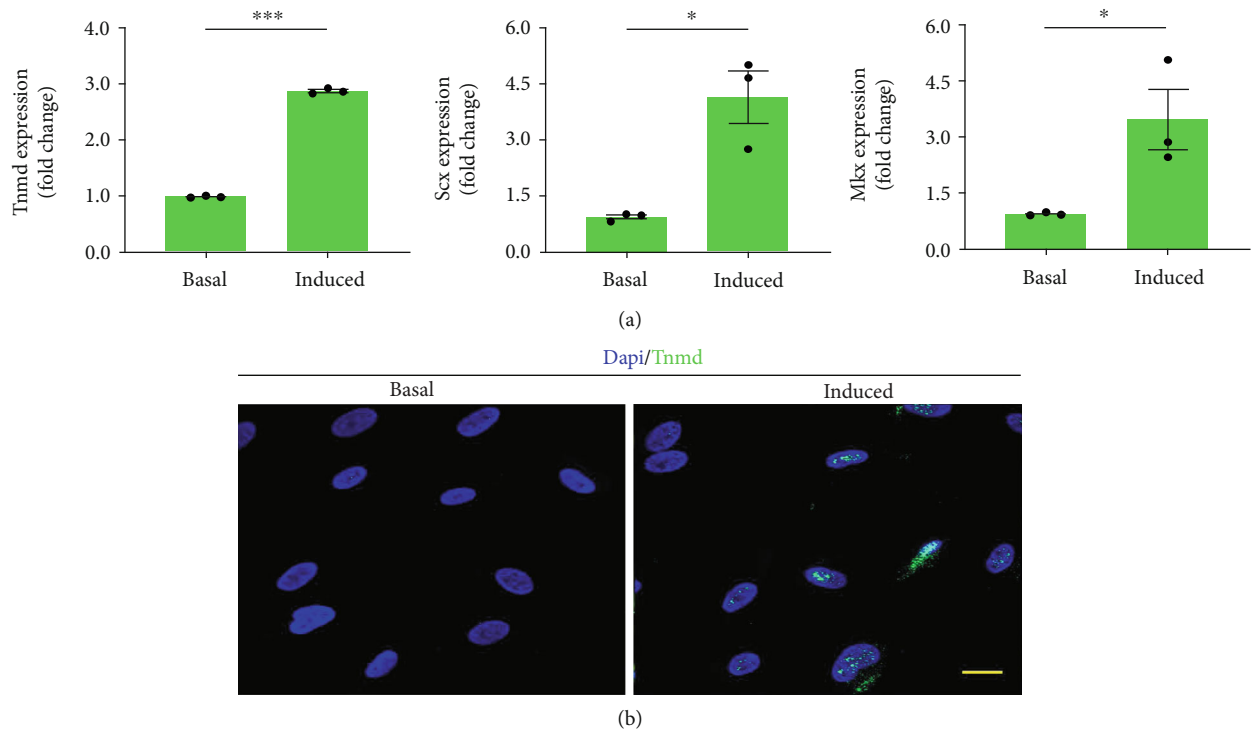


FIGURE 7: Tenogenic differentiation of urine-derived cells in vitro. (a) Tenogenic gene (Tnmd, Scx, and Mlx) expression compared between tenogenic medium and its respective basal cultures. \* $p < 0.05$ , \*\* $p < 0.01$ , \*\*\* $p < 0.001$ . Tnmd, tenomodulin; Scx, scleraxis; Mlx, mohawk. (b) The Tnmd protein expression of the urine-derived cells after 7 days of tenogenic induction. Scale bars = 15  $\mu$ m.

into osteogenesis, chondrogenesis, adipogenesis, and tenogenesis under a specific induction. The successful isolation of USCs from canine urine may help us preliminarily evaluate the efficacy of USCs-based therapy in a preclinical canine model for clinical management of tissue injuries.

### Data Availability

The data used to support the findings of this study are included in the article.

### Conflicts of Interest

The authors declare no competing financial interests.

### Authors' Contributions

H.L. and C.C. designed the experiments. Y.X. and Y.C. performed the experiments and analyzed the data. T.Z. and Y.X. wrote the manuscript. M.L., Q.S., T.Q., J.H., and J. L. assisted in the experiments and preparation of the manuscript. C.C. and J. L. supervised the study. Yan Xu and Tao Zhang contributed equally to this work.

### Acknowledgments

This work was supported by the National Natural Science Foundation of China (Nos. 81730068, 81902220 and 81902192), the Natural Science Foundation of Hunan Province of China (No. 2017JJ2006 and 2018JJ3814),

and the China Postdoctoral Science Foundation (No. 2019M652809). The authors extend their sincere thanks to Prof. Hui Xie in Xiangya Hospital, Central South University, for sharing the protocol of human urine-derived stem cells isolation.

### References

- [1] M. N. Pantelic and L. M. Larkin, "Stem cells for skeletal muscle tissue engineering," *Tissue Engineering. Part B, Reviews*, vol. 24, no. 5, pp. 373–391, 2018.
- [2] M. T. Langhans, S. Yu, and R. S. Tuan, "Stem cells in skeletal tissue engineering: technologies and models," *Current Stem Cell Research & Therapy*, vol. 11, no. 6, pp. 453–474, 2016.
- [3] C. Brown, C. McKee, S. Bakshi et al., "Mesenchymal stem cells: cell therapy and regeneration potential," *Journal of Tissue Engineering and Regenerative Medicine*, vol. 13, no. 9, pp. 1738–1755, 2019.
- [4] S. E. Haynesworth, J. Goshima, V. M. Goldberg, and A. I. Caplan, "Characterization of cells with osteogenic potential from human marrow," *Bone*, vol. 13, no. 1, pp. 81–88, 1992.
- [5] J. U. N. G. U. YOO, T. R. A. C. I. S. BARTHEL, K. E. I. T. A. NISHIMURA et al., "The chondrogenic potential of human bone-marrow-derived mesenchymal progenitor cells," *The Journal of Bone and Joint Surgery. American Volume*, vol. 80, no. 12, pp. 1745–1757, 1998.
- [6] Q. W. Wang, Z. L. Chen, and Y. J. Piao, "Mesenchymal stem cells differentiate into tenocytes by bone morphogenetic protein (BMP) 12 gene transfer," *Journal of Bioscience and Bioengineering*, vol. 100, no. 4, pp. 418–422, 2005.

- [7] Y. H. Choi, A. Kurtz, and C. Stamm, "Mesenchymal stem cells for cardiac cell therapy," *Human Gene Therapy*, vol. 22, no. 1, pp. 3–17, 2011.
- [8] R. N. Bearden, S. S. Huggins, K. J. Cummings, R. Smith, C. A. Gregory, and W. B. Saunders, "In-vitro characterization of canine multipotent stromal cells isolated from synovium, bone marrow, and adipose tissue: a donor-matched comparative study," *Stem Cell Research & Therapy*, vol. 8, no. 1, p. 218, 2017.
- [9] X. Wang, Y. Wang, W. Gou, Q. Lu, J. Peng, and S. Lu, "Role of mesenchymal stem cells in bone regeneration and fracture repair: a review," *International Orthopaedics*, vol. 37, no. 12, pp. 2491–2498, 2013.
- [10] J. Pak, J. H. Lee, W. A. Kartolo, and S. H. Lee, "Cartilage regeneration in human with adipose tissue-derived stem cells: current status in clinical implications," *BioMed Research International*, vol. 2016, Article ID 4702674, 12 pages, 2016.
- [11] M. Qasim, D. S. Chae, and N. Y. Lee, "Bioengineering strategies for bone and cartilage tissue regeneration using growth factors and stem cells," *Journal of Biomedical Materials Research. Part A*, vol. 108, no. 3, pp. 394–411, 2019.
- [12] Z. C. Hao, S. Z. Wang, X. J. Zhang, and J. Lu, "Stem cell therapy: a promising biological strategy for tendon-bone healing after anterior cruciate ligament reconstruction," *Cell Proliferation*, vol. 49, no. 2, pp. 154–162, 2016.
- [13] P. Y. Neo, T. K. H. Teh, A. S. R. Tay et al., "Stem cell-derived cell-sheets for connective tissue engineering," *Connective Tissue Research*, vol. 57, no. 6, pp. 428–442, 2016.
- [14] S. Xie, Y. Zhou, Y. Tang et al., "Book-shaped decellularized tendon matrix scaffold combined with bone marrow mesenchymal stem cells-sheets for repair of achilles tendon defect in rabbit," *Journal of Orthopaedic Research*, vol. 37, no. 4, pp. 887–897, 2019.
- [15] X. Ji, M. Wang, F. Chen, and J. Zhou, "Urine-derived stem cells: the present and the future," *Stem Cells International*, vol. 2017, Article ID 4378947, 8 pages, 2017.
- [16] L. Chen, L. Li, F. Xing et al., "Human urine-derived stem cells: potential for cell-based therapy of cartilage defects," *Stem Cells International*, vol. 2018, Article ID 4686259, 14 pages, 2018.
- [17] D. Hatsushika, T. Muneta, T. Nakamura et al., "Repetitive allogeneic intraarticular injections of synovial mesenchymal stem cells promote meniscus regeneration in a porcine massive meniscus defect model," *Osteoarthritis and Cartilage*, vol. 22, no. 7, pp. 941–950, 2014.
- [18] S. C. O. T. T. P. BRUDER, K. A. R. L. H. KRAUS, V. I. C. T. O. R. M. GOLDBERG, and S. U. D. H. A. KADIYALA, "The effect of implants loaded with autologous mesenchymal stem cells on the healing of canine segmental bone defects," *The Journal of Bone and Joint Surgery. American Volume*, vol. 80, no. 7, pp. 985–996, 1998.
- [19] M. Horie, M. D. Driscoll, H. W. Sampson et al., "Implantation of allogenic synovial stem cells promotes meniscal regeneration in a rabbit meniscal defect model," *The Journal of Bone and Joint Surgery. American Volume*, vol. 94, no. 8, pp. 701–712, 2012.
- [20] X. Xia, K. F. Chan, G. T. Y. Wong et al., "Mesenchymal stem cells promote healing of nonsteroidal anti-inflammatory drug-related peptic ulcer through paracrine actions in pigs," *Science translational medicine*, vol. 11, no. 516, p. eaat7455, 2019.
- [21] S. O. Canapp, D. A. Canapp, V. Ibrahim, B. J. Carr, C. Cox, and J. G. Barrett, "The use of adipose-derived progenitor cells and platelet-rich plasma combination for the treatment of supraspinatus tendinopathy in 55 dogs: a retrospective study," *Frontiers in Veterinary Science*, vol. 3, p. 61, 2016.
- [22] R. Storb, R. B. Epstein, T. C. Graham, and E. D. Thomas, "Methotrexate regimens for control of graft-versus-host disease in dogs with allogeneic marrow grafts," *Transplantation*, vol. 9, no. 3, pp. 240–246, 1970.
- [23] H. G. Prentice, H. A. Blacklock, G. Janossy et al., "Depletion of T lymphocytes in donor marrow prevents significant graft-versus-host disease in matched allogeneic leukaemic marrow transplant recipients," *Lancet*, vol. 1, no. 8375, pp. 472–476, 1984.
- [24] G. Socie and B. R. Blazar, "Acute graft-versus-host disease: from the bench to the bedside," *Blood*, vol. 114, no. 20, pp. 4327–4336, 2009.
- [25] I. Kiviranta, M. Tammi, J. Jurvelin, A. M. Säämänen, and H. J. Helminen, "Moderate running exercise augments glycosaminoglycans and thickness of articular cartilage in the knee joint of young beagle dogs," *Journal of Orthopaedic Research*, vol. 6, no. 2, pp. 188–195, 1988.
- [26] B. A. Bockstahler, M. Skalicky, C. Peham, M. Müller, and D. Lorinson, "Reliability of ground reaction forces measured on a treadmill system in healthy dogs," *Veterinary Journal*, vol. 173, no. 2, pp. 373–378, 2007.
- [27] A. J. Schreiner, J. P. Stannard, C. R. Cook et al., "Comparison of meniscal allograft transplantation techniques using a pre-clinical canine model," *Journal of Orthopaedic Research*, 2020.
- [28] M. I. Wits, G. C. Tobin, M. D. Silveira et al., "Combining canine mesenchymal stromal cells and hyaluronic acid for cartilage repair," *Genetics and Molecular Biology*, vol. 43, no. 1, p. e20190275, 2020.
- [29] J. E. Adams, M. E. Zobitz, J. S. Reach Jr., K.-N. An, and S. P. Steinmann, "Rotator cuff repair using an acellular dermal matrix graft: an in vivo study in a canine model," *Arthroscopy: The Journal of Arthroscopic & Related Surgery*, vol. 22, no. 7, pp. 700–709, 2006.
- [30] J. L. Cook, P. A. Smith, J. P. Stannard et al., "A canine hybrid double-bundle model for study of arthroscopic ACL reconstruction," *Journal of Orthopaedic Research*, vol. 33, no. 8, pp. 1171–1179, 2015.
- [31] J. B. Volpon, "Nonunion using a canine model," *Archives of Orthopaedic and Trauma Surgery*, vol. 113, no. 6, pp. 312–317, 1994.
- [32] J. Harding, R. M. Roberts, and O. Mirochnitchenko, "Large animal models for stem cell therapy," *Stem Cell Research & Therapy*, vol. 4, no. 2, p. 23, 2013.
- [33] A. M. Hoffman and S. W. Dow, "Concise review: stem cell trials using companion animal disease models," *Stem Cells*, vol. 34, no. 7, pp. 1709–1729, 2016.
- [34] M. Dominici, K. Le Blanc, I. Mueller et al., "Minimal criteria for defining multipotent mesenchymal stromal cells. The International Society for Cellular Therapy position statement," *Cytotherapy*, vol. 8, no. 4, pp. 315–317, 2006.
- [35] K. A. Russell, N. H. C. Chow, D. Dukoff et al., "Characterization and Immunomodulatory effects of canine adipose tissue- and bone marrow-derived mesenchymal stromal cells," *PLoS One*, vol. 11, no. 12, p. e0167442, 2016.
- [36] A. Sasaki, M. Mizuno, N. Ozeki et al., "Canine mesenchymal stem cells from synovium have a higher chondrogenic potential than those from infrapatellar fat pad, adipose tissue, and bone marrow," *PLoS One*, vol. 13, no. 8, p. e0202922, 2018.

- [37] A. B. T. Hill, J. Therrien, J. M. Garcia, and L. C. Smith, "Mesenchymal-like stem cells in canine ovary show high differentiation potential," *Cell Proliferation*, vol. 50, no. 6, p. e12391, 2017.
- [38] E. Zucconi, N. M. Vieira, D. F. Bueno et al., "Mesenchymal stem cells derived from canine umbilical cord vein—a novel source for cell therapy studies," *Stem Cells and Development*, vol. 19, no. 3, pp. 395–402, 2010.
- [39] G. Bento, A. K. Shafiqullina, A. A. Rizvanov, V. A. Sardão, M. P. Macedo, and P. J. Oliveira, "Urine-derived stem cells: applications in regenerative and predictive medicine," *Cells*, vol. 9, no. 3, p. 573, 2020.
- [40] C. Wu, L. Chen, Y.-z. Huang et al., "Comparison of the proliferation and differentiation potential of human urine-, placenta decidua basalis-, and bone marrow-derived stem cells," *Stem Cells International*, vol. 2018, Article ID 7131532, 2018.
- [41] J. Guan, J. Zhang, H. Li et al., "Human urine derived stem cells in combination with  $\beta$ -TCP can be applied for bone regeneration," *PLoS One*, vol. 10, no. 5, p. e0125253, 2015.
- [42] A. J. Chen, J. K. Pi, J. G. Hu et al., "Identification and characterization of two morphologically distinct stem cell subpopulations from human urine samples," *Science China. Life Sciences*, vol. 63, no. 5, pp. 712–723, 2020.
- [43] J. Liu, M. Wu, G. Feng, R. Li, Y. Wang, and J. Jiao, "Down-regulation of LINC00707 promotes osteogenic differentiation of human bone marrow-derived mesenchymal stem cells by regulating DKK1 via targeting miR-103a-3p," *International Journal of Molecular Medicine*, vol. 46, no. 3, pp. 1029–1038, 2020.
- [44] F. Nie, W. Zhang, Q. Cui, Y. Fu, H. Li, and J. Zhang, "Kaempferol promotes proliferation and osteogenic differentiation of periodontal ligament stem cells via Wnt/ $\beta$ -catenin signaling pathway," *Life Sciences*, vol. 258, p. 118143, 2020.
- [45] H. Carmona, H. Valadez, Y. Yun, J. Sankar, L. Estala, and F. A. Gomez, "Development of microfluidic-based assays to estimate the binding between osteocalcin (BGLAP) and fluorescent antibodies," *Talanta*, vol. 132, pp. 676–679, 2015.
- [46] M. Furuhashi and G. S. Hotamisligil, "Fatty acid-binding proteins: role in metabolic diseases and potential as drug targets," *Nature Reviews. Drug Discovery*, vol. 7, no. 6, pp. 489–503, 2008.
- [47] P. Tontonoz and B. M. Spiegelman, "Fat and beyond: the diverse biology of PPAR $\gamma$ ," *Annual Review of Biochemistry*, vol. 77, no. 1, pp. 289–312, 2008.
- [48] E. D. Rosen and B. M. Spiegelman, "PPAR $\gamma$ : a nuclear regulator of metabolism, differentiation, and cell growth," *The Journal of Biological Chemistry*, vol. 276, no. 41, pp. 37731–37734, 2001.
- [49] P. Tontonoz, E. Hu, R. A. Graves, A. I. Budavari, and B. M. Spiegelman, "mPPAR  $\gamma$  2: tissue-specific regulator of an adipocyte enhancer," *Genes & Development*, vol. 8, no. 10, pp. 1224–1234, 1994.
- [50] M. Pei, J. Li, Y. Zhang, G. Liu, L. Wei, and Y. Zhang, "Expansion on a matrix deposited by nonchondrogenic urine stem cells strengthens the chondrogenic capacity of repeated-passage bone marrow stromal cells," *Cell and Tissue Research*, vol. 356, no. 2, pp. 391–403, 2014.
- [51] J. J. Guan, X. Niu, F. X. Gong et al., "Biological characteristics of human-urine-derived stem cells: potential for cell-based therapy in neurology," *Tissue Engineering. Part A*, vol. 20, no. 13-14, pp. 1794–1806, 2014.
- [52] S. Bharadwaj, G. Liu, Y. Shi et al., "Multipotential differentiation of human urine-derived stem cells: potential for therapeutic applications in urology," *Stem Cells*, vol. 31, no. 9, pp. 1840–1856, 2013.
- [53] P. Gao, P. Han, D. Jiang, S. Yang, Q. Cui, and Z. Li, "Effects of the donor age on proliferation, senescence and osteogenic capacity of human urine-derived stem cells," *Cytotechnology*, vol. 69, no. 5, pp. 751–763, 2017.
- [54] H. S. Kang, S. H. Choi, B. S. Kim et al., "Advanced properties of urine derived stem cells compared to adipose tissue derived stem cells in terms of cell proliferation, immune modulation and multi differentiation," *Journal of Korean Medical Science*, vol. 30, no. 12, pp. 1764–1776, 2015.
- [55] W. Zarychta-Wiśniewska, A. Burdzinska, A. Kulesza et al., "Bmp-12 activates tenogenic pathway in human adipose stem cells and affects their immunomodulatory and secretory properties," *BMC Cell Biology*, vol. 18, no. 1, p. 13, 2017.
- [56] L. Dai, X. Hu, X. Zhang et al., "Different tenogenic differentiation capacities of different mesenchymal stem cells in the presence of BMP-12," *Journal of Translational Medicine*, vol. 13, no. 1, p. 200, 2015.
- [57] H. Liu, S. Zhu, C. Zhang et al., "Crucial transcription factors in tendon development and differentiation: their potential for tendon regeneration," *Cell and Tissue Research*, vol. 356, no. 2, pp. 287–298, 2014.
- [58] C. Shukunami, A. Takimoto, M. Oro, and Y. Hiraki, "Scleraxis positively regulates the expression of tenomodulin, a differentiation marker of tenocytes," *Developmental Biology*, vol. 298, no. 1, pp. 234–247, 2006.

## Review Article

# The Potential Use of Mesenchymal Stem Cells and Their Derived Exosomes as Immunomodulatory Agents for COVID-19 Patients

Faisal A. Alzahrani <sup>1</sup>, Islam M. Saadeldin <sup>2,3</sup>, Abrar Ahmad <sup>1</sup>, Dipak Kumar <sup>4</sup>,  
Esam I. Azhar,<sup>5</sup> Arif Jamal Siddiqui <sup>6</sup>, Bassem Kurdi <sup>7</sup>, Abdulrahim Sajini <sup>8</sup>,  
Abdulmajeed F. Alrefaei <sup>9</sup>, and Sadaf Jahan <sup>10</sup>

<sup>1</sup>Department of Biochemistry, Faculty of Science, Embryonic Stem Cell Unit, King Fahad Center for Medical Research, King Abdulaziz University, Jeddah, Saudi Arabia

<sup>2</sup>Department of Physiology, Faculty of Veterinary Medicine, Zagazig University, Zagazig 44519, Egypt

<sup>3</sup>Department of Animal Production College of Food and Agriculture Science, King Saud University, Riyadh 11451, Saudi Arabia

<sup>4</sup>Zoology Department, KKM College, Munger University, Jamui, India

<sup>5</sup>Department of Medical Laboratories, College of Applied Medical Sciences, King Abdulaziz University, Jeddah, Saudi Arabia

<sup>6</sup>Department of Biology, College of Science, University of Hail, Hail, Saudi Arabia

<sup>7</sup>Department of Pediatrics, Faculty of Medicine, King Abdulaziz University, Jeddah, Saudi Arabia

<sup>8</sup>Department of Biomedical Engineering, Khalifa University of Science and Technology, Abu Dhabi, UAE

<sup>9</sup>Jamoum University College, Department of Biology, University of Umm Al-Qura, Saudi Arabia

<sup>10</sup>College of Applied Medical Science, Majmaah University, Al Majmaah, Saudi Arabia

Correspondence should be addressed to Sadaf Jahan; [jahan149@gmail.com](mailto:jahan149@gmail.com)

Received 6 June 2020; Revised 22 July 2020; Accepted 27 August 2020; Published 24 September 2020

Academic Editor: Huseyin Sumer

Copyright © 2020 Faisal A. Alzahrani et al. This is an open access article distributed under the Creative Commons Attribution License, which permits unrestricted use, distribution, and reproduction in any medium, provided the original work is properly cited.

A novel severe acute respiratory syndrome coronavirus (SARS-CoV-2) causing lethal acute respiratory disease emerged in December 2019. The World Health Organization named this disease “COVID-19” and declared it a pandemic on March 11, 2020. Many studies have shown that mesenchymal stem cells (MSCs) and their exosomes (MSCs-Exo), which are isolated from allogenic bone marrow stem cells, significantly lower the risk of alveolar inflammation and other pathological conditions associated with distinct lung injuries. For example, in acute respiratory distress syndrome (ARDS) and pneumonia patients, MSCs-Exo and MSCs provide similar healing properties and some clinical trials have used cell-based inhalation therapy which show great promise. MSCs and MSCs-Exo have shown potential in clinical trials as a therapeutic tool for severely affected COVID-19 patients when compared to other cell-based therapies, which may face challenges like the cells’ sticking to the respiratory tract epithelia during administration. However, the use of MSCs or MSCs-Exo for treating COVID-19 should strictly adhere to the appropriate manufacturing practices, quality control measurements, preclinical safety and efficacy data, and the proper ethical regulations. This review highlights the available clinical trials that support the therapeutic potential of MSCs or MSCs-Exo in severely affected COVID-19 patients.

## 1. Introduction

A lethal acute respiratory tract disease caused by a novel severe acute respiratory syndrome (SARS) coronavirus emerged at the end of 2019 in Wuhan, China [1–3]. The first outbreaks in China 13.8% suffered severe disease and 6.1% required critical care [4]. Since that outbreak, the World Health Organization

(WHO) named the disease Coronavirus Disease “COVID-19” and declared it a pandemic on March 11, 2020 [5]. It is caused by an RNA virus (ssRNA) 50–200 nm in diameter that is composed of four structural proteins: nucleocapsid protein, spike protein, envelope protein, and membrane protein [1].

As COVID-19 cases emerged, the pertaining symptoms were associated with severe respiratory tract infections and



inflammations. At first, the infections were thought to be part of the normal, seasonal flu. However, after many failed attempts to control the infectious virus, it was identified as a different virus with similar symptoms to other respiratory viral diseases. Patients probably were first infected with the virus through a wholesale market of seafood and other non-vegetarian food items; the first patients worked at the market or made purchases there regularly. As more cases were identified, the market was closed with immediate effect, and all required steps were adopted to avoid further spreading of infections due to the highly contagious nature of the virus [4].

The causative virus was found to have a 5% genetic association with SARS as part of a subset of beta coronaviruses [6]. The WHO identified the virus as severe acute respiratory syndrome coronavirus-2 (SARS-CoV-2) and recommended that the disease resulting in the current outbreak should be explained as “2019-nCoV acute respiratory disease” (2019 novel coronavirus acute respiratory disease). The nomenclature for the virus was confirmed by the International Committee on Taxonomy of Viruses (ICOTV) as SARS-CoV-2 [7].

Rapid replication of SARS-CoV-2 is believed to occur after the onset of infection and severe inflammatory responses due to cytokine storms have been observed. This subsequent inflammatory response damages alveolar epithelia and capillary endothelial cells, resulting in interstitial and alveolar edema and impaired pulmonary functions. Such damage leads to acute hypoxic respiratory failure and results in acute respiratory distress syndrome (ARDS). People older than 50 years are at a high risk for COVID-19-induced pneumonia, and the WHO has estimated the mortality rate of SARS-CoV-2 to be ~3.7% [8].

Due to its appearance under an electron microscope, which is like a solar corona, the SARS-CoV-2 family was named *Coronaviridae*. The subfamily *Orthocoronavirinae* is zoonotic and is further categorized into the following genera: alpha, beta, gamma, and delta coronaviruses. Coronaviruses are varied and have single-strand (ss), positive-sense RNA (+RNA) [7]. Enzyme lactate dehydrogenase levels and neutrophil counts are used as disease identification markers for SARS viruses [9]. Evidence suggests that bats and birds are the primary hosts for these coronaviruses, and many studies have suggested that coronaviruses can infect bats, birds, cats, dogs, lions, pigs, mice, horses, and whales, as well as humans. Genomic and serologic data have confirmed that camels and bats can act as intermediate hosts for humans for Middle East Respiratory Syndrome Coronavirus (MERS-CoV) and SARS-CoV, respectively.

Phylogenetic studies of the complete RNA-dependent RNA polymerase (RdRp) gene have shown that SARS-CoV-2 is different from SARS-CoV; therefore, SARS-CoV-2 has been identified in the subgenus *Sarbecovirus* [7]. The genomic studies of SARS-CoV-2 have revealed its similarity to bat-derived coronavirus strains, such as bat-SL-CoVZC45 and bat-SLCoVZXC21, the virus that caused the SARS outbreak in 2003 [7]. Evidence has also revealed that SARS-CoV-2 survives on distinct surfaces. For example, the virus can persist for 3 hours in aerosol and up to 72 hours on stainless steel, plastic, cardboard, and copper surfaces [10].

One of the guidelines recently released by the National Health and Medical Commission indicated that SARS-CoV-2 severe cases generally impart severe pneumonia accompanied by difficulty in breathing after one week of illness [11, 12]. Severe cases quickly progress to ARDS, septic shock, and multiple organ dysfunction syndrome (MODS), which are challenging to manage medically [13]. As mentioned previously, COVID-19 causes a severe secretion of cytokines in the lung region, thereby damaging the alveolar epithelia and capillary endothelial cells. The immunomodulatory effect of the therapeutic agents can reverse this reaction and thus protect the lungs from severe damage [14].

The containment, management, and treatment of the disease have challenged both clinicians and researchers in different fields of biomedicine. As of the finalization of this manuscript, no positive or promising treatment against SARS-CoV-2 has been found, although many streamlined therapies are on the way. However, the side effects of some pharmaceutical drugs that have been used to try to control the disease have been observed and drugs are effective in some individuals, while they fail in others. Convalescent plasma therapy also showed some promise [15–17]. Researchers are also working on a vaccine against COVID-19 but still have a long way to go. Therefore, based on the research and generated data, immediate therapy that does not negatively impact the health of the patients is still needed to overcome the crisis.

Stem cell research and therapy have given hope to both researchers and clinicians. Previous studies have shown that stem cell therapy is a promising treatment for numerous diseases and conditions, such as neurodegeneration, diabetes, and cancer. [18, 19]. Recently, mesenchymal stem cells (MSCs) have been introduced as a potential therapeutic approach for treating SARS-CoV-2 [19]. MSCs suppress viral infections by releasing specific cytokines; these features are intrinsically present while the MSCs reside in their niche before being isolated from the source tissue [20]. Therefore, MSCs and their exosomes (MSCs-Exo) are expected to survive even when transplanted into a patient with a confirmed SARS-CoV-2 infection (NCT04276987). Due to the ambiguity of MSC therapy in treating SARS-CoV-2, the reported clinical trials are being reviewed to present the information to researchers of the stem cell-based therapy. This review focuses on approaches to improve patients' immunological response against SARS-CoV-2 infection using MSCs and/or MSCs-Exo therapy.

## 2. Covid-19 Diagnosis and Pathogenesis

Initially, SARS-CoV-2 infection presents mild symptoms that are similar to diseases caused by other respiratory viruses [21]. The timeline between exposure and appearance of the first symptoms ranges from 1 to 14 days [4], and epidemiological studies have revealed that SARS-CoV-2 may be transmitted during the pre-symptomatic incubation period [22]. Indeed, virologic studies using reverse transcriptase-polymerase chain reaction (RT-PCR) have detected large quantities of the SARS-CoV-2 viral RNA among persons with asymptomatic and pre-symptomatic SARS-CoV-2 infections

[23]. The risk of transmission is not yet clear due to the uncertain degree of SARS-CoV-2 viral RNA shedding. However, it is thought to be greatest in symptomatic patients since viral shedding is at its peak at symptom onset and gradually declines over time (up to several weeks) [22–24].

The symptoms of SARS-CoV-2 infection may involve a dry cough, sore throat, tiredness, high fever, anorexia, myalgia, and nasal congestion among others [25]. These symptoms begin increasing gradually, leading to difficulty in breathing and need for hospitalization as they progress. Less than 10% of symptomatic patients have reported headaches, confusion, hemoptysis, rhinorrhea, sore throat, vomiting, and diarrhea [26]. Some persons with SARS-CoV-2 may experience gastrointestinal symptoms, such as diarrhea and nausea, before the onset of fever and lower respiratory tract problems [27]. About 80% of symptomatic patients do not require medical assistance or hospitalization. The rate of mortality reported among patients admitted to the ICU has varied, ranging from 39 to 72%. Survivors have a median hospitalization period of 10–13 days [4].

Two other lethal coronaviruses, SARS-CoV and MERS-CoV, have been found to induce an excessive and unusual immune response of the host cells similar to SARS-CoV-2 [28]. However, unlike SARS-CoV-2, infections caused by these viruses are always accompanied by cytokine storms (an encroachment of the immune system cells and their activating compounds, such as cytokines) that subsequently result in ARDS, thereby producing multiple organ failure and/or death [8]. Even in patients treated for cytokine storms in the ICU, continued inflammation leads to severe pulmonary fibrosis, causing lung dysfunction and substantially reducing the quality of life [8]. The pathogenesis of SARS-CoV-2 is less clear, and many avenues for new therapeutic strategies are being explored and unfortunately, nothing is reliable at this time.

### 3. Immunomodulation by Mesenchymal Stem Cells and/or Their Exosomes

Therapeutic applications of stem cells for a variety of disorders have been explored. As a result, the number of clinical trials conducted with MSCs has increased exponentially over the past few years. MSCs are the most efficient and postindigenous stem cells as they are self-renewable and able to differentiate into multiple genealogies [29, 30]. These stem cells possess atypical characteristics, such as easy isolation and harvesting procedures, pliability, and intrinsic movement toward an injured area (i.e., the process of homing) [31–33]. MSCs have shown antiapoptotic and anti-inflammatory actions in the administrated tissues, and through paracrine secretions, MSCs are responsible for immunomodulatory effects [34, 35]. Furthermore, they are capable of activating other resident stem cells to be utilized in the healing process and can stimulate neo-angiogenesis, tissue repair, and cell survival in surrounding tissues [36] by facilitating tissue regeneration through mechanisms involving their inherent self-renewal and multiple differentiations. These capabilities have rendered MSCs biologically significant and clinically useful for research. Notably, MSCs are free from any ethical

issues and constraints enabling their universal application. MSC therapy has been effectively utilized to cure some disorders, including degenerative, inflammatory, and metabolic diseases, and it has been used to repair and regenerate damaged or lost tissues [30, 31, 37, 38]. Moreover, the therapy has been found to be applicable for treating cancer [39] as well as neurodegenerative disorders [40].

Every stem cell, including MSCs, has a distinctive and intrinsic homing property that moves it toward the site of inflammation in the body. Various studies have indicated that stem cells can repair damaged or diseased tissues, ease inflammation, and modulate the immune system so that the patients' quality of life is improved. These stem cells influence tissue repair via paracrine activities or by direct cell-to-cell contacts. In the case of injury, MSCs migrate toward the injured area, where they generate numerous cells and play an important role in healing via high multiplication, differentiation immunomodulation, and neovascularization induction [36, 37, 41, 42]. Based on their use in successful transplantation therapy, the stem cells are considered a single arrow that can hit multiple targets (i.e., various diseases), resulting in novel therapeutic outcomes [29].

Exosomes are released from all kinds of cells, including stem cells [43]. They have shown molecular similarity with their mother cells; therefore, it has been hypothesized that MSCs-Exo can be administered to the affected area for neovascularization and tissue repair [41]. Exosomes are membrane-enclosed extracellular vesicles (EVs) that have a diameter ranging from 30 to 100 nm. Studies of exosomes have reported that they are stable at low storage temperatures for long periods [44], and this survival rate and stability make them superior to the parent cell [45, 46]. Furthermore, when compared to cellular therapy, exosomes and EVs provide an appealing, prudent, and promising therapeutic strategy because they lack nuclei, which frees them from the risk of tumor formation and any kind of mutation [47]. Despite lacking a nucleus, exosomes have all the essential growth factors and biological signals that help restore damaged tissues [48, 49]. Indeed, analysis of exosomes' genomics and proteomics data found that the quality of their mRNA, miRNA, tRNA, and protein is first rate [50–53].

Experimental studies have shown the efficacy of MSCs and MSCs-Exo in treating pathological conditions, including reducing lung inflammation. For example, when MSCs and MSCs-Exo were injected into pneumonia patients, the pertaining trials exhibited nearly similar therapeutic effects [54, 55]. On the other hand, cell-based inhalation therapy for treating lung infections has also progressed to clinical trials [56, 57]. Additionally, some studies have suggested the immunomodulatory effects of MSCs and MSCs-Exo. An animal model of bronchopulmonary dysplasia showed that exosomes derived from both the umbilical cord and bone marrow reduced inflammation, fibrosis, pulmonary hypertension, and pulmonary vascular modeling, thereby improving lung function [38]. The mechanism involved in these improvements may have been a modulation of the phenotype of macrophages with an increase in the number of immunosuppressive M2 macrophages [38]. Furthermore, peripheral blood mononuclear cells (PBMC) were isolated

from asthmatic patients and treated with bone marrow MSCs-Exo in *in vitro* conditions; this treatment increased the expression of interleukin-10 (IL-10) and transformed growth factor beta 1 (TGF- $\beta$ 1), thus enhancing the function of immunosuppressive regulatory T cells [58]. Moreover, exosomes taken from adipose tissue-derived MSCs were found to reduce atopic dermatitis in an *in vivo* mouse model; this effect was mediated through a reduction in the levels of inflammatory cytokines, eosinophils, infiltrated mast cells, IgE, and CD86+ and CD206+ cells [59].

In a skin-defect mouse model, exosomes from umbilical cord MSCs were found to reduce scar formation and accumulation of myofibroblasts [60], while a rat skin burn model showed that exosomes from umbilical cord MSCs both enhanced the ability of skin wounds to reepithelialize and promoted the ability of skin cells to proliferate and survive [61]. Another study using the rat skin burn model found that umbilical cord MSCs-Exo reduced burn-induced inflammation; this was attributed to the expression of exosomal miRNA-181c [62]. Interestingly, in an *in vivo* model of skeletal muscle injury, bone marrow MSCs-Exo were found to enhance the regeneration of skeletal muscle, which was attributed partly to miRNAs contained in the exosomes [63]. Additionally, pathological damage due to inflammation in a chronic graft-versus-host-disease mouse model was found to be ameliorated by treatment with bone marrow MSCs-Exo through a reduction in the activation and infiltration of CD4+ T cells, suppression of T helper 17 cells, reduction in inflammatory cytokines, and increase in the levels of regulatory T cells [64].

Various studies have estimated that MSCs play a crucial role in tissue regeneration and immunomodulation through their paracrine activity. Moreover, MSCs facilitate antiapoptotic activity, impeding the fibrosis of tissues. One study showed the ability of MSCs to reduce microbial-induced lung injuries in an *in vivo* mice model; they imparted significant contribution against H9N2 and H5N1 viruses in *in vivo* mouse models by reducing the hypersecretion of cytokines into the lungs [65].

The International Society for Cellular and Gene Therapies (ISCT) and the International Society for Extracellular Vesicles (ISEV) do not currently endorse the use of EVs or exosomes for any purpose in COVID-19 due to some valid points before administration to the COVID-19 patients. Although the ISCT and ISEV encourage research and trials of MSCs-Exo, they suggest strict handling and precautionary measures while using MSCs-Exo-related therapies to avoid failure and risk to the subject's health.

The source of the MSCs-Exo is also important as MSCs are a heterogeneous cell entity that can be obtained from different tissues. Even if they are obtained from identical tissues, they may display clone-specific functional differences [66]. Side-by-side comparison of four MSCs-Exo preparations harvested from the conditioned media of different donor-derived bone marrow MSCs showed significant variations in cytokine content (Kordelas et al. 2014). Additionally, the correlation with MSCs' therapeutic potency is poorly understood, and researchers must identify the exact mechanistic action [67].

Like some other viruses, the novel coronavirus enters the host cell through the angiotensin-converting enzyme 2 (ACE2) receptor on the host cell's surface [68]. ACE2 receptors are abundantly present in human blood vessels and act as a cardioregulator. In the lungs, these receptors are present on the alveolar type II cells (AT2). This is the reason that coronavirus mostly attacks the cells of the capillary-permeated lungs [69]. Additionally, the virus can affect any other organ where ACE2 receptors are present, such as the kidneys. Indeed, multiorgan failure in severe cases can even result in patients' deaths.

In this case, MSCs can be deployed to ameliorate SARS-CoV-2-induced hyperinflammation and pathology through their anti-inflammatory activity. As ACE2 receptors are absent on MSCs, MSCs cannot be targeted by COVID-19. Thus, MSCs can be a reliable treatment for overcoming lung injuries and can be involved in the antiviral pathway [70]. Additionally, MSCs can interact with most of the cells of the immune system, such as B cells, T cells, neutrophils, natural killer (NK) cells, dendritic cells (DCs), and macrophages, and thereby moderate these cells' response to pathogens [58, 66]. Moreover, MSCs are stimulated by inflammatory cytokines only when inflammation levels are uncontrollably high. Furthermore, MSC-released cytokines can prohibit neutrophil dissemination and improve macrophage differentiation [71]. Additionally, they can release EVs containing microRNAs, mRNAs, DNA, proteins, and other metabolites that can specifically be delivered into host lung cells, thereby promoting the regeneration and restoration of lung structures and functions [72]. With such astonishing properties, MSCs-Exo could prove to be a promising therapy for COVID-19. The pathogenesis and rescue therapy of MSCs are presented in Figure 1.

#### 4. Recent Studies and Clinical Trials Using Stem Cells against COVID-19-Induced Pathogenesis

Cell-based clinical trials using stem cells—especially MSCs and MSCs-Exo from variable sources like adipose tissue, umbilical cord blood (UCB), Wharton's jelly, and bone marrow—in the treatment of ARDS are undergoing. Indeed, some of the ongoing clinical trials have yet to submit their final reports (see Table 1). The safety of MSC application is being documented, and most reports show low mortality and morbidity rates in COVID-19 patients [73]. One study reported the effectiveness of MSC therapeutic strategies against threatening COVID-19-induced immune system reactions [74]. Moreover, Leng et al. [75] used MSCs to treat seven cases (two common, four severe, and one critically severe case). They showed improvement in the pulmonary functional outcome of all seven patients in day 2 of MSC injection without any adverse effects. Furthermore, Sengupta et al. [76] demonstrated significant reversal of hypoxia and reversal of cytokine storm in patients hospitalized with severe COVID-19 following a single intravenous injection of bone marrow-derived exosomes (ExoFlo), with no adverse effects associated with the treatment. Although the number of COVID-19 patients who underwent MSC or MSC-Exo treatment is very limited and there is a lack of studies elucidating



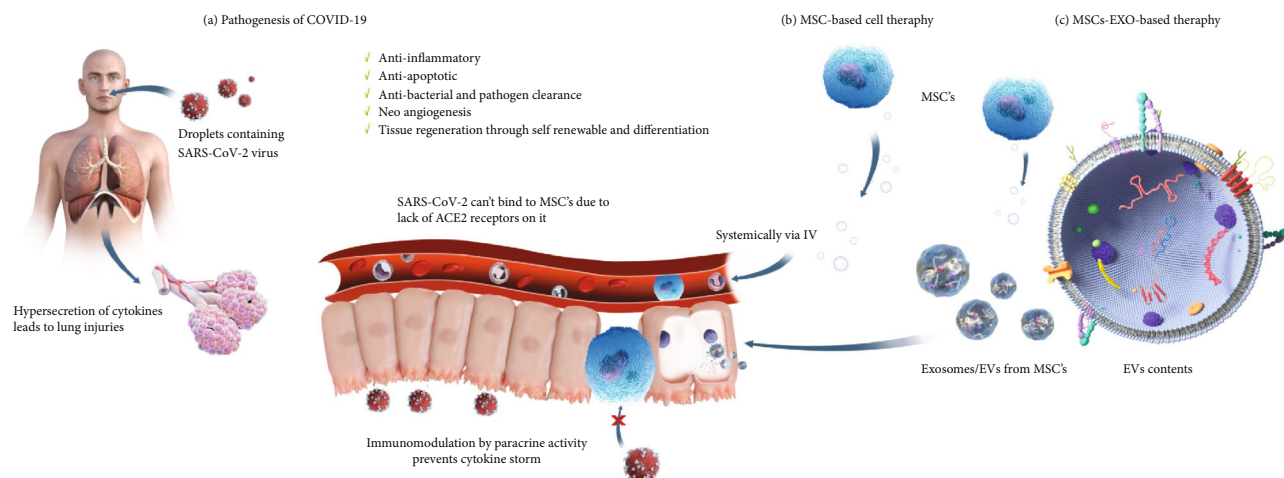


FIGURE 1: Pathogenesis of COVID-19 and stem-cell-based therapy. (a). SARS-CoV-2 enters into the human body via droplets from infected patients. In human cells, SARS-CoV-2 binds with the ACE2 receptors present on host cells and initiates a cytokine storm. This storm results in severe lung injury. (b). MSCs. (c). MSCs-Exo or EVs are considered a possible future treatment due to many of their properties, such as a lack of ACE2 receptors (which prevents a cytokine storm) and immune modulation and restoration of damaged cells due to their essential growth factors and metabolites, see Supplemental Video 1 for the proposed mechanism of MSCs-Exo in treating COVID-19 symptoms.

the underlying mechanisms, these studies showed the potential application of MSC therapy for severe COVID-19 cases. It is worth noted that risks associated with MSC transfusion appear to be uncommon. However, the potential risks might include failure of the cells to work as expected, potential for MSCs to multiply or change into inappropriate cell types, product contamination, growth of tumors, infections, thrombus formation, and administration site reactions [77, 78]. Fortunately, MSC-Exo can overcome these potential risks as they cannot replicate or differentiate [79].

Doctors and researchers from the UAE, USA, Iran, and Jordan are working on stem cell-based therapies for COVID-19, and these ongoing clinical trials are providing important information for the fight against COVID-19. Many studies have shown that MSCs-Exo treat ARDS by suppressing inflammation via modulating the immune systems and thus protect alveolar epithelial cells [54]. MSCs have also shown a positive impact against COVID-19-induced infection (ClinicalTrials.gov, Identifier: NCT04361942); they were found to be efficacious in reducing nonproductive inflammation and in promoting lung regeneration in phase 2 clinical trials (ClinicalTrials.gov, Identifier: NCT03608592), as well as in patients with ARDS in other clinical trials. The clinical trials are listed in Table 1, which summarizes the ongoing clinical trials, their country of origin, their current phase, and the possible working timeline. As shown in the table, some studies are still in the first phase, while others are in their second and third phases.

The recovery of patients is also documented through ClinicalTrials.gov, Identifier NCT04366063. The mortality rate in SARS-CoV-2-related severe ARDS is high despite treatment with antivirals, glucocorticoids, immunoglobulins, and mechanical ventilation. Preclinical and clinical evidence has indicated that MSCs migrate to the lungs and respond to the proinflammatory lung environment by releasing anti-inflammatory factors. Thus, they reduce the proliferation of

proinflammatory cytokines while modulating regulatory T cells and macrophages to promote the resolution of inflammation [58]. Therefore, MSCs may have the potential to increase patients' survival by managing COVID-19 induced ARDS.

The primary objective of the phase-three trial is to appraise the potency and protection of the combination of the MSC remestemcel-L and standard of care compared to the placebo and standard of care in patients with ARDS due to SARS-CoV-2. Additionally, the trial is aimed at monitoring the effect of MSCs on inflammatory biomarkers (ClinicalTrials.gov Identifier: NCT04371393). Earlier research showed that MSCs could significantly reduce inflammatory cell infiltration in lung tissue and prevent lung tissue damage [58, 65], and previous trials (IRCT20200217046526N1) reported the safety of three injections of MSCs in patients infected with COVID-19. The clinical trials also show that MSC administration strongly improves the anti-inflammatory reactions in the body in COVID-19 patients [80]. A recent study (ClinicalTrials.gov, Identifier: NCT04346368) also mentioned the immunomodulatory effect of intravenously administered bone marrow MSCs, which modulated the lung microenvironment in COVID-19 patients. Critically ill COVID-19 patients with ARDS (mild or moderate) will be enrolled in this clinical trial. This multicenter trial will have 60 patients, and all patients in all groups will receive conventional therapy for virus treatment and supportive care for ARDS.

## 5. Summary and Conclusions

Wuhan has reported multiple cases of pneumonia patients infected with the novel coronavirus since December 2019. As of May 22, 2020, 5,223,401 cases of COVID-19 (per the applied case definitions and testing strategies in the affected countries) and 335,205 deaths have been reported (source: <https://www.worldometers.com>). In the future, the total number of cases in the world may exceed 10 million, and



TABLE 1: The available clinical trials (<https://clinicaltrials.gov/>) using MSCs and/or MSCs-Exo to treat COVID-19 patients (last accessed on July 21, 2020).

Status	Study title	Interventions	Country	Registered no.
Recruiting	Treatment of COVID-19 patients using Wharton's jelly-mesenchymal stem cells	WJ-MSCs	Jordan	NCT04313322
Completed	Study evaluating the safety and efficacy of autologous non-hematopoietic peripheral blood stem cells in COVID-19	Autologous nonhematopoietic peripheral blood stem cells (NHPBSC)	United Arab Emirates	NCT04473170
Not yet recruiting	Autologous adipose-derived stem cells (AdMSCs) for COVID-19	Autologous adipose-derived stem cells	United States	NCT04428801
Recruiting	Mesenchymal stem cell infusion for COVID-19 infection	Mesenchymal stem cells	Pakistan	NCT04444271
Recruiting	Safety and efficacy study of allogeneic human dental pulp mesenchymal stem cells to treat severe COVID-19 patients	Allogeneic human dental pulp stem cells (BSH BTC & Utooth BTC)	China	NCT04336254
Not yet recruiting	Safety and efficacy of mesenchymal stem cells in the management of severe COVID-19 pneumonia	Umbilical cord-derived mesenchymal stem cells	Spain	NCT04429763
Recruiting	MSCs in COVID-19 ARDS	Mesenchymal stromal cells	United States	NCT04371393
Recruiting	Human umbilical cord mesenchymal stem cells (MSCs) therapy in ARDS (ARDS)	Umbilical cord-derived mesenchymal stem cell (UCMSCs) suspension	China	NCT03608592
Recruiting	Mesenchymal stem cell for acute respiratory distress syndrome due for COVID-19	Infusion IV of mesenchymal stem cells	Mexico	NCT04416139
Not yet recruiting	NestaCell® mesenchymal stem cell to treat patients with severe COVID-19 pneumonia	NestaCell®	Brazil	NCT04315987
Enrolling by invitation	A randomized, double-blind, placebo-controlled clinical trial to determine the safety and efficacy of Hope Biosciences Allogeneic Mesenchymal Stem Cell Therapy (HB-adMSCs) to provide protection against COVID-19	HB-adMSCs	United States	NCT04348435
Active, not recruiting	Use of mesenchymal stem cells in acute respiratory distress syndrome caused by COVID-19	Mesenchymal stem cells derived from Wharton jelly of umbilical cords	Mexico	NCT04456361
Recruiting	Clinical trial to assess the safety and efficacy of intravenous administration of allogeneic adult mesenchymal stem cells of expanded adipose tissue in patients with severe pneumonia due to COVID-19	Allogeneic and expanded adipose tissue-derived mesenchymal stem cells	Spain	NCT04366323
Enrolling by invitation	A clinical trial to determine the safety and efficacy of Hope Biosciences Autologous Mesenchymal Stem Cell Therapy (HB-adMSCs) to provide protection against COVID-19	HB-adMSCs	United States	NCT04349631
Not yet recruiting	Novel coronavirus induced severe pneumonia treated by dental pulp mesenchymal stem cells	Dental pulp mesenchymal stem cells	China	NCT04302519
Recruiting	Mesenchymal stem cell treatment for pneumonia patients infected with COVID-19	MSCs	China	NCT04252118
Not yet recruiting	Bone marrow-derived mesenchymal stem cell treatment for severe patients with coronavirus disease 2019 (COVID-19)	BM-MSCs	China	NCT04346368
Active, not recruiting	Treatment with human umbilical cord-derived mesenchymal stem cells for severe corona virus disease 2019 (COVID-19)	UC-MSCs	China	NCT04288102
Not yet recruiting	Study of human umbilical cord mesenchymal stem cells in the treatment of severe COVID-19	UC-MSCs	China	NCT04273646
Recruiting	Efficacy of intravenous infusions of stem cells in the treatment of COVID-19 patients	Intravenous infusions of stem cells	Pakistan	NCT04437823

TABLE 1: Continued.

Status	Study title	Interventions	Country	Registered no.
Enrolling by invitation	Treatment of Covid-19 associated pneumonia with allogenic pooled olfactory mucosa-derived Mesenchymal stem cells	Allogenic pooled olfactory mucosa-derived mesenchymal stem cells	Belarus	NCT04382547
Recruiting	Clinical research of human mesenchymal stem cells in the treatment of COVID-19 pneumonia	UC-MSCs	China	NCT04339660
Active, not recruiting	Safety and effectiveness of mesenchymal stem cells in the treatment of pneumonia of coronavirus disease 2019	Mesenchymal stem cells	China	NCT04371601
Recruiting	Mesenchymal stem cell therapy for SARS-CoV-2-related acute respiratory distress syndrome	Cell therapy protocol 1 Cell therapy protocol 2	Iran	NCT04366063
Active, not recruiting	Role of immune and inflammatory response in recipients of allogeneic haematopoietic stem cell transplantation (SCT) affected by severe COVID19		United Kingdom	NCT04349540
Recruiting	Administration of allogenic UC-MSCs as adjuvant therapy for critically-ill COVID-19 patients	Umbilical cord mesenchymal stem cells	Indonesia	NCT04457609
Recruiting	Use of UC-MSCs for COVID-19 patients	Umbilical cord mesenchymal stem cells	United States	NCT04355728
Recruiting	Efficacy and safety study of allogeneic HB-adMSCs for the treatment of COVID-19	HB-adMSC	United States	NCT04362189
Recruiting	Clinical use of stem cells for the treatment of Covid-19	MSC treatment	Turkey	NCT04392778
Not yet recruiting	Stem cell educator therapy treat the viral inflammation in COVID-19	Combination product: stem cell educator-treated mononuclear cells apheresis	United States	NCT04299152
Recruiting	Treatment of coronavirus COVID-19 pneumonia (pathogen SARS-CoV-2) with cryopreserved allogeneic P_MMSCs and UC-MMSCs	Placenta-derived MMSCs; cryopreserved placenta-derived multipotent mesenchymal stromal cells	Ukraine	NCT04461925
Not yet recruiting	BAttLe against COVID-19 using mesenchymal stromal cells	Allogeneic and expanded adipose tissue-derived mesenchymal stromal cells	United States	NCT04348461
Not yet recruiting	Safety and efficacy of intravenous Wharton's jelly derived mesenchymal stem cells in acute respiratory distress syndrome due to COVID 19	Wharton's jelly-derived mesenchymal stem cells	Colombia	NCT04390152
Not yet recruiting	Use of hUC-MSC product (BX-U001) for the treatment of COVID-19 with ARDS	Human umbilical cord mesenchymal stem cells	United States	NCT04452097
Recruiting	Pediatrics HOT COVID-19 database in NY tristate		United States	NCT04445402
Not yet recruiting	Using PRP and cord blood in treatment of Covid -19	Stem cells	Egypt	NCT04393415
Not yet recruiting	Study of the safety of therapeutic Tx with Immunomodulatory MSC in adults with COVID-19 infection requiring mechanical ventilation	BM-Allo.MSC	United States	NCT04397796
Recruiting	Safety and efficacy of CAStem for severe COVID-19 associated with/without ARDS	CAStem	China	NCT04331613
Recruiting	Mesenchymal stromal cell therapy for the treatment of acute respiratory distress syndrome	Mesenchymal stromal stem cells—KI-MSC-PL-205	Sweden	NCT04447833

TABLE 1: Continued.

Status	Study title	Interventions	Country	Registered no.
Not yet recruiting	Mesenchymal stem cells (MSCs) in inflammation-resolution programs of coronavirus disease 2019 (COVID-19) induced acute respiratory distress syndrome (ARDS)	MSC	Germany	NCT04377334
Recruiting	Efficacy and safety evaluation of mesenchymal stem cells for the treatment of patients with respiratory distress due to COVID-19	XCEL-UMC-BETA	Spain	NCT04390139
Not yet recruiting	Cellular immuno-therapy for COVID-19 acute respiratory distress syndrome—vanguard	Mesenchymal stromal cells	Canada	NCT04400032
Not yet recruiting	ACT-20 in patients with severe COVID-19 pneumonia	ACT-20-MSC	United States	NCT04398303
Not yet recruiting	Safety and feasibility of allogenic MSC in the treatment of COVID-19	Mesenchymal stromal cell infusion	Brazil	NCT04467047
Recruiting	Repair of acute respiratory distress syndrome by stromal cell administration (REALIST) (COVID-19)	Human umbilical cord-derived CD362 enriched MSCs	United Kingdom	NCT03042143
Not yet recruiting	Mesenchymal stromal cells for the treatment of SARS-CoV-2 induced acute respiratory failure (COVID-19 disease)	Mesenchymal stromal cells	United States	NCT04345601
Recruiting	Treatment of severe COVID-19 pneumonia with allogeneic mesenchymal stromal cells (COVID_MSV)	Mesenchymal stromal cells	Spain	NCT04361942
Recruiting	Double-blind, multicenter, study to evaluate the efficacy of PLX PAD for the treatment of COVID-19	PLX-PAD	United States	NCT04389450
Recruiting	Umbilical cord(UC)-derived Mesenchymal stem cells(MSCs) treatment for the 2019-novel coronavirus (nCOV) pneumonia	UC-MSCs	China	NCT04269525
Recruiting	Cell therapy using umbilical cord-derived mesenchymal stromal cells in SARS-CoV-2-related ARDS	Umbilical cord Wharton's jelly-derived human	France	NCT04333368
Recruiting	MultiStem administration for COVID-19 induced ARDS (MACoVIA)	MultiStem	United States	NCT04367077
Not yet recruiting	Multiple dosing of mesenchymal stromal cells in patients with ARDS (COVID-19)	Mesenchymal stromal cells	United States	NCT04466098
Not yet recruiting	A pilot clinical study on inhalation of mesenchymal stem cells exosomes treating severe novel coronavirus pneumonia	MSCs-derived exosomes	China	NCT04276987
Not yet recruiting	A study to collect bone marrow for process development and production of BM-MSC to treat severe COVID19 pneumonitis	Bone marrow harvest	United Kingdom	NCT04397471
Not yet recruiting	Organicell flow for patients with COVID-19	Organicell flow (human amniotic fluid contain growth factors, cytokines, and chemokines as well as other extracellular vesicles/ nanoparticles derived from amniotic stem and epithelial cells)	United States	NCT04384445

deaths may be around 3.4% of the total cases in most countries. Based on current data, 10–15% of the affected individuals will develop a severe form of the disease, requiring hospitalization and respiratory support. Thus, the COVID-19 pandemic is a public health emergency.

At present, no effective therapeutic strategy against COVID-19-induced pneumonia exists, especially for the severe and critical cases, and immediate therapy with mini-

mal side effects is needed to overcome the crisis. Preclinical and clinical data support the investigational use of MSCs-Exo/EVs because of their anti-inflammatory and immunomodulatory responses. Moreover, lack of ethical restrictions, high availability, and easy isolation procedures are the key benefits of using MSCs-Exo-based therapy.

Intravenously infused stem cells provide a reliable alternative in terms of accumulation on the targeted site,

multiplication, and differentiation due to paracrine activity. As the lungs are the primary organ infected by COVID-19, intravenous administration of MSCs-Exo may target the lungs to rescue the infected site from severe injury by providing immunomodulatory effects. Moreover, the noninvasive and economical qualities of MSCs make them an attractive therapeutic candidate for COVID-19.

The purpose of this review was to investigate the efficiency and safety of MSCs, especially MSCs-Exo, in treating patients with severe pneumonia infected with SARS-CoV-2. As recently recommended, MSCs should also be clinically validated for treating severe cases of MERS, for which mortality rates are up to 34% [74, 81]. Based on the clinical trials on COVID-19, this review encourages further research into the use of MSCs and/or EVs for treating COVID-19 after strictly following appropriate manufacturing procedures, quality control measurements, preclinical safety and efficacy data, and proper ethical regulations.

### Data Availability

All data are available in the manuscript.

### Conflicts of Interest

The authors declare that there is no conflict of interests regarding the publication of this paper.

### Authors' Contributions

Faisal A. Alzahrani and Islam M. Saadeldin contributed equally to this work.

### Acknowledgments

This research was supported by King Abdulaziz City for Science and Technology (KACST) under project number 5-20-01-009-0067. Special thanks also to Mister Ahmed Al-Zahrani for producing the figure.

### Supplementary Materials

Video. 1: this video show the possible mechanism of MSCs-Exo for treating COVID-19 symptoms. (*Supplementary Materials*)

### References

- [1] N. Zhu, D. Zhang, W. Wang et al., "A novel coronavirus from patients with pneumonia in China, 2019," *New England Journal of Medicine*, vol. 382, no. 8, pp. 727–733, 2020.
- [2] CDC COVID-19 Response Team, S. Bialek, E. Boundy et al., "Severe outcomes among patients with coronavirus disease 2019 (COVID-19)—United States, February 12–March 16, 2020," *MMWR. Morbidity and Mortality Weekly Report*, vol. 69, no. 12, pp. 343–346, 2020.
- [3] A. E. Gorbalenya, S. C. Baker, R. S. Baric et al., "Severe acute respiratory syndrome-related coronavirus: The species and its viruses – a statement of the Coronavirus Study Group," *BioRxiv*, 2020.
- [4] R. Verity, L. C. Okell, I. Dorigatti et al., "Estimates of the severity of coronavirus disease 2019: a model-based analysis," *The Lancet Infectious Diseases*, vol. 20, no. 6, pp. 669–677, 2020.
- [5] V. J. Munster, M. Koopmans, N. van Doremalen, D. van Riel, and E. de Wit, "A novel coronavirus emerging in China — key questions for impact assessment," *New England Journal of Medicine*, vol. 382, no. 8, pp. 692–694, 2020.
- [6] L.-s. Wang, Y.-r. Wang, D. Ye, and Q. Liu, "review of the 2019 novel coronavirus (SARS-CoV-2) based on current evidence," *International journal of antimicrobial agents*, vol. 55, no. 6, article 105948, 2020.
- [7] H. Wang, X. Li, T. Li et al., "The genetic sequence, origin, and diagnosis of SARS-CoV-2," *European journal of clinical microbiology & infectious diseases : official publication of the European Society of Clinical Microbiology*, vol. 39, no. 9, pp. 1629–1635, 2020.
- [8] P. Mehta, D. F. McAuley, M. Brown et al., "COVID-19: consider cytokine storm syndromes and immunosuppression," *The Lancet*, vol. 395, no. 10229, pp. 1033–1034, 2020.
- [9] Y. Han, H. Zhang, S. Mu et al., "Lactate dehydrogenase, a risk factor of severe COVID-19 patients," *medRxiv*, 2020.
- [10] R. Suman, M. Javaid, A. Haleem, R. Vaishya, S. Bahl, and D. Nandan, "Sustainability of coronavirus on different surfaces," *Journal of Clinical and Experimental Hepatology*, vol. 10, no. 4, pp. 386–390, 2020.
- [11] S. G. Campbell and T. Marrie, "Diagnosis and treatment of community-acquired pneumonia," in *Evidence-Based Emergency Medicine*, pp. 100–102, 2008.
- [12] S. P. Adhikari, S. Meng, Y.-J. Wu et al., "Epidemiology, causes, clinical manifestation and diagnosis, prevention and control of coronavirus disease (COVID-19) during the early outbreak period: a scoping review," *Infectious diseases of poverty*, vol. 9, no. 1, p. 29, 2020.
- [13] T. Singhal, "A review of coronavirus disease-2019 (COVID-19)," *The Indian Journal of Pediatrics*, vol. 87, no. 4, pp. 281–286, 2020.
- [14] C. Rodriguez and C. Veciana, "The global helminth belt and COVID-19: the new eosinophilic link," *Qeios*, 2020.
- [15] L. Chen, J. Xiong, L. Bao, and Y. Shi, "Convalescent plasma as a potential therapy for COVID-19," *The Lancet Infectious Diseases*, vol. 20, no. 4, pp. 398–400, 2020.
- [16] K. Duan, B. Liu, C. Li et al., "Effectiveness of convalescent plasma therapy in severe COVID-19 patients," *Proceedings of the National Academy of Sciences*, vol. 117, no. 17, pp. 9490–9496, 2020.
- [17] C. Shen, Z. Wang, F. Zhao et al., "Treatment of 5 critically ill patients with COVID-19 with convalescent plasma," *Journal of the American Medical Association*, vol. 323, no. 16, p. 1582, 2020.
- [18] A. Pen and U. B. Jensen, "Current status of treating neurodegenerative disease with induced pluripotent stem cells," *Acta Neurologica Scandinavica*, vol. 135, no. 1, pp. 57–72, 2017.
- [19] D. Gerace, R. Martiniello-Wilks, N. T. Nassif, B. Ren, and A. M. Simpson, "Ex vivo Expanded Murine Mesenchymal Stem Cells as Targets for the Generation of a Cell Replacement Therapy for Type 1 Diabetes," *77th Scientific Sessions of the American-Diabetes-Association*, 2017.
- [20] S. H. Nile, A. Nile, J. Qiu, L. Li, X. Jia, and G. Kai, "COVID-19: pathogenesis, cytokine storm and therapeutic potential of



- interferons,” *Cytokine & Growth Factor Reviews*, vol. 53, pp. 66–70, 2020.
- [21] H. M. Ashour, W. F. Elkhatib, M. Rahman, and H. A. Elshabrawy, “Insights into the recent 2019 novel coronavirus (SARS-CoV-2) in light of past human coronavirus outbreaks,” *Pathogens*, vol. 9, no. 3, p. 186, 2020.
- [22] P. Wikramaratna, R. S. Paton, M. Ghafari, and J. Lourenco, “Estimating false-negative detection rate of SARS-CoV-2 by RT-PCR,” *Medrxiv*, 2020.
- [23] A. W. Byrne, D. McEvoy, A. Collins et al., “Inferred duration of infectious period of SARS-CoV-2: rapid scoping review and analysis of available evidence for asymptomatic and symptomatic COVID-19 cases,” *medRxiv*, 2020.
- [24] X. Wang, H. Yao, X. Xu et al., “Limits of Detection of 6 Approved RT-PCR Kits for the Novel SARS-Coronavirus-2 (SARS-CoV-2),” *Clinical Chemistry*, vol. 66, no. 7, pp. 977–979, 2020.
- [25] J. Krajewska, W. Krajewski, K. Zub, and T. Zatoński, “COVID-19 in otolaryngologist practice: a review of current knowledge,” *European Archives of Oto-Rhino-Laryngology*, vol. 277, no. 7, pp. 1885–1897, 2020.
- [26] M. Khalili, M. Karamouzian, N. Nasiri, S. Javadi, A. Mirzazadeh, and H. Sharifi, “Epidemiological characteristics of COVID-19: a systemic review and meta-analysis,” *Epidemiology Infection*, vol. 148, 2020.
- [27] L. Pan, M. Mu, P. Yang et al., “Clinical characteristics of COVID-19 patients with digestive symptoms in Hubei, China: a descriptive, cross-sectional, multicenter study,” *The American journal of gastroenterology*, vol. 115, no. 5, pp. 766–773, 2020.
- [28] E. Prompetchara, C. Ketloy, and T. Palaga, “Immune responses in COVID-19 and potential vaccines: lessons learned from SARS and MERS epidemic,” *Asian Pacific Journal of Allergy and Immunology*, vol. 38, no. 1, pp. 1–9, 2020.
- [29] S. Viswanathan, Y. Shi, J. Galipeau et al., “Mesenchymal stem versus stromal cells: International Society for Cell & Gene Therapy (ISCT®) Mesenchymal Stromal Cell committee position statement on nomenclature,” *Cytotherapy*, vol. 21, no. 10, pp. 1019–1024, 2019.
- [30] A. I. Caplan, “Mesenchymal stem cells,” *Journal of orthopaedic research*, vol. 9, no. 5, pp. 641–650, 1991.
- [31] W. Lin, L. Xu, S. Zwingersberger, E. Gibon, S. B. Goodman, and G. Li, “Mesenchymal stem cells homing to improve bone healing,” *Journal of orthopaedic translation*, vol. 9, pp. 19–27, 2017.
- [32] P. Conaty, L. S. Sherman, Y. Naaldijk, H. Ulrich, A. Stolzing, and P. Rameshwar, “Methods of mesenchymal stem cell homing to the blood–brain barrier,” in *Somatic Stem Cells*, pp. 81–91, Springer, 2018.
- [33] S. Grad, S. Wangler, M. Peroglio et al., “Homing of mesenchymal stem cells into degenerative intervertebral disc: effect on disc cell survival,” *Orthopaedic Proceedings*, vol. 101-B, Supplement 10, 2019.
- [34] N. Su, P.-L. Gao, K. Wang, J.-Y. Wang, Y. Zhong, and Y. Luo, “Fibrous scaffolds potentiate the paracrine function of mesenchymal stem cells: a new dimension in cell-material interaction,” *Biomaterials*, vol. 141, pp. 74–85, 2017.
- [35] G. Zheng, R. Huang, G. Qiu et al., “Mesenchymal stromal cell-derived extracellular vesicles: regenerative and immunomodulatory effects and potential applications in sepsis,” *Cell and tissue research*, vol. 374, no. 1, pp. 1–15, 2018.
- [36] A. Pansky, B. Roitzheim, and E. Tobiasch, “Differentiation potential of adult human mesenchymal stem cells,” *Clinical Laboratory*, vol. 53, no. 1–2, pp. 81–84, 2007.
- [37] A. Carreras, I. Almendros, J. M. Montserrat, D. Navajas, and R. Farre, “Mesenchymal stem cells reduce inflammation in a rat model of obstructive sleep apnea,” *Respiratory physiology & neurobiology*, vol. 172, no. 3, pp. 210–212, 2010.
- [38] G. R. Willis, A. Fernandez-Gonzalez, J. Anastas et al., “Mesenchymal stromal cell exosomes ameliorate experimental bronchopulmonary dysplasia and restore lung function through macrophage immunomodulation,” *American Journal of Respiratory and Critical Care Medicine*, vol. 197, no. 1, pp. 104–116, 2018.
- [39] S. Mandal, F. Arfuso, G. Sethi, A. Dharmarajan, and S. Warriar, “Encapsulated human mesenchymal stem cells (eMSCs) as a novel anti-cancer agent targeting breast cancer stem cells: development of 3D primed therapeutic MSCs,” *The international journal of biochemistry & cell biology*, vol. 110, pp. 59–69, 2019.
- [40] S. Jahan, D. Kumar, A. Kumar et al., “Neurotrophic factor mediated neuronal differentiation of human cord blood mesenchymal stem cells and their applicability to assess the developmental neurotoxicity,” *Biochemical and biophysical research communications*, vol. 482, no. 4, pp. 961–967, 2017.
- [41] K. Pill, S. Hofmann, H. Redl, and W. Holnthoner, “Vascularization mediated by mesenchymal stem cells from bone marrow and adipose tissue: a comparison,” *Cell regeneration*, vol. 4, no. 1, p. 4:8, 2015.
- [42] S. T. Lee, K. Chu, K. H. Jung et al., “Anti-inflammatory mechanism of intravascular neural stem cell transplantation in haemorrhagic stroke,” *Brain*, vol. 131, no. 3, pp. 616–629, 2008.
- [43] L. Cheng, K. Zhang, S. Wu, M. Cui, and T. Xu, “Focus on mesenchymal stem cell-derived exosomes: opportunities and challenges in cell-free therapy,” *Stem cells international*, vol. 2017, 10 pages, 2017.
- [44] N. Kumeda, Y. Ogawa, Y. Akimoto, H. Kawakami, M. Tsujimoto, and R. Yanoshita, “Characterization of membrane integrity and morphological stability of human salivary exosomes,” *Biological and Pharmaceutical Bulletin*, vol. 40, no. 8, pp. 1183–1191, 2017.
- [45] F. A. Alzahrani, M. A. El-Magd, A. Abdelfattah-Hassan et al., “Potential effect of exosomes derived from cancer stem cells and MSCs on progression of DEN-induced HCC in rats,” *Stem Cells International*, vol. 2018, Article ID 8058979, 17 pages, 2018.
- [46] L. Lv, Q. Zeng, S. Wu et al., “Chapter 8 - exosome-based translational nanomedicine: the therapeutic potential for drug delivery,” in *Mesenchymal Stem Cell Derived Exosomes*, Y. Tang and B. Dawn, Eds., pp. 161–176, Academic Press, Boston, 2015.
- [47] C. Liu and C. Su, “Design strategies and application progress of therapeutic exosomes,” *Theranostics*, vol. 9, no. 4, pp. 1015–1028, 2019.
- [48] M. Adamiak, G. Cheng, S. Bobis-Wozowicz et al., “Induced pluripotent stem cell (iPSC)-derived extracellular vesicles are safer and more effective for cardiac repair than iPSCs,” *Circulation research*, vol. 122, no. 2, pp. 296–309, 2018.
- [49] M. Nishiga, H. Guo, and J. C. Wu, “Induced pluripotent stem cells as a biopharmaceutical factory for extracellular vesicles,” *European heart journal*, vol. 39, no. 20, pp. 1848–1850, 2018.
- [50] R. C. Lai, S. S. Tan, B. J. Teh et al., “Proteolytic potential of the MSC exosome proteome: implications for an exosome-

- mediated delivery of therapeutic proteasome,” *International Journal of Proteomics*, vol. 2012, 14 pages, 2012.
- [51] T. S. Chen, R. C. Lai, M. M. Lee, A. B. H. Choo, C. N. Lee, and S. K. Lim, “Mesenchymal stem cell secretes microparticles enriched in pre-microRNAs,” *Nucleic acids research*, vol. 38, no. 1, pp. 215–224, 2010.
- [52] H. Valadi, K. Ekström, A. Bossios, M. Sjöstrand, J. J. Lee, and J. O. Lötvall, “Exosome-mediated transfer of mRNAs and microRNAs is a novel mechanism of genetic exchange between cells,” *Nature cell biology*, vol. 9, no. 6, pp. 654–659, 2007.
- [53] S. R. Baglio, K. Rooijers, D. Koppers-Lalic et al., “Human bone marrow-and adipose-mesenchymal stem cells secrete exosomes enriched in distinctive miRNA and tRNA species,” *Stem cell research & therapy*, vol. 6, no. 1, 2015.
- [54] F. F. Cruz and P. R. M. Rocco, “Stem-cell extracellular vesicles and lung repair,” *Stem Cell Investigation*, vol. 4, no. 9, p. 78, 2017.
- [55] Y. Li, Z. Yin, J. Fan, S. Zhang, and W. Yang, “The roles of exosomal miRNAs and lncRNAs in lung diseases,” *Signal Transduction and Targeted Therapy*, vol. 4, no. 1, 2019.
- [56] B. H. Yahaya, “ID2008 Aerosol-based cell delivery as an innovative treatment for lung diseases,” *Biomedical Research and Therapy*, vol. 4, p. 41, 2017.
- [57] E. Kardia, N. S. S. A. Halim, and B. H. Yahaya, “Aerosol-based cell therapy for treatment of lung diseases,” *Stem Cell Heterogeneity*, pp. 243–255, 2016.
- [58] Y. M. Du, Y. X. Zhuansun, R. Chen, L. Lin, Y. Lin, and J. G. Li, “Mesenchymal stem cell exosomes promote immunosuppression of regulatory T cells in asthma,” *Experimental Cell Research*, vol. 363, no. 1, pp. 114–120, 2018.
- [59] B. S. Cho, J. O. Kim, D. H. Ha, and Y. W. Yi, “Exosomes derived from human adipose tissue-derived mesenchymal stem cells alleviate atopic dermatitis,” *Stem Cell Research & Therapy*, vol. 9, no. 1, p. 187, 2018.
- [60] S. Fang, C. Xu, Y. Zhang et al., “Umbilical cord-derived mesenchymal stem cell-derived exosomal microRNAs suppress myofibroblast differentiation by inhibiting the transforming growth factor- $\beta$ /SMAD2 pathway during wound healing,” *Stem Cells Translational Medicine*, vol. 5, no. 10, pp. 1425–1439, 2016.
- [61] B. Zhang, M. Wang, A. Gong et al., “HucMSC-exosome mediated-Wnt4 signaling is required for cutaneous wound healing,” *Stem Cells*, vol. 33, no. 7, pp. 2158–2168, 2015.
- [62] X. Li, L. Liu, J. Yang et al., “Exosome derived from human umbilical cord mesenchymal stem cell mediates MiR-181c attenuating burn-induced excessive inflammation,” *eBioMedicine*, vol. 8, pp. 72–82, 2016.
- [63] Y. Nakamura, S. Miyaki, H. Ishitobi et al., “Mesenchymal-stem-cell-derived exosomes accelerate skeletal muscle regeneration,” *FEBS Letters*, vol. 589, no. 11, pp. 1257–1265, 2015.
- [64] P. Lai, X. Chen, L. Guo et al., “A potent immunomodulatory role of exosomes derived from mesenchymal stromal cells in preventing cGVHD,” *Journal of Hematology & Oncology*, vol. 11, no. 1, p. 135, 2018.
- [65] Y. Li, J. Xu, W. Shi et al., “Mesenchymal stromal cell treatment prevents H9N2 avian influenza virus-induced acute lung injury in mice,” *Stem cell research & therapy*, vol. 7, no. 1, p. 159, 2016.
- [66] P. Martínez-Peinado, S. Pascual-García, E. Roche, and J. M. Sempere-Ortells, “Differences of clonogenic mesenchymal stem cells on immunomodulation of lymphocyte subsets,” *Journal of Immunology Research*, vol. 2018, 11 pages, 2018.
- [67] V. Börger, D. J. Weiss, J. D. Anderson et al., “International Society for Extracellular Vesicles and International Society for Cell and Gene Therapy statement on extracellular vesicles from mesenchymal stromal cells and other cells: considerations for potential therapeutic agents to suppress coronavirus disease-19,” *Cytotherapy*, vol. 22, no. 9, pp. 482–485, 2020.
- [68] L. Du, Y. He, Y. Zhou, S. Liu, B.-J. Zheng, and S. Jiang, “The spike protein of SARS-CoV—a target for vaccine and therapeutic development,” *Nature Reviews Microbiology*, vol. 7, no. 3, pp. 226–236, 2009.
- [69] K. Kuba, Y. Imai, T. Ohto-Nakanishi, and J. M. Penninger, “Trilogy of ACE2: a peptidase in the renin-angiotensin system, a SARS receptor, and a partner for amino acid transporters,” *Pharmacology & therapeutics*, vol. 128, no. 1, pp. 119–128, 2010.
- [70] A. K. Shetty, “Mesenchymal stem cell infusion shows promise for combating coronavirus (COVID-19)-induced pneumonia,” *Aging and disease*, vol. 11, no. 2, pp. 462–464, 2020.
- [71] B. Fazekas and M. D. Griffin, “Mesenchymal stromal cell-based therapies for acute kidney injury: progress in the last decade,” *Kidney International*, vol. 97, no. 6, pp. 1130–1140, 2020.
- [72] S. L. Maas, X. O. Breakefield, and A. M. Weaver, “Extracellular vesicles: unique intercellular delivery vehicles,” *Trends in cell biology*, vol. 27, no. 3, pp. 172–188, 2017.
- [73] M. Tobaiqy, M. Qashqary, S. Al-Dahery et al., “Therapeutic management of patients with COVID-19: a systematic review,” *Infection Prevention in Practice*, vol. 2, no. 3, article 100061, 2020.
- [74] A. Zumla, F.-S. Wang, G. Ippolito et al., “Reducing mortality and morbidity in patients with severe COVID-19 disease by advancing ongoing trials of mesenchymal stromal (stem) cell (MSC) therapy - achieving global consensus and visibility for cellular host-directed therapies,” *International Journal of Infectious Diseases*, vol. 96, pp. 431–439, 2020.
- [75] Z. Leng, R. Zhu, W. Hou et al., “Transplantation of ACE2(-) mesenchymal stem cells improves the outcome of patients with COVID-19 pneumonia,” *Aging and Disease*, vol. 11, no. 2, pp. 216–228, 2020.
- [76] V. Sengupta, S. Sengupta, A. Lazo, P. Woods, A. Nolan, and N. Bremer, “Exosomes derived from bone marrow mesenchymal stem cells as treatment for severe COVID-19,” *Stem Cells and Development*, vol. 29, no. 12, pp. 747–754, 2020.
- [77] P. CfDca, *Stem cell and exosome products*, 2020, July 2020 <https://www.cdca.gov/hai/outbreaks/stem-cell-products.html>.
- [78] S. S. Raza, P. Seth, and M. A. Khan, “Primed’ mesenchymal stem cells: a potential novel therapeutic for COVID19 patients,” *Stem Cell Reviews and Reports*, vol. 2020, pp. 1–10, 2020.
- [79] A. Tsuchiya, S. Takeuchi, T. Iwasawa et al., “Therapeutic potential of mesenchymal stem cells and their exosomes in severe novel coronavirus disease 2019 (COVID-19) cases,” *Inflammation and Regeneration*, vol. 40, no. 1, 2020.
- [80] Q. Ye, B. Wang, and J. Mao, “The pathogenesis and treatment of the ‘cytokine storm’ in COVID-19,” *The Journal of infection*, vol. 80, no. 6, pp. 607–613, 2020.
- [81] Z. A. Memish, S. Perlman, M. D. Van Kerkhove, and A. Zumla, “Middle East respiratory syndrome,” *The Lancet*, vol. 395, no. 10229, pp. 1063–1077, 2020.

## Research Article

# Myocardin-Related Transcription Factor A (MRTF-A) Regulates the Balance between Adipogenesis and Osteogenesis of Human Adipose Stem Cells

Laura Hyväri,<sup>1,2</sup> Sari Vanhatupa,<sup>1</sup> Heidi T. Halonen,<sup>3</sup> Minna Kääriäinen ,<sup>4</sup>  
and Susanna Miettinen <sup>1,2</sup>

<sup>1</sup>Adult Stem Cell Group, Faculty of Medicine and Health Technology, Tampere University, Tampere, Finland

<sup>2</sup>Research, Development and Innovation Centre, Tampere University Hospital, Tampere, Finland

<sup>3</sup>Computational Biophysics and Imaging Group, Faculty of Medicine and Health Technology, Tampere University, Tampere, Finland

<sup>4</sup>Department of Plastic and Reconstructive Surgery, Tampere University Hospital, Tampere, Finland

Correspondence should be addressed to Susanna Miettinen; [susanna.miettinen@tuni.fi](mailto:susanna.miettinen@tuni.fi)

Received 7 June 2020; Revised 19 August 2020; Accepted 26 August 2020; Published 22 September 2020

Academic Editor: Huseyin Sumer

Copyright © 2020 Laura Hyväri et al. This is an open access article distributed under the Creative Commons Attribution License, which permits unrestricted use, distribution, and reproduction in any medium, provided the original work is properly cited.

Previous studies have demonstrated that myocardin-related transcription factor A (MRTF-A) generates a link between the dynamics of the actin cytoskeleton and gene expression with its coregulator, serum response factor (SRF). MRTF-A has also been suggested as a regulator of stem cell differentiation. However, the role of MRTF-A in human mesenchymal stem cell differentiation remains understudied. We aimed to elucidate whether MRTF-A is a potential regulator of human adipose stem cell (hASC) differentiation towards adipogenic and osteogenic lineages. To study the role of MRTF-A activity in the differentiation process, hASCs were cultured in adipogenic and osteogenic media supplemented with inhibitor molecules CCG-1423 or CCG-100602 that have been shown to block the expression of MRTF-A/SRF-activated genes. Our results of image-based quantification of Oil Red O stained lipid droplets and perilipin 1 staining denote that MRTF-A inhibition enhanced the adipogenic differentiation. On the contrary, MRTF-A inhibition led to diminished activity of an early osteogenic marker alkaline phosphatase, and export of extracellular matrix (ECM) proteins collagen type I and osteopontin. Also, quantitative Alizarin Red staining representing ECM mineralization was significantly decreased under MRTF-A inhibition. Image-based analysis of Phalloidin staining revealed that MRTF-A inhibition reduced the F-actin formation and parallel orientation of the actin filaments. Additionally, MRTF-A inhibition affected the protein amounts of  $\alpha$ -smooth muscle actin ( $\alpha$ -SMA), myosin light chain (MLC), and phosphorylated MLC suggesting that MRTF-A would regulate differentiation through SRF activity. Our results strongly indicate that MRTF-A is an important regulator of the balance between osteogenesis and adipogenesis of hASCs through its role in mediating the cytoskeletal dynamics. These results provide MRTF-A as a new interesting target for guiding the stem cell differentiation in tissue engineering applications for regenerative medicine.

## 1. Introduction

The actin cytoskeleton of a cell is continuously modified to allow dynamic cell functions such as stem cell differentiation [1, 2]. Actin dynamics are accomplished by continuous actin turnover and treadmilling regulated by Rho GTPase RhoA-Rho-associated coiled-coil kinase (Rho-ROCK) pathway [3, 4]. RhoA-ROCK pathway has also been reported to regulate the fate decision of mesenchymal stem cells (MSCs) [1, 2, 5].

However, the role of ROCK downstream effector myocardin-related transcription factor A (MRTF-A) in the regulation of MSC differentiation remains less studied. MRTF-A, also known as megakaryocyte acute leukemia protein (MAL) and megakaryoblastic leukemia (MKL1), belongs to the myocardin family [6, 7] and is found in numerous embryonic and adult tissues [8]. MRTF-A generates a unique link between actin dynamics and gene expression because the activity of MRTF-A is controlled by the balance between



monomeric G-actin and the polymerized filamentous F-actin. At low actin polymerization state, MRTF-A is inactive as it is reversibly bound to cytoplasmic or nuclear G-actin through N-terminal RPEL repeats. On the other hand, when actin filament assembly is stimulated by Rho-ROCK activity, MRTF-A is released from its repressive complex with G-actin [7, 9, 10]. In the nucleus, an active MRTF-A works as a transcription coactivator of serum response factor (SRF) to activate transcription of contractile and cytoskeletal genes including alpha-, beta-, and gamma actins, integrin  $\beta$ 1, vinculin; cofilin 1; talin 1; myosin heavy chains; and myosin light chain 9 [6–8, 11].

Recently, studies have linked MRTF-A to regulation of adipogenesis through its ability to respond to actin dynamics [12]. Adipogenic differentiation towards white adipose tissue (WAT) has been reported to involve cytoskeletal changes towards rounder cell morphology, which in mature adipocytes allows optimal lipid storage [13, 14]. Adipogenesis is regulated through sequential activation of transcription factors, of which peroxisome proliferator-activated receptor gamma (PPAR $\gamma$ ) is considered the key adipocyte-specific master switch [13–16]. Interestingly, PPAR $\gamma$  has been found to be one of the targets through which MRTF-A regulates adipogenesis [17, 18]. Nobusue and coworkers reported that depletion of MRTF-A with RNAi method enhanced PPAR $\gamma$  in murine cells [12]. To support this finding, McDonald and coworkers observed that MRTF-A and SRF were down-regulated during adipogenesis of murine embryo fibroblasts, and reciprocally, cells genetically manipulated to express MRTF-A and SRF displayed hindered adipogenesis [19]. Similarly, in a study of Mikkelsen and coworkers, SRF overexpression inhibited adipogenesis, whereas RNAi-mediated knockdown of SRF enhanced adipogenesis in mouse preadipocytes [20]. In addition to regulation of WAT, MRTF-A has been reported to regulate the browning of WAT containing mitochondria and uncoupling protein 1- (UCP1-) rich cells found in brown and beige adipose tissue [17, 19].

Adipogenesis and osteogenesis have been found mutually exclusive in MSC differentiation [2, 5, 15]. Thus, we hypothesized if MRTF-A would as well reciprocally guide the differentiation fate decision. The MSC osteogenesis is controlled by a master regulator runt-related transcription factor 2 (RUNX2), which regulates the osteoblast-specific gene expression of alkaline phosphatase (ALP), osteopontin (OPN), and osteocalcin (OCN) [15, 21]. The actin cytoskeleton is also modified during osteoblast formation: angular shape, well-defined stress fibers, but also increased actin polymerization have been reported [1, 22, 23]. To date, the existing literature addressing MRTF-A in osteogenic differentiation is sparse. Bian and coworkers implicated the regulatory effect of MRTF-A on osteogenic differentiation potential in rodent MSCs [24]. In their study, MRTF-A knockout mice had inferior bone development compared with wild type, and bone marrow mesenchymal stem cells (BMSCs) isolated from the knockout mice had decreased osteogenesis *in vitro* [24]. Supporting these findings, also, SRF-deficient mice have been reported to have reduced bone mineral density and bone formation rate [25].

Our study aimed to investigate the role of MRTF-A coregulator in guiding the differentiation commitment of human adipose stem cells (hASCs). Human ASCs are multipotential MSCs with the capacity to give rise to mesenchymal tissues such as fat, bone, and cartilage and have immunomodulatory properties making them suitable to be used in regenerative medicine [26]. Our approach to study the role of MRTF-A in the regulation of differentiation fate was to use two molecular inhibitors described by Evelyn and coworkers targeted to MRTF-A/SRF-mediated gene transcription, a first-generation inhibitor CCG-1423 [27] and a second-generation analog CCG-100602 [28]. CCG-100602 was designed and synthesized to improve the potency and attenuate the cytotoxicity of the lead compound by molecular modifications to the chemical structure of CCG-1423 [28–30]. The molecular target of CCG-1423 has been proposed to be the N-terminal basic domain of MRTF-A which acts as a functional nuclear localization signal (NLS) [31]. In contrast, the biological activity of the related compound CCG-100602 remains unidentified. We cultured hASCs in basic culture medium (BM) and differentiated the cells using adipogenic and osteogenic culture media, AM and OM, respectively, with or without inhibitor supplementation. Adipogenesis and osteogenesis were studied using analyses of early and late markers of differentiation, immunocytochemical staining of both intracellular and extracellular matrix (ECM) proteins, and image-based analysis methods. In addition, the F-actin formation, orientation of actin filaments, and actin-related proteins were studied to evaluate the role of MRTF-A in mediating the cytoskeletal responses during differentiation. To the best of our knowledge, this is the first study elucidating the role of MRTF-A in the regulation of the balance between hASC adipogenic and osteogenic differentiation courses. Since hASCs have been increasingly used in the clinical setting, the detailed understanding of their molecular mechanisms is of great value.

## 2. Materials and Methods

**2.1. hASC Isolation and Culture.** The hASCs used in the study were isolated from adipose tissue samples of six female donors aged 40–63 (Md = 51) with their written informed consent in accordance with the Regional Ethics Committee of the Expert Responsibility area of Tampere University Hospital, Tampere, Finland (ethical approval R15161). More detailed donor information is given in Table S1. The isolation protocol has been described previously [32, 33]. Briefly, the adipose tissue was digested mechanically and enzymatically (Collagenase type I; Thermo Fisher Scientific; Waltham, MA, USA), centrifuged, and filtrated to separate the stem cells.

The isolated hASCs were cultured adhering to a Nunclon Delta surface polystyrene culture flask (Thermo Fisher Scientific). Human ASCs were expanded and cultured in basic culture medium, designated as BM, containing 5% human serum (GE Healthcare; Chicago, IL, USA, or BioWest; Nuaille, France) and 1% antibiotics (Penicillin/Streptomycin; Lonza, Basel, Switzerland) in Minimum Essential Medium  $\alpha$ , no nucleosides (MEM  $\alpha$ ), or Dulbecco's Modified Eagle



Medium/Ham's Nutrient Mixture F-12, no glutamine (DMEM/F-12) (both media from Thermo Fisher Scientific). 1% GlutaMax (Thermo Fisher Scientific) was added when using DMEM/F-12. The cells were passaged when reaching 70–80% confluency and detached using TrypLE Select (Thermo Fisher Scientific).

**2.2. Flow Cytometry Analysis of Immunophenotype.** The hASCs used in the study were characterized by flow cytometry (FACSaria; BD Biosciences, Erembodegem, Belgium) at passage 1 to evaluate their immunophenotype. Human ASCs (10 000 cells/sample) were single stained with monoclonal antibodies: CD14-PE-Cy7, CD19-PE-Cy7, CD45RO-APC, CD73-PE, CD90-APC (aforementioned antibodies from BD Biosciences, Franklin Lakes, NJ, USA), CD11a-APC, CD105-PE (R&D Systems Inc., Minneapolis, MN, USA), CD34-APC, and HLA-DR-PE (Immunotools GmbH, Friesoythe, Germany). Fluorescence level greater than 99% was considered positive.

**2.3. Differentiation Media and Inhibitors.** Human ASCs were induced with differentiation culture media and the MRTF-A inhibitors 24 h after plating the cells for experiments. Osteogenic differentiation was accomplished with osteogenic medium (OM) consisting of BM supplemented with 200  $\mu$ M L-ascorbic acid 2-phosphate, 10 mM  $\beta$ -glycerophosphate, and 5 nM dexamethasone (DEX) (reagents from Sigma-Aldrich, Saint Louis, MO, USA). For adipogenic differentiation, hASCs were cultured in adipogenic medium (AM) containing BM supplemented with 1  $\mu$ M DEX, 17  $\mu$ M pantothenate, 33  $\mu$ M biotin (from Sigma-Aldrich), and 100 nM insulin (Thermo Fisher Scientific). 0.25 mM 3-isobutyl-1-methylxanthine (IBMX; Sigma-Aldrich) was added to AM once at the beginning of differentiation. MRTF-A inhibition was carried out by supplementing BM, OM, and AM with one of two inhibitor molecules targeted to MRTF-A/SRF signaling. We used a first-generation inhibitor CCG-1423 (Selleck Chemicals; Houston, TX, USA) and a second-generation analog CCG-100602 (Cayman Chemical Company; Ann Arbor, MI, USA). BM, OM, and AM without inhibitors were used as controls. Media and inhibitors were changed twice a week during the experiments.

**2.4. Cell Viability.** The inhibitor effect on the viability of hASCs was analyzed with LIVE/DEAD™ Viability/Cytotoxicity Kit for mammalian cells (Invitrogen™; Thermo Fisher Scientific). The cells were seeded on CellBIND culture plates (Corning) in the density of 260 cells/cm<sup>2</sup> and cultured 7 days in BM, OM, or AM conditions and the media supplemented with 3  $\mu$ M, 8  $\mu$ M, 15  $\mu$ M, or 30  $\mu$ M CCG-100602 or 15  $\mu$ M, 20  $\mu$ M, 25  $\mu$ M, or 30  $\mu$ M CCG-1423. After the 7-day culture, staining was done as described previously [34], but using a 30 min incubation time for the staining solution. Briefly, the cells were washed with Dulbecco's Phosphate-Buffered Saline (DPBS; Lonza) and stained with a working solution of 0.5  $\mu$ M calcein-AM and 0.25  $\mu$ M ethidium homodimer-1 (EthD-1) in DPBS for 30 min at room temperature. After staining, fresh DPBS was changed to the wells, and the viable green-

stained (calcein-AM) and dead red-stained (EthD-1) cells were immediately imaged.

**2.5. Proliferation and ALP Activity.** The proliferation of hASCs was analyzed using CyQUANT™ assay (Invitrogen™; Thermo Fisher Scientific). The hASCs were seeded on CellBIND culture plates (Corning) in the density of 260 cells/cm<sup>2</sup> and cultured for 7 days or 14 days in BM, OM, or AM conditions supplemented with 15, 20, or 25  $\mu$ M CCG-1423 inhibitor or 10 or 12  $\mu$ M CCG-100602 inhibitor. BM, OM, and AM without inhibitors were used as controls. The hASCs were lysed into 0.1% Triton X-100 buffer (Sigma-Aldrich). After a freeze-thaw cycle, the proliferation of hASCs was studied with CyQUANT GR-Dye in lysis buffer, and the fluorescence was measured with a microplate reader at 480/520 nm (Wallac Victor 1420 Multilabel Counter; Perkin Elmer, Waltham, MA, USA).

The activity of ALP, an early marker of osteogenic differentiation, was studied from the same samples as proliferation, but only the samples cultured in BM and OM conditions were studied. The lysed samples were analyzed with a colorimetric assay, as described before [35]. Briefly, the samples were incubated 15 min 37°C in a working solution containing 1:1 10.8  $\mu$ M phosphatase substrate and 1.5 M alkaline buffer solution. After incubation, the reaction was halted using 1.0 M sodium hydroxide (all reagents from Sigma-Aldrich). Absorbances were measured at 405 nm.

**2.6. Alizarin Red Staining and Quantification of Mineralization.** Late osteogenic differentiation was evaluated by assessing the calcium accumulation with Alizarin Red (AR) staining. The hASCs were seeded 260 cells/cm<sup>2</sup> on CellBIND plates (Corning) and cultured 21 days in BM or OM conditions with or without CCG-1423 and CCG-100602 inhibitors. At day 21, the cells were fixed with 70% ethanol and stained with 2% Alizarin Red S solution (pH 4.1–4.3; Sigma-Aldrich) for 10 min. After staining, wells were washed with deionized water and 70% ethanol and dried. Samples were photographed with Olympus OM-D E-M5 Mark II camera with M. Zuiko 60 mm macro lens (Olympus; Tokyo, Japan). Quantification of the staining was done by eluting the dye into 100 mM cetylpyridinium chloride (Sigma-Aldrich) for 3.5 h and measuring the absorbances at 544 nm.

**2.7. Oil Red O Staining.** Adipogenesis was studied by assessing the accumulation of lipid droplets with Oil Red O (ORO) staining. The hASCs were seeded 260 cells/cm<sup>2</sup> on CellBIND plates (Corning) and cultured for 21 days in BM or AM conditions. The media were supplemented with 15 or 20  $\mu$ M CCG-1423 or 10 or 12  $\mu$ M CCG-100602 inhibitors. BM and AM without inhibitors were used as controls. At day 21, the cells were fixed with 4% paraformaldehyde (PFA; Sigma-Aldrich), rinsed with deionized water, and pretreated with 60% isopropanol (2-propanol, Merck, Darmstadt, Germany). The cells were stained with 0.2% ORO staining solution for 15 min, counterstained 5 min with 1:2000 4',6-diamidino-2-phenylindole (DAPI; Sigma-Aldrich) in deionized water, and washed several times.

**2.8. Immunocytochemical and Phalloidin Staining.** The hASCs were seeded 1000 cells/cm<sup>2</sup> into chambered polymer coverslips (ibiTreat  $\mu$ -slide 8-well chamber; IbiDi GmbH, Gräfelting, Germany) and cultured in BM, OM, or AM supplemented with 20  $\mu$ M CCG-1423 or 12  $\mu$ M CCG-100602. The culture period was 7 days for Phalloidin staining, 14 days for immunocytochemical staining (ICC) of collagen type I (COL-1), and 21 days for ICC staining of osteopontin (OPN) and perilipin 1 (Plin1). After culture, hASCs were washed with PBS (Lonza), fixed 15 min with 0.2% triton X-100 in PFA (Sigma-Aldrich), and blocked with 1% Bovine serum albumin (BSA; Sigma-Aldrich) in PBS. The samples were incubated with primary antibodies, washed, and incubated with secondary antibodies supplemented with Phalloidin-TRITC. After washes, the samples were counterstained with DAPI. Detailed reagent information is given in Table 1. Negative controls are presented in Figure S2.

**2.9. Fluorescence Imaging.** LIVE/DEAD-, ORO-, ICC-, and Phalloidin-stained hASC samples were imaged under an inverted microscope Olympus IX51 (Olympus) equipped with fluorescence unit and camera (DP30BW). Fluorescence images were taken using Alexa 488, Alexa 546, and DAPI filters, and 4, 10, 20, or 40x objectives. The ORO-, ICC- (COL-1, OPN, and Plin1), and Phalloidin-stained samples for quantification of mean intensity were imaged keeping the exposure times constant between the samples of different culture conditions. On the contrary, the LIVE/DEAD- and Phalloidin-stained samples for image-based analysis of actin orientation were imaged by adjusting optimal exposure times for each image to ensure visibility of the cells and the actin filaments, respectively. The image processing was done with Adobe Photoshop CC (Adobe; San Jose, CA, USA) or Fiji [36].

**2.10. Image-Based Quantification of Lipid Droplet Area.** Lipid droplet formation was quantified based on image analysis of ORO-stained samples with a custom analysis pipeline designed for CellProfiler (version 2.0.0, 64-bit Windows) [37]. The same protocol was used as described previously [5], but 0.1 and 1.0 were set as lower and upper bounds for lipid area segmentation, and 15 pixels was set as a threshold for exclusion of lipid droplet areas smaller than 5  $\mu$ m in diameter.

**2.11. Image-Based Analysis of F-Actin Intensity and Orientation.** In an effort to analyze the formation of actin filaments, the Phalloidin- and DAPI-stained 40x fluorescence images of hASCs were analyzed with Fiji [36]. Briefly, the mean intensity of Phalloidin in each condition was measured, and the nuclei count of corresponding images was analyzed for normalization of the intensities.

For the analysis of actin orientation, 20x fluorescence images of Phalloidin-stained hASCs were analyzed with CytoSpectre 1.2 spectral analysis tool [38]. In brief, the images were analyzed with default settings, but specifying image magnification (20x) and camera pixel size (6.45  $\mu$ m). The software was used to calculate the circular variance describing the isotropy of orientation distribution in the

image field. Circular variance is bounded in the interval [0, 1], where a value closer to zero signifies distribution along the same direction (anisotropy), and a value closer to one designates spread distribution (isotropy) [38, 39].

**2.12. Western Blotting and Immunodetection.** Western blotting was performed to detect the protein expression of inhibitor-treated hASCs. The cells were seeded 5000 cells/cm<sup>2</sup> in CellBIND 6-well plate (Corning) and cultured 7 days in BM, OM, or AM supplemented with 20  $\mu$ M CCG-1423 or 12  $\mu$ M CCG-100602. Samples were washed with PBS (Lonza), lysed with 2x LAEMMLI sample buffer (Bio-Rad; Hercules, CA, USA), and separated with sodium dodecyl sulfate polyacrylamide gel electrophoresis. After separation, the proteins were transferred onto 0.2  $\mu$ m polyvinylidene fluoride (PVDF) membrane using Trans-Blot Turbo Ready-to-assemble transfer Kit (Bio-Rad). The PVDF membranes were blocked with 5% nonfat milk powder in Tris-buffered saline (TBS) supplemented with 0.05% Tween 20 (Sigma-Aldrich). Membranes were incubated with primary antibodies followed by washing steps (0.5%, 0.1%, and 0.05% Tween 20 in TBS) and secondary antibody incubation (antibodies, dilutions, and incubation times are presented in Table 2). After similar washing steps, proteins of interest were detected with chemiluminescence (ECL Prime Western Blotting Detection Reagent; GE Healthcare, Little Chalfont, UK), and the membranes were imaged with Chemi Doc MP System (Bio-Rad). Semiquantitative analysis of immunoblotted protein amounts was performed with Image J [40] to show the protein levels of MRTF-A,  $\alpha$ -SMA, pMLC, and MLC normalized with  $\beta$ -actin representing the cell amount in different culture conditions.

**2.13. Statistical Analysis.** Statistical significances were analyzed separately within each culture media (BM, OM, or AM) by comparing the inhibited conditions to the control condition without the inhibitors. MRTF-A inhibitor effects on cell proliferation (CyQUANT, 4 donors), ALP activity (4 donors), quantitative Alizarin Red staining (3 donors), and image-based analysis of actin (2 donors) and ORO (4 donors) were evaluated. All quantitative results are presented as mean and standard deviation (SD). Nonparametric Kruskal-Wallis and Mann-Whitney tests were performed using GraphPad Prism version 5.02 (GraphPad Software; La Jolla, CA, USA), followed by Bonferroni post hoc test. *N* values represent the number of parallel samples or images analyzed. The differences with  $p \leq 0.05$  were considered significant.

### 3. Results

**3.1. hASC Characterization.** The cells were identified as mesenchymal based on their plastic adherence, differentiation potential towards adipogenic and osteogenic lineages, and the surface marker expression pattern conveying the criteria given by the International Society for Cellular Therapy [41]. The expression of CD73, CD90, and CD105 was positive ( $\geq 95\%$  cells), and there was a lack of expression of CD11a, CD14, CD19, CD45, and HLA-DR ( $\leq 2\%$  positive cells).

TABLE 1: Reagents used in cytochemical staining.

Antibody type	Antibody	Host species	Dilution	Incubation
Primary	Anti-Collagen I (ab90395) <sup>1</sup>	Mouse	1 : 2000	+4°C, overnight
Primary	Anti-Osteopontin (ab8448) <sup>1</sup>	Rabbit	1 : 100	+4°C, overnight
Primary	Anti-Perilipin-1 (ab3526) <sup>1</sup>	Rabbit	1 : 600	+4°C, overnight
Secondary	Anti-mouse IgG Alexa fluor 488 (A11029) <sup>2</sup>	Goat	1 : 500	+4°C, 45 min
Secondary	Anti-rabbit IgG Alexa fluor 488 (A21206) <sup>2</sup>	Donkey	1 : 500	+4°C, 45 min
—	Phalloidin–Tetramethylrhodamine B isothiocyanate (TRITC) <sup>3</sup>	—	1 : 500	+4°C, 45 min
—	DAPI <sup>3</sup>	—	1 : 2000	RT, 5 min

<sup>1</sup>Abcam, Cambridge, United Kingdom. <sup>2</sup>Thermo Fisher Scientific. <sup>3</sup>Sigma-Aldrich.

TABLE 2: Primary and secondary antibodies used in immunodetection.

Antibody type	Antibody	Host species	Dilution	Incubation
Primary	Anti-MKL1/MRTF-A (14760S) <sup>1</sup>	Rabbit	1 : 800	+4°C, overnight
Primary	Anti-MLC (3672S) <sup>1</sup>	Rabbit	1 : 500	+4°C, overnight
Primary	Anti-pMLC (3671S) <sup>1</sup>	Rabbit	1 : 500	+4°C, overnight
Primary	anti- $\alpha$ -SMA (14968S) <sup>1</sup>	Rabbit	1 : 1000	+4°C, overnight
Primary	Anti- $\beta$ -actin (sc47778) <sup>2</sup>	Mouse	1 : 2000	RT, 1 h
Secondary	Anti-rabbit IgG-HRP (7074S) <sup>1</sup>	Goat	1 : 2000	RT, 1 h
Secondary	Anti-mouse IgG-HRP (sc2005) <sup>2</sup>	Goat	1 : 2000	RT, 1 h

<sup>1</sup>Cell Signaling Technology, Danvers, Massachusetts, USA. <sup>2</sup>Santa Cruz Biotechnology, Dallas, Texas, USA.

The expression of hematopoietic marker CD34 was the modest, but previous studies have linked this elevation to the early passage of ASCs that declines when the cells are passaged [14, 42, 43]. Detailed surface marker expressions, their standard deviations, and fluorophore information are given in Table S2.

**3.2. Viability and Proliferation.** We first examined the role of MRTF-A in hASC adhesion and viability by using two inhibitor molecules (CCG-1423 and CCG-100602) in BM, OM, and AM cultures. A selection of concentrations of both inhibitors was used to find optimal concentrations for cell viability. Based on the representative LIVE/DEAD-stained images of adherent hASCs in Figure 1(a), there were viable green-stained cells, but no dead cells, in all culture conditions. The number of adherent cells decreased as a response to increasing inhibitor amount. With CCG-100602, the effect was also dependent on the culture media because the OM condition supported the viability over BM and AM conditions.

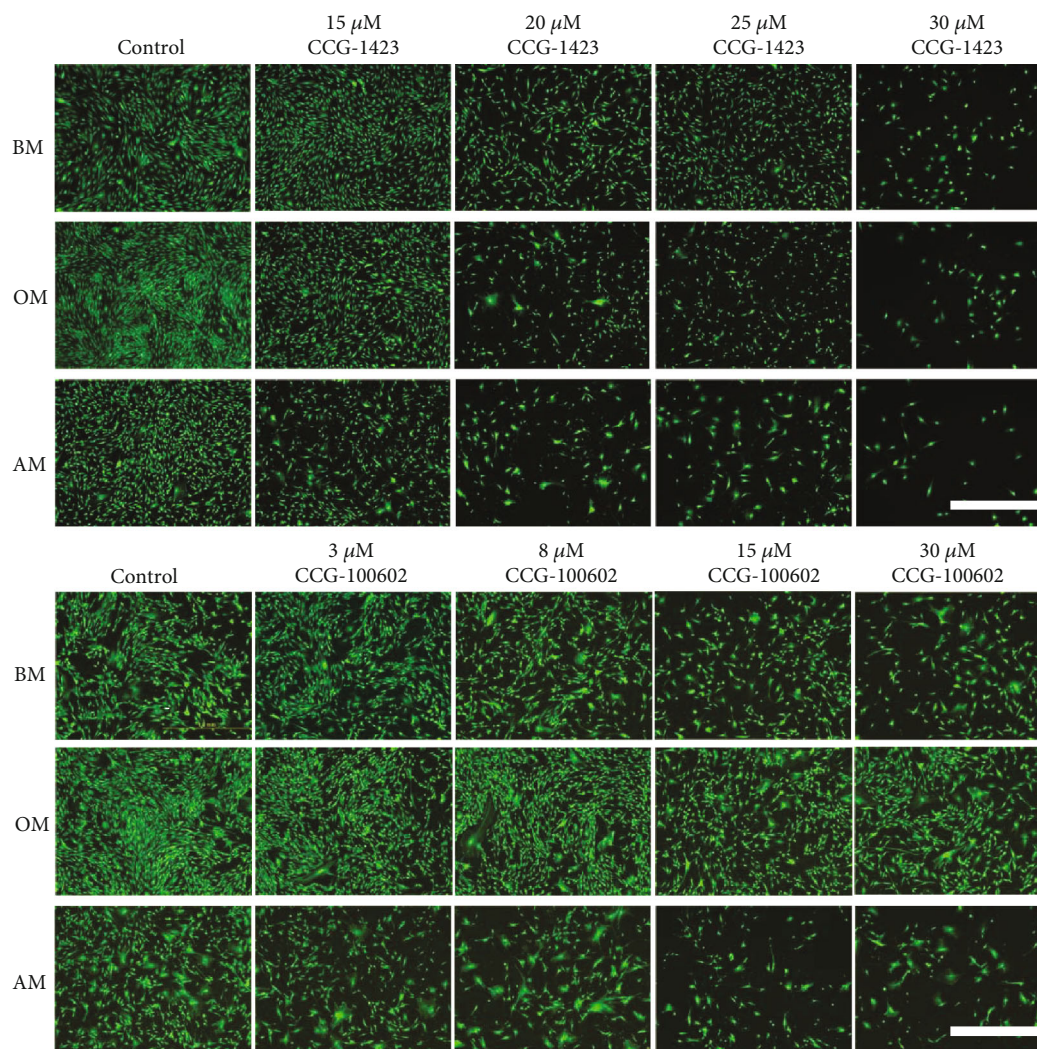
Cell proliferation, analyzed with CyQUANT assay, aligned with the viability results. Figures 1(b) and 1(c) show that the inhibitors had a dose-dependent effect on the cellular nucleic acid bound fluorescent GR-Dye denoting cell number. The inhibitor effect accumulated over time, and more significant reductions in cell amounts were seen after 14 days of culture. The hASCs in AM were more sensitive to inhibition, and lower inhibitor concentrations led to significantly reduced cell amount already at day 7.

**3.3. Adipogenic Differentiation.** We next investigated the significance of MRTF-A activity on the adipogenic potential of hASCs using ORO staining of cytoplasmic neutral lipids after

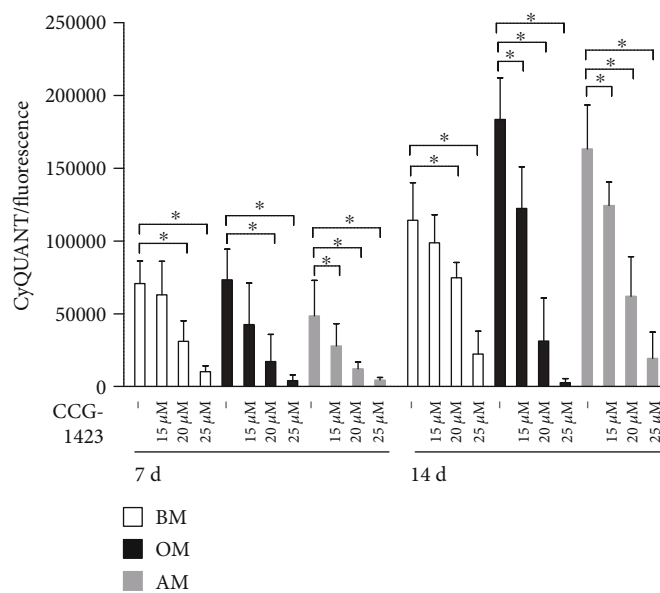
21 days of culture in BM or AM conditions supplemented with 15 or 20  $\mu$ M CCG-1423 or 10 or 12  $\mu$ M CCG-100602. The representative ORO- and DAPI-stained fluorescence images are shown in Figure 2(a). The lipid droplet accumulation was also quantified by analyzing the total ORO-stained area, as well as the area of lipid droplet clusters exceeding 5  $\mu$ m in diameter to demonstrate the adipogenic maturation (Figure 2(b)). BM condition contained small red-stained lipid droplets, and both inhibitors significantly increased the size of the individual droplets. Noticeable adipogenic differentiation with large matured droplets was obtained in the AM condition, but the enlarged, clustered lipid droplets were quite scarce in AM control. MRTF-A inhibition significantly enhanced both the total area of lipid droplets and the proportion of large droplets in AM condition. However, despite their abundance, the MRTF-A inhibitor-induced lipid droplets were not as clustered as in AM control but rather more separated. Interestingly, 15  $\mu$ M CCG-1423 and 10  $\mu$ M CCG-100602 were found more optimal concentrations in supporting the hASC maturation.

Adipogenic differentiation was further assessed with ICC staining of adipogenic marker Plin1 (Figure 2(c)). The inhibitor treatment enhanced Plin1 production of the hASCs in BM condition. Plin1 staining was stronger in AM conditions, and the staining intensity was relatively the same in control AM and with inhibition. The zoom images revealed large lipid droplets covered with Plin1 in the AM supplemented with MRTF-A inhibitors. However, these structures were absent in the AM control condition. In addition, quantitative real-time PCR (qRT-PCR) analysis was done to study the effect of MRTF-A inhibition on a genetic level using one donor cell line (Table S3 and Figure S1). We found that the





(a)



(b)

FIGURE 1: Continued.



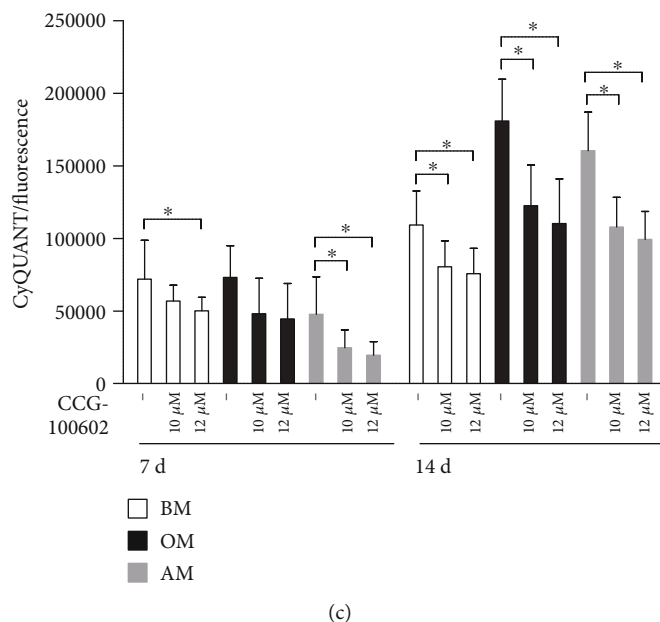


FIGURE 1: Effect of MRTF-A inhibition on viability and proliferation of hASCs. (a) Representative fluorescence images of LIVE/DEAD-stained hASCs. hASCs were cultured 7 d in BM, OM, or AM supplemented with 15, 20, 25, or 30  $\mu\text{M}$  CCG-1423 or 3, 8, 15, or 30  $\mu\text{M}$  CCG-100602 inhibitor, after which LIVE/DEAD analysis was performed. Green dye represents living cells (Alexa 488 filter), and a negligible number of dead cells are stained with red dye (Alexa 546). Scale bar 1.0 mm, same scale in every image. (b, c) Proliferation of hASCs at 7 and 14 d was analyzed with the CyQUANT method. The hASCs were cultured in BM, OM, or AM supplemented with 15, 20, or 25  $\mu\text{M}$  CCG-1423 inhibitor (b) or 10 or 12  $\mu\text{M}$  CCG-100602 inhibitor (c).  $N = 12$ , independent biological replicates from 4 donors. 5% significance level was used in the statistical analysis, and the comparisons were made within a culture condition by comparing the inhibitor concentrations with the untreated medium control. BM: basic medium; OM: osteogenic medium; AM: adipogenic medium.

MRTF-A inhibitors led to enhanced or unaffected human adipocyte fatty acid-binding protein (*AP2*) expression, but both inhibitors had a downregulating effect on leptin (*LEP*) in AM condition.

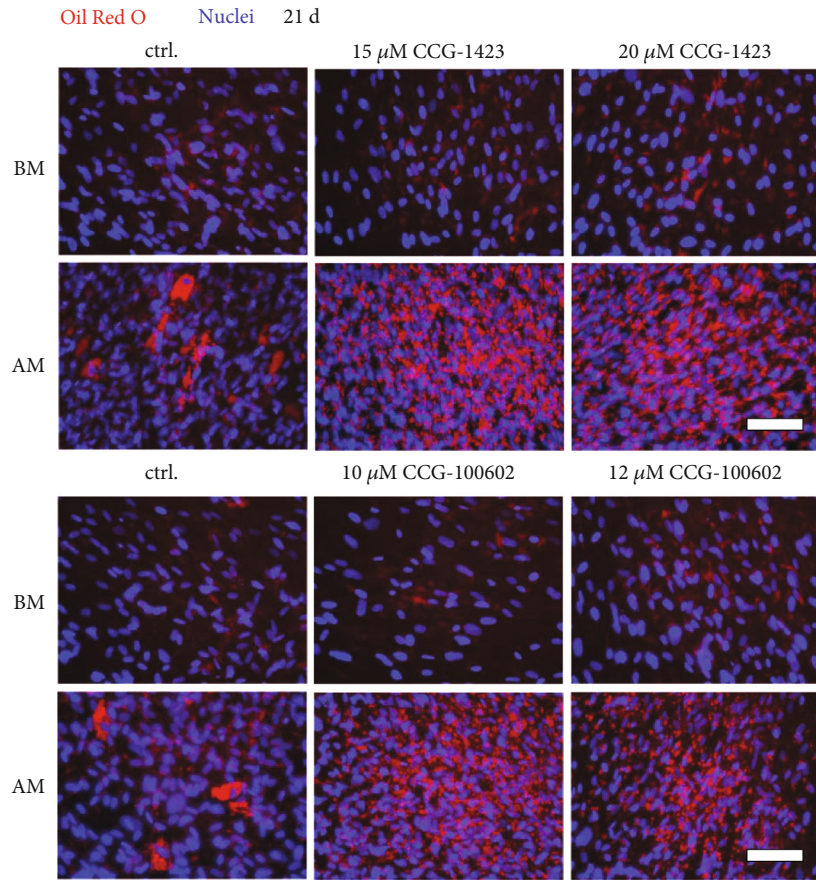
**3.4. Osteogenic Differentiation.** We evaluated the early osteogenic potential of MRTF-A inhibitor-treated hASCs by measuring the activity of ALP, at day 7 and 14 time points in BM or OM conditions. Figures 3(a) and 3(b) show that the ALP activity remained relatively low at day 7, and its activity rose within the culture period. The ALP activity was elevated in OM control condition at day 14, but decreased dose-dependently with MRTF-A inhibition in both BM and OM conditions. The activity was significantly reduced in OM with only 25  $\mu\text{M}$  CCG-1423, whereas the next-generation inhibitor CCG-100602 reduced ALP significantly with both concentrations. Additionally, the gene expression of an early osteogenic marker gene runt-related transcription factor 2a (*RUNX2A*) was decreased with CCG-1423 when analyzed with qRT-PCR (Table S3 and Figure S1).

The osteogenesis-related formation of secreted ECM proteins was analyzed by COL-1 staining at day 14. In BM, although the level of staining remained modest, inhibition of MRTF-A slightly increased COL-1 synthesis and processing in the endoplasmic reticulum (ER) and Golgi network (Figure 3(c)). In OM, however, COL-1 staining was considerably stronger, and the protein was secreted into ECM to form fibrous structures in the control condition. COL-1 production was lower in OM conditions with MRTF-A inhibitors,

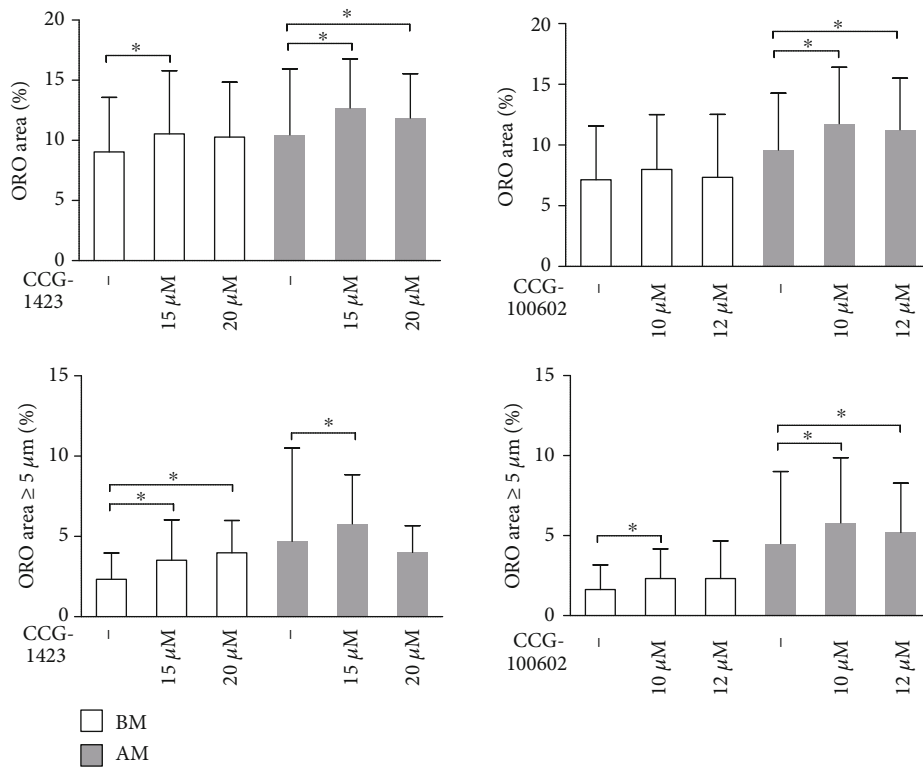
and the protein was sequestered to the intracellular membranes.

The ability of the hASCs to differentiate further towards osteoblasts was evaluated by AR staining of calcium deposits at day 21 for the assessment of ECM mineralization (Figures 4(a) and 4(b)). AR staining was low in BM conditions, as hypothesized, and the polystyrene control for AR staining was clear (data not shown). In OM control condition, the hASCs showed calcium accumulation as represented by the strong red staining of the samples. Inhibition of MRTF-A signaling by CCG-1423 or CCG100602 resulted in a significant dose-dependent reduction of mineral formation in the OM condition. Late osteogenesis was also analyzed by ICC staining of OPN. As displayed in Figure 4(c), the hASCs produced OPN independent of the culture condition. However, cells in OM without inhibitors were producing and secreting OPN to the ECM unlike the other culture conditions. Interestingly, MRTF-A inhibition confined OPN in the intracellular space.

**3.5. Actin-Related Proteins and Cytoskeleton.** The role of MRTF-A in the synthesis of actin-related proteins was assessed by Western blotting and immunodetection of MRTF-A,  $\beta$ -actin,  $\alpha$ -SMA, pMLC, and MLC at day 7 (Figure 5 and Figure S3). Based on the band size and intensity, the total protein amount of  $\beta$ -actin was relatively constant in the studied culture conditions, and the inhibitor effect on the protein level of MRTF-A varied in different culture media. However, MRTF-A inhibition predominantly



(a)



(b)

FIGURE 2: Continued.

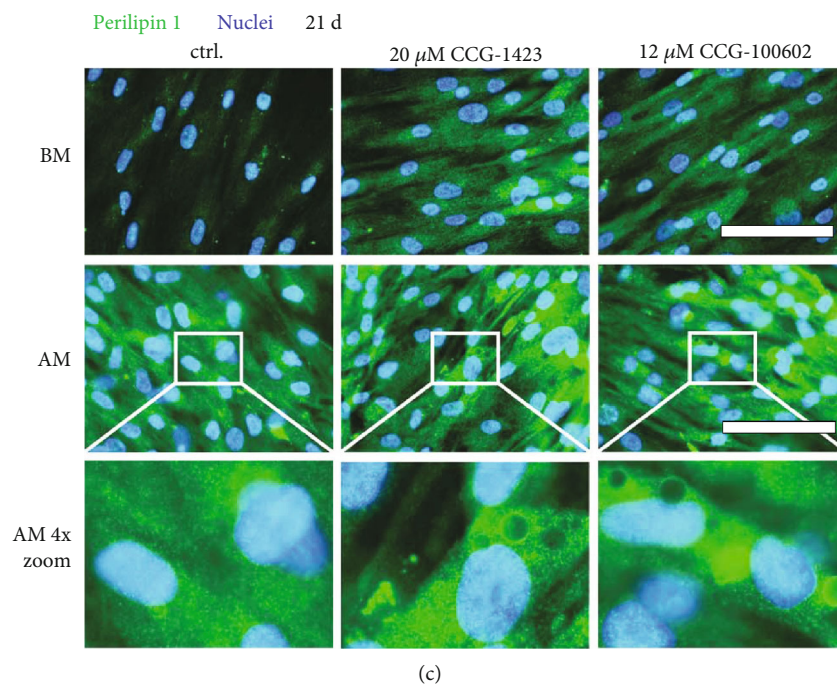


FIGURE 2: Adipogenesis of hASCs treated with MRTF-A inhibitors at 21 d. hASCs were cultured 21 d in BM or AM conditions supplemented with 15 or 20  $\mu\text{M}$  CCG-1423 or 10 or 12  $\mu\text{M}$  CCG-100602 inhibitors and stained with ORO method. (a) Representative fluorescence images of hASCs stained with ORO for intracellular lipid accumulation followed by nuclei staining with DAPI. Fluorescence images were taken with Alexa 546 for ORO (red) and DAPI (blue) filters, and 20x magnification. Scale bars 100  $\mu\text{m}$ . (b) Lipid droplet areas were quantified from the ORO-stained fluorescence images with a custom analysis pipeline designed for CellProfiler. The graphs present the total ORO-stained area or lipid droplet clusters with a diameter of over 5  $\mu\text{m}$  as percentages of the total image area.  $N = 36$  for BM +20  $\mu\text{M}$  CCG-1423 and AM +20  $\mu\text{M}$  CCG-1423, other conditions  $N = 59 - 63$  images (15 independent biological replicates from 4 donors). (c) Representative Plin1- and DAPI-stained samples of MRTF-A inhibitor-treated hASCs at 21 d imaged with a fluorescence microscope using Alexa 488 for Plin1 (green) and DAPI (blue) filters, and 40x magnification. The lowest row represents 4x digital zoom of the white rectangles in AM images. Scale bars 100  $\mu\text{m}$ . BM: basic medium; AM: adipogenic medium; ORO: Oil Red O.

decreased the amount of SRF-regulated proteins  $\alpha$ -SMA, MLC, and the phosphorylated form pMLC, although the culture media supplements also played a role on protein expression. We found that both inhibitors reduced the  $\alpha$ -SMA protein amount in BM and AM conditions, but in OM condition, only CCG-1423 reduced  $\alpha$ -SMA. MLC and its phosphorylated form pMLC were induced in OM, and their protein levels were lower in BM and AM conditions.

In order to study the cytoskeleton of MRTF-A inhibitor-treated hASCs in BM, OM, and AM conditions, the F-actin of the cells was stained with Phalloidin-TRITC (Figure 6(a)). The hASCs were fibroblastic and spindle-like in BM and OM control conditions. MRTF-A inhibition forced the cells to adopt more spread morphology with less coherently aligned cytoskeleton. Additionally, the inhibitor treatment led to decreased mean Phalloidin intensity in every culture media (Figure 6(b)). The inhibitor effect was the most prevalent in AM condition where the mean intensity values normalized with nuclei count of corresponding images were significantly reduced (Figure 6(c)). The circular variance, i.e., the isotropy of the actin filament orientations, was the lowest in BM and OM control conditions, meaning that the actin filaments were the most parallel-aligned (Figure 6(d), representative images in Figure S4). Based on quantitation, MRTF-A inhibition significantly increased the circular variance of the actin filaments in BM condition, and a

similar trend was found in OM and AM conditions. The adipogenic culture medium itself resulted in less fibroblastic morphology compared with BM and OM.

#### 4. Discussion

The dynamic behavior of the actin cytoskeleton is central in many cellular processes, including stem cell commitment into various differentiation lineages. Importantly, the changes in cell morphology have also been proposed to guide the differentiation. [1, 2] Actin dynamics are accomplished by actin turnover through the reversible polymerization of actin monomers into filaments. The ratio of G-actin and F-actin, in turn, regulates the activity of MRTF-A, which has been suggested as a direct link between the dynamic changes of actin cytoskeleton and regulation of gene activity [7]. Our previous study demonstrated that Rho-ROCK signaling, a central regulator of actin cytoskeleton, plays a switch like role in hASC commitment towards osteogenesis or adipogenesis [5]. This prompted us to question whether ROCK downstream target MRTF-A would also have a similar regulatory function in the lineage commitment of human ASCs.

The role of MRTF-A- and SRF-mediated transcription in regulation of differentiation has been previously studied mostly with genomic methods such as gain and loss of function of the MRTF-A gene in rodents [12, 19, 24]. Our



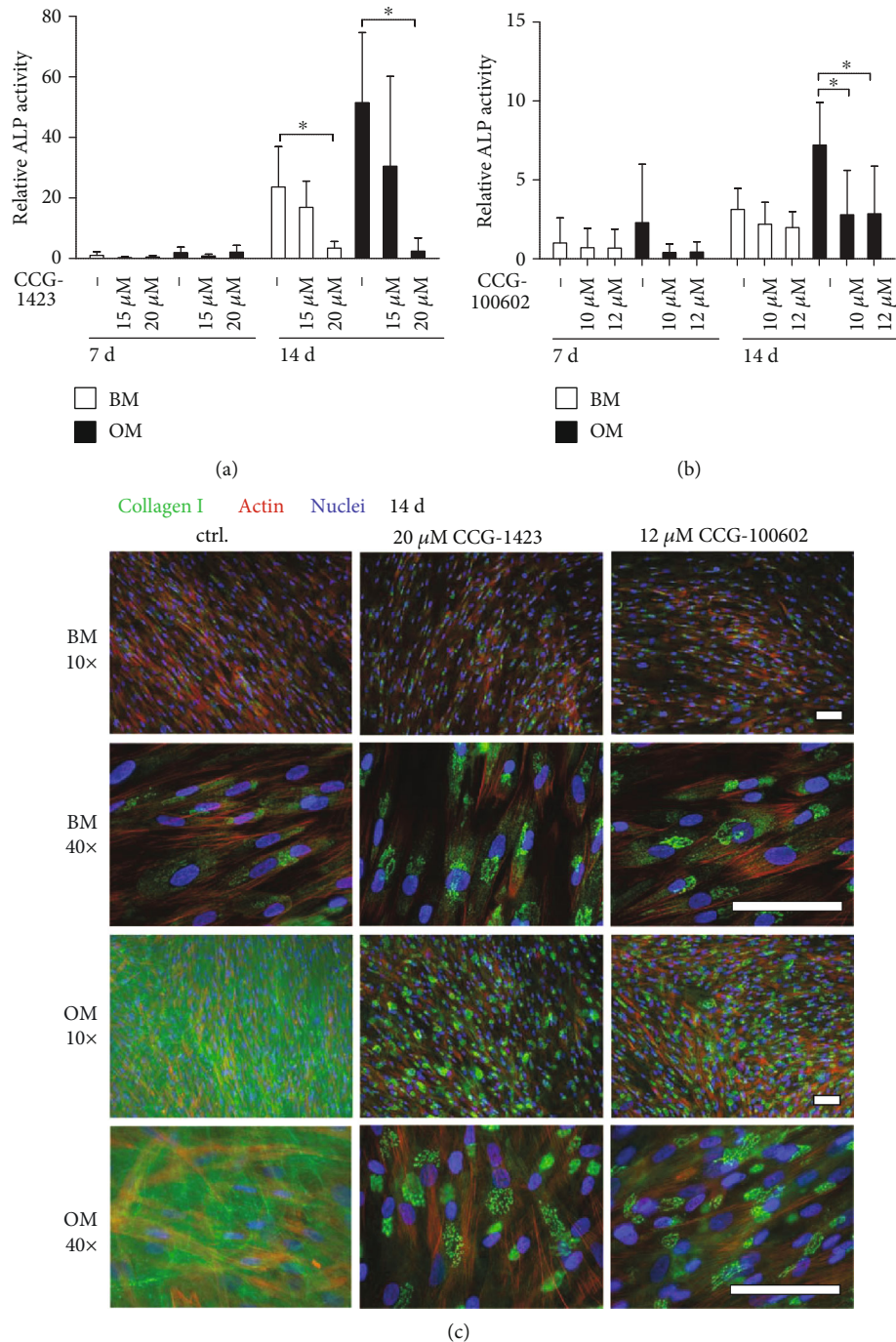


**FIGURE 3:** Early osteogenesis of MRTF-A inhibitor-treated hASCs. The hASCs were cultured in BM or OM supplemented with CCG-1423 (a) or CCG-100602 (b) inhibitors in addition to medium controls. ALP activity was analyzed with ALP assay at 7 d and 14 d. The ALP absorbance values were normalized with corresponding CyQUANT results, and the results are presented relative to the 7 d BM sample.  $N = 12$ , independent biological replicates from 4 donors. Significance level 5%. (c) Representative images of COL-1 (Alexa 488, green)-, actin (Alexa 546, red)-, and nuclei (DAPI, blue)-stained hASCs at 14 d, after culture with 20  $\mu$ M CCG-1423 or 12  $\mu$ M CCG-100602. Images with 10x and 40x magnifications are provided to give an overall view and a more detailed view of intracellular localization of COL-1. Scale bars 100  $\mu$ m. BM: basic medium; OM: osteogenic medium.

approach using MRTF-A inhibition with two pharmacological compounds CCG-1423 [27] and its analog CCG-100602 [28, 30] let us carry on a three-week cell cultures, typical for human MSC *in vitro* differentiation studies, under the influence of the inhibitors. We began by optimizing the functional

inhibitor concentrations without cytotoxic effects to hASCs because no prior data was available. Both inhibitors had dose-dependent decreasing effect on cell adhesion and viability, as studied with LIVE/DEAD assay. Based on the CyQUANT analysis of cell proliferation, the inhibitors



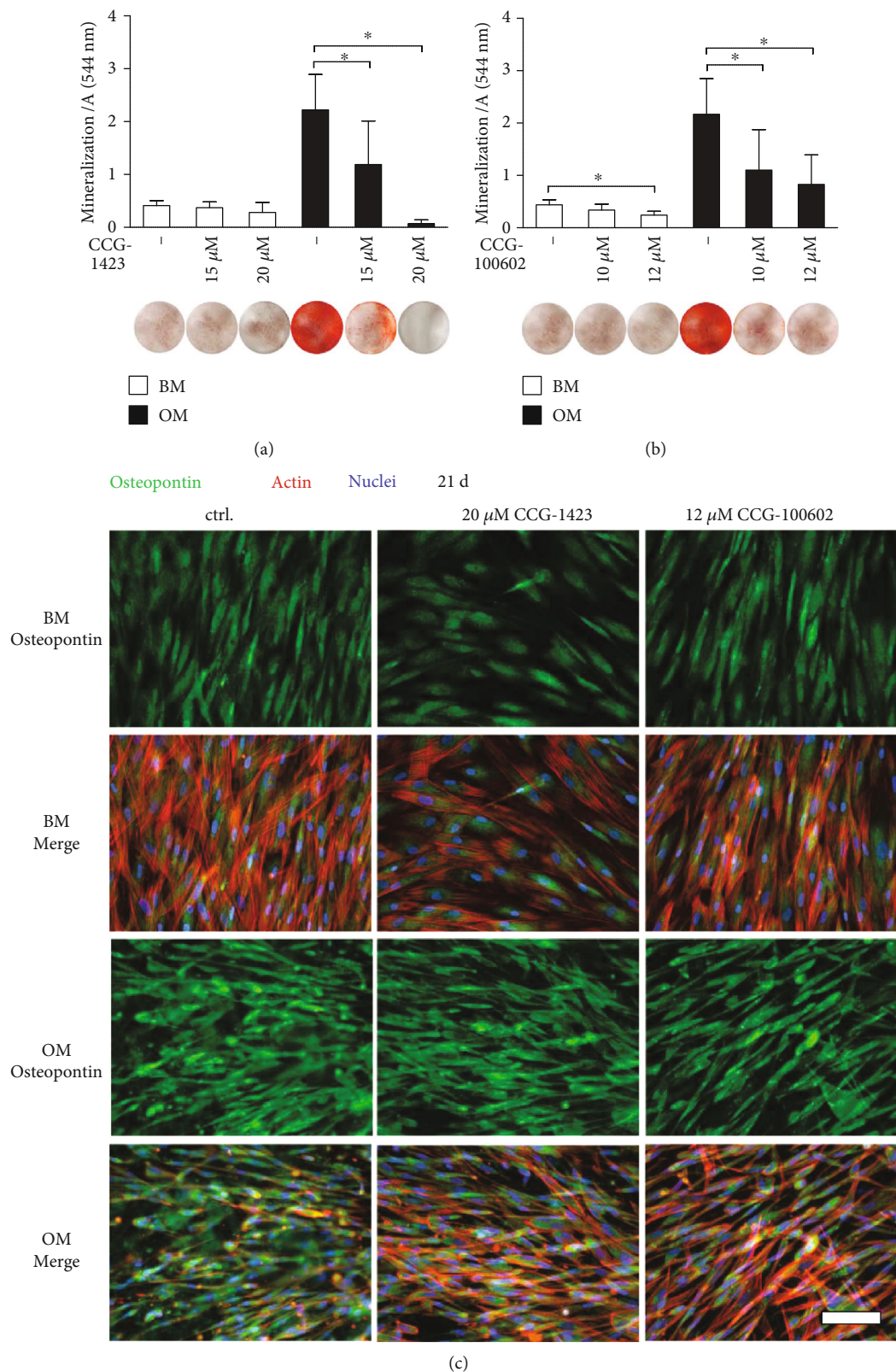


FIGURE 4: Late osteogenesis of MRTF-A inhibitor-treated hASCs. Matrix mineralization of hASCs was analyzed with AR staining after 21 d of culture with CCG-1423 (a) or CCG-100602 (b) inhibitors. Quantitative results of AR staining are presented as graphs, and corresponding representative images of the stained wells (area 1.9 cm<sup>2</sup>) are displayed below the columns, bright red dye represents mineral. *N* = 9, independent biological replicates from 3 donors. Significance level 5%. (c) Representative OPN-stained samples of MRTF-A inhibitor-treated hASCs at 21 d. The cells were imaged with a fluorescence microscope using Alexa 488 for OPN (green), Alexa 546 for actin (red), and DAPI (blue) filters, and 20x magnification. Scale bar 100  $\mu$ m, same scale in every image. BM: basic medium; OM: osteogenic medium.

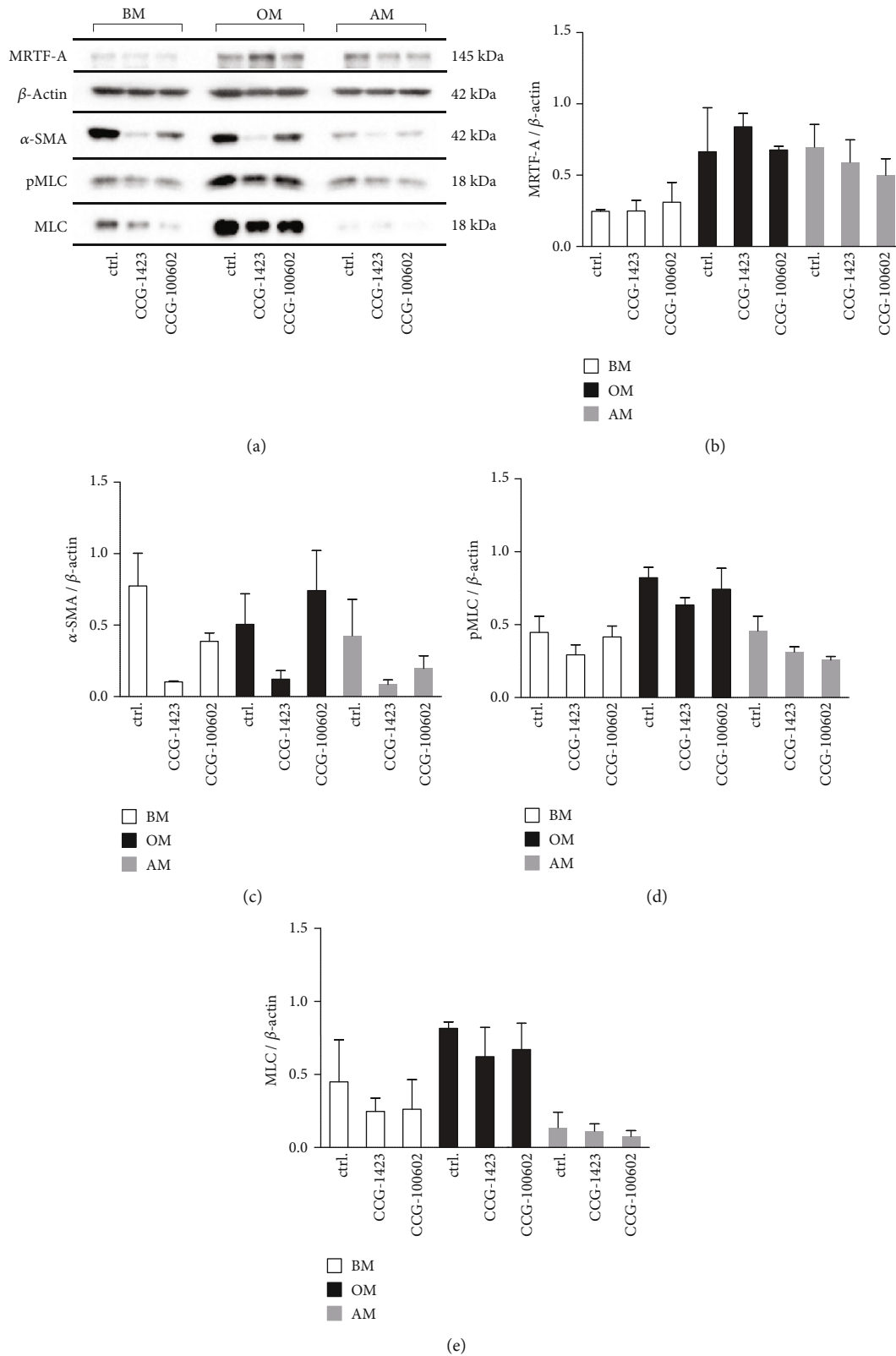


FIGURE 5: Intracellular protein levels of MRTF-A,  $\beta$ -actin,  $\alpha$ -SMA, pMLC, and MLC as a response to MRTF-A inhibition. hASCs were cultured 7 d in BM, OM, or AM media supplemented with 20  $\mu$ M CCG-1423 or 12  $\mu$ M CCG-100602. (a) Representative WB results of immunoblotted MRTF-A,  $\beta$ -actin,  $\alpha$ -SMA, pMLC, and MLC. Semiquantitative results of MRTF-A (b),  $\alpha$ -SMA (c), pMLC (d), and MLC (e) normalized with  $\beta$ -actin. MRTF-A and  $\alpha$ -SMA:  $N=2$  independent experiments, 2 donors; pMLC and MLC:  $N=4$  independent experiments, 2 donors. BM: basic medium; OM: osteogenic medium; AM: adipogenic medium.

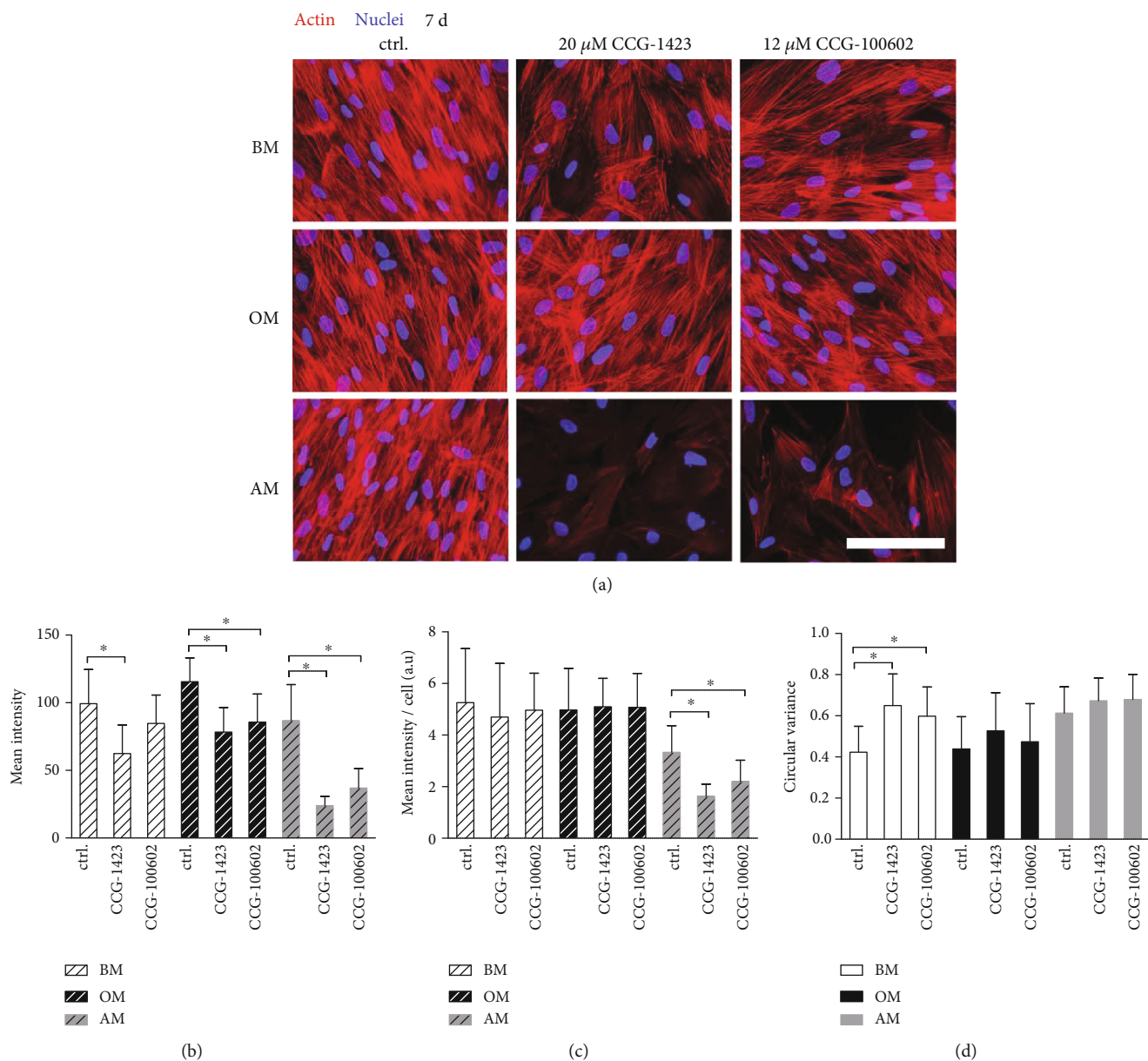


FIGURE 6: F-actin intensity and orientation of MRTF-A inhibitor-treated hASCs. hASCs were cultured 7 d in BM, OM, or AM media supplemented with 20  $\mu\text{M}$  CCG-1423 or 12  $\mu\text{M}$  CCG-100602. (a) Representative images of Phalloidin- and DAPI-stained hASCs imaged with Alexa 546 for actin (red) and DAPI for nuclei (blue) filters using 40x magnification and constant exposure time. Scale bar 100  $\mu\text{m}$ . Image-based analysis done with Fiji of mean Phalloidin intensity (b) and mean intensity normalized with nuclei number (c) of the samples described in (a).  $N = 18$ -25 images, 4 independent biological replicates from 2 donors. Significance level 5%. (d) Image-based analysis of actin orientation done with CytoSpectre 1.2 spectral analysis tool. Phalloidin-stained hASCs were imaged with 20x magnification and optimally adjusted exposure times from the same biological replicates as above (representative images in Figure S4).  $N = 16$ -27 images. Significance level 5%. BM: basic medium; OM: osteogenic medium; AM: adipogenic medium.

decreased cell number concentration-dependently, and the cell response was cumulative over time. The inhibitor effect was also dependent on the culture medium.

Previous *in vivo* and *in vitro* studies have suggested that MRTF-A and SRF transcription factors have a negative role in regulation of adipogenesis. This means that MRTF-A activity or overexpression is linked to decreased adipogenesis, whereas knockdown or diminished MRTF-A signaling to enhanced adipogenic differentiation fate [12, 18–20, 24]. As expected, we found that inhibition of MRTF-A activity sup-

ported the adipogenesis of hASCs. Based on ORO staining of neutral lipids and the quantitative analysis of lipid droplet area, inhibitor treatment stimulated adipogenic commitment, and large lipid droplets were detected throughout the culture area. MRTF-A inhibition also supported the maturation process, characterized with the enlargement and fusion of individual droplets [16]. In AM control with unaffected MRTF-A activity, the lipid droplets formed scarce, unevenly distributed clusters.

We also studied the adipogenesis with ICC staining of Plin1, which is one of the perilipin family proteins of the



phospholipid monolayer shielding the lipid droplet hydrophobic core [13, 44, 45]. Intense staining of Plin1 was found in all AM conditions, although large droplets with Plin1 on the surface were only detected in MRTF-A inhibitor-treated hASCs. It is possible that some lipid droplets were lost during the staining protocols, because mature adipocytes lose their attachment to the culture platform [14]. In basic culture medium, MRTF-A inhibitor enhanced Plin1 production of hASCs. Furthermore, the lipid droplet size was slightly increased, indicating that the molecular intervention was enough to support adipogenesis even without adipogenic culture supplements. Our results are in coherence with previous findings that Plin1 is one of the PPAR $\gamma$  target genes that is upregulated by MRTF-A depletion in mouse preadipocytes [12].

Recent studies have identified the phenotype of the MRTF-A regulated adipocytes, and their identity was reported to equivalent beige (also called brite) adipocytes [17, 19]. These adipocytes have characteristics of both white and brown adipose tissue; they are multilocular- and mitochondria-rich adipocytes involved in energy dissipation and thermogenic activities [46]. McDonald and coworkers found that the circulating levels of leptin were diminished in the MRTF-A knockout mice compared with the wild type littermates [19]. There is also some evidence that the human adipokine leptin is more associated with white adipose tissue than brown phenotype [47]. Our results of gene expression show that *LEP* was strongly expressed in the adipogenic control condition and markedly downregulated with MRTF-A inhibition. Additionally, the organization of the maturing lipid droplets was different from the typical fat vacuole clusters forming under adipogenic supplements. Therefore, the phenotype of hASCs with MRTF-A inhibition could be somewhat beige-like. However, the molecular identity of these cells will remain to be determined.

Next, we asked if the enhanced adipogenic differentiation with MRTF-A inhibition was linked to a reciprocal reduction in the osteogenic potential of hASCs. Our goal was to carefully study whether early osteogenesis, ECM production, and matrix mineralization were regulated by MRTF-A. Unlike adipogenesis, the relation of MRTF-A and osteogenesis has been demonstrated previously only in one study to our knowledge. Bian and coworkers showed *in vivo* and *in vitro* that the bone development and expression of osteogenic markers, respectively, were negatively affected by the loss of MRTF-A function in mice [24]. SRF knockout has been also reported to decrease the activity of early osteogenic markers RUNX2 and ALP [25]. Likewise, based on our results, MRTF-A inhibition significantly reduced the ALP protein activity stimulated by osteogenic culture condition in hASCs, and *RUNX2A* gene expression was hindered with CCG-1423.

Production and secretion of extracellular proteins and mineralization of ECM are an important part of skeletal development, bone remodeling, and homeostasis [48]. Therefore, we stained two constituents of the organic phase of ECM: COL-1, which provides the elasticity and flexibility to bone [48] and OPN, a regulator of matrix remodeling and tissue calcification [49]. Bian and coworkers found that MRTF-A knockout mice had lower protein expression of

COL-1 and OPN [24]. As presumed, we discovered that COL-1 and OPN synthesis and secretion were enhanced by hASCs in OM condition. However, our results revealed an interesting phenomenon that these proteins were sequestered in intracellular space with MRTF-A inhibition. To study the role of MRTF-A in osteogenic maturation, we examined ECM mineral accumulation with qualitative and quantitative AR analyses. Osteogenic media-induced mineralization was significantly and concentration-dependently reduced with both MRTF-A inhibitors. The decreased ECM mineralization has also been previously reported with MRTF-A or SRF knockout murine cells [24, 25]. These results together denote that the activity of MRTF-A is important in the different stages of the osteogenic commitment of hASCs.

Finally, the actin cytoskeleton and synthesis of actin-related proteins were studied to elucidate the role of MRTF-A in regulating the differentiation fate decision of hASCs by mediating the actin dynamics. Dramatic cytoskeletal changes have been reported to occur early in the differentiation process of the fibroblastic and spindle-like mesenchymal precursor cells into mesenchymal lineages to drive the formation of specialized tissues [1, 2, 14, 50]. Nobusue and coworkers proposed that adipogenesis would require disruption of actin stress fibers and subsequent formation of MRTF-A and G-actin complexes [12]. We discovered that MRTF-A inhibition significantly decreased the coherency of actin orientation of hASCs in BM condition, and a similar trend was seen in the intensity of Phalloidin staining representing F-actin. MRTF-A inhibition also reduced the synthesis of  $\alpha$ -SMA and MLC indicating to SRF-dependent regulation. Importantly, these cytoskeletal changes were related to the observed moderate enhancement of adipogenesis in BM condition. The adipogenic culture supplements and MRTF-A inhibition caused the hASCs to adopt more spread morphology with reduced parallel alignment of the actin filaments. Furthermore, the observed significant reduction in actin polymerization but relatively unaffected cellular protein level of  $\beta$ -actin may suggest that MRTF-A inhibition altered the ratio between G-actin and F-actin. Similar inhibitory effect on F-actin was also demonstrated recently in human intestinal myofibroblasts with CCG-100602 [51]. During osteogenesis, the hASC morphology was relatively spindle-like with predominant parallel actin filaments traversing the entire length of the cells. MRTF-A inhibition decreased the F-actin formation, the parallel-alignment of actin filaments, and the expression of SRF-regulated MLC and pMLC in OM condition. When activated, pMLC is involved in the formation of actomyosin complex contributing to the enhanced intracellular tension, linked to osteogenic course [1, 22]. Thus, the inhibitor-mediated changes in the cytoskeletal and protein level were linked to the suppressed osteogenic outcome. These results signify that MRTF-A regulates the differentiation fate of hASCs together with the biochemical cues by coupling the actin dynamics and target gene expression.

## 5. Conclusions

In summary, we have provided evidence that MRTF-A transcription cofactor is an important regulator of the inverse balance between adipogenesis and osteogenesis of hASCs.



Our results showing that MRTF-A inhibitors enhance the lipid droplet formation and maturation indicate that MRTF-A is a negative regulator of adipogenesis. Reciprocally, our novel findings of reduced osteogenesis as a response to MRTF-A inhibition highlight the necessity of MRTF-A activity on the osteogenic outcome of hASCs *in vitro*. MRTF-A translates the cytoskeletal changes to gene transcription via SRF and provides an essential temporarily coupled regulatory signaling node in stem cell differentiation. This study adds to the knowledge on the regulation of differentiation lineage commitment in human stem cells and provides further insight into molecular targets for pharmacological intervention to guide the differentiation fate into the desired direction.

### Data Availability

The data supporting the results of this study is available upon request from the corresponding author.

### Conflicts of Interest

The authors declare that there are no conflicts of interest regarding the publication of this paper.

### Acknowledgments

The authors thank Ms. Anna-Maija Honkala, Ms. Sari Kallio-koski, and M.Sc. Kimmo Kartasalo, Tampere University, for their valuable technical assistance. The authors acknowledge the Biocenter Finland and Tampere Imaging Facility for the service. This study was financially supported by the Finnish Cultural Foundation, Ester and Uuno Kokki Fund, Jane and Aatos Erkko Foundation, and the Doctoral Programme in Biomedicine and Biotechnology, Tampere University. This study was partly supported by the Competitive State Research Financing of the Expert Responsibility area of Tampere University Hospital, Business Finland, and the Academy of Finland.

### Supplementary Materials

Table S1: hASC donor information. Table S2: hASC characterization by surface marker expression. Table S3: primer sequences and accession numbers for qRT-PCR. Figure S1: relative gene expression of *AP2*, *LEP*, and *RUNX2A*. Figure S2: negative controls of the immunocytochemical staining. Figure S3: Western blot and immunodetection of MRTF-A,  $\beta$ -actin,  $\alpha$ -SMA, pMLC, and MLC of a replicate donor cell line. Figure S4: representative images of hASC for image-based analysis of actin orientation. (*Supplementary Materials*)

### References

- [1] K. A. Kilian, B. Bugarija, B. T. Lahn, and M. Mrksich, "Geometric cues for directing the differentiation of mesenchymal stem cells," *Proceedings of the National Academy of Sciences*, vol. 107, no. 11, pp. 4872–4877, 2010.
- [2] R. McBeath, D. M. Pirone, C. M. Nelson, K. Bhadriraju, and C. S. Chen, "Cell shape, cytoskeletal tension, and RhoA regulate late stem cell lineage commitment," *Developmental Cell*, vol. 6, no. 4, pp. 483–495, 2004.
- [3] K. Riento and A. J. Ridley, "Rocks: multifunctional kinases in cell behaviour," *Nature Reviews Molecular Cell Biology*, vol. 4, pp. 446–456, 2003.
- [4] E. K. Yim and M. P. Sheetz, "Force-dependent cell signaling in stem cell differentiation," *Stem Cell Research & Therapy*, vol. 3, no. 5, p. 41, 2012.
- [5] L. Hyväri, M. Ojansivu, M. Juntunen, K. Kartasalo, S. Miettinen, and S. Vanhatupa, "Focal adhesion kinase and ROCK signaling are switch-like regulators of human adipose stem cell differentiation towards osteogenic and adipogenic lineages," *Stem Cells International*, vol. 2018, Article ID 2190657, 13 pages, 2018.
- [6] F. Miralles, G. Posern, A. Zaromytidou, and R. Treisman, "Actin dynamics control SRF activity by regulation of its coactivator MAL," *Cell*, vol. 113, no. 3, pp. 329–342, 2003.
- [7] E. N. Olson and A. Nordheim, "Linking actin dynamics and gene transcription to drive cellular motile functions," *Nature Reviews Molecular Cell Biology*, vol. 11, no. 5, pp. 353–365, 2010.
- [8] D. Z. Wang, S. Li, D. Hockemeyer et al., "Potentiation of serum response factor activity by a family of myocardin-related transcription factors," *Proceedings of the National Academy of Sciences*, vol. 99, no. 23, pp. 14855–14860, 2002.
- [9] M. K. Vartiainen, S. Guettler, B. Larijani, and R. Treisman, "Nuclear actin regulates dynamic subcellular localization and activity of the SRF cofactor MAL," *Science*, vol. 316, no. 5832, pp. 1749–1752, 2007.
- [10] J. Weissbach, F. Schikora, A. Weber, M. Kessels, and G. Posern, "Myocardin-related transcription factor A activation by competition with WH2 domain proteins for actin binding," *Molecular and Cellular Biology*, vol. 36, no. 10, pp. 1526–1539, 2016.
- [11] Y. Sun, K. Boyd, W. Xu et al., "Acute myeloid leukemia-associated Mkl1 (Mrtf-a) is a key regulator of mammary gland function," *Molecular and Cellular Biology*, vol. 26, pp. 5809–5826, 2006.
- [12] H. Nobusue, N. Onishi, T. Shimizu et al., "Regulation of MKL1 via actin cytoskeleton dynamics drives adipocyte differentiation," *Nature Communications*, vol. 5, article 3368, 2014.
- [13] M. A. de la Rosa Rodriguez and S. Kersten, "Regulation of lipid droplet-associated proteins by peroxisome proliferator-activated receptors," *Biochimica et Biophysica Acta (BBA) - Molecular and Cell Biology of Lipids*, vol. 1862, no. 10, pp. 1212–1220, 2017.
- [14] B. Galateanu, S. Dinescu, A. Cimpean, A. Dinischiotu, and M. Costache, "Modulation of adipogenic Conditions for prospective use of hADSCs in adipose tissue engineering," *International Journal of Molecular Sciences*, vol. 13, no. 12, pp. 15881–15900, 2012.
- [15] A. W. James, "Review of signaling pathways governing MSC osteogenic and adipogenic differentiation," *Scientifica*, vol. 2013, Article ID 684736, 17 pages, 2013.
- [16] S. M. Niemelä, S. Miettinen, Y. Konttinen et al., "Fat tissue: views on reconstruction and exploitation," *Journal of Craniofacial Surgery*, vol. 18, pp. 325–335, 2007.
- [17] M. Rosenwald, V. Efthymiou, L. Opitz, and C. Wolfrum, "SRF and MKL1 independently inhibit brown adipogenesis," *PLoS One*, vol. 12, article e0170643, 2017.
- [18] K. Swärd, K. G. Stenkula, C. Rippe, A. Alajbegovic, M. F. Gomez, and S. Albinsson, "Emerging roles of the myocardin

- family of proteins in lipid and glucose metabolism,” *The Journal of Physiology*, vol. 594, no. 17, pp. 4741–4752, 2016.
- [19] M. McDonald, C. Li, H. Bian, B. Smith, M. Layne, and S. Farmer, “Myocardin-related transcription factor A regulates conversion of progenitors to beige adipocytes,” *Cell*, vol. 160, no. 1–2, pp. 105–118, 2015.
- [20] T. S. Mikkelsen, Z. Xu, X. Zhang et al., “Comparative epigenomic analysis of murine and human adipogenesis,” *Cell*, vol. 143, no. 1, pp. 156–169, 2010.
- [21] M. J. Biggs and M. J. Dalby, “Focal adhesions in osteoneogenesis,” *Proceedings of the Institution of Mechanical Engineers, Part H: Journal of Engineering in Medicine*, vol. 224, no. 12, pp. 1441–1453, 2010.
- [22] X. Ambriz, P. de Lanerolle, and J. R. Ambrosio, “The mechanobiology of the actin cytoskeleton in stem cells during differentiation and interaction with biomaterials,” *Stem Cells International*, vol. 2018, Article ID 2891957, 11 pages, 2018.
- [23] H. Sonowal, A. Kumar, J. Bhattacharyya, P. K. Gogoi, and B. G. Jaganathan, “Inhibition of actin polymerization decreases osteogenic differentiation of mesenchymal stem cells through p38 MAPK pathway,” *Journal of Biomedical Science*, vol. 20, p. 71, 2013.
- [24] H. Bian, J. Z. Lin, C. Li, and S. R. Farmer, “Myocardin-related transcription factor A (MRTFA) regulates the fate of bone marrow mesenchymal stem cells and its absence in mice leads to osteopenia,” *Molecular Metabolism*, vol. 5, no. 10, pp. 970–979, 2016.
- [25] J. Chen, K. Yuan, X. Mao, J. M. Miano, H. Wu, and Y. Chen, “Serum response factor regulates bone formation via IGF-1 and Runx2 signals,” *Journal of Bone and Mineral Research*, vol. 27, no. 8, pp. 1659–1668, 2012.
- [26] M. Patrikoski, J. Sivula, H. Huhtala et al., “Different culture conditions modulate the immunological properties of adipose stem cells,” *Stem Cells Translational Medicine*, vol. 3, pp. 1220–1230, 2014.
- [27] C. R. Evelyn, S. M. Wade, Q. Wang et al., “CCG-1423: a small-molecule inhibitor of RhoA transcriptional signaling,” *Molecular Cancer Therapeutics*, vol. 6, no. 8, pp. 2249–2260, 2007.
- [28] C. R. Evelyn, J. L. Bell, J. G. Ryu et al., “Design, synthesis and prostate cancer cell-based studies of analogs of the Rho/MKL1 transcriptional pathway inhibitor, CCG-1423,” *Bioorganic & Medicinal Chemistry Letters*, vol. 20, no. 2, pp. 665–672, 2010.
- [29] L. A. Johnson, E. S. Rodansky, A. J. Haak, S. D. Larsen, R. R. Neubig, and P. D. Higgins, “Novel Rho/MRTF/SRF inhibitors block matrix-stiffness and TGF- $\beta$ -induced fibrogenesis in human colonic myofibroblasts,” *Inflammatory Bowel Diseases*, vol. 20, no. 1, pp. 154–165, 2014.
- [30] B. Watanabe, S. Minami, H. Ishida et al., “Stereospecific inhibitory effects of CCG-1423 on the cellular events mediated by myocardin-related transcription factor A,” *PLoS One*, vol. 10, no. 8, article e0136242, 2015.
- [31] K. Hayashi, B. Watanabe, Y. Nakagawa, S. Minami, and T. Morita, “RPEL proteins are the molecular targets for CCG-1423, an inhibitor of Rho signaling,” *PLoS One*, vol. 9, no. 2, article e89016, 2014.
- [32] J. Gimble and F. Guilak, “Adipose-derived adult stem cells: isolation, characterization, and differentiation potential,” *Cytotherapy*, vol. 5, no. 5, pp. 362–369, 2003.
- [33] B. Lindroos, S. Boucher, L. Chase et al., “Serum-free, xeno-free culture media maintain the proliferation rate and multipotentiality of adipose stem cells in vitro,” *Cytotherapy*, vol. 11, no. 7, pp. 958–972, 2009.
- [34] M. Ojansivu, X. Wang, L. Hyväri et al., “Bioactive glass induced osteogenic differentiation of human adipose stem cells is dependent on cell attachment mechanism and mitogen-activated protein kinases,” *European Cells and Materials*, vol. 35, pp. 54–72, 2018.
- [35] L. Tirkkonen, S. Haimi, S. Huttunen et al., “Osteogenic medium is superior to growth factors in differentiation of human adipose stem cells towards bone-forming cells in 3D culture,” *European Cells and Materials*, vol. 25, pp. 144–158, 2013.
- [36] J. Schindelin, I. Arganda-Carreras, E. Frise et al., “Fiji: an open-source platform for biological-image analysis,” *Nature Methods*, vol. 9, pp. 676–682, 2012.
- [37] L. Kametsky, T. R. Jones, A. Fraser et al., “Improved structure, function and compatibility for CellProfiler: modular high-throughput image analysis software,” *Bioinformatics*, vol. 27, no. 8, pp. 1179–1180, 2011.
- [38] K. Kartasalo, R. P. Polonen, M. Ojala et al., “CytoSpectre: a tool for spectral analysis of oriented structures on cellular and subcellular levels,” *BMC Bioinformatics*, vol. 16, no. 1, p. 344, 2015.
- [39] P. Berens, “CircStat: AMATLABToolbox for circular statistics,” *Journal of Statistical Software*, vol. 31, no. 10, 2009.
- [40] C. A. Schneider, W. S. Rasband, and K. W. Eliceiri, “NIH image to ImageJ: 25 years of image analysis,” *Nature Methods*, vol. 9, no. 7, pp. 671–675, 2012.
- [41] M. Dominici, K. Le Blanc, I. Mueller et al., “Minimal criteria for defining multipotent mesenchymal stromal cells. The International Society for Cellular Therapy position statement,” *Cytotherapy*, vol. 8, no. 4, pp. 315–317, 2006.
- [42] J. B. Mitchell, K. McIntosh, S. Zvonice et al., “Immunophenotype of human adipose-derived cells: temporal changes in stromal-associated and stem cell-associated markers,” *Stem Cells*, vol. 24, no. 2, pp. 376–385, 2006.
- [43] M. J. Varma, R. G. Breuls, T. E. Schouten et al., “Phenotypical and functional characterization of freshly isolated adipose tissue-derived stem cells,” *Stem Cells and Development*, vol. 16, no. 1, pp. 91–104, 2007.
- [44] A. R. Kimmel and C. Sztalryd, “The perilipins: major cytosolic lipid droplet-associated proteins and their roles in cellular lipid storage, mobilization, and systemic homeostasis,” *Annual Review of Nutrition*, vol. 36, no. 1, pp. 471–509, 2016.
- [45] A. R. Thiam and M. Beller, “The why, when and how of lipid droplet diversity,” *Journal of Cell Science*, vol. 130, no. 2, pp. 315–324, 2017.
- [46] J. Wu, P. Boström, L. M. Sparks et al., “Beige adipocytes are a distinct type of thermogenic fat cell in mouse and human,” *Cell*, vol. 150, no. 2, pp. 366–376, 2012.
- [47] A. M. Cypess, A. P. White, C. Vernochet et al., “Anatomical localization, gene expression profiling and functional characterization of adult human neck brown fat,” *Nature Medicine*, vol. 19, no. 5, pp. 635–639, 2013.
- [48] A. Infante and C. I. Rodriguez, “Osteogenesis and aging: lessons from mesenchymal stem cells,” *Stem Cell Research & Therapy*, vol. 9, p. 244, 2018.
- [49] C. De Fusco, A. Messina, V. Monda et al., “Osteopontin: relation between adipose tissue and bone homeostasis,” *Stem Cells International*, vol. 2017, Article ID 4045238, 6 pages, 2017.

- [50] R. Sordella, W. Jiang, G. C. Chen, M. Curto, and J. Settleman, "Modulation of Rho GTPase signaling regulates a switch between adipogenesis and myogenesis," *Cell*, vol. 113, no. 2, pp. 147–158, 2003.
- [51] Y. J. Choi, J. B. Koo, H. Y. Kim et al., "Umbilical cord/placenta-derived mesenchymal stem cells inhibit fibrogenic activation in human intestinal myofibroblasts via inhibition of myocardin-related transcription factor A," *Stem Cell Research & Therapy*, vol. 10, no. 1, pp. 291–298, 2019.

## Research Article

# Differentiation Potential of Early- and Late-Passage Adipose-Derived Mesenchymal Stem Cells Cultured under Hypoxia and Normoxia

Ashley G. Zhao <sup>1</sup>, Kiran Shah <sup>1,2</sup>, Julien Freitag<sup>2,3,4</sup>, Brett Cromer <sup>1</sup>,  
and Huseyin Sumer <sup>1</sup>

<sup>1</sup>Department of Chemistry and Biotechnology, Faculty of Science, Engineering and Technology, Swinburne University of Technology, John St, Hawthorn VIC 3122, Australia

<sup>2</sup>Magellan Stem Cells P/L, 116-118 Thames St, Box Hill VIC 3129, Australia

<sup>3</sup>Melbourne Stem Cell Centre, Box Hill, VIC 3129, Australia

<sup>4</sup>Charles Sturt University, School of Biomedical Science, Albury, NSW 2640, Australia

Correspondence should be addressed to Huseyin Sumer; [hsumer@swin.edu.au](mailto:hsumer@swin.edu.au)

Received 2 July 2020; Revised 25 August 2020; Accepted 28 August 2020; Published 18 September 2020

Academic Editor: Stefania Cantore

Copyright © 2020 Ashley G. Zhao et al. This is an open access article distributed under the Creative Commons Attribution License, which permits unrestricted use, distribution, and reproduction in any medium, provided the original work is properly cited.

With an increasing focus on the large-scale expansion of mesenchymal stem cells (MSCs) required for clinical applications for the treatment of joint and bone diseases such as osteoarthritis, the optimisation of conditions for *in vitro* MSC expansion requires careful consideration to maintain native MSC characteristics. Physiological parameters such as oxygen concentration, media constituents, and passage numbers influence the properties of MSCs and may have major impact on their therapeutic potential. Cells grown under hypoxic conditions have been widely documented in clinical use. Culturing MSCs on large scale requires bioreactor culture; however, it is challenging to maintain low oxygen and other physiological parameters over several passages in large bioreactor vessels. The necessity to scale up the production of cells *in vitro* under normoxia may affect important attributes of MSCs. For these reasons, our study investigated the effects of normoxic and hypoxic culture condition on early- and late-passage adipose-derived MSCs. We examined effect of each condition on the expression of key stem cell marker genes POU5F1, NANOG, and KLF4, as well as differentiation genes RUNX2, COL1A1, SOX9, COL2A1, and PPARG. We found that expression levels of stem cell marker genes and osteogenic and chondrogenic genes were higher in normoxia compared to hypoxia. Furthermore, expression of these genes reduced with passage number, with the exception of PPARG, an adipose differentiation marker, possibly due to the adipose origin of the MSCs. We confirmed by flow cytometry the presence of cell surface markers CD105, CD73, and CD90 and lack of expression of CD45, CD34, CD14, and CD19 across all conditions. Furthermore, *in vitro* differentiation confirmed that both early- and late-passage adipose-derived MSCs grown in hypoxia or normoxia could differentiate into chondrogenic and osteogenic cell types. Our results demonstrate that the minimal standard criteria to define MSCs as suitable for laboratory-based and preclinical studies can be maintained in early- or late-passage MSCs cultured in hypoxia or normoxia. Therefore, any of these culture conditions could be used when scaling up MSCs in bioreactors for allogeneic clinical applications or tissue engineering for the treatment of joint and bone diseases such as osteoarthritis.

## 1. Introduction

Mesenchymal stem cells (MSCs) are multipotent cells, originally derived from the embryonic mesenchyme, and able to differentiate into connective tissues such as bone, fat, cartilage, tendon, and muscle [1, 2]. These cells are

ubiquitous and reside in various tissues and organs for self-repair and tissue homeostasis [3]. They can be isolated from bone marrow, periosteum, trabecular bone, adipose tissue, synovium, skeletal tissue, blood, brain, spleen, liver, kidney, lung, bone marrow, muscle, thymus, pancreas, blood vessels, and deciduous teeth [4, 5]. MSCs can self-



renew, have immunosuppressive properties, and intrinsically secrete a wide range of bioactive molecules [6, 7]. MSCs have significant clinical value and have been used in cardiovascular, neural, and orthopaedic therapeutic applications such as osteoarthritis. To date, there are 1,052 clinical trials registered for various medical conditions exploring the therapeutic benefits of MSCs in a broad range of diseases (<http://clinicaltrials.gov>). Furthermore, MSCs derived from adipose tissue show great promise for the treatment of degenerative diseases such as osteoarthritis [8, 9]. Collectively, this activity demonstrates the therapeutic potential of MSCs, widely acknowledged by researchers worldwide.

Human MSCs are heterogeneous and can be obtained from many sources via different isolation, culture, and expansion methods. There are also a variety of different approaches to characterise these cells [10]. This has caused some difficulty in comparing study outcomes and has led to controversial results. Consequently, the Mesenchymal Stem Cell Committee of the International Society for Cellular Therapy (ISCT) has provided three minimal standard criteria to define MSCs for laboratory-based investigation and pre-clinical studies, based on adherent properties, self-renewal, expression of surface markers, and multilineage differentiation capacity [10]. Firstly, MSCs must be plastic-adherent in tissue culture flasks. Secondly, more than 95% of MSC population must express CD105, CD73, and CD90 and lack expression (less than 2% population) of CD45, CD34, CD14 or CD11b, CD79a or CD19, and HLA class II. Third, MSCs must be able to differentiate into osteoblasts, adipocytes, and chondroblasts *in vitro* with standard differentiation conditions.

MSCs are functionally heterogeneous and often present in limited numbers in the human body [1, 11]. Their *in vitro* expansion for clinical dosage has become a necessity and warrants large-scale production of MSCs prior to implantation. The proliferative properties of MSCs are robust but the lack of standard methods for isolation, the different sources of MSC, and variation in both culture conditions and the number of passages may result in less than optimal cells for clinical purposes. The impact of *in vitro* culture conditions on cellular attributes of MSCs is an important factor to consider for cell therapy. Several studies have described changes in the biology of the cells, including physiological and genetic changes caused by varying tissue *ex vivo* cell culture parameters such as seeding density, media nutrients, length of culture, shear force when culturing in bioreactors, pH, temperature, and oxygen percentage [12–14]. Culture conditions can have an impact on gene expression, the proteome and cellular organization [15, 16]. All these physicochemical parameters are important and careful cell culture optimisation, with these parameters in mind, must be performed in order to produce optimal cells for therapy that have close functional similarity to native stem cells *in vivo*.

Of these parameters, oxygen level in cell culture has been described in the literature as having a significant influence on MSC characteristics. Oxygen tension acts both as a metabolic substrate and a powerful signalling molecule to regulate the

proliferation and differentiation properties of stem cells [17]. Quiescent MSCs in their natural niches are tightly controlled and maintained to protect them from oxidative damage at a physiological low oxygen tension [18] and mainly rely on anaerobic glycolysis to support ATP production [19]. However, MSC expansion is often conducted in normoxic conditions (21% O<sub>2</sub>), which is about 4–10 folds greater than their natural physiological environment [20, 21]. Cultured MSCs under high oxygen conditions or normoxia would switch from anaerobic glycolysis to the mitochondrial oxidative phosphorylation which might be harmful for cellular function [22]. Differential culturing of MSCs under hypoxia and normoxia does not seem to affect immune-phenotypic features or cellular plasticity, but does seem to affect cell morphology and complexity, as well as mitochondrial activity [23]. Culturing MSCs at a larger scale may require a bioreactor and increased passaging, however, and it may be challenging to maintain low oxygen and other physiological parameters over several passages. It is unclear what the effects of oxygen concentration are on stem cell marker expression and multipotency.

Hypoxia is one of the key parameters described to exert effects on several cellular activities in MSCs during osteogenic and chondrogenic differentiation [17]. During chondrogenesis, low oxygen tension (5%) inhibits the proliferation of MSCs but increases the total collagen, protein, and glycosaminoglycan synthesis [24]. Other studies support this reduced proliferation rate of MSCs in hypoxic conditions, as well as showing reduced adipogenic and osteogenic differentiation potentials [25]. Nevertheless, there was no significant difference between normoxia (21% oxygen) and hypoxia (2% oxygen) in the cell surface expression of the markers CD73, CD90, CD105, CD106, CD146, and MHC class I, which is measured by flow cytometry. As mammalian tissue has much lower oxygen concentration than atmospheric conditions, ranging from 1 to 7% in cartilage, bone marrow, and 10–13% in arteries lungs and liver [26], low oxygen culture is mostly used *in vitro*. It is believed that low oxygen is able to maintain normal cellular functions such as cell growth, differentiation, and cell migration [26–29].

Nevertheless, the impact of oxygen tension on cultured MSCs remains controversial, due to conflicting results, although these discrepancies might be due to other differences in culture conditions or different sources of MSCs. Therefore, further comparative analyses on *in vitro* cultured cells under normoxic and hypoxic culture conditions are needed to determine the effects on MSC stemness, particularly for large-scale systems such as bioreactors for clinical use. Although bone marrow-derived MSCs were the first identified and have been extensively studied [1], harvesting from bone marrow is a limiting factor as it is a painful procedure and produces only a low yield of MSCs. An alternative source of MSCs from the adipose tissue can be obtained by a minimally invasive procedure and can achieve a 100 to 500-folds greater yield than from the bone. It is now an accepted alternative source of MSCs, leading to changes in medical practices and regenerative medicine [30, 31]. The current study is aimed at comparing the characteristics of early- and late-passage adipose-derived MSCs, which is used

for the treatment of osteoarthritis and cultured under hypoxic or normoxic conditions. From this comparison, we aimed to determine whether late-passage MSCs grown in normoxic culture conditions could be a reliable, safe, and effective source of cells for regenerative medicine and tissue engineering for applications such as osteoarthritis. We determined whether early- and late-passage MSCs cultured in hypoxia or normoxia maintain the minimal standard criteria for MSCs, set by the ISCT, for laboratory-based investigation and preclinical studies.

## 2. Material and Methods

**2.1. Cell Culture.** Adipose tissue was harvested by liposuction by a qualified clinician with ethics approval and written consent (Monash University Human Research Ethics Committee number CF 14/2230 2014001175 and registered clinical trial registration: Australian New Zealand Clinical Trials Registry - ACTRN12617000638336.). The adipose tissue was then processed in a clean room facility. In brief, the minced adipose tissue was digested with collagenase to release the stromal vascular fraction (SVF) from mature adipocytes. The stromal vascular fraction (SVF) was cultured in the flask as passage 0. The plastic-adherent adipose-derived MSCs were harvested away from floating SVF cells. MSCs were cultured in basal medium with 2 mM glutamine with 5% FBS (Invitrogen) and grown under hypoxic (2% O<sub>2</sub>) or normoxic (~21% O<sub>2</sub>) conditions for up to nine passages. Subculturing by trypsinisation was performed when MSCs reached approximately 80% confluence. The four sample groups were MSCs cultured in hypoxic conditions, harvested at passage 5 (P5H) or at passage 9 (P9H), or cultured in normoxic conditions, harvested at passage 5 (P5N) or passage 9 (P9N).

MSCs were differentiated into chondrocytes or osteocytes by culturing in Chondrocyte Differentiation Reagent ATCC® PCS-500-051™ for 19 days, or Osteocyte Differentiation Reagent ATCC® PCS-500-052™ for 21 days, respectively. In brief, samples were cultured in 6-well culture plates with a half media change every 3–4 days. Osteogenic differentiation was confirmed by Alizarin Red S staining. Cells were fixed with 4% formaldehyde for 30 mins and then rinsed twice with distilled water, stained with Alizarin Red S solution for 3 minutes, and rinsed three times in distilled water before imaging. Chondrogenic differentiation was confirmed by Alcian Blue staining. Cells were fixed with 4% formaldehyde for 30 mins and then rinsed once with DPBS, stained with Alcian Blue solution prepared in 0.1 N HCl for 30 minutes, and then rinsed three times with 0.1 N HCl. Then, 2 ml of distilled water was added into each well to neutralize the samples before imaging.

**2.2. Quantitative Real-Time PCR and Statistical Analysis.** Total RNA was extracted from cell samples, using a RNeasy Mini Kit (Cat#74104, Qiagen), according to the manufacturer's instructions. The concentration and quality of the extracted RNA were measured using a NanoDrop2000 Spectrophotometer (Thermo Scientific). 5 µg of RNA from each sample was transcribed into cDNA using Tetro cDNA Syn-

thesis Kit (Bioline) following manufacturer's instructions. Primers used for gene expression analysis, listed in Table 1, have been published previously [32].

qRT-PCR was performed by using SsoAdvanced™ Universal SYBR Green Supermix kit (ThermoFisher Scientific). Three independent experiments were performed in triplicate, with GAPDH as the reference gene. The reaction mix preparation and thermal cycling protocol were followed according to SsoAdvanced™ Universal SYBR Green Supermix kit. A Bio-Rad CFX96™ system was used for thermal cycling, with initial denaturing at 95°C for 30 sec, then 40 cycles of denaturing at 95°C for 10 sec, annealing and extension at 59°C for 30 sec, and Melt-Curve Analysis from 65°C to 95°C with 0.5°C increment. Statistical analysis was performed by one-way ANOVA; the P5H samples were set to a value of 1 and used as a reference to determine a statistical significance.

**2.3. Flow Cytometry.** In brief,  $0.5 \times 10^6$  MSCs were resuspended in 500 µL of FACS buffer (1% BSA and 0.1% EDTA in phosphate-buffered saline (PBS)) and incubated for 30 minutes at 4°C with 1:500 dilution of antibodies, CD73 (Cat# 11073942), CD90 (Cat# 25090942), CD105 (Cat# 12105742), or CD14 (Cat# 11014942), CD19 (Cat# 25019382), CD34 (Cat# 25034942), and CD45 (Cat# MHCD4531) from ThermoFisher Scientific, respectively. After washing twice with 1 mL of FACS buffer, the labelled MSCs were resuspended in 500 µL of FACS buffer and subjected to flow cytometry (Attune NxT, Life Technologies) to analyse surface markers.

## 3. Results

To determine the effect of oxygen concentration during culture on MSC properties, we cultured MSCs under different oxygen conditions for different numbers of passages. Initially, primary adipose-derived MSCs were cultured under GMP conditions under hypoxia (2% O<sub>2</sub>) up to passage 4. The plastic-adherent cells were subjected to flow cytometry analysis for the CD markers CD73, CD90, CD105, CD14, CD19, CD34, and CD45, to confirm their MSC phenotype before cryopreservation. The cells were then further subcultured under hypoxic or normoxic conditions and harvested at either passage 5 or 9 and frozen for later analysis. This gave rise to four sample groups that were further analysed: MSCs cultured in hypoxic conditions and harvested at passage 5 (P5H) or at passage 9 (P9H), or cultured in normoxic conditions and harvested at passage 5 (P5N) or at passage 9 (P9N).

RNA samples from the four sample groups under normoxia and hypoxia conditions at early and late were analysed by qRT-PCR. Genes were organised into four groups—pluripotent genes, osteogenic genes, chondrogenic, and adipogenic genes. The relative quantification  $2^{-\Delta\Delta CT}$  method was used to calculate the relative amount of mRNA templates in each of the test samples from ( $C_T$  (target, test),  $C_T$  (target, calibrator),  $C_T$  (GAPDH, test),  $C_T$  (GAPDH, calibrator)) four  $C_T$  values in triplicate [33]. The housekeeping gene *GAPDH* was employed as the reference gene and the low passage sample under hypoxia, P5H, served as the calibrator. The target gene expression in all other samples is thus

TABLE 1: The information of the specific genes.

Gene marker type	Name of gene primer	Gene name	Accession number	Forward and reverse sequences	PCR product length (bps)
Housekeeping	Glyceraldehyde-3-phosphate dehydrogenase	<i>GAPDH</i>	NM_002046.5	F: ATGTTTCGTCATGGGTGTGAA R: TGTGGTCATGAGTCCTTCCA	144
	POU class 5 homeobox	<i>POU5F1</i>	NM_002701.5	F: GCAATTTGCCAAGCTCCTGAA R: AGCTAAGCTGCAGAGCCTCAAAG	141
Pluripotent gene	Nanog homeobox	<i>NONAG</i>	NM_024865.3	F: CAACTGGCCGAAGAATAGCAATG R: TGGTTGCTCCAGGTTGAATTGTT	159
	Kruppel-like factor 4	<i>KLF4</i>	NM_004235.5	F: AAGAGTTCCCATCTCAAGGCACA R: GGGCGAATTTCCATCCACAG	91
Osteogenic gene	Runt-related transcription factor 2	<i>RUNX2</i>	NM_004348.3	F: ATGTGTTTGTTCAGCAGCA R: TCCCTAAAGTCACTCGGTATGTGTA	195
	Collagen type I alpha 1 chain	<i>COL1A1</i>	NM_000088	F: GCTACCCAACTTGCCCTTCATG R: TGCAGTGGTAGGTGATGTTCTGA	168
Chondrogenic gene	SRY-box 9	<i>SOX9</i>	NM_000346.3	F: TGTATCACTGAGTCATTTGCAGTGT R: AAGGTCTGTCAGTGGGCTGAT	187
	Collagen type II alpha 1 chain	<i>COL2A1</i>	NM_001844.4	F: TGAAGGTTTTCTGCAACATGGA R: TTGGGAACGTTTGTCTGGATT	67
Adipogenic gene	Peroxisome proliferator-activated receptor gamma	<i>PPARG</i>	NM_005037.5	F: TGGAATTAGATGACAGCGACTTGG R: CTGGAGCAGCTTGGCAAACA	182

represented as an increase or decrease relative to the calibrator. Since cDNAs were synthesised from RNAs by one cycle of PCR amplification, the gene expression analysis results represent the relative amount of mRNA templates in the test sample. The errors were calculated from the standard deviations carried by the triplicate  $C_T$  values using the standard propagation of the error methods.

The relative gene expression for pluripotent marker genes *KLF4*, *NANOG*, and *POU5F1* (*Oct-4*) are shown in Figure 1. The *KLF4* gene was expressed at markedly higher levels ( $p < 0.01$ ) in MSCs cultured in normoxia than in hypoxia. The levels of *KLF4* increased 2.1-folds with increased passage number from 5 to 9 in hypoxia ( $p < 0.05$ ), while it decreased 0.7-folds in normoxia ( $p < 0.05$ ). Likewise, *NANOG* and *POU5F1* (*Oct-4*) genes were expressed slightly higher under normoxia than in hypoxia, but the change was much smaller than for *KLF4*. Under both hypoxic and normoxic conditions, the expression of *NANOG* and *POU5F1* (*Oct-4*) decreased with the increasing passage number.

We next turned to gene markers of lineage-specific differentiation. An examination of relative expression of osteogenic marker genes *RUNX2* and *COL1A1* revealed little change with passage number under hypoxia (Figure 1). *COL1A1* also had no significant change with passage number under normoxia; however, the *RUNX2* gene was considerably higher in normoxic culture conditions relative to hypoxic conditions and was significantly higher ( $p < 0.05$ ) at the earlier passage. Expression of the chondrogenic marker genes *Sox9* and *COL2A1* was found to remain relatively low in hypoxia, while *Sox9* expression was significantly higher in normoxia when compared to hypoxia ( $p < 0.01$ ) and decreased 0.45-folds with increased passage number. Overall expression of osteogenic and chondrogenic genes reduced with passage number. In contrast, expression of the

adipogenic marker gene *PPARG* was increased markedly in normoxia relative to hypoxia ( $p < 0.01$ ). Expression of *PPARG* also increased with passage number in MSCs cultured in both hypoxia and normoxia ( $p < 0.01$ ). Overall, the expression levels of pluripotent, osteogenic, chondrogenic, and adipogenic marker genes were higher in normoxia when compared to equivalent hypoxia condition. The expression levels for genes reduced with passage number, except for *PPARG* which increased with passage number in cells grown in both hypoxia and normoxia.

Next, we determined the effect of oxygen tension and passage number on MSC cell surface protein markers. High expression of surface markers CD105, CD73, and CD90 are important criteria for the classification and clinical use of MSCs. Flow cytometry was employed to determine the presence of these proteins using the fluorescent antibodies anti-CD105 PE, anti-CD73 FITC, and anti-CD90 PE Cy7. All samples showed high expression of each of the cell surface markers by flow cytometry, relative to unlabelled controls (Figure 2), indicating that the cells retain these positive markers of MSCs at both early and late passages when cultured in either hypoxia and normoxia. Interestingly, the level of CD105 detected on the cell surface was markedly higher for cells grown in normoxia than for those grown in hypoxia. To further confirm MSC state, negative markers of MSCs, CD14, CD45, CD34, and CD 19 were tested by flow cytometry using anti-CD14 FITC, anti-CD45 PerCP, anti-CD34-RPE, and anti-CD19 PE-Cy7 antibodies, respectively. All cell samples were negative for each of these cell surface markers by flow cytometry, overlapping closely with unstained controls (Figure 2). This further confirms that cells grown under both hypoxia and normoxia, and at early and late passage, meet the standard criteria set by the ISCT to define MSCs for laboratory-based investigation and preclinical studies.

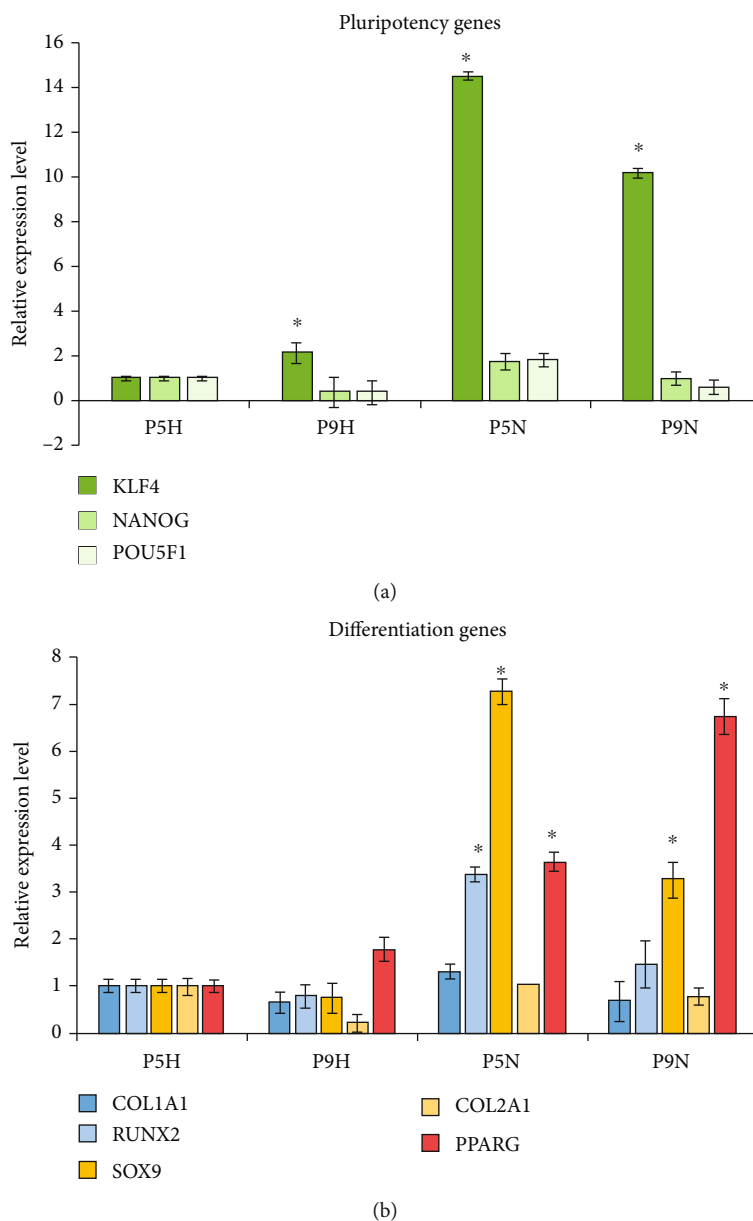


FIGURE 1: Relative gene expression levels by qRT-PCR for cells cultured under hypoxia and normoxia. (a) qRT-PCR for pluripotency genes *KLF4*, *NANOG*, and *POU5F1*. (b) qRT-PCR for MSC differentiation genes; osteogenic markers *COL1A1* and *RUNX2*, chondrogenic markers *SOX9* and *COL2A1*, and adipogenic marker *PPARG*. Relative expression levels are expressed using the *GAPDH* as the reference gene, and values were normalized to P5H; error bars represent SD. Statistically significant difference,  $p < 0.05$ , shown by \* for relative expression level when compared to P5H sample.

A final characteristic of MSCs is that they can differentiate into multiple lineages under the appropriate conditions *in vivo* and *in vitro*. Thus, we determined the chondrogenic and osteogenic differentiation potential of the adipose-derived MSCs. Osteogenic differentiation was induced for 19 days before staining with Alizarin Red S to test for calcium accumulation. Osteogenic differentiation was confirmed in the culture dishes for all culture conditions, relative to undifferentiated controls, by red staining as well as the beginning of mineral deposits in the form of discrete precipitate foci/nodules (Figures 3(a)–3(e)). This osteogenic differentiation was further analysed under higher magnification

on coverslips, where Alzerin Red S staining for calcium accumulation was more evident (Figures 3(f)–3(j)). Although both early- and late-passage MSCs grown under normoxia and hypoxia showed differentiation potential, cells grown under hypoxia appeared to have increased calcium mineralisation (Figures 3(d) and 3(e)). Alternatively, chondrogenic differentiation was induced for 21 days, before being stained with Alcian Blue to show proteoglycan accumulation. Imaging of cell monolayers in culture dishes revealed positive staining of Alcian Blue for all culture conditions compared to controls (Figures 4(a)–4(e)). The chondrogenic differentiation was further analysed under higher magnification on



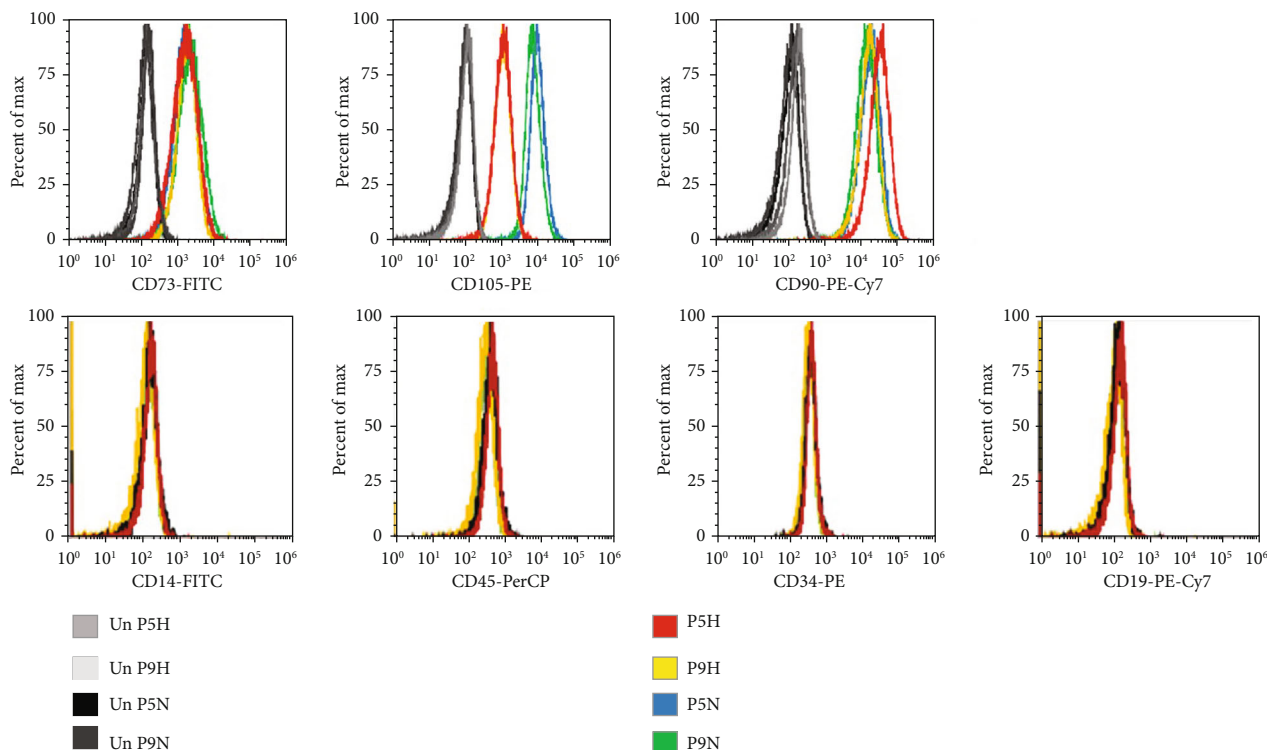


FIGURE 2: Flow cytometry of CD cell surface markers for cells cultured under hypoxia and normoxia. The positive CD markers for MSCs as detected by the fluorescent antibodies anti-CD73 FITC, anti-CD105 PE, and anti-CD90 PE Cy7. The negative markers of MSCs were detected using anti-CD14 FITC, anti-CD45 PerCP, anti-CD34-R-PE, and anti-CD19 PE-Cy7 antibodies. Unstained cell for each condition was used as negative controls.

coverslips whereby Alcian Blue staining for chondrocytes and proteoglycans was more evident (Figures 4(f)–4(j)).

#### 4. Discussion

MSCs have significant clinical value and have been used in a number of autologous therapeutic applications. MSCs have anti-inflammatory and immunosuppressive properties and could also be used in allogeneic transplantation but this would require large numbers of cells [2, 28, 34]. However, for safety purposes, a low *in vitro* passage number of less than 5 is generally used for MSCs in clinical applications [35]. The challenge for allogeneic cell therapies, as well as tissue engineering applications, is that low passage MSCs might not yield enough cells for these applications where larger numbers of stem cells are needed. One potential source of allogeneic MSCs is from adipose tissue. There are a large number of liposuction surgeries performed every year around the world, where adipose tissue is removed and discarded as medical waste. This excess adipose tissue could serve as a valuable source of MSCs with implied extensive potential for allogeneic therapeutics and tissue engineering [16]. In this study, we focused on adipose-derived MSCs which originally reside at low oxygen concentration (<4%) [36] and investigated the effects of oxygen tension and passage number to determine whether they retain their stem cell properties. We compared four samples: passage 5 and 9 MSCs cultured in hypoxic conditions, P5H and P9H, respec-

tively, and passage 5 and 9 MSCs cultured in normoxic condition, P5N and P9N, respectively. These samples were then characterised by qRT-PCR, flow cytometry of CD markers, and differentiation potential.

Firstly, the relative gene expression in each sample was determined using the relative quantification  $2^{-\Delta\Delta CT}$  method. The housekeeping gene *GAPDH* was employed as reference gene as it has comparably stable expression [37], and the P5H sample was used as a calibrator. Three pluripotency marker genes, POU class 5 homeobox 1 (*POU5F1*) gene, Nanog homeobox (*Nanog*) gene, and Kruppel-like factor 4 (*KLF4*) genes, were analysed for their expression by qRT-PCR quantification. *POU5F1* gene, also known as *Oct-4*, encodes a transcription factor containing a POU homeodomain involved in embryonic development and stem cell pluripotency [38]. *NANOG* encodes a DNA binding homeobox transcription factor involved in ESC proliferation, renewal, and pluripotency, which can also block stem cell differentiation [39]. *KLF4* gene encodes a Kruppel family transcription factor involved in diverse cellular processes to regulate cell proliferation, differentiation, and acts a suppressor of p53 gene expression [40, 41]. The roles of *Oct-4* and *NANOG* are to maintain MSC properties, keeping MSCs in proliferative and undifferentiated states, while *KLF4* regulates the cell cycle. This study has shown that adipose-derived MSCs expressed the classical pluripotency-related genes *NANOG*, *Oct-4*, and *KLF4*. Cells grown in normoxia had a higher expression of the genes

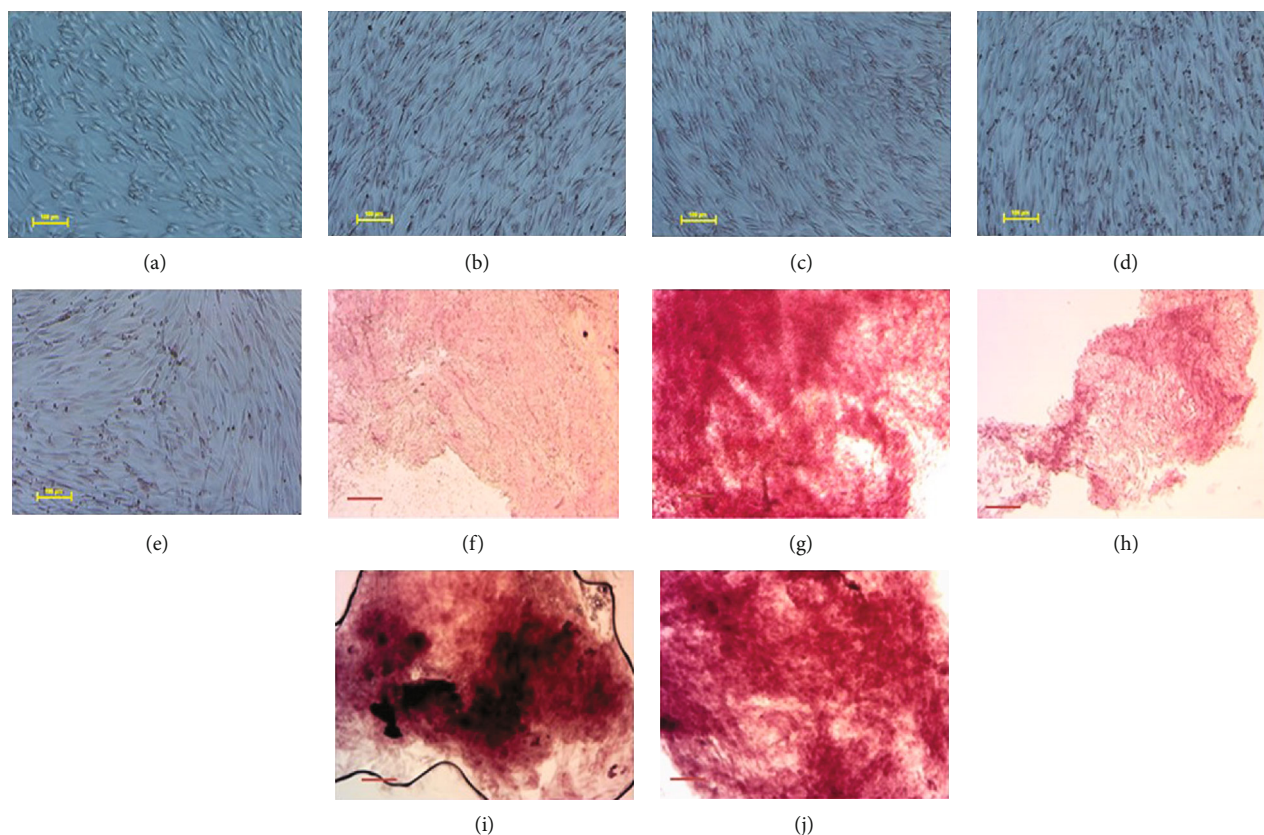


FIGURE 3: Osteogenic differentiation of MSCs cultured under hypoxia and normoxia. Alizarin Red S staining for cells differentiated for 19 days imaged in (a–e) culture wells and (f–j) on coverslips. (a) Negative control, (b) passage 5 hypoxia (P5H), (c) passage 9 hypoxia (P9H), (d) passage 5 normoxia (P5N), and (e) passage 9 normoxia (P9H). Scale bar 100  $\mu\text{m}$ .

than those grown in hypoxia. These results are in line with a study demonstrating that 2,232 genes which involved in development, morphogenesis, cell adhesion, and proliferation were upregulated more than three-folds in MSCs under normoxic culture condition [42]. Additionally, hypoxia has been shown to inhibit the expression of stemness genes in MSCs such as *Oct-4* gene [43]. This is in contrast to other reports whereby hypoxia enhanced stemness gene expression [26, 36, 44–46]. Furthermore, we observed a reduction *NANOG* and *Oct-4* genes' expression with an increased passage number, both in hypoxia and normoxia. This finding corresponds with previous studies in which the expression of two major pluripotent genes *Oct-4* and *NANOG* were expressed at higher level at early passage and reduced with passage number [47, 48]. Additionally, we found that *KLF4* was expressed much higher compared to *NANOG* and *Oct-4*, and was also much higher under normoxia. Furthermore, the increased expression of *KLF4* with passage number under hypoxia is in line with previous reports of young versus old human BM-MSCs [49], while the reduction in *KLF4* expression under hypoxia versus normoxia has also been previously reported [17]. These results taken together suggest that culturing MSCs under normoxia activates *KLF4* to regulate the cell cycle and maintain MSCs in their proliferative and undifferentiated state.

The relative expression for the chondrogenic, osteogenic, and adipogenic genes were also analysed. Firstly, the chondrogenic genes *SRY-box 9 (SOX9)* and *Collagen type II alpha 1 chain (COL2A1)* levels decreased with passage number. The *COL2A1* gene encodes the alpha 1 chain of type II collagen—a fibrillar collagen found in cartilage and *SOX9* is a master regulator of chondrogenesis [50]. These results concur with previous studies, which showed the chondrogenic differentiation potential reduced at higher passage [47, 51, 52]. Next, the adipogenic gene, peroxisome proliferator-activated receptor gamma (*PPARG*) gene, was analysed. It encodes a member of the peroxisome proliferator-activated receptor subfamily of nuclear receptor gamma and is a regulator of adipocyte differentiation. *PPARG* gene expression increased with passage number for both hypoxia and normoxia, with higher levels detected in normoxia overall. This is inconsistent with previous studies, which have shown that MSCs have a reduced capacity for adipogenic differentiation with increasing passage number [52]. The adipose origin of the MSCs used in this study may be an explanation for this apparent contradiction. In a previous study, bone marrow derived-MSCs differentiated readily into osteoblasts and adipose-derived MSCs into adipocytes [53]. Finally, the osteogenic gene expression for the Runt-related transcription factor 2 (*RUNX2*) and *Collagen*

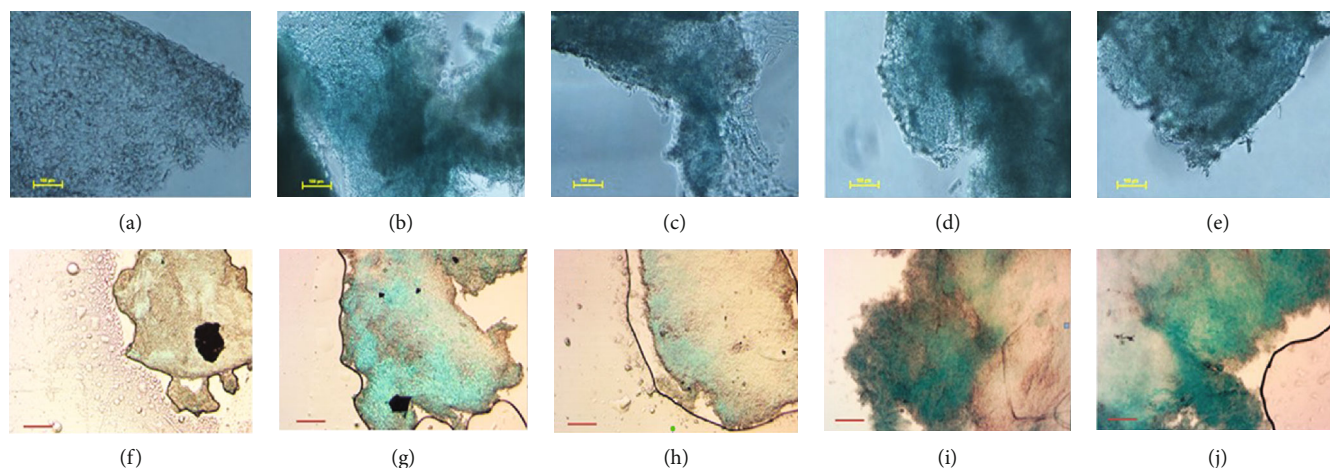


FIGURE 4: Chondrogenic differentiation of MSCs cultured under hypoxia and normoxia. Alcian Blue staining for cells differentiated for 21 days imaged in (a–e) culture wells and (f–j) on coverslips. (a) Negative control, (b) passage 5 hypoxia (P5H), (c) passage 9 hypoxia (P9H), (d) passage 5 normoxia (P5N), and (e) passage 9 normoxia (P9H). Scale bar 100  $\mu\text{m}$ .

type I alpha 1 chain (*COL1A1*) genes were also determined. Both genes decreased with passage number, consistent with previous published results [48, 52].

The presence or absence of CD cell surface markers is also important criteria for MSCs. We determined the levels of both positive and negative MSC markers by flow cytometry and qRT-PCR. As a minimum, it has been suggested that at least two positive and two negative markers are required for MSC phenotyping [54]. We found that the three positive CD markers CD105, CD73, and CD90 were present at high levels in all samples, as determined by flow cytometry. Interestingly, CD105 was higher in normoxia when compared to cells cultured under hypoxia; the reduced levels of MSC surface marker expression of CD105 and CD44 have also been reported for MSC cultured in hypoxia for greater than 48 hrs [55]. These studies concluded that the consequences of the downregulation of CD105, which is an adhesive molecule and part of the TGF $\beta$  receptor complex, remain to be determined. Additionally, our findings for the negative MSC CD markers CD14, CD45, CD34, and CD19 were confirmed to be absent across all conditions. Taken together, our results indicate that adipose-derived MSCs grown in both hypoxia and normoxia and at early and late passage meet the minimum CD phenotype requirements for laboratory-based investigation and clinical applications [35].

MSCs also have the ability to differentiate into many different cell types. Here, we demonstrated the ability of adipose-derived MSCs to differentiate into osteocytes and chondrocytes under all culture conditions. Firstly, following 19 days of osteogenic differentiation MSCs grown under hypoxia and normoxia were shown to be able differentiate into osteocytes. Positive Alizarin Red S staining and calcium accumulation were detected in both early- and late-passage cells and is in line with the previous results [56, 57]. Additionally, chondrogenic differentiation was induced for 21 days, before being stained with Alcian Blue to confirm MSC differentiation into chondrocytes [58, 59]. Proteoglycan accumulation and deposits were observed for cells cultured in all conditions, confirming chondrogenic differentiation potential of

both early- and late-passage MSCs cultured under hypoxia or normoxia.

Although the effects of hypoxia on MSCs have been well studied, there are conflicting reports on its effect on differentiation. For example, hypoxia inhibits osteogenic and adipogenic differentiation capacity of MSCs [25, 60–64] and attenuates MSC chondrogenesis [65]. In contrast, others have shown that hypoxia promotes osteogenic, adipogenic, and chondrogenic differentiation potential of MSCs [26, 66, 67]. Furthermore, hypoxia enhances osteogenesis but inhibits adipogenesis of MSCs [68]. The variation in reports, especially for adipose-derived MSCs, might be caused by different cultivation condition as hypoxia has been shown to effect these cells more [21]. Furthermore, it is important to take into account the normal physiological state [69, 70]. The focus of our study was to determine whether late-passage MSCs grown in normoxic culture conditions could be a reliable, safe, and effective source of cells for regenerative medicine and tissue engineering for applications such as osteoarthritis. We confirmed that late-passage adipose-derived MSCs cultured under normoxia retained both chondrogenic and osteogenic differentiation potential.

In summary, we compared the effects of culturing adipose-derived MSCs in hypoxia and normoxia. We found that the expression levels of pluripotent, osteogenic, chondrogenic, and adipogenic genes were higher in normoxia when compared to hypoxia, and expression levels reduced with passage number. Despite these gene expression changes, we showed that cells grown under all conditions met the phenotypic requirements for both positive and negative CD markers by flow cytometry. Furthermore, the MSCs were confirmed to maintain the ability to differentiate into both osteogenic and chondrogenic cell types. Our findings demonstrate that cells grown under both hypoxia and normoxia, and at early and late passage, meet the standard criteria set by the ISCT to define MSCs for laboratory-based investigation and preclinical studies. Therefore, these culture conditions could be used when scaling up MSC cell culture in bioreactors, if large numbers of cells are required for allogeneic



clinical applications or tissue engineering for the treatment of joint and bone diseases such as osteoarthritis.

## Data Availability

No data were used to support this study.

## Conflicts of Interest

Authors have no conflicts of interest.

## Acknowledgments

This research is supported by an Australian Government Research Training Program (RTP) Scholarship.

## References

- [1] M. F. Pittenger, A. M. Mackay, S. C. Beck et al., "Multilineage potential of adult human mesenchymal stem cells," *Science*, vol. 284, no. 5411, pp. 143–147, 1999.
- [2] R. M. Samsonraj, M. Raghunath, V. Nurcombe, J. H. Hui, A. J. van Wijnen, and S. M. Cool, "Concise review: multifaceted characterization of human mesenchymal stem cells for use in regenerative medicine," *Stem Cells Translational Medicine*, vol. 6, no. 12, pp. 2173–2185, 2017.
- [3] A. Klimczak and U. Kozłowska, "Mesenchymal Stromal Cells and Tissue-Specific Progenitor Cells: Their Role in Tissue Homeostasis," *Stem Cells International*, vol. 2016, Article ID 4285215, 11 pages, 2016.
- [4] F. P. Barry and J. M. Murphy, "Mesenchymal stem cells: clinical applications and biological characterization," *International Journal of Biochemistry and Cell Biology*, vol. 36, no. 4, pp. 568–584, 2004.
- [5] L. da Silva Meirelles, P. C. Chagastelles, and N. B. Nardi, "Mesenchymal stem cells reside in virtually all post-natal organs and tissues," *Journal of Cell Science*, vol. 119, no. 11, pp. 2204–2213, 2006.
- [6] A. I. Caplan and J. E. Dennis, "Mesenchymal stem cells as trophic mediators," *Journal of Cellular Biochemistry*, vol. 98, no. 5, pp. 1076–1084, 2006.
- [7] L. da Silva Meirelles, A. I. Caplan, and N. B. Nardi, "In search of the in vivo identity of mesenchymal stem cells," *Stem Cells*, vol. 26, no. 9, pp. 2287–2299, 2008.
- [8] K. Shah, T. Drury, I. Roic et al., "Outcome of Allogeneic Adult Stem Cell Therapy in Dogs Suffering from Osteoarthritis and Other Joint Defects," *Stem Cells International*, vol. 2018, Article ID 7309201, 7 pages, 2018.
- [9] K. Shah, A. G. Zhao, and H. Sumer, "New Approaches to Treat Osteoarthritis with Mesenchymal Stem Cells," *Stem Cells International*, vol. 2018, Article ID 5373294, 9 pages, 2018.
- [10] M. Dominici, K. Le Blanc, I. Mueller et al., "Minimal criteria for defining multipotent mesenchymal stromal cells. The International Society for Cellular Therapy position statement," *Cytotherapy*, vol. 8, no. 4, pp. 315–317, 2006.
- [11] M. Faustini, M. Bucco, T. Chlapanidas et al., "Nonexpanded mesenchymal stem cells for regenerative medicine: yield in stromal vascular fraction from adipose tissues," *Tissue Engineering Part C-Methods*, vol. 16, no. 6, pp. 1515–1521, 2010.
- [12] J. J. Bara, R. G. Richards, M. Alini, and M. J. Stoddart, "Concise review: bone marrow-derived mesenchymal stem cells change phenotype following in vitro culture: implications for basic research and the clinic," *Stem Cells*, vol. 32, no. 7, pp. 1713–1723, 2014.
- [13] D. Brindley, K. Moorthy, J. H. Lee, C. Mason, H. W. Kim, and I. Wall, "Bioprocess forces and their impact on cell behavior: implications for bone regeneration therapy," *Journal of Tissue Engineering*, vol. 2011, 2011.
- [14] P. A. Sotiropoulou, S. A. Perez, M. Salagianni, C. N. Baxevasis, and M. Papamichail, "Characterization of the optimal culture conditions for clinical scale production of human mesenchymal stem cells," *Stem Cells*, vol. 24, no. 2, pp. 462–471, 2006.
- [15] M. E. Bernardo, A. M. Cometa, D. Pagliara et al., "Ex vivo expansion of mesenchymal stromal cells," *Best Practice and Research: Clinical Haematology*, vol. 24, no. 1, pp. 73–81, 2011.
- [16] J. M. Gimble, A. J. Katz, and B. A. Bunnell, "Adipose-derived stem cells for regenerative medicine," *Circulation Research*, vol. 100, no. 9, pp. 1249–1260, 2007.
- [17] L. Basciano, C. Nemos, B. Foliguet et al., "Long term culture of mesenchymal stem cells in hypoxia promotes a genetic program maintaining their undifferentiated and multipotent status," *BMC Cell Biology*, vol. 12, no. 1, p. 12, 2011.
- [18] K. Naka, T. Muraguchi, T. Hoshii, and A. Hirao, "Regulation of reactive oxygen species and genomic stability in hematopoietic stem cells," *Antioxidants & Redox Signaling*, vol. 10, no. 11, pp. 1883–1894, 2008.
- [19] K. Ito and T. Suda, "Metabolic requirements for the maintenance of self-renewing stem cells," *Nature Reviews Molecular Cell Biology*, vol. 15, no. 4, pp. 243–256, 2014.
- [20] D. C. Chow, L. A. Wenning, W. M. Miller, and E. T. Papoutsakis, "Modeling pO<sub>2</sub> distributions in the bone marrow hematopoietic compartment. II. Modified Kroghian models," *Biophysical Journal*, vol. 81, no. 2, pp. 685–696, 2001.
- [21] T. Ma, W. L. Grayson, M. Frohlich, and G. Vunjak-Novakovic, "Hypoxia and stem cell-based engineering of mesenchymal tissues," *Biotechnology Progress*, vol. 25, no. 1, pp. 32–42, 2009.
- [22] J. C. Estrada, C. Albo, A. Benguria et al., "Culture of human mesenchymal stem cells at low oxygen tension improves growth and genetic stability by activating glycolysis," *Cell Death and Differentiation*, vol. 19, no. 5, pp. 743–755, 2012.
- [23] A. Pezzi, B. Amorin, Á. Laureano et al., "Effects of hypoxia in long-term in vitro expansion of human bone marrow derived mesenchymal stem cells," *Journal of Cellular Biochemistry*, vol. 118, no. 10, pp. 3072–3079, 2017.
- [24] D. W. Wang, B. Fermor, J. M. Gimble, H. A. Awad, and F. Guilak, "Influence of oxygen on the proliferation and metabolism of adipose derived adult stem cells," *Journal of Cellular Physiology*, vol. 204, no. 1, pp. 184–191, 2005.
- [25] C. Holzwarth, M. Vaegler, F. Gieseke et al., "Low physiologic oxygen tensions reduce proliferation and differentiation of human multipotent mesenchymal stromal cells," *BMC Cell Biology*, vol. 11, no. 1, p. 11, 2010.
- [26] S. P. Hung, J. H. Ho, Y. R. V. Shih, T. Lo, and O. K. Lee, "Hypoxia promotes proliferation and osteogenic differentiation potentials of human mesenchymal stem cells," *Journal of Orthopaedic Research*, vol. 30, no. 2, pp. 260–266, 2012.
- [27] W. L. Grayson, F. Zhao, B. Bunnell, and T. Ma, "Hypoxia enhances proliferation and tissue formation of human mesenchymal stem cells," *Biochemical and Biophysical Research Communications*, vol. 358, no. 3, pp. 948–953, 2007.



- [28] L. da Silva Meirelles, A. M. Fontes, D. T. Covas, and A. I. Caplan, "Mechanisms involved in the therapeutic properties of mesenchymal stem cells," *Cytokine & Growth Factor Reviews*, vol. 20, no. 5-6, pp. 419-427, 2009.
- [29] I. Rosova, M. Dao, B. Capoccia, D. Link, and J. A. Nolte, "Hypoxic preconditioning results in increased motility and improved therapeutic potential of human mesenchymal stem cells," *Stem Cells*, vol. 26, no. 8, pp. 2173-2182, 2008.
- [30] J. K. Fraser, I. Wulur, Z. Alfonso, and M. H. Hedrick, "Fat tissue: an underappreciated source of stem cells for biotechnology," *Trends in Biotechnology*, vol. 24, no. 4, pp. 150-154, 2006.
- [31] P. A. Zuk, M. Zhu, P. Ashjian et al., "Human adipose tissue is a source of multipotent stem cells," *Molecular Biology of the Cell*, vol. 13, no. 12, pp. 4279-4295, 2002.
- [32] A. Dudakovic, E. Camilleri, S. M. Riestler et al., "High-resolution molecular validation of self-renewal and spontaneous differentiation in clinical-grade adipose-tissue derived human mesenchymal stem cells," *Journal of Cellular Biochemistry*, vol. 115, no. 10, pp. 1816-1828, 2014.
- [33] J. S. Yuan, A. Reed, F. Chen, and C. N. Stewart, "Statistical analysis of real-time PCR data," *BMC Bioinformatics*, vol. 7, no. 1, 2006.
- [34] K. McIntosh, S. Zvonic, S. Garrett et al., "The immunogenicity of human adipose-derived cells: temporal changes in vitro," *Stem Cells*, vol. 24, no. 5, pp. 1246-1253, 2006.
- [35] L. de Girolamo, E. Lucarelli, G. Alessandri et al., "Mesenchymal stem/stromal cells: a new "cells as drugs" paradigm. Efficacy and critical aspects in cell therapy," *Current Pharmaceutical Design*, vol. 19, no. 13, pp. 2459-2473, 2013.
- [36] W. K. Z. Wan Safwani, J. R. Choi, K. W. Yong, I. Ting, N. A. Mat Adenan, and B. Pinguan-Murphy, "Hypoxia enhances the viability, growth and chondrogenic potential of cryopreserved human adipose-derived stem cells," *Cryobiology*, vol. 75, pp. 91-99, 2017.
- [37] E. Ragni, M. Viganò, P. Rebulli, R. Giordano, and L. Lazzari, "What is beyond a qRT-PCR study on mesenchymal stem cell differentiation properties: how to choose the most reliable housekeeping genes," *Journal of Cellular and Molecular Medicine*, vol. 17, no. 1, pp. 168-180, 2013.
- [38] G. L. Shi and Y. Jin, "Role of Oct4 in maintaining and regaining stem cell pluripotency," *Stem Cell Research & Therapy*, vol. 1, no. 5, p. 39, 2010.
- [39] A. Saunders, F. Faiola, and J. L. Wang, "Concise review: pursuing self-renewal and pluripotency with the stem cell factor Nanog," *Stem Cells*, vol. 31, no. 7, pp. 1227-1236, 2013.
- [40] A. M. Ghaleb and V. W. Yang, "Krüppel-like factor 4 (KLF4): what we currently know," *Gene*, vol. 611, pp. 27-37, 2017.
- [41] C. S. Park, A. Lewis, T. Chen, and D. Lacorazza, "Concise review: regulation of self-renewal in normal and malignant hematopoietic stem cells by Krüppel-Like factor 4," *Stem Cells Translational Medicine*, vol. 8, no. 6, pp. 568-574, 2019.
- [42] S. Ohnishi, T. Yasuda, S. Kitamura, and N. Nagaya, "Effect of hypoxia on gene expression of bone marrow-derived mesenchymal stem cells and mononuclear cells," *Stem Cells*, vol. 25, no. 5, pp. 1166-1177, 2007.
- [43] H. Y. Ren, Y. Cao, Q. J. Zhao et al., "Proliferation and differentiation of bone marrow stromal cells under hypoxic conditions," *Biochemical and Biophysical Research Communications*, vol. 347, no. 1, pp. 12-21, 2006.
- [44] N. E. B. Ahmed, M. Murakami, S. Kaneko, and M. Nakashima, "The effects of hypoxia on the stemness properties of human dental pulp stem cells (DPSCs)," *Scientific Reports*, vol. 6, no. 1, 2016.
- [45] C. Fotia, A. Massa, F. Boriani, N. Baldini, and D. Granchi, "Hypoxia enhances proliferation and stemness of human adipose-derived mesenchymal stem cells," *Cytotechnology*, vol. 67, no. 6, pp. 1073-1084, 2015.
- [46] S. Y. Kwon, S. Y. Chun, Y. S. Ha et al., "Hypoxia enhances cell properties of human mesenchymal stem cells," *Tissue Engineering and Regenerative Medicine*, vol. 14, no. 5, pp. 595-604, 2017.
- [47] E. Pierantozzi, B. Gava, I. Manini et al., "Pluripotency regulators in human mesenchymal stem cells: expression of NANOG but not of OCT-4 and SOX-2," *Stem Cells and Development*, vol. 20, no. 5, pp. 915-923, 2011.
- [48] C. C. Tsai and S. C. Hung, "Functional roles of pluripotency transcription factors in mesenchymal stem cells," *Cell Cycle*, vol. 11, no. 20, pp. 3711-3712, 2012.
- [49] J. Dong, Z. Zhang, H. Huang et al., "miR-10a rejuvenates aged human mesenchymal stem cells and improves heart function after myocardial infarction through KLF4," *Stem Cell Research & Therapy*, vol. 9, no. 1, pp. 1-16, 2018.
- [50] J. C. Robins, N. Akeno, A. Mukherjee et al., "Hypoxia induces chondrocyte-specific gene expression in mesenchymal cells in association with transcriptional activation of Sox9," *Bone*, vol. 37, no. 3, pp. 313-322, 2005.
- [51] A. Banfi, A. Muraglia, B. Dozin, M. Mastrogiacomo, R. Cancedda, and R. Quarto, "Proliferation kinetics and differentiation potential of ex vivo expanded human bone marrow stromal cells: implications for their use in cell therapy," *Experimental Hematology*, vol. 28, no. 6, pp. 707-715, 2000.
- [52] R. Izadpanah, C. Trygg, B. Patel et al., "Biologic properties of mesenchymal stem cells derived from bone marrow and adipose tissue," *Journal of Cellular Biochemistry*, vol. 99, no. 5, pp. 1285-1297, 2006.
- [53] M. Al-Nbaheen, R. Vishnubalaji, D. Ali et al., "Human stromal (mesenchymal) stem cells from bone marrow, adipose tissue and skin exhibit differences in molecular phenotype and differentiation potential," *Stem Cell Reviews and Reports*, vol. 9, no. 1, pp. 32-43, 2013.
- [54] P. Bourin, B. A. Bunnell, L. Casteilla et al., "Stromal cells from the adipose tissue-derived stromal vascular fraction and culture expanded adipose tissue-derived stromal/stem cells: a joint statement of the International Federation for Adipose Therapeutics and Science (IFATS) and the International Society for Cellular Therapy (ISCT)," *Cytotherapy*, vol. 15, no. 6, pp. 641-648, 2013.
- [55] B. Antebi, L. A. Rodriguez, K. P. Walker et al., "Short-term physiological hypoxia potentiates the therapeutic function of mesenchymal stem cells," *Stem Cell Research & Therapy*, vol. 9, no. 1, p. 265, 2018.
- [56] W. Wagner, P. Horn, M. Castoldi et al., "Replicative senescence of mesenchymal stem cells: a continuous and organized process," *PLoS ONE*, vol. 3, no. 5, p. e2213, 2008.
- [57] M. E. Wall, S. H. Bernacki, and E. G. Lobo, "Effects of serial passaging on the adipogenic and osteogenic differentiation potential of adipose-derived human mesenchymal stem cells," *Tissue Engineering*, vol. 13, no. 6, pp. 1291-1298, 2007.

- [58] J. D. Kretlow, Y. Q. Jin, W. Liu et al., "Donor age and cell passage affects differentiation potential of murine bone marrow-derived stem cells," *BMC Cell Biology*, vol. 9, no. 1, p. 60, 2008.
- [59] S. Tsutsumi, A. Shimazu, K. Miyazaki et al., "Retention of multilineage differentiation potential of mesenchymal cells during proliferation in response to FGF," *Biochemical and Biophysical Research Communications*, vol. 288, no. 2, pp. 413–419, 2001.
- [60] C. Fehrer, R. Brunauer, G. Laschober et al., "Reduced oxygen tension attenuates differentiation capacity of human mesenchymal stem cells and prolongs their lifespan," *Aging Cell*, vol. 6, no. 6, pp. 745–757, 2007.
- [61] J. H. Lee and D. M. Kemp, "Human adipose-derived stem cells display myogenic potential and perturbed function in hypoxic conditions," *Biochemical and Biophysical Research Communications*, vol. 341, no. 3, pp. 882–888, 2006.
- [62] P. Malladi, Y. Xu, M. Chiou, A. J. Giaccia, and M. T. Longaker, "Effect of reduced oxygen tension on chondrogenesis and osteogenesis in adipose-derived mesenchymal cells," *American Journal of Physiology-Cell Physiology*, vol. 290, no. 4, pp. C1139–C1146, 2006.
- [63] I. H. Park, K. H. Kim, H. K. Choi et al., "Constitutive stabilization of hypoxia-inducible factor alpha selectively promotes the self-renewal of mesenchymal progenitors and maintains mesenchymal stromal cells in an undifferentiated state," *Experimental and Molecular Medicine*, vol. 45, no. 9, p. e44, 2013.
- [64] K. Tamama, H. Kawasaki, S. S. Kerpedjieva, J. J. Guan, R. K. Ganju, and C. K. Sen, "Differential roles of hypoxia inducible factor subunits in multipotential stromal cells under hypoxic condition," *Journal of Cellular Biochemistry*, vol. 112, no. 3, pp. 804–817, 2011.
- [65] M. C. Ronziere, E. Perrier, F. Mallein-Gerin, and A. M. Freyria, "Chondrogenic potential of bone marrow- and adipose tissue-derived adult human mesenchymal stem cells," *Bio-Medical Materials and Engineering*, vol. 20, no. 3-4, pp. 145–158, 2010.
- [66] D. K. Taheem, D. A. Foyt, S. Loaiza et al., "Differential regulation of human bone marrow mesenchymal stromal cell chondrogenesis by hypoxia inducible Factor-1 $\alpha$  hydroxylase inhibitors," *Stem Cells*, vol. 36, no. 9, pp. 1380–1392, 2018.
- [67] C. C. Tsai, Y. J. Chen, T. L. Yew et al., "Hypoxia inhibits senescence and maintains mesenchymal stem cell properties through down-regulation of E2A-p21 by HIF-TWIST," *Blood*, vol. 117, no. 2, pp. 459–469, 2011.
- [68] M. Wagegg, T. Gaber, F. L. Lohanatha et al., "Hypoxia promotes osteogenesis but suppresses adipogenesis of human mesenchymal stromal cells in a hypoxia-inducible factor-1 dependent manner," *Plos One*, vol. 7, no. 9, p. e46483, 2012.
- [69] W. Chen, Y. Zhuo, D. Duan, and M. Lu, "Effects of hypoxia on differentiation of mesenchymal stem cells," *Current Stem Cell Research & Therapy*, vol. 15, no. 4, pp. 332–339, 2020.
- [70] R. Das, H. Jahr, G. van Osch, and E. Farrell, "The role of hypoxia in bone marrow-derived mesenchymal stem cells: considerations for regenerative medicine approaches," *Tissue Engineering Part B-Reviews*, vol. 16, no. 2, pp. 159–168, 2010.

## Research Article

# A Xeno-Free Strategy for Derivation of Human Umbilical Vein Endothelial Cells and Wharton's Jelly Derived Mesenchymal Stromal Cells: A Feasibility Study toward Personal Cell and Vascular Based Therapy

Hataiwan Kunkanjanawan,<sup>1</sup> Tanut Kunkanjanawan,<sup>2</sup> Veerapol Khemarangsarn,<sup>2</sup> Rungrueng Yodsheewan ,<sup>3</sup> Kasem Theerakittayakorn,<sup>4</sup> and Rangsun Parnpai <sup>4</sup>

<sup>1</sup>Medeze Research and Development Co., Ltd, 28/9 Moo 8, Phutthamonthon Sai 4 Rd., Krathum Lom, Sam Phran, Nakhon Pathom 73220, Thailand

<sup>2</sup>Medeze Stem Cell Co., Ltd, 28/9 Moo 8, Phutthamonthon Sai 4 Rd., Krathum Lom, Sam Phran, Nakhon Pathom 73220, Thailand

<sup>3</sup>Department of Pathology, Faculty of Veterinary Medicine, Kasetsart University, 1 Moo 6, Kamphaeng Saen, Nakhon Pathom 73140, Thailand

<sup>4</sup>Embryo Technology and Stem Cell Research Center, School of Biotechnology, Suranaree University of Technology, 111 University Avenue, Muang Nakhon Ratchasima, Nakhon Ratchasima 30000, Thailand

Correspondence should be addressed to Rangsun Parnpai; rangsun@g.sut.ac.th

Received 26 June 2020; Revised 17 August 2020; Accepted 24 August 2020; Published 7 September 2020

Academic Editor: Sangho Roh

Copyright © 2020 Hataiwan Kunkanjanawan et al. This is an open access article distributed under the Creative Commons Attribution License, which permits unrestricted use, distribution, and reproduction in any medium, provided the original work is properly cited.

Coinplantation of endothelial cells (ECs) and mesenchymal stromal cells (MSCs) into the transplantation site could be a feasible option to achieve a sufficient level of graft-host vascularization. To find a suitable source of tissue that provides a large number of high-quality ECs and MSCs suited for future clinical application, we developed a simplified xeno-free strategy for isolation of human umbilical vein endothelial cells (HUVECs) and Wharton's jelly-derived mesenchymal stromal cells (WJ-MSCs) from the same umbilical cord. We also assessed whether the coculture of HUVECs and WJ-MSCs derived from the same umbilical cord (autogenic cell source) or from different umbilical cords (allogenic cell sources) had an impact on *in vitro* angiogenic capacity. We found that HUVECs grown in 5 ng/ml epidermal growth factor (EGF) supplemented xeno-free condition showed higher proliferation potential compared to other conditions. HUVECs and WJ-MSCs obtained from this technic show an endothelial lineage (CD31 and von Willebrand factor) and MSC (CD73, CD90, and CD105) immunophenotype characteristic with high purity, respectively. It was also found that only the coculture of HUVEC/WJ-MSC, but not HUVEC or WJ-MSC mono-culture, provides a positive effect on vessel-like structure (VLS) formation, *in vitro*. Further investigations are needed to clarify the pros and cons of using autogenic or allogenic source of EC/MSC in tissue engineering applications. To the best of our knowledge, this study offers a simple, but reliable, xeno-free strategy to establish ECs and MSCs from the same umbilical cord, a new opportunity to facilitate the development of personal cell-based therapy.

## 1. Introduction

Since blood supply is an essential factor that holds the great effect on graft survival and host tissue integration, various approaches promoting vascularization have been developed in the field of tissue engineering research. Among these,

cotransplantation of multiple cell types (i.e., adipose-derived stem cells and human umbilical vein endothelial cells; HUVECs) has proven to yield a superiority effect on neovascularization in an adipogenesis mouse models [1]. This finding is in accordance with Ma et al. (2014), who showed that coculture of human adipose tissue-derived or

human bone marrow-derived mesenchymal stromal cells (MSCs) with HUVECs resulted in vessel-like structure (VLS) formation after *in vivo* implantation, either on day 3 or on day 7, in athymic mouse models [2]. However, although the beneficial effects between MSCs and ECs have been reported [3–5], these studies were performed on MSCs and ECs derived from the different individuals, as an allogenic cell source. Little is known about the angiogenic capacity of MSCs and ECs coculturing especially when those cells derived from the same (autogenic) source.

Human umbilical cord (hUC) is a unique niche that contains abundant source of postnatal stem cells (such as haematopoietic stem cells and MSCs) and ECs (such as HUVECs) [3, 4, 6]. Several groups have reported various protocols for the isolation of Wharton's jelly-derived mesenchymal stromal cells (WJ-MSCs) from hUC using animal-free or so-called xeno-free culture system [7–10]. Xeno-free culture system refers to the cell cultivation processes that avoid the use of animal-associated supplement, such as fetal bovine serum (FBS) and porcine trypsin, due to an awareness on contamination; both from xenogenic compound and microorganism. Nowadays, xeno-free culture strategy includes, but not limit to, the use of human blood derivatives (such as human serum and human platelet lysate), microbial recombinant proteins, and chemically defined media [11]. Indeed, the advantage of xeno-free culture system is not only to eliminate the risk of zoonosis but also to promote self-renewal ability and multilineage differentiation potential [7, 12, 13]. Over the past few decades, numerous studies illustrate the great value of MSCs in the field of tissue engineering and regenerative medicine through their differentiation potential, ability to homing and engraftment, and paracrine factors secretion [14]. However, one of the major obstacles to transfer this upcoming technology to clinical use is the culture system that the cells have been established. Therefore, to comply with the long-term safety requirements for cell-based therapy, xeno-free established cells have become a preferred source of cell-based product suited for future clinical application [15].

To creating a new opportunity to facilitate the development of personal cell and vascular-based therapy, the objectives of this study are to isolate and expand HUVECs and WJ-MSCs from the same umbilical cord using the defined xeno-free strategies and to determine how the coculture of autogenic and allogenic HUVEC/WJ-MSC contribute to the angiogenic capacity, *in vitro*.

## 2. Materials and Methods

**2.1. Chemicals and Media.** All reagents were purchased from Sigma-Aldrich (St. Louis, MO, USA) unless otherwise stated.

**2.2. Isolation of HUVECs and WJ-MSCs.** In this study, ethical approval was granted by the Ethics Committee for Researches Involving Human Subjects, Suranaree University of Technology (EC-62-81), Nakhon Ratchasima, Thailand. After receiving the signed informed consents from the parents, the umbilical cords ( $N = 3$ ) were collected and processed at Medeze stem cell laboratory within 24 hrs after

delivery. In all experiments, cells were maintained in a humidified atmosphere of 37°C and 5% CO<sub>2</sub> incubator.

HUVECs were isolated from umbilical vein as described previously [16], with some modification. Briefly, the collected umbilical cords were sterilized by ethanol and rinsed twice by phosphate-buffered saline (PBS). Then, the umbilical vein was filled with 0.2% collagenase (xeno-free grade, EMD Millipore; Cat. No. SCR139) and incubated at room temperature for 30 min. After that, the cells were collected and cultured on 25 cm<sup>2</sup> tissue culture flask (Corning). Three different media were examined for their effects on HUVECs isolation: (a) commercial xeno-culture (nonxeno-free) system composed of basal medium 200 (Invitrogen) supplemented with low serum growth supplements (LSGS kit, contain 2% v/v FBS, Invitrogen); (b) xeno-free culture system composed of M199/EBSS (Hyclone) containing 10% human serum (HS), 2 mM L-glutamine, 10 ng/ml basic fibroblast growth factor (bFGF, Prospec), 5 U/ml heparin (xeno-free grade, Life science production), 100 U/ml penicillin, and 100 µg/ml streptomycin (Millipore); (c) xeno-free culture system (B) supplemented with 5 ng/ml epidermal growth factor (EGF, Prospec). These 3 conditions were next referred as LSGS, xeno-free+bFGF, and xeno-free+bFGF+EGF, respectively. On the following day, the media were changed to remove cell debris. The culture media were refreshed every 3–4 days.

After HUVECs isolation, the same umbilical cord was subjected to isolate WJ-MSCs by using tissue explant method. In brief, the umbilical vein was mechanically excised and removed. Then, the umbilical cord matrix was cut into 2–3 mm thick and cultured on 20 µg/ml human fibronectin coated tissue culture plate. WJ-MSCs were maintained in αMEM (Hyclone) supplemented with 10% HS, 100 U/ml penicillin, and 100 µg/ml streptomycin. The culture media were refreshed every 3–4 days.

At 90% confluence, the HUVECs and WJ-MSCs were subcultured by TrypLE Express (Invitrogen) and used for subsequent studies. For future use, HUVECs and WJ-MSCs were frozen in freezing medium consisting of culture medium plus 10% dimethylsulfoxide (Wak-Chemie Medical GmbH) and 20% (v/v) human serum albumin solution (Baxter). The frozen aliquots were then stored in vapor phase liquid nitrogen.

**2.3. Immunocytochemical Staining.** The expression of key endothelial markers, including CD31 (PECAM-1) and von Willebrand factor (vWf), was used to qualitatively analyzed HUVECs cell lines ( $N = 3$ ) obtained from each condition. At passage 3, HUVECs were seeded onto 4-well tissue culture plate (Nunc) and fixed with 4% paraformaldehyde after reaching confluence. Then, cells were washed and blocked with 10% fetal bovine serum in 0.25% Triton X-100 for 1 hr. The cells were incubated with the primary antibodies against human CD31 (1:200, Abcam) and human vWf (1:200, Abcam) overnight at 4°C. Subsequently, cells were washed and incubated for 1 hr with appropriate Alexa 488 (Invitrogen)/DyLight 594 (Thermo Fisher Scientific) conjugated secondary antibody. After washing, cell nuclei were stained with 4',6-diamidino-2-phenylindole (DAPI, Biolegend) for 10 min at room temperature.



Finally, the cells were observed under an inverted fluorescent microscope.

**2.4. Expansion Potential of HUVECs under Different Culture Conditions.** To compare expansion potential in each culture condition, growth kinetics of HUVECs (from passage 4 to passage 6) obtained from LSGS, xeno-free+bFGF, and xeno-free+bFGF+EGF conditions were quantified as described previously [17], with some modifications. Briefly, HUVECs ( $N = 3$ ) were plated at 10,000 cells/cm<sup>2</sup> and cultured under their originated condition for 72 hrs. Then, cells from each group were collected, stained with 0.4% trypan blue (Invitrogen), and counted by Countess™ Automated Cell Counter (Invitrogen). Each condition was performed in duplicate. Population doubling (PD) was calculated using equation (1). NH is the harvested cell number, and NI is the initial cell number.

$$PD = \frac{\log_{10}NH - \log_{10}NI}{\log_{10}2}. \quad (1)$$

**2.5. Flow Cytometry Analysis.** The purities of HUVECs (at passage 3 and passage 6, each passage  $N = 3$ ) and WJ-MSCs (at passage 3,  $N = 3$ ) were taken for flow cytometry analysis. The following antihuman antibodies were used according to the manufacturer's instructions. For HUVECs, cells were stained with anti-CD31-FITC, anti-CD105-PE, and anti-CD45-FITC. For WJ-MSCs, cells were stained with anti-CD73-APC, anti-CD90-FITC, anti-CD105-PE, and anti-CD45-FITC. All antibodies were purchased from BD Bioscience. Corresponding isotype immunoglobulins were used as negative control. Single-cell suspensions of  $1 \times 10^5$  cells were incubated with the appropriate concentration antibodies for 20 min at room temperature. Then, cells were washed and resuspended in 500  $\mu$ L PBS and analyzed using CytoFLEX flow cytometer (Beckman Coulter). At least 10,000 events were acquired, and the results were analyzed using CytExpert software.

**2.6. In vitro 2D-Angiogenic Capacity and Immunocytochemical Staining.** An *in vitro* angiogenic capacities of monocultures and cocultures of autogenic and allogenic HUVECs/WJ-MSCs (1:1 cell ratio) were determined by 2-dimensional (2D) culture ( $N = 3$ ), as previously described [2] with some modifications. In the autogenic group, HUVECs and WJ-MSCs derived from the single umbilical cord were cocultured together. In the allogenic group, HUVECs and WJ-MSCs derived from the different umbilical cords were cocultured together. A total number of  $2 \times 10^5$  cells were seeded and cultured in basal medium 200 supplemented with LSGS on 0.2% gelatin-coated 4-well tissue culture plates. At day 3, samples were washed by PBS and fixed with 4% paraformaldehyde for 20 minutes.

For immunocytochemical staining, 5% normal goat serum was used as a blocking solution for 1 hr at room temperature. After that, samples were incubated with rabbit anti-human CD31 polyclonal antibody (1:80, Abcam) at 4°C, overnight. After three times washing by 0.05% PBS-Tween, the goat anti-rabbit conjugated-horseradish peroxidase (1:1000, Abcam) was added into the cultured wells for 1 hr

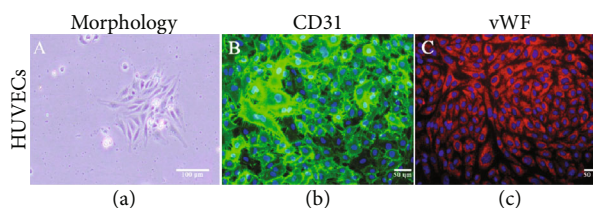


FIGURE 1: Growth colony and the expression of endothelial cell markers of isolated HUVECs. A typical cobblestone-like colony was observed after 24 hours culture (a). A representative image of (b) CD31 (green) and (c) vWF (red) was detected in HUVECs regardless of their cultivated condition. Nuclei of the cells were indicated by 4',6-diamidino-2-phenylindole staining. Studies were performed on three independent cell lines with duplicates. Scale bar: 100  $\mu$ m (a) and 50  $\mu$ m (b, c).

at room temperature. After washing, 3,3'-Diaminobenzidine (DAB) was used as substrate, and hematoxylin was next applied for nuclear staining. The stained cells were observed, and the photos were taken by using an inverted microscope.

**2.7. Statistical Analysis.** All experiments were performed on 3 different cell lines with duplicate. Data were expressed as mean  $\pm$  SEM. Statistical analysis was performed by SPSS software using one-way ANOVA and paired, two-tailed Student's *t*-test. A *P* value was considered statistically significant different at  $P < 0.05$ .

### 3. Results

**3.1. Xeno-Free System Support the Isolation and Expansion of HUVECs and WJ-MSCs.** To obtain multiple cell types potentially useful for cell and vascular based therapy, we first examined the possibility of isolation of HUVECs and WJ-MSCs from single umbilical cord using a well-defined xeno-free culture system compared with commercially available xeno-containing culture medium. In this study, we were able to obtain both HUVEC and WJ-MSC cell lines from all donors under tested culture conditions. Based on phase-contrast microscopic appearance, HUVECs from all three conditions demonstrated a classical cobblestone-like morphology (Figure 1(a)) with no significant difference observed. After reaching confluence of primary culture, HUVECs from all three conditions were able to be passaged, expanded in monolayer culture, and cryopreserved for future usage. At passage 3, the expressions of endothelial-specific markers were first confirmed by indirect immunofluorescence staining. We found that the expressions of CD31 and vWF were detected in HUVECs obtained from all three conditions (Figures 1(b) and 1(c)).

After 7-14 days of culture, adherent fibroblast-like cell populations were grown out from the edge of WJ explants. These cells also had the ability to expand and can be cryopreserved for future study. Therefore, by using a simple tissue explant technic, the rest of the umbilical cord can still be used as a source of WJ-MSCs.

**3.2. Xeno-Free Culture System Accelerated the Proliferation Potential of HUVECs.** We next evaluated the effect of media

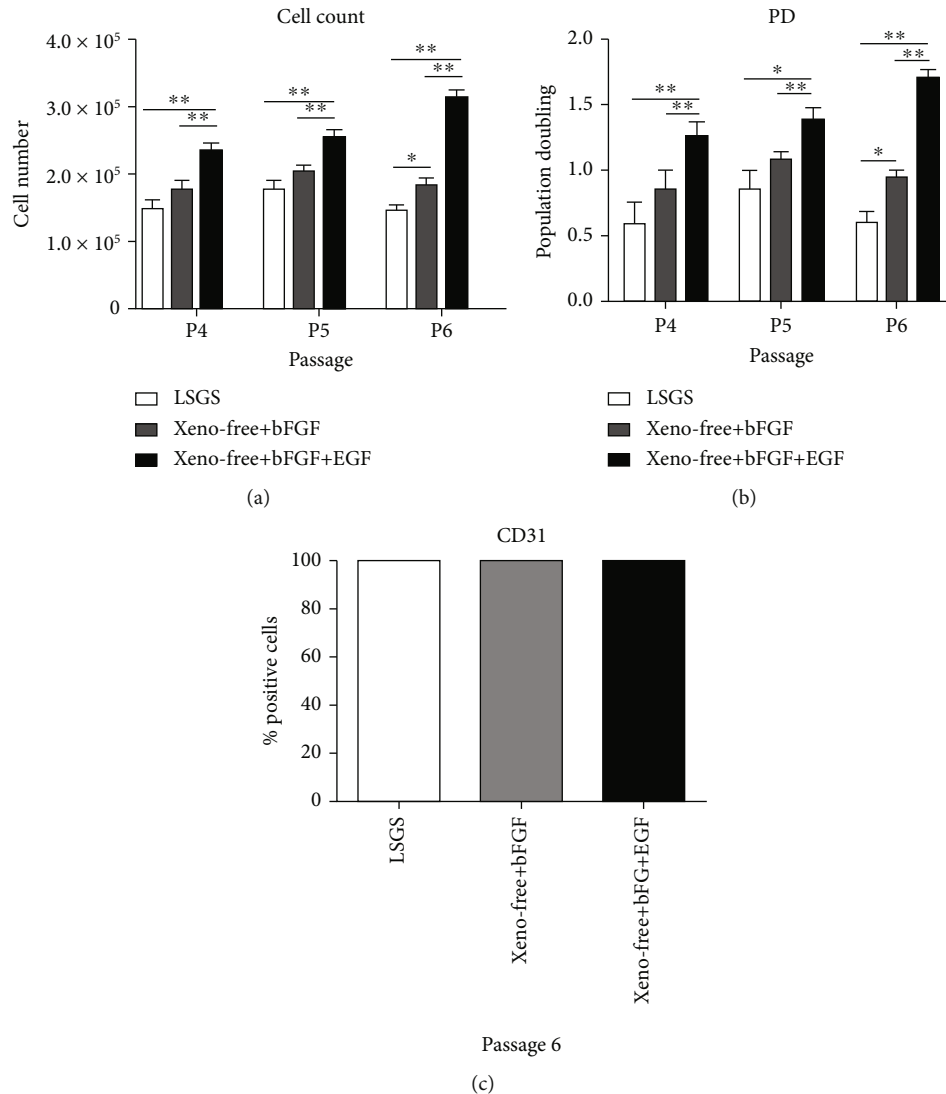


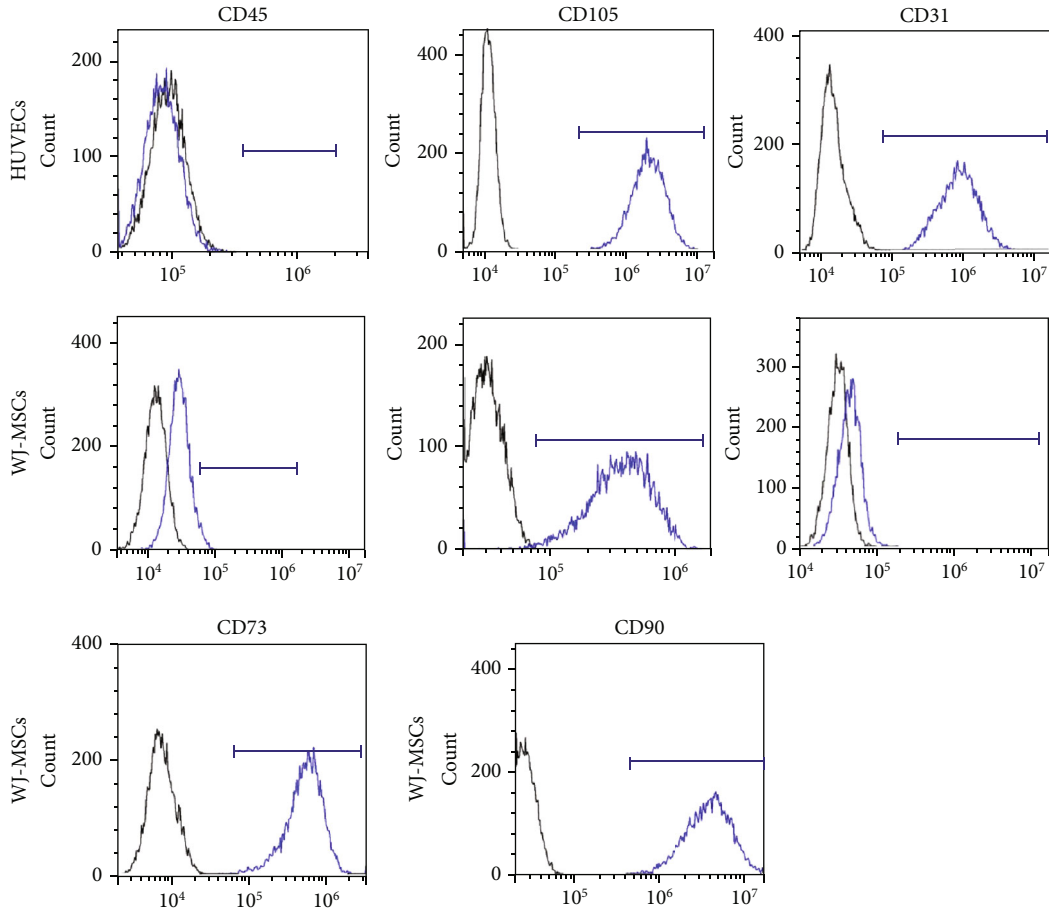
FIGURE 2: Effects of different culture constituents on growth kinetics and endothelial marker maintenance of HUVECs. Comparison of LSGS, xeno-free+bFGF, and xeno-free+bFGF+EGF culture media on cell proliferation (a) and population doubling (b) at passage 4, 5, and 6. At passage 6, HUVECs obtained from all three conditions still maintain the expression of CD31 (c). Data were expressed as mean  $\pm$  SEM ( $N = 3$ ). Significant differences at \* $P < 0.05$  and \*\* $P < 0.01$ .

constituent and supplement on the proliferation of HUVECs isolated from all three conditions: LSGS, xeno-free+bFGF, and xeno-free+bFGF+EGF. We found that HUVECs cultured in xeno-free+bFGF+EGF condition exhibited a higher proliferation activity than the other media tested ( $P < 0.01$ ; Figure 2(a)). As shown by population doubling plots (P4 and P6 ( $P < 0.01$ ) and P5 ( $P < 0.05$ ); Figure 2(b)), the accelerated expansions of HUVECs under xeno-free+bFGF+EGF condition were observed at all-time point assessed. Moreover, it was noteworthy that the expression of CD31 remained stable for HUVECs obtained from all three conditions after 6 passages (Figure 2(c)). Based on these experimental findings, HUVECs isolated under xeno-free+bFGF+EGF condition were then selected for the subsequent experiment.

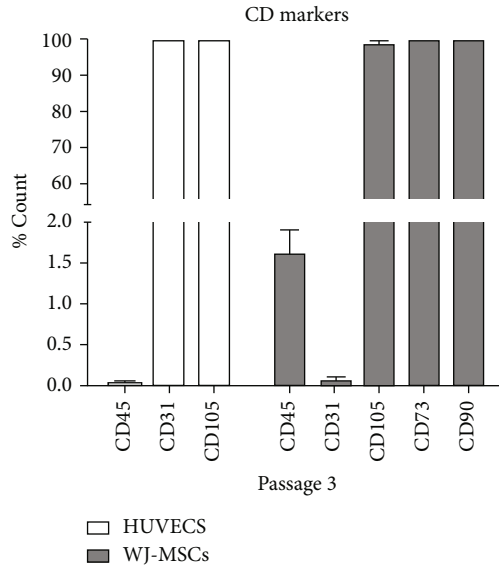
### 3.3. Expanded HUVECs and WJ-MSCs Showed Their Immunophenotype Characteristics with High Purity. Since

cell purity is one of the key parameters required for cellular therapy products, we next performed flow cytometry analysis for both HUVECs and WJ-MSCs obtained by our technics. At passage 3, the percentage of CD31<sup>+</sup> ( $99.96\% \pm 0.05\%$ ), CD105<sup>+</sup> ( $99.70\% \pm 0.13\%$ ), and CD45<sup>-</sup> ( $0.01\% \pm 0.02\%$ ) cells indicated that HUVECs isolated under xeno-free+bFGF+EGF condition possess endothelial lineage characteristics [18] with more than 99% purity (Figures 3(a) and 3(b)). And, WJ-MSCs isolated from the remaining umbilical cord were fulfill the classical MSC immunophenotype [19]; cells were positive for CD73 ( $99.72\% \pm 0.15\%$ ), CD90 ( $99.75\% \pm 0.21\%$ ), and CD105 ( $98.83\% \pm 0.65\%$ ) and were negative for CD45 ( $1.61\% \pm 0.54\%$ ) (Figures 3(a) and 3(b)).

### 3.4. In vitro 2-Dimensional Coculture of HUVECs/WJ-MSCs Exhibited a Vessel-Like Structure. To assess whether cocultured of ECs and WJ-MSCs has positive effects on



(a)



(b)

FIGURE 3: Purification of HUVECs and WJ-MSCs obtained by using a single umbilical cord with xeno-free cell isolation and expansion strategy. (a) Representative flow cytometry analysis of expanded HUVECs and WJ-MSCs stained with antibodies directed against human antigens specific for pan leukocyte (CD45), ECs (CD31), and MSCs: CD105, CD73, and CD90. (b) Percentage of HUVECs (light bar) and WJ-MSC-s (gray bar) stained positive for endothelial and MSC markers. Data were expressed as mean  $\pm$  SEM ( $N = 3$ ).

angiogenicity, HUVECs obtained from xeno-free+bFGF +EGF condition were then cocultured with WJ-MSCs for 3

days. Immunostaining of CD31 was used to confirm the endothelial lineage phenotype of the structure. We found

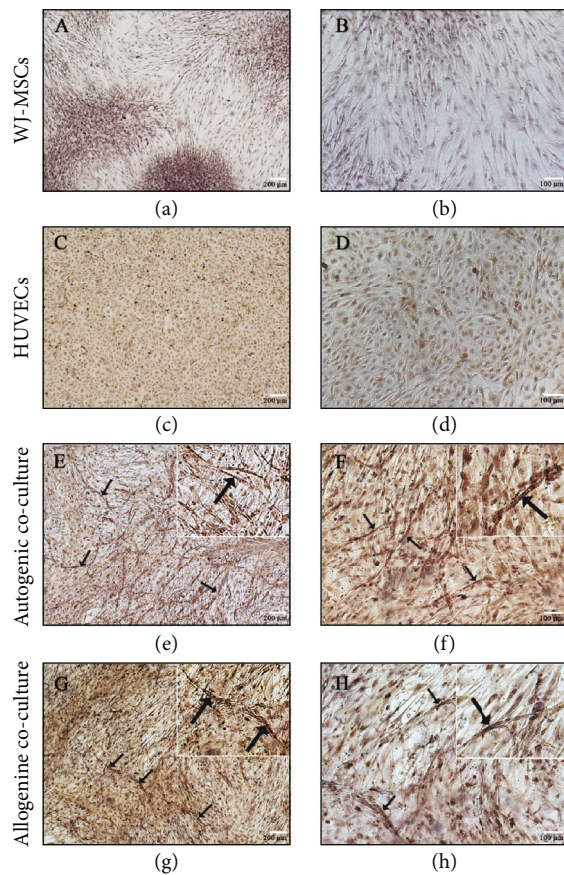


FIGURE 4: Vessel-like structure formation in 2-dimensional (2D) culture. After 3 days cultured in endothelial growth media, WJ-MSCs (a, b), HUVECs (c, d), autogenic (e, f), and allogenic (g, h) HUVECs/WJ-MSCs coculture were stained with antibodies directed against human CD31 (brown). Arrows indicated CD31 stained VLS in both of autogenic and allogenic HUVECs/WJ-MSCs coculture condition. Scale bar: 200  $\mu\text{m}$  (a, c, e, and g) and 100  $\mu\text{m}$  (b, d, f, and h).

that the vessel-like structures (VLS) stained positively for CD31 were observed only in HUVECs/WJ-MSCs coculture in both of autologous (Figures 4(e) and 4(f)) and allogenic (Figures 4(g) and 4(h)) coculture conditions. In contrast, none of VLS was identified in HUVECs (Figures 4(c) and 4(d)) and WJ-MSCs (Figures 4(a) and 4(b)) monoculture.

#### 4. Discussion

To achieve a desirable therapeutic outcome in the field of stem cells and tissue engineering, multidisciplinary factors should be taken into consideration, for example, a performance of engineered tissues, an appropriate structural/scaffold support, and a sufficient oxygen and nutrient supply of engineered tissue. [20]. To overcome the problem of inadequate blood supply, several strategies that promote graft-host vascularization have been employed: (i) direct derivation of proangiogenic growth factors such as vascular endothelial growth factor, fibroblast growth factor, and platelet-derived growth factors [21]; (ii) the transplantation of multiple cells types (i.e., endothelial progenitor cells;

EPCs, ECs, and MSCs) [2, 5, 22, 23]; and (iii) the use of vascular-inductive biocompatible scaffolds combined with stem/progenitor cells [24]. ECs can be isolated from different types of blood vessels, such as arteries, veins, and capillaries [25]. For instance, autologous EC sources are internal mammary artery, saphenous vein, and skin tissue [26, 27]. However, harvesting of autologous ECs is usually not possible because of the invasive collection procedure, poor tissue quality cause by preexisting conditions of the patient, and limited proliferation potential of the isolated cells. hUC, as HUVEC origin, in contrast, offers a high-quality EC source that is readily available after a child's birth. The advantages of HUVECs beyond other EC source include sample accessibility, uncomplacate isolation process, and availability of published data [27].

In the present study, the attention has been drawn to the use of cells obtained from hUC, a potential cell source that is routinely discarded after birth. Apart from its ethical acceptance and painless collection procedure, hUC provides the unique niche of multiple types of cell (i.e., WJ-MSCs [4], ECs, and EPCs from umbilical cord vein [28, 29]) that provide a mutual support mechanism through their inheritance distinct functions, multilineage differentiation potentials, and neovascularization [30, 31]. Here, we report for the first time that HUVECs and WJ-MSCs can be obtained from the same umbilical cord using a simple 2-step technic, the first enzymatic digestion of the umbilical vein followed by mechanical explant of Wharton's jelly tissue. This technic utilized the fact that hUC contains different types of multipotent progenitor cells, and these cells itself have a natural barrier to prevent cell line cross-contamination during the isolation process. We also demonstrated that medium comprised of 10% human serum, an appropriate xeno-free alternative of FBS, could be used to support the expansion, until cryopreservation, of HUVECs and WJ-MSCs. To get the superior expansion condition for HUVECs, we found that the addition of 5 ng/ml EGF yielded a better proliferation potential when compared with the standard xeno-free+bFGF culture condition and nonxeno-free LSGS culture condition, respectively. The results of flow cytometry analysis showed that both HUVECs and WJ-MSCs obtained by this technic possess the immunophenotype characteristic of endothelial and MSCs with more than 99% and 98% purity, respectively. This is in accordance with the previous report that hUC can be used as a source for vascular cell bank [16]. It is worth mentioning that, besides the establishment of xeno-free culture system for both WJ-MSCs and HUVECs, our findings fulfill the attempt to establish therapeutic applicable cell bank [32–36] by offering a possibility to set up “two-in-one” (two cell types in one sample) autogenic cell bank.

The ability of ECs and MSCs on neovascularization is also a topic of interest in the field of stem cells and tissue engineering. A number of studies have proven that different sources of MSCs (e.g., bone marrow-derived and adipose tissue-derived MSCs) provide beneficial effects on vascular tube formation of ECs via stabilization of ECs network and secretion of vasculogenic growth factor, such as hepatocyte growth factor [37, 38]. However, the promising results of those studies obtained from the coculturing of allogenic cell



sources, which might be less attractive considering in personalized cell therapy [39]. In this study, we found that only coculture of HUVECs/WJ-MSCs was able to form VLS after 3 days culture in endothelial culture medium. These implied the angiogenic supporting effect of HUVECs and WJ-MSCs in both of autogenic and allogenic cell source conditions. Although, we were not able to perform the quantitative comparison between VLS degree derived from autogenic and allogenic cell source conditions. Our preliminary results provide compelling evidence that the coculturing of the autogenic and allogenic HUVECs/WJ-MSCs give rise to the different level of VLS formation. Further investigations on molecular interactions, a quantitative assay of VLS formation, and an *in vivo* functional study of these cells are needed to clarify which combination (autogenic or allogenic cell source) should be considered before moving from the bench to the bedside.

In conclusion, the defined xeno-free strategy proposed by this study offers a simple, but reliable, approach to establish the autogenic HUVECs and WJ-MSCs that are suited for future personal clinical application.

## Data Availability

Source data used to support the findings of this study are available from the corresponding author upon request.

## Conflicts of Interest

HK, TK, and VK are employees of Medeze group Co., Ltd. The remaining authors declare that they have no financial interest in the products described in this article.

## Acknowledgments

The authors would like to thank Prapot Tanthaisong, Salinee Jumsanong, Sarinya Yindee, Nudjaree Wiengin, and Sudarat Waengern for their assistance in laboratory work. This work was supported by Medeze group Co., Ltd. Kasem Theerakittayakorn was supported by SUT Postgraduate research fellowships.

## References

- [1] V. Haug, N. Torio-Padron, G. B. Stark, G. Finkenzeller, and S. Strassburg, "Comparison between endothelial progenitor cells and human umbilical vein endothelial cells on neovascularization in an adipogenesis mouse model," *Microvascular Research*, vol. 97, pp. 159–166, 2015.
- [2] J. Ma, F. Yang, S. K. Both et al., "In vitro and in vivo angiogenic capacity of BM-MSCs/HUVECs and AT-MSCs/HUVECs cocultures," *Biofabrication*, vol. 6, no. 1, 2014.
- [3] B. Baudin, A. Bruneel, N. Bosselut, and M. Vaubourdoille, "A protocol for isolation and culture of human umbilical vein endothelial cells," *Nature Protocols*, vol. 2, no. 3, pp. 481–485, 2007.
- [4] H. S. Wang, S. C. Hung, S. T. Peng et al., "Mesenchymal stem cells in the Wharton's jelly of the human umbilical cord," *Stem Cells*, vol. 22, no. 7, pp. 1330–1337, 2004.
- [5] N. Sakata, N. K. Chan, J. Chrisler, A. Obenaus, and E. Hathout, "Bone marrow cell co-transplantation with islets improves their vascularization and function," *Transplantation*, vol. 89, no. 6, pp. 686–693, 2010.
- [6] H. E. Broxmeyer, G. W. Douglas, G. Hango et al., "Human umbilical cord blood as a potential source of transplantable hematopoietic stem/progenitor cells," *Proceedings of the National Academy of Sciences of the United States of America*, vol. 86, no. 10, pp. 3828–3832, 1989.
- [7] M. C. Corotchi, M. A. Popa, A. Remes, L. E. Sima, I. Gussi, and M. L. Plesu, "Isolation method and xeno-free culture conditions influence multipotent differentiation capacity of human Wharton's jelly-derived mesenchymal stem cells," *Stem Cell Research & Therapy*, vol. 4, no. 4, p. 81, 2013.
- [8] P. Venugopal, S. Balasubramanian, A. S. Majumdar, and M. Ta, "Isolation, characterization, and gene expression analysis of Wharton's jelly-derived mesenchymal stem cells under xeno-free culture conditions," *Stem Cells Cloning*, vol. 4, pp. 39–50, 2011.
- [9] I. Hartmann, T. Hollweck, S. Haffner et al., "Umbilical cord tissue-derived mesenchymal stem cells grow best under GMP-compliant culture conditions and maintain their phenotypic and functional properties," *Journal of Immunological Methods*, vol. 363, no. 1, pp. 80–89, 2010.
- [10] T. Hatlapatka, P. Moretti, A. Lavrentieva et al., "Optimization of culture conditions for the expansion of umbilical cord-derived mesenchymal stem or stromal cell-like cells using xeno-free culture conditions," *Tissue Engineering. Part C, Methods*, vol. 17, no. 4, pp. 485–493, 2011.
- [11] M. Cimino, R. M. Gonçalves, C. C. Barrias, and M. C. L. Martins, "Xeno-free strategies for safe human mesenchymal stem/stromal cell expansion: supplements and coatings," *Stem Cells International*, vol. 2017, Article ID 6597815, 13 pages, 2017.
- [12] J. Jung, N. Moon, J. Y. Ahn et al., "Mesenchymal stromal cells expanded in human allogenic cord blood serum display higher self-renewal and enhanced osteogenic potential," *Stem Cells and Development*, vol. 18, no. 4, pp. 559–572, 2009.
- [13] L. K. Boland, A. J. Burand, D. T. Boyt et al., "Nature vs. Nurture: Defining the Effects of Mesenchymal Stromal Cell Isolation and Culture Conditions on Resiliency to Palmitate Challenge," *Frontiers in Immunology*, vol. 10, 2019.
- [14] T. Zhao, F. Sun, J. Liu et al., "Emerging role of mesenchymal stem cell-derived exosomes in regenerative medicine," *Current Stem Cell Research & Therapy*, vol. 14, no. 6, pp. 482–494, 2019.
- [15] D. G. Halme and D. A. Kessler, "FDA regulation of stem-cell-based therapies," *The New England Journal of Medicine*, vol. 355, no. 16, pp. 1730–1735, 2006.
- [16] B. Polchow, K. Kebbel, G. Schmiedeknecht et al., "Cryopreservation of human vascular umbilical cord cells under good manufacturing practice conditions for future cell banks," *Journal of Translational Medicine*, vol. 10, no. 1, p. 98, 2012.
- [17] U. Nekanti, L. Mohanty, P. Venugopal, S. Balasubramanian, S. Totey, and M. Ta, "Optimization and scale-up of Wharton's jelly-derived mesenchymal stem cells for clinical applications," *Stem Cell Research*, vol. 5, no. 3, pp. 244–254, 2010.
- [18] M. H. Strijbos, J. Kraan, M. A. den Bakker, B. N. Lambrecht, S. Sleijfer, and J. W. Gratama, "Cells meeting our

- immunophenotypic criteria of endothelial cells are large platelets,” *Cytometry. Part B, Clinical Cytometry*, vol. 72, no. 2, pp. 86–93, 2007.
- [19] M. Dominici, K. le Blanc, I. Mueller et al., “Minimal criteria for defining multipotent mesenchymal stromal cells. The International Society for Cellular Therapy position statement,” *Cytotherapy*, vol. 8, no. 4, pp. 315–317, 2006.
- [20] E. A. Phelps and A. J. García, “Engineering more than a cell: vascularization strategies in tissue engineering,” *Current Opinion in Biotechnology*, vol. 21, no. 5, pp. 704–709, 2010.
- [21] J. C. Y. Chung and D. Shum-Tim, “Neovascularization in tissue engineering,” *Cell*, vol. 1, no. 4, pp. 1246–1260, 2012.
- [22] S. Koob, N. Torio-Padron, G. B. Stark, C. Hannig, Z. Stankovic, and G. Finkenzyler, “Bone formation and neovascularization mediated by mesenchymal stem cells and endothelial cells in critical-sized calvarial defects,” *Tissue Engineering. Part A*, vol. 17, no. 3-4, pp. 311–321, 2011.
- [23] S. Afra and M. M. Matin, “Potential of mesenchymal stem cells for bioengineered blood vessels in comparison with other eligible cell sources,” *Cell and Tissue Research*, vol. 380, no. 1, pp. 1–13, 2020.
- [24] E. Jabbarzadeh, T. Starnes, Y. M. Khan et al., “Induction of angiogenesis in tissue-engineered scaffolds designed for bone repair: a combined gene therapy–cell transplantation approach,” *Proceedings of the National Academy of Sciences of the United States of America*, vol. 105, no. 32, pp. 11099–11104, 2008.
- [25] A. Krüger-Genge, A. Blocki, R. P. Franke, and F. Jung, “Vascular endothelial cell biology: an update,” *International Journal of Molecular Sciences*, vol. 20, no. 18, p. 4411, 2019.
- [26] S. Kim and H. von Recum, “Endothelial stem cells and precursors for tissue engineering: cell source, differentiation, selection, and application,” *Tissue Engineering Part B: Reviews*, vol. 14, no. 1, pp. 133–147, 2008.
- [27] I. Kocherova, A. Bryja, P. Mozdziaik et al., “Human umbilical vein endothelial cells (HUVECs) co-culture with osteogenic cells: from molecular communication to engineering prevascularised bone grafts,” *Journal of Clinical Medicine*, vol. 8, no. 10, p. 1602, 2019.
- [28] P. K. Schaefermeier, N. Cabeza, J. C. Besser et al., “Potential cell sources for tissue engineering of heart valves in comparison with human pulmonary valve cells,” *ASAIO Journal*, vol. 55, no. 1, pp. 86–92, 2009.
- [29] Y. Mou, Z. Yue, H. Zhang et al., “High quality in vitro expansion of human endothelial progenitor cells of human umbilical vein origin,” *International Journal of Medical Sciences*, vol. 14, no. 3, pp. 294–301, 2017.
- [30] M. W. Merx, A. Zerneck, E. A. Liehn et al., “Transplantation of human umbilical vein endothelial cells improves left ventricular function in a rat model of myocardial infarction,” *Basic Research in Cardiology*, vol. 100, no. 3, pp. 208–216, 2005.
- [31] E. Jover, M. Fagnano, G. Angelini, and P. Madeddu, “Cell Sources for Tissue Engineering Strategies to Treat Calcific Valve Disease,” *Frontiers in Cardiovascular Medicine*, vol. 5, 2018.
- [32] S. E. Tannenbaum, O. Singer, Y. Gil et al., “Hadassah, provider of “regulatory-ready” pluripotent clinical-grade stem cell banks,” *Stem Cell Research*, vol. 42, p. 101670, 2020.
- [33] G. R. Diaferia, M. Cardano, M. Cattaneo et al., “The science of stem cell biobanking: investing in the future,” *Journal of Cellular Physiology*, vol. 227, no. 1, pp. 14–19, 2012.
- [34] D. T. Harris, “Stem cell banking for regenerative and personalized medicine,” *Biomedicine*, vol. 2, no. 1, pp. 50–79, 2014.
- [35] S. Bardelli, “Stem cell biobanks,” *Journal of Cardiovascular Translational Research*, vol. 3, no. 2, pp. 128–134, 2010.
- [36] E. Abranches, S. Spyrou, and T. Ludwig, “GMP banking of human pluripotent stem cells: a US and UK perspective,” *Stem Cell Research*, vol. 45, p. 101805, 2020.
- [37] K. Pill, S. Hofmann, H. Redl, and W. Holnthoner, “Vascularization mediated by mesenchymal stem cells from bone marrow and adipose tissue: a comparison,” *Cell Regeneration*, vol. 4, no. 1, p. 4:8, 2015.
- [38] K. Pill, J. Melke, S. Mühleder et al., “Microvascular networks from endothelial cells and mesenchymal stromal cells from adipose tissue and bone marrow: a comparison,” *Frontiers in Bioengineering and Biotechnology*, vol. 6, 2018.
- [39] G. Meza, D. Urrejola, N. Saint Jean et al., “Personalized cell therapy for pulpitis using autologous dental pulp stem cells and leukocyte platelet-rich fibrin: a case report,” *Journal of Endodontics*, vol. 45, no. 2, pp. 144–149, 2019.

## Review Article

# Dental Tissue-Derived Human Mesenchymal Stem Cells and Their Potential in Therapeutic Application

Lu Gan,<sup>1</sup> Ying Liu,<sup>1</sup> Dixin Cui,<sup>1</sup> Yue Pan,<sup>1</sup> Liwei Zheng,<sup>1</sup> and Mian Wan <sup>2</sup>

<sup>1</sup>State Key Laboratory of Oral Diseases and National Clinical Research Center for Oral Diseases and Department of Pediatric Dentistry, West China Hospital of Stomatology, Sichuan University, Chengdu, Sichuan 610041, China

<sup>2</sup>State Key Laboratory of Oral Diseases and National Clinical Research Center for Oral Diseases and Department of Cariology and Endodontics, West China Hospital of Stomatology, Sichuan University, Chengdu, Sichuan 610041, China

Correspondence should be addressed to Mian Wan; [mianwan@scu.edu.cn](mailto:mianwan@scu.edu.cn)

Received 26 June 2020; Accepted 15 July 2020; Published 1 September 2020

Academic Editor: Sangho Roh

Copyright © 2020 Lu Gan et al. This is an open access article distributed under the Creative Commons Attribution License, which permits unrestricted use, distribution, and reproduction in any medium, provided the original work is properly cited.

Human mesenchymal stem cells (hMSCs) are multipotent cells, which exhibit plastic adherence, express specific cell surface marker spectrum, and have multi-lineage differentiation potential. These cells can be obtained from multiple tissues. Dental tissue-derived hMSCs (dental MSCs) possess the ability to give rise to mesodermal lineage (osteocytes, adipocytes, and chondrocytes), ectodermal lineage (neurocytes), and endodermal lineages (hepatocytes). Dental MSCs were first isolated from dental pulp of the extracted third molar and till now they have been purified from various dental tissues, including pulp tissue of permanent teeth and exfoliated deciduous teeth, apical papilla, periodontal ligament, gingiva, dental follicle, tooth germ, and alveolar bone. Dental MSCs are not only easily accessible but are also expandable *in vitro* with relative genomic stability for a long period of time. Moreover, dental MSCs have exhibited immunomodulatory properties by secreting cytokines. Easy accessibility, multi-lineage differentiation potential, and immunomodulatory effects make dental MSCs distinct from the other hMSCs and an effective tool in stem cell-based therapy. Several preclinical studies and clinical trials have been performed using dental MSCs in the treatment of multiple ailments, ranging from dental diseases to nondental diseases. The present review has summarized dental MSC sources, multi-lineage differentiation capacities, immunomodulatory features, its potential in the treatment of diseases, and its application in both preclinical studies and clinical trials. The regenerative therapeutic strategies in dental medicine have also been discussed.

## 1. Introduction

Human mesenchymal stem cells (hMSCs) are multipotent cells isolated from various tissues, including bone marrow, adipose tissue, umbilical cord, and dental tissue. These cells share similar properties: being plastic-adherent, expressing a specific cell surface marker spectrum (CD73+, CD90+, CD105+, CD34-, CD45-, CD11b-, CD14-, CD19-, CD79a-, and human leucocyte antigen-DR-), and possessing the ability to give rise to osteoblasts, chondrocytes, and adipocytes. hMSCs are highly accessible and expandable *in vitro* with genomic stability. Furthermore, these cells have the remarkable potential of multipotent differentiation, as they not only could differentiate into mesodermal lineages (adipocytes, osteocytes, and chondrocytes) but also could transdifferentiate

into ectodermal lineages (neurocytes) and endodermal lineages (hepatocytes and pancreocytes). All these characteristics make them promising stem cell sources for regenerative therapy, but their clinical applications have been limited due to questionable safety issues, inconclusive quality control, unaccomplished clinical-grade production, and incomplete understanding of the mechanism regulating these hMSCs [1–4].

To address this, scientists worldwide have been searching for safe, effective, and easily accessible stem cell sources with great differentiation potential for regenerative medicine. Dental MSCs, which show typical MSC features, have been found in various dental tissues, ranging from discarded extracted teeth to their attached tissues [5–7]. These cells are not only easily accessible but are also expandable with relative genomic stability for a long period of time. Notably,

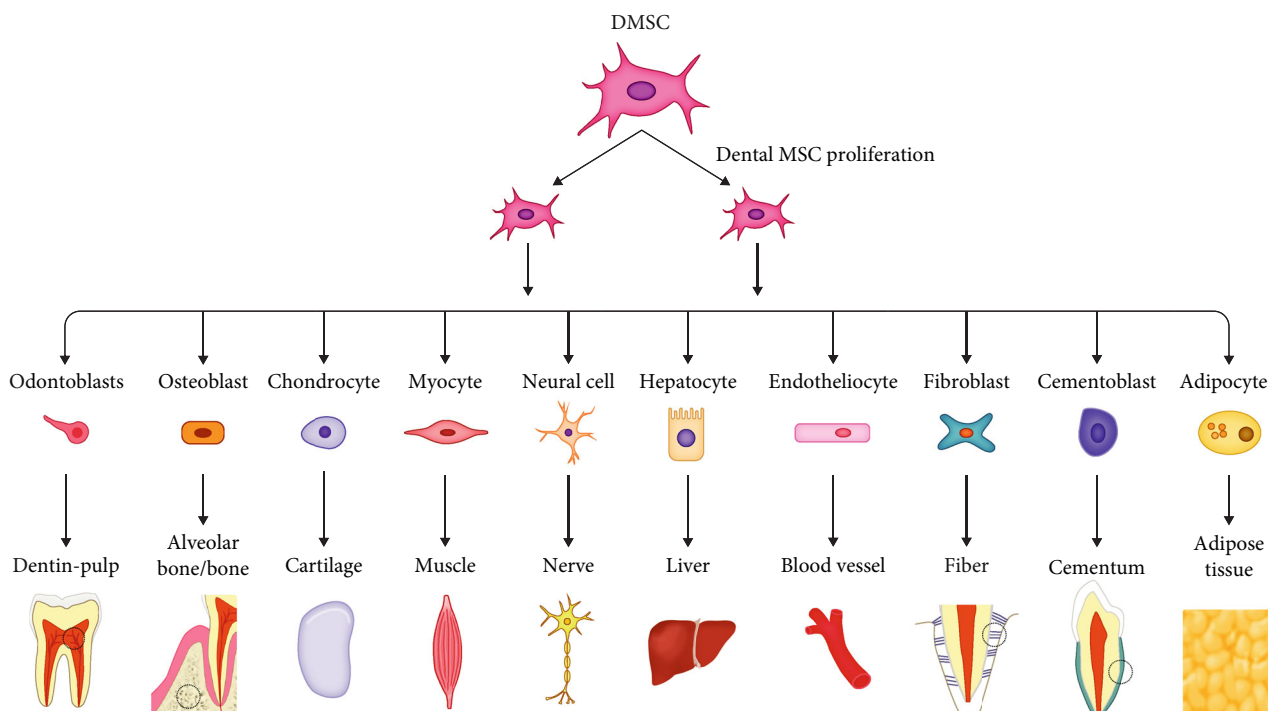


FIGURE 1: Multilineage differentiation capacity of dental MSCs.

apart from mesodermal lineages, they have the ability to transdifferentiate into ectodermal and endodermal lineages [5, 8–12] (Figure 1). Moreover, dental MSCs exhibit immunomodulatory properties by secreting cytokines and immune receptors [13]. All these characteristics of dental MSCs make them distinct from other hMSCs, and they can be applied in stem cell-based therapy. Several preclinical studies and clinical trials were performed using dental MSCs in the treatment of dental diseases and nondental diseases like neurodegenerative diseases and autoimmune and orthopedic disorders [14–18].

The present review has summarized dental MSC sources, multi-lineage differentiation potential, immunomodulatory features, its potential in the treatment of diseases, and its application in both preclinical studies and clinical trials. The regenerative therapeutic strategies in dental medicine have also been discussed.

## 2. Dental Mesenchymal Stem Cells (Dental MSCs)

The existence of dental MSCs was suggested by the formation of tertiary dentin following dental caries or trauma. The first efficient population of dental MSCs was reported from the dental pulp tissue of an extracted third molar [19]. Later on, cells that possess characteristics of MSCs were isolated from the pulp tissue of exfoliated deciduous teeth [20], apical papilla [21], periodontal ligament [22], gingiva [23], dental follicle [24, 25], tooth germ [26], and alveolar bone [27]. These cell populations exhibit heterogeneity, i.e., distinct cell surface markers, proliferation rate, and differentiation poten-

tial, which has been reviewed by Zhou et al. [28], suggesting their diverse functions and applications in clinic.

**2.1. Stem Cells from Dental Pulp.** The first dental MSC population, human dental pulp stem cells (hDPSCs), was isolated from the dental pulp tissue of impacted third molars. These cells exhibit MSC properties, including high proliferation, multi-lineage differentiation potential, as well as immunomodulatory properties [19, 29]. Substantial studies have documented the odontogenic differentiation potential of hDPSCs, i.e., hDPSCs generated a dentin-pulp-like organoid with Matrigel *in vitro* and induced mineralized reparative dentin formation with hydroxyapatite (HA)/tricalcium phosphate (TCP) ceramic particles *in vivo* [19, 30–32]. Attributing to the origin of the neural crest, hDPSCs show remarkable neurogenic potential compared with human bone marrow stem cells (BMMSCs). The higher expression level of neurotrophins like nerve growth factor (NGF) and longer axons were detected in hDPSCs cultured with a microfluidic coculture system containing trigeminal neurons. Neurospheres were also generated by hDPSCs upon specific differentiation conditions [33–35]. The ability of hDPSCs to differentiate into endothelial cells and their angiogenic potential have also been reported, as hDPSCs were found to secrete vascular endothelial growth factors (VEGF) and generate visible blood vessels in three-dimensional- (3D-) printed HA constructs [36]. Their capabilities of neurogenic and angiogenic differentiation made a great contribution to the whole pulp regeneration. Implanted hDPSCs gave rise to 3D pulp tissue with vascular and nerve reconstruction in the empty root canal of traumatized permanent incisors [37]. hDPSCs could also differentiate into osteoblasts and



further regenerate bone tissue, due to expressing several typical osteoblastic markers, such as alkaline phosphatase (ALP), osteopontin (OPN), and osteocalcin (OCN) [38]. Newly formed bone was found following the application of the bioengineered constructs of hDPSCs with poly- $\epsilon$ -caprolactone- (PCL-) biphasic calcium phosphate (BCP) scaffolds. hDPSCs could also differentiate into other cell lineages, such as adipocytes, chondroblasts, hepatocytes, and cardiomyocytes. The high plasticity of hDPSCs makes them an ideal stem cell source for stem cell-based therapy, which has been thoroughly reviewed by Mortada *et al.* [29].

Then, stem cells from the dental pulp tissue of exfoliated deciduous teeth were purified with a similar method for hDPSC isolation. Analogous to hDPSCs, cultured stem cells from exfoliated deciduous teeth (SHEDs) are capable of differentiating into various cell types, such as osteocytes, chondrocytes, adipocytes, odontoblasts, endothelial cells, and hepatocytes [20]. However, due to the developmental differences between deciduous and permanent teeth, SHEDs present different features from hDPSCs, for instance, a higher proliferative capability, more cell-population doublings, a sphere-like cluster formation, and a distinctive osteoinductive capacity [20]. For odontogenic differentiation potential, SHEDs are able to differentiate into odontoblasts and form dentin-like tissue or pulp-like tissue, instead of a complete dentin-pulp-like complex [20, 39]. When combined with collagen type I, hDPSCs formed the functional dental pulp tissue in the full-length root canal. The newly formed pulp tissue contained functional odontoblasts, which regenerated tubular dentin tissue [40]. Following neural inductive culture, SHEDs presented higher expression levels of neuronal and glial cell markers than hDPSCs, such as  $\beta$ -III-tubulin, tyrosine-hydroxylase (TH), microtubule-associated protein 2 (MAP2), and Nestin. Dopaminergic (DAergic) neurons could be produced by SHED-derived neurospheres in a DAergic induction system [41]. Additionally, SHEDs could act as neuroprotector agents to promote neural functional recovery through paracrine effects and inhibit glial scar formation after spinal cord contusion [42]. Conditioned media (CM) derived from SHEDs, containing various neurotrophic factors, enhanced peripheral sciatic nerve regeneration with axon regeneration and remyelination, which improved motor functions thus preventing muscle atrophy [43]. These multifaceted neural regeneration activities render SHEDs as an optimal cellular source to improve the injured nerve. For osteogenic potential, SHEDs induced new bone formation *in vivo* by recruiting host osteogenic cells, rather than differentiating into osteoblasts which happened *in vitro* [20]. Larger osteoids and more collagen fibers were formed by SHEDs with poly(lactic-co-glycolic acid) (PLGA) membrane transplantation as compared to DPSCs and BMMSCs [44].

In addition to striking multi-lineage differentiation potential, the immunomodulatory effects have been reported in MSCs from dental pulp tissue, which may function through correcting the underlying pathological immune responses. hDPSCs have been suggested to regulate local immune response by suppressing the expression of metalloproteinases (MMPs) including MMP3 and MMP13 and to inhibit acute rejection of allograft by releasing transforming

growth factor-beta (TGF- $\beta$ ) [45]. Dai *et al.* found that SHEDs suppressed the CD4+ T cell-driven responses via inhibiting the proliferation of T lymphocytes and the upregulated ratio of Th1/Th2 by inducing the expansion of Treg cells [46]. Local injection of SHEDs increased the number of anti-inflammatory CD206+ M2 macrophages and altered the cytokine expression profiles in periodontal tissues with periodontitis [47].

**2.2. Stem Cells from the Apical Papilla (SCAPs).** During tooth development, dental papilla derived from the ectomesenchyme ultimately converts into the dental pulp tissue and migrate to locations around the apex [48]. Root development and apical closure could still be observed in immature permanent teeth suffering from periapical periodontitis or abscess. These clinical phenomena suggested that a population of MSCs might reside in apical papilla. SCAPs were isolated from third molar root apical papilla, which contains fewer blood vessels and cells than dental pulp tissue [21, 48].

SCAPs have shown a greater potential to regenerate dentin than DPSCs, since they have higher proliferation with greater telomerase activity, suggesting that SHED is a cell source for odontoblasts responsible for the production of dentin [21]. Previous studies have confirmed that SCAPs are capable of differentiating into odontoblast-like cells and form a typical dentin-like structure on the surface of HA/TCP [21, 48]. Larger areas of mineralized nodules positive to Alizarin Red were formed by SCAPs with culture medium containing L-ascorbate-2-phosphate [48]. When SCAPs mixed with host cells, odontoblasts positive for dentin sialophosphoprotein (DSPP) and dentin matrix protein 1 (DMP1) and ectopic formation of vascularized pulp-like tissue were detected in mice molars [49]. A greater migration ability assessed by scratch assay enhanced their capacity for dentin regeneration by cell homing [21]. Considering their role in root development, SCAPs have been suggested to possess a significant potential for root regeneration. A functional bioroot with periodontal ligament tissue was generated in the alveolar socket of a minipig following transplantation of human SCAPs and periodontal ligament stem cells (PDLSCs). Additionally, SHEDs showed a PDL-related marker *in vitro* and exhibited greater mineralization capacity on account of higher expression levels of ALP, bone sialoprotein (BSP), and OCN expression compared to PDLSCs [50]. Therefore, SCAPs have been considered as a promising alternative source for periodontal tissue regeneration. Their potential for angiogenesis has also been confirmed in 3D-printed HA scaffolds. Derived from the cranial neural crest, SCAPs possess neurogenic differentiation potential similar to DPSCs and SHEDs. After transplantation of the human apical papilla tissue into the injured spinal cord in rats, improvements were observed in gait and glial reactivity [51]. Besides, SCAPs may be a potential immunotherapeutic tool for immunological diseases due to their low immunogenicity and capability of inhibiting T cell proliferation [52].

**2.3. Periodontal Ligament Stem Cells (PDLSCs).** Periodontal ligament (PDL) is a soft connective tissue, which contains progenitor cells that maintain tissue homeostasis and

regeneration of periodontal tissues [22, 53]. PDLSCs were isolated from the attached PDL of the extracted third molar with expression of two early MSC markers STRO-1 and CD146/MUC18 and higher levels of scleraxis, a tendon-specific transcription factor, compared to DPSCs [22].

The potential for the cementogenic/osteogenic differentiation of PDLSCs has been shown by the formation of calcified nodules and expression of ALP, matrix extracellular protein (MEPE), BSP, OCN, and TGF- $\beta$  receptor I [22]. Human PDLSCs have been demonstrated to be a reliable source for the fabrication of 3D PDL tissues [54]. Typical cementum/PDL-like structures, including Sharpey's fiber-like tissue, were generated after the transplantation of human PDLSCs into the rat periodontal lesion sites [22]. PDLSCs also contribute to root regeneration. When combined with SCAPs, they generated a collagen fiber which anchored into the newly formed cementum on the surface of the HA/TCP carrier, and formed a functional root supporting a porcelain crown [21]. Extracellular vesicles (EVs) released by PDLSCs have also been reported to possess osteogenic properties and promote bone regeneration. Collagen membranes with PDLSC-EV transplantation showed osteoid formation with an osteoblast-like structure on the host native bone side and new bone irregularly arranged in the implant site of rats subjected to calvarial defects. Neural crest-derived PDLSCs spontaneously express neural protein markers as Nestin and growth associated protein-43 (GAP-43) upon xeno-free culture conditions [55]. In addition to previously demonstrated adipocytes and chondrogenic cells, several studies sequentially reported the differentiation potential of PDLSCs toward endothelial cells, cardiac myocytes, islet-like cells, and retinal ganglion-like cells [11].

Based on immunosuppression, low immunogenicity, and the ability to produce a vast array of cytokines, PDLSCs and their products have the potential to treat inflammatory disorders and autoimmune diseases. Ding *et al.* found the PDLSCs failed to express HLA-II DR and costimulatory molecules and possessed marked immunosuppression via PGE2-induced T-cell anergy [56].

**2.4. Gingival-Derived Mesenchymal Stem Cells (GMSCs).** A population of progenitor cells or stem cells has been identified in the spinous layer of human gingiva, an easily accessible tissue from remnants or discarded tissues following routine dental procedures, namely GMSCs.

The osteogenic differentiation of GMSCs was determined by formed deposits with positive Alizarin Red S staining and upregulated expression of OCN *in vitro*, while their ability for osteogenic differentiation has not been observed *in vivo* [23]. However, recent evidence has shown that EVs derived from GMSCs exhibit significant osteogenic properties as revealing high expression levels of RUNX2 and BMP2/4 and abundant extracellular matrix (ECM) and nodules of new bone formation [57]. Transplantation of GMSCs formed connective-like tissues expressing collagen I, which is absent in DPSCs or PDLSCs [23]. Human fetal GMSCs have an ability for gingival differentiation automatically *in vivo* because they may contain more precursor cells to differentiate into gingival cells. After having been transplanted into the gingiva

defects of rats, human GMSCs generated new tissue like normal gingiva [58]. GMSCs are capable of neurogenic differentiation since they are positive for glial fibrillary acidic protein (GFAP), neurofilament (NF-M), and  $\beta$ -tubulin III upon neural differentiation conditions [23]. GMSC spheroids have shown differentiation potential into both neuronal and Schwann-like cells with a 3D-collagen scaffold. And 3D bio-printed grafts with GMSCs formed nerve tissue with a normal size at the defect of rat facial nerves and showed higher therapeutic potential on facial palsy. These findings have demonstrated that GMSCs present promising potential for nerve regeneration and functional recovery [59]. Besides, they could also differentiate into adipocytes, chondrocytes and endothelial cells [23, 60].

Importantly, GMSCs have distinctive immunomodulatory functions, as they could suppress peripheral blood mononuclear cells (PBMCs) and upregulate IFN- $\gamma$ -induced indoleamine 2,3-dioxygenase (IDO) and IL-10. Spheroid-derived GMSCs displayed the capability to enhance the secretion of several chemokines and cytokines and improved resistance to oxidative stress-induced apoptosis. They have been reported to attenuate chemotherapy-induced oral mucositis [61].

**2.5. Dental Follicle Stem Cells (DFSCs).** The dental follicle (DF) is responsible for forming alveolar bone and the root-bone interface in tooth development; it is an ectomesenchymal tissue that contains progenitor cells (PCs) for periodontal ligament cells, cementoblasts, and osteoblasts [24, 25, 28]. These PCs were isolated from the dental follicle of the extracted third molars, characterized by expressed undifferentiated cell markers Notch-1 and Nestin, namely DFSCs [24, 25].

DFSCs express a higher level of insulin-like growth factors (IGF-2) compared to hMSCs and exhibit higher proliferation potential and colony-forming ability compared with SHEDs, DPSCs, and PDLSCs, suggesting their potential in regenerative medicine [24, 25, 62, 63]. Their superior osteogenic properties have been reported by several studies. DFSCs show higher expression levels of osteogenic-related markers such as RUNX2 and ALP compared to SHEDs and DPSCs [62]. Long-term culture of DFSCs with differentiation inductive medium have demonstrated that they have the potential to differentiate into osteoblasts expressing BSP and OCN and form calcium deposits [24, 25]. DFSCs are more immature than PDLSCs. There is less heterochromatin in the nucleus and fewer organelles and bundles of microfilaments in the cytoplasm of DFSCs than in the cytoplasm of PDLSCs on ultrastructural comparison [63]. The higher expression of DSPP in DFSCs has shown its preferable potential for odontogenic differentiation and dentin regeneration compared to PDLSCs. And they generated complete dentin including dentin, predentin, and calcospherites upon the induction of treated dentin matrix (TDM) [11]. The properties of periodontal differentiation of DFSCs have also been demonstrated. They are able to form fibrous membrane PDL-like structures or calcified nodules with bone- or cementum-like structures under *in vitro* conditions, suggesting their potential for periodontal differentiation [24, 25]. Upon *in vivo* transplantation, DFSCs derived from the apical

end of human developing root could produce a cementum/PDL-like complex characterized by a thin layer of cementum-like tissues and PDL-like collagen fibers inserted perpendicularly into the newly formed cementum-like deposits [25]. These findings suggest that DFSCs are a promising alternative source for bioroot engineering.

Furthermore, the immunomodulatory effects of DFSCs also favor their therapeutic potential to treat autoimmune, inflammatory, and allergic diseases. Compared with SHEDs and DPSCs, DFSCs stimulated by IFN- $\gamma$  remarkably increased the number of CD4+FOXP3+ Treg cells and suppressed the proliferation and apoptosis of peripheral blood mononuclear cells (PBMCs) [62, 64].

**2.6. Tooth Germ Stem Cells (TGSCs).** In the bell stage, tooth germ consists of three components including enamel organ, dental mesenchymal cells (dental papilla or pulp), and dental follicle. The progenitor cell populations of dental mesenchymal cells, named TGSCs, have been isolated and identified from human third molar tooth germ [26]. The expression of DSPP has confirmed the odontogenic differentiation of TGSCs with the treatment of BMP2 and BMP7 [65].

The osteogenic differentiation capability of TGSCs has been demonstrated, as new bone formation was obtained in the pore area of the HA/TGSC implants. TGSCs have the potential to regenerate cartilage tissue, which is attributed to their chondrogenic differentiation ability upon induction. After TGSCs attached to 3D biological scaffolds, abundant hyaline cartilage-specific extracellular matrix (ECM) and collagen type II expression were found [66]. TGSCs were also able to differentiate into hepatocytes under hepatic induction. This was indicated by the expression of the liver-specific albumin gene, positive staining for albumin protein, and morphological change [26]. In rats with injured liver, transplantation of differentiated TGSCs could suppress the liver hydroxyproline content and reduce areas of damage, therefore suppressing liver fibrosis and steatonecrosis [26], suggesting that TGSCs are useful in cytotherapy for liver diseases.

**2.7. Alveolar Bone-Derived Mesenchymal Stem Cells (ABMSCs).** BMMSCs have been isolated from various bone tissues such as the ilium by an invasive procedure, namely, marrow aspiration. Alternatively, collecting ABMSCs from alveolar bone during the course of dental surgery is providing a new isolation method with a few extra invasive interventions [27]. ABMSCs have favorable osteogenic differentiation potential comparable to BMMSCs but a weaker potential to differentiate into chondrocytes or adipocytes [27]. New bone has been detected in a rabbit critical-size mandibular bone defect model with transplants which consist of ABMSCs and  $\beta$ -TCP [67]. ABMSCs also have the potential for bone tissue regeneration, and their potential to reconstruct alveolar bone will contribute to improving periodontal defects.

### 3. Dental MSC-Based Therapy for Dental Diseases

Considering the multi-lineage potential, dental MSCs are suggested as promising cells for the treatment of dental dis-

eases. Therefore, there have been a variety of therapeutic applications in dental medicine, ranging from preclinical studies (Table 1) to initial clinical trials (Table 2).

**3.1. Endodontic Diseases.** Dental caries and tooth trauma are common diseases associated with the teeth, which destroys the rigid structure of the teeth, both the enamel and dentin, resulting in pulp necrosis and periapical disease. For mature permanent teeth, the current routine clinical treatment is traditional root canal therapy based on pulpectomy, which involves the removal of damaged dental pulp tissue, enlargement of the root canal, and filling of the sterile canal with artificial filling materials [68]. When immature permanent teeth suffer from necrotic pulp/apical periodontitis, tooth development would be arrested, resulting in immature teeth with a thin root dentin and open apices. These teeth need to be treated with special measures based on pulpectomy, including the traditional apexification procedure and an apical mineral trioxide aggregate (MTA) plug [32]. Despite the wide implementation of the current routine treatment, the lack of biological dentin/pulp or dentin-pulp complex and the limitations of existing materials may lead to a great risk of serious reinfection and tooth fracture, thereby resulting in a poor survival rate for teeth. Therefore, the biological regeneration of dentin and pulp could be an ideal and alternative solution to replace defective dental structures in modern dental medicine. Based on different pulp conditions, several novel ideas for dentin-pulp complex and dental pulp regeneration therapy are presented [32]. Firstly, for local regeneration of the dentin-pulp complex following pulpotomy, combining dental MSCs with growth factors or platelet-rich plasma (PRP) is a promising solution to induce DPSCs and capillaries from the residual root pulp tissue and regenerate dentin tissue. Secondly, for a complete regeneration of the dentin-pulp complex for devital tooth after pulpectomy or pulp necrosis, cell homing and cell transplantation are utilized to achieve regeneration of the entire dental pulp for adult permanent teeth or revascularization for immature permanent teeth. However, the traditional revascularization approach fails to regenerate the dentin-pulp complex, unlike novel tissue engineering [68]. With various types of stem cells identified and remarkable breakthroughs in tissue engineering, numerous researches on dental MSC-mediated dentin and dental pulp regeneration have been carried out in animal models and human clinical trials [32].

**3.1.1. Dentin Regeneration.** The composite construct made up of porcine SHEDs and  $\beta$ -TCP scaffold has been directly capped on the created chamber roof defects in the premolars of swine, showing that almost complete dentin regeneration was observed with the newly formed dentin-like structure performing sparse porosity and certain thickness. It is indicated that the novel therapy based on dental MSCs significantly regenerated the dentin-like structure and is useful in direct pulp capping [69]. Subsequent research explored hDPSC-mediated dentin regeneration. hDPSCs were cultured onto the human dentin treated by ethylene diamine tetra-acetic acid and citric acid (hTD) and then implanted in the mouse model.

TABLE 1: Preclinical studies on treatment of dental diseases based on dental MSCs.

Disease target	Type of dental MSCs or their secretions	Animal model	Experiment design			Results or outcome			Reference
			Cell density Administration	Biomaterials/scaffolds	Growth factors	Time	Tissue regeneration	Effect evaluation and safety assessment	
Endodontic diseases	hDPSCs	Nude mice	$3 \times 10^4$ Subcutaneous transplantation	Human treated dentin (hTD)	—	4, 6, and 8 weeks	Dentin-like tissue	IHE: DSPP, DMP1, and human mitochondria antibodies [70]	
	hDPSCs	Nude mice	$2 \times 10^6$ Subcutaneous injection 100 $\mu$ L	Nanofibrous spongy microspheres (NF-SMS)	Odontogenic medium	6 weeks	Dentin-like tissue	IHE: DSPP Safety: NF-SMS almost completely degraded [71]	
	hDPSCs modified by PDGF-BB	Mice	— Subcutaneous transplantation	Porous CPC scaffolds	—	12 weeks	Dentin-pulp complex	Positive markers in IHE: DSPP and PDGF-BB protein secreted endogenous stem/progenitor cell homing [72]	
	Canine DPSCs	Beagle dogs Pulpotomy	$1 \times 10^7$ Autologous transplantation	Absorbable gelatin sponge	Simvastatin (SIM)	10 weeks	Coronal pulp	RGE: closure of the root apex and thickening of the root canal wall HE: regenerated pulp filling in nearly the entire pulp cavity with odontoblastic cells [75]	
	Porcine DPSCs	Minipigs Pulpotomy	$2 \times 10^7$ Autologous transplantation Pulp chamber	Injectable nanopeptide hydrogel	—	21 days	Failed No pulp	Micro-CT: reparative mineralized bridge in the residual pulp; failure of partial pulp regeneration [76]	
	Swine DPSCs	Miniswine	$2 \times 10^7$ Autologous/allogeneic transplantation Root canal	Injectable hyaluronic acid (HyA) gel or collagen TE gel	—	3~5 months	Dentin-like pulp-like	IHE: DSPP, DMP1, BSP, and Nestin HE: regeneration of vascularized pulp-like tissue with a layer of newly deposited dentin-like tissue or osteodentin along the canal walls. Safety: no overcalcification of the pulp canal space after 5 months of follow-up [71]	
	Canine mobilized DPSCs	Dogs	$2 \times 10^7$ Autologous transplantation Root canal	Drug-approved collagen	Granulocyte colony-stimulating factor (G-CSF)	14~180 days	Functional dental pulp	HE: regenerative pulp with well vasculature and innervation on day 14 RG: complete obliteration of the enlarged apical portion and lateral and coronal dentin formation Laser Doppler: functional recovery of pulpal blood flow after 90 days Pulp vitality: positive response on day 180 Safety: no adverse effects on both the whole and local [77]	
	Pig DPSCs	Minipig	DPSC aggregates Autologous transplantation Root canals	—	—	3 months	Whole pulp tissue	HE: regenerated pulp tissue containing an odontoblast layer and blood vessels IHE: NeuN [79]	



TABLE 1: Continued.

Disease target	Type of dental MSCs or their secretions	Experiment design				Results or outcome		Reference	
		Animal model	Cell density Administration	Biomaterials/scaffolds	Growth factors	Time	Tissue regeneration		Effect evaluation and safety assessment
Human SCAPs	Human SCAPs	Minipig	$2 \times 10^6$ Local injection Periodontal defect	—	—	12 weeks	Periodontal tissue	Clinical assessments: PD, GR, and AL loss values decrease CT scan: alveolar bone regeneration HE: remarkable regeneration of periodontal tissues (Sharpey's fibers, periodontal ligament, and cementum)	[84]
		Rat	Transplantation Periodontal defect	Collagen sponge	—	4 weeks	Periodontal tissue	Micro-CT: alveolar bone regeneration, decreased exposed root surface area HE: new periodontal tissue formation, dense fibrous connective tissues, periodontal ligament, osteoblast-like cells, small islet-like bone clusters, more united crestal bone	[103]
Periodontal diseases	SFRP2-human SCAPs	Miniature pig	$2 \times 10^6$ Local injection Periodontal defect	—	—	12 weeks	Periodontal tissue	Clinical assignment: values of probing depth, gingival recession, and attachment loss Micro-CT: alveolar bone regeneration HE: increased tissue regeneration (increased height of newborn alveolar bone, and mature and thicker new cementum, periodontal ligament, and Sharpey's fibers)	[85]
		Rat	PDLSC- amnion	Amnion	—	4 weeks	Periodontal tissue	Micro-CT images: new bone formation HE: cementum-like, narrow connective tissues, PDL-like tissues	[86]
	Human GMSC-CM	Rat	Transplantation	Collage membrane	—	1, 2, and 4 weeks	Periodontal tissue	HE: newly formed periodontal tissue IHE: TNF- $\alpha$ , IL-1 $\beta$ , IL-10, BSP-II, and Runx2	[87]

DSPP: dentin sialophosphoprotein; DMPI: dentin matrix protein 1; HE: hematoxylin and eosin; IHE: immunohistochemical stains; PDGF: platelet-derived growth factor; RG: radiographic examination; BSP: bone sialoprotein; DAPI: 4',6-diamidino-2-phenylindole; PD: probing depth; GR: gingival recession; AL: attachment loss; CM: conditioned medium; SFRPs: secreted frizzled-related proteins; Amnion: decellularized amniotic membrane.

TABLE 2: Current clinical studies on treatment of dental diseases based on dental MSCs.

Application	Source of dental MSCs	Size	Cells	Therapeutic strategy	Growth factor	Delivery approach	Follow-up time	Outcome	Reference
Irreversible pulpitis	Mobilized hDPSCs from 3rd molar	5	Passage 7	—	G-CSF 300 ng	Autologous transplantation	1, 2, 4, 12, 24, 28, and 32 weeks	No adverse events EPT: positive response at 4 weeks MRI: SI in the root canal approached that of the normal pulp in untreated controls after 24 weeks CBCT: lateral dentin formation in three cases at 28 weeks	[37]
Dental trauma with pulp necrosis	hDPSCs from deciduous canine teeth	26	Two hDPSC aggregates containing $1 \times 10^8$ /ml	—	Extracellular matrix	Autologous implantation	1, 3, 6, 9, 12, and 24 months	No significant side effects after 12 months Digital RVG: continued root development EPT: decrease in sensation thresholds CBCT: apical foramen width decreased, the length of the treated tooth root increased Laser Doppler flowmetry: increase in vascular formation Histology staining: regeneration of 3D whole dental pulp tissue	[79]
Irreversible pulpitis	hDPSCs from inflamed pulp	1	$1 \times 10^6$ /ml	Membrane of collagen	Leukocyte platelet-rich fibrin (L-PRF)	Autologous implantation	6 and 36 months	Remaining free of any symptoms Periapical radiographs: a normal periapical area CBCT: intact periapical bone structures Sensitivity: delayed response to cold EPT: responsive Laser Doppler flowmetry: low blood perfusion	[80]
Periodontal intrabony defects	hDPSCs	11	Micrograft containing cells	Collagen sponge	—	Autologous implantation	6 and 12 months	No adverse events Clinical measurements: PD reduction, CAL increased, pocket closure, gingival improvement	[90]
Periodontal intrabony defects	hDPSCs	15	Micrograft containing cells	Collagen sponge	—	Autologous implantation	6 and 12 months	Radiographs: intrabony defect decreased No adverse events.	[91]
Periodontal disease	hDPSCs	1	$5 \times 10^6$ /ml	Collagen sponge	—	Allogeneic grafting	3 and 6 months	Clinical measurements: PD reduction, CAL gain Radiographs: bone defect fill No signs or symptoms of rejection. Clinical evaluation: tooth mobility, periodontal pocket depth decreased CBCT: bone defect area significantly reduced	[92]

G-CSF: granulocyte colony-stimulating factor; EPT: electric pulp vitality testing; CBCT: cone beam computed tomography; SI: signal intensity; RVG: radiovisiography; PD: probing depth; CAL: clinical attachment level; PPD: probing pocket depth; BOP: bleeding on probing.

Formation of dentin-like tissues expressing specific dentin markers demonstrated that hDPSCs could be induced by hTD to regenerate the complete dentin tissue *in vivo* [70]. Meanwhile, hDPSCs were seeded onto a novel injectable cell carrier named nanofibrous spongy microspheres (NF-SMS). The result showed that a supported dentin-like tissue was generated in nude mice [71]. However, the narrow root foramen/limited tissue infiltration and blood supply would hold back the application of dental MSCs in clinic. A combination of some powerful growth factors and stem cells could serve as an alternative solution. Zhang *et al.* modified hDPSCs by over-expressing platelet-derived growth factor- (PDGF-) BB, which is a potent mitogenic factor as a mediator in wound healing and tissue repair, and obtained more dentin-like mineralized tissue similar to tooth dentin tissue *in vivo*. Further studies demonstrated that PDGF-BB-modified hDPSCs facilitated stem cell homing via the PI3K/Akt pathway and improved hDPSC-mediated dentin-pulp complex regeneration [72]. Lastly, a novel dentin-pulp-like organoid was developed by constructs mixed with hDPSCs and Matrigel in an odontogenic differentiation medium. The organoid demonstrated a biologically active response to biodentine supplements and suggested hDPSCs as a future approach for tooth regeneration [33]. Although scientific evidence shows a positive trend to dentin regeneration using dental MSCs, especially hDPSCs in animal models, there is a lack of persuasive evidence of clinical trials up to now.

**3.1.2. Pulp/Dentin-Pulp-Like Regeneration.** Dental pulp plays an indispensable role in maintaining homeostasis of the tooth, but its capacity of self-repair is highly limited. Hopefully, recent preclinical and clinical studies on cell homing and autogenous/allogeneic dental MSCs transplantation have provided further evidence of dental pulp regeneration. Depending on the clinical situation, there are mainly two cell-based pulp-regeneration strategies, partial dental pulp regeneration and whole pulp tissue regeneration [73]. A tentative experiment achieved rat DPSC-mediated partial dental pulp regeneration in rat molars after pulpotomy, suggesting that the remaining healthy pulp tissue could be recoverable and may have the potential to regenerate the lost portion of the dental pulp tissue [74]. Subsequent researches were performed in large animal models to test the feasibility of this regenerative approach. In a beagle dog model, Jia *et al.* transplanted canine DPSCs (cDPSCs) pretreated with simvastatin into immature premolars treated by pulpotomy. Then, regenerated coronal pulp was found filling nearly the entire pulp chamber with newly formed dentin and odontoblastic cells seen in the regenerated area, suggesting that coronal dental pulp regeneration could be realizable by cDPSCs transplantation [75]. Nevertheless, a study implanted pDPSCs/hydrogel into premolars and molars after pulpotomy in a minipig model and only found reparative dentinogenesis without dental pulp regeneration, highlighting the necessity for further investigations to develop a favorable regenerative microenvironment [76].

In recent years, there is growing concern about cell-based regenerative therapy for pulpless teeth. Moreover, several clinical studies are currently underway to confirm the efficacy

and safety of stem cell-based regenerative therapy. Inspiring outcomes have been reported for the whole dental pulp regeneration. Nakashima *et al.* developed a composite of drug-approved collagen scaffold and clinical-grade human mobilized DPSCs (MDPSCs) induced by granulocyte colony-stimulating factor (G-CSF) and achieved complete dental pulp regeneration by autologous transplantation with the composite in the mature teeth of dogs after pulpectomy. Similar to the healthy dental pulp tissue, regenerative pulp-like tissue presented good vasculature, innervation, odontoblast-like cells, and recovered function. Moreover, rare adverse effects confirmed the safety of cell therapy for dental pulp regeneration. A notable finding is that there were no significant age-related changes in biological properties and the stability of human MDPSCs *in vitro* and *in vivo* [77]. Then, this team performed a pilot clinical study to further demonstrate the availability and clinical safety of autologous transplantation of MDPSCs in pulpectomized teeth [37]. Functional dentin formation was observed by cone beam computed tomography (CBCT) in three of the five patients. Further study showed that variable sizes hDPSCs constructs possess the ability of self-organizing and can fill the human tooth root canal to regenerate blood vessel-rich pulp-like tissues after implantation in the subcutaneous space of mice [78]. Much more significantly, whole functional dental pulp tissue regeneration in a minipig was observed after pig DPSC aggregates were implanted into young permanent incisors. And newly formed dental pulp tissue containing an odontoblast layer and blood vessels as well as the expression of neuron markers NeuN indicated that functional dental pulp regeneration could be achieved in a large preclinical animal model [79]. Recently, Xuan *et al.* performed a randomized clinical controlled trial for treating immature permanent teeth injuries due to trauma. Taking apexification as a control group, this study demonstrated that not only could hDPSCs implantation regenerate 3D dental pulp tissue with blood vessels and sensory nerves but it could also show better efficacy and safety of hDPSCs implantation [79]. The majority of MSC-based endodontic treatments were performed in immature permanent teeth of adult patients. Interestingly, a recent case showed a personalized cell therapy in tooth #28 with symptomatic irreversible pulpitis in a 50-year-old man. As reported, hDPSCs were isolated from the inflamed dental pulp tissue of the diseased tooth #28. Combined with leukocyte platelet-rich fibrin (L-PRF) from the patient's blood, expanded hDPSCs were introduced into the prepared root canal. There was a positive response to an electric pulp test and a vitality test after a follow-up period of 36 months, which indicated that this MSC-based therapeutic method contributed to dental pulp regeneration [80].

**3.2. Periodontal Diseases.** Periodontitis leads to the damage of periodontal tissue including gingiva, cementum, ligament, and alveolar bone [81]. At present, periodontitis is routinely treated by debridement, surgery involving mechanical means, and guided tissue regeneration (GTR), which remain unsatisfactory due to rare regeneration [82]. The ultimate therapeutic goal for periodontal diseases is to regenerate lost

periodontal tissues. To address this, cell-based tissue regeneration has become one of the optimal periodontal therapies [81]. Several outstanding reviews have summarized the progress of cell-based regeneration of periodontal tissues [82, 83]. In the current review, we focus on the advance of dental MSC-based therapy for periodontal diseases, particularly periodontitis.

Previous studies of dental MSC-based therapy for periodontal tissue regeneration mainly focus on PDLSCs and DPSCs, but the source of PDLSCs is limited. A recent study discovered that SCAPs could serve as an alternative cell source for periodontitis treatment. Human SCAPs were injected subperiosteally to the surface of bone around the periodontitis defects in minipigs. It demonstrated that local injection of SCAPs improved gingival status and enhanced both bone and cementum regeneration [84]. With the discovery of key factors that maintain the function of SCAPs in periodontal treatment, subsequently, a strategy of gene modification has been studied by Li *et al.* By comparative investigation, they found that SCAPs overexpressing with SFRP2 promoted SCAP-mediated bone, PDL, and cementum regeneration in a minipig periodontitis model [85]. Recently a novel method named cell transfer technology was devised, in which cells were transferred onto a scaffold surface. With this new approach, Iwasaki *et al.* transferred human PDLSCs to the decellularized amniotic membrane (amnion) and transplanted the PDLSC-amnion into a rat with a created dehiscence-type periodontal defect. Newly generated cementum, PDL, and bone were detected, suggesting dental MSC-based treatment as a proposed new technology for periodontal diseases [86]. Conditioned medium generated by dental MSC culture (dental MSC-CM), which contains growth factors, cytokines, and other active substances, is considered as another new trend in periodontal tissue regeneration. Cell-free dental MSC-CM is more convenient and safer to apply in clinic than cell-based therapy. Qiu *et al.* transplanted collagen membranes loaded with concentrated GMSC-CM and PDLSC-CM into the buccal periodontal defects of molars in rats. More newly formed periodontal tissues were observed in both GMSC-CM and PDLSC-CM [87].

Following supporting evidence provided by numerous animal studies, the first human clinical trial was carried out to treat periodontal osseous defects in three patients through autologous *ex vivo* PDLSCs transplantation [88]. Later researchers devised a novel approach with stem cell assistance in the periodontal tissue regeneration technique (SAI-PRT) bypassing *ex vivo* PDLSCs. In a case report, researchers transplanted the transferable mass consisting of gelatin sponge and soft tissue harboring PDLSCs scraped from cementum and the alveolar socket of the third molar into the intrabony defect of another molar in the same patient. Then, they obtained clinical success with the reduction of probing pocket depth and the recovery of attachment over the evaluation of one year. Although the study is not certain about the number and viability of immediate PDLSCs transplantation, SAI-PRT might be a constructive avenue in the treatment of periodontal osseous defects [89]. Meanwhile, Aimetti *et al.* reported serial cases to explore the clinical

potential effects of the application of hDPSCs to treat deep intrabony defects via regenerative therapy. A total of 11 periodontitis patients with intrabony defects received treatment including a minimally invasive flap and autologous hDPSCs loaded on a collagen sponge. Significant clinical improvements and rare adverse effects were observed in a one-year follow-up [90]. Then, the team performed a randomized controlled clinical trial to evaluate the effectiveness of the novel therapeutic strategy as studied above. A remarkable reduction of probing depth (PD), a gain of clinical attachment, and the filling of bone defects in a test group further suggested that this cytotherapeutic approach based on PDLSCs engineering is a safe and innovative strategy to treat severe periodontal defects [91]. Moreover, a case report presented the effect of allogeneic hDPSCs transplantation in periodontal tissue regeneration of an aged periodontitis patient. hDPSCs were obtained from the dental pulp tissue of a 7-year-old donor and expanded. During periodontal surgery of the mesial circumferential bone defect, hDPSCs were seeded into a lyophilized collagen-polyvinylpyrrolidone sponge. After the allogeneic graft, the patient exhibited improved clinical manifestation without any sign of rejection. It is indicated that allogeneic hDPSCs transplantation could induce periodontal tissue regeneration [92].

**3.3. Therapeutic Strategies in MSC-Based Dental Medicine.** Due to their excellent potential for multi-lineage differentiation, dental MSCs are considered as an ideal source for tissue engineering and regenerative dental medicine. To date, researchers are looking for a feasible, safe, and effective approach for regenerative and translational dentistry [16]. Three feasible regenerative strategies based on dental MSCs have been proposed to treat dental diseases in clinic (Figure 2).

**3.3.1. Scaffold-Supported Tissue Engineering.** Generally, the principles of tissue engineering are based on three elements, including stem cells with multi-lineage differentiation potential, scaffolds as carriers for stem cells, and bioactive molecules inducing differentiation [93]. Dental MSCs are regarded as ideal cells for dental tissue engineering since they possess a shared embryological origin with craniofacial tissue [94]. Biocompatible scaffolds provide a favorable 3D micro-environment for stem cells, which regulate proliferation and differentiation [16]. In regenerative dentistry, current dominating attempts and studies of scaffold-supported tissue engineering include regeneration of dentin, dental pulp, and periodontal tissue and formation of bioroot. In a miniswine model, Zhu *et al.* transplanted autologous and allogeneic swine DPSCs carried by a bioscaffold hydrogel into the root canal space of the miniswine. Orthotopic vascularized pulp-like tissue regeneration was achieved with newly generated dentin-like tissue or osteodentin along the canal walls [95]. Similarly, a study used a root-shaped HA/TCP scaffold with allogeneic swine DPSCs, which was wrapped by a vitamin C-induced allogeneic PDLSC sheet and implanted into the jaw bone socket in swine and successfully regenerated a functional bioroot with a dentinal tubule-like structure and a functional PDL-like structure after six months [96]. Recently, a cell-laden hydrogel encapsulating GMSCs was used to



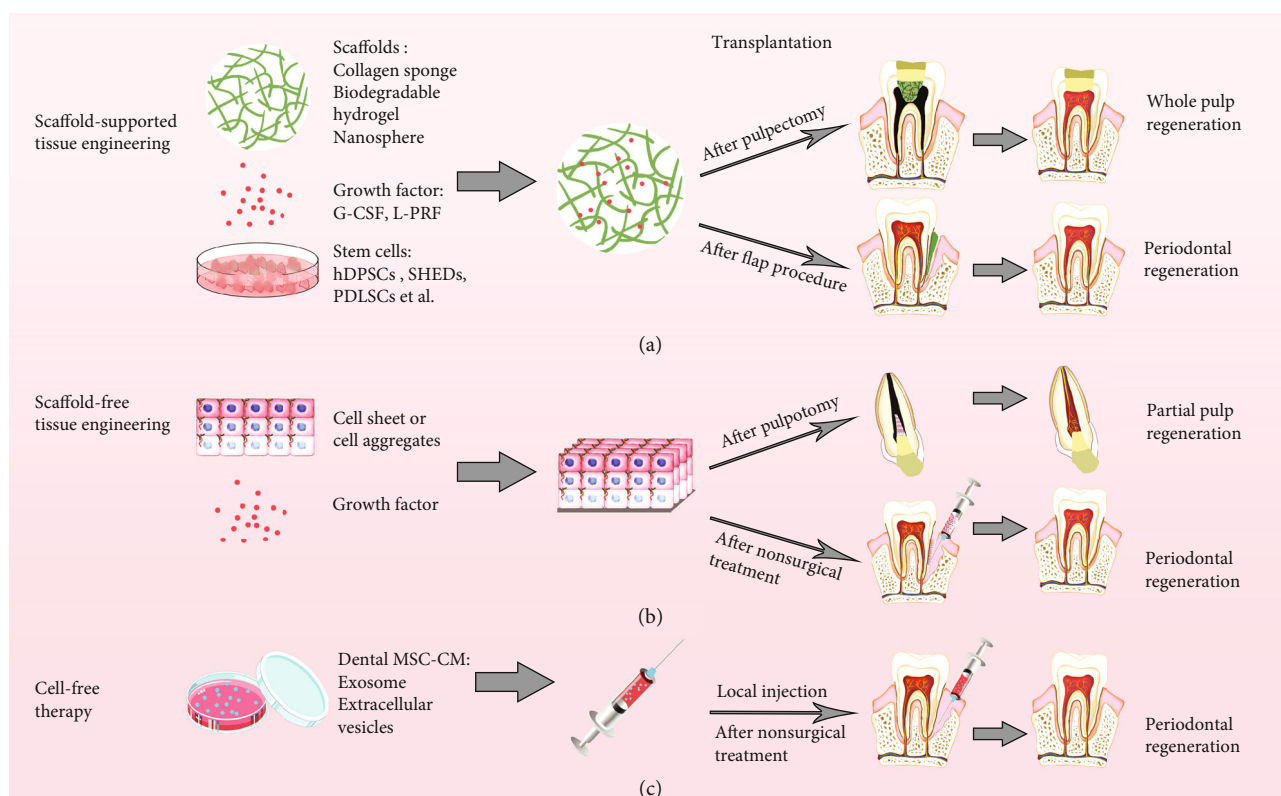


FIGURE 2: Three therapeutic strategies of endodontic and periodontal diseases using dental MSCs. (a) Dental tissue regeneration through a classic tissue engineering model, consisting of dental MSCs, supporting biomaterial scaffolds, and growth factors. (b) Dental tissue regeneration by tissue engineering without scaffolds. (c) Dental tissue regeneration with a cell-free approach using conditioned medium (CM) with exosomes and/or extracellular vesicles (EVs) secreted by dental MSCs.

promote craniofacial bone tissue regeneration. This study showed complete bone regeneration around ailing dental implants in rat peri-implantitis [97]. To achieve dentine-pulp complex regeneration, the optimal protocols should integrate cells, biomaterials, and growth factors. However, there are still several issues related to long-term safety and effectiveness, such as host immune rejection, degradation, and potential infection.

**3.3.2. Scaffold-Free Strategies for Tissue Engineering.** Based on the formation of tridimensional cell-to-cell aggregates without any other external support, scaffold-free technologies avoid the unknown risks of using biomaterials. Two scaffold-free strategies have caught the eye of researchers, which are cell sheets and cell injection. As a unique method of cell processing via culturing in temperature-responsive cell culture dishes or in ascorbic acid, cell sheets have been widely explored and applied in regenerative dentistry [16, 98]. PDLSC cell sheets were autologously transplanted into the denuded root surface in a canine model with a one-wall intrabony defect, and periodontal tissue regeneration was remarkably observed with both cementum and PDL fibers after eight weeks [99]. Cell injection might be a common treatment for periodontal disorders because it is a minimally invasive process. Local injection of allogeneic SCAPs has been shown effective for treating periodontitis by the promotion of periodontal tissue regeneration in a miniature

pig model [84]. However, the cell injection approach, independent from the use of any scaffold or biomolecule, has some practical issues, for instance, the risk of losing cell properties in the aseptis storage period and a small application range.

**3.3.3. Cell Homing or Cell-Free Therapy.** Cell homing is a cell-free approach to repair or regenerate tissue through active recruitment of host endogenous cells to the injured region, mainly via bioactive molecules. Compared with stem cell engraftment, cell homing may evade many hurdles in clinical translation of cell transplantation, including tumorigenicity, antigenicity, host rejection, and infection associated with cell-based therapies [100]. Exosome secreted by dental MSCs could act as paracrine signalers in cell homing. The exosome is one of EVs containing cytokines and microRNAs and plays a vital role in stem cell-based therapy by releasing molecules in target tissues [16]. Furthermore, dental MSCs may provide the secretome/CM with future regenerative therapeutic applications. Compared with the therapy using dental MSCs, dental MSC-CM, which is cell free, exhibits remarkable biological properties, including higher safety, migration activity, and greater ability of odontoblastic differentiation [101]. In a recent work, PDLSC-CM was transplanted into surgically created periodontal defects in a rat, and it was found that PDLSC-CM containing extracellular matrix proteins, enzymes, angiogenic factors, growth factors, and

cytokines enhanced periodontal regeneration by suppressing the inflammatory response via TNF- $\alpha$  production [102]. The dental MSC-mediated cell-free therapeutic approach is an appealing approach for treating dental diseases and has predominance over cell-based therapy despite some limitations in it. The bioactive molecules involve secretomes released by various populations, and their mechanisms need to be further understood.

#### 4. Dental MSC-Based Therapy for Nondental Diseases

**4.1. Other Oral Diseases.** The present therapeutic application of dental MSCs is not limited to endodontic and periodontal diseases. Recently, dental MSC-based therapy for other oral diseases has been proposed in animals and humans, such as craniofacial bone defects, progressive temporomandibular joint (TMJ) arthritis, facial nerve lesions, taste bud loss, and Sjogren's syndrome.

The craniofacial bone defect could be repaired by bone regeneration with dental MSCs [96, 103]. In a well-established rat model with peri-implantitis, GMSC-laden adhesive alginate hydrogels were injected into the bony defect sites around implants, which increased implant survival and the amount of recovered bone [96]. Dental MSCs also hold promise for the treatment of facial nerve injury. Recent experimental evidence showed that a novel method to treat crush injury of rats' facial nerve is via a single application of human SHEDs immediately, which could promote a positive local effect on neuroprotection and remyelination in 2 weeks [104].

A further important application of dental MSCs is for the treatment of TMJ disorders. Common TMJ arthritis often leads to sustained synovitis, cartilage and bone destruction, and pain. Considering the potential immunomodulatory features of human DPSCs, Cui *et al.* tried to locally inject hDPSCs into the articular cavity to treat rat TMJ arthritis. It was found that DPSCs relieved hyperalgesia and synovial inflammation, attenuated cartilage and matrix degradation, and promoted bone regeneration [105]. Dental MSCs have been suggested to promote taste bud regeneration and have promising potential applications in postsurgery tongue reconstruction of patients with tongue cancer [106]. Interestingly, recent work has also suggested that SHEDs exert a protective effect on the secretory function of the salivary gland and exhibit therapeutic potential for the improvement of hyposalivation in Sjogren's syndrome [107].

**4.2. Extraoral Diseases.** Besides widespread application for treating oral diseases, as a powerful autologous stem cell source, dental MSCs also have great therapeutic potential for the treatment of multiple systemic ailments. A recent review has summarized the extensive usage of hDPSCs in the cell-therapeutic paradigm shift to treat various diseases [18]. Other dental MSCs have also been applied in the treatment of extraoral diseases like neurodegenerative diseases and autoimmune and orthopedic disorders. Dental MSCs have a remarkable potential to treat neural diseases such as spinal cord injury (SCI) and peripheral nerve injury, like sci-

atic nerve and superior laryngeal nerve (SLN) injury, owing to their ability to differentiate into neural-like cells and regenerate neural tissue [107]. SCI is a severe traumatic central nervous system disease resulting in the damage of sensory and motor functions. It has been demonstrated by recent studies that dental MSCs could facilitate functional improvement after SCI in animal models [108–111]. For instance, SHED-CM loaded in collagen hydrogel was injected into the injury site and gained higher Basso, Beattie, and Bresnahan (BBB) scores which suggested that this new cell-free therapeutic approach is conducive to sensory and motor function recovery of SCI [110]. Peripheral nerve injury following traumatic accidents or surgical complications is a severe clinical problem resulting in sensory disturbances, paralysis, and locomotive disability. Because dental MSCs present a great privilege in neurogenic differentiation, they are a hopeful cell source to treat injured peripheral nerves, like the sciatic nerve and SLN [111–113]. For example, the sciatic nerve could be regenerated and repaired after hDPSC implantation or exosome derived from GMSC transplantation in a rat model with sciatic nerve defects [112, 113]. Besides, Tsuruta *et al.* established a novel animal model of SLN injury, which was characterized as having weight loss and drinking behavior changes. The therapeutic effects of systemic administration of SHED-CM in this model showed functional recovery of the SLN and axonal regeneration [114]. Furthermore, hDPSCs have been suggested as an appropriate stem cell source for stroke treatment and acute cerebral ischemia [115, 116].

Also, dental MSCs play an important role in bone and cartilage tissue engineering. Campos *et al.* treated noncritical defects in an ovine model with the biomaterial Bonelike and hDPSCs, and obtained significant radiographic and microscopical evidence of improved bone regeneration [117]. hDPSCs also have been used to treat full-thickness articular cartilage defects. hDPSCs and PRP scaffolds were transplanted into full-thickness cartilage defects in rabbits, resulting in a significant improvement of impaired cartilage and formation of articular cartilage with hyaline-like and fibrocartilaginous tissue [118].

Furthermore, dental MSCs might be another choice for systemic lupus erythematosus (SLE) therapy and are also effective in reducing a kidney glomerular lesion and perivascular inflammation infiltration [119]. And dental MSCs are able to treat diabetes by obtaining insulin-producing cells or improving diabetic polyneuropathy [119, 120].

#### 5. Conclusion

Dental MSCs have been a precious stem cell source in regenerative medicine and have a great therapeutic application potential not only in oral diseases but also in various extraoral diseases. Here, a lot of evidence has demonstrated that dental MSCs are capable of multi-lineage differentiation and are conducive for regenerating and repairing dental tissue. Moreover, some clinical trials with dental MSCs have been completed and demonstrated the efficacy and safety of dental MSC-based therapy for oral diseases. However, these studies are limited, with a limited number of patients and a

rather short-term follow-up, so more clinical trials are required before they can be applied effectively and safely in clinic. In addition to a significant potential in dental medicine, dental MSCs have already been considered as an alternative source for nerve and bone regeneration and have therapeutic potential for treating various diseases, such as neural impairment, stroke, bone and cartilage defects, SLE, and diabetes. However, thoroughly understanding the regulatory mechanism of dental MSCs is required before their wide application in clinic.

## Conflicts of Interest

The authors declare that there are no conflicts of interest regarding the publication of this paper.

## Authors' Contributions

Lu Gan and Ying Liu contributed equally to this work.

## Acknowledgments

This work was supported by National Natural Science Foundation of China (NSFC) Grant 81800929 and Sichuan Science and Technology Program 2019JDR0096 to Mian Wan; National Natural Science Foundation of China (NSFC) Grant 81771033 and Clinical Research Project/Foundation of West China Hospital of Stomatology Grant LCYJ2019-24 to Liwei Zheng; and Preeminent Youth Fund of Sichuan Province Grant 2016JQ0054 to Liwei Zheng.

## References

- [1] M. F. Pittenger, A. M. Mackay, S. C. Beck et al., "Multilineage potential of adult human mesenchymal stem cells," *Science*, vol. 284, no. 5411, pp. 143–147, 1999.
- [2] F. Gao, S. M. Chiu, D. A. L. Motan et al., "Mesenchymal stem cells and immunomodulation: current status and future prospects," *Cell Death & Disease*, vol. 7, no. 1, article e2062, 2016.
- [3] R. Berebichez-Fridman and P. R. Montero-Olvera, "Sources and clinical applications of mesenchymal stem cells: state-of-the-art review," *Sultan Qaboos University Medical Journal*, vol. 18, no. 3, pp. 264–e277, 2018.
- [4] Y. Han, X. Li, Y. Zhang, Y. Han, F. Chang, and J. Ding, "Mesenchymal stem cells for regenerative medicine," *Cell*, vol. 8, no. 8, p. 886, 2019.
- [5] G. T.-J. Huang, S. Gronthos, and S. Shi, "Mesenchymal stem cells derived from dental tissues vs. those from other sources: their biology and role in regenerative medicine," *Journal of Dental Research*, vol. 88, no. 9, pp. 792–806, 2009.
- [6] P. T. Sharpe, "Dental mesenchymal stem cells," *Development*, vol. 143, no. 13, pp. 2273–2280, 2016.
- [7] E. P. Chalisserry, S. Y. Nam, S. H. Park, and S. Anil, "Therapeutic potential of dental stem cells," *Journal of Tissue Engineering*, vol. 8, 2016.
- [8] G. Varga and G. Gerber, "Mesenchymal stem cells of dental origin as promising tools for neuroregeneration," *Stem Cell Research & Therapy*, vol. 5, no. 2, p. 61, 2014.
- [9] R. Patil, B. M. Kumar, W.-J. Lee et al., "Multilineage potential and proteomic profiling of human dental stem cells derived from a single donor," *Experimental Cell Research*, vol. 320, no. 1, pp. 92–107, 2014.
- [10] J. Fujiyoshi, H. Yamaza, S. Sonoda et al., "Therapeutic potential of hepatocyte-like-cells converted from stem cells from human exfoliated deciduous teeth in fulminant Wilson's disease," *Scientific Reports*, vol. 9, no. 1, article 1535, 2019.
- [11] O. Trubiani, J. Pizzicannella, S. Caputi et al., "Periodontal ligament stem cells: current knowledge and future perspectives," *Stem Cells and Development*, vol. 28, no. 15, pp. 995–1003, 2019.
- [12] K. Iohara, L. Zheng, H. Wake et al., "A novel stem cell source for vasculogenesis in ischemia: subfraction of side population cells from dental pulp," *Stem Cells*, vol. 26, no. 9, pp. 2408–2418, 2008.
- [13] J. Liu, F. Yu, Y. Sun et al., "Concise reviews: characteristics and potential applications of human dental tissue-derived mesenchymal stem cells," *Stem Cells*, vol. 33, no. 3, pp. 627–638, 2015.
- [14] G. Orsini, P. Pagella, and T. A. Mitsiadis, "Modern trends in dental medicine: an update for internists," *The American Journal of Medicine*, vol. 131, no. 12, pp. 1425–1430, 2018.
- [15] Q. Zhai, Z. Dong, W. Wang, B. Li, and Y. Jin, "Dental stem cell and dental tissue regeneration," *Frontiers of Medicine*, vol. 13, no. 2, pp. 152–159, 2019.
- [16] M. Tatullo, B. Codispoti, F. Paduano, M. Nuzzolese, and I. Makeeva, "Strategic tools in regenerative and translational dentistry," *International Journal of Molecular Sciences*, vol. 20, no. 8, article 1879, 2019.
- [17] P. Stanko, U. Altanerova, J. Jakubchova, V. Repiska, and C. Altaner, "Dental mesenchymal stem/stromal cells and their exosomes," *Stem Cells International*, vol. 2018, Article ID 8973613, 8 pages, 2018.
- [18] Y. Yamada, S. Nakamura-Yamada, K. Kusano, and S. Baba, "Clinical potential and current progress of dental pulp stem cells for various systemic diseases in regenerative medicine: a concise review," *International Journal of Molecular Sciences*, vol. 20, no. 5, article 1132, 2019.
- [19] S. Gronthos, M. Mankani, J. Brahim, P. G. Robey, and S. Shi, "Postnatal human dental pulp stem cells (DPSCs) in vitro and in vivo," *Proceedings of the National Academy of Sciences of the United States of America*, vol. 97, no. 25, pp. 13625–13630, 2000.
- [20] M. Miura, S. Gronthos, M. Zhao et al., "SHED: stem cells from human exfoliated deciduous teeth," *Proceedings of the National Academy of Sciences of the United States of America*, vol. 100, no. 10, pp. 5807–5812, 2003.
- [21] W. Sonoyama, Y. Liu, D. Fang et al., "Mesenchymal stem cell-mediated functional tooth regeneration in swine," *PLoS One*, vol. 1, no. 1, article e79, 2006.
- [22] B.-M. Seo, M. Miura, S. Gronthos et al., "Investigation of multipotent postnatal stem cells from human periodontal ligament," *The Lancet*, vol. 364, no. 9429, pp. 149–155, 2004.
- [23] Q. Zhang, S. Shi, Y. Liu et al., "Mesenchymal stem cells derived from human gingiva are capable of immunomodulatory functions and ameliorate inflammation-related tissue destruction in experimental colitis," *Journal of Immunology*, vol. 183, no. 12, pp. 7787–7798, 2009.
- [24] C. Morscheck, W. Götz, J. Schierholz et al., "Isolation of precursor cells (PCs) from human dental follicle of wisdom teeth," *Matrix Biology*, vol. 24, no. 2, pp. 155–165, 2005.



- [25] C. Han, Z. Yang, W. Zhou et al., "Periapical follicle stem cell: a promising candidate for cementum/periodontal ligament regeneration and bio-root engineering," *Stem Cells and Development*, vol. 19, no. 9, pp. 1405–1415, 2010.
- [26] E. Ikeda, K. Yagi, M. Kojima et al., "Multipotent cells from the human third molar: feasibility of cell-based therapy for liver disease," *Differentiation*, vol. 76, no. 5, pp. 495–505, 2008.
- [27] T. Matsubara, K. Suardita, M. Ishii et al., "Alveolar bone marrow as a cell source for regenerative medicine: differences between alveolar and iliac bone marrow stromal cells," *Journal of Bone and Mineral Research*, vol. 20, no. 3, pp. 399–409, 2005.
- [28] T. Zhou, J. Pan, P. Wu et al., "Dental follicle cells: roles in development and beyond," *Stem Cells International*, vol. 2019, Article ID 9159605, 17 pages, 2019.
- [29] I. Mortada and R. Mortada, "Dental pulp stem cells and osteogenesis: an update," *Cytotechnology*, vol. 70, no. 5, pp. 1479–1486, 2018.
- [30] E. Anitua, M. Troya, and M. Zalduendo, "Progress in the use of dental pulp stem cells in regenerative medicine," *Cytotechnology*, vol. 20, no. 4, pp. 479–498, 2018.
- [31] S. Sohn, Y. Park, S. Srikanth et al., "The role of ORAI1 in the odontogenic differentiation of human dental pulp stem cells," *Journal of Dental Research*, vol. 94, no. 11, pp. 1560–1567, 2015.
- [32] G. S. da Silva, M. S. Moreira, K. A. Fukushima et al., "Current evidence of tissue engineering for dentine regeneration in animal models: a systematic review," *Regenerative Medicine*, vol. 15, no. 2, pp. 1345–1360, 2020.
- [33] S. Y. Jeong, S. Lee, W. H. Choi, J. H. Jee, H.-R. Kim, and J. Yoo, "Fabrication of dentin-pulp-like organoids using dental-pulp stem cells," *Cell*, vol. 9, no. 3, p. 642, 2020.
- [34] P. Pagella, S. Miran, E. Neto, I. Martin, M. Lamghari, and T. A. Mitsiadis, "Human dental pulp stem cells exhibit enhanced properties in comparison to human bone marrow stem cells on neurites outgrowth," *The FASEB Journal*, vol. 34, no. 4, pp. 5499–5511, 2020.
- [35] Y. Kawase-Koga, Y. Fujii, D. Yamakawa, M. Sato, and D. Chikazu, "Identification of neurospheres generated from human dental pulp stem cells in xeno-/serum-free conditions," *Regenerative Therapy*, vol. 14, pp. 128–135, 2020.
- [36] J. Jung, J.-W. Kim, H.-J. Moon, J. Y. Hong, and J. K. Hyun, "Characterization of neurogenic potential of dental pulp stem cells cultured in xeno/serum-free condition: *in vitro* and *in vivo* assessment," *Stem Cells International*, vol. 2016, Article ID 6921097, 12 pages, 2016.
- [37] M. Nakashima, K. Iohara, M. Murakami et al., "Pulp regeneration by transplantation of dental pulp stem cells in pulpitis: a pilot clinical study," *Stem Cell Research & Therapy*, vol. 8, no. 1, p. 61, 2017.
- [38] P. Hilkens, A. Bronckaers, J. Ratajczak, P. Gervois, E. Wolfs, and I. Lambrechts, "The angiogenic potential of DPSCs and SCAPs in an *in vivo* model of dental pulp regeneration," *Stem Cells International*, vol. 2017, Article ID 2582080, 14 pages, 2017.
- [39] M. M. Cordeiro, Z. Dong, T. Kaneko et al., "Dental pulp tissue engineering with stem cells from exfoliated deciduous teeth," *Journal of Endodontics*, vol. 34, no. 8, pp. 962–969, 2008.
- [40] V. Rosa, Z. Zhang, R. H. M. Grande, and J. E. Nör, "Dental pulp tissue engineering in full-length human root canals," *Journal of Dental Research*, vol. 92, no. 11, pp. 970–975, 2013.
- [41] J. Wang, X. Wang, Z. Sun et al., "Stem cells from human exfoliated deciduous teeth can differentiate into dopaminergic neuron-like cells," *Stem Cells and Development*, vol. 19, no. 9, pp. 1375–1383, 2010.
- [42] F. Nicola, M. R. Marques, F. Odorcyk et al., "Stem cells from human exfoliated deciduous teeth modulate early astrocyte response after spinal cord contusion," *Molecular Neurobiology*, vol. 56, no. 1, pp. 748–760, 2019.
- [43] Y. Sugimura-Wakayama, W. Katagiri, M. Osugi et al., "Peripheral nerve regeneration by secretomes of stem cells from human exfoliated deciduous teeth," *Stem Cells and Development*, vol. 24, no. 22, pp. 2687–2699, 2015.
- [44] K. Nakajima, R. Kunimatsu, K. Ando et al., "Comparison of the bone regeneration ability between stem cells from human exfoliated deciduous teeth, human dental pulp stem cells and human bone marrow mesenchymal stem cells," *Biochemical and Biophysical Research Communications*, vol. 497, no. 3, pp. 876–882, 2018.
- [45] K. H. Kwack, J. M. Lee, S. H. Park, and H. W. Lee, "Human dental pulp stem cells suppress alloantigen-induced immunity by stimulating T cells to release transforming growth factor beta," *Journal of Endodontics*, vol. 43, no. 1, pp. 100–108, 2017.
- [46] Y.-Y. Dai, S.-Y. Ni, K. Ma, Y.-S. Ma, Z.-S. Wang, and X.-L. Zhao, "Stem cells from human exfoliated deciduous teeth correct the immune imbalance of allergic rhinitis via Treg cells *in vivo* and *in vitro*," *Stem Cell Research & Therapy*, vol. 10, no. 1, p. 39, 2019.
- [47] X. Gao, Z. Shen, M. Guan et al., "Immunomodulatory role of stem cells from human exfoliated deciduous teeth on periodontal regeneration," *Tissue Engineering Part A*, vol. 24, no. 17–18, pp. 1341–1353, 2018.
- [48] W. Sonoyama, Y. Liu, T. Yamaza et al., "Characterization of the apical papilla and its residing stem cells from human immature permanent teeth: a pilot study," *Journal of Endodontics*, vol. 34, no. 2, pp. 166–171, 2008.
- [49] C. Pelissari, A. F. C. Paris, A. Mantesso, and M. Trierveiler, "Apical papilla cells are capable of forming a pulplike tissue with odontoblastlike cells without the use of exogenous growth factors," *Journal of Endodontics*, vol. 44, no. 11, pp. 1671–1676, 2018.
- [50] K. Chen, H. Xiong, Y. Huang, and C. Liu, "Comparative analysis of *in vitro* periodontal characteristics of stem cells from apical papilla (SCAP) and periodontal ligament stem cells (PDLSCs)," *Archives of Oral Biology*, vol. 58, no. 8, pp. 997–1006, 2013.
- [51] P. De Berdt, J. Vanacker, B. Ucakar et al., "Dental apical papilla as therapy for spinal cord injury," *Journal of Dental Research*, vol. 94, no. 11, pp. 1575–1581, 2015.
- [52] G. Ding, Y. Liu, Y. An et al., "Suppression of T cell proliferation by root apical papilla stem cells *in vitro*," *Cells, Tissues, Organs*, vol. 191, no. 5, pp. 357–364, 2010.
- [53] C. A. G. McCulloch and A. H. Melcher, "Cell density and cell generation in the periodontal ligament of mice," *The American Journal of Anatomy*, vol. 167, no. 1, pp. 43–58, 1983.
- [54] T. Iwata, M. Yamato, Z. Zhang et al., "Validation of human periodontal ligament-derived cells as a reliable source for cytotherapeutic use," *Journal of Clinical Periodontology*, vol. 37, no. 12, pp. 1088–1099, 2010.
- [55] O. Trubiani, S. Guarnieri, F. Diomedede et al., "Nuclear translocation of PKC $\alpha$  isoenzyme is involved in neurogenic



- commitment of human neural crest-derived periodontal ligament stem cells,” *Cellular Signalling*, vol. 28, no. 11, pp. 1631–1641, 2016.
- [56] G. Ding, Y. Liu, W. Wang et al., “Allogeneic periodontal ligament stem cell therapy for periodontitis in swine,” *Stem Cells*, vol. 28, no. 10, pp. 1829–1838, 2010.
- [57] F. Diomedea, A. Gugliandolo, P. Cardelli et al., “Three-dimensional printed PLA scaffold and human gingival stem cell-derived extracellular vesicles: a new tool for bone defect repair,” *Stem Cell Research & Therapy*, vol. 9, no. 1, p. 104, 2018.
- [58] J. Li, S.-q. Xu, K. Zhang et al., “Treatment of gingival defects with gingival mesenchymal stem cells derived from human fetal gingival tissue in a rat model,” *Stem Cell Research & Therapy*, vol. 9, no. 1, p. 27, 2018.
- [59] Q. Zhang, P. D. Nguyen, S. Shi, J. C. Burrell, D. K. Cullen, and A. D. le, “3D bio-printed scaffold-free nerve constructs with human gingiva-derived mesenchymal stem cells promote rat facial nerve regeneration,” *Scientific Reports*, vol. 8, no. 1, article 6634, 2018.
- [60] K. M. Fawzy El-Sayed and C. E. Dörfer, “Gingival mesenchymal stem/progenitor cells: a unique tissue engineering gem,” *Stem Cells International*, vol. 2016, Article ID 7154327, 16 pages, 2016.
- [61] Q. Zhang, A. L. Nguyen, S. Shi et al., “Three-dimensional spheroid culture of human gingiva-derived mesenchymal stem cells enhances mitigation of chemotherapy-induced oral mucositis,” *Stem Cells and Development*, vol. 21, no. 6, pp. 937–947, 2012.
- [62] S. Yildirim, N. Zibandeh, D. Genc, E. M. Ozcan, K. Goker, and T. Akkoc, “The comparison of the immunologic properties of stem cells isolated from human exfoliated deciduous teeth, dental pulp, and dental follicles,” *Stem Cells International*, vol. 2016, Article ID 4682875, 15 pages, 2016.
- [63] Y. Tian, D. Bai, W. Guo et al., “Comparison of human dental follicle cells and human periodontal ligament cells for dentin tissue regeneration,” *Regenerative Medicine*, vol. 10, no. 4, pp. 461–479, 2015.
- [64] S. Tomic, J. Djokic, S. Vasilijic et al., “Immunomodulatory properties of mesenchymal stem cells derived from dental pulp and dental follicle are susceptible to activation by toll-like receptor agonists,” *Stem Cells and Development*, vol. 20, no. 4, pp. 695–708, 2011.
- [65] P. N. Taşlı, S. Aydın, M. E. Yalvaç, and F. Şahin, “Bmp 2 and bmp 7 induce odonto- and osteogenesis of human tooth germ stem cells,” *Applied Biochemistry and Biotechnology*, vol. 172, no. 6, pp. 3016–3025, 2014.
- [66] A. C. Calikoglu Koyuncu, G. Gurel Pekozer, M. Ramazanoglu, G. Torun Kose, and V. Hasirci, “Cartilage tissue engineering on macroporous scaffolds using human tooth germ stem cells,” *Journal of Tissue Engineering and Regenerative Medicine*, vol. 11, no. 3, pp. 765–777, 2017.
- [67] X. Wang, H. Xing, G. Zhang et al., “Restoration of a Critical Mandibular Bone Defect Using Human Alveolar Bone-Derived Stem Cells and Porous Nano-HA/Collagen/PLA Scaffold,” *Stem Cells International*, vol. 2016, Article ID 8741641, 13 pages, 2016.
- [68] T. Morotomi, A. Washio, and C. Kitamura, “Current and future options for dental pulp therapy,” *The Japanese Dental Science Review*, vol. 55, no. 1, pp. 5–11, 2019.
- [69] Y. Zheng, X. Y. Wang, Y. M. Wang et al., “Dentin regeneration using deciduous pulp stem/progenitor cells,” *Journal of Dental Research*, vol. 91, no. 7, pp. 676–682, 2012.
- [70] H. L. B. Tran and V. N. Doan, “Human dental pulp stem cells cultured onto dentin derived scaffold can regenerate dentin-like tissue in vivo,” *Cell and Tissue Banking*, vol. 16, no. 4, pp. 559–568, 2015.
- [71] R. Kuang, Z. Zhang, X. Jin et al., “Nanofibrous spongy microspheres enhance odontogenic differentiation of human dental pulp stem cells,” *Advanced Healthcare Materials*, vol. 4, no. 13, pp. 1993–2000, 2015.
- [72] M. Zhang, F. Jiang, X. Zhang et al., “The effects of platelet-derived growth factor-BB on human dental pulp stem cells mediated dentin-pulp complex regeneration,” *Stem Cells Translational Medicine*, vol. 6, no. 12, pp. 2126–2134, 2017.
- [73] G. T. J. Huang, “Pulp and dentin tissue engineering and regeneration: current progress,” *Regenerative Medicine*, vol. 4, no. 5, pp. 697–707, 2009.
- [74] J.-B. Souron, A. Petiet, F. Decup et al., “Pulp cell tracking by radionuclide imaging for dental tissue engineering,” *Tissue Engineering Part C: Methods*, vol. 20, no. 3, pp. 188–197, 2014.
- [75] W. Jia, Y. Zhao, J. Yang et al., “Simvastatin Promotes Dental Pulp Stem Cell-induced Coronal Pulp Regeneration in Pulpotomized Teeth,” *Journal of Endodontics*, vol. 42, no. 7, pp. 1049–1054, 2016.
- [76] F. Mangione, M. EzEldeen, C. Bardet et al., “Implanted dental pulp cells fail to induce regeneration in partial pulpotomies,” *Journal of Dental Research*, vol. 96, no. 12, pp. 1406–1413, 2017.
- [77] M. Nakashima and K. Iohara, “Mobilized dental pulp stem cells for pulp regeneration: initiation of clinical trial,” *Journal of Endodontics*, vol. 40, no. 4, pp. S26–S32, 2014.
- [78] Y. Itoh, J. I. Sasaki, M. Hashimoto, C. Katata, M. Hayashi, and S. Imazato, “Pulp regeneration by 3-dimensional dental pulp stem cell constructs,” *Journal of Dental Research*, vol. 97, no. 10, pp. 1137–1143, 2018.
- [79] K. Xuan, B. Li, H. Guo et al., “Deciduous autologous tooth stem cells regenerate dental pulp after implantation into injured teeth,” *Science Translational Medicine*, vol. 10, no. 455, article eaaf3227, 2018.
- [80] G. Meza, D. Urrejola, N. Saint Jean et al., “Personalized cell therapy for pulpitis using autologous dental pulp stem cells and leukocyte platelet-rich fibrin: a case report,” *Journal of Endodontics*, vol. 45, no. 2, pp. 144–149, 2019.
- [81] D. F. Kinane, P. G. Stathopoulou, and P. N. Papapanou, “Periodontal diseases,” *Nature Reviews Disease Primers*, vol. 3, no. 1, article 17038, 2017.
- [82] T. Ouchi and T. Nakagawa, “Mesenchymal stem cell-based tissue regeneration therapies for periodontitis,” *Regenerative Therapy*, vol. 14, pp. 72–78, 2020.
- [83] J. Nuñez, F. Vignoletti, R. G. Caffesse, and M. Sanz, “Cellular therapy in periodontal regeneration,” *Periodontology 2000*, vol. 79, no. 1, pp. 107–116, 2019.
- [84] G. Li, N. Han, X. Zhang et al., “Local injection of allogeneic stem cells from apical papilla enhanced periodontal tissue regeneration in minipig model of periodontitis,” *BioMed Research International*, vol. 2018, Article ID 3960798, 8 pages, 2018.

- [85] G. Li, N. Han, H. Yang et al., "SFRP2 promotes stem cells from apical papilla-mediated periodontal tissue regeneration in miniature pig," *Journal of Oral Rehabilitation*, 2019.
- [86] K. Iwasaki, K. Akazawa, M. Nagata et al., "The fate of transplanted periodontal ligament stem cells in surgically created periodontal defects in rats," *International Journal of Molecular Sciences*, vol. 20, no. 1, p. 192, 2019.
- [87] J. Qiu, X. Wang, H. Zhou et al., "Enhancement of periodontal tissue regeneration by conditioned media from gingiva-derived or periodontal ligament-derived mesenchymal stem cells: a comparative study in rats," *Stem Cell Research & Therapy*, vol. 11, no. 1, p. 42, 2020.
- [88] F. Feng, K. Akiyama, Y. Liu et al., "Utility of PDL progenitors for in vivo tissue regeneration: a report of 3 cases," *Oral Diseases*, vol. 16, no. 1, pp. 20–28, 2010.
- [89] K. L. Vandana, H. Ryana, and P. J. Dalvi, "Autologous periodontal stem cell assistance in periodontal regeneration technique (SAI-PRT) in the treatment of periodontal intrabony defects: a case report with one-year follow-up," *Journal of Dental Research, Dental Clinics, Dental Prospects*, vol. 11, no. 2, pp. 123–126, 2017.
- [90] M. Aimetti, F. Ferrarotti, M. Gamba, M. Giraudi, and F. Romano, "Regenerative treatment of periodontal intrabony defects using autologous dental pulp stem cells: a 1-year follow-up case series," *The International Journal of Periodontics & Restorative Dentistry*, vol. 38, no. 1, pp. 51–58, 2018.
- [91] F. Ferrarotti, F. Romano, M. N. Gamba et al., "Human intrabony defect regeneration with micrografts containing dental pulp stem cells: a randomized controlled clinical trial," *Journal of Clinical Periodontology*, vol. 45, no. 7, pp. 841–850, 2018.
- [92] B. Hernández-Monjaraz, E. Santiago-Osorio, E. Ledesma-Martínez, A. Alcauter-Zavala, and V. M. Mendoza-Núñez, "Retrieval of a periodontally compromised tooth by allogeneic grafting of mesenchymal stem cells from dental pulp: a case report," *The Journal of International Medical Research*, vol. 46, no. 7, pp. 2983–2993, 2018.
- [93] D. Hughes and B. Song, "Dental and nondental stem cell based regeneration of the craniofacial region: a tissue based approach," *Stem Cells International*, vol. 2016, Article ID 8307195, 20 pages, 2016.
- [94] X. Zhu, J. Liu, Z. Yu et al., "A miniature swine model for stem cell-based de novo regeneration of dental pulp and dentin-like tissue," *Tissue Engineering Part C: Methods*, vol. 24, no. 2, pp. 108–120, 2018.
- [95] F. Wei, T. Song, G. Ding et al., "Functional tooth restoration by allogeneic mesenchymal stem cell-based bio-root regeneration in swine," *Stem Cells and Development*, vol. 22, no. 12, pp. 1752–1762, 2013.
- [96] M. M. Hasani-Sadrabadi, P. Sarrion, S. Pouraghaei et al., "An engineered cell-laden adhesive hydrogel promotes craniofacial bone tissue regeneration in rats," *Science Translational Medicine*, vol. 12, no. 534, article eaay6853, 2020.
- [97] H. Bakhtiar, A. Mazidi S, S. Mohammadi Asl et al., "The role of stem cell therapy in regeneration of dentine-pulp complex: a systematic review," *Progress in Biomaterials*, vol. 7, no. 4, pp. 249–268, 2018.
- [98] L. Hu, Y. Liu, and S. Wang, "Stem cell-based tooth and periodontal regeneration," *Oral Diseases*, vol. 24, no. 5, pp. 696–705, 2018.
- [99] Y. Tsumanuma, T. Iwata, K. Washio et al., "Comparison of different tissue-derived stem cell sheets for periodontal regeneration in a canine 1-wall defect model," *Biomaterials*, vol. 32, no. 25, pp. 5819–5825, 2011.
- [100] S. Eramo, A. Natali, R. Pinna, and E. Milia, "Dental pulp regeneration via cell homing," *International Endodontic Journal*, vol. 51, no. 4, pp. 405–419, 2018.
- [101] S. El Moshy, I. A. Radwan, D. Rady et al., "Dental stem cell-derived secretome/conditioned medium: the future for regenerative therapeutic applications," *Stem Cells International*, vol. 2020, Article ID 7593402, 29 pages, 2020.
- [102] M. Nagata, K. Iwasaki, K. Akazawa et al., "Conditioned medium from periodontal ligament stem cells enhances periodontal regeneration," *Tissue Engineering Part A*, vol. 23, no. 9–10, pp. 367–377, 2017.
- [103] R. T. Stuepp, P. B. Delben, F. Modolo, A. G. Trentin, R. C. Garcez, and M. T. Biz, "Human dental pulp stem cells in rat mandibular bone defects," *Cells, Tissues, Organs*, vol. 207, no. 3–4, pp. 138–148, 2020.
- [104] D. M. Saez, R. T. Sasaki, D. d. O. Martins, M. Chacur, I. Kerkis, and M. C. P. da Silva, "Rat facial nerve regeneration with human immature dental pulp stem cells," *Cell Transplantation*, vol. 28, no. 12, pp. 1573–1584, 2019.
- [105] S. J. Cui, T. Zhang, Y. Fu et al., "DPSCs attenuate experimental progressive TMJ arthritis by inhibiting the STAT1 pathway," *Journal of Dental Research*, vol. 99, no. 4, pp. 446–455, 2020.
- [106] Y. Zhang, S. Shi, Q. Xu, Q. Zhang, R. M. Shanti, and A. D. Le, "SIS-ECM laden with GMSC-derived exosomes promote taste bud regeneration," *Journal of Dental Research*, vol. 98, no. 2, pp. 225–233, 2019.
- [107] D. Wang, Y. Wang, W. Tian, and J. Pan, "Advances of tooth-derived stem cells in neural diseases treatments and nerve tissue regeneration," *Cell Proliferation*, vol. 52, no. 3, article e12572, 2019.
- [108] Y. Xu, M. Chen, T. Zhang et al., "Spinal cord regeneration using dental stem cell-based therapies," *Acta Neurobiologiae Experimentalis*, vol. 79, no. 4, pp. 319–327, 2019.
- [109] S. Kabatas, C. S. Demir, E. Civelek et al., "Neuronal regeneration in injured rat spinal cord after human dental pulp derived neural crest stem cell transplantation," *Bratislava Medical Journal*, vol. 119, no. 3, pp. 143–151, 2018.
- [110] R. Asadi-Golshan, V. Razban, E. Mirzaei et al., "Sensory and motor behavior evidences supporting the usefulness of conditioned medium from dental pulp-derived stem cells in spinal cord injury in rats," *Asian Spine Journal*, vol. 12, no. 5, pp. 785–793, 2018.
- [111] C. Prado, P. Fratini, G. de Sá Schiavo Matias et al., "Combination of stem cells from deciduous teeth and electroacupuncture for therapy in dogs with chronic spinal cord injury: a pilot study," *Research in Veterinary Science*, vol. 123, pp. 247–251, 2019.
- [112] Y. Okuwa, T. Toriumi, H. Nakayama et al., "Transplantation effects of dental pulp-derived cells on peripheral nerve regeneration in crushed sciatic nerve injury," *Journal of Oral Science*, vol. 60, no. 4, pp. 526–535, 2018.
- [113] F. Rao, D. Zhang, T. Fang et al., "Exosomes from Human Gingiva-Derived Mesenchymal Stem Cells Combined with Biodegradable Chitin Conduits Promote Rat Sciatic Nerve Regeneration," *Stem Cells International*, vol. 2019, Article ID 2546367, 12 pages, 2019.

- [114] T. Tsuruta, K. Sakai, J. Watanabe, W. Katagiri, and H. Hibi, "Dental pulp-derived stem cell conditioned medium to regenerate peripheral nerves in a novel animal model of dysphagia," *PLoS One*, vol. 13, no. 12, article e0208938, 2018.
- [115] M. R. Gancheva, K. L. Kremer, S. Gronthos, and S. A. Koblar, "Using dental pulp stem cells for stroke therapy," *Frontiers in Neurology*, vol. 10, p. 422, 2019.
- [116] C. Nito, K. Sowa, M. Nakajima et al., "Transplantation of human dental pulp stem cells ameliorates brain damage following acute cerebral ischemia," *Biomedicine & Pharmacotherapy*, vol. 108, pp. 1005–1014, 2018.
- [117] J. M. Campos, A. C. Sousa, A. R. Caseiro et al., "Dental pulp stem cells and Bonelike® for bone regeneration in ovine model," *Regenerative Biomaterials*, vol. 6, no. 1, pp. 49–59, 2019.
- [118] X. Tang, W. Li, X. Wen et al., "Transplantation of dental tissue-derived mesenchymal stem cells ameliorates nephritis in lupus mice," *Annals of Translational Medicine*, vol. 7, no. 7, p. 132, 2019.
- [119] B. Xu, D. Fan, Y. Zhao et al., "Three-dimensional culture promotes the differentiation of human dental pulp mesenchymal stem cells into insulin-producing cells for improving the diabetes therapy," *Frontiers in Pharmacology*, vol. 10, article 1576, 2020.
- [120] E. Miura-Yura, S. Tsunekawa, K. Naruse et al., "Secreted factors from cultured dental pulp stem cells promoted neurite outgrowth of dorsal root ganglion neurons and ameliorated neural functions in streptozotocin-induced diabetic mice," *Journal of Diabetes Investigation*, vol. 11, no. 1, pp. 28–38, 2020.

## Research Article

# Peripheral Circulation and Astrocytes Contribute to the MSC-Mediated Increase in IGF-1 Levels in the Infarct Cortex in a dMCAO Rat Model

Xiaobo Li,<sup>1</sup> Wenxiu Yu,<sup>1</sup> Yunqian Guan,<sup>2,3</sup> Haiqiang Zou,<sup>4</sup> Zhaohui Liang,<sup>1</sup> Min Huang,<sup>1</sup> Renchao Zhao,<sup>1</sup> Chunsong Zhao,<sup>2,3</sup> Zhenhua Ren,<sup>2,3</sup> and Zhiguo Chen<sup>2,3</sup> 

<sup>1</sup>Department of Neurology, Northern Jiangsu People's Hospital, Clinical Medical School of Yangzhou University, Yangzhou, China

<sup>2</sup>Cell Therapy Center, Beijing Institute of Geriatrics, Xuanwu Hospital Capital Medical University, National Clinical Research Center for Geriatric Diseases, Key Laboratory of Neurodegenerative Diseases, Ministry of Education, Beijing 100053, China

<sup>3</sup>Center of Neural Injury and Repair, Beijing Institute for Brain Disorders, Beijing 100069, China

<sup>4</sup>Department of Neurology, The General Hospital of Guangzhou Military Command, Guangzhou, China

Correspondence should be addressed to Zhiguo Chen; [chenzhiguo@gmail.com](mailto:chenzhiguo@gmail.com)

Received 17 May 2020; Revised 31 July 2020; Accepted 10 August 2020; Published 1 September 2020

Academic Editor: Huseyin Sumer

Copyright © 2020 Xiaobo Li et al. This is an open access article distributed under the Creative Commons Attribution License, which permits unrestricted use, distribution, and reproduction in any medium, provided the original work is properly cited.

**Background and Purpose.** Previously, we found that insulin-like growth factor-1 (IGF-1) levels in the infarct cortex in the acute phase of distal middle cerebral artery occlusion (dMCAO) rats are increased by intravenous infusion of allogeneic mesenchymal stem/stromal cells (MSCs). CD68+ microglia and NeuN+ neurons are part, but not all, of the sources of IGF-1. The present study is aimed at exploring the respective contributions of brain endogenous Iba-1+ microglia, GFAP+ astrocytes, infiltrated neutrophils, lymphocytes and monocytes/macrophages, and peripheral circulation, to the increased IGF-1 level in the infarct cortex after MSC infusion. **Materials and Methods.** Ischemic brain injury was induced by dMCAO in Sprague-Dawley rats. The transplantation group received MSC infusion 1 h after dMCAO. Expression of IGF-1 in GFAP+ astrocytes, Iba-1+ microglia/macrophages, CD3+ lymphocytes, Ly6C+ monocytes/macrophages, and neutrophil elastase (NE)+ neutrophils was examined to determine the contribution of these cells to the increase of IGF-1. ELISA was performed to examine IGF-1 levels in blood plasma at days 2, 4, and 7 after ischemia onset. **Results.** In total, only 5-6% of Iba-1+ microglia were colabeled with IGF-1 in the infarct cortex, corpus callosum, and striatum at day 2 post-dMCAO. MSC transplantation did not lead to a higher proportion of Iba-1+ cells that coexpressed IGF-1. In the infarct cortex, all Iba-1+/IGF-1+ double-positive cells were also positive for CD68. In the infarct, corpus callosum, and striatum, the majority (50-80%) of GFAP+ cells were colabeled with ramified IGF-1 signals. The number of GFAP+/IGF-1+ cells was further increased following MSC treatment. In the infarct cortex, approximately 15% of IGF-1+ cells were double-positive for CD3. MSC treatment reduced the number of infiltrated CD3+/IGF-1+ cells by 70%. In the infarct, few Ly6C+ monocytes/macrophages or NE+ neutrophils expressed IGF-1, and MSC treatment did not induce a higher percentage of these cells that coexpressed IGF-1. The IGF-1 level in peripheral blood plasma was significantly higher in the MSC group than in the ischemia control group. **Conclusion.** The MSC-mediated increase in IGF-1 levels in the infarct cortex mainly derives from two sources, astrocytes in brain and blood plasma in periphery. Manipulating the IGF-1 level in the peripheral circulation may lead to a higher level of IGF-1 in brain, which could be conducive to recovery at the early stage of dMCAO.



## 1. Introduction

Insulin-like growth factor-1 (IGF-1) is a member of the insulin gene family [1]. In addition to regulating cerebral development, neurogenesis, cognition, and memory function [2], IGF-1 is also an important player during the damage and recovery processes in ischemic stroke [3, 4].

It has been widely recognized that neuroinflammation plays a critical role in brain injuries and neurodegeneration. The role of IGF-1 in the central nervous system (CNS) is, to a large extent, due to its ability to regulate immune cells in brain, such as microglia and infiltrated macrophages.

Microglia are important players in both innate immunity and adaptive immunity. The polarization of microglia is associated with the pathogenesis of a number of inflammatory disorders, such as the acute and chronic damage after stroke. Several *in vitro* studies revealed a direct anti-inflammatory effect of IGF-1 on microglia [5, 6]. Accumulating evidence suggests that IGF-1 may also modulate microglial phenotypes; for example, an increase in IGF-1 levels promotes the switch to the M2 phenotype [7]. Macrophages can also be regulated by IGF-1. In peripheral tissues, IGF-1 impacts macrophagic functions and leads to down-regulation of proinflammatory cytokines and a change in disease progression [8, 9].

Astrocytes can also produce IGF-1 and are positive for IGF-1 receptors [10, 11]. Addition of IGF-1 to the *in vitro* culture of astrocytes promotes astrocyte growth and formation of glycogen [12]. Overexpression of IGF-1 by astrocytes through an AAV-mediated delivery improves outcome in a rat stroke model [13]. Astrocyte-derived IGF-1 can also protect neurons from kainic acid- (KA-) induced excitotoxicity in an astrocyte-neuron coculture system, and the rescue effect is abrogated by adding IGF-1R inhibitor [14].

By using ELISA in a previous study, we reported an increased level of IGF-1 in the ischemic core and peri-infarct striatum in dMCAO rats at 48 h after intravenous (i.v.) infusion of rat bone marrow-derived MSCs [10]. MSC treatment leads to a higher level of IGF-1 compared to dMCAO rats without MSC infusion. By using immunostaining, we found that IGF-1 signals are mainly located in the infarct area. A minority of IGF-1 signals colocalize with NeuN+ neurons and CD68+-activated microglia in infarcts; nonetheless, quantitative analysis showed that these cells cannot account for all of the IGF-1-positive signals [15]. Other contributors in the brain and periphery (IGF-1 can cross the blood-brain barrier (BBB) [16–18]) to the increased IGF-1 signals in the brain warrant further investigation. In this study, we surveyed a wide spectrum of cell types that included Iba-1+ microglia, GFAP+ astrocytes, infiltrated immune cells such as CD3+ lymphocytes, neutrophil elastase (NE)+ neutrophils, and Ly6C+ monocytes/macrophages, as well as the peripheral circulation, to determine their contribution to the increased IGF-1 level in the brain.

## 2. Materials and Methods

**2.1. dMCAO Model.** The performance of allogeneic bone marrow MSC (BMSC) culture, infusion, dMCAO model

establishment, and behavioral tests have been described in our previous study [19].

In brief, primary cultures of bone marrow stromal cells were obtained from donor young adult male rats, and BMSCs were isolated as previously described [15, 19]. Animals were anesthetized with 3.5% isoflurane and then maintained with 1.0–2.0% isoflurane in N<sub>2</sub>O:O<sub>2</sub> (2:1). One-hour posts ischemia, randomly selected rats received BMSC infusion. Approximately 1 × 10<sup>6</sup> BMSCs in 1 mL of vehicle (1 mL of saline) were slowly injected over a 5 min period into each rat via the tail vein.

In total, 100 wild-type Sprague-Dawley rats were purchased from Vital River Laboratory Animal Technology (Beijing, China). All animal protocols were in accordance with the Guidelines for the Care and Use of Experimental Animals and approved by the Institutional Animal Care and Use Committee of Capital Medical University. All experimental animals were housed in a specific pathogen-free rodent barrier facility at the Xuanwu Hospital Capital Medical University, on a 12 h light:12 h darkness cycle with food and water ad libitum.

Ten Sprague-Dawley rats were used for harvesting bone marrow MSCs. Ninety Sprague-Dawley rats were divided into three groups: “sham”, “ischemia”, and “ischemia+MSCs” with 30 rats in each group. And for each group, 3 time points—days 2, 4, and 7 posts ischemia—were chosen with 10 rats used for each time point.

**2.2. IGF-1 Measurement in Blood Plasma.** Blood was collected in heparinized tubes from the abdominal aorta. Subsequently, the blood samples were centrifuged at 1000×g for 10 min at room temperature, and the resulting plasma was obtained. The plasma was apportioned into 0.5 mL aliquots and stored at -80°C for further use.

IGF-1 levels were determined by ELISA using the R&D systems quantitative rat IGF-1 immunoassay kit (Minneapolis, MN, USA), which demonstrates high cross-reactivity with rat IGF-1. Plasma samples were diluted in the calibrator diluent provided in the kit at 1:10. The results were presented as ng/mL in undiluted plasma.

**2.3. Brain Immunohistochemistry and Counting under Confocal Microscopy.** Immunohistochemistry and cell counting were performed as previously described [15, 19, 20].

Confocal images were acquired using a Leica TCS SP5 II AOBS laser scanning confocal microscope. The section thickness was 40 μm to minimize the possibility of cell body overlap in the z-axis. FITC or Cy3 fluorescence was acquired with an excitation wavelength of 633 nm and detection at 648–712 nm. Cy5 was detected with an excitation wavelength of 488 nm and detection at 501–542 nm.

**2.4. Quantification and Statistical Analysis.** As described in our previous study [15, 19], the selection of sections for each rat and the demarcation of the counting area in the infarct cortex were in accordance with the work published by Gelosa et al. [21]. In brief, we outlined the counting area in the dorsal infarct cortex which was 2 mm adjacent to the boundary line between the normal and infarct areas

(Supplementary Figure 1). The counting area in the striatum and corpus callosum was also demonstrated in the Supplementary Figure 1.

IGF-1-positive cells in the brain were counted in 4 coronal sections from each rat (40  $\mu\text{m}$  thickness, 480  $\mu\text{m}$  interval, located between -2.0 mm and 2.0 mm to bregma); for each slide, 2 squares of images were captured under a microscope with a view field set as 800  $\times$  800  $\mu\text{m}$  (200x).

Eight fields of view were digitalized under a 20x objective, and the number of positive cells was summed for IGF-1-positive cells that coexpressed Iba-1, GFAP, CD3, Ly6C, or neutrophil elastase (NE). The proportion of all IGF-1+ cells that were double-positive for each lineage marker was calculated and averaged.

Data were presented as the mean  $\pm$  standard error of the mean (SEM). The comparisons were analyzed by one-way analysis of variance (one-way ANOVA) and Bonferroni-Dunnnett corrections using SPSS 19.0. The level of significance of all comparisons was set at  $p < 0.05$ .

### 3. Results

**3.1. Iba-1+ Microglia/Macrophages Are Not the Main Source of IGF-1 in the Infarct Cortex.** Microglia at an activated state vs. resting state assume different morphologies and marker expression profiles. The activated microglia stain positive for CD68 (Figure 1), and both activated and resting stage microglia are positive for Iba-1. In our previous studies, we reported that CD68+ microglia express IGF-1 in the brain of a stroke model [15, 19]. In the present study, we continued to look into a wider range of microglia population—Iba-1+ cells, with regard to IGF-1 expression.

By immunostaining, we found that IGF-1 signals were almost absent in the brain cortex in the sham group (data not shown). In the ischemia control group at day 2 after ischemia, Iba-1 and IGF-1 signals were mainly localized in the cortical infarct area, specifically the inner infarct border zone (Figures 1(a)–1(d)).

Interestingly, although the distribution patterns of Iba-1+ cells and IGF-1+ cells were similar (Figures 1(a)–1(d)), double-positive cells were only occasionally observed (Figure 1(e)).

In this study, the counts of Iba-1+/IGF-1+ cells were similar to those of CD68+/IGF-1+ cells in the infarct cortex, suggesting that IGF-1 expression in the Iba-1+ cell population might come from the CD68+/IGF-1+ double-positive cells. By triple immunostaining, we verified that the Iba-1+/IGF-1+ cells were indeed CD68+ cells (Figures 1(f)–1(h), arrow) in the infarct area of the cortex. The CD68-/Iba-1+ microglial cells were negative for IGF-1.

After MSC infusion, both IGF-1+ and Iba-1+ signals were still detected in the inner border zone of the infarct area (Figures 1(i)–1(l)). The quantities of Iba-1+/IGF+ double-positive cells, together with the percentages of Iba-1+/IGF-1+ double-positive cells among the total Iba-1+ cells or IGF-1+ cells, respectively (4.40  $\pm$  1.49/view field, 6.93  $\pm$  3.61%, and 8.55  $\pm$  3.62%), were all increased compared to those of the ischemia group (2.93  $\pm$  2.08/view field, 5.34  $\pm$  3.93%, and 6.60  $\pm$  4.84%).

In the infarct area, the CD68+ cells still expressed IGF-1 (Figure 1(m) and 1(n)), and the triple staining results confirmed that the Iba-1+/IGF-1+ cells were mostly CD68+ (Figures 1(o) and 1(p)). These results suggested that in the infarct area, IGF-1 expression in the Iba-1+ cell population was derived from the CD68+/IGF-1+ double-positive cells.

The quantities of Iba-1+/IGF-1+ double-positive cells in the brain infarct area, both before and after MSC infusion, were very low, indicating that Iba-1+ cells may not be the major source of IGF-1 in the ischemic cortex.

**3.2. Iba-1+ Microglia/Macrophages Are Not the Main Source of IGF-1 in the Striatum and Corpus Callosum.** In the sham group, no significant IGF-1+ signals were detected in the striatum or corpus callosum (data not shown).

Two days after ischemia onset, IGF-1+ signals were found scattered in the striatum and corpus callosum (Figures 2(a)–2(d)). Although the distribution patterns of Iba-1+ cells and IGF-1+ cells were similar (Figures 2(a)–2(d) and Figures 2(e)–2(h)), the quantity of Iba-1+/IGF-1+ double-positive cells remained very low (4.53  $\pm$  2.03/view field) (Figures 2(g)–2(h)). The percentages of Iba-1+/IGF-1+ cells among the total Iba-1+ cells or IGF-1+ cells were 7.83  $\pm$  3.50% and 9.22  $\pm$  4.62%, respectively.

CD68+ cells represent an activated subpopulation of microglia and were detected to be positive for IGF-1 (Figures 2(e) and 2(f)). The expression patterns of IGF-1 in microglia differed in striatum and corpus callosum vs. in infarct cortex; in striatum and corpus callosum, Iba-1+/IGF-1+ double-positive cells were not limited to CD68+ cell population, and 30–40% of the Iba-1+/IGF-1+ double-positive cells stained negative for CD68 (Figures 2(g) and 2(h)).

In the striatum and corpus callosum, neither the distribution patterns of IGF-1+ and Iba-1+ cells (Figures 2(i)–2(l)) nor the quantity of double-labeled cells (5.40  $\pm$  1.96/view field) was significantly changed by MSC treatment (Figures 2(m) and 2(n)). The double-positive cells were highlighted in a magnified view (Figures 2(o) and 2(p)). In addition, MSC infusion did not change the percentages of Iba-1+/IGF-1+ double-positive cells among the total Iba-1+ (9.92  $\pm$  5.21%) or IGF-1+ cells (11.39  $\pm$  4.59%).

Taken together, Iba-1+/IGF-1+ cells constituted a small part of the IGF-1+ cells in the infarct area, striatum, and corpus callosum, suggesting that the Iba-1+ cell population is not the main source of IGF-1.

**3.3. GFAP+ Astrocytes Are the Main Cell Source of IGF-1 in Infarct Area.** Previously, we found that in the ischemia brain cortex of dMCAO model, IGF-1 was partially expressed by NeuN+ neurons and CD68+ microglia/macrophages. On top of that, a significant number of other IGF-1-expressing cells existed, which included cells with a ramified morphology, reminiscent of GFAP+ astrocytes.

Due to the similarity in the morphology and distribution pattern of IGF-1+ signals and GFAP+ astrocytes in the ischemic hemisphere, double fluorescent immunostaining was employed to examine the spatial relationship of these two markers.

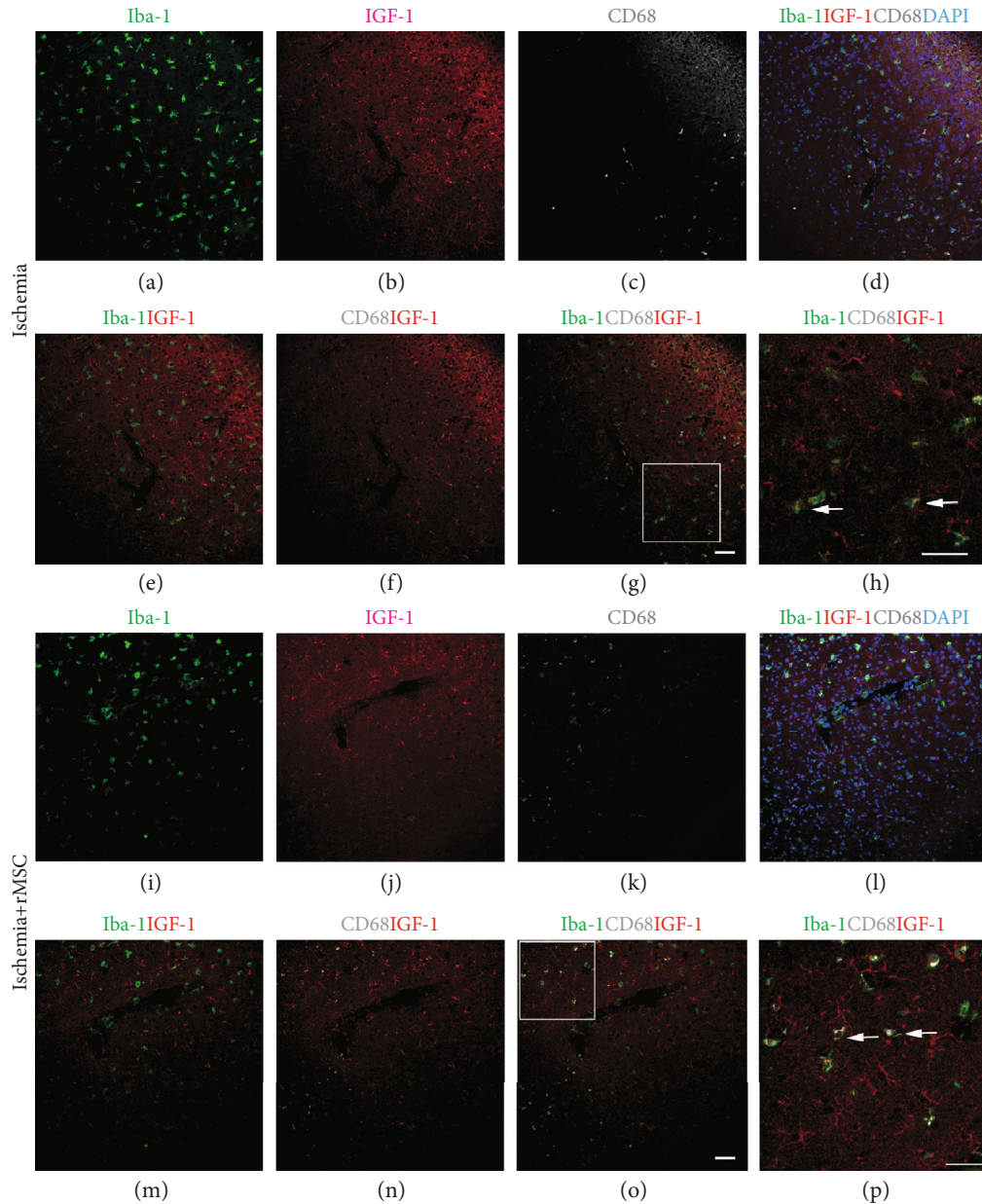


FIGURE 1: The distribution of Iba-1+, IGF-1+, and CD68+ cells in the infarct area with and without MSC infusion. (a–h) Without MSC transplantation, the distribution of IGF-1+ and Iba-1+ cells in the infarct area. (i–p) With MSC transplantation, the distribution of IGF-1+ and Iba-1+ cells in the infarct area. (a, i) Iba-1 staining in green. (b, j) IGF-1 staining in red. (c, k) CD68 staining in white. (d, l) Merged image of Iba-1, IGF-1, CD68, and blue DAPI nuclear staining. (e, m) Merged image of Iba-1 and IGF-1. Very few Iba-1+/IGF-1+ cells were scattered in the infarct area. (f, n) Merged image of CD68 and IGF-1. (g, o) Merged image of Iba-1, CD68, and IGF-1. (h) (square in (g)) and (p) (square in (o)) The IGF-1/Iba-1+ cells were CD68 positive, while the CD68-/Iba-1+ cells were negative for IGF-1. Arrow: IGF-1, Iba-1, and CD68 triple-labeled cells. Scale bar, 50  $\mu$ m.

As shown in Figure 3, an increased level of astrogliosis was observed 48 h following dMCAO (Figures 3(e)–3(h)) compared to sham controls (Figures 3(a)–3(d)). Following MSC treatment, the number of GFAP+ astrocytes ( $42.3 \pm 5.2$ /view field) was slightly but significantly reduced compared to that in the ischemia control group ( $48.43 \pm 9.67$ /view field). However, the quantity of GFAP+/IGF-1+ double-positive cells in the infarct area increased following infusion of MSCs (Figures 3(i)–3(l)) from  $24.47 \pm 6.17$ /view field in the ischemia vehicle group to  $31.03 \pm 5.22$ /view field

( $p < 0.01$ ) in the MSC group. The double-positive cells were highlighted in a magnified view (Figures 3(m) and 3(n)). As a net result, the percentage of GFAP+/IGF-1+ double-positive cells among the GFAP+ astrocytes was significantly increased from  $50.79 \pm 8.97\%$  in the ischemia control group to  $78.70 \pm 20.11\%$  in the MSC group (Figure 3(o)). This suggested that MSC treatment had induced more astrocytes to express IGF-1.

The above data suggested that GFAP+ astrocytes present in the infarct area of dMCAO rats were the main source of



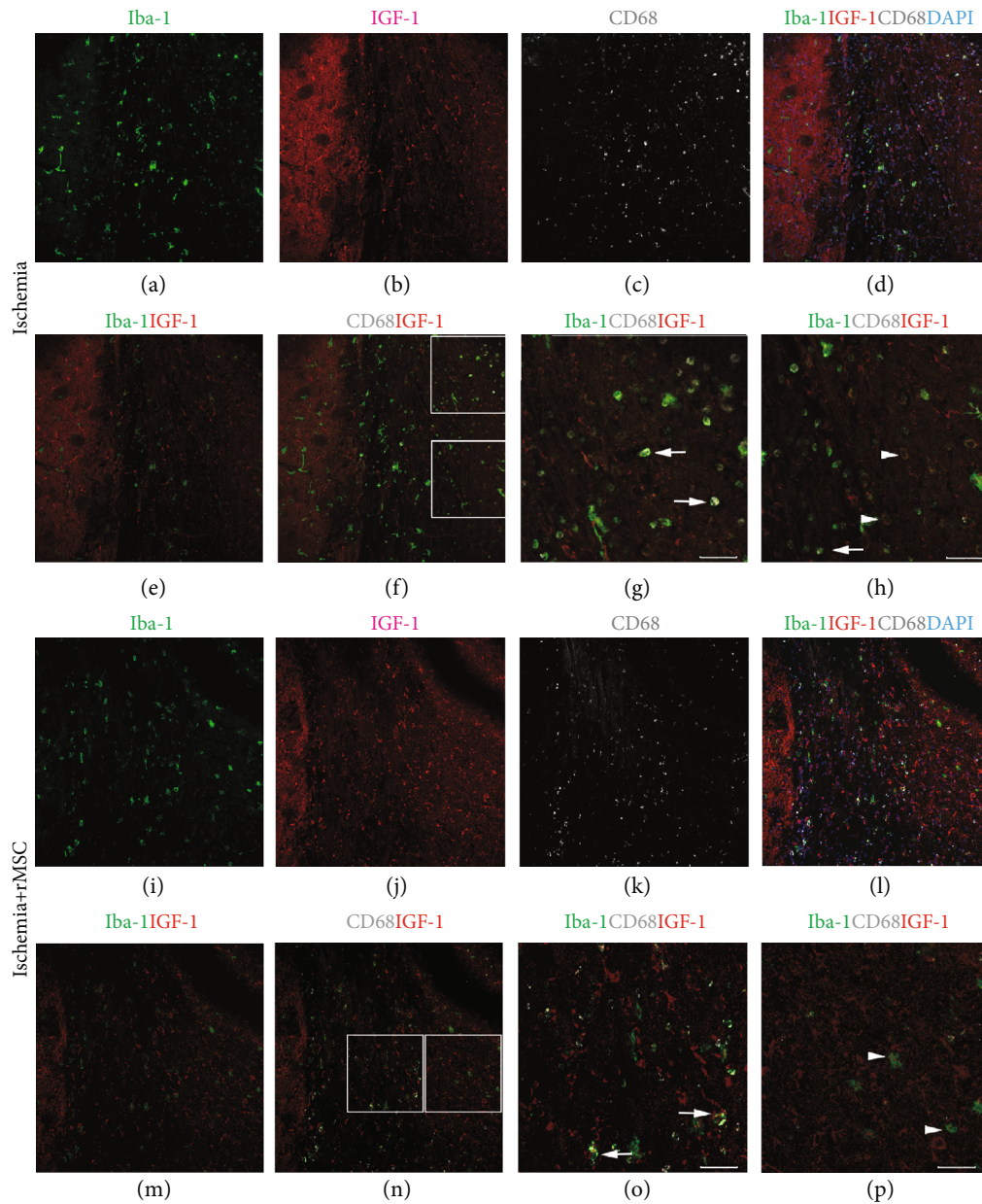


FIGURE 2: The distribution of Iba-1+, IGF-1+, and CD68+ cells in the striatum and corpus callosum with and without MSC infusion. (a–h) Without MSC transplantation, the distribution patterns of IGF-1+ and Iba-1+ cells in the corpus callosum are similar. (i–p) With MSC transplantation, the distribution of IGF-1+ and Iba-1+ cells in the corpus callosum. (a, i) Iba-1 staining in green. (b, j) IGF-1 staining in red. (c, k) CD68 staining in white. (d, l) DAPI nuclear staining in blue merged with Iba-1, IGF-1, and CD68. (e, m) Merged image of Iba-1+ and IGF-1+. (f, n) Merged image of CD68, Iba-1, and IGF-1. Iba-1+/IGF-1+ double-positive cells could be found. (g, o) Merged image of Iba-1, IGF-1, and CD68. (g, o) (upper square in (f)) and (h) (lower square in (f)) The quantity of Iba-1+/IGF-1+ cells in the striatum and corpus callosum was not increased by MSC transplantation. The majority of Iba-1+/IGF-1+ double-positive cells were CD68+. (o) (left square in (n)) and (p) (right square in (n)) The difference in striatum vs. cortex was that IGF-1 expression was not limited to CD68+ cells. There were Iba-1+/IGF-1+ double-positive cells that were negative for CD68. Arrow: IGF-1, Iba-1, and CD68 triple-labeled cells; arrowhead: IGF-1+Iba-1+ double-positive but CD68 negative cells. Scale bar, 50  $\mu$ m.

IGF-1, since  $57.64 \pm 12.93\%$  of IGF-1+ cells in the ischemia group and  $68.44 \pm 23.42\%$  in the MSC infusion group were GFAP+ astrocytes (Figure 3(o)).

**3.4. GFAP+ Astrocytes Are the Main Source of IGF-1 in the Striatum and Corpus Callosum.** In addition to the infarct cortex, numerous GFAP+ astrocytes and a few IGF-1+ cells were

detected in the striatum and corpus callosum of sham group (Figures 4(a)–4(d)).

Compared to the ischemia control group (Figures 4(e)–4(h)), MSC infusion induced a slightly but significantly reduced number of GFAP+ astrocytes (from  $36.4 \pm 9.72/\text{view field}$  to  $31.4 \pm 4.54/\text{view field}$ ) (Figures 4(i)–4(l)), but an increased number of GFAP+/IGF-1+ double-positive cells



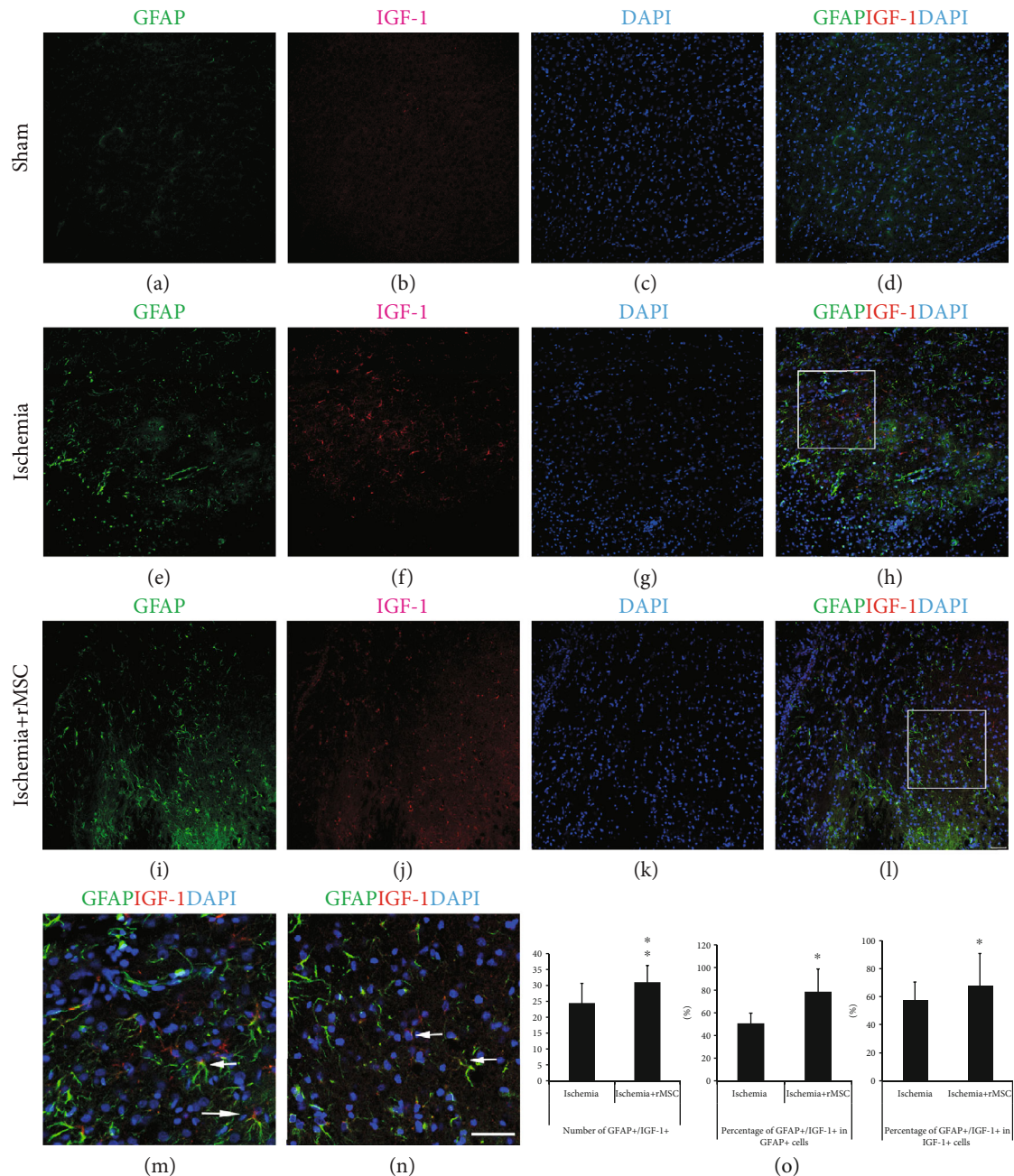


FIGURE 3: MSC treatment reduces the quantity of GFAP+ cells but increases the number of IGF-1+/GFAP+ cells in the infarct. (a–d) In the sham group, a few GFAP+ cells could be found in the brain cortex. (e–h) In the infarct area of the ischemia control group, the number of GFAP+ and IGF-1+ cells both increased. (i–l) In the infarct area, MSC treatment decreased GFAP+ cell quantity but increased the number of cells double positive for GFAP and IGF-1. (a, e, and i) GFAP staining. (b, f, and j) IGF-1. (c, g, and k) DAPI nuclear staining. (d, h, and l) Double-stained GFAP+/IGF-1+ cells. (m, n) (squares in (h, l)) The amplified view of GFAP+/IGF-1+ cells. (o) After MSC transplantation, the quantity of GFAP+/IGF-1+ double-positive cells and the percentages among all IGF-1+ or GFAP+ cells increased. Scale bar, 50  $\mu$ m.

(from  $21.7 \pm 3.78$ /view field to  $27.27 \pm 3.43$ /view field) (Figures 4(i)–4(l), and 4(o)). The double-positive cells were highlighted in a magnified view (Figures 4(m) and 4(n)). The proportion of astrocytes that coexpressed IGF-1 was enhanced from  $62.20 \pm 12.12\%$  to  $87.45 \pm 8.64\%$ .

GFAP+ astrocytes present in the striatum and corpus callosum might be the main sources of IGF-1 expression in that area, in that GFAP+/IGF-1+ double-positive cells constituted

up to  $72.66 \pm 8.98\%$  of IGF-1+ cells in the ischemia group, which was significantly increased to  $81.22 \pm 9.70\%$  in the MSC group (Figure 4(o)).

**3.5. CD3+/IGF-1+ Cells Increase Significantly after Ischemia and Are Decreased with MSC Treatment.** In the brain cortex of the sham group, few CD3+ lymphocytes were detected (Figures 5(a)–5(d)). In the ischemia control group, a markedly

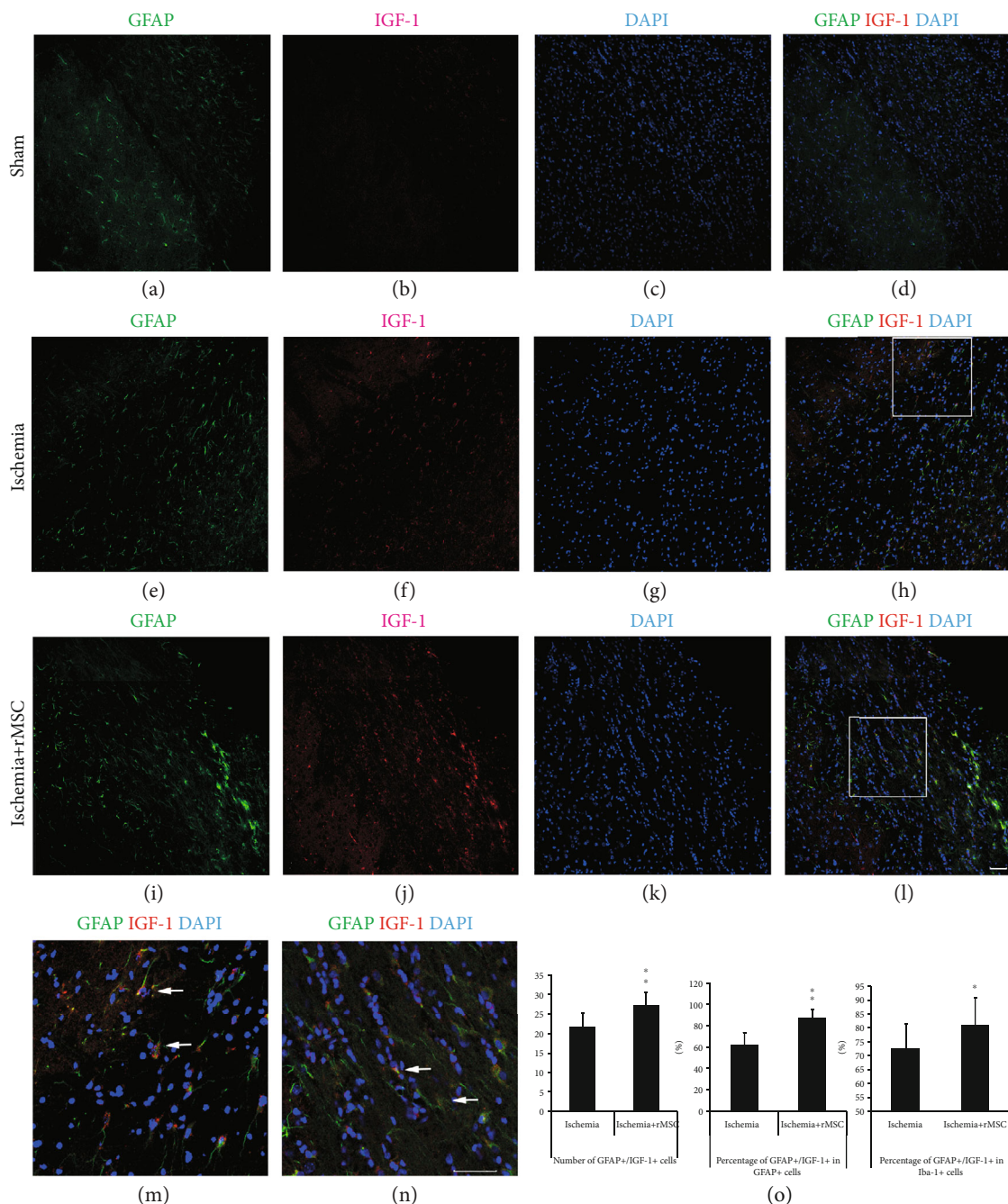


FIGURE 4: MSC treatment decreases the quantity of GFAP+ cells but increases GFAP+/IGF-1+ cells in the ipsilateral striatum and corpus callosum. (a–d) In the striatum and corpus callosum of the sham group, IGF-1 signals were rarely found. (e–h) In the striatum and corpus callosum of the ischemia control group, both IGF-1 and GFAP signals were increased. (i–l) After MSC transplantation, more GFAP+/IGF-1+ cells were observed in the striatum and corpus callosum. (a, e, and i) GFAP staining. (b, f, and j) IGF-1. (c, g, and k) DAPI nuclear staining. (d, h, and l) Double-stained GFAP+/IGF-1+ cells. (m, n) (squares in (h, l)) The amplified view of GFAP+/IGF-1+ cells. (o) The histogram of GFAP+/IGF-1+ cell quantity and percentages in the ischemia group and MSC transplantation group ( $*p < 0.05$ ,  $**p < 0.01$ , compared with the ischemia vehicle group). Arrow: double-labeled cells. Scale bar, 50  $\mu\text{m}$ .

larger number of CD3+ cells were observed in the infarct area (Figures 5(e)–5(h)). Double staining revealed that CD3+/IGF-1+ cells were mainly distributed in the inner border zone of the infarct area (Figures 5(e)–5(h)).

MSC treatment reduced the quantity of CD3+/IGF-1+ cells that had infiltrated into the brain from  $11.20 \pm 2.95$  per view field in the ischemia group to  $6.6 \pm 1.28$  in the MSC

group (Figures 5(i)–5(l)). The double-positive cells were highlighted in a magnified view (Figures 5(m) and 5(n)). MSC treatment also reduced the proportion of CD3+ cells that coexpressed IGF-1 from  $35.62 \pm 14.46\%$  before MSC treatment to  $27.54 \pm 7.86\%$  after treatment (Figures 5(i)–5(l) and 5(o)).

In the ischemia group, the percentage of CD3+/IGF-1+ cells among IGF-1+ cells was  $26.46 \pm 8.91\%$ , which was



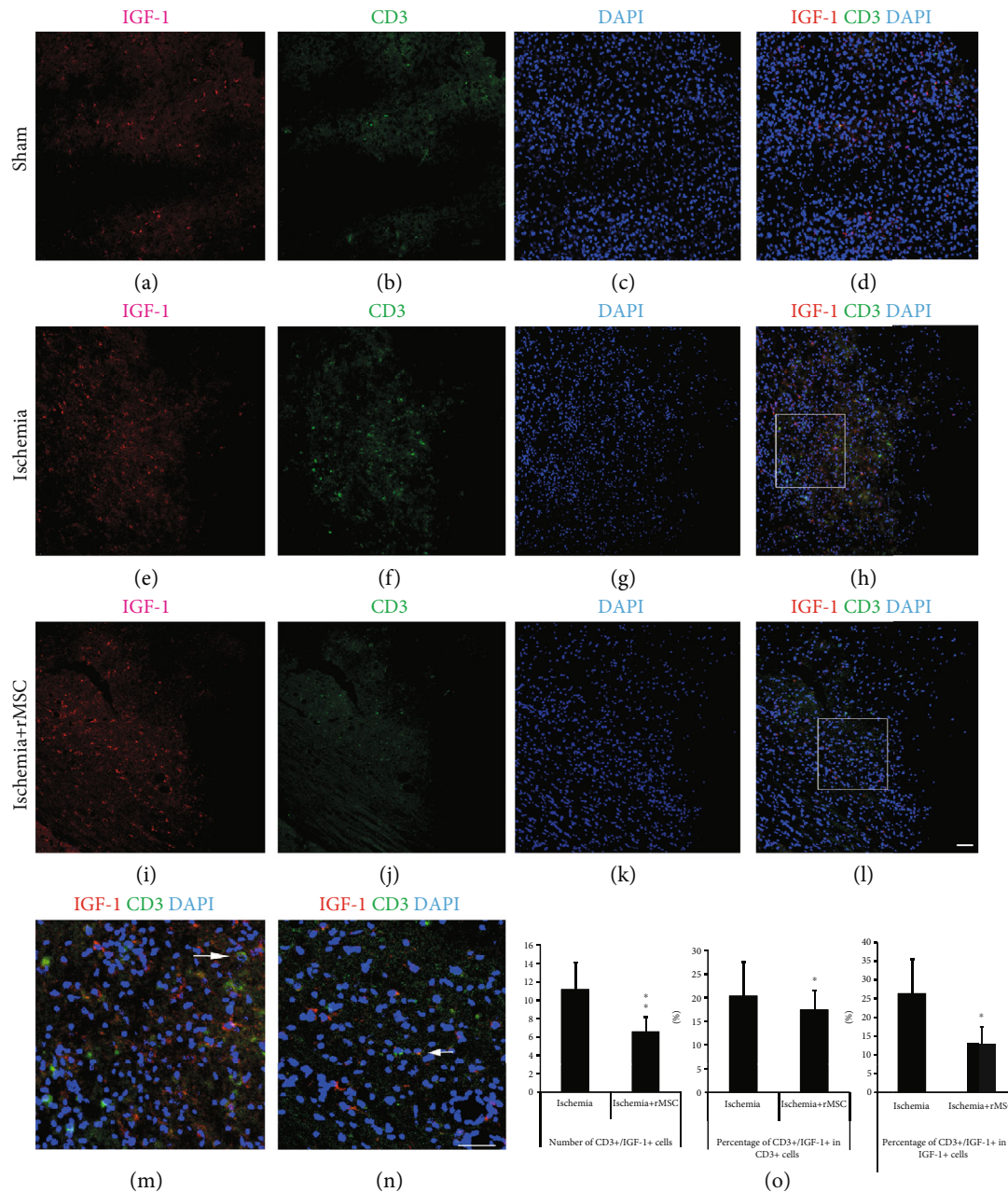


FIGURE 5: CD3+ cells that express IGF-1 in the infarct area are reduced by MSC treatment. (a–d) In the sham group, CD3+ lymphocytes were barely observed in the brain. (e–h) CD3+ and CD3+/IGF-1+ cells increased significantly in the infarct area of the ischemia control group. (i–l) The number of CD3+ and CD3+/IGF-1+ cells in the infarct area was reduced dramatically by MSC transplantation. (a, e, and i) CD3 staining. (b, f, and j) IGF-1. (c, g, and k) DAPI nuclear staining. (d, h, and l) Double-stained CD3+/IGF-1+ cells. (m, n) (insets in (h, l)) The amplified view of CD3+/IGF-1+ cells in the ischemia and MSC transplantation groups. (o) The histogram of CD3+/IGF-1+ cell quantity and percentages in the ischemia group and MSC transplantation group (\* $p < 0.05$ , \*\* $p < 0.01$ , compared with the ischemia vehicle group). Arrow: double-labeled cells. Scale bar, 50  $\mu\text{m}$ .

dramatically reduced by MSC infusion to  $13.14 \pm 4.38\%$  (Figures 5(i)–5(l) and 5(o)).

**3.6. Limited Contribution from Ly6C+ Monocytes/Macrophages to IGF-1 Expression.** In our previous study, we reported that both Ly6C+ infiltrated monocytes/macrophages and brain-derived neurotrophic factor (BDNF) immunostaining are mainly located in the infarct boundary

zone. The Ly6C+ cells are the main source of BDNF [19]. In the present study, we continued to investigate the contribution of infiltrated Ly6C+ cells to IGF-1 expression.

At day 2 after dMCAO, Ly6C+ infiltrated monocytes/macrophages were found mainly in the inner border zone of the infarct. Ly6C+ signals were scattered around but rarely colocalized within the cytoplasm of IGF-1-expressing cells (Figures 6(a)–6(d)). In the inner infarct border zone, there

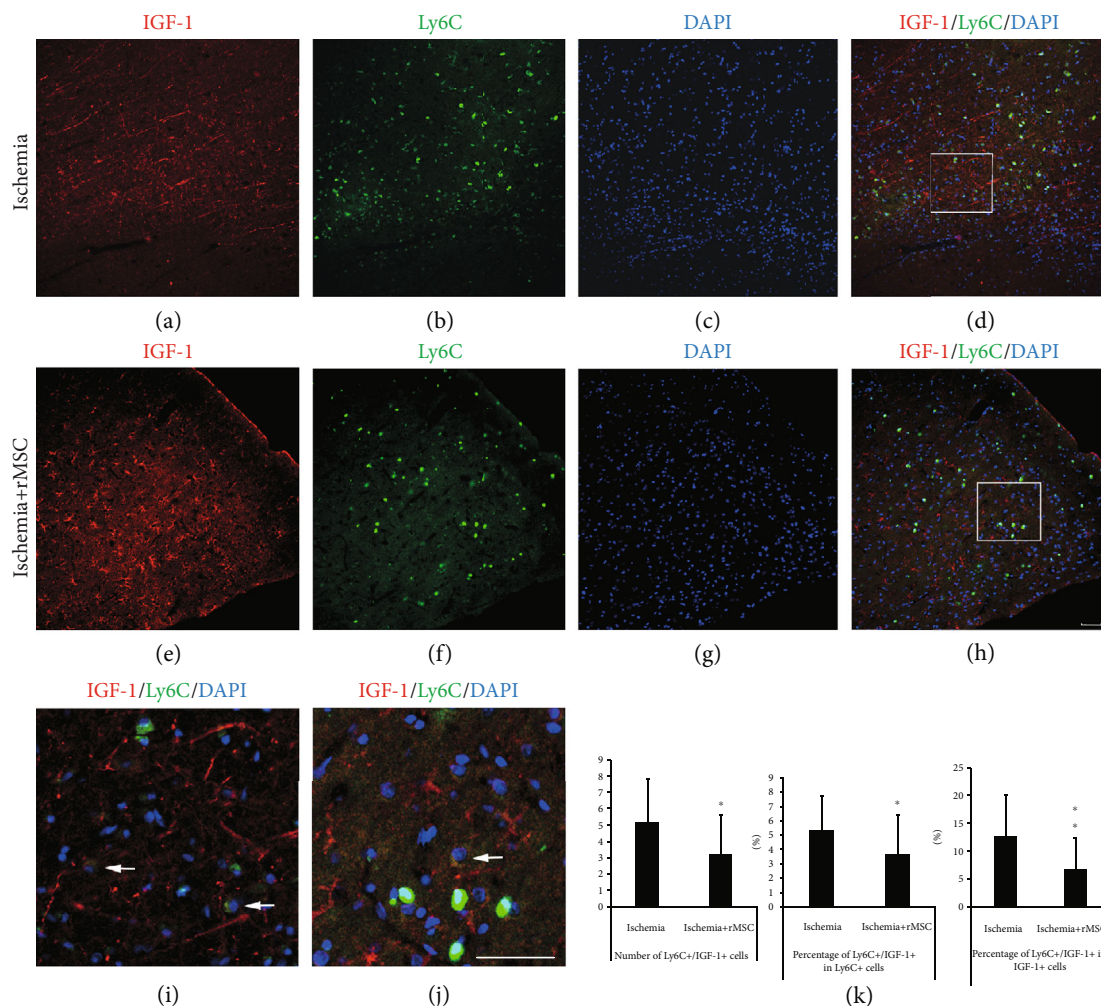


FIGURE 6: MSC treatment reduces the number of infiltrated Ly6C+ cells that express IGF-1. (a–d) In the ischemia control group, Ly6C+ and Ly6C+/IGF-1+ cells were mainly located in the infarct areas. The quantity of Ly6C+ cells that expressed IGF-1 in the ischemia core cortex of the ipsilateral brain was very small. (e–h) After MSC infusion, the distribution of Ly6C+ and IGF-1+ cells was still restricted in the infarct area of the ipsilateral cortex. MSC infusion reduced the quantity of Ly6C+ cells infiltrated into the brain and decreased the percentage of Ly6C+ cells that coexpressed IGF-1. (a, e) IGF-1 staining. (b, f) Ly6C staining. (c, g) DAPI nuclear staining. (d, h) Double-stained Ly6C+/IGF-1+ cells. (i) (inset in (d)) In the inner infarct boundary zone of the ischemia group, the amplified view of Ly6C+/IGF-1+ cells. (j) (inset in (h)) In the MSC transplantation group, the amplified view of Ly6C+/IGF-1+ cells. (k) The histogram of Ly6C+/IGF-1+ cell quantity and percentages in the ischemia group and MSC transplantation group (\* $p < 0.05$ , \*\* $p < 0.01$ , compared with the ischemia vehicle group). Arrow: Ly6C+/IGF-1+ double-labeled cells. Scale bar, 50  $\mu\text{m}$ .

were  $5.20 \pm 2.63$  Ly6C+/IGF-1+ cells per view field; only  $5.38 \pm 2.34\%$  of Ly6C+ cells coexpressed IGF-1, and  $12.67 \pm 7.72\%$  of IGF-1+ cells coexpressed Ly6C+ (Figures 6(a)–6(d) and 6(k)).

MSC treatment not only reduced the number of Ly6C+/IGF-1+ cells to  $3.20 \pm 2.43$ /view field but also decreased the percentage of Ly6C+/IGF-1+ cells among the Ly6C+ population to  $3.64 \pm 2.78\%$  (Figures 6(e)–6(h)). The double-positive cells were highlighted in a magnified view (Figures 6(i) and 6(j)). The percentage of Ly6C+/IGF-1+ cells among the IGF-1+ cells decreased accordingly to  $6.71 \pm 5.74\%$  (Figures 6(e)–6(h) and 6(k)).

Taken together, these results indicated that only a small portion of Ly6C+ monocytes/macrophages were capable of expressing IGF-1, and Ly6C+ cells in this

experimental setting were probably not the main cellular source of IGF-1 expression.

**3.7. NE+ Neutrophils Do Not Express IGF-1.** Few NE+ neutrophils were detected in the brains of the sham group (data not shown). In the dMCAO model, NE+ neutrophils existed in both the ischemia control group (Figures 7(a)–7(d)) and the MSC treatment group (Figures 7(e)–7(h)). However, no NE+ neutrophils coexpressing IGF-1 were observed, suggesting that NE+ neutrophils were not the source of IGF-1 in this experimental setting.

**3.8. The Plasma Level of IGF-1 Is Increased following MSC Treatment.** The concentration of IGF-1 in the blood plasma ( $172.7 \pm 35.9$  ng/mL) of ischemia group was lower than that



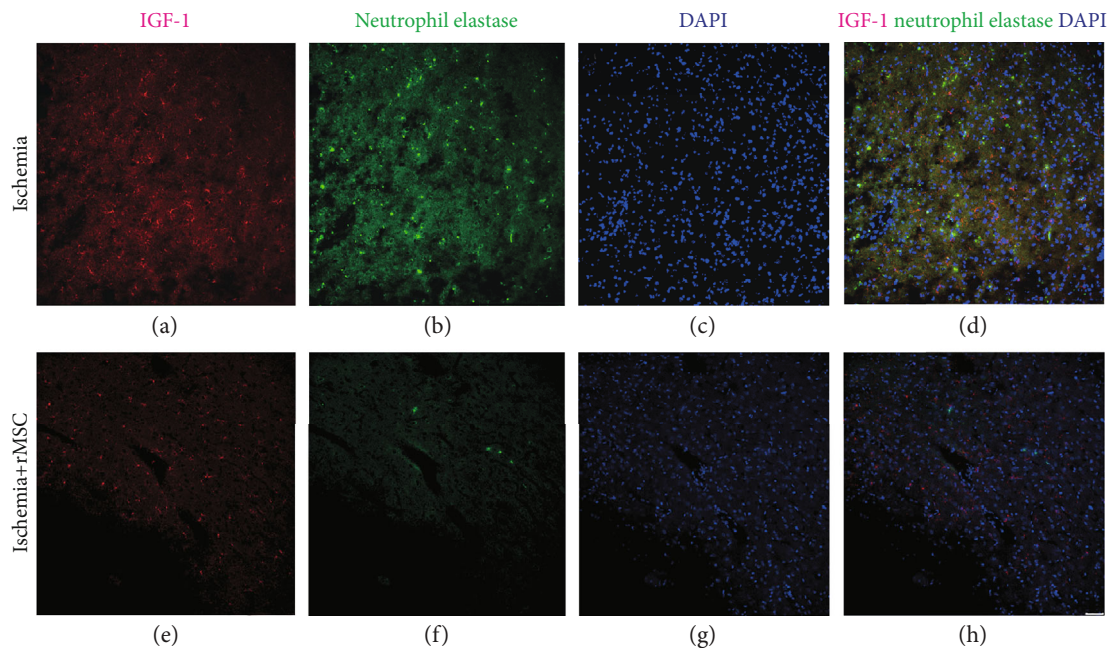


FIGURE 7: NE+ neutrophils in the ischemia core cortex are not the main source of IGF-1. (a–d) In the infarct boundary zone of the ischemia group, immunohistological examination showed strong expression of neutrophil elastase (NE), a marker for neutrophils, mainly located inside the entire cerebral ischemia core cortex but not in the striatum or corpus callosum. No double staining of NE+/IGF-1 cells were found. (e–h) NE+ cell number was reduced in the infarct area 2 days after MSC transplantation. No double-stained NE+/IGF-1+ cells were observed in the transplantation group. (a, e) IGF-1 staining. (b, f) Neutrophil elastase staining. (c, g) DAPI nuclear staining. (d, h) Merged images of neutrophil elastase, IGF-1, and DAPI. Scale bar, 50  $\mu\text{m}$ .

of sham group ( $246.9 \pm 44.5$  ng/mL). Forty-eight hours following MSC treatment in dMCAO rats, the IGF-1 level in blood plasma was significantly augmented to  $206.5 \pm 30.3$  ng/mL (Figure 8(a)).

Similarly, the concentrations of IGF-1 in the ischemia group were  $178.2 \pm 33.5$  ng/mL and  $188.7 \pm 34.5$  ng/mL at days 4 and 7, respectively, which were significantly increased following MSC treatment to  $233.1 \pm 18.9$  ng/mL ( $p < 0.05$ ) and  $245.8 \pm 25.7$  ng/mL, respectively ( $p < 0.05$ ) (Figures 8(b) and 8(c)).

#### 4. Discussion

IGF-1 has been implicated as a potential neuroprotective agent in hypoxia-ischemia-induced damage [20, 22]. Previously, by using ELISA on nonperfused brain tissues, we reported that IGF-1 concentrations increase in ischemia core and striatum in dMCAO model at 48 h after MSC infusion; yet levels of other neurotrophic factors, such as glial cell line-derived neurotrophic factor (GDNF) and vascular endothelial growth factor (VEGF) are not changed compared to those of the ischemia vehicle group at 2, 4, and 7 days after ischemia onset and MSC infusion [15].

In the previous study, we reported that IGF-1 signals are mainly ( $\sim 60\%$ ) located in the cortex infarct area. A smaller proportion ( $\sim 40\%$ ) of IGF-1 signals are detected in the striatum and corpus callosum. In the infarct area, IGF-1 signals are colocalized with NeuN and CD68, the markers of neurons and activated microglia/macrophages, respectively; but all of these cells together only contribute

to a small part of the entire IGF-1+ signals [15]. These results strongly suggest that there are other cell types as the source(s) of IGF-1 in the ischemia ipsilateral hemisphere. In the present study, we examined additional possible sources in the brain and periphery and found that astrocytes and peripheral circulation may be the main contributors to the increased level of IGF-1.

Due to the autofluorescence problem caused by blood cells, brain section staining is usually performed on transcardially perfused animals. IGF-1 is a factor that can readily cross the BBB. The consequence of perfusion is that IGF-1 diffused in the CSF and extracellular matrix would have been washed away, and only intracellular IGF-1 could be detected by staining on brain sections. This caveat may lead to an underrepresentation of IGF-1+ signals on perfused brain sections.

Upon brain injury, astrocytes are activated, which leads to phagocytosis, antigen processing and presentation, and the production of both neurotrophic and cytotoxic factors. Astrocytes are also a heterogeneous population, and reactions of astrocytes may depend on the nature of the activating stimulus and the microenvironment.

During ischemic injury, astrocytes were activated and upregulated expression of IGF-1 (Figures 3 and 4). MSC treatment induced astrocytes to further enhance IGF-1 expression without increasing the number of activated astrocytes (Figures 3 and 4). The molecular cues that promoted astrocytic expression of IGF-1 remained to be addressed.

Astrocytes are considered to play dual functions in neuroinflammation. On the one hand, astrocytes can produce

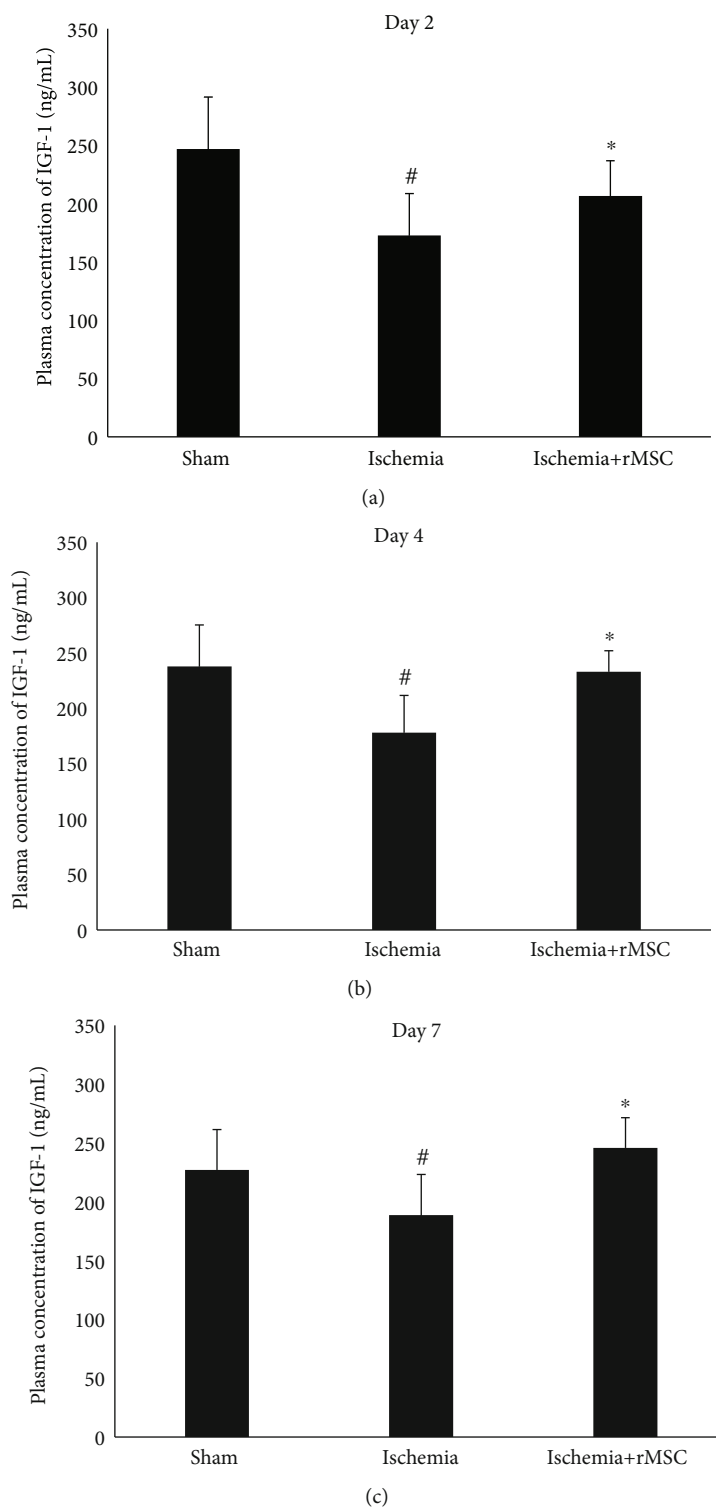


FIGURE 8: IGF-1 plasma levels at days 2, 4, and 7 after dMCAO and MSC infusion. (a–c) Two, 4, and 7 days after MSC infusion.

neurotrophic factors including nerve growth factor (NGF), BDNF, and IGF-1 [23]. On the other hand, activated astrocytes may release cytotoxic factors, such as reactive oxygen and nitrogen species (superoxide anion, nitric oxide) and toxic amino acids [24]. It was proposed by some researchers that astrocytes could be categorized into polarized A1 and

alternatively A2 status [25]. Yet how MSC treatment may impact this A1 vs. A2 balance remains unknown and warrants further investigation.

In the present study, a majority (50–80%) of GFAP+ astrocytes were IGF-1+. Upregulation of IGF-1 in the brain may further facilitate astrocytes to generate IGF-1. IGF-1

gene therapy can reduce the reactivity of astrocytes in response to proinflammatory stimuli *in vitro* [26] and exert neuroprotective and neuroreparative actions in experimental animal models of hypoxia and stroke [27–29]. Our results suggest that IGF-1 may mediate a positive feedback loop in the regulation of astrocytes. Further studies are needed to investigate the detailed mechanisms underlying the interaction between astrocytes and IGF-1 in dMCAO models.

IGF-1 is able to cross the BBB; therefore, it is important to examine the peripheral levels of IGF-1 as well. The primary site of IGF-1 production in peripheral organs is the liver, but IGF-1 is not required for postnatal body growth in mice [30]. Blood-derived IGF-1 was increased by MSC treatment at days 2, 4, and day 7 in this study. The results suggest that MSC treatment-mediated changes of IGF-1 levels in blood may be an important mechanism leading to an increased level of IGF-1 in the brain. In some studies where MSC was infused through an intravenous route, no MSCs are observed in brain but the therapeutic and neuroprotective effects remain obvious, implying an indirect function through peripheral mediators [31].

It is unclear how MSC infusion induces upregulation of IGF-1 in the periphery and whether this increase of IGF-1 results from a direct effect of MSCs on hepatocytes. If manipulation of circulating IGF-1 levels at the acute phase of dMCAO can affect disease outcome, future therapeutic strategies may be contemplated in this direction for treatment of stroke.

## Abbreviations

BBB:	Blood-brain barrier
BDNF:	Brain-derived neurotrophic factor
dMCAO:	Distal middle cerebral artery occlusion
FGF2:	Fibroblast growth factor-2
GDNF:	Glial cell line-derived neurotrophic factor
IGF-1:	Insulin-like growth factor-1
KA:	Kainic acid
NE:	Neutrophil elastase
NGF:	Nerve growth factor
VEGF:	Vascular endothelial growth factor.

## Data Availability

The data used in the manuscript supporting the conclusions of the study can be accessed by email request.

## Conflicts of Interest

The authors declare that there is no conflict of interest regarding the publication of this paper.

## Authors' Contributions

Xiaobo Li, Wenxiu Yu, and Yunqian Guan contributed equally to this work.

## Acknowledgments

This work was supported by the Stem Cell and Translation National Key Project (2016YFA0101403), National Natural Science Foundation of China (81371377, 81973351, 81671186, 81661130160, 81422014, and 81561138004), Beijing Municipal Natural Science Foundation (7172055 and 5142005), Beijing Talents Foundation (2017000021223TD03), Support Project of High-level Teachers in Beijing Municipal Universities in the Period of 13th Five-year Plan (CIT&TCD20180333), Beijing Medical System High Level Talent Award (2015-3-063), Beijing Municipal Health Commission Fund (PXM2020\_026283\_000005), Beijing One Hundred, Thousand, and Ten Thousand Talents Fund (2018A03), the Royal Society-Newton Advanced Fellowship (NA150482), and Science and technology project item in social development area of Guangdong Province (2014A020212563).

## Supplementary Materials

Supplementary Figure 1: schematic demonstration of the counting areas. The cerebral infarct area from a rat in the “ischemia control” group was indicated by staining with triphenyltetrazolium chloride (TTC). Rectangles indicate the areas where cell counting was performed. (*Supplementary Materials*)

## References

- [1] M. L. Adamo, X. Ma, C. L. Ackert-Bicknell, L. R. Donahue, W. G. Beamer, and C. J. Rosen, “Genetic increase in serum insulin-like growth factor-I (IGF-I) in C3H/HeJ compared with C57BL/6J mice is associated with increased transcription from the IGF-I exon 2 promoter,” *Endocrinology*, vol. 147, no. 6, pp. 2944–2955, 2006.
- [2] S. Komoly, L. D. Hudson, H. D. Webster, and C. A. Bondy, “Insulin-like growth factor I gene expression is induced in astrocytes during experimental demyelination,” *Proceedings of the National Academy of Sciences of the United States of America*, vol. 89, no. 5, pp. 1894–1898, 1992.
- [3] W. H. Lee, J. A. Clemens, and C. A. Bondy, “Insulin-like growth factors in the response to cerebral ischemia,” *Molecular and Cellular Neurosciences*, vol. 3, no. 1, pp. 36–43, 1992.
- [4] C. Bondy, H. Werner, C. T. Roberts Jr., and D. LeRoith, “Cellular pattern of type-I insulin-like growth factor receptor gene expression during maturation of the rat brain: comparison with insulin-like growth factors I and II,” *Neuroscience*, vol. 46, no. 4, pp. 909–923, 1992.
- [5] K. J. Allahdadi, T. A. de Santana, G. C. Santos et al., “IGF-1 overexpression improves mesenchymal stem cell survival and promotes neurological recovery after spinal cord injury,” *Stem Cell Research & Therapy*, vol. 10, no. 1, p. 146, 2019.
- [6] A. Nadjar, O. Berton, S. Guo et al., “IGF-1 signaling reduces neuro-inflammatory response and sensitivity of neurons to MPTP,” *Neurobiology of Aging*, vol. 30, no. 12, pp. 2021–2030, 2009.
- [7] J. P. Barrett, A. M. Minogue, A. Falvey, and M. A. Lynch, “Involvement of IGF-1 and Akt in M1/M2 activation state in bone marrow-derived macrophages,” *Experimental Cell Research*, vol. 335, no. 2, pp. 258–268, 2015.

- [8] S. Sukhanov, Y. Higashi, S. Y. Shai et al., "IGF-1 reduces inflammatory responses, suppresses oxidative stress, and decreases atherosclerosis progression in ApoE-deficient mice," *Arteriosclerosis, Thrombosis, and Vascular Biology*, vol. 27, no. 12, pp. 2684–2690, 2007.
- [9] T. Hijikawa, M. Kaibori, Y. Uchida et al., "Insulin-like growth factor 1 prevents liver injury through the inhibition of TNF- $\alpha$  and iNOS induction in D-galactosamine and LPS-treated rats," *Shock*, vol. 29, no. 6, pp. 740–747, 2008.
- [10] N. C. Chisholm and F. Sohrabji, "Astrocytic response to cerebral ischemia is influenced by sex differences and impaired by aging," *Neurobiology of Disease*, vol. 85, pp. 245–253, 2016.
- [11] I. Ocran, K. L. Valentino, I. F. Eng, R. L. Hintz, D. M. Wilson, and R. G. Rosenfeld, "Structural and immunohistochemical characterization of insulin-like growth factor I and II receptors in the murine central nervous system," *Endocrinology*, vol. 123, no. 2, pp. 1023–1034, 1988.
- [12] W. Kum, S. Q. Zhu, S. K. S. Ho, J. D. Young, and C. S. Cockram, "Effect of insulin on glucose and glycogen metabolism and leucine incorporation into protein in cultured mouse astrocytes," *Glia*, vol. 6, no. 4, pp. 264–268, 1992.
- [13] A. K. Okoreeh, S. Bake, and F. Sohrabji, "Astrocyte-specific insulin-like growth factor-1 gene transfer in aging female rats improves stroke outcomes," *Glia*, vol. 65, no. 7, pp. 1043–1058, 2017.
- [14] W. Chen, B. He, W. Tong, J. Zeng, and P. Zheng, "Astrocytic insulin-like growth factor-1 protects neurons against excitotoxicity," *Frontiers in Cellular Neuroscience*, vol. 13, p. 298, 2019.
- [15] X. Li, M. Huang, R. C. Zhao et al., "Intravenously delivered allogeneic mesenchymal stem cells bidirectionally regulate inflammation and induce neurotrophic effects in distal middle cerebral artery occlusion rats within the first 7 days after stroke," *Cellular Physiology and Biochemistry*, vol. 46, no. 5, pp. 1951–1970, 2018.
- [16] E. Carro, C. Spuch, J. L. Trejo, D. Antequera, and I. Torres-Aleman, "Choroid plexus megalin is involved in neuroprotection by serum insulin-like growth factor I," *The Journal of Neuroscience*, vol. 25, no. 47, pp. 10884–10893, 2005.
- [17] S. Gubbi, G. F. Quipildor, N. Barzilai, D. M. Huffman, and S. Milman, "40 Years of IGF1: IGF1: the Jekyll and Hyde of the aging brain," *Journal of Molecular Endocrinology*, vol. 61, no. 1, pp. T171–T185, 2018.
- [18] W. Pan and A. J. Kastin, "Interactions of IGF-1 with the blood-brain barrier in vivo and in situ," *Neuroendocrinology*, vol. 72, no. 3, pp. 171–178, 2000.
- [19] Y. Guan, X. Li, W. Yu et al., "Intravenous transplantation of mesenchymal stem cells reduces the number of infiltrated Ly6C<sup>+</sup> Cells but enhances the proportions positive for BDNF, TNF- $1\alpha$ , and IL- $1\beta$  in the infarct cortices of dMCAO rats," *Stem Cells International*, vol. 2018, Article ID 9207678, 14 pages, 2018.
- [20] J. Guan, L. Bennet, P. D. Gluckman, and A. J. Gunn, "Insulin-like growth factor-1 and post-ischemic brain injury," *Progress in Neurobiology*, vol. 70, no. 6, pp. 443–462, 2003.
- [21] P. Gelsa, D. Lecca, M. Fumagalli et al., "Microglia is a key player in the reduction of stroke damage promoted by the new antithrombotic agent Ticagrelor," *Journal of Cerebral Blood Flow & Metabolism*, vol. 34, no. 6, pp. 979–988, 2014.
- [22] S. Wrigley, D. Arafa, and D. Tropea, "Insulin-like growth factor 1: at the crossroads of brain development and aging," *Frontiers in Cellular Neuroscience*, vol. 11, p. 14, 2017.
- [23] A. R. Filous and J. Silver, "Targeting astrocytes in CNS injury and disease: a translational research approach," *Progress in Neurobiology*, vol. 144, pp. 173–187, 2016.
- [24] A. Becerra-Calixto and G. P. Cardona-Gomez, "The role of astrocytes in neuroprotection after brain stroke: potential in cell therapy," *Frontiers in Molecular Neuroscience*, vol. 10, p. 88, 2017.
- [25] S. A. Liddelow, K. A. Guttenplan, L. E. Clarke et al., "Neurotoxic reactive astrocytes are induced by activated microglia," *Nature*, vol. 541, no. 7638, pp. 481–487, 2017.
- [26] M. J. Bellini, C. B. Hereñú, R. G. Goya, and L. M. Garcia-Segura, "Insulin-like growth factor-I gene delivery to astrocytes reduces their inflammatory response to lipopolysaccharide," *Journal of Neuroinflammation*, vol. 8, no. 1, p. 21, 2011.
- [27] Q. Liu, J. Z. Guan, Y. Sun et al., "Insulin-like growth factor 1 receptor-mediated cell survival in hypoxia depends on the promotion of autophagy via suppression of the PI3K/Akt/mTOR signaling pathway," *Molecular Medicine Reports*, vol. 15, no. 4, pp. 2136–2142, 2017.
- [28] W. Zhu, Y. Fan, T. Frenzel et al., "Insulin growth factor-1 gene transfer enhances neurovascular remodeling and improves long-term stroke outcome in mice," *Stroke*, vol. 39, no. 4, pp. 1254–1261, 2008.
- [29] Y. Liu, X. Wang, W. Li et al., "A sensitized IGF1 treatment restores corticospinal axon-dependent functions," *Neuron*, vol. 95, no. 4, pp. 817–833.e4, 2017, e4.
- [30] K. Sjogren, J. L. Liu, K. Blad et al., "Liver-derived insulin-like growth factor I (IGF-I) is the principal source of IGF-I in blood but is not required for postnatal body growth in mice," *Proceedings of the National Academy of Sciences of the United States of America*, vol. 96, no. 12, pp. 7088–7092, 1999.
- [31] H. Chi, Y. Guan, F. Li, and Z. Chen, "The effect of human umbilical cord mesenchymal stromal cells in protection of dopaminergic neurons from apoptosis by reducing oxidative stress in the early stage of a 6-OHDA-induced Parkinson's disease model," *Cell Transplant*, vol. 28, Supplement 1, pp. 87S–99S, 2019.



## Review Article

# Spatial Distributions, Characteristics, and Applications of Craniofacial Stem Cells

Geru Zhang,<sup>1</sup> Qiwen Li,<sup>1</sup> Quan Yuan,<sup>1,2</sup> and Shiwen Zhang <sup>1,2</sup>

<sup>1</sup>State Key Laboratory of Oral Diseases and National Clinical Research Center for Oral Diseases, West China Hospital of Stomatology, Sichuan University, Chengdu, China

<sup>2</sup>Department of Oral Implantology, West China Hospital of Stomatology, Sichuan University, Chengdu, China

Correspondence should be addressed to Shiwen Zhang; [sw.zhang2018@scu.edu.cn](mailto:sw.zhang2018@scu.edu.cn)

Received 20 May 2020; Revised 29 July 2020; Accepted 1 August 2020; Published 29 August 2020

Academic Editor: Sangho Roh

Copyright © 2020 Geru Zhang et al. This is an open access article distributed under the Creative Commons Attribution License, which permits unrestricted use, distribution, and reproduction in any medium, provided the original work is properly cited.

Stem cells play an irreplaceable role in the development, homeostasis, and regeneration of the craniofacial bone. Multiple populations of tissue-resident craniofacial skeletal stem cells have been identified in different stem cell niches, including the cranial periosteum, jawbone marrow, temporomandibular joint, cranial sutures, and periodontium. These cells exhibit self-renewal and multidirectional differentiation abilities. Here, we summarized the properties of craniofacial skeletal stem cells, based on their spatial distribution. Specifically, we focused on the *in vivo* genetic fate mapping of stem cells, by exploring specific stem cell markers and observing their lineage commitment in both the homeostatic and regenerative states. Finally, we discussed their application in regenerative medicine.

## 1. Introduction

The reconstruction of craniofacial bone defects is more challenging than that of the limb bone, as it requires both functional and esthetic recovery. Traditional therapies to regenerate craniofacial bone, including autologous bone grafts, allografts, and xenografts [1–3], exhibit different limitations and often fail to meet the demands of recovery [4–6]. Stem cell-guided regenerative medicine is an alternative that is currently the most promising approach to solve this problem.

Mesenchymal stem cells (MSCs) are groups of cells residing in different tissues and niches, such as the bone marrow, adipose tissue, teeth, and umbilical cord tissue. MSCs have been extensively used in tissue repair, organ reconstruction, immunomodulation, and even in the treatment of disease [7–11]. In addition, self-cell-constituted implantation results in reduced immunogenicity, and the molecules excreted from MSCs are beneficial for tissue recovery [12, 13]. The combination of MSCs with bioscaffolds further promoted MSC-based therapy by guiding MSC proliferation and migration [14].

To identify and isolate MSCs easily *in vitro*, the International Society for Cellular Therapy has proposed three

criteria to define MSCs [15]. First, the isolated cells can adhere to plastic plates when cultured *in vitro*. Second, the cells express the CD73, CD90, and CD105 surface markers but not CD34, CD45, CD14 or CD11b, CD79a or CD19, and HLA-DR. Third, the cells can differentiate into osteocytes, chondrocytes, and adipocytes. In addition to *in vitro* characterization, the recent application and improvement of the fluorescent reporter mouse system and lineage tracing technique make the *in vivo* study of stem cells feasible [16]. Importantly, the *in vivo* study of stem cells can aid in accurately recapitulating the niche-dependent functions and interactions of stem cells.

MSCs from bones, including the bone marrow, periosteum, growth plate, and calvarium, have been the most thoroughly studied. It is now recognized that bone MSCs are highly heterogeneous populations that display variable self-renewal and differentiation potential. MSCs that commit to skeletal lineages and express selective surface markers (e.g., leptin receptor, PDGFR $\alpha$ , nestin, Cxcl12, Hox11, PTHrP, Sca1, Ctsk, Axin2, and Gli1) are now defined as skeletal stem cells (SSCs). Craniofacial SSCs are subgroups of cells residing in the calvarium, maxillary and mandibular bones, and

tooth-supporting tissue. These cells display the basic characteristics of SSCs and are capable of self-renewal and multilineage differentiation. They can regenerate oral tissues and repair critical defects of craniofacial bones [17–20]. However, craniofacial SSCs are distinct from long bone SSCs, which might result from the different developmental origins and stem cell microenvironments/niches. The craniofacial bone originates from the mesoderm and neural crest, and the bony structure is formed by intramembranous ossification. Long bones, on the other hand, mainly originate from the mesoderm and are formed by endochondral ossification [20, 21]. In addition, the craniofacial bone is a flat bone with limited bone marrow, but the long bone is enriched with the bone marrow. Hematopoiesis-depleted or hematopoiesis-enriched environments result in totally different stem cell niches. Therefore, craniofacial SSCs are different from SSCs in long bones or other tissues. Interestingly, studies have shown that SSCs/MSCs from craniofacial bones exhibit superior osteogenic properties compared with long bone SSCs/MSCs in craniofacial tissue reconstruction [22–24]. A pioneering study also found that postnatal lineage-restricted craniofacial SSCs reverted to their embryonic plastic state and regained a neural crest cell phenotype in response to mandibular distraction for jaw regeneration [25]. Identifying subpopulations and illustrating the properties of craniofacial SSCs are thus crucial to stem cell-guided regenerative medicine.

In this review, we summarize the cranial and maxillofacial tissues in which stem cells reside as well as the characteristics of these stem cells and advancements in their applications.

## 2. Periosteum

The surface of the bone is covered by the periosteum, which is a 50–150  $\mu\text{m}$  two-layer membrane with an abundance of nerves and blood vessels (Figure 1). The outer fibrous layer is adjacent to the surrounding soft fibrous and muscular tissue, while the inner layer is highly vascularized and provides a niche for progenitor cells [26, 27]. A large number of studies have already shown that precursor cells residing in the craniofacial bone periosteum play an important role in bone regeneration [28]. For a long time, no specific cell marker was available to identify and isolate craniofacial periosteum-derived stem cells (PSCs) [28, 29]. Recently, two specific surface makers (Ctsk<sup>+</sup> and Mx1<sup>+</sup> $\alpha$ SMA<sup>+</sup>) have been identified.

Cathepsin K (CTSK) has long been regarded as a specific marker for osteoclasts. Using *Ctsk-mGFP* transgenic mice to trace cell lineages combined with single-cell RNA sequencing, Debnath et al. identified Ctsk<sup>+</sup> periosteum stem cells as both long bone and calvarial periosteal skeletal stem cells (PSCs). Ctsk<sup>+</sup> PSCs are capable of self-renewal, colony formation, and multilineage differentiation. Interestingly, Ctsk<sup>+</sup> PSCs are highly plastic, as they can mediate not only intramembranous ossification but also endochondral ossification in response to bone injury [30]. In 2019, Park et al. observed that a group of postnatal long-term Mx1<sup>+</sup> $\alpha$ SMA<sup>+</sup> periosteal stem cells contributed significantly to the injury repair of bone defects. In addition to being capable of self-renewal and clonal multipotency, Mx1<sup>+</sup> $\alpha$ SMA<sup>+</sup> PSCs can migrate toward the

injury site in response to a CCR5 ligand- (CCL5-) dependent mechanism, as visualized by *in vivo* real-time imaging of the calvarium [31].

## 3. Craniofacial Bone Marrow

Given that jawbones and teeth in the craniofacial system originate from the cranial neural crest, marrow stem cells in jawbones are considered to have characteristics different from those of long bone MSCs. Studies have been performed to compare the similarities and differences between stem cells in the craniofacial, axial, and appendicular regions. Human MSCs in the jawbone and iliac crest have been the most commonly studied, as these sites are ideal for marrow aspiration. Akintoye et al. cultured jawbone MSCs and iliac crest MSCs from the same individual and found that jawbone MSCs displayed a higher proliferation rate, delayed senescence, and greater differentiation potential. *In vivo* transplantation results showed that jawbone MSCs formed more bone, whereas iliac crest MSCs formed more compacted bone along with hematopoietic tissue [32]. Using tube formation assays and 3D fibrin vasculogenic tests, Du et al. found that jawbone MSCs showed stronger angiogenic propensities than iliac crest MSCs when they were cocultured with human umbilical vein endothelial cells (HUVECs). Coculture with jawbone MSCs allowed HUVECs to form more tube-like structures *in vitro* and larger vessels *in vivo* [33]. The increase in the expression of the basic fibroblast growth factor (bFGF) by jawbone MSCs is the key factor contributing to angiogenesis. However, the chondrogenic and adipogenic potential of jawbone MSCs is weaker than that of iliac crest MSCs [34, 35].

Several populations of SSCs in the long bone marrow were identified, including leptin-receptor-expressing (LepR<sup>+</sup>) SSCs, nestin-expressing (Nestin<sup>+</sup>) SSCs, Gremlin 1-expressing (Grem1<sup>+</sup>) SSCs, glioma-associated oncogene 1-expressing (Gli1<sup>+</sup>) SSCs, and CD45<sup>+</sup>Ter119<sup>-</sup>Tie2<sup>-</sup>AlphaV<sup>+</sup>Thy6C3<sup>-</sup>CD105<sup>-</sup>CD200<sup>+</sup> SSCs [36–39]. However, their identity and function in the craniofacial bone remain unclear. We recently identified a quiescent population of tissue-resident LepR<sup>+</sup> SSCs in jawbone marrow that became activated in response to tooth extraction and contributed to intramembranous bone formation [40]. Using *LepR-Cre; tdTomato; Col2.3-GFP* reporter mice, we found that these LepR<sup>+</sup> cells remained quiescent in the physiological state and gradually increased in activity with age. External stimuli such as tooth extraction activated LepR<sup>+</sup> SSCs, which rapidly proliferated and differentiated into Col2.3-expressing osteoblasts, contributing significantly to extraction socket repair. Ablation of LepR<sup>+</sup> SSCs with diphtheria toxin dramatically impaired the bone healing process. A mechanistic study showed that alveolar LepR<sup>+</sup> SSCs are responsive to parathyroid hormone/parathyroid hormone I receptor (PTH/PTH1R) signaling. Knockout of *Pth1r* in the LepR<sup>+</sup> cell lineage disrupted the bone formation process.

## 4. Temporomandibular Joint

The temporomandibular joint (TMJ) is located between the temporal bone and the mandible. It is one of the most frequently used joints in humans and is the only diarthrosis

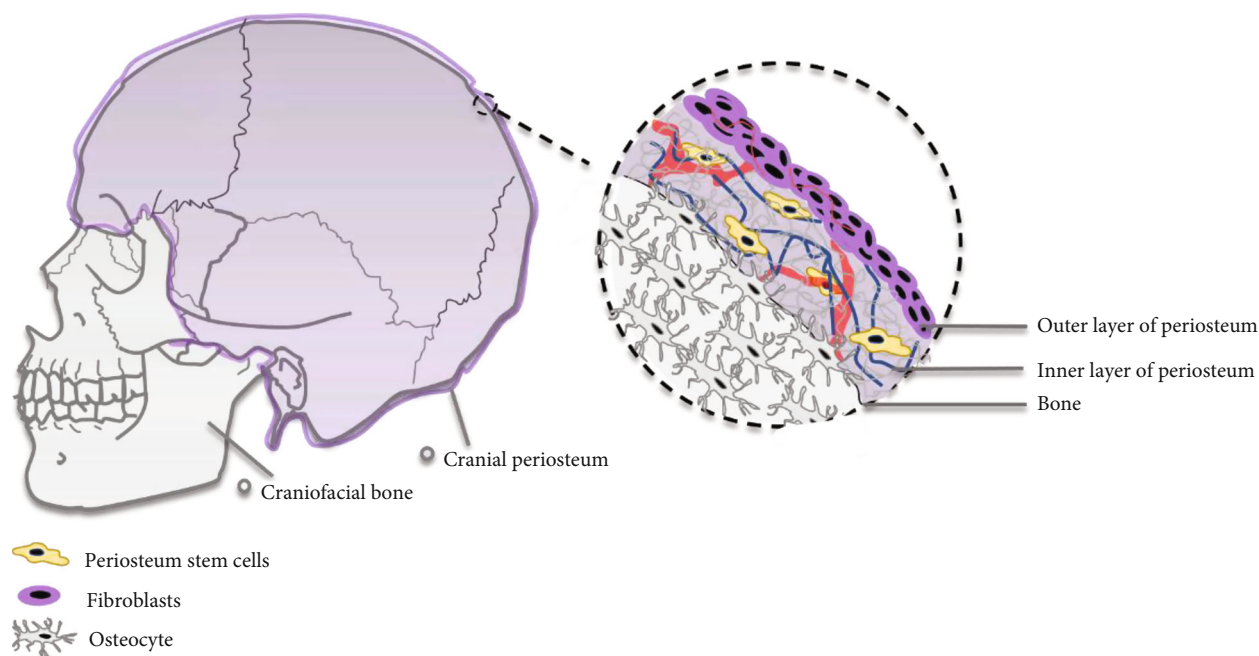


FIGURE 1: Stem cell distribution in the cranial bone. The stem cells are located in the inner layer of calvarium periosteum.

in the stomatognathic system. The occurrence of TMJ osteoarthritis is highly prevalent in humans, yet the regenerative capacity of condylar cartilage is limited. Therefore, identifying and isolating stem cells in the TMJ is crucial for osteoarthritis amelioration and regeneration.

Two types of stem cells reside in the TMJ (Figure 2). One type is TMJ synovium-derived stem cells, and the other type is fibrocartilage stem cells (FCSCs). In 2011, Liu et al. isolated and cultured stem cells from human TMJ synovial fluid and found that these cells exhibit fibroblastic and spindle shapes. Flow cytometry analysis showed that these cells express MSC markers and could be induced to differentiate toward osteogenic, chondrogenic, adipogenic, and neurogenic lineages. Thus, these synovium-derived cells are stem cells [41]. Koyama et al. found STRO-1- and CD146-expressing stem cells in the TMJ synovial fluid of patients with temporomandibular joint disorder. These cells showed great potential to differentiate into chondrocytes, osteoblasts, adipocytes, and neurons [42]. Stem cells were also isolated from the radiolucent zone of TMJ ankylosis patients, but they had a slower proliferation rate and lower osteogenic differentiation capacity than BMSCs [43]. In 2014, Sun et al. isolated synovial fragment cells from the synovial fluid of temporomandibular disease patients and revealed the multilineage differentiation capacity of this group of cells [44]. Fibrocartilage stem cells (FCSCs) reside in the superficial zone of condylar cartilage. A single FCSC could generate a cartilage anlage, which then undergoes autogenous bone formation and supports a hematopoietic microenvironment. Wnt signaling impairs the FCSC niche and results in cartilage degeneration. Intra-articular injection of the Wnt inhibitor sclerostin reconstructed the stem cell niche and repaired TMJ injury, indicating a potential therapeutic strategy for patients with fibrocartilage defects and disease [45].

## 5. Sutures

In summary, the flexible connection between paired calvarial bones permits the deformation of the skull during birth, directs the growth of the skull, and acts as a shock absorber that can cushion the load of mastication (Figure 3). Humans and mice both have four sutures. Metopic sutures (called interfrontal sutures in mice) and sagittal sutures are vertically distributed, and the osteogenic fronts about each other. Coronal sutures and lambdoid sutures are horizontally distributed, and their osteogenic fronts overlap with each other. Unossified sutures are recognized as the bone growth center of the postnatal skull vault [46], where the new bone precipitates at the edges of the bone front. Premature closure of the suture could lead to craniosynostosis. Studies have demonstrated a unique stem cell niche in cranial sutures, where multiple populations of several subpopulations of suture mesenchymal stem cells (SuSCs) were identified, including Gli1-positive (Gli1<sup>+</sup>) cells, Axin2-expressing (Axin2<sup>+</sup>) cells, and postnatal Prx1-expressing (Prx1<sup>+</sup>) cells [46–49]. All these cells possess the ability for self-renewal and continually produce skeletal cell descendants. Clonal expansion analysis demonstrated that SuSCs were capable of forming bones during calvarial development. SuSCs expand dramatically in the damaged site and contribute directly to skeletal repair; the nearer the cells are to the sutures, the better the recovery is [46, 50]. However, the spatiotemporal properties of SuSCs differ. During the early stage of postnatal development, Gli1<sup>+</sup> cells were distributed throughout the periosteum, dura, and sutures, whereas Axin2<sup>+</sup> cells and Prx1<sup>+</sup> cells appeared only in the sutures. At 4 weeks of age, all of the SuSCs were restricted to the sutures. Gli1<sup>+</sup> SuSCs were capable of trilineage differentiation into chondrocytes, osteoblasts, and adipocytes; Axin2<sup>+</sup> SuSCs mainly gave rise to the chondro- and osteolineages, whereas Prx1<sup>+</sup> SuSCs

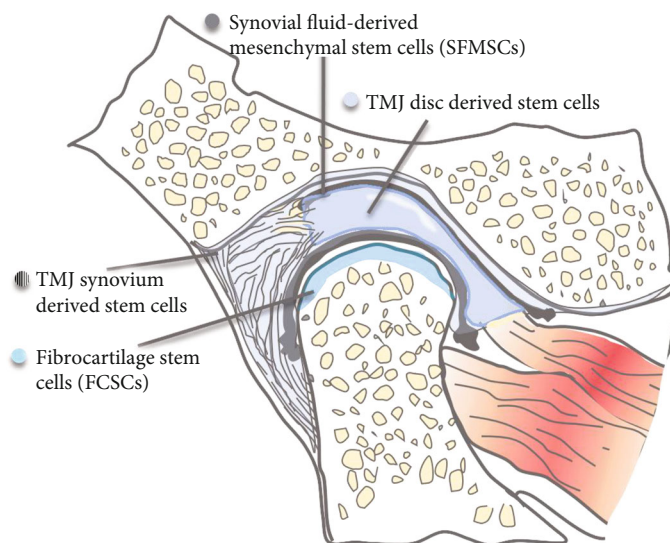


FIGURE 2: Stem cell distribution in TMJ. Stem cells are located in the synovial fluid, synovium, disc of TMJ, and surface zone of condylar cartilage.

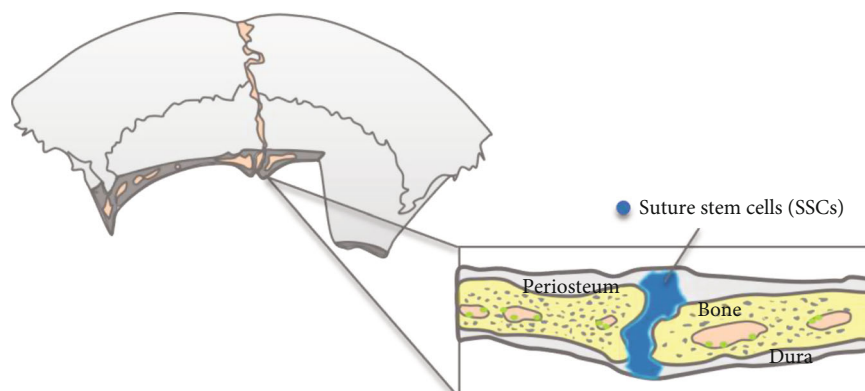


FIGURE 3: Stem cell distribution in sutures.

could only differentiate into osteoblasts. Depletion of  $Gli1^+$  or  $Axin2^+$  cells but not  $Prx1^+$  SuSCs caused craniosynostosis. Additional comparisons of the three types of cells are listed in Table 1.

## 6. Periodontium

The tooth is a hard tissue containing a vascularized and nerve-rich pulp chamber and is surrounded by the tooth-supporting periodontium, including the periodontal ligament, cementum, and alveolar bone. Multiple stem cell niches exist in dental tissues, as teeth are uniquely shaped and are subject to complicated microenvironments with occlusal force and microorganisms [53]. To date, more than seven kinds of dental stem cells have been found, including dental pulp stem cells (DPSCs) [54], human exfoliated deciduous teeth (SHED) [55], periodontal ligament stem cells (PDLSCs) [56], dental follicle progenitor cells (DFPCs) [57], stem cells from dental apical papilla (SCAP) [58], tooth germ stem cells (TGSCs) [59], gingival mesenchymal stem cells (GMSCs) [60], and human natal dental pulp stem cells (NDP-SCs) (Figure 4) [61]. All of them are capable of self-renewal, proliferation, and multi-

directional differentiation [62]. Among them, PDLSCs are the only kind of stem cells that can differentiate into osteoblasts *in vivo* and contribute to the construction of alveolar bone and tooth extraction sockets.

As reported in 2004, Seo et al. isolated and identified PDLSCs from human impacted wisdom teeth for the first time [56]. In addition to wisdom teeth, PDLSCs can be extracted from permanent tooth root surfaces [63], deciduous tooth [64–66], or even inflammatory periodontal tissues [67]. However, PDLSCs derived from different environments display different properties related to proliferation and osteogenic potential. For example, studies have found that PDLSCs from deciduous teeth promote osteoclastogenesis and lead to root absorption [68]. PDLSCs from inflammatory tissue are predisposed to a pathological local microenvironment [69]. The regulatory mechanism of PDLSC biological behavior remains to be revealed.

To exploit the osteogenic potential of PDLSCs, the osteogenic mechanism of PDLSCs needs to be clarified. It has been reported that antidifferentiation noncoding RNA (ANCR) [70], long noncoding RNAs (lncRNAs) [71], and microRNA-182 and microRNA-214 [72, 73] regulate the proliferation



TABLE 1: The subpopulations of suture mesenchymal stem cells and their characteristics.

Cell types		Gli1 <sup>+</sup> cells [50, 51]	Axin2 <sup>+</sup> cells [46]	Postnatal Prx1 <sup>+</sup> cells [52]
Distribution	Early stage	All over the periosteum, dura, and the craniofacial sutures	In the calvarial sutures	In the calvarial sutures
	One month after birth	Self-renewal	Only in the sutures	/
	Self-renewal		Slow-cycling cells	
Stemness	Contribution to other tissues	Suture mesenchyme, periosteum, dura mater, and parts of the calvarial bones	Suture mesenchyme and bone matrix near the osteogenic fronts	All calvarial tissues, except bone marrow osteoblasts
	Ability to repair the defect	Unequivocal and potentially exclusive contribution of the sutural mesenchyme to calvarial injury repair		
Ablation		Craniosynostosis	Craniosynostosis	Did not result in craniosynostosis or any other major craniofacial phenotype
MSC markers		CD90, CD73, CD44, Sca1, and CD146	LepR	Pdgfra and Mcam/CD146 (upregulation), Ccne2, Mcm4, and Pcna (downregulation), Itga2, Itga3, and Itga6
Differentiation	Osteoblasts	+	+ (upon external stimulation)	+ (stimulated with recombinant WNT3A)
	Chondrocytes	+	+ (upon external stimulation)	/
	Adipocytes	+	/	/
Foundation of each study		Gli1 is the master transcriptional factor of hedgehog signaling and is indispensable for bone development and homeostasis. Gli1 <sup>+</sup> stem cells have been identified in canine and long bones.	Axin2 plays an irreplaceable role in the Wnt, BMP, and FGF signaling pathways; Axin2 knockout mice showed craniosynostosis.	Prx1 was previously shown to be highly expressed during limb bud formation and craniofacial development.

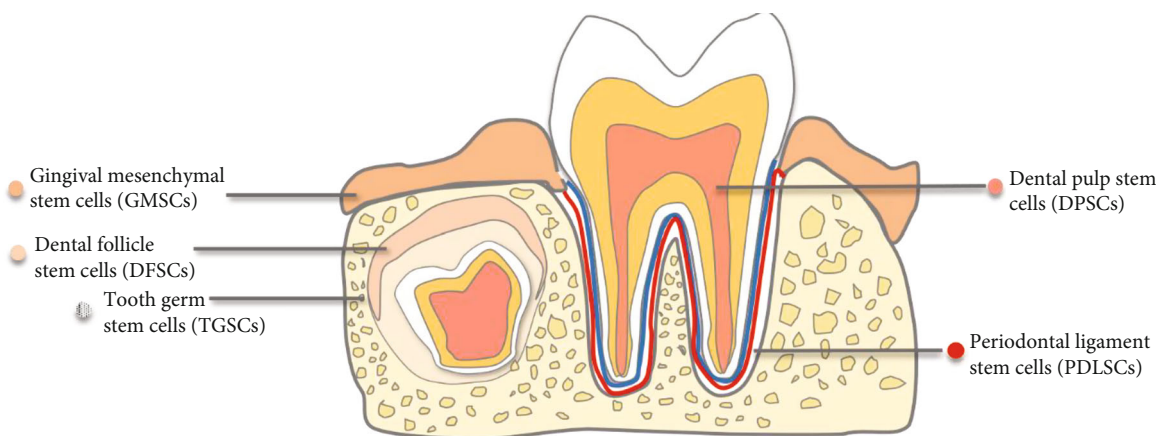


FIGURE 4: Stem cell distribution in dental tissues. Stem cells are located in gingiva, dental follicle, tooth germ, dental pulp, and periodontal ligament.

and osteogenic differentiation of PDLSCs. He et al. [74] and Yan et al. [75] found that hypoxia and cannabinoid receptor I (CB1) could alter the activity of PDLSCs through the p38/MAPK pathway. Meanwhile, the PI3K-AKT-mTOR pathway [76] and NF-κB axis [77] are also involved in the modula-

tion of PDLSCs. In clinical practice, additional topics, such as how metformin contributes to the osteogenic potential of PDLSCs [78] and how nicotine [79, 80] and *Porphyromonas gingivalis* [81] weaken the osteogenic potential of PDLSCs, remain to be investigated.

PDLSCs exhibit high potential for tissue regeneration and are capable of giving rise to osteoblast-/cementoblast-like cells, adipocytes, chondrogenic cells, neurogenic lineage cells, endothelial cells, cardiac myocytes, and Schwann cells *in vitro* [62]. For stem cell identity and fate commitment, Roguljic and colleagues identified  $\alpha$ SMA as a marker of PDLSCs *in vivo* [82].  $\alpha$ SMA<sup>+</sup> PDLSCs expanded over time and mainly gave rise to cells in the apical region. Following periodontal ligament injury, PDLSCs proliferated and generated mature cementoblasts, osteoblasts, and fibroblasts within the periodontium. However,  $\alpha$ SMA<sup>+</sup> PDLSCs only made minor contributions to periodontium homeostasis and repair. Yuan and colleagues used Axin2 to track progenitor cells in the periodontal ligament and reported that PDLSCs are responsive to Wnt signaling [83]. Axin2<sup>+</sup> PDLSCs remain quiescent under physiological conditions and differentiate into osteoblastic cells for alveolar bone repair when tooth extraction injury occurs. Most recently, using genetic fate mapping, Men et al. identified Gli1<sup>+</sup> PDLSCs in adult mouse molars that gave rise to periodontal ligament, alveolar bone, and cementum in both the homeostatic state and during injury repair [84]. Gli1<sup>+</sup> PDLSCs are enriched in the apical tooth region and surround the neurovascular bundle, and they are activated by canonical Wnt signaling. Sclerostin secreted by alveolar bone osteocytes inhibits Wnt signaling. Occlusal force can inhibit sclerostin secretion. Therefore, a feedback loop that regulates stem cell activities is present in the stem cell niche, where occlusal force-mediated inhibition of sclerostin secretion by alveolar bone osteocytes promotes Gli1<sup>+</sup> cell maintenance and activation. The authors also compared other stem cell markers with Gli1. They concluded that labeling of Gli1 more efficiently identified PDLSCs compared to labeling of  $\alpha$ SMA, LepR, NG2, and Pdgfra. Using an inducible Cre system and immunostaining, they also reported that LepR<sup>+</sup>, NG2<sup>+</sup>, and Pdgfra<sup>+</sup> cells are descendants of Gli1<sup>+</sup> cells in the periodontal ligament.

## 7. Application of Craniofacial Stem Cells

Stem cells for tissue regeneration have been widely exploited and are mainly applied in three ways: direct transplantation of a specific type of stem cells, combined application of different types of stem cells, and the use of stem cells in combination with biological scaffolds. However, the regenerative techniques used in the long bone cannot be easily extended to craniofacial applications because the microenvironment of craniofacial tissue is quite different from that of the long bone. Oral pathological factors (e.g., microorganisms, nicotine, and bisphosphonate) greatly affect the biological behavior of craniofacial stem cells. For instance, Kim et al. found that excessive nicotine intake will induce the vacuolation of jawbone MSCs and impair their proliferation and differentiation capacity [85]. Akintoye et al. found that jawbone MSC self-renewal and proliferation ability were impaired when the MSCs were treated with bisphosphonate, which might be associated with the pathogenesis of bisphosphonate-associated osteonecrosis. Therefore, to minimize potential damage, the use of appropriate ways to amplify and induce stem cells to differentiate toward the osteoblast lineage is particularly important. Wang et al. reported that vitamin C and vitamin D were ideal stimu-

lants of craniofacial PDLSCs for osteoblast differentiation *in vitro* [26]. Naung et al. proposed a protocol to cultivate palate periosteum-derived MSCs in serum-free and xeno-free medium, which could become a useful source of MSCs for clinical applications [86]. Moreover, a recent study found that induced pluripotent stem cells (iPSCs) generated from human jaw periosteum cells expressed MSC markers and possessed strong mineralization ability [87].

The application of MSCs for regenerative medicine should be performed with caution because the stem cells obtained and expanded with plastic culture are highly heterogeneous and might not be intrinsically multipotent [88]. It should be noted that the minimal criteria, including adherence to the plastic plate, induction of multidirectional differentiation, and detection of appropriate surface marker profiles, are not sufficient to identify *bona fide* stem cells [89]. Some quiescent stem cells might not readily adhere to the plastic, and the heterogeneous cell mixture contains lineage-committed stem cells that give rise to cells of native tissue origin. For instance, bone marrow stem cells show an intrinsic propensity for differentiation toward osteolineages [90]. The surface markers of bone marrow stem cells are specific for fibroblast-like cells rather than stem cells [88]. Therefore, *in vivo* clonal assays and fate mapping are essential to identify *bona fide* stem cells [38]. Future studies are warranted to identify the stem cell properties of craniofacial stem cells, which will benefit clinical applications.

## 8. Conclusions

This review describes the stem cells found in the craniofacial periosteum, craniofacial bone marrow, TMJ, cranial suture, and periodontal ligament. Craniofacial stem cells express specific cell surface determinants, possess a low self-renewal rate, and show multidifferentiation ability. They rapidly proliferated and differentiated into osteoblasts in response to injury. In addition, craniofacial tissues are easily obtained from human jawbones with minimal invasiveness when clinicians perform implant surgeries, tooth extractions, and periodontal surgeries. All these results indicated that craniofacial stem cells are an ideal resource for tissue engineering.

However, the current research on craniofacial stem cells is still inadequate and lacks depth. Specific cell markers for the isolation of stem cells are still lacking. *In vivo* clonal assays and lineage fate mapping are warranted in future studies, which could facilitate the therapeutic application of craniofacial stem cells *in vivo* and in the clinic.

## Conflicts of Interest

The authors declare that they have no competing interests.

## Authors' Contributions

Geru Zhang and Qiwen Li contributed equally to this work.

## Acknowledgments

This work was supported by grants from the National Natural Science Foundation of China (Grant Number: NSFC

81901042) and China Postdoctoral Science Foundation (Grant Number: 2019M653443) to Shiwen Zhang.

## References

- [1] K. S. Boehm, M. al-Taha, A. Morzycki, O. A. Samargandi, S. al-Youha, and M. R. LeBlanc, "Donor site morbidities of iliac crest bone graft in craniofacial surgery: a systematic review," *Annals of Plastic Surgery*, vol. 83, no. 3, pp. 352–358, 2019.
- [2] W. Zhang and P. C. Yelick, "Craniofacial tissue engineering," *Cold Spring Harbor Perspectives in Medicine*, vol. 8, no. 1, 2018.
- [3] J. A. Fearon, D. Griner, K. Dittthakaseem, and M. Herbert, "Autogenous bone reconstruction of large secondary skull defects," *Plastic and Reconstructive Surgery*, vol. 139, no. 2, pp. 427–438, 2017.
- [4] J. C. Melville, V. A. Mañón, C. Blackburn, and S. Young, "Current methods of maxillofacial tissue engineering," *Oral and Maxillofacial Surgery Clinics of North America*, vol. 31, no. 4, pp. 579–591, 2019.
- [5] Y. Fillingham and J. Jacobs, "Bone grafts and their substitutes," *The Bone & Joint Journal*, vol. 98-B, 1\_Supple\_A, pp. 6–9, 2016.
- [6] R. Dimitriou, E. Jones, D. McGonagle, and P. V. Giannoudis, "Bone regeneration: current concepts and future directions," *BMC Medicine*, vol. 9, no. 1, 2011.
- [7] A. Andrzejewska, B. Lukomska, and M. Janowski, "Concise review: mesenchymal stem cells: from roots to boost," *Stem Cells*, vol. 37, no. 7, pp. 855–864, 2019.
- [8] X. Fu, G. Liu, A. Halim, Y. Ju, Q. Luo, and G. Song, "Mesenchymal stem cell migration and tissue repair," *Cell*, vol. 8, no. 8, p. 784, 2019.
- [9] J. Galipeau and L. Sensébé, "Mesenchymal stromal cells: clinical challenges and therapeutic opportunities," *Cell Stem Cell*, vol. 22, no. 6, pp. 824–833, 2018.
- [10] R. Yang, T. Yu, and Y. Zhou, "Interplay between craniofacial stem cells and immune stimulus," *Stem Cell Research & Therapy*, vol. 8, no. 1, p. 147, 2017.
- [11] J. L. Spees, R. H. Lee, and C. A. Gregory, "Mechanisms of mesenchymal stem/stromal cell function," *Stem Cell Research & Therapy*, vol. 7, no. 1, p. 125, 2016.
- [12] C. Harrell, C. Fellabaum, N. Jovicic, V. Djonov, N. Arsenijevic, and V. Volarevic, "Molecular mechanisms responsible for therapeutic potential of mesenchymal stem cell-derived secretome," *Cell*, vol. 8, no. 5, p. 467, 2019.
- [13] M. De Luca, A. Aiuti, G. Cossu, M. Parmar, G. Pellegrini, and P. G. Robey, "Advances in stem cell research and therapeutic development," *Nature Cell Biology*, vol. 21, no. 7, pp. 801–811, 2019.
- [14] A. Ho-Shui-Ling, J. Bolander, L. E. Rustom, A. W. Johnson, F. P. Luyten, and C. Picart, "Bone regeneration strategies: engineered scaffolds, bioactive molecules and stem cells current stage and future perspectives," *Biomaterials*, vol. 180, pp. 143–162, 2018.
- [15] M. Dominici, K. le Blanc, I. Mueller et al., "Minimal criteria for defining multipotent mesenchymal stromal cells. The International Society for Cellular Therapy position statement," *Cytotherapy*, vol. 8, no. 4, pp. 315–317, 2006.
- [16] M. Kassem and P. Bianco, "Skeletal stem cells in space and time," *Cell*, vol. 160, no. 1-2, pp. 17–19, 2015.
- [17] F. Kawecki, W. P. Clafshenkel, M. Fortin, F. A. Auger, and J. Fradette, "Biomimetic tissue-engineered bone substitutes for maxillofacial and craniofacial repair: the potential of cell sheet technologies," *Advanced Healthcare Materials*, vol. 7, no. 6, article e1700919, 2018.
- [18] P. T. Sharpe, "Dental mesenchymal stem cells," *Development*, vol. 143, no. 13, pp. 2273–2280, 2016.
- [19] J. Liu, F. Yu, Y. Sun et al., "Concise reviews: characteristics and potential applications of human dental tissue-derived mesenchymal stem cells," *Stem Cells*, vol. 33, no. 3, pp. 627–638, 2015.
- [20] H. Zhao and Y. Chai, "Stem cells in teeth and craniofacial bones," *Journal of Dental Research*, vol. 94, no. 11, pp. 1495–1501, 2015.
- [21] D. Wang, J. R. Gilbert, X. Zhang, B. Zhao, D. F. E. Ker, and G. M. Cooper, "Calvarial versus long bone: implications for tailoring skeletal tissue engineering," *Tissue Engineering Part B: Reviews*, vol. 26, no. 1, pp. 46–63, 2020.
- [22] B. Hernández-Monjaraz, E. Santiago-Osorio, A. Monroy-García, E. Ledesma-Martínez, and V. Mendoza-Núñez, "Mesenchymal stem cells of dental origin for inducing tissue regeneration in periodontitis: a mini-review," *International Journal of Molecular Sciences*, vol. 19, no. 4, p. 944, 2018.
- [23] M. Yang, H. Zhang, and R. Gangolli, "Advances of mesenchymal stem cells derived from bone marrow and dental tissue in craniofacial tissue engineering," *Current Stem Cell Research & Therapy*, vol. 9, no. 3, pp. 150–161, 2014.
- [24] D. L. Alge, D. Zhou, L. L. Adams et al., "Donor-matched comparison of dental pulp stem cells and bone marrow-derived mesenchymal stem cells in a rat model," *Journal of Tissue Engineering and Regenerative Medicine*, vol. 4, no. 1, pp. 73–81, 2010.
- [25] R. C. Ransom, A. C. Carter, A. Salhotra et al., "Mechanoreponsive stem cells acquire neural crest fate in jaw regeneration," *Nature*, vol. 563, no. 7732, pp. 514–521, 2018.
- [26] Y.-L. Wang, A. Hong, T.-H. Yen, and H.-H. Hong, "Isolation of mesenchymal stem cells from human alveolar periosteum and effects of vitamin D on osteogenic activity of periosteum-derived cells," *Journal of Visualized Experiments*, vol. 135, article e57166, 2018.
- [27] O. D. de Lageneste, A. Julien, R. Abou-Khalil et al., "Periosteum contains skeletal stem cells with high bone regenerative potential controlled by periostin," *Nature Communications*, vol. 9, no. 1, 2018.
- [28] Z. Lin, A. Fateh, D. M. Salem, and G. Intini, "Periosteum," *Journal of Dental Research*, vol. 93, no. 2, pp. 109–116, 2013.
- [29] S. Mouraret, E. von Kaeppler, C. Bardet et al., "The potential for vertical bone regeneration via maxillary periosteal elevation," *Journal of Clinical Periodontology*, vol. 41, no. 12, pp. 1170–1177, 2014.
- [30] S. Debnath, A. R. Yallowitz, J. McCormick et al., "Discovery of a periosteal stem cell mediating intramembranous bone formation," *Nature*, vol. 562, no. 7725, pp. 133–139, 2018.
- [31] L. C. Ortinau, H. Wang, K. Lei et al., "Identification of functionally distinct Mx1+ $\alpha$ SMA+ periosteal skeletal stem cells," *Cell Stem Cell*, vol. 25, no. 6, pp. 784–796.e5, 2019.
- [32] S. O. Akintoye, T. Lam, S. Shi, J. Brahim, M. T. Collins, and P. G. Robey, "Skeletal site-specific characterization of orofacial and iliac crest human bone marrow stromal cells in same individuals," *Bone*, vol. 38, no. 6, pp. 758–768, 2006.
- [33] Y. Du, F. Jiang, Y. Liang et al., "The angiogenic variation of skeletal site-specific human BMSCs from same alveolar cleft

- patients: a comparative study," *Journal of Molecular Histology*, vol. 47, no. 2, pp. 153–168, 2016.
- [34] M. Kanawa, A. Igarashi, K. Fujimoto et al., "Genetic markers can predict chondrogenic differentiation potential in bone marrow-derived mesenchymal stromal cells," *Stem Cells International*, vol. 2018, Article ID 9530932, 9 pages, 2018.
- [35] T. Matsubara, K. Suardita, M. Ishii et al., "Alveolar bone marrow as a cell source for regenerative medicine: differences between alveolar and iliac bone marrow stromal cells," *Journal of Bone and Mineral Research*, vol. 20, no. 3, pp. 399–409, 2005.
- [36] B. O. Zhou, R. Yue, M. M. Murphy, J. G. Peyer, and S. J. Morrison, "Leptin-receptor-expressing mesenchymal stromal cells represent the main source of bone formed by adult bone marrow," *Cell Stem Cell*, vol. 15, no. 2, pp. 154–168, 2014.
- [37] D. L. Worthley, M. Churchill, J. T. Compton et al., "Gremlin 1 identifies a skeletal stem cell with bone, cartilage, and reticular stromal potential," *Cell*, vol. 160, no. 1–2, pp. 269–284, 2015.
- [38] C. K. F. Chan, E. Y. Seo, J. Y. Chen et al., "Identification and specification of the mouse skeletal stem cell," *Cell*, vol. 160, no. 1–2, pp. 285–298, 2015.
- [39] Y. Shi, G. He, W. C. Lee, J. A. McKenzie, M. J. Silva, and F. Long, "Gli1 identifies osteogenic progenitors for bone formation and fracture repair," *Nature Communications*, vol. 8, no. 1, p. 2043, 2017.
- [40] D. Zhang, S. Zhang, J. Wang et al., "LepR-expressing stem cells are essential for alveolar bone regeneration," *Journal of Dental Research*, no. article 002203452093283, 2020.
- [41] Z. Liu, X. Long, J. Li, L. Wei, Z. Gong, and W. Fang, "Differentiation of temporomandibular joint synovial mesenchymal stem cells into neuronal cells in vitro: an in vitro study," *Cell Biology International*, vol. 35, no. 1, pp. 87–91, 2011.
- [42] N. Koyama, Y. Okubo, K. Nakao, K. Osawa, K. Fujimura, and K. Bessho, "Pluripotency of mesenchymal cells derived from synovial fluid in patients with temporomandibular joint disorder," *Life Sciences*, vol. 89, no. 19–20, pp. 741–747, 2011.
- [43] E. Xiao, J. M. Li, Y. B. Yan et al., "Decreased osteogenesis in stromal cells from radiolucent zone of human TMJ ankylosis," *Journal of Dental Research*, vol. 92, no. 5, pp. 450–455, 2013.
- [44] Y. P. Sun, Y. H. Zheng, W. J. Liu, Y. L. Zheng, and Z. G. Zhang, "Synovium fragment-derived cells exhibit characteristics similar to those of dissociated multipotent cells in synovial fluid of the temporomandibular joint," *PLoS One*, vol. 9, no. 7, article e101896, 2014.
- [45] M. C. Embree, M. Chen, S. Pylawka et al., "Exploiting endogenous fibrocartilage stem cells to regenerate cartilage and repair joint injury," *Nature Communications*, vol. 7, no. 1, 2016.
- [46] T. Maruyama, J. Jeong, T. J. Sheu, and W. Hsu, "Stem cells of the suture mesenchyme in craniofacial bone development, repair and regeneration," *Nature Communications*, vol. 7, no. 1, 2016.
- [47] E. Durham, R. N. Howie, N. Larson, A. LaRue, and J. Cray, "Pharmacological exposures may precipitate craniosynostosis through targeted stem cell depletion," *Stem Cell Research*, vol. 40, p. 101528, 2019.
- [48] E. L. Durham, R. N. Howie, R. Houck et al., "Involvement of calvarial stem cells in healing: a regional analysis of large cranial defects," *Wound Repair and Regeneration*, vol. 26, no. 5, pp. 359–365, 2018.
- [49] D. H. Doro, A. E. Grigoriadis, and K. J. Liu, "Calvarial suture-derived stem cells and their contribution to cranial bone repair," *Frontiers in Physiology*, vol. 8, p. 956, 2017.
- [50] S. Park, H. Zhao, M. Urata, and Y. Chai, "Sutures possess strong regenerative capacity for calvarial bone injury," *Stem Cells and Development*, vol. 25, no. 23, pp. 1801–1807, 2016.
- [51] H. Zhao, J. Feng, T. V. Ho, W. Grimes, M. Urata, and Y. Chai, "The suture provides a niche for mesenchymal stem cells of craniofacial bones," *Nature Cell Biology*, vol. 17, no. 4, pp. 386–396, 2015.
- [52] K. Wilk, S. C. A. Yeh, L. J. Mortensen et al., "Postnatal calvarial skeletal stem cells expressing PRX1 reside exclusively in the calvarial sutures and are required for bone regeneration," *Stem Cell Reports*, vol. 8, no. 4, pp. 933–946, 2017.
- [53] S. O. Akintoye, "The distinctive jaw and alveolar bone regeneration," *Oral Diseases*, vol. 24, no. 1–2, pp. 49–51, 2018.
- [54] S. Gronthos, M. Mankani, J. Brahim, P. G. Robey, and S. Shi, "Postnatal human dental pulp stem cells (DPSCs) in vitro and in vivo," *Proceedings of the National Academy of Sciences of the United States of America*, vol. 97, no. 25, pp. 13625–13630, 2000.
- [55] M. Miura, S. Gronthos, M. Zhao et al., "SHED: stem cells from human exfoliated deciduous teeth," *Proceedings of the National Academy of Sciences of the United States of America*, vol. 100, no. 10, pp. 5807–5812, 2003.
- [56] B.-M. Seo, M. Miura, S. Gronthos et al., "Investigation of multipotent postnatal stem cells from human periodontal ligament," *Lancet*, vol. 364, no. 9429, pp. 149–155, 2004.
- [57] C. Morscheck, W. Götz, J. Schierholz et al., "Isolation of precursor cells (PCs) from human dental follicle of wisdom teeth," *Matrix Biology*, vol. 24, no. 2, pp. 155–165, 2005.
- [58] W. Sonoyama, Y. Liu, T. Yamaza et al., "Characterization of the apical papilla and its residing stem cells from human immature permanent teeth: a pilot study," *Journal of Endodontia*, vol. 34, no. 2, pp. 166–171, 2008.
- [59] E. Ikeda, K. Yagi, M. Kojima et al., "Multipotent cells from the human third molar: feasibility of cell-based therapy for liver disease," *Differentiation*, vol. 76, no. 5, pp. 495–505, 2008.
- [60] Q. Z. Zhang, W. R. Su, S. H. Shi et al., "Human gingiva-derived mesenchymal stem cells elicit polarization of m2 macrophages and enhance cutaneous wound healing," *Stem Cells*, vol. 28, no. 10, pp. 1856–1868, 2010.
- [61] E. Karaöz, B. N. Doğan, A. Aksoy et al., "Isolation and in vitro characterisation of dental pulp stem cells from natal teeth," *Histochemistry and Cell Biology*, vol. 133, no. 1, pp. 95–112, 2010.
- [62] S. Aydin and F. Sahin, "Stem cells derived from dental tissues," *Advances in Experimental Medicine and Biology*, vol. 1144, pp. 123–132, 2019.
- [63] F. M. Chen, L. N. Gao, B. M. Tian et al., "Treatment of periodontal intrabony defects using autologous periodontal ligament stem cells: a randomized clinical trial," *Stem Cell Research & Therapy*, vol. 7, no. 1, 2016.
- [64] L. Winning, I. A. El Karim, and F. T. Lundy, "A comparative analysis of the osteogenic potential of dental mesenchymal stem cells," *Stem Cells and Development*, vol. 28, no. 15, pp. 1050–1058, 2019.
- [65] M. Khoshhal, I. Amiri, and L. Gholami, "Comparison of in vitro properties of periodontal ligament stem cells derived from permanent and deciduous teeth," *Journal of Dental Research, Dental Clinics, Dental Prospects*, vol. 11, no. 3, pp. 140–148, 2017.
- [66] J. S. Song, S. O. Kim, S. H. Kim et al., "In vitro and in vivo characteristics of stem cells derived from the periodontal ligament



- of human deciduous and permanent teeth," *Tissue Engineering. Part A*, vol. 18, no. 19-20, pp. 2040–2051, 2012.
- [67] N. Liu, S. Shi, M. Deng et al., "High levels of  $\beta$ -catenin signaling reduce osteogenic differentiation of stem cells in inflammatory microenvironments through inhibition of the noncanonical Wnt pathway," *Journal of Bone and Mineral Research: the official journal of the American Society for Bone and Mineral Research*, vol. 26, no. 9, pp. 2082–2095, 2011.
- [68] B. Li, Y. Zhang, Q. Wang et al., "Periodontal ligament stem cells modulate root resorption of human primary teeth via Runx2 regulating RANKL/OPG system," *Stem Cells and Development*, vol. 23, no. 20, pp. 2524–2534, 2014.
- [69] H. Kato, Y. Taguchi, K. Tominaga, M. Umeda, and A. Tanaka, "Porphyromonas gingivalis LPS inhibits osteoblastic differentiation and promotes pro-inflammatory cytokine production in human periodontal ligament stem cells," *Archives of Oral Biology*, vol. 59, no. 2, pp. 167–175, 2014.
- [70] Q. Jia, W. Jiang, and L. Ni, "Down-regulated non-coding RNA (lncRNA-ANCR) promotes osteogenic differentiation of periodontal ligament stem cells," *Archives of Oral Biology*, vol. 60, no. 2, pp. 234–241, 2015.
- [71] L. Wang, F. Wu, Y. Song et al., "Long noncoding RNA related to periodontitis interacts with miR-182 to upregulate osteogenic differentiation in periodontal mesenchymal stem cells of periodontitis patients," *Cell Death & Disease*, vol. 7, no. 8, article e2327, 2016.
- [72] F. Cao, J. Zhan, X. Chen, K. Zhang, R. Lai, and Z. Feng, "miR-214 promotes periodontal ligament stem cell osteoblastic differentiation by modulating Wnt/ $\beta$ -catenin signaling," *Molecular Medicine Reports*, vol. 16, no. 6, pp. 9301–9308, 2017.
- [73] X. Gu, M. Li, Y. Jin, D. Liu, and F. Wei, "Identification and integrated analysis of differentially expressed lncRNAs and circRNAs reveal the potential ceRNA networks during PDLSC osteogenic differentiation," *BMC Genetics*, vol. 18, no. 1, p. 100, 2017.
- [74] Y. He, C. X. Jian, H. Y. Zhang et al., "Hypoxia enhances periodontal ligament stem cell proliferation via the MAPK signaling pathway," *Genetics and Molecular Research*, vol. 15, no. 4, 2016.
- [75] W. Yan, Y. Cao, H. Yang et al., "CB1 enhanced the osteo/dentinogenic differentiation ability of periodontal ligament stem cells via p38 MAPK and JNK in an inflammatory environment," *Cell Proliferation*, vol. 52, no. 6, article e12691, 2019.
- [76] X. Y. Xu, X. T. He, J. Wang et al., "Role of the P2X7 receptor in inflammation-mediated changes in the osteogenesis of periodontal ligament stem cells," *Cell Death & Disease*, vol. 10, no. 1, p. 20, 2019.
- [77] Y. Xu, C. Ren, X. Zhao, W. Wang, and N. Zhang, "microRNA-132 inhibits osteogenic differentiation of periodontal ligament stem cells via GDF5 and the NF- $\kappa$ B signaling pathway," *Pathology - Research and Practice*, vol. 215, no. 12, p. 152722, 2019.
- [78] R. Zhang, Q. Liang, W. Kang, and S. Ge, "Metformin facilitates the proliferation, migration, and osteogenic differentiation of periodontal ligament stem cells in vitro," *Cell Biology International*, vol. 44, no. 1, pp. 70–79, 2019.
- [79] Z. Chen and H. L. Liu, "Restoration of miR-1305 relieves the inhibitory effect of nicotine on periodontal ligament-derived stem cell proliferation, migration, and osteogenic differentiation," *Journal of Oral Pathology & Medicine*, vol. 46, no. 4, pp. 313–320, 2017.
- [80] T. K. Ng, L. Huang, D. Cao et al., "Cigarette smoking hinders human periodontal ligament-derived stem cell proliferation, migration and differentiation potentials," *Scientific Reports*, vol. 5, no. 1, p. 7828, 2015.
- [81] L. L. Ramenzoni, G. Russo, M. D. Moccia, T. Attin, and P. R. Schmidlin, "Periodontal bacterial supernatants modify differentiation, migration and inflammatory cytokine expression in human periodontal ligament stem cells," *PLoS One*, vol. 14, no. 7, article e0219181, 2019.
- [82] H. Roguljic, B. G. Matthews, W. Yang, H. Cvija, M. Mina, and I. Kalajzic, "In vivo identification of periodontal progenitor cells," *Journal of Dental Research*, vol. 92, no. 8, pp. 709–715, 2013.
- [83] X. Yuan, X. Pei, Y. Zhao, U. S. Tulu, B. Liu, and J. A. Helms, "A Wnt-responsive PDL population effectuates extraction socket healing," *Journal of Dental Research*, vol. 97, no. 7, pp. 803–809, 2018.
- [84] Y. Men, Y. Wang, Y. Yi et al., "Gli1+ periodontium stem cells are regulated by osteocytes and occlusal force," *Developmental Cell*, 2020.
- [85] B. S. Kim, S. J. Kim, H. J. Kim et al., "Effects of nicotine on proliferation and osteoblast differentiation in human alveolar bone marrow-derived mesenchymal stem cells," *Life Sciences*, vol. 90, no. 3-4, pp. 109–115, 2012.
- [86] N. Y. Naung, W. Duncan, R. D. Silva, and D. Coates, "Localization and characterization of human palatal periosteum stem cells in serum-free, xeno-free medium for clinical use," *European Journal of Oral Sciences*, vol. 127, no. 2, pp. 99–111, 2019.
- [87] F. Umrath, H. Steinle, M. Weber et al., "Generation of iPSCs from jaw periosteal cells using self-replicating RNA," *International Journal of Molecular Sciences*, vol. 20, no. 7, p. 1648, 2019.
- [88] T. H. Ambrosi, M. T. Longaker, and C. K. F. Chan, "A revised perspective of skeletal stem cell biology," *Frontiers in Cell and Development Biology*, vol. 7, p. 189, 2019.
- [89] P. Bianco and P. G. Robey, "Skeletal stem cells," *Development*, vol. 142, no. 6, pp. 1023–1027, 2015.
- [90] A. Rauch, A. K. Haakonsson, J. G. S. Madsen et al., "Osteogenesis depends on commissioning of a network of stem cell transcription factors that act as repressors of adipogenesis," *Nature Genetics*, vol. 51, no. 4, pp. 716–727, 2019.

## Review Article

# Mesenchymal Stem Cell-Derived Extracellular Vesicles and Their Therapeutic Potential

Ashley G. Zhao <sup>1</sup>, Kiran Shah <sup>1,2</sup>, Brett Cromer <sup>1</sup> and Huseyin Sumer <sup>1</sup>

<sup>1</sup>Department of Chemistry and Biotechnology, Faculty of Science, Engineering and Technology, Swinburne University of Technology, John St., Hawthorn VIC 3122, Australia

<sup>2</sup>Magellan Stem Cells P/L, 116-118 Thames St., Box Hill VIC 3129, Australia

Correspondence should be addressed to Huseyin Sumer; [hsumer@swin.edu.au](mailto:hsumer@swin.edu.au)

Received 30 June 2020; Revised 27 July 2020; Accepted 5 August 2020; Published 24 August 2020

Academic Editor: Cinzia Allegrucci

Copyright © 2020 Ashley G. Zhao et al. This is an open access article distributed under the Creative Commons Attribution License, which permits unrestricted use, distribution, and reproduction in any medium, provided the original work is properly cited.

Extracellular vesicles (EVs) are cell-derived membrane-bound nanoparticles, which act as shuttles, delivering a range of biomolecules to diverse target cells. They play an important role in maintenance of biophysiological homeostasis and cellular, physiological, and pathological processes. EVs have significant diagnostic and therapeutic potentials and have been studied both *in vitro* and *in vivo* in many fields. Mesenchymal stem cells (MSCs) are multipotent cells with many therapeutic applications and have also gained much attention as prolific producers of EVs. MSC-derived EVs are being explored as a therapeutic alternative to MSCs since they may have similar therapeutic effects but are cell-free. They have applications in regenerative medicine and tissue engineering and, most importantly, confer several advantages over cells such as lower immunogenicity, capacity to cross biological barriers, and less safety concerns. In this review, we introduce the biogenesis of EVs, including exosomes and microvesicles. We then turn more specifically to investigations of MSC-derived EVs. We highlight the great therapeutic potential of MSC-derived EVs and applications in regenerative medicine and tissue engineering.

## 1. Extracellular Vesicles

Extracellular vesicles (EVs) bearing nucleic acids, proteins, and lipids can be released into the extracellular space from eukaryotic cells, as well as from some prokaryotic cells [1]. These released EVs are lipid bilayer-bound nanoparticles and are found in many biological fluids such as serum, cerebrospinal fluid, saliva, urine, nasal secretions, and breast milk. They can also be collected in cell culture medium. Originally, EVs were regarded as cellular waste [2] but since have been shown to play important biological roles in cellular homeostasis and the spreading of biomolecules to neighbouring cells and tissues. Transported biomolecules can contribute to normal physiology or disease states or could be therapeutics to be delivered to damaged cells and tissues. For these reasons, EVs show significant potential in biotechnology [3–5]. Many different names have been used for extracellular vesicles, following several independent discoveries, which have led to confusing nomenclature. As the extracellular vesicle field has grown tremendously over the

past few decades, the International Society for Extracellular Vesicles (ISEV) was launched in 2011, with the aim of advancing extracellular vesicle research globally. The term “extracellular vesicles” (EVs) was introduced by ISEV to describe preparations of vesicles isolated from biofluids and cell cultures [3]. Based on their size and biogenesis, EVs could be classified into three main subclasses: exosomes (40–120 nm), microvesicles (50–1000 nm), and apoptotic bodies (500–2000 nm) [6]. Both microvesicles and apoptotic bodies are directly shed from the plasma membrane but via different cellular processes, whereas exosomes are generated by the endocytic pathway and are originally considered to play a particularly important role in cell-to-cell communication [7].

## 2. Exosomes

The term exosome was first used to describe membrane nanovesicles released from mammalian reticulocytes through the endosomal pathway in the 1980s [8–10]. Exosomes were

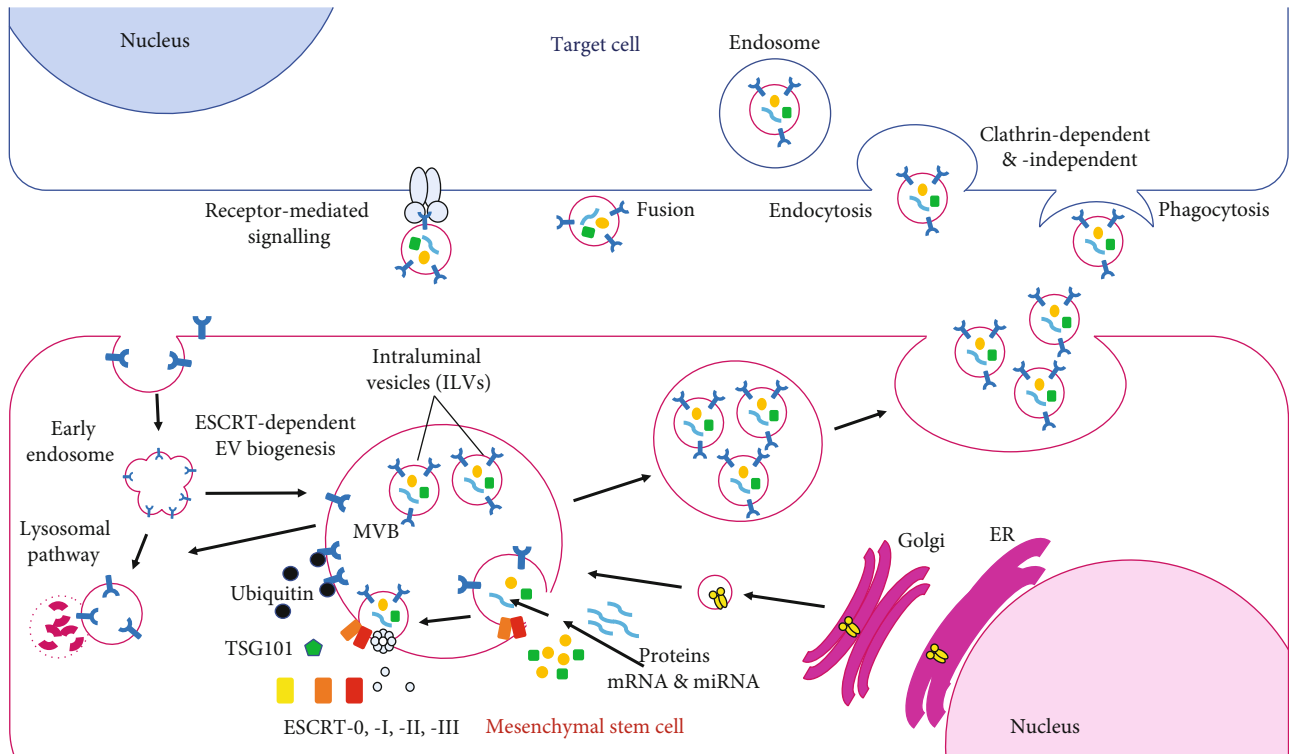


FIGURE 1: Extracellular vesicle biogenesis; ILVs invaginate from the outer endosomal membrane to bud into the lumen of endosomes through ESCRT-dependent/independent machineries during the maturation of MVB from the early endosome. Matured MVB is then transported to the cell periphery and fuses with the plasma membrane to release ILVs (exosomes). Exosomes together with microvesicles enter the target cells through signalling, fusion, and endocytosis pathways.

originally thought to be waste products released by cells. In the subsequent decades, further research identified that exosomes have an important function as transport vehicles and can act to stimulate immune suppression of tumor growth [11, 12]. One of the important discoveries in the field was the presence of nucleic acids-mRNA and miRNA in exosomes and hence the ability to alter specific gene expression and protein translation in recipient cells [13]. Today, exosomes are recognised to play an important role in intercellular communication through transfer of proteins, lipids, and nucleic acids into recipient cells [6, 14, 15] (Figure 1).

**2.1. Exosome Biogenesis.** Many cellular processes are involved in the generation of exosomes. These include the production of microvesicular bodies (MVBs) and formation of intraluminal vesicles (ILVs) during early endosomal maturation into MVBs. This is followed by trafficking and fusion of MVBs with the plasma membrane, releasing ILVs extracellularly as exosomes [16]. Several cellular mechanisms are involved in the formation of ILVs and maturation of MVBs, including the Endosomal Sorting Complex Required for Transport (ESCRT) which involves both ESCRT-dependent and ESCRT-independent transport mechanisms, described below.

The best-described mechanism for the formation of ILVs is the ESCRT-dependent machinery [17, 18]. ILVs are formed from early endosomes by the inward budding of the limiting membrane and then scission of the narrow neck to release the bud into the endosomal lumen as a vesicle. ESCRT

proteins sort ubiquitinated proteins into these buds [19]. The role of the four ESCRT complexes ESCRT-0, ESCRT-I, ESCRT-II, and ESCRT-III in the formation of ILVs in the interior of MVBs was well-described in the early 2000s [20–22]. The ESCRT-dependent mechanism starts from the interaction of the ESCRT-0 complex with ubiquitylated proteins, which are organized by clathrin into specialized endosomal subdomains [23]. Then, direct interaction between ESCRT-0 and TSG101 of the ESCRT-I complex recruits ESCRT-I and ESCRT-II and starts the inward budding of the ILVs into the lumen of the MVBs.

The ESCRT-I/ESCRT-II system is one core part of the ESCRT machinery, which functions as one branch of the ESCRT pathway to feed into ESCRT-III and the Vps4 scission machinery [19]. ESCRT-II recruits the ESCRT-III complex to develop a curved membrane-binding surface and line tubules extended away from the cytoplasm [24]. ESCRT-III also recruits the associated protein Alix for the recruitment of the deubiquitinating enzyme Doa4 [25]. Finally, ESCRT-associated proteins Vps4 and Vta1 cleave the ILV into free vesicles and disassemble ESCRT complexes [17]. Some ESCRT components and accessory proteins such as TSG101, HRS, and ALIX are retained in the ILVs and become important protein markers of exosomes. However, it is not clear whether they are specific markers for exosomes since ESCRT-I/II/III and their accessory molecules are associated with various other budding and membrane scission processes, such as microvesicle release, wound repair on the plasma membrane, neuron pruning, membrane abscission

in cytokinesis, nucleus envelope reformation, and cellular autophagy processes [19]. Alternatively, ESCRT-0 has been specifically implicated in exosome secretion and is not yet described in plasma membrane budding and scission processes. Therefore, ESCRT-0 components might be more specific markers to demonstrate endosomal origin [26].

Interestingly, ILVs can still form in MVBs via ESCRT-independent mechanisms [27]. Many studies suggest that ESCRT-independent mechanisms are involved in ILV formation and exosome biogenesis. The ESCRT-independent mechanisms involve lipids (ceramide, cholesterol, and PLD2), tetraspanins, syntenins, or heat-shock proteins [23, 28–31]. For example, depleted ESCRT subunits such as Hrs, TSG101, Alix, or Vps4 and exosomes enriched in protein-lipid protein (PLP) and CD63 were still secreted through a ceramide-dependent sorting mechanism [15, 27]. Even though many studies have described significant contributions to ILV formation pathways, exosome biogenesis is still not exhaustively studied. Therefore, since current knowledge of exosome biogenesis is not fully specific to exosome secretion and is also not shown in all cell types [26], further studies on exosome biogenesis are still needed.

Once late endosomes become fully mature MVBs, they are transported to the cell periphery and fuse with the plasma membrane to release ILVs as exosomes [1, 32, 33]. The mechanisms of MVB mobilization, docking, and fusion involve a large network of proteins, including the actin cytoskeleton, microtubules, and associated molecular motors such as kinesins and myosins, molecular switches (small GTPases), tethering factors, and SNARE proteins [7, 32, 34–38]. Proteins and protein complexes organise the tethers and work together with Rab proteins to direct the vesicle targeting [34]. The activated Rab proteins (Rab GTPases) such as Rab7, Rab11, Rab27, and related Ral-1 regulate vesicle formation, trafficking, and fusion. They control movement through interaction of the vesicles with cytoskeletal components, tethering/docking these vesicles to the cell periphery [32, 37, 39–41].

MVB trafficking requires actin and microtubule cytoskeletons and motor proteins to transport and tether MVBs to the plasma membrane [33]. After docking of MVBs to the plasma membrane, soluble N-ethylmaleimide-sensitive factor attachment protein receptors (SNAREs) regulate the fusion of the MVB lipid bilayer with the plasma membrane to release ILVs [36]. SNAREs are the core fusion engine in membrane fusion and are recycled after each fusion event [35]. SNARE proteins are classified into four subfamilies based on their SNARE motifs; Qa-, Qb-, Qc-(t-), and R- (v-) SNAREs, which are highly conserved and diverged early in eukaryotic evolution [42]. They are assembled in a *trans* configuration and formed as helical core complexes, mediated by the SNARE motifs. The assembly starts at the N termini of the SNARE motif followed by a zipper-like fashion towards the C-terminal membrane anchors. The function of SNARE complexes is to provide the mechanical force exerted on the membrane to proceed with the fusion of two lipid bilayers and then distort membranes to form a fusion pore releasing ILVs of MVBs into the extracellular environment as exosomes [35].

### 3. Microvesicles

Similar to exosomes, many types of machinery are involved in microvesicle biogenesis. Unlike exosome biogenesis which has been intensively studied, microvesicle biogenesis has only recently started to emerge as a focus of study [43]. Microvesicles, also classified as ectosomes, are directly generated from the plasma membrane [44]. Microvesicles are generated by the formation of outward buds in specific sites of the membrane and then released into the extracellular space by fission [45]. Several molecular rearrangements are involved including changes in lipid and protein composition and even  $\text{Ca}^{2+}$  level at the specific sites of the membrane to elicit membrane budding [46, 47].  $\text{Ca}^{2+}$  level changes alter the lipid composition of the plasma membrane, and the externalization of phosphatidylserine also plays a role in microvesicle formation [48].

Microvesicles have also been shown to be enriched in cholesterol and are raised from cholesterol-rich lipid rafts [49]. Furthermore, the depletion of cholesterol significantly reduces microvesicle shedding. Other factors such as molecular rearrangements in the plasma membrane, cell shape maintenance proteins, cytoskeletal elements, and their regulators are also involved in microvesicle biogenesis [50]. The regulators of actin dynamics, RhoA (a member of the small GTPases family), and its downstream-associated protein ROCK and LIM kinases are essential for microvesicle biogenesis [51]. A calcium-dependent enzyme, calpain, which regulates cytoskeletal proteins is involved in microvesicle shedding [52]. Inhibition of calpain could suppress PAK1/1 activation to decrease polymerization of actin, formation of filopodia, and furthermore interfere with the generation of microvesicles. ARF6 also plays a key role in microvesicle formation and shedding [53]. ARF6-GTP-dependent activation of phospholipase D recruits the extracellular signal-regulated kinase (ERK) to the plasma membrane, and then ERK phosphorylates and activates myosin light-chain kinase (MLCK) which is an important regulator of actin polymerization and myosin activity. This process is essential for microvesicle release, and inhibition of ARF6 could block microvesicle shedding. Both exosomes and microvesicles play important roles in physiological and pathological cellular processes.

### 4. EV Function

Endosomal exosomes were considered as the main mediators that affect recipient cells. However, it is difficult to efficiently separate exosomes from other subtypes of EVs by current isolation methods, so it is difficult to definitively assign a function to a particular type of vesicle. Furthermore, not only do the formation and secretion of ILVs employ multiple mechanisms, resulting in heterogeneous exosomes, but other EVs also overlap in their biophysical properties [54]. Moreover, there is currently no consensus on markers to distinguish exosomes from other EVs.

The techniques used to isolate small EVs result in a heterogeneous mix of sizes, origin, and molecular composition, with an unknown portion of them being exosomes [55]. Therefore, they may contain a mixture of endosomal and



nonendosomal small EVs [56] and even some nonvesicular molecules such as various dense lipoproteins [57]. Nevertheless, many studies have discovered a significant function of EVs to target cells and demonstrated their potential in many pathophysiological fields such as cancer, immune responses, various diseases, and regenerative therapeutics [5, 6]. Even though there are many studies that describe the function of exosomes, most of these studies may contain a mixture of EVs with different subtypes due to their preparation method, so the observed function, assigned to exosomes, may be elicited by multiple EV types [26].

EVs carry proteins, lipids, and nucleic acids and can be released by most cells and taken up by recipient cells to trigger various phenotypic effects [58]. The lipid bilayer of EVs can protect their content, transit through the extracellular fluid, and internalise into recipient cells. Different recipient cell types take up heterogeneous EVs through different pathways which are highly specialised and specific processes [59]. EVs bind to appropriate receptors on target cells through receptor-ligand interaction and enter these cells through three major EV uptake pathways: signalling, fusion, and endocytosis [43, 59].

Many studies have shown the diverse biological functions of EVs. EVs released by B lymphocytes present MHC-peptide complexes to specific T cells which suggested that EVs played a role in adaptive immune responses [60, 61]. Proteins and mRNAs of EVs can be transferred into target cells, and mRNAs can be translated into corresponding proteins [62]. For example, selective mRNAs and miRNAs were found in mast cell EVs and involved in the immune response [13].

Genetic communication between cells might also occur via the trafficking of EVs through the systemic circulation, similar to how hormones impact their recipient cells. EVs derived from stem cells play a pivotal role in tissue regeneration [63, 64]. EVs not only play important roles in many aspects of biology such as intercellular vesicle traffic, immunity, neurobiology, and microbiology but also have important roles in disease pathogenesis such as tumor progression, neurodegenerative propagation, and HIV and prion spread [6, 65]. For example, tumor cells can release EVs into the microenvironment to elicit tumor progression via numerous mechanisms such as promoting angiogenesis, suppressing immune responses, and tumor cell migration in metastases [65, 66]. More recently, mesenchymal stem cells have been shown to be prolific producers of EVs and have been investigated for their potential therapeutic applications.

## 5. Mesenchymal Stem Cells and EVs

Mesenchymal stem cells (MSCs) are multipotent stem cells derived from mesenchyme, which develops from the mesoderm [67]. MSCs are capable of self-renewal and differentiation into skeletal and connective tissues such as the bone, fat, cartilage, and muscle [68]. The main roles of resident MSCs in adults are self-repair and to maintain cellular tissue homeostasis. Due to their plastic adherence properties when cultured *in vitro*, MSCs can be easily isolated from various

organs and tissues such as the bone marrow, adipose tissue, muscle tissue, skin, teeth, periosteum, trabecular bone, synovium, skeletal tissues, brain, spleen, liver, kidney, thymus, pancreas, and blood vessels [68, 69]. MSCs are considered to be ideal candidates for tissue regeneration and tissue engineering, and interest in their biological roles and clinical potential has dramatically increased over the last three decades [70].

There are over two thousand clinical trials registered on ClinicalTrials.gov investigating therapeutic applications of MSCs in many diseases, such as bronchopulmonary dysplasia, multiple sclerosis, autoimmune diseases, Alzheimer's disease, liver diseases, osteoarthritis, kidney disease, myocardial infarction, and graft versus host disease. Initially, the therapeutic applications of MSCs were investigated to replace injured cells, based on their differentiation potential. However, less than 1% of the transplanted MSCs could reach the target tissue, such as the infarcted myocardium in treatment of myocardial infarction [71]. Nonetheless, MSCs restored heart function more rapidly compared to the slow and inefficient differentiation process of cardiomyocytes [72]. MSCs have also been shown to be effective in treating degenerative diseases such as osteoarthritis for both animals and humans [73, 74]. Furthermore, it has been demonstrated that MSCs can be effective in the modulation of immune responses, anti-inflammatory affect, tissue repair, and regeneration in many therapeutic applications *in vitro* and *in vivo*. Therefore, MSCs are proposed to exert their beneficial effects by paracrine secretion rather than from their differentiation [75, 76], for which most MSC clinical trials were rationalized. However, to date, none of the identified soluble secreted mediators alone are able to sufficiently mediate the MSC therapeutic effects [77]. Subsequently, many studies have shown that the paracrine effects of MSCs were mediated in part by the secretion of EVs [63, 78]. Thus, extracellular vesicles derived from MSCs might be a safer cell-free alternative to cell therapy [79]. More recently, the research focus on the mechanism of therapeutic action of MSCs, which was previously attributed to their differentiation and paracrine efficacy, has now focused on the role of EVs. MSC-derived EVs play an important role in the regulation of normal physiological, tissue regenerative, and pathological propagation processes, and MSCs are considered to be prolific producers of EVs when compared to other cell types [80].

MSC-derived EVs have been shown to contain at least 730 different proteins [81]. These proteins reflected both features of MSCs and EVs. For example, 53 proteins of MSC-derived EVs were related to self-renewal genes associated with MSCs, and 25 proteins were differentiation genes of MSCs. In their study, Kim et al. (2014) showed that MSC-derived EV proteins included not only surface markers of MSCs but also MSC-specific proteins involved in signalling pathways to facilitate self-renewal and differentiation. MSC-derived EVs also contain proteins associated with EV biogenesis, trafficking, docking, and fusion. Furthermore, EV proteins such as the surface receptor PDGFRB, EGFR, and PLAU; signalling molecules of RAS-MAPK, RHO, and CDC42 pathways; cell adhesion molecules; and additional MSC antigens are associated with promotion and

modulation of MSC therapeutic potential. These proteins may play a role in the efficacy of MSC-derived EVs in tissue repair and tissue regeneration. Even though EV miRNAs were estimated to be less than one copy per EV [82], some EVs might be enriched with certain miRNAs. 171 miRNAs were identified in MSC-derived EVs [83]. The most abundant 23 miRNAs could target 5481 genes to regulate many specific pathways and biological processes, such as miR-130a-3p and miR-199a, which induce cellular proliferation, promote angiogenesis, and inhibit apoptosis. Furthermore, the proteome of purified MSC exosomes as profiled by mass spectrometry and antibody arrays contains 938 unique gene products found in the exosome database website <http://exocarta.org> that encompass a wide range of biochemical and cellular processes including cellular communication, structure and mechanics, inflammation, exosome biogenesis, tissue repair and regeneration, and metabolism [84].

## 6. Therapeutic Applications of Mesenchymal Stem Cell-Derived Extracellular Vesicles

To date, the therapeutic potential of MSC-derived EVs has been studied in both animal models and various clinical applications for many disease areas, such as cardiovascular disease, acute kidney injury, liver disease, lung disease, cutaneous wound healing, and cancer suppression [72, 85–87]. EVs have also been tested as potential diagnostic tools, anti-tumor therapeutics, drug delivery vehicles, and vaccines [85, 88]. Here, we focus on the therapeutic potential of MSC-derived EVs in a number of applications in regenerative medicine.

One of the first reports of MSC-derived EVs was of those derived from human bone marrow MSCs. These EVs had a beneficial impact on tubular epithelial cells through delivering mRNA cargo to activate regenerative programmes and resulted in recovery from acute kidney injury *in vitro* and *in vivo* [89]. Furthermore, intravenous administration of human MSC-derived EVs had the same efficacy as MSCs themselves on the treatment of acute kidney injury by inhibiting apoptosis and stimulating tubular cell proliferation in a rat model [86]. They also protected the kidney from the development of chronic injury, which highlights the potential of MSC-derived EVs for regenerative medicine.

Recent studies include the use of MSC-derived EVs for the treatment of a number of neuropathological diseases, such as multiple sclerosis [90] and Alzheimer's disease [91]. In a mouse model of multiple sclerosis, the mice were treated with saline, placenta MSCs, and low-dose ( $1.0 \times 10^7$ ) or high-dose ( $1.0 \times 10^{10}$ ) human placenta MSC-derived EVs. [90]. Both MSCs and MSC-derived EVs showed regenerative effects and prevented oligodendroglia degradation and demyelination, resulting in motor function improvement. Importantly, animals treated with high-dose MSC-derived EVs or MSCs showed similar clinical outcomes, demonstrating that MSC-derived EVs possess the same therapeutic potential as MSCs. Another preclinical study showed that MSC-derived EVs could be a therapeutic strategy for the treatment of currently incurable Alzheimer's disease [91].

After 28 days of injection of  $10 \mu\text{g}$  EVs and  $1 \times 10^6$  MSCs separately into two groups of mice with induced Alzheimer's disease, both groups had similar beneficial effects in improvement of neurogenesis and cognitive function.

MSC-derived EVs are capable of reducing the infarct size of myocardial injury through modulating the injured tissue environment, inducing angiogenesis, promoting proliferation, and preventing apoptosis [63]. The therapeutic effects of MSC-derived EVs on myocardial infarction have been demonstrated in a mouse model [92]. MSC-derived EVs could reduce infarct size to preserve cardiac function for an extended period through rapid activation of multiple cardioprotective pathways.

The function of MSC EVs in cartilage repair has been studied by investigation of the effects of human MSC-derived EVs on chondrocyte survival *in vitro* [93]. The chondrocytes could quickly endocytose the labelled MSC-derived EVs and rapidly phosphorylate AKT and ERK in chondrocytes within 1 hour to elicit the cellular proliferation of chondrocytes. MSC-derived EVs enhanced regeneration of the damaged cartilage through inducing proliferation, migration, and matrix synthesis of chondrocytes, attenuating apoptosis and modulating immune reactivity. Furthermore, intra-articular injection of  $100 \mu\text{g}/100 \mu\text{l}$  of embryonic MSC-derived EVs could efficiently repair osteochondral defects in a rat model [94]. The results from the MSC-derived EV treatment group showed hyaline cartilage regeneration by the end of 12 weeks. In contrast, the defects of controls treated with PBS were filled with fibrous and noncartilaginous tissue. Additionally, there were no adverse inflammatory responses in this experiment. In a preclinical study, the efficacy of MSC-derived EVs secreted from synovial membrane was compared to induced MSC-derived EVs in the treatment of mouse osteoarthritis (OA) [95]. Intra-articular injection of only  $8 \mu\text{l}$  of EVs ( $1.0 \times 10^{10}/\text{ml}$ ), from either source, into collagenase-induced OA mice attenuated OA. MSC-derived EVs showed a more significant effect than synovial membrane MSC-derived EVs. Furthermore, EVs from adipose tissue-derived MSCs could repair damaged cartilage through increasing the proliferation and migration of chondrocytes in a rat model of OA [96]. These numerous studies demonstrate the possibility of treating chronic conditions with MSC-derived EVs to address current unmet medical needs.

### 6.1. Alternate Therapeutic Delivery Methods of MSC-Derived EVs.

As researchers have begun to unlock the therapeutic potential of MSC-derived EVs in the field of regenerative medicine, alternate delivery methods are being explored. These include the encapsulation of EVs in hydrogels or incorporation into biodegradable scaffolds such as polylactide (PLA) and polyethyleneimine (PEI). These methodologies represent ways of cell-free delivery methods with the benefits of MSCs, which can be sustained over long periods of time.

Hydrogels are a 3D network of polymers with hydrophilic properties that can swell in an aqueous solution and absorb biologic fluids and therefore have the potential to act as delivery vectors in tissue engineering. A biodegradable hydrogel was used to encapsulate ES cell-differentiated MSC-

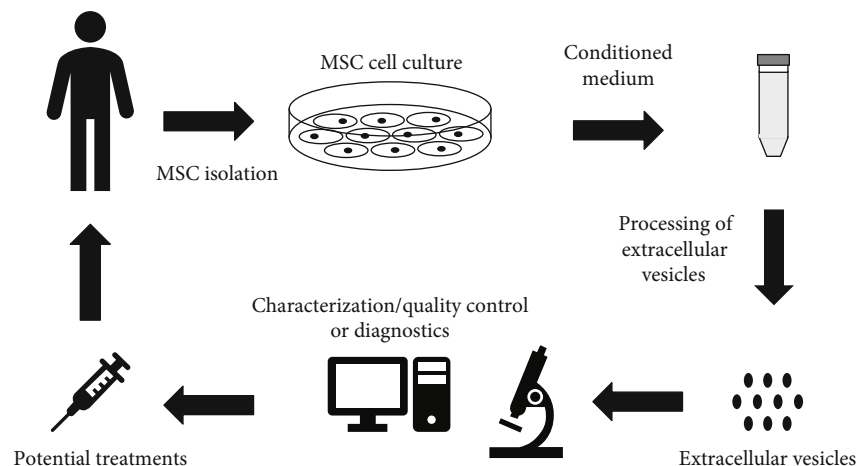


FIGURE 2: Workflow of MSC-derived EVs for therapeutic and diagnostic applications. MSCs can be isolated from patients from a variety of tissues. MSCs are cultured *in vitro*, and the conditioned culture medium is collected and subjected to extracellular vesicle isolation and/or purification. The isolated MSC-derived EVs can be used for diagnostic purposes or undergo quality control before being used in autologous and/or allogeneic therapeutics.

derived EVs in a rat hepatic regeneration model [97]. The EVs were encapsulated in PEG hydrogels, which acted as a sustained-release EV depot to treat liver disease in rats [97]. The MSC-derived EV-laden hydrogels could gradually release EVs and result in accumulation in the liver for one month, compared to 24-hour clearance after conventional bolus injection. This study not only demonstrated the anti-apoptosis, antifibrosis, and regenerative properties of MSC-derived EVs but also demonstrated a sustained systemic delivery method which could be employed for treatment of a variety of diseases.

Alternatively, EVs can be incorporated into solid 3D scaffolds when modelling structures such as bone. In a rat model of calvaria bone tissue damage, MSC-derived EVs were delivered on 3D PLA and PEI scaffolds to determine their ability to repair bone lesions [98]. Human MSCs, MSC-derived EVs, and 3D PLA or PEI-engineered EVs were evaluated in a number of combinations for their capability for bone defect regeneration *in vitro* and *in vivo*. It was found that there was more host tissue in-growth in the implant of 3D-PLA+MSC EV and 3D-PLA+EV+MSC samples than 3D-printed PLA scaffolds only and 3D-PLA+MSC samples. Abundant ECM, formation of nodules, and visible blood vessels in 3D-PLA+MSC EV, 3D-PLA+EV+MSC, 3D-PLA+PEI-EV, and 3D-PLA+PEI-EV+MSC samples were reported. This finding demonstrates that MSC-derived EVs could contribute to osteogenic regeneration, improve the mineralization process, and develop an extensive vascular network. Furthermore, the calvarial bone defect was completely repaired in 3D-PLA+EV+MSC, 3D-PLA+PEI-EV, and 3D-PLA+PEI-EV+MSC samples when evaluated for up to 16 weeks, which demonstrates the potential of MSC-derived tissue engineering for the treatment of bone defects. In another study on cartilage regeneration, MSC-derived EVs were evaluated using 3D-printed ECM and Gelatin-Methacryloyl (GelMA) hydrogels in a rabbit OA model [99]. The 3D-printed ECM/GelMA/EV scaffold had the best therapeutic effect in cartilage regeneration when compared to 3D-printed GelMA and 3D-printed

ECM/GelMA scaffolds. The defect region with the 3D-printed radially oriented ECM/GelMA/EVs had facilitated cartilage regeneration and repaired tissue with a mixture of fibrocartilage and hyaline-like cartilage. These studies suggest a promising application of MSC-derived EVs in 3D printing for tissue engineering of bone and cartilage.

**6.2. Clinical Trials Using MSC-Derived EVs.** Overall, MSC-derived EVs have been evaluated for their therapeutic potential for the treatment of various diseases both *in vitro* and in animal models. Based on these results and findings, a number of clinical trials have begun to evaluate the therapeutic potential of MSC-derived EVs for the treatment of particular diseases and the procedure similar as in Figure 2. Using the key search words of “exosomes” and “extracellular vesicles” in the clinical trials website (<https://clinicaltrials.gov/>) reveals 172 and 51 registered clinical trials, respectively. Although some of these studies include MSC-derived EVs, very few clinical studies have been published. MSC-derived EVs have improved therapy-refractory graft-versus-host disease (GvHD) in patients [80]. These MSC-derived EVs were isolated from allogeneic MSC-cultured medium and delivered to steroid-refractory GvHD patients in escalating doses. The clinical GvHD symptoms significantly declined shortly after the start of MSC-derived EV treatment. The GvHD patients were stable and had no side effects. Another clinical trial displayed efficacy outcomes using EVs derived from umbilical cord MSCs to treat chronic kidney disease [100]. These results demonstrated that MSC-derived EVs could safely improve the inflammatory immune reaction and overall kidney function in chronic kidney disease patients through MSC EV administration in two doses, the first intravenous and the second intra-arterial.

Based on the preclinical and clinical studies, human MSC-derived EVs are considered as promising products in regenerative medicine and tissue engineering. Many studies have compared the beneficial effects of MSCs and MSC-derived EVs and showed that they had similar therapeutic



outcomes. This indicates that MSC-derived EVs possess the same therapeutic potential as MSCs. The use of MSC-derived EVs might serve as an alternative, cell-free therapy over MSC transplantation for tissue regeneration [81] and have “off-the-shelf” therapeutic potential. Furthermore, clinical applications of MSC-derived EVs are advantageous over MSC cell-based therapy, as they have lower immunogenicity, capacity to cross biological barriers, and less safety concerns, such as the possibility of MSC differentiation or tumor generation [88, 101, 102]. The preclinical results using MSC EVs in tissue engineering have given exciting promise to their use as powerful tools as therapies to tackle a wide range of unmet disease burden.

Despite the progress in the field, the EV isolation method may yield different EV subtypes as they coexist but may differ in their functional properties [103]. The heterogeneity of MSCs which include tri-, bi-, and unipotent populations [104] needs to be addressed as they may impact on therapeutic outcomes of trials using EVs derived from different MSC populations. Not only are EVs highly heterogeneous, but they also have shown to result in various outcomes; stressed MSCs cultured in serum-deprived media secrete tumor-supportive EVs [105], and therefore, some caution is advised when using MSC-derived EVs for regenerative applications and more research is required. It should also be noted that some of the clinical studies have been terminated without publication. Furthermore, some experiments have demonstrated better results when using MSCs and MSC-derived EVs together, compared to the cells or EVs alone [90, 98]. Other considerations include the dose requirement, as some studies required higher doses of EVs or multidose injections to achieve significant therapeutic outcome [90, 100]. Another shortcoming is the half-life of EVs. Cellular therapies using MSCs are able to continuously release the beneficial paracrine factors (including EVs), while EVs have a relatively short half-life and therefore might be unable to retain sufficient levels present at the defect region [103]. However, this drawback might be offset by using alternate delivery methods such as bioengineered scaffolds, such as PEI, encapsulation with PEG hydrogels, or GelMA to maintain the sustained release of the MSC-derived EVs [97–99]. These bioengineering techniques for EV delivery might open up new avenues for therapeutic application.

Along with rapid development of the EV field, MSC-derived EVs have gained significant attention for their use in regenerative medicine. MSC-derived EVs bearing proteins, lipids, and RNAs could impact the target cells to exert their therapeutic effects. The cellular fate of EVs is still not well understood [26], and many questions of MSC-derived EV biodistribution are unanswered. Furthermore, the therapeutic mechanism of MSC-derived EVs still remains elusive [106]. Many MSC-derived EV studies *in vitro* and *in vivo* have verified that they are capable of enhancing tissue repair and mediating regeneration in various diseases and enhancing therapeutic outcomes. MSC-derived EVs have the theoretical advantages of being a safer regenerative tool when compared to cell-based therapies. However, we are in the early stage of using MSC-derived EVs in regenerative medicine. Standardised techniques for culture conditions and

large-scale culturing, effective isolation, optimal dosing, and safe storage need to be methodically determined before large-scale clinical applications. We believe that MSC-derived EVs hold great promise in cell-free therapy, with the potential to be applied in a wide range of diseases.

## Conflicts of Interest

The authors have no conflicts of interest.

## Acknowledgments

This research is supported by an Australian Government Research Training Program (RTP) Scholarship.

## References

- [1] M. Colombo, G. Raposo, and C. Thery, “Biogenesis, secretion, and intercellular interactions of exosomes and other extracellular vesicles,” *Annual Review of Cell and Developmental Biology*, vol. 30, no. 1, pp. 255–289, 2014.
- [2] R. M. Johnstone, M. Adam, J. R. Hammond, L. Orr, and C. Turbide, “Vesicle formation during reticulocyte maturation-association of plasma-membrane activities with released vesicles (exosomes),” *Journal of Biological Chemistry*, vol. 262, no. 19, pp. 9412–9420, 1987.
- [3] S. J. Gould and G. Raposo, “As we wait: coping with an imperfect nomenclature for extracellular vesicles,” *Journal of Extracellular Vesicles*, vol. 2, no. 1, 2013.
- [4] P. D. Stahl and G. Raposo, “Extracellular vesicles: exosomes and microvesicles, integrators of homeostasis,” *Physiology*, vol. 34, no. 3, pp. 169–177, 2019.
- [5] M. Yáñez-Mó, P. R.-M. Siljander, Z. Andreu et al., “Biological properties of extracellular vesicles and their physiological functions,” *Journal of Extracellular Vesicles*, vol. 4, no. 1, 2015.
- [6] S. E. L. Andaloussi, I. Mäger, X. O. Breakefield, and M. J. A. Wood, “Extracellular vesicles: biology and emerging therapeutic opportunities,” *Nature Reviews Drug Discovery*, vol. 12, no. 5, pp. 347–357, 2013.
- [7] G. Raposo and W. Stoorvogel, “Extracellular vesicles: exosomes, microvesicles, and friends,” *Journal of Cell Biology*, vol. 200, no. 4, pp. 373–383, 2013.
- [8] B. T. Pan and R. M. Johnstone, “Fate of the transferrin receptor during maturation of sheep reticulocytes *in vitro*: selective externalization of the receptor,” *Cell*, vol. 33, no. 3, pp. 967–978, 1983.
- [9] C. Harding, J. Heuser, and P. Stahl, “Endocytosis and intracellular processing of transferrin and colloidal gold-transferrin in rat reticulocytes: demonstration of a pathway for receptor shedding,” *European Journal of Cell Biology*, vol. 35, no. 2, pp. 256–263, 1984.
- [10] B. T. Pan, K. Teng, C. Wu, M. Adam, and R. M. Johnstone, “Electron-microscopic evidence for externalization of the transferrin receptor in vesicular form in sheep reticulocytes,” *Journal of Cell Biology*, vol. 101, no. 3, pp. 942–948, 1985.
- [11] G. Raposo, H. W. Nijman, W. Stoorvogel et al., “B lymphocytes secrete antigen-presenting vesicles,” *Journal of Experimental Medicine*, vol. 183, no. 3, pp. 1161–1172, 1996.
- [12] L. Zitvogel, A. Regnault, A. Lozier et al., “Eradication of established murine tumors using a novel cell-free vaccine:



- dendritic cell derived exosomes,” *Nature Medicine*, vol. 4, no. 5, pp. 594–600, 1998.
- [13] H. Valadi, K. Ekström, A. Bossios, M. Sjöstrand, J. J. Lee, and J. O. Lötvall, “Exosome-mediated transfer of mRNAs and microRNAs is a novel mechanism of genetic exchange between cells,” *Nature Cell Biology*, vol. 9, no. 6, pp. 654–659, 2007.
- [14] S. Mathivanan, H. Ji, and R. J. Simpson, “Exosomes: extracellular organelles important in intercellular communication,” *Journal of Proteomics*, vol. 73, no. 10, pp. 1907–1920, 2010.
- [15] M. Simons and G. Raposo, “Exosomes - vesicular carriers for intercellular communication,” *Current Opinion in Cell Biology*, vol. 21, no. 4, pp. 575–581, 2009.
- [16] N. P. Hessvik and A. Llorente, “Current knowledge on exosome biogenesis and release,” *Cellular and Molecular Life Sciences*, vol. 75, no. 2, pp. 193–208, 2018.
- [17] P. I. Hanson and A. Cashikar, “Multivesicular body morphogenesis,” *Annual Review of Cell and Developmental Biology*, vol. 28, no. 1, pp. 337–362, 2012.
- [18] J. H. Hurley, “ESCRT complexes and the biogenesis of multivesicular bodies,” *Current Opinion in Cell Biology*, vol. 20, no. 1, pp. 4–11, 2008.
- [19] J. H. Hurley, “ESCRTs are everywhere,” *EMBO Journal*, vol. 34, no. 19, pp. 2398–2407, 2015.
- [20] D. J. Katzmann, C. J. Stefan, M. Babst, and S. D. Emr, “Vps27 recruits ESCRT machinery to endosomes during MVB sorting,” *Journal of Cell Biology*, vol. 162, no. 3, pp. 413–423, 2003.
- [21] M. Babst, D. J. Katzmann, W. B. Snyder, B. Wendland, and S. D. Emr, “Endosome-associated complex, ESCRT-II, recruits transport machinery for protein sorting at the multivesicular body,” *Developmental Cell*, vol. 3, no. 2, pp. 283–289, 2002.
- [22] D. J. Katzmann, M. Babst, and S. D. Emr, “Ubiquitin-dependent sorting into the multivesicular body pathway requires the function of a conserved endosomal protein sorting complex, ESCRT-I,” *Cell*, vol. 106, no. 2, pp. 145–155, 2001.
- [23] R. C. Piper and D. J. Katzmann, “Biogenesis and function of multivesicular bodies,” *Annual Review of Cell and Developmental Biology*, vol. 23, no. 1, pp. 519–547, 2007.
- [24] P. I. Hanson, R. Roth, Y. Lin, and J. E. Heuser, “Plasma membrane deformation by circular arrays of ESCRT-III protein filaments,” *Journal of Cell Biology*, vol. 180, no. 2, pp. 389–402, 2008.
- [25] W. M. Henne, N. J. Buchkovich, and S. D. Emr, “The ESCRT pathway,” *Developmental Cell*, vol. 21, no. 1, pp. 77–91, 2011.
- [26] M. Mathieu, L. Martin-Jaular, G. Lavieu, and C. Théry, “Specificities of secretion and uptake of exosomes and other extracellular vesicles for cell-to-cell communication,” *Nature Cell Biology*, vol. 21, no. 1, pp. 9–17, 2019.
- [27] F. M. Goni and A. Alonso, “Biophysics of sphingolipids I. Membrane properties of sphingosine, ceramides and other simple sphingolipids,” *Biochimica et Biophysica Acta (BBA) - Biomembranes*, vol. 1758, no. 12, pp. 1902–1921, 2006.
- [28] J. Kowal, M. Tkach, and C. Théry, “Biogenesis and secretion of exosomes,” *Current Opinion in Cell Biology*, vol. 29, pp. 116–125, 2014.
- [29] K. Trajkovic, C. Hsu, S. Chiantia et al., “Ceramide triggers budding of exosome vesicles into multivesicular endosomes,” *Science*, vol. 319, no. 5867, pp. 1244–1247, 2008.
- [30] G. van Niel, S. Charrin, S. Simoes et al., “The tetraspanin CD63 regulates ESCRT-independent and -dependent endosomal sorting during melanogenesis,” *Developmental Cell*, vol. 21, no. 4, pp. 708–721, 2011.
- [31] M. F. Baietti, Z. Zhang, E. Mortier et al., “Syndecan-syntenin-ALIX regulates the biogenesis of exosomes,” *Nature Cell Biology*, vol. 14, no. 7, pp. 677–685, 2012.
- [32] V. Hyenne, A. Apaydin, D. Rodriguez et al., “RAL-1 controls multivesicular body biogenesis and exosome secretion,” *Journal of Cell Biology*, vol. 211, no. 1, pp. 27–37, 2015.
- [33] E. Granger, G. McNee, V. Allan, and P. Woodman, “The role of the cytoskeleton and molecular motors in endosomal dynamics,” *Seminars in Cell & Developmental Biology*, vol. 31, pp. 20–29, 2014.
- [34] H. Cai, K. Reinisch, and S. Ferro-Novick, “Coats, tethers, Rabs, and SNAREs work together to mediate the intracellular destination of a transport vesicle,” *Developmental Cell*, vol. 12, no. 5, pp. 671–682, 2007.
- [35] R. Jahn and R. H. Scheller, “SNAREs - engines for membrane fusion,” *Nature Reviews Molecular Cell Biology*, vol. 7, no. 9, pp. 631–643, 2006.
- [36] K. Essandoh and G.-C. Fan, “Chapter 1 - insights into the mechanism of exosome formation and secretion A2 - Tang, Yaoliang,” in *Mesenchymal Stem Cell Derived Exosomes*, B. Dawn, Ed., pp. 1–19, Academic Press, Boston, MA, USA, 2015.
- [37] M. Zerial and H. McBride, “Rab proteins as membrane organizers,” *Nature Reviews Molecular Cell Biology*, vol. 2, no. 2, pp. 107–117, 2001.
- [38] H. Stenmark, “Rab GTPases as coordinators of vesicle traffic,” *Nature Reviews Molecular Cell Biology*, vol. 10, no. 8, pp. 513–525, 2009.
- [39] A. Savina, M. Vidal, and M. I. Colombo, “The exosome pathway in K562 cells is regulated by Rab11,” *Journal of Cell Science*, vol. 115, no. 12, pp. 2505–2515, 2002.
- [40] C. Hsu, Y. Morohashi, S. I. Yoshimura et al., “Regulation of exosome secretion by Rab35 and its GTPase-activating proteins TBC1D10A-C,” *Journal of Cell Biology*, vol. 189, no. 2, pp. 223–232, 2010.
- [41] M. Ostrowski, N. B. Carmo, S. Krumeich et al., “Rab27a and Rab27b control different steps of the exosome secretion pathway,” *Nature Cell Biology*, vol. 12, no. 1, pp. 19–30, 2010.
- [42] D. Fasshauer, R. B. Sutton, A. T. Brunger, and R. Jahn, “Conserved structural features of the synaptic fusion complex: SNARE proteins reclassified as Q- and R-SNAREs,” *Proceedings of the National Academy of Sciences of the United States of America*, vol. 95, no. 26, pp. 15781–15786, 1998.
- [43] G. van Niel, G. D’Angelo, and G. Raposo, “Shedding light on the cell biology of extracellular vesicles,” *Nature Reviews Molecular Cell Biology*, vol. 19, no. 4, pp. 213–228, 2018.
- [44] H. F. G. Heijnen, A. E. Schiel, R. Fijnheer, H. J. Geuze, and J. J. Sixma, “Activated platelets release two types of membrane vesicles: microvesicles by surface shedding and exosomes derived from exocytosis of multivesicular bodies and alpha-granules,” *Blood*, vol. 94, no. 11, pp. 3791–3799, 1999.
- [45] J. Ratajczak, M. Wysoczynski, F. Hayek, A. Janowska-Wieczorek, and M. Z. Ratajczak, “Membrane-derived microvesicles: important and underappreciated mediators of cell-to-cell communication,” *Leukemia*, vol. 20, no. 9, pp. 1487–1495, 2006.

- [46] A. Piccin, W. G. Murphy, and O. P. Smith, "Circulating microparticles: pathophysiology and clinical implications," *Blood Reviews*, vol. 21, no. 3, pp. 157–171, 2007.
- [47] E. Pap, É. Pállinger, M. Pásztói, and A. Falus, "Highlights of a new type of intercellular communication: microvesicle-based information transfer," *Inflammation Research*, vol. 58, no. 1, pp. 1–8, 2009.
- [48] K. Al-Nedawi, B. Meehan, and J. Rak, "Microvesicles: messengers and mediators of tumor progression," *Cell Cycle*, vol. 8, no. 13, pp. 2014–2018, 2009.
- [49] I. del Conde, C. N. Shrimpton, P. Thiagarajan, and J. A. López, "Tissue-factor-bearing microvesicles arise from lipid rafts and fuse with activated platelets to initiate coagulation," *Blood*, vol. 106, no. 5, pp. 1604–1611, 2005.
- [50] V. R. Minciacchi, M. R. Freeman, and D. Di Vizio, "Extracellular vesicles in cancer: exosomes, microvesicles and the emerging role of large oncosomes," *Seminars in Cell & Developmental Biology*, vol. 40, pp. 41–51, 2015.
- [51] B. Li, M. A. Antonyak, J. Zhang, and R. A. Cerione, "RhoA triggers a specific signaling pathway that generates transforming microvesicles in cancer cells," *Oncogene*, vol. 31, no. 45, pp. 4740–4749, 2012.
- [52] M. Crespin, C. Vidal, F. Picard, C. Lacombe, and M. Fontenay, "Activation of PAK1/2 during the shedding of platelet microvesicles," *Blood Coagulation & Fibrinolysis*, vol. 20, no. 1, pp. 63–70, 2009.
- [53] V. Muralidharan-Chari, J. Clancy, C. Plou et al., "ARF6-regulated shedding of tumor cell-derived plasma membrane microvesicles," *Current Biology*, vol. 19, no. 22, pp. 1875–1885, 2009.
- [54] B. Mateescu, E. J. K. Kowal, B. W. M. van Balkom et al., "Obstacles and opportunities in the functional analysis of extracellular vesicle RNA - an ISEV position paper," *Journal of Extracellular Vesicles*, vol. 6, no. 1, 2017.
- [55] K. W. Witwer, E. I. Buzás, L. T. Bemis et al., "Standardization of sample collection, isolation and analysis methods in extracellular vesicle research," *Journal of Extracellular Vesicles*, vol. 2, no. 1, 2013.
- [56] J. Kowal, G. Arras, M. Colombo et al., "Proteomic comparison defines novel markers to characterize heterogeneous populations of extracellular vesicle subtypes," *Proceedings of the National Academy of Sciences of the United States of America*, vol. 113, no. 8, pp. E968–E977, 2016.
- [57] N. Karimi, A. Cvjetkovic, S. C. Jang et al., "Detailed analysis of the plasma extracellular vesicle proteome after separation from lipoproteins," *Cellular and Molecular Life Sciences*, vol. 75, no. 15, pp. 2873–2886, 2018.
- [58] G. Raposo and P. D. Stahl, "Extracellular vesicles: a new communication paradigm?," *Nature Reviews Molecular Cell Biology*, vol. 20, no. 9, pp. 509–510, 2019.
- [59] L. A. Mulcahy, R. C. Pink, and D. R. F. Carter, "Routes and mechanisms of extracellular vesicle uptake," *Journal of Extracellular Vesicles*, vol. 3, no. 1, 2014.
- [60] A. Bobrie, M. Colombo, G. Raposo, and C. Théry, "Exosome secretion: molecular mechanisms and roles in immune responses," *Traffic*, vol. 12, no. 12, pp. 1659–1668, 2011.
- [61] C. Théry, M. Ostrowski, and E. Segura, "Membrane vesicles as conveyors of immune responses," *Nature Reviews Immunology*, vol. 9, no. 8, pp. 581–593, 2009.
- [62] J. Ratajczak, K. Miekus, M. Kucia et al., "Embryonic stem cell-derived microvesicles reprogram hematopoietic progenitors: evidence for horizontal transfer of mRNA and protein delivery," *Leukemia*, vol. 20, no. 5, pp. 847–856, 2006.
- [63] R. C. Lai, F. Arslan, M. M. Lee et al., "Exosome secreted by MSC reduces myocardial ischemia/reperfusion injury," *Stem Cell Research*, vol. 4, no. 3, pp. 214–222, 2010.
- [64] M. Z. Ratajczak, M. Kucia, T. Jadczyk et al., "Pivotal role of paracrine effects in stem cell therapies in regenerative medicine: can we translate stem cell-secreted paracrine factors and microvesicles into better therapeutic strategies?," *Leukemia*, vol. 26, no. 6, pp. 1166–1173, 2012.
- [65] H. Haga, I. K. Yan, K. Takahashi, J. Wood, A. Zubair, and T. Patel, "Tumour cell-derived extracellular vesicles interact with mesenchymal stem cells to modulate the microenvironment and enhance cholangiocarcinoma growth," *Journal of Extracellular Vesicles*, vol. 4, no. 1, article 24900, 2015.
- [66] J. Rak and A. Guha, "Extracellular vesicles - vehicles that spread cancer genes," *BioEssays*, vol. 34, no. 6, pp. 489–497, 2012.
- [67] F. P. Barry and J. M. Murphy, "Mesenchymal stem cells: clinical applications and biological characterization," *International Journal of Biochemistry and Cell Biology*, vol. 36, no. 4, pp. 568–584, 2004.
- [68] P. Bianco, "Mesenchymal stem cells," *Annual Review of Cell and Developmental Biology*, vol. 30, no. 1, pp. 677–704, 2014.
- [69] L. da Silva Meirelles, P. C. Chagastelles, and N. B. Nardi, "Mesenchymal stem cells reside in virtually all post-natal organs and tissues," *Journal of Cell Science*, vol. 119, no. 11, pp. 2204–2213, 2006.
- [70] A. Klimczak and U. Kozłowska, "Mesenchymal stromal cells and tissue-specific progenitor cells: their role in tissue homeostasis," *Stem Cells International*, vol. 2016, Article ID 4285215, 11 pages, 2016.
- [71] I. M. Barbash, P. Chouraqui, J. Baron et al., "Systemic delivery of bone marrow-derived mesenchymal stem cells to the infarcted myocardium," *Circulation*, vol. 108, no. 7, pp. 863–868, 2003.
- [72] R. C. Lai, T. S. Chen, and S. K. Lim, "Mesenchymal stem cell exosome: a novel stem cell-based therapy for cardiovascular disease," *Regenerative Medicine*, vol. 6, no. 4, pp. 481–492, 2011.
- [73] K. Shah, A. G. Zhao, and H. Sumer, "New approaches to treat osteoarthritis with mesenchymal stem cells," *Stem Cells International*, vol. 2018, 9 pages, 2018.
- [74] K. Shah, T. Drury, I. Roic et al., "Outcome of allogeneic adult stem cell therapy in dogs suffering from osteoarthritis and other joint defects," *Stem Cells International*, vol. 2018, 7 pages, 2018.
- [75] S. R. Baglio, K. Rooijers, D. Koppers-Lalic et al., "Human bone marrow- and adipose-mesenchymal stem cells secrete exosomes enriched in distinctive miRNA and tRNA species," *Stem Cell Research & Therapy*, vol. 6, no. 1, 2015.
- [76] L. da Silva Meirelles, A. M. Fontes, D. T. Covas, and A. I. Caplan, "Mechanisms involved in the therapeutic properties of mesenchymal stem cells," *Cytokine & Growth Factor Reviews*, vol. 20, no. 5–6, pp. 419–427, 2009.
- [77] S. Ghannam, C. Bouffi, F. Djouad, C. Jorgensen, and D. Noël, "Immunosuppression by mesenchymal stem cells: mechanisms and clinical applications," *Stem Cell Research & Therapy*, vol. 1, no. 1, p. 2, 2010.
- [78] S. Bruno, C. Grange, F. Collino et al., "Microvesicles derived from mesenchymal stem cells enhance survival in a lethal

- model of acute kidney injury,” *PLoS One*, vol. 7, no. 3, article e33115, 2012.
- [79] A. Tieu, M. Slobodian, D. A. Fergusson et al., “Methods and efficacy of extracellular vesicles derived from mesenchymal stromal cells in animal models of disease: a preclinical systematic review protocol,” *Systematic Reviews*, vol. 8, no. 1, p. 322, 2019.
- [80] L. Kordelas, V. Rebmann, A. K. Ludwig et al., “MSC-derived exosomes: a novel tool to treat therapy-refractory graft-versus-host disease,” *Leukemia*, vol. 28, no. 4, pp. 970–973, 2014.
- [81] H. S. Kim, D. Y. Choi, S. J. Yun et al., “Proteomic analysis of microvesicles derived from human mesenchymal stem cells,” *Journal of Proteome Research*, vol. 11, no. 2, pp. 839–849, 2012.
- [82] J. R. Chevillet, Q. Kang, I. K. Ruf et al., “Quantitative and stoichiometric analysis of the microRNA content of exosomes,” *Proceedings of the National Academy of Sciences of the United States of America*, vol. 111, no. 41, pp. 14888–14893, 2014.
- [83] S. W. Ferguson, J. Wang, C. J. Lee et al., “The microRNA regulatory landscape of MSC-derived exosomes: a systems view,” *Scientific Reports*, vol. 8, no. 1, p. 1419, 2018.
- [84] C. Gallina, V. Turinetto, and C. Giachino, “A new paradigm in cardiac regeneration: the mesenchymal stem cell secretome,” *Stem Cells International*, vol. 2015, Article ID 765846, 10 pages, 2015.
- [85] S. Rani, A. E. Ryan, M. D. Griffin, and T. Ritter, “Mesenchymal stem cell-derived extracellular vesicles: toward cell-free therapeutic applications,” *Molecular Therapy*, vol. 23, no. 5, pp. 812–823, 2015.
- [86] S. Gatti, S. Bruno, M. C. Deregibus et al., “Microvesicles derived from human adult mesenchymal stem cells protect against ischaemia-reperfusion-induced acute and chronic kidney injury,” *Nephrology Dialysis Transplantation*, vol. 26, no. 5, pp. 1474–1483, 2011.
- [87] C. Akyurekli, Y. le, R. B. Richardson, D. Fergusson, J. Tay, and D. S. Allan, “A systematic review of preclinical studies on the therapeutic potential of mesenchymal stromal cell-derived microvesicles,” *Stem Cell Reviews and Reports*, vol. 11, no. 1, pp. 150–160, 2015.
- [88] G. Natasha, B. Gundogan, A. Tan et al., “Exosomes as immunotherapeutic nanoparticles,” *Clinical Therapeutics*, vol. 36, no. 6, pp. 820–829, 2014.
- [89] S. Bruno, C. Grange, M. C. Deregibus et al., “Mesenchymal stem cell-derived microvesicles protect against acute tubular injury,” *Journal of the American Society of Nephrology*, vol. 20, no. 5, pp. 1053–1067, 2009.
- [90] K. Clark, S. Zhang, S. Barthe et al., “Placental mesenchymal stem cell-derived extracellular vesicles promote myelin regeneration in an animal model of multiple sclerosis,” *Cell*, vol. 8, no. 12, p. 1497, 2019.
- [91] E. E. Reza-Zaldivar, M. A. Hernández-Sapiéns, Y. K. Gutiérrez-Mercado et al., “Mesenchymal stem cell-derived exosomes promote neurogenesis and cognitive function recovery in a mouse model of Alzheimer’s disease,” *Neural Regeneration Research*, vol. 14, no. 9, pp. 1626–1634, 2019.
- [92] F. Arslan, R. C. Lai, M. B. Smeets et al., “Mesenchymal stem cell-derived exosomes increase ATP levels, decrease oxidative stress and activate PI3K/Akt pathway to enhance myocardial viability and prevent adverse remodeling after myocardial ischemia/reperfusion injury,” *Stem Cell Research*, vol. 10, no. 3, pp. 301–312, 2013.
- [93] S. Zhang, S. J. Chuah, R. C. Lai, J. H. P. Hui, S. K. Lim, and W. S. Toh, “MSC exosomes mediate cartilage repair by enhancing proliferation, attenuating apoptosis and modulating immune reactivity,” *Biomaterials*, vol. 156, pp. 16–27, 2018.
- [94] S. Zhang, W. C. Chu, R. C. Lai, S. K. Lim, J. H. P. Hui, and W. S. Toh, “Exosomes derived from human embryonic mesenchymal stem cells promote osteochondral regeneration,” *Osteoarthritis and Cartilage*, vol. 24, no. 12, pp. 2135–2140, 2016.
- [95] Y. Zhu, Y. Wang, B. Zhao et al., “Comparison of exosomes secreted by induced pluripotent stem cell-derived mesenchymal stem cells and synovial membrane-derived mesenchymal stem cells for the treatment of osteoarthritis,” *Stem Cell Research & Therapy*, vol. 8, no. 1, p. 64, 2017.
- [96] C. H. Woo, H. K. Kim, G. Y. Jung et al., “Small extracellular vesicles from human adipose-derived stem cells attenuate cartilage degeneration,” *Journal of Extracellular Vesicles*, vol. 9, no. 1, 2020.
- [97] S. Mardpour, M. H. Ghanian, H. Sadeghi-abandansari et al., “Hydrogel-mediated sustained systemic delivery of mesenchymal stem cell-derived extracellular vesicles improves hepatic regeneration in chronic liver failure,” *ACS Applied Materials & Interfaces*, vol. 11, no. 41, pp. 37421–37433, 2019.
- [98] F. Diomedea, A. Gugliandolo, P. Cardelli et al., “Three-dimensional printed PLA scaffold and human gingival stem cell-derived extracellular vesicles: a new tool for bone defect repair,” *Stem Cell Research & Therapy*, vol. 9, no. 1, p. 104, 2018.
- [99] P. Chen, L. Zheng, Y. Wang et al., “Desktop-stereolithography 3D printing of a radially oriented extracellular matrix/mesenchymal stem cell exosome bioink for osteochondral defect regeneration,” *Theranostics*, vol. 9, no. 9, pp. 2439–2459, 2019.
- [100] W. Nassar, M. el-Ansary, D. Sabry et al., “Umbilical cord mesenchymal stem cells derived extracellular vesicles can safely ameliorate the progression of chronic kidney diseases,” *Biomaterials Research*, vol. 20, no. 1, 2016.
- [101] S. R. Baglio, D. M. Pegtel, and N. Baldini, “Mesenchymal stem cell secreted vesicles provide novel opportunities in (stem) cell-free therapy,” *Frontiers in Physiology*, vol. 3, p. 359, 2012.
- [102] R. W. Y. Yeo, R. C. Lai, B. Zhang et al., “Mesenchymal stem cell: an efficient mass producer of exosomes for drug delivery,” *Advanced Drug Delivery Reviews*, vol. 65, no. 3, pp. 336–341, 2013.
- [103] T. Lener, M. Gimona, L. Aigner et al., “Applying extracellular vesicles based therapeutics in clinical trials - an ISEV position paper,” *Journal of Extracellular Vesicles*, vol. 4, no. 1, 2015.
- [104] R. M. Samsonraj, M. Raghunath, V. Nurcombe, J. H. Hui, A. J. van Wijnen, and S. M. Cool, “Concise review: multifaceted characterization of human mesenchymal stem cells for use in regenerative medicine,” *Stem Cells Translational Medicine*, vol. 6, no. 12, pp. 2173–2185, 2017.
- [105] K. C. Vallabhaneni, P. Penfornis, S. Dhule et al., “Extracellular vesicles from bone marrow mesenchymal stem/stromal cells transport tumor regulatory microRNA, proteins, and metabolites,” *Oncotarget*, vol. 6, no. 7, pp. 4953–4967, 2015.
- [106] A. Gowen, F. Shahjin, S. Chand, K. E. Odegard, and S. V. Yelamanchili, “Mesenchymal stem cell-derived extracellular vesicles: challenges in clinical applications,” *Frontiers in Cell and Developmental Biology*, vol. 8, 2020.

## Research Article

# Bone Marrow Concentrate in the Treatment of Aneurysmal Bone Cysts: A Case Series Study

**Lorenzo Andreani, Sheila Shytaj , Elisabetta Neri, Fabio Cosseddu, Antonio D'Arienzo, and Rodolfo Capanna**

*Azienda Ospedaliera Universitaria Pisana, Via Paradisa 2, Pisa 56124, Italy*

Correspondence should be addressed to Sheila Shytaj; [s.shytaj@studenti.unipi.it](mailto:s.shytaj@studenti.unipi.it)

Received 26 June 2020; Accepted 10 August 2020; Published 21 August 2020

Academic Editor: Heinrich Sauer

Copyright © 2020 Lorenzo Andreani et al. This is an open access article distributed under the Creative Commons Attribution License, which permits unrestricted use, distribution, and reproduction in any medium, provided the original work is properly cited.

*Introduction.* A recent attractive option regarding mesenchymal stem cells (MSC) application is the treatment of bone cystic lesions and in particular aneurysmal bone cysts (ABC), in order to stimulate intrinsic healing. We performed a retrospective evaluation of the results obtained at our institution. *Methods.* The study group consisted of 46 cases with an average follow-up of 33 months. Forty-two patients underwent percutaneous treatment as the first approach; four patients had curettage as first treatment. In all cases, autologous bone marrow concentrate (BMC) was associated too. The healing status was followed up through a plain radiograph 45 days and 2 months after the procedure. *Results and Conclusions.* At the final follow-up, thirty-six patients healed with a Neer type II aspect, nine healed with a type I aspect, and one patient was not classified having total hip arthroplasty. Bone marrow concentrate is easy to obtain and to manipulate and can be immediately available in a clinical setting. We can assert that the use of BMC must be encouraged being harmless and having an unquestionable high osteogenic and healing potential in bone defects.

## 1. Introduction

In the past 30 years, many studies have confirmed the potentials and plasticity of the so-called mesenchymal stem cells (MSC): they have been shown to reside within the connective tissues of most organs and can differentiate into osteogenic, adipogenic, and chondrogenic lineages under appropriate conditions [1–3]. These features have led to an increasing application of MSC in the orthopaedic field, especially when a strong regenerative capacity applied through a minimally invasive approaches is required. A simple method to have MSC is the bone marrow concentrate (BMC) obtained through autologous bone marrow aspiration and centrifugation. Local application of BMC is one of the current available treatments of bone defects and in particular of cystic lesions [4, 5]. Among them aneurysmal bone cysts (ABC) are uncommon osteolytic lesions, usually eccentric, with a hyperplastic behaviour often arising in the long bones of young people, being rare after 30 years of age [6]. The treatment approach to ABC has evolved in the past years ranging

from radiotherapy to resection. More recently, less invasive procedures such as complete or partial curettage, and various substance injections seemed to be promising [7, 8]. We performed a retrospective evaluation of the results obtained at our institution after aneurysmal bone cyst percutaneous treatment with application of BMC in order to understand if the use of bone marrow stem cells actually gives benefits.

## 2. Material and Methods

We present a retrospective study involving 57 patients with diagnosis of aneurysmal bone cyst, treated at our institution between January 2013 and June 2019. The following exclusion criteria were applied: secondary ABC, initial treatment in other institution, and incomplete radiographic evaluation. Eight patients were excluded according to the following criteria: 2 ABC associated to chondroblastoma, 3 patient who had initial treatment in another hospital, and 6 patients for the absence of complete radiographic evaluation available. The study group consisted of 46 patients with an average



TABLE 1: ABC anatomical location.

Location	
Proximal humerus	14
Humeral diaphysis	8
Pelvis	3
Femur diaphysis	6
Proximal femur	13
Calcaneus	2

TABLE 2: Enneking classification.

Inactive	Intact, well-defined margins
Active	Incomplete margins but well-defined lesion
Aggressive	Poorly defined margins with reactive bone formation

follow-up of 33 months. Forty-two patients underwent percutaneous treatment as first approach; four patients had curettage as first treatment. The patients enrolled performed a plain radiograph before intervention, and the following radiographic variables were assessed: affected bone, staging according to the Enneking system [9], and location according to the Capanna classification [10]. In all cases, the diagnosis was obtained through a histopathological study of specimens collected intraoperatively. All of the procedures were performed using sedation and local anaesthesia or under general anaesthesia with an aseptic technique. The percutaneous injections were performed introducing a Jamshidi needle, under fluoroscopic guide, into the lesion. The content of the cyst was then aspirated and sent for histopathologic evaluation; subsequently, the chosen drugs were injected into the lesion. The injected substances were: vitamin C, atossiclerol (0, 25%), methylprednisolone acetate, and autologous bone marrow concentrate (BMC). The two lesions treated with curettage were filled with bone chips enriched with the same substances aforementioned. The BMC was obtained through aspiration of bone marrow from the ipsilateral iliac crest and centrifugation in a dedicated RegenKit® device. The healing status was followed up through a plain radiograph 45 days after the procedure and then 2 months after. According to the modified Neer classification [11], the procedure was repeated if no satisfactory healing of the lesion occurred after 2 months, i.e. if the radiolucent area was  $\geq 50\%$  of the lesion diameter or in case of relapse.

### 3. Results

The mean age at diagnosis was 13.8 with a male prevalence (31 males, 15 females). The anatomical location, collected in Table 1, shows a predominant distribution in the proximal metaphysis of long bones and in the pelvis. The cysts were classified in inactive, active, and aggressive according to the Enneking staging of musculoskeletal tumours as shown in Table 2: they were all active, except for one that was an aggressive lesion. According to the Capanna staging (Table 3), all patients had type II lesions, i.e., central and affecting the entire diameter of the bone, except for two cases

TABLE 3: Capanna classification.

Type	Morphological features
I	Central lesion
II	Central lesion involving the entire bone diameter
III	Eccentric lesion
IV	Subperiosteal lesion
V	Subperiosteal lesion extending to soft tissues

having eccentric lesion, defined as type III. Thirty-six patients healed after the first treatment; among them, four had an open curettage and the cavity was filled with bone chips and autologous BMC. Of the remaining ten patients, seven healed with 2 percutaneous injections; of the remaining two, 3 had percutaneous injection and one had a resection with total hip replacement. Healing was assessed using the modified Neer classification (Table 4) used for unicameral bone cyst treatment: at the final follow-up, thirty-six patients healed with a type II aspect, nine healed with a type I aspect, and one patient was not classified having total hip arthroplasty.

### 4. Discussion

The application of bone marrow concentrate (BMC) in the treatment of aneurysmal bone cysts (ABC) is a quite new procedure. The use of BMC to fill bony defects is well known, with a success rate that seems to be related to the number of progenitors in the graft [12]. ABC are reactive and locally aggressive lesions having osteolytic, hyperplastic, hyperemic, and hemorrhagic features; they are uncommon and rarely present after 30 years of age. Aneurysmal bone cyst-like modifications can be observed also in other pathological conditions, in malignant tumours such as telangiectatic osteosarcoma, and this eventuality must be ruled out through the histological study of specimens [6]. The aim of ABC treatment is to arrest their potentially high destructive capability. In the past years, different approaches have been proposed for ABC treatment ranging from resection to mini-invasive percutaneous procedures, and still today, there is no consensus on the best treatment [13–15]. However, the analysis of ABC pathogenesis and natural history, although not completely understood, can be helpful to chose the most appropriate treatment. It was long thought that ABC's cause was a vascular impairment due to abnormal venous circulation with osteoclast activation and local bone resorption; a more recent clonal theory overtook the vascular theory: the origin of the lesion seems to be associated with a translocation of USP6 oncogene on chromosome 17 [16, 17]. This finding confirms the oncological nature of ABC and therefore their high evolutivity: as for other musculoskeletal tumors, ABC can be classified as inactive, active, and aggressive and their evolution proceeds in phases. The initial osteolysis can evolve to cortical destruction and periosteal reaction creating a bulky bone; the appearance of septa attests a stabilization and remodelling attempt that in a few cases can lead to spontaneous resolution. In other cases, ABC assume an aggressive and destructive behaviour; however, the reason

TABLE 4: Modified Neer classification.

TYPE	Description
I	Cyst healed with radiolucent area < 1 cm
II	Cyst healed with radiolucent area < 50% of diameter and enough cortical thickness
III	Persistent cyst with radiolucent area > 50% of diameter with thin cortical rim
IV	Recurrent cysts in the obliterated area or increased residual radiolucent area

that shifts to a stabilizing or a destructive pattern is still unknown [7, 18]. Delloye et al. were among the first to report two cases of ABC treated with BMC: the rationale underlying this treatment was in the inductive properties of mesenchymal stems cells [19]. Many studies have already confirmed that BMC, particularly, if obtained through iliac crest aspiration, is rich in mesenchymal cells that seem to represent the source of osteoblastic elements during growth, remodelling, and bone reparative processes [20–22]. Moreover, ABCs are subject to continuous reparative processes in a cavity filled with blood that provides an ideal environment for mesenchymal cells to express their inductive capacities. Therefore, the aim of our treatment was to induce spontaneous ossification of ABC through a minimally invasive procedure. Currently, there is no consensus on the ideal treatment of ABC. For eccentric and aggressive lesions, located in expendable bones like the proximal fibula or pubic ramus, many authors have advocate resection as treatment of choice, reporting very low recurrence rates [23, 24]. According to other authors, curettage with or without bone grafting seems to be the best choice, reporting acceptable recurrence rates with a much better functional outcome than resection [25, 26]. More recently, in consideration of patients' young age and with better understanding of ABC pathogenesis, less-invasive procedures are gaining more success: percutaneous embolization, isolated intracystic injection of demineralized bone powder, bone marrow, calcitonin and Ethibloc are some examples [27–29]. Docquier and Delloye reported good results inducing ABCs' healing with intralesional implantation, through a mini-invasive access, of a bone paste made of autogenic bone marrow and allogenic bone powder: the goal of this treatment was to interrupt the destructive osteoclastic process and promote spontaneous bone regeneration [7]. In our series, with the technique described, we obtained a full recovery after only one treatment in more than 50% of our cases; the remaining had a maximum of two other procedures except for one patient, affected by a lesion involving the femoral head in contact with the articular cartilage that eventually underwent prosthetic replacement. Only four patients received curettage as first treatment since they had wide lesions ; they both reported a Neer II grade at follow-up. As regards percutaneous approach, we believe that, given the age of patients affected by this condition, the proposed treatment avoids extensive surgery and blood loss and can be repeatable with minor discomfort for the patient. Moreover, we did not report any complication, including superficial or deep infection, fracture, or other adverse reactions, both at the harvest site and at the application site: this confirmed the safety of the procedure used.

Nevertheless, even if the results obtained are promising, the number of cases is exiguous and a larger group is necessary to confirm the validity of this procedure ; perhaps with a greater number of patients a stratification based on anatomical location and cyst dimension would be feasible and would help in the choice of the best treatment.

## 5. Conclusions

Even if affected by the limitation of a relatively small number of patients, our case series proves that bone marrow concentrate is easy to obtain and to manipulate, and can be immediately available in a clinical setting; it offered good results with no complications. We believe that cavitary lesions like ABCs are ideal settings for using mesenchymal cells since they act as a biological chamber where the healing processes can be potentiated by the presence of blood and growth factors that stimulate differentiation of an osteogenic lineage.

## Data Availability

The data sets used and/or analysed during the current study are available from the corresponding author on reasonable request.

## Consent

Written consent was obtained from all patients included in this study (or their parents for underaged patients).

## Conflicts of Interest

The authors declare that they have no competing interests.

## References

- [1] A. J. Friedenstein, S. Piatelyk II, and K. V. Petrakova, "Osteogenesis in transplants of bone marrow cells," *Journal of Embryology and Experimental Morphology*, vol. 16, no. 3, pp. 381–390, 1966.
- [2] A. J. Friedenstein, R. K. Chailakhjan, and K. S. Lalykina, "The development of fibroblast colonies in monolayer cultures of guinea-pig bone marrow and spleen cells," *Cell and Tissue Kinetics*, vol. 3, no. 4, pp. 393–403, 1970.
- [3] M. Owen and A. J. Friedenstein, "Stromal stem cells: marrow-derived osteogenic precursors," *Ciba Foundation Symposium*, vol. 136, pp. 42–60, 1988.
- [4] P. De Biase, D. A. Campanacci, G. Beltrami et al., "Scaffolds combined with stem cells and growth factors in healing of pseudotumoral lesions of bone," *International Journal of*

- Immunopathology and Pharmacology*, vol. 24, no. 1, Supplement 2, pp. 11–15, 2011.
- [5] M. Jäger, M. Herten, U. Fochtmann et al., “Bridging the gap: bone marrow aspiration concentrate reduces autologous bone grafting in osseous defects,” *Journal of Orthopaedic Research*, vol. 29, no. 2, pp. 173–180, 2011.
  - [6] M. Campanacci, *Bone and Soft Tissue Tumors*, Springer, 2013.
  - [7] P. L. Docquier and C. Delloye, “Treatment of aneurysmal bone cysts by introduction of demineralized bone and autogenous bone marrow,” *The Journal of Bone and Joint Surgery American Volume*, vol. 87, no. 10, pp. 2253–2258, 2005.
  - [8] J. Cottalorda and S. Bourelle, “Current treatments of primary aneurysmal bone cysts,” *Journal of Pediatric Orthopaedics. Part B*, vol. 15, no. 3, pp. 155–167, 2006.
  - [9] W. F. Enneking, S. S. Spanier, and M. A. Goodman, “A system for the surgical staging of musculoskeletal sarcoma,” *Clinical Orthopaedics and Related Research*, vol. 153, pp. 106–120, 1980.
  - [10] R. Capanna, G. Bettelli, R. Biagini, P. Ruggieri, F. Bertoni, and M. Campanacci, “Aneurysmal cysts of long bones,” *Italian Journal of Orthopaedics and Traumatology*, vol. 11, no. 4, pp. 409–417, 1985.
  - [11] C. S. Neer 2nd, K. C. Francis, R. C. Marcove, J. Terz, and P. N. Carbonara, “Treatment of unicameral bone cyst. A follow-up study of one hundred seventy-five cases,” *The Journal of Bone and Joint Surgery American Volume*, vol. 48, no. 4, pp. 731–745, 1966.
  - [12] P. Hernigou, A. Poignard, F. Beaujean, and H. Rouard, “Percutaneous autologous bone-marrow grafting for nonunions influence of the number and concentration of progenitor cells,” *The Journal of Bone and Joint Surgery. American Volume*, vol. 87, no. 7, pp. 1430–1437, 2005.
  - [13] P. Flont, M. Kolacinska-Flont, and K. Niedzielski, “A comparison of cyst wall curettage and en bloc excision in the treatment of aneurysmal bone cysts,” *World Journal of Surgical Oncology*, vol. 11, p. 109, 2013.
  - [14] F. O. Abuhassan and A. O. Shannak, “Subperiosteal resection of aneurysmal bone cysts of the distal fibula,” *Journal of Bone and Joint Surgery. British Volume (London)*, vol. 91-B, no. 9, pp. 1227–1231, 2009.
  - [15] N. K. Garg, H. Carty, H. P. Walsh, J. C. Dorgan, and C. E. Bruce, “Percutaneous Ethibloc injection in aneurysmal bone cysts,” *Skeletal Radiology*, vol. 29, no. 4, pp. 211–216, 2000.
  - [16] G. P. Nielsen, J. A. Fletcher, and A. M. Oliveira, “Aneurysmal bone cyst,” in *WHO Classification of Tumours of Softtissue and Bone*, B. J. A. Fletcher, P. C. W. Hogendoorn, and F. Mertens, Eds., pp. 348–349, IARC, Lyon, 2013.
  - [17] Y. Ye, L. M. Pringle, A. W. Lau et al., “TRE17/USP6 oncogene translocated in aneurysmal bone cyst induces matrix metalloproteinase production via activation of NF- $\kappa$ B,” *Oncogene*, vol. 29, no. 25, pp. 3619–3629, 2010.
  - [18] J. Malghem, B. Maldague, W. Esselinckx, P. De Nayer, and A. Vincent, “Spontaneous healing of aneurysmal bone cysts. A report of three cases,” *The Journal of Bone and Joint Surgery. British volume*, vol. 71-B, no. 4, pp. 645–650, 1989.
  - [19] C. Delloye, P. De Nayer, J. Malghem, and H. Noel, “Induced healing of aneurysmal bone cysts by demineralized bone particles. A report of two cases,” *Archives of Orthopaedic and Trauma Surgery*, vol. 115, no. 3-4, pp. 141–145, 1996.
  - [20] S. P. Bruder, D. J. Fink, and A. I. Caplan, “Mesenchymal stem cells in bone development, bone repair, and skeletal regeneration therapy,” *Journal of Cellular Biochemistry*, vol. 56, no. 3, pp. 283–294, 1994.
  - [21] M. Owen, “Lineage of osteogenic cells and their relationship to the stromal system,” in *Bone and Mineral*, W. A. Peck, Ed., vol. 3, pp. 1–25, Elsevier, Amsterdam, 1985.
  - [22] R. O. Oreffo and J. T. Triffitt, “Future potentials for using osteogenic stem cells and biomaterials in orthopedics,” *Bone*, vol. 25, no. 2, pp. 5S–9S, 1999.
  - [23] M. Campanacci, R. Capanna, and P. Picci, “Unicameral and aneurysmal bone cysts,” *Clinical Orthopaedics*, vol. 204, pp. 25–36, 1986.
  - [24] J. Cottalorda, R. Kohler, and F. Lorge, “Aggressive aneurysmal bone cyst of the humerus in a child,” *Revue de Chirurgie Orthopédique et Réparatrice de l'Appareil Moteur*, vol. 90, no. 6, pp. 577–580, 2004.
  - [25] A. M. Vergel de Dios, J. R. Bond, T. C. Schives, R. A. McLeod, and K. K. Unni, “Aneurysmal bone cyst. A clinicopathologic study of 238 cases,” *Cancer*, vol. 69, no. 12, pp. 2921–2931, 1992.
  - [26] B. P. Tillmann, D. C. Dahlin, P. R. Lipscomb, and J. R. Steewart, “Aneurysmal bone cysts, analysis of 95 cases,” *Mayo Clinic Proceedings*, vol. 43, pp. 478–495, 1968.
  - [27] J. Cottalorda and S. Bourelle, “Aneurysmal bone cyst in 2006,” *Revue de Chirurgie Orthopédique et Réparatrice de l'Appareil Moteur*, vol. 93, no. 1, pp. 5–16, 2007.
  - [28] L. Amendola, L. Simonetti, C. E. Simoes, S. Bandiera, F. de Iure, and S. Boriani, “Aneurysmal bone cyst of the mobile spine: the therapeutic role of embolization,” *European Spine Journal*, vol. 22, no. 3, pp. 533–541, 2013.
  - [29] C. Adamsbaum, E. Mascard, J. M. Guinebretière, G. Kalifa, and J. Dubouset, “Intralesional Ethibloc injections in primary aneurysmal bone cysts: an efficient and safe treatment,” *Skeletal Radiology*, vol. 32, no. 10, pp. 559–566, 2003.

## Research Article

# Dental Pulp Mesenchymal Stem Cells as a Treatment for Periodontal Disease in Older Adults

Beatriz Hernández-Monjaraz,<sup>1</sup> Edelmiro Santiago-Osorio,<sup>2</sup> Edgar Ledesma-Martínez,<sup>2</sup> Itzen Aguiñiga-Sánchez,<sup>2</sup> Norma Angélica Sosa-Hernández,<sup>2</sup> and Víctor Manuel Mendoza-Núñez <sup>1</sup>

<sup>1</sup>Research Unit on Gerontology, FES Zaragoza, National Autonomous University of Mexico, 09230 Mexico City, Mexico

<sup>2</sup>Haematopoiesis and Leukaemia Laboratory, Research Unit on Cell Differentiation and Cancer, FES Zaragoza, National Autonomous University of Mexico, 09230 Mexico City, Mexico

Correspondence should be addressed to Víctor Manuel Mendoza-Núñez; mendovic@unam.mx

Received 18 June 2020; Revised 23 July 2020; Accepted 30 July 2020; Published 18 August 2020

Academic Editor: Sangho Roh

Copyright © 2020 Beatriz Hernández-Monjaraz et al. This is an open access article distributed under the Creative Commons Attribution License, which permits unrestricted use, distribution, and reproduction in any medium, provided the original work is properly cited.

Periodontal disease (PD) is one of the main causes of tooth loss and is related to oxidative stress and chronic inflammation. Although different treatments have been proposed in the past, the vast majority do not regenerate lost tissues. In this sense, the use of dental pulp mesenchymal stem cells (DPMSCs) seems to be an alternative for the regeneration of periodontal bone tissue. A quasi-experimental study was conducted in a sample of 22 adults between 55 and 64 years of age with PD, without uncontrolled systemic chronic diseases. Two groups were formed randomly: (i) experimental group (EG)  $n = 11$ , with a treatment based on DPMSCs; and a (ii) control group (CG)  $n = 11$ , without a treatment of DPMSCs. Every participant underwent clinical and radiological evaluations and measurement of bone mineral density (BMD) by tomography. Saliva samples were taken as well, to determine the total concentration of antioxidants, superoxide dismutase (SOD), lipoperoxides, and interleukins (IL), before and 6 months after treatment. All subjects underwent curettage and periodontal surgery, the EG had a collagen scaffold treated with DPMSCs, while the CG only had the collagen scaffold placed. The EG with DPMSCs showed an increase in the BMD of the alveolar bone with a borderline statistical significance (baseline  $638.82 \pm 181.7$  vs. posttreatment  $781.26 \pm 162.2$  HU,  $p = 0.09$ ). Regarding oxidative stress and inflammation markers, salivary SOD levels were significantly higher in EG (baseline  $1.49 \pm 0.96$  vs.  $2.14 \pm 1.12$  U/L posttreatment,  $p < 0.05$ ) meanwhile  $IL1\beta$  levels had a decrease (baseline  $1001.91 \pm 675.5$  vs. posttreatment  $722.3 \pm 349.4$  pg/ml,  $p < 0.05$ ). Our findings suggest that a DPMSCs treatment based on DPMSCs has both an effect on bone regeneration linked to an increased SOD and decreased levels of  $IL1\beta$  in aging subjects with PD.

## 1. Introduction

Periodontal disease (PD) is an infectious and inflammatory alteration that affects the supporting tissues of the teeth and, when treatment is not appropriate or adequate, it can cause the loss of these [1]. PD presents an immune and anti-inflammatory response caused by antigenic substances from bacteria in the subgingival biofilm; however, the exacerbated host response is ineffective, and therefore chronic inflammation is maintained [2].

During the acute phase of PD, the presence of bacteria, and especially the lipopolysaccharides in your cell wall, attracts macrophages, leukocytes, and neutrophils to the area of infection. The latter contain enzymes such as NADPH oxidase and myeloperoxidase to produce reactive oxygen species (ROS) that help fight pathogens [3, 4].

Under normal conditions, antioxidant mechanisms protect tissues from damage by ROS secreted by neutrophils. However, if the body's antioxidant capacity is insufficient, oxidative stress (OxS) occurs, which is an imbalance between



ROS and antioxidants in favor of the former, causing tissue damage [5].

OxS causes oxidation of important enzymes, stimulates the release of proinflammatory interleukins, lipid peroxidation, and DNA, and protein damage. These mechanisms affect the gingival tissues, the periodontal ligament, the root cementum, and the alveolar bone that support the tooth [6, 7].

A prevalence of PD is estimated at around 11% within the world population [8]. This frequency and its complications increase as age increases. In this sense, the prevalence in people over 40 years is higher than 30%. Among the main alterations of this disease can be mentioned the loss of teeth and chewing problems. This disease can even impact social conditions like decreasing self-esteem and affecting social relationships [9].

The infectious and inflammatory processes of PD are closely related to systemic diseases, such as cardiovascular diseases, diabetes mellitus, arthritis, obesity, and Alzheimer's disease [10–12]. In this respect, both these biological alterations and social repercussions may cause a risk of systemic diseases and an overall life quality reduction of the individual. Thus, it is essential to give timely and effective treatment for PD. A high percentage of adults in the aging process with PD require surgical treatment; nevertheless, the results are not entirely satisfactory because the regeneration of the lost tissue is not achieved [13].

For this reason, new therapeutic alternatives have been proposed, amid them, the grafting of dental pulp mesenchymal stem cells (DPMSCs), have shown successful results in preclinical investigations [14–17], yet there are few clinical human studies [18].

The dental pulp cells originate from the neural crest. During the embryonic period, the interaction between oral ectodermal epithelial cells and mesenchymal stem cells (MSCs) leads to the formation of various structures. First, the enamel organ is formed. Then, the papilla and dental follicle are formed. MSCs give rise to other components of the tooth, such as dentin, pulp, cementum, and the periodontal ligament [19]. DPMSCs are the MSCs that lodge in the papilla at the level of the pulp chamber, where they remain until teeth are exfoliated. Given its characteristics, this cell niche is easily accessible, because its morbidity is limited after harvesting and it is considered a suitable candidate for cell-based tissue engineering strategies. Furthermore, it has a wide expansion rate, the potential to differentiate into cells from multiple cells, organs, systems [20, 21], and without having a malignant phenotype [22].

In addition, it has been shown in preclinical studies that DPMSCs differentiate into cementoblast-like cells, adipocytes, and collagen-forming cells, with the ability to generate cement-like material from periodontal tissue [23]. Hence, they could be used in the treatment of PD. Still, despite its qualities and favorable results, both *in vitro* and *in vivo* [24] studies on the use of DPMSCs in humans with PD are limited [18].

So, the objective of this study was to determine the effect of a DPMSC treatment both the clinical improvement and regeneration of periodontic bone tissue and their relationship

with the markers of chronic inflammation and oxidative stress of people in the aging process with PD.

## 2. Materials and Methods

**2.1. Experimental Design.** A quasi-experimental study with 22 patients with PD was designed. The subjects' age range was between 55 to 64 years old. All were volunteers, of both sexes, healthy or with controlled chronic diseases during the last 12 months, without osteoporosis or horizontal periodontal bone defects.

The research protocol was approved by the Ethics Committee of the National Autonomous University of Mexico (UNAM), Zaragoza (25/11/SO/3.4.1.), and registered in ISRCTN12831118. This study was performed in accordance with the Declaration of Helsinki, and all participants signed the written informed consent.

After a first screening, 48 patients were excluded from the final sample because they did not meet the inclusion criteria ( $n = 37$ ), declined to participate ( $n = 3$ ), or did not attend the first appointment ( $n = 8$ ). Thus, for this study, 22 patients with periodontitis were finally enrolled.

The volunteers who met the inclusion and exclusion criteria underwent nonsurgical treatment, in order to control the acute phase of the disease and to manipulate the tissues. This treatment consisted of hygienic-dietary instructions and scaling and root planing. Enrolled subjects were randomly divided into 2 groups (Figure 1). For the experimental group (EG), a collagen scaffold plus  $5 \times 10^6$  of DPMSCs was placed by periodontal surgery. On the other hand, for the control group (CG), only collagen scaffolding without cells was placed. Both groups underwent probing, mobility, bone mineral density, and saliva sampling to determine the Total Antioxidants Status (TAS), superoxide dismutase (SOD), lipoperoxides (LPO), and interleukins (IL) levels.

**2.2. Cell Culture.** Mesenchymal stem cells were obtained from the dental pulp of three donors (two male patients ages 7 and 8 and a 10-year-old patient) after their parents' signed the written informed consent. All the samples were obtained under aseptic conditions and under the strict criteria of good manufacturing practices, using animal-origin free reagents.

The procedure for all samples was as follows. The dental pulp was gently extracted from the teeth and immersed in a digestive solution (3 mg/ml collagenase type I plus 4 mg/ml dispase in Minimum Essential Medium-Alpha (MEM- $\alpha$ ) (Life Technologies, Grand Island, New York United States of America) for 1 hour at 37° C. After the dental pulp had been digested, it was dissociated and centrifuged at 497 G for 5 minutes. After centrifugation, it was resuspended in MEM- $\alpha$  and incubated at 37° C until 80% confluence was reached. The cells were analyzed by flow cytometry, and differentiation tests were performed for osteogenic, adipogenic, and chondrogenic lineages (Figure 2). The present findings were consistent with the criteria of the International Society of Cell Therapy for mesenchymal stem cells [25].

**2.3. Treatment.** Before the intervention, rinses were indicated for 2 minutes with 0.12% chlorhexidine. After performing

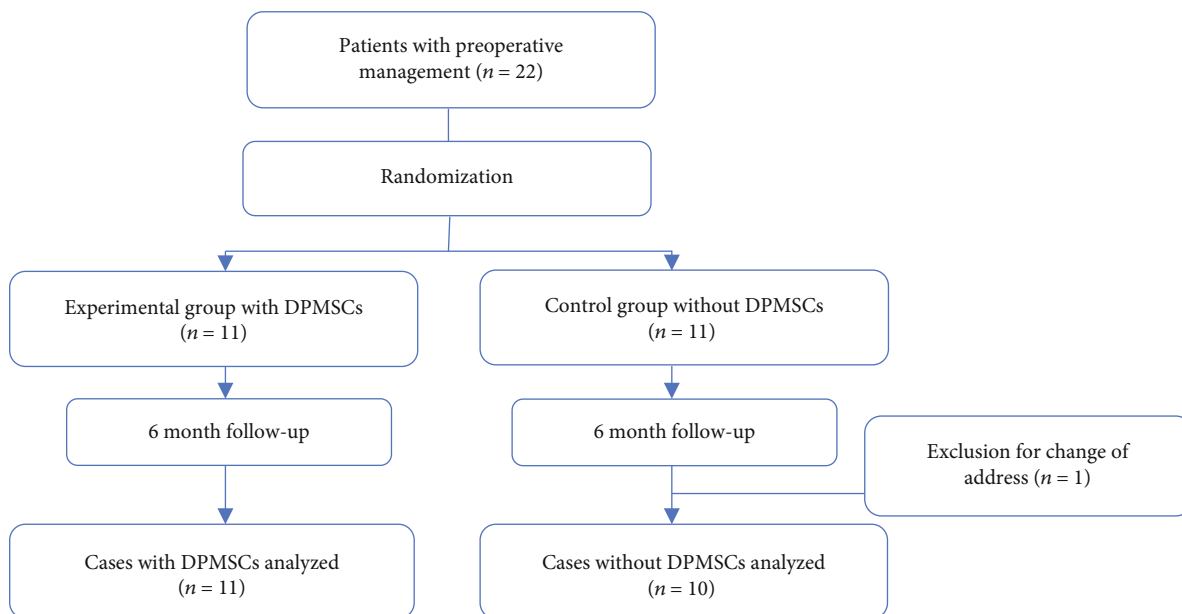


FIGURE 1: General scheme for study tracking.

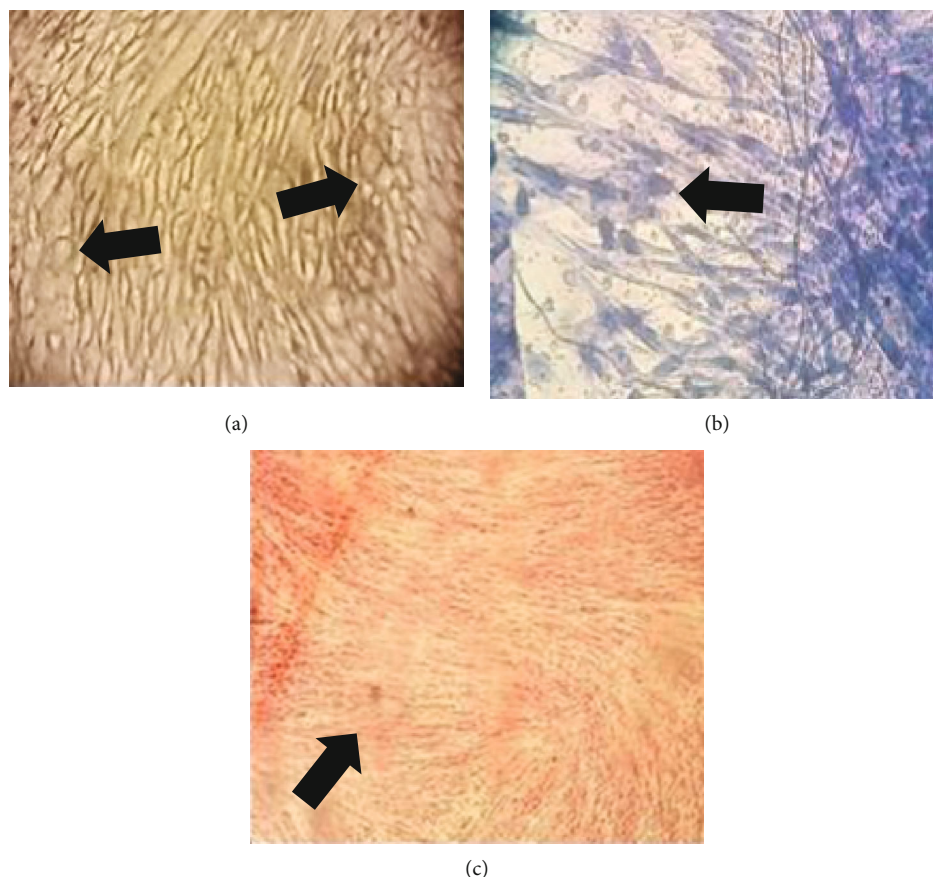


FIGURE 2: Representative images showing *in vitro* differentiation of multiple mesenchymal stem cell lineages from dental pulp obtained from a 7-year-old donor: (a) Red oil staining showing lipid deposits (arrows), indicative of adipogenic lineage; (b) alcian blue staining showing glycosaminoglycan deposits (arrows), indicative of chondrogenic lineage; and (c) alizarin red staining showing more densely stained areas with mineral deposits (arrows), indicative of osteogenic lineage; (all images, original magnification  $\times 40$ ).

asepsis of the area with benzalkonium chloride, locoregional anesthesia was applied through lidocaine and adrenaline infiltrations 1 : 50,000 to continue surgical access in the area of the periodontal bone defect using a flap technique, which consisted of in making an initial incision parallel to the longitudinal axis of the teeth, with a scalloped design and vertical discharge incisions. Then, a mucoperiosteal flap was raised, which was necessary to allow access to the root and bone surfaces. The root surfaces were smoothed with an ultrasonic reamer, the granulation tissue was peeled off, and the area was irrigated with saline water. Once the surface was cleaned, the bone defect was filled with lyophilized polyvinylpyrrolidone sponge® (clg-PVP) in 0.5 cm<sup>2</sup> fragments with an Adson forceps soaked in chlorhexidine gel. Subsequently, the EG patients had 5 × 10<sup>6</sup> DPMSCs dripped suspended in 200 ml of PBS, while the CG only received 200 ml of PBS without DPMSCs. Finally, in both groups, collagen membranes (Biomed extend®) were placed and the flap was sutured with Viacryl®. A drop of periacril was placed, and finally Coepack® was added to the area to protect the wound (Figure 3).

To control pain and edema, 100 mg nimesulide was indicated at the end of the intervention and 12 hours later. Finally, the stability of the patient was ensured, and care instructions were given. The need to control the biofilm in the areas during the first 2 weeks was explained to the patient by means of rinsing with chlorhexidine solution for 2 minutes twice a day; the use of Tebodont® toothpaste and dental cleaning with the curaprox surgical brush®. Weekly check-ups were scheduled to monitor the healing process. Surgical cement was removed after 7 days, and a tomography was performed 3 and 6 months after surgery.

**2.4. Statistical Analysis.** The data was analyzed using descriptive statistics, where we determined the mean and standard deviation (SD) and perform the Mann Whitney *U* test. A value of <0.05 is considered statistically significant. Values were determined using the SPSS statistical analysis program, version 20.0.

### 3. Results

**3.1. General.** Sociodemographic characteristics and teeth were involved in the study are presented in Table 1.

**3.2. Effect of DPMSCs on Clinical Parameters.** In Table 2, we show that both the group to which collagen plus DPMSCs was placed and the group to which only collagen was placed demonstrated an increase in bone mineral density; however, the increase in the DPMSCs group is almost twice more than the group without cells (with DPMSCs, 142.442 ± 19.5 vs. without DPMSCs, 50.262 ± 9.1 HU) with a borderline statistical significance (*p* = 0.09). Similarly, regarding the depth of periodontal defect (DPD), a statistically significant clinical improvement was observed in the group with DPMSCs compared to the group with no cells placed (with DPMSCs, -3.32 ± 0.12 vs. without DPMSCs, -1.80 ± 0.15 mm, *p* < 0.001).

Regarding the degree of dental mobility, 100% of the patients in the group with DPMSCs and in the group without

DPMSCs stopped having grade III mobility; nevertheless, 73% of the first group changed from grade III to grade I, in contrast to 40% observed in the group that did not have DPMSCs grafts (Table 2).

On the other hand, Figure 4 shows the tomographic and radiological images of a case of a patient in the group with DPMSCs and another in the group without DPMSCs, where a bone type filler was more clinically evident in the first group compared to the second was observed. In other words, the quantitative results agree with what was observed in the tomographies, where the presence of radiopaque tissue in the area of the periodontal defect is seen (Figure 3).

**3.3. Effect of DPMSC on Oxidative Stress Levels.** Regarding the oxidative stress markers in saliva, it was observed that after treatment with DPMSCs, there is a statistically significant increase in SOD (baseline, 1.49 ± 0.96 vs. posttreatment, 2.14 ± 1.12 U/L, *p* < 0.05) in the group with DPMSCs (Table 3).

**3.4. Effect of DPMSC on Levels of Proinflammatory Interleukins.** Likewise, in relation to the effect of DPMSCs on the concentration of interleukins IL-1β, IL-6, IL-8, IL-10, and TNF-α, it was found that the group to which DPMSCs were placed had a decrease in IL-1β (baseline, 1001.91 ± 675.53 vs. posttreatment, 722.30 ± 349.45 pg/ml, *p* < 0.05) and that IL-6 also increased when grafting DPMSCs (baseline, 11.31 ± 5.76 vs. posttreatment, 28.06 ± 18.43 pg/ml, *p* = 0.06) (Table 4).

Finally, during the recovery period, the patients had no complications, only minimal pain controlled with pain relievers.

## 4. Discussion

Periodontal disease is a consequence of an exacerbated immune response generated by the body to the excessive accumulation of Gram-negative bacteria [26]. The direct or indirect degradation of the collagen of the extracellular matrix collagen in PD is the result of the activation of proteases and phagocytosis. Furthermore, the release of proinflammatory interleukins is also disproportionately stimulated through NF-κB activation and PG-E2 production by lipid peroxidation and superoxide release, which is related to bone resorption [27].

In order to treat PD, several treatments have been proposed; yet, scientific community continues to looking for one method that allows the regeneration of the periodontium. Regeneration of periodontal tissues lost through PD is a true challenge because the alveolar bone, cementum, and periodontal ligament must be restored to their original architecture and physiology. For this reason, mesenchymal stem cells (MSCs) allogeneic transplantation such as dental pulp mesenchymal stem cells derived from deciduous teeth (DPMSCs) is a good option for treating PD [28].

DPMSCs have been shown *in vitro* to be able to differentiate into the necessary cells to repair tissues and also target inflamed areas while secreting anti-inflammatory interleukins that modulate the response of the immune system





FIGURE 3: Representative images showing the intervention. (a) Periodontal defect is shown; (b) exposure of the periodontal defect before treatment; (c) placement of the collagen scaffolding; (d) placement of the DPMSCs; (e) placement of the membrane; and (f) sutured flap.

[29]. Conversely, some preclinical trials suggest that MSCs have antioxidant potential and, consequently, the ability to reduce the OxS that occurs during inflammation in PD [30, 31].

In this context, promising results have been found reported *in vitro* [32–34] and in animal models [14–17, 35–43]; even so, human research to support clinical application is limited [44–47].

Human studies about DPMSC and PD are generally been conducted in young patients. However, the problem is that PD occurs mainly in people over the age of 40, in which most cells, including those of periodontal tissue, go into senescence [28].

Additionally, although DPMSCs have multiple functions, they decrease with age [48]. Thus, performing an autogenous graft, (with cells from the same individual), involves two important limitations: The first one is the ethical complication of extracting the pulp from a healthy tooth trying to rescue another with periodontal damage disease. And secondly, even if the DPMSCs were obtained from the patient, probably his cells would have already gone into senescence due to the changes that take place during the aging process [28].

Therefore, a useful alternative is to opt for MSCs from a young exogenous source or from children, in order to overcome the limitations of aged tissues and repair them. This, altogether with the low immunogenicity of the DPMSCs



TABLE 1: Demographic data and characteristics of the study population.

Characteristics	With DPMSCs	Without DPMSCs	Total
No. of subjects, <i>n</i>	11	10	21
Age (y), mean $\pm$ SD	59.1 $\pm$ 5.12	59.7 $\pm$ 5.25	59.4 $\pm$ 5.19
Gender, <i>n</i> (%)			
Female	4 (63.6)	3 (40)	7 (33.3)
Male	7 (36.4)	7 (70)	14 (66.7)
Education (y), mean $\pm$ SD	11.72 $\pm$ 3.64	12.0 $\pm$ 3.71	11.8 $\pm$ 3.68
Systemic diseases, <i>n</i> (%)			
Yes	3 (27.3)	4 (40)	7 (33.3)
No	8 (72.7)	6 (60)	14 (66.7)
Regular medication, <i>n</i> (%)			
Yes	3 (27.3)	4 (40)	7 (33.3)
No	8 (72.7)	6 (60)	14 (66.7)
Teeth involved, <i>n</i> (%)			
Maxilla incisor	1 (9)	0 (0)	1 (4.8)
Maxilla canine	0 (0)	0 (0)	0 (0)
Maxilla premolar	0 (0)	1 (1)	1 (4.8)
Maxilla molar	0 (0)	1 (1)	1 (4.8)
Mandible incisor	2 (18)	0 (0)	2 (9.5)
Mandible canine	0 (0)	0 (0)	0 (0)
Mandible premolar	1 (9)	1 (1)	2 (9.5)
Mandible molar	7 (64)	7 (7)	14 (66.6)

Values show mean  $\pm$  standard deviation. DPMSCs: dental pulp mesenchymal stem cells; EG: experimental group; CG: control group.

and its easy obtaining prompted us to choose them to carry out the present study.

Accordingly, we present the results of the effect of DPMSCs on a collagen scaffold for the regeneration of periodontal tissues in aging patients with vertical bone defects caused by PD.

The therapeutic effects related to the regeneration of periodontal tissue were evaluated through radiographic images, clinical parameters (as has been proposed in the clinical setting) [44–47], and also with the measurement of bone mineral density (BMD) through tomography [49]. In this sense, in our study, an increase in BMD twice more was observed in the group with DPMSCs compared to the group without them, with borderline statistical significance.

In this regard, the tissue formation within the bone defect of our patients may be due to the fact that DPMSCs differentiate rapidly in osteoblasts and endotheliocytes [50], which allows the formation of bone and the blood vessels necessary to irrigate the newformed tissue. Besides, it has been observed that the DPMSCs placed in bone defects express bone morphogenic proteins 2 (BMP2), which in turn produce a greater amount of bone, which is later mineralized, as reported by Liu et al. (2011) and Aimetti et al. (2014), who observed by radiographs, that after the placement of an MSCs graft,

the defect had been completely filled by a bone-like tissue [51, 52].

The increase in BMD with DPMSCs could be caused by two mechanisms. The first is explained by differentiation and proliferation of DPMSCs from the donor within the recipient's tissues, and the second mechanism is through a complex cellular communication system between grafted DPMSCs and receptor periodontal tissue cells, which are aged and damaged [24]. To complement the images showing new bone formation, it would be useful to determine markers such as BALP, Trap5b, Ntx, Ctx, and MMP-8 that indicate the rate of bone remodelling formation, resorption, and regulation in the long term [53].

Regarding Depth of Periodontal Defect (DPD), in our study, a statistically significant decrease was observed in the group with DPMSCs compared to the group without them. This suggests that the DPMSCs promote cell proliferation resulting in an increase in both the gingival tissue and the underlying one, which causes its insertion to be located more coronally. This finding is consistent with what was previously reported by our research group, in a clinical case [54] and with other studies done by Aimetti et al. (2014), who described a clinical case with a periodontal defect, treated by MSCs obtained from one of the third molars of the same patient, whereas after one year of intervention it was observed that DPD had decreased and the degree of mobility was also reduced [52]. This is due to the fact that both the regeneration of the gingival sulcus epithelium and bone tissue formation, favoring that the epithelial adhesion is more coronally repositioned; thus, reducing DPD as indicated by Sculean et al. (2004), in a study with infraosseous defects in humans [55].

Concerning radiographic analysis, in our study, an increase in the area of the periodontal defect was observed, which is consistent with various preclinical and clinical trials, whose reports were that after the placement of different types of MSCs, a radiopaque area was observed radiographically in the bone defect coronal part [43–47, 54].

On the contrary, MSCs have both enzymatic and non-enzymatic biological mechanisms, which help in neutralizing ROS and correcting the damage caused to the proteome and genome by OxS, thereby, efficient management of OxS is guaranteed [56]. Since OxS is closely related to PD, in our study, we evaluated the concentrations of lipoperoxides, total antioxidants, and also superoxide dismutase (SOD). In this regard, it was observed that 6 months after the placement of the DPMSCs graft, there was a statistically significant increase in the concentration of SOD compared to the group that was not treated with DPMSCs. This is consistent with other studies that have shown that MSCs increase SOD levels, supporting the proposed antioxidant effect of MSCs [57].

On this subject, some studies have shown that MSCs can resist high levels of OxS and its induced death. This is related to the reduction in apoptosis and the ability of MSCs to process peroxide and peroxynitrite, since the latter is associated with the activity of SOD1, SOD2, CAT, and GPX1 enzymes in MSCs and a high level of intracellular GSx [30]. Furthermore, MSCs express a high level of methionine and sulfoxide

TABLE 2: Effect of DPMSCs on clinical parameters by treatment group.

Parameter	With DPMSCs ( <i>n</i> = 11)			Without DPMSCs ( <i>n</i> = 10)			<i>p</i>
	Basal	6 months	Difference EG	Basal	6 months	Difference CG	
BMD (HU)	638.82 ± 181.7	781.26 ± 162.2	142.442 ± 19.5	620.49 ± 143.5	670.76 ± 134.4	50.262 ± 9.1	0.098
DPD (mm)	5.66 ± 0.41	2.34 ± 0.29*	-3.32 ± 0.12	5.58 ± 0.38	3.78 ± 0.53	-1.80 ± 0.15	0.001
Dental mobility							
Grade III (%)	10 (90)	0 (0)		7 (70)	0 (0)		
Grade II (%)	1 (10)	3 (27)		3 (30)	6 (60)		
Grade I (%)	0 (0)	8 (73)		0 (0)	4 (40)		

Values show mean ± standard deviation. Mann-Whitney *U* and Wilcoxon test, \**p* < 0.05. DPMSCs: dental pulp mesenchymal stem cells; BMD: bone mineral density; HU: Hunsfield units; DPD: Depth of Periodontal Defect (DPD). EG: experimental group; CG: control group.

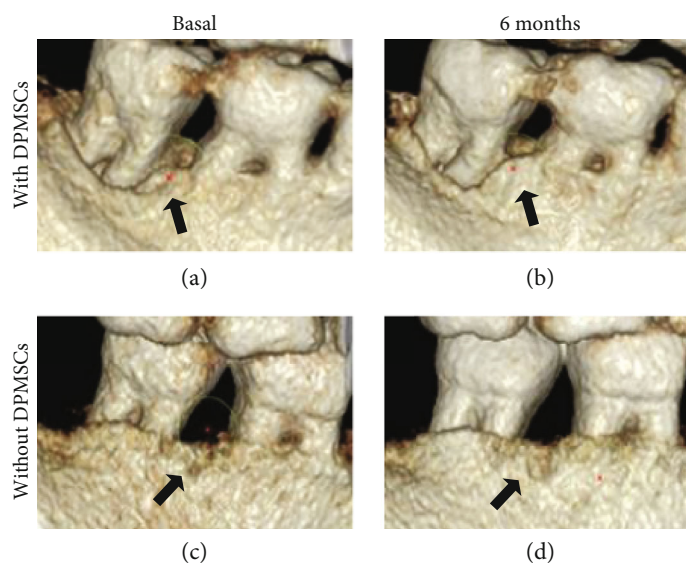


FIGURE 4: Cone beam volumetric tomography and radiography in which the growth of bone tissue is observed in the EG with DPMSCs (a, b) and the CG without DPMSCs (c, d).

TABLE 3: Oxidative stress markers in saliva prior to DPMSCs placement and 6 months after that.

Parameter	With DPMSCs ( <i>n</i> = 11)			Without DPMSCs ( <i>n</i> = 10)			<i>p</i>
	Basal	6 months	Difference EG	Basal	6 months	Difference CG	
TAS (mmol/L)	0.598 ± 0.21	0.757 ± 0.32	0.159 ± 0.35	0.591 ± 0.29	0.640 ± 0.49	0.049 ± 0.36	0.618
SOD (U/L)	1.49 ± 0.96	2.14 ± 1.12*	0.647 ± 0.73	1.386 ± 0.70	1.100 ± 0.57	-0.276 ± 0.65	0.047
LPO (μmol/L)	0.0791 ± 0.02	0.0448 ± 0.35	-0.031 ± 0.04	0.0677 ± 0.03	0.0610 ± 0.03	-0.006 ± 0.03	0.225

Values show mean ± standard deviation. Mann-Whitney *U* test, \**p* < 0.05. DPMSCs: dental pulp mesenchymal stem cells; TAS: Total Antioxidant Status; SOD: superoxide dismutase; LPO: lipoperoxides. EG: experimental group; CG: control group.

reductase A; the last one acting as an important enzyme for repairing oxidized proteins and for recovering methionine residues that act as preserve the free-radical sink. [58].

Although treatment with MSCs can prevent decreased SOD activity [59], it is important to mention that both the synthesis and the release of SOD by MSCs are synergistically regulated by inflammatory mediators such as TNF- $\alpha$  and INF- $\gamma$  preventing damage tissue [60]. In this regard, it has been shown that the correct proliferation, migration, and

maturation of DPMSCs depend on the molecules found in the environment and on genetic control [61]. The combined action of signal transduction that is induced by some interleukins determines that DPMSCs differentiate into an osteogenic lineage [62, 63]. Additionally, it is known that high concentrations of proinflammatory interleukins play a fundamental role in the breakdown of periodontal tissue [64].

Although, a genetic expression analysis has proposed the predominant effect of MSCs treatment on the activation of

TABLE 4: Proinflammatory interleukins concentrations (pg/ml) in saliva samples prior to and after DPMSCs placement.

Parameter	With DPMSCs ( <i>n</i> = 11)			Without DPMSCs ( <i>n</i> = 10)			<i>p</i>
	Basal	6 months	Difference EG	Basal	6 months	Difference CG	
TNF- $\alpha$	8.91 $\pm$ 3.04	7.66 $\pm$ 3.37	-1.24 $\pm$ 1.41	9.276 $\pm$ 5.98	7.80 $\pm$ 5.78	-1.28 $\pm$ 1.79	0.844
IL-6	11.31 $\pm$ 5.76	28.06 $\pm$ 18.43	16.74 $\pm$ 5.88	20.13 $\pm$ 15.57	22.43 $\pm$ 18.40	2.30 $\pm$ 4.00	0.067
IL-1 $\beta$	1001.91 $\pm$ 657.53	722.30 $\pm$ 349.45*	-279.61 $\pm$ 167.51	1238.18 $\pm$ 779.95	1543.92 $\pm$ 827.15	305.73 $\pm$ 256.11	0.039
IL-10	2.92 $\pm$ 0.91	2.80 $\pm$ 0.48	-0.112 $\pm$ 0.212	2.62 $\pm$ 0.61	3.36 $\pm$ 0.56	-2.58 $\pm$ 0.19	0.268
IL-8	1270.92 $\pm$ 670.64	1145.72 $\pm$ 805.99	-125.19 $\pm$ 364.71	1497.27 $\pm$ 1339.83	827.27 $\pm$ 632.15	-670.0 $\pm$ 326.30	0.417

Values show mean  $\pm$  standard error. Mann-Whitney *U* test, \**p* < 0.05. DPMSCs: dental pulp mesenchymal stem cells; IL: interleukin; TNF- $\alpha$ : tumor necrosis factor alpha; EG: experimental group; CG: control group.

inflammatory pathways “normalizing” inflammation levels [65]. In this regard, in the present investigation, a statistically significant decrease in the levels of IL-1 $\beta$  was observed in the group to which the DPMSCs were placed compared to the group without them. This interleukin is closely related to the existence and severity of PD. This statement is in agreement with several studies that affirm that IL-1 $\beta$  is synthesized by several cell lines of periodontal tissue and that it occupies a central position among the mediators of the inflammatory cascade during PD [66–68]. It is undeniable that the increase in IL-1 $\beta$  production is associated with the development of periodontal disease [69] and that the use of inhibitors of this cytokine contributes to the reduction of periodontal bone loss in primates [70], so it is suggested that the monitoring of IL1 $\beta$  levels is a useful approach for determining therapeutic outcomes and a potential target treatments for PD [69, 71]. Therefore, our findings support the hypothesis that not only stem cells reduce the concentration of IL-1 $\beta$  but also favor an increase in bone regeneration in patients with periodontal disease.

Having said that, although high levels of IL-1 $\beta$  are associated with PD, it is also true that early IL-1 $\beta$  effectively induces mesenchymal stem cells to differentiate into osteoblasts and tissue to become mineralized [72]. Consequently, it would be advisable in future studies to carry out a short-term evaluation after the placement of the DPMSCs.

Also, it has been reported that after the administration of MSCs, the inflammatory microenvironment is promoted to an anti-inflammatory one, by inhibiting the production of proinflammatory cytokines (such as TNF- $\alpha$  and IL-6) and regulating endothelial permeability. These effects can be mediated by paracrine mechanisms that control the inflammation cascade [73]. IL-6 is involved in the differentiation of DPMSCs towards preosteoblasts [74]. For this reason, it is possible that it intervenes in the regeneration of the periodontium [64, 68]. In this regard, in our study, IL-6 concentrations showed a decrease with a tendency to difference in the group treated with DPMSCs.

On the other hand, in our research, it was observed that the patients treated with DPMSCs had no signs or symptoms of rejection, which is consistent with previous clinical studies that indicate that none of the patients had adverse effects on mesenchymal stem cell grafting, since these are cells have immunosuppressive activity, allowing them to be used allogeneically in the treatment of various diseases [75, 76]. Sim-

ilarly, our results agree with those of the study by Feng et al. (2010), who observed that patients who underwent periodontal ligament cells had a beneficial effect on periodontal defects and had an uncomplicated healing of the gum during the first 3 weeks [45].

This may be related to the fact that MSCs suppress the proliferation of CD4<sup>+</sup>, CD8<sup>+</sup>, B cells, and natural killer T cells [65]. They also induce the proliferation of CD4/CD25 regulatory T cells (Tregs), when cocultured with blood mononuclear cells, and can activate macrophages influencing them to differentiate into an anti-inflammatory immunophenotype [77–80].

The immunomodulatory capacity of MSCs is an important property exploited for the treatment of diseases related to inflammation, such as PD, because they can regulate both the innate and adaptive immune response [81–83].

Some studies suggest that MSCs can inhibit activation of T lymphocytes, natural killer cells, and dendritic cells [84], and that type 1 dendritic cells are induced by MSCs to reduce TNF- $\alpha$  secretion and type dendritic cells 2 to increase IL-10 secretion [85, 86]. Likewise, Th1 cells reduce the secretion of INF- $\gamma$  and Th2 cells increase the secretion of IL-4 [87], which induces a higher immune tolerance a phenotype [88].

MSCs can suppress immune reactions both *in vitro* and *in vivo* [89] because they express low levels of the Major Histocompatibility Complex (MHC) I antigens and do not express MHC II. Accordingly, it is proposed that MSCs have an “immunological privilege” that allows them to be used in allogeneic transplants without problems [90].

Studies with autologous and allogeneic MSCs reveal that these produce soluble factors such as TGF- $\beta$  and hepatocyte growth factor that suppress lymphocyte proliferation [91]. In incipient clinical trials where MSCs are used allogeneically, they have been shown to have good tolerance and to not induce an immune response when transplanted into an unrelated receptor [92, 93], as observed in our study. In this sense, preclinical and clinical studies applying MSC reveal beneficial effects to solve different pathologies, but that does not exclude some risks of acute problems (such as immune-mediated reaction and embolic phenomenon), intermediate problems (like graft versus host disease and secondary infection), and long-term problems (as risk of malignancy), due to controversial results on these risks [94], it is recommended to monitor the long-term safety of MSC use, quality control,

and clinical-grade production that includes cell viability, endotoxin, and oncogenic assays [95].

Finally, our findings show a therapeutic advantage in the application of mesenchymal stem cells in vertical defects, bone neof ormation, antioxidant, and anti-inflammatory activity compared to conventional treatment. Hence, DP MSC treatment could be a more effective therapeutic option for the recovery of connective tissues around the tooth, which have been lost due to PD. Although it is important to point out that one limitation of the study was the reduced sample size, likewise, the groups were not proportionally divided by age and sex, so the influence of these variables could not be evaluated. In addition, the study follow-up was only at 6 months, and the effectiveness of the treatment cannot be assured any longer. In this sense, although the potential risks of MSC administration cannot be completely ruled out in our study, the function of MSCs appears to be mediated through a “hit and run” mechanism rather than through a sustained engraftment in the injured tissues. The low degree of MSC engraftment may limit the long-term advantages of MSC therapy [96]. Also, both the localized issue of periodontal disease and of the therapeutic procedure proposed here could act in favor rather than to the detriment of the patient’s health.

## 5. Conclusions

Our findings suggest that a DP MSCs treatment has an effect on periodontal bone regeneration in periodontal disease in aging people, linked to an increased superoxide dismutase, and decreased proinflammatory interleukins. Therefore, we conclude that a DP MSCs treatment can be a useful option to regenerate the lost tissues in periodontal disease.

## Data Availability

The data used to support the findings of this study are available from the corresponding author upon request.

## Conflicts of Interest

There are no conflicts of interest.

## Acknowledgments

Posgrado en Ciencias Biológicas, UNAM y Consejo Nacional de Ciencia y Tecnología (CONACyT) CVU: 412849/262614. The authors appreciate the clinical support of Andrés Alcauter-Zavala and Carlos Andrés Rosas Sánchez in the language review. This project was supported by a grant from the Secretaría de Educación, Ciencia, Tecnología e Innovación de la Ciudad de México SECITI/042/2018 “Red colaborativa de Investigación Traslacional para el Envejecimiento Saludable de la Ciudad de México (RECITES).” Also, it was supported by Dirección General de Asuntos del Personal Académico, Universidad Nacional Autónoma de México (DGAPA, UNAM), PAPIIT IN221815, and Posgrado en Ciencias Biológicas, UNAM.

## References

- [1] F. C. Irani, R. R. Wassall, and P. M. Preshaw, “Impact of periodontal status on oral health-related quality of life in patients with and without type 2 diabetes,” *Journal of Dentistry*, vol. 43, no. 5, pp. 506–511, 2015.
- [2] G. Hajishengallis, “Immunomicrobial pathogenesis of periodontitis: keystone pathogens, pathobionts, and host response,” *Trends in Immunology*, vol. 35, no. 1, pp. 3–11, 2014.
- [3] B. Syndergaard, M. al-Sabbagh, R. J. Kryscio et al., “Salivary biomarkers associated with gingivitis and response to therapy,” *Journal of Periodontology*, vol. 85, no. 8, pp. e295–e303, 2014.
- [4] N. Nizam, P. Gümüş, J. Pitkänen, T. Tervahartiala, T. Sorsa, and N. Buduneli, “Serum and salivary matrix metalloproteinases, neutrophil elastase, myeloperoxidase in patients with chronic or aggressive periodontitis,” *Inflammation*, vol. 37, no. 5, pp. 1771–1778, 2014.
- [5] M. Greabu, A. Totan, D. Miricescu, R. Radulescu, J. Virlan, and B. Calenic, “Hydrogen sulfide, oxidative stress and periodontal diseases: a concise review,” *Antioxidants (Basel)*, vol. 5, no. 1, p. 3, 2016.
- [6] M. Fredriksson, A. Gustafsson, B. Asman, and K. Bergström, “Hyper-reactive peripheral neutrophils in adult periodontitis: generation of chemiluminescence and intracellular hydrogen peroxide after in vitro priming and FcγR stimulation,” *Journal of Clinical Periodontology*, vol. 25, no. 5, pp. 394–398, 1998.
- [7] A. Sharma and S. Sharma, “Reactive oxygen species and antioxidants in periodontics: a review,” *International journal of Dental clinics*, vol. 3, no. 2, pp. 44–47, 2011.
- [8] N. J. Kassebaum, E. Bernabé, M. Dahiya, B. Bhandari, C. J. L. Murray, and W. Marcenes, “Global burden of severe periodontitis in 1990–2010: a systematic review and meta-regression,” *Journal of Dental Research*, vol. 93, no. 11, pp. 1045–1053, 2014.
- [9] P. E. Petersen and H. Ogawa, “The global burden of periodontal disease: towards integration with chronic disease prevention and control,” *Periodontology 2000*, vol. 60, no. 1, pp. 15–39, 2012.
- [10] J. Otomo-Corgel, J. J. Pucher, M. P. Rethman, and M. A. Reynolds, “State of the science: chronic periodontitis and systemic health,” *The Journal of Evidence-Based Dental Practice*, vol. 12, no. 3, pp. 20–28, 2012.
- [11] H. Mawardi, L. Elbadawi, and S. Sonis, “Current understanding of the relationship between periodontal and systemic diseases,” *Saudi Medical Journal*, vol. 36, no. 2, pp. 150–158, 2015.
- [12] P. S. Rahajoe, M. Smit, G. Schuurmans et al., “Increased IgA anti-citrullinated protein antibodies in the periodontal inflammatory exudate of healthy individuals compared to rheumatoid arthritis patients,” *Journal of Clinical Periodontology*, vol. 47, no. 5, pp. 552–560, 2020.
- [13] D. F. Kinane, P. G. Stathopoulou, and P. N. Papapanou, “Periodontal diseases,” *Nature Reviews. Disease Primers*, vol. 3, no. 1, p. 17038, 2017.
- [14] S. Otaki, S. Ueshima, K. Shiraishi et al., “Mesenchymal progenitor cells in adult human dental pulp and their ability to form bone when transplanted into immunocompromised mice,” *Cell Biology International*, vol. 31, no. 10, pp. 1191–1197, 2007.
- [15] X. Fu, L. Jin, P. Ma, Z. Fan, and S. Wang, “Allogeneic stem cells from deciduous teeth in treatment for periodontitis in miniature swine,” *Journal of Periodontology*, vol. 85, no. 6, pp. 845–851, 2014.





- [16] X. Gao, Z. Shen, M. Guan et al., "Immunomodulatory role of stem cells from human exfoliated deciduous teeth on periodontal regeneration," *Tissue Engineering. Part A*, vol. 24, no. 17-18, pp. 1341–1353, 2018.
- [17] Y. Q. Qiao, L. S. Zhu, S. J. Cui, T. Zhang, R. L. Yang, and Y. H. Zhou, "Local administration of stem cells from human exfoliated primary teeth attenuate experimental periodontitis in mice," *The Chinese Journal of Dental Research*, vol. 22, no. 3, pp. 157–163, 2019.
- [18] B. Hernández-Monjaraz, E. Santiago-Osorio, A. Monroy-García, E. Ledesma-Martínez, and V. Mendoza-Núñez, "Mesenchymal stem cells of dental origin for inducing tissue regeneration in periodontitis: a mini-review," *International Journal of Molecular Sciences*, vol. 19, no. 4, p. 944, 2018.
- [19] C. M. Sedgley and T. M. Botero, "Dental stem cells and their sources," *Dental Clinics of North America*, vol. 56, no. 3, pp. 549–561, 2012.
- [20] Y. Y. Jo, H. J. Lee, S. Y. Kook et al., "Isolation and characterization of postnatal stem cells from human dental tissues," *Tissue Engineering*, vol. 13, no. 4, pp. 767–773, 2007.
- [21] J. Han, D. Menicanin, S. Gronthos, and P. M. Bartold, "Stem cells, tissue engineering and periodontal regeneration," *Australian Dental Journal*, vol. 59, Suppl 1, pp. 117–1130, 2014.
- [22] T. Okajcekova, J. Strnadel, M. Pokusa et al., "A comparative in vitro analysis of the osteogenic potential of human dental pulp stem cells using various differentiation conditions," *International Journal of Molecular Sciences*, vol. 21, no. 7, p. 2280, 2020.
- [23] B. M. Kinaia, S. M. A. Chogle, A. M. Kinaia, and H. E. Goodis, "Regenerative therapy: a periodontal-endodontic perspective," *Dental Clinics of North America*, vol. 56, no. 3, pp. 537–547, 2012.
- [24] E. Ledesma-Martínez, V. M. Mendoza-Núñez, and E. Santiago-Osorio, "Mesenchymal stem cells for periodontal tissue regeneration in elderly patients," *The Journals of Gerontology. Series A, Biological Sciences and Medical Sciences*, vol. 74, no. 9, pp. 1351–1358, 2019.
- [25] M. Dominici, K. le Blanc, I. Mueller et al., "Minimal criteria for defining multipotent mesenchymal stromal cells. The International Society for Cellular Therapy position statement," *Cytotherapy*, vol. 8, no. 4, pp. 315–317, 2006.
- [26] J. L. Dzink, A. C. R. Tanner, A. D. Haffajee, and S. S. Socransky, "Gram negative species associated with active destructive periodontal lesions," *Journal of Clinical Periodontology*, vol. 12, no. 8, pp. 648–659, 1985.
- [27] I. L. C. Chapple and J. B. Matthews, "The role of reactive oxygen and antioxidant species in periodontal tissue destruction," *Periodontol 2000*, vol. 43, no. 1, pp. 160–232, 2007.
- [28] E. Ledesma-Martínez, V. M. Mendoza-Núñez, and E. Santiago-Osorio, "Mesenchymal stem cells derived from dental pulp: a review," *Stem Cells International*, vol. 2016, Article ID 4709572, 12 pages, 2016.
- [29] L. Hao, H. Sun, J. Wang, T. Wang, M. Wang, and Z. Zou, "Mesenchymal stromal cells for cell therapy: besides supporting hematopoiesis," *International Journal of Hematology*, vol. 95, no. 1, pp. 34–46, 2012.
- [30] S. M. Shalaby, A. S. el-Shal, S. H. Abd-Allah et al., "Mesenchymal stromal cell injection protects against oxidative stress in *Escherichia coli*-induced acute lung injury in mice," *Cytotherapy*, vol. 16, no. 6, pp. 764–775, 2014.
- [31] T. Sun, G. Z. Gao, R. F. Li et al., "Bone marrow-derived mesenchymal stem cell transplantation ameliorates oxidative stress and restores intestinal mucosal permeability in chemically induced colitis in mice," *American Journal of Translational Research*, vol. 7, no. 5, pp. 891–901, 2015.
- [32] S. Gronthos, M. Mankani, J. Brahim, P. G. Robey, and S. Shi, "Postnatal human dental pulp stem cells (DPSCs) in vitro and in vivo," *Proceedings of the National Academy of Sciences*, vol. 97, no. 25, pp. 13625–13630, 2000.
- [33] M. Miura, S. Gronthos, M. Zhao et al., "SHED: stem cells from human exfoliated deciduous teeth," *Proceedings of the National Academy of Sciences*, vol. 100, no. 10, pp. 5807–5812, 2003.
- [34] S. Shi, P. M. Bartold, M. Miura, B. M. Seo, P. G. Robey, and S. Gronthos, "The efficacy of mesenchymal stem cells to regenerate and repair dental structures," *Orthodontics & Craniofacial Research*, vol. 8, no. 3, pp. 191–199, 2005.
- [35] T. Iwata, M. Yamato, H. Tsuchioka et al., "Periodontal regeneration with multi-layered periodontal ligament-derived cell sheets in a canine model," *Biomaterials*, vol. 30, no. 14, pp. 2716–2723, 2009.
- [36] Y. Liu, Y. Zheng, G. Ding et al., "Periodontal ligament stem cell-mediated treatment for periodontitis in miniature swine," *Stem Cells*, vol. 26, no. 4, pp. 1065–1073, 2008.
- [37] R. D'Aquino, A. De Rosa, V. Lanza et al., "Human mandible bone defect repair by the grafting of dental pulp stem/progenitor cells and collagen sponge biocomplexes," *European Cells and Materials*, vol. 18, pp. 75–83, 2009.
- [38] G. Ding, Y. Liu, W. Wang et al., "Allogeneic periodontal ligament stem cell therapy for periodontitis in swine," *Stem Cells*, vol. 28, no. 10, pp. 1829–1838, 2010.
- [39] J.-Y. Park, S. H. Jeon, and P.-H. Choung, "Efficacy of periodontal stem cell transplantation in the treatment of advanced periodontitis," *Cell Transplantation*, vol. 20, no. 2, pp. 271–286, 2011.
- [40] L. Wang, H. Shen, W. Zheng et al., "Characterization of stem cells from alveolar periodontal ligament," *Tissue Engineering. Part A*, vol. 17, no. 7-8, pp. 1015–1026, 2011.
- [41] F. F. Suaid, F. V. Ribeiro, T. R. L. E. S. Gomes et al., "Autologous periodontal ligament cells in the treatment of class III furcation defects: a study in dogs," *Journal of Clinical Periodontology*, vol. 39, no. 4, pp. 377–384, 2012.
- [42] J. Nuñez, S. Sanz-Blasco, F. Vignoletti et al., "Periodontal regeneration following implantation of cementum and periodontal ligament-derived cells," *Journal of Periodontal Research*, vol. 47, no. 1, pp. 33–44, 2012.
- [43] S. Portron, A. Soueidan, A.-C. Marsden et al., "Periodontal regenerative medicine using mesenchymal stem cells and biomaterials: a systematic review of pre-clinical studies," *Dental Materials Journal*, vol. 38, no. 6, pp. 867–883, 2019.
- [44] A. Pérez-Borrego, L. Domínguez-Rodríguez, Z. T. Ilisástigui-Ortueta, and P. Hernández-Ramírez, "Utilización de células madre en el tratamiento de defectos óseos periodontales," *Revista Cubana de Estomatología*, vol. 46, no. 4, pp. 108–116, 2009.
- [45] F. Feng, K. Akiyama, Y. Liu et al., "Utility of PDL progenitors for in vivo tissue regeneration: a report of 3 cases," *Oral Diseases*, vol. 16, no. 1, pp. 20–28, 2010.
- [46] F. Carini, G. B. Menchini Fabris, E. Biagi, A. Salvade', L. Sbordone, and M. G. Baldoni, "Estudio experimental sobre la utilización de células madre humanas en la terapia de los

- defectos periodontales: resultados preliminares,” *Avances en Periodoncia e Implantología Oral*, vol. 23, no. 2, pp. 97–107, 2011.
- [47] F. Ferrarotti, F. Romano, M. N. Gamba et al., “Human intrabony defect regeneration with micrografts containing dental pulp stem cells: a randomized controlled clinical trial,” *Journal of Clinical Periodontology*, vol. 45, no. 7, pp. 841–850, 2018.
- [48] C. Raggi and A. C. Berardi, “Mesenchymal stem cells, aging and regenerative medicine,” *Muscles Ligaments Tendons J*, vol. 2, no. 3, pp. 239–242, 2012.
- [49] D. Goodarzi Pour, E. Romoozi, and Y. Soleimani Shayesteh, “Accuracy of cone beam computed tomography for detection of bone loss,” *J Dent (Tehran)*, vol. 12, no. 7, pp. 513–523, 2015.
- [50] C. Mangano, A. de Rosa, V. Desiderio et al., “The osteoblastic differentiation of dental pulp stem cells and bone formation on different titanium surface textures,” *Biomaterials*, vol. 31, no. 13, pp. 3543–3551, 2010.
- [51] H. C. Liu, L. L. E. D. S. Wang et al., “Reconstruction of alveolar bone defects using bone morphogenetic protein 2 mediated rabbit dental pulp stem cells seeded on nano-hydroxyapatite/collagen/poly(L-lactide),” *Tissue Engineering Part A*, vol. 17, no. 19–20, pp. 2417–2433, 2011.
- [52] M. Aimetti, F. Ferrarotti, L. Cricenti, G. M. Mariani, and F. Romano, “Autologous dental pulp stem cells in periodontal regeneration: a case report,” *International Journal of Periodontics & Restorative Dentistry*, vol. 34, Supplement 3, pp. 27–33, 2014.
- [53] U. K. Gursoy, E. Könönen, S. Huuononen et al., “Salivary type I collagen degradation end-products and related matrix metalloproteinases in periodontitis,” *Journal of Clinical Periodontology*, vol. 40, no. 1, pp. 18–25, 2013.
- [54] B. Hernández-Monjaraz, E. Santiago-Osorio, E. Ledesma-Martínez, A. Alcauter-Zavala, and V. M. Mendoza-Núñez, “Retrieval of a periodontally compromised tooth by allogeneic grafting of mesenchymal stem cells from dental pulp: a case report,” *The Journal of International Medical Research*, vol. 46, no. 7, pp. 2983–2993, 2018.
- [55] A. Sculean, A. Stavropoulos, P. Windisch, T. Keglevich, T. Karring, and I. Gera, “Healing of human intrabony defects following regenerative periodontal therapy with a bovine-derived xenograft and guided tissue regeneration,” *Clinical Oral Investigations*, vol. 8, no. 2, pp. 70–74, 2004.
- [56] A. Valle-Prieto and P. A. Conget, “Human mesenchymal stem cells efficiently manage oxidative stress,” *Stem Cells and Development*, vol. 19, no. 12, pp. 1885–1893, 2010.
- [57] W. A. Silva, D. T. Covas, R. A. Panepucci et al., “The profile of gene expression of human marrow mesenchymal stem cells,” *Stem Cells*, vol. 21, no. 6, pp. 661–669, 2003.
- [58] A. B. Salmon, V. I. Pérez, A. Bokov et al., “Lack of methionine sulfoxide reductase A in mice increases sensitivity to oxidative stress but does not diminish life span,” *The FASEB Journal*, vol. 23, no. 10, pp. 3601–3608, 2009.
- [59] F. da Costa Gonçalves, M. Grings, N. S. Nunes et al., “Antioxidant properties of mesenchymal stem cells against oxidative stress in a murine model of colitis,” *Biotechnology Letters*, vol. 39, no. 4, pp. 613–622, 2017.
- [60] K. Kemp, K. Hares, E. Mallam, K. J. Heesom, N. Scolding, and A. Wilkins, “Mesenchymal stem cell-secreted superoxide dismutase promotes cerebellar neuronal survival,” *Journal of Neurochemistry*, vol. 114, no. 6, pp. 1569–1580, 2010.
- [61] I. Thesleff and P. Nieminen, “Tooth morphogenesis and cell differentiation,” *Current Opinion in Cell Biology*, vol. 8, no. 6, pp. 844–850, 1996.
- [62] Y. Ohata and K. Ozono, “Bone and stem cells. The mechanism of osteogenic differentiation from mesenchymal stem cell,” *Clinical Calcium*, vol. 24, no. 4, pp. 501–508, 2014.
- [63] S. J. Dangaria, Y. Ito, X. Luan, and T. G. H. Diekwisch, “Successful periodontal ligament regeneration by periodontal progenitor preseeded on natural tooth root surfaces,” *Stem Cells and Development*, vol. 20, no. 10, pp. 1659–1668, 2011.
- [64] J. L. Ebersole, D. R. Dawson, L. A. Morford, R. Peyyala, C. S. Miller, and O. A. González, “Periodontal disease immunology: ‘double indemnity’ in protecting the host,” *Periodontology 2000*, vol. 62, no. 1, pp. 163–202, 2013.
- [65] S. H. J. Mei, J. J. Haitisma, C. C. Dos Santos et al., “Mesenchymal stem cells reduce inflammation while enhancing bacterial clearance and improving survival in sepsis,” *American Journal of Respiratory and Critical Care Medicine*, vol. 182, no. 8, pp. 1047–1057, 2010.
- [66] S. Pitaru, C. A. G. McCulloch, and S. A. Narayanan, “Cellular origins and differentiation control mechanisms during periodontal development and wound healing,” *Journal of Periodontal Research*, vol. 29, no. 2, pp. 81–94, 1994.
- [67] R. Teles, F. Teles, J. Frias-López, B. Paster, and A. Haffajee, “Lessons learned and unlearned in periodontal microbiology,” *Periodontology 2000*, vol. 62, no. 1, pp. 95–162, 2013.
- [68] G. Hajishengallis, T. Maekawa, T. Abe, E. Hajishengallis, and J. D. Lambris, “Complement involvement in periodontitis: molecular mechanisms and rational therapeutic approaches,” *Advances in Experimental Medicine and Biology*, vol. 865, pp. 57–74, 2015.
- [69] K. Aral, M. R. Milward, Y. Kapila, A. Berdeli, and P. R. Cooper, “Inflammasomes and their regulation in periodontal disease: a review,” *Journal of Periodontal Research*, vol. 55, no. 4, pp. 473–487, 2020.
- [70] T. W. Oates, D. T. Graves, and D. L. Cochran, “Clinical, radiographic and biochemical assessment of IL-1/TNF-alpha antagonist inhibition of bone loss in experimental periodontitis,” *Journal of Clinical Periodontology*, vol. 29, no. 2, pp. 137–143, 2002.
- [71] J. T. Marchesan, M. S. Girnary, K. Moss et al., “Role of inflammasomes in the pathogenesis of periodontal disease and therapeutics,” *Periodontology 2000*, vol. 82, no. 1, pp. 93–114, 2019.
- [72] K. Sonomoto, K. Yamaoka, K. Oshita et al., “Interleukin-1 $\beta$  induces differentiation of human mesenchymal stem cells into osteoblasts via the Wnt-5a/receptor tyrosine kinase-like orphan receptor 2 pathway,” *Arthritis and Rheumatism*, vol. 64, no. 10, pp. 3355–3363, 2012.
- [73] W. L. Tai, Z. X. Dong, D. D. Zhang, and D. H. Wang, “Therapeutic effect of intravenous bone marrow-derived mesenchymal stem cell transplantation on early-stage LPS-induced acute lung injury in mice,” *Journal of Southern Medical University*, vol. 32, no. 3, pp. 283–290, 2012.
- [74] N. Nowwarote, W. Sukarawan, P. Pavasant, and T. Osathanon, “Basic fibroblast growth factor regulates REX1 expression via IL-6 in stem cells isolated from human exfoliated deciduous teeth,” *Journal of Cellular Biochemistry*, vol. 118, no. 6, pp. 1480–1488, 2017.
- [75] Z. Li, C. M. Jiang, S. An et al., “Immunomodulatory properties of dental tissue-derived mesenchymal stem cells,” *Oral Diseases*, vol. 20, no. 1, pp. 25–34, 2014.

- [76] Y.-H. Kang, H.-J. Lee, S.-J. Jang et al., “Immunomodulatory properties and *in vivo* osteogenesis of human dental stem cells from fresh and cryopreserved dental follicles,” *Differentiation*, vol. 90, no. 1-3, pp. 48–58, 2015.
- [77] S. Aggarwal and M. F. Pittenger, “Human mesenchymal stem cells modulate allogeneic immune cell responses,” *Blood*, vol. 105, no. 4, pp. 1815–1822, 2005.
- [78] A. Corcione, F. Benvenuto, E. Ferretti et al., “Human mesenchymal stem cells modulate B-cell functions,” *Blood*, vol. 107, no. 1, pp. 367–372, 2006.
- [79] K. Le Blanc and O. Ringdén, “Immunomodulation by mesenchymal stem cells and clinical experience,” *Journal of Internal Medicine*, vol. 262, no. 5, pp. 509–525, 2007.
- [80] J. Kim and P. Hematti, “Mesenchymal stem cell-educated macrophages: a novel type of alternatively activated macrophages,” *Experimental Hematology*, vol. 37, no. 12, pp. 1445–1453, 2009.
- [81] S. R. R. Hall, K. Tsoyi, B. Ith et al., “Mesenchymal stromal cells improve survival during sepsis in the absence of heme oxygenase-1: the importance of neutrophils,” *Stem Cells*, vol. 31, no. 2, pp. 397–407, 2013.
- [82] D. Noël, F. Djouad, C. Bouffi, D. Mrugala, and C. Jorgensen, “Multipotent mesenchymal stromal cells and immune tolerance,” *Leukemia & Lymphoma*, vol. 48, no. 7, pp. 1283–1289, 2009.
- [83] K. Le Blanc, I. Rasmusson, B. Sundberg et al., “Treatment of severe acute graft-versus-host disease with third party haploidentical mesenchymal stem cells,” *Lancet*, vol. 363, no. 9419, pp. 1439–1441, 2004.
- [84] S. Beyth, Z. Borovsky, D. Mevorach et al., “Human mesenchymal stem cells alter antigen-presenting cell maturation and induce T-cell unresponsiveness,” *Blood*, vol. 105, no. 5, pp. 2214–2219, 2005.
- [85] W. Zhang, W. Ge, C. Li et al., “Effects of mesenchymal stem cells on differentiation, maturation, and function of human monocyte-derived dendritic cells,” *Stem Cells and Development*, vol. 13, no. 3, pp. 263–271, 2004.
- [86] B. Zhang, R. Liu, D. Shi et al., “Mesenchymal stem cells induce mature dendritic cells into a novel Jagged-2 dependent regulatory dendritic cell population,” *Blood*, vol. 113, no. 1, pp. 46–57, 2009.
- [87] A. Graziano, R. D’Aquino, G. Laino et al., “Human CD34+ stem cells produce bone nodules *in vivo*,” *Cell Proliferation*, vol. 41, no. 1, pp. 1–11, 2008.
- [88] P. Batten, P. Sarathchandra, J. W. Antoniwi et al., “Human mesenchymal stem cells induce T cell anergy and downregulate T cell allo-responses via the TH2 pathway: relevance to tissue engineering human heart valves,” *Tissue Engineering*, vol. 12, no. 8, pp. 2263–2273, 2006.
- [89] M. Krampera, A. Pasini, G. Pizzolo, L. Cosmi, S. Romagnani, and F. Annunziato, “Regenerative and immunomodulatory potential of mesenchymal stem cells,” *Current Opinion in Pharmacology*, vol. 6, no. 4, pp. 435–441, 2006.
- [90] E. Zappia, S. Casazza, E. Pedemonte et al., “Mesenchymal stem cells ameliorate experimental autoimmune encephalomyelitis inducing T-cell anergy,” *Blood*, vol. 106, no. 5, pp. 1755–1761, 2005.
- [91] M. Di Nicola, C. Carlo-Stella, M. Magni et al., “Human bone marrow stromal cells suppress T-lymphocyte proliferation induced by cellular or nonspecific mitogenic stimuli,” *Blood*, vol. 99, no. 10, pp. 3838–3843, 2002.
- [92] J. M. Ryan, F. P. Barry, J. M. Murphy, and B. P. Mahon, “Mesenchymal stem cells avoid allogeneic rejection,” *Journal of Inflammation*, vol. 2, no. 1, p. 8, 2005.
- [93] E. M. Horwitz, P. L. Gordon, W. K. K. Koo et al., “Isolated allogeneic bone marrow-derived mesenchymal cells engraft and stimulate growth in children with osteogenesis imperfecta: implications for cell therapy of bone,” *Proceedings of the National Academy of Sciences*, vol. 99, no. 13, pp. 8932–8937, 2002.
- [94] W. Lin, L. Huang, Y. Li et al., “Mesenchymal stem cells and cancer: clinical challenges and opportunities,” *BioMed Research International*, vol. 2019, Article ID 2820853, 12 pages, 2019.
- [95] P. Saeedi, R. Halabian, and A. A. I. Fooladi, “A revealing review of mesenchymal stem cells therapy, clinical perspectives and modification strategies,” *Stem Cell Investigation*, vol. 6, p. 34, 2019.
- [96] L. von Bahr, I. Batsis, G. Moll et al., “Analysis of tissues following mesenchymal stromal cell therapy in humans indicates limited long-term engraftment and no ectopic tissue formation,” *Stem Cells*, vol. 30, no. 7, pp. 1575–1578, 2012.

## Research Article

# IL-37 Gene Modification Enhances the Protective Effects of Mesenchymal Stromal Cells on Intestinal Ischemia Reperfusion Injury

Dejun Kong <sup>1,2</sup>, Yonghao Hu,<sup>1,2</sup> Xiang Li,<sup>1,2</sup> Dingding Yu,<sup>1,2</sup> Hongyue Li,<sup>1,2</sup> Yiming Zhao,<sup>1,2</sup> Yafei Qin,<sup>1,2</sup> Wang Jin,<sup>1,2</sup> Baoren Zhang,<sup>1,2</sup> Bo Wang,<sup>3</sup> Hongda Wang,<sup>1,2</sup> Guangming Li,<sup>1,2</sup> and Hao Wang <sup>1,2</sup>

<sup>1</sup>Department of General Surgery, Tianjin Medical University General Hospital, Tianjin, China

<sup>2</sup>Tianjin General Surgery Institute, Tianjin, China

<sup>3</sup>Department of Paediatric Surgery, Tianjin Medical University General Hospital, Tianjin, China

Correspondence should be addressed to Hao Wang; [hwangca272@hotmail.com](mailto:hwangca272@hotmail.com)

Received 7 May 2020; Revised 15 July 2020; Accepted 24 July 2020; Published 8 August 2020

Academic Editor: Jun Liu

Copyright © 2020 Dejun Kong et al. This is an open access article distributed under the Creative Commons Attribution License, which permits unrestricted use, distribution, and reproduction in any medium, provided the original work is properly cited.

**Background.** Ischemia reperfusion injury (IRI) is the major cause of intestinal damage in clinic. Although either mesenchymal stromal cells (MSCs) or interleukin 37 (IL-37) shows some beneficial roles to ameliorate IRI, their effects are limited. In this study, the preventative effects of IL-37 gene-modified MSCs (IL-37-MSCs) on intestinal IRI are investigated. **Methods.** Intestinal IRI model was established by occluding the superior mesenteric artery for 30 minutes and then reperused for 72 hours in rats. Forty adult male Sprague-Dawley rats were randomly divided into the sham control, IL-37-MSC-treated, MSC-treated, recombinant IL-37- (rIL-37-) treated, and untreated groups. Intestinal damage was assessed by H&E staining. The levels of gut barrier function factors (diamine oxidase and D-Lactate) and inflammation cytokine IL-1 $\beta$  were assayed using ELISA. The synthesis of tissue damage-related NLRP3 inflammasome and downstream cascade reactions including cleaved caspase-1, IL-1 $\beta$ , and IL-18 was detected by western blot. The mRNA levels of proinflammatory mediators IL-6 and TNF- $\alpha$ , which are downstream of IL-1 $\beta$  and IL-18, were determined by qPCR. Data were analyzed by one-way analysis of variance (ANOVA) after the normality test and followed by post hoc analysis with the least significant difference (LSD) test. **Results.** IL-37-MSCs were able to migrate to the damaged tissue and significantly inhibit intestinal IRI. As compared with MSCs or the rIL-37 monotherapy group, IL-37-MSC treatment both improved gut barrier function and decreased local and systemic inflammation cytokine IL-1 $\beta$  level in IRI rats. In addition, tissue damage-related NLRP3 and downstream targets (cleaved caspase-1, IL-1 $\beta$ , and IL-18) were significantly decreased in IRI rats treated with IL-37-MSCs. Furthermore, IL-1 $\beta$ - and IL-18-related proinflammatory mediator IL-6 and TNF- $\alpha$  mRNA expressions were all significantly decreased in IRI rats treated with IL-37-MSCs. **Conclusion.** The results suggest that IL-37 gene modification significantly enhances the protective effects of MSCs against intestinal IRI. In addition, NLRP3-related signaling pathways could be associated with IL-37-MSC-mediated protection.

## 1. Introduction

Intestinal ischemia reperfusion injury (IRI), one of the major causes of clinical acute intestine necrosis, is a life-threatening disease with high mortality and disability [1]. Intestinal IRI is common in multiple diseases including vascular occlusion, hemorrhagic shock, trauma, and small bowel transplantation

[2, 3]. However, currently, there is no effective treatment available besides surgical intervention, and thus, a novel treatment is urgently needed [4].

The underlying mechanisms of intestinal IRI are complicated, and diverse factors are involved in the process [1]. Briefly, intestinal IRI is often correlated with circulatory diseases in the gastrointestinal system involving the superior



mesenteric artery (SMA), weak innate immunity, weak adaptive immunity, and high levels of inflammation. At the early stage of ischemia, the endothelial barrier is destroyed resulting in an increase in vascular permeability. Simultaneously, reactive oxygen species (ROS) can be excessively produced. After ROS production, reperfusion upregulates the release of ROS, consequently disrupting normal ATP generation. Excessive ROS also cause severe oxidative stress, which can promote DNA damage, endothelial dysfunction, and local inflammatory responses. On the basis of ischemia, reperfusion triggers the release of intracellular and extracellular damage-associated molecular pattern molecules (DAMPs), resulting in the accumulation of inflammatory cells such as monocytes and dendritic cells [5].

The NOD-like receptor protein 3 (NLRP3) is a member of pattern recognition receptors and plays a key role in inflammatory responses via formation of an intracellular multiprotein complex known as NLRP3 inflammasome, which is the best characterized of all other inflammasomes [6]. Inflammasomes are important signal platforms in detecting sterile stressors and pathogenic microorganisms such as some DAMPs, which activate and release the highly proinflammatory cytokines interleukin  $1\beta$  (IL- $1\beta$ ) and interleukin 18 (IL-18). In this process, ROS, as a kind of DAMPs, was excessively produced during IRI and then promotes NLRP3 inflammasome activation [7], subsequently assisting conversion of pro-caspase-1 into cleaved caspase-1; the activation of caspase-1 can upregulate the production and secretion of the cytokines such as IL- $1\beta$  and IL-18 by cleavage of pro-IL- $1\beta$  and pro-IL-18. At the same time, activation of inflammasome-associated inflammatory caspase-1 drives cleavage of the proapoptosis factor, gasdermin D, generating an N-terminal fragment that oligomerizes to form pores on the cell membrane and causes programmed cell death known as pyroptosis [8–11]. In previous studies, NLRP3 can be activated by different mediators such as DAMPs and/or PAMPs *in vivo*, and NLRP3 plays a crucial role in the development of IRI in various organs [7, 12, 13]. Therefore, inhibiting NLRP3 inflammasome activation may play a protective role in IRI.

Mesenchymal stromal cells (MSCs) are a group of stem cells derived from the embryonic mesoderm, which can differentiate into various kinds of cells [4, 14, 15]. MSCs have the proliferative, pluripotent, and immunomodulatory potentials that can help repair damaged tissues and improve tissue microenvironment [16]. Accumulating evidence has demonstrated that MSC treatment could alleviate IRI in various organs by inhibiting intensive inflammation, apoptosis, generations of oxidative stress, ROS, and immune overreactivity [17, 18].

Interleukin 37 (IL-37) is a novel cytokine that recently characterized a member in the IL-1 family, which plays a key role in limiting excessive and runaway inflammatory responses via suppressing both innate and adaptive immunity [19–21]. It has been demonstrated that a knockdown of endogenous IL-37 in human peripheral blood mononuclear cells results in increased production of several proinflammatory cytokines [22]. Human IL-37 transgenic mice are protected against metabolic syndrome, systemic inflam-

mation reaction, DSS-induced colitis, and acute myocardial infarction. As an immunomodulatory factor, IL-37 has been tested in IRI models such as myocardial and renal IRI [23, 24].

Although MSCs and IL-37 could protect organs against IRI, their roles are limited for many reasons [25, 26]. Thus, it is necessary to combine them together to enhance their individual therapeutic effects. In this study, we successfully conducted IL-37 gene-modified MSCs and investigated their combined effects on the prevention of intestinal IRI and explored potential mechanisms of prevention.

## 2. Materials and Methods

**2.1. Animals.** Male Sprague-Dawley (SD) rats weighing 250–300 g were purchased from China National Institute for Food and Drug Control and were placed in a standard temperature environment, provided a standard diet, and provided water in the Animal Care Facility of Tianjin General Surgery Institute. All animal experimental operations were approved by the Institute of Animal Care and Use Committee at Tianjin Medical University and performed in accordance with the Guide for the Care and Use of Laboratory Animals.

**2.2. Isolation and Culture of MSCs.** MSCs were prepared according to the protocol described previously [4]. Briefly, in order to harvest the adipose tissue surrounding the inguens, rats were sacrificed and soaked in 75% alcohol for 10 min. Then, 200–300  $\mu$ L sterile PBS was added to every 0.5 g adipose tissue to prevent dehydration. The tissue was cut into  $<1\text{ mm}^3$  pieces, followed by the addition of type I collagenase solution (1 mg/mL, Solarbio, Beijing, China). The resulting tissue solution was placed in tubes which were subsequently placed on a shaker and incubated with constant agitation for 60 minutes (37°C, 200 rpm). Next, an equal volume of serum-containing medium was added to terminate digestion of the tissue. After that, the solution was centrifuged (1800 rpm, 5 min), the supernatant was discarded, and the remaining cells were washed twice with PBS. Lastly, cells were inoculated in a 15% fetal bovine serum (FBS, Hyclone, Tauranga, New Zealand) containing  $\alpha$ -MEM medium (Hyclone, Tauranga, New Zealand) and 1% penicillin/streptomycin (Solarbio, Beijing, China) and subcultured after 7–10 days. MSCs were identified through detection of the cell's morphology and the cells' surface markers.

**2.3. Preparation and Identification of IL-37-MSCs.** The construction of the vector expressing IL-37 (NM\_014439, IL-37 isoform b, which is best characterized, Ubi-MCS-3FLAG-SV40-EGFP-IRES-puromycin vector was used in this study, Ubi and SV40 here are promoters, FLAG and EGFP are marker genes, and MCS is a multiple cloning site), the required sequencing (results are shown in the supplement), and the lentiviral packaging were supported by GeneChem Inc., Shanghai, China. We conducted lentiviral transfection of MSCs according to the protocol provided by GeneChem Inc. (the vector lacking IL-37 was used as control). Lentiviral transfection is done with a suitable multiplicity of infection (MOI = 200, ratio of lentivirus to cell number) inside a

biological safety cabinet. The cells then were observed under an inverted fluorescence microscope at 72 hours posttransfection, and IL-37 expression was identified by immunofluorescence (IF, details are shown in methods of immunofluorescence).

Furthermore, IL-37-MSCs were subjected to drug screening using a 1  $\mu$ g/mL puromycin (Solarbio, Beijing, China) solution to obtain high-purity IL-37-MSCs. Flow cytometry was performed on the resulting IL-37-MSCs before treatment to ensure cell purity and quality.

**2.4. Flow Cytometry Analysis.** The positive rate for markers of MSCs and IL-37-MSCs was analyzed by using flow cytometric analysis. In brief, MSCs were stained with fluorescent antibodies, including anti-CD29-FITC, anti-CD45-PE, anti-CD79a-PE, and anti-CD90-FITC (eBioscience, San Diego, USA), according to the manufacturer's instruction. The percentages of various markers of MSCs were analyzed using the FlowJo software.

**2.5. Immunofluorescence.** We used immunofluorescence (IF) technology to identify IL-37 expression in IL-37-MSCs to ensure successful transfection; MSCs (negative control with lentiviral transfection which express GFP while lacking IL-37) were used as control. Briefly, first of all, MSCs were cultured on the slides pretreated with polylysine overnight. Then, cells were treated with 4% paraformaldehyde (PFA) for 30 minutes and subsequently treated with 0.1% Triton-X (Solarbio, Beijing, China) for 2 minutes. After that, cells were treated with 5% BSA for 30 minutes to reduce nonspecific antibody binding. Next, anti-IL-37 antibody (dilution at 1:250, Abcam, Cambridge, UK) was added to the slides for the night; after being washed three times by PBS, the cy3-conjugated goat anti-rabbit secondary antibody was added for half an hour and washed three times with PBS again. DAPI (Thermo Fisher Scientific, Waltham, USA) was added dropwise before the coverslip was placed over the slides. Lastly, the slides were observed under a fluorescence microscope.

**2.6. Experimental Groups.** To test the effects of IL-37-MSCs on protecting against intestinal IRI, SD rats were randomly assigned to five groups ( $n = 8$  each group): sham control group, IL-37-MSC-treated IRI group, MSC-treated IRI group, recombinant IL-37- (rIL-37-) treated (PeproTech, New Jersey, US) IRI group, and untreated IRI group. In the beginning, rats got intraperitoneal injection of pentobarbital sodium (50 mg/kg), heating pad was used to maintain their temperature, and abdomen hair was removed. After abdominal disinfection, SMA was isolated by a midline incision into the abdominal cavity. In the sham control group, rats were only operated by opening and closing the abdomen, without clipping the SMA. In other groups, the roof of SMA was clipped for 30 min then recovered reperfusion. After restoring the blood supply and closing the incision,  $2 \times 10^6$  IL-37-MSCs,  $2 \times 10^6$  MSCs, 2  $\mu$ g rIL-37 (based on efficacy assessments from our preexperimental results, 2  $\mu$ g each rat was used in this study), and 1 mL PBS were separately injected into tail veins of the SD rats. Rats were maintained

by continuous monitoring with a temperature-controlled self-regulated heating system after operation. After reperfusion for 72 hours, all rats were sacrificed for IRI assessment.

**2.7. Tracing of Infused IL-37-MSCs.** As IL-37-MSCs express GFP protein, we detected fluorescent protein expression in the damaged tissue to identify whether IL-37-MSCs could migrate to the injured intestine. The ileums were embedded in OCT to freeze the relevant section, and then, slides were observed under a fluorescent microscope to detect GFP expression.

**2.8. Histology.** To evaluate the impact of IL-37-MSC transplantation on the severity of intestinal IRI, the ileum was collected for assessment [27]. Intestine specimens were fixed in 10% formalin for 72 hours, then embedded in paraffin with correct orientation position of the crypt to villus axis and sectioned at 5  $\mu$ m for hematoxylin and eosin (H&E) staining to assess the severity of injury site. Chiu's score grading was used as standard: 0, normal villi of the small intestinal mucosa; 1, Gruenhagen's space under the intestinal mucosal epithelium in the villus axis, often accompanied by capillary congestion; 2, intestinal mucosal epithelium elevation from the intrinsic membrane and expansion of the intestinal subepithelial space; 3, large intestinal mucosal epithelium elevation, villus lodging to both sides, part of the villus shed; 4, villus and lamina detachment, bare capillaries dilate, an increase in the composition of lamina propria cell components; and 5, lamina propria is digested, bleeding or ulcers form [14, 28]. The slides from each sample and each slide with five fields at a magnification  $\times 100$  were observed by a professional pathologist, and the average scores of each group were calculated. The samples were randomly assigned to the pathologist and the experimental groups were blinded.

**2.9. Enzyme-Linked Immunosorbent Assay (ELISA).** D-Lactic acid (D-Lac) and diamine oxidase (DAO) in the serum were used to assess the gut barrier function [29]. IL-1 $\beta$  in the tissue and serum was used to assess the local and systemic inflammation activity. DAO, D-Lac ELISA kits (Senbeijia, Nanjing, China), and IL-1 $\beta$  ELISA kit (DAKEWE, Shenzhen, China) were used to evaluate the levels of local and systemic inflammation in the serum or tissue. All operations were conducted according to the manufacturer's recommended protocol.

**2.10. Real-Time PCR.** Total RNA was obtained from ileum tissue by using RNAprep Pure Tissue Kit (Tiangen, Beijing, China), and reverse transcription was performed by FastQuant RT Super Mix (Tiangen, Beijing, China); mRNA expression was quantified by 2x SYBR Green qPCR Master Mix (Bimake, Houston, TX, USA). In the reaction system,  $\beta$ -actin was used as an internal normalizing gene, and mRNA expression was analyzed by comparing cycles of threshold (Ct value) of  $2^{-\Delta\Delta Ct}$ . The primer sequences used were as follows:  $\beta$ -actin forward: 5'-GTTG ACAT CCGT AAAG AC-3', reverse: 5'-TGGA AGGT GGAC AGTG AG-3'; TNF- $\alpha$  forward: 5'-ACAC ACGA GACG CTGA AGTA-3', reverse: 5'-GGAA CAGT CTGG GAAG TCT-3'; and IL-6 forward:

5'-CTCA TTCT GTCT CGAG CCCA-3', reverse: 5'-CTGT GAAG TCTC CTCT CCGG-3'.

**2.11. Western Blot.** Ileum tissues were homogenized, and the resulting total protein was extracted by RIPA lysis mixed with PMSF (Solarbio, Beijing, China). Then, 50  $\mu$ g of protein per sample was subjected to 7.5%, 10%, or 15% sodium dodecyl sulfate polyacrylamide gel electrophoresis (SDS-PAGE, Solarbio, Beijing, China). After overnight incubation at 4°C with anti-NLRP3 antibody (dilution at 1:1000, Abcam, Cambridge, UK), anti-caspase-1 antibody (dilution at 1:300, Santa Cruz, Oregon, USA, SC-398715), anti-IL-1 $\beta$  antibody (dilution at 1:600, Bioss, Beijing, China), anti-IL-18 antibody (dilution at 1:600, Bioss, Beijing, China), anti- $\beta$ -actin antibody (dilution at 1:2000, Servicebio, Wuhan, China), and anti-HSP-90 antibody (dilution at 1:1000, Santa Cruz, Oregon, USA), the membranes with blotted proteins were then incubated with HRP-conjugated goat anti-rabbit secondary antibody (dilution at 1:2000, CST, Boston, USA) or rat anti-mouse secondary antibody (dilution at 1:2000, Servicebio, Wuhan, China) for an hour at room temperature. After washing three times with TBST, the electrochemiluminescence solution (ECL, Millipore, Massachusetts, USA) was added to the membranes, and then, the membranes were exposed to the exposure machine (ChemiScope series, Cline Science Instruments Co., Ltd), and the resulting images were recorded and analyzed.

**2.12. Statistics.** Data were expressed as mean  $\pm$  SD, and the differences among multiple groups were analyzed using one-way analysis of variance (ANOVA) after the normality test and followed by post hoc analysis with the least significant difference (LSD) test. Throughout the text, figures, and legends, the following terminologies are used to denote statistical significance: \* $p$  < 0.05; \*\* $p$  < 0.01; and \*\*\* $p$  < 0.001.

### 3. Results

**3.1. Characterization of MSCs and IL-37-MSCs.** After passage 2, MSCs showed spindle-shaped, fibroblast-like morphology and exhibited colony-forming abilities (Figure 1(a)). At passage 3, MSCs were detected and demonstrated high levels of expression of CD29 and CD90, but no expression of CD45 and CD79a (Figure 1(b)). At 72 hours posttransfection, the expression of GFP fluorescent protein was observed under a fluorescence microscope (Figure 1(c)). In addition, IL-37 expression was found in IL-37-MSCs but not in MSCs, as expected. After passing through the puromycin drug screening, the GFP-positive rate was above 99.8% measured by flow cytometry before cell treatment which met our needs (Figure 1(d)).

**3.2. Transplanted IL-37-MSCs Could Migrate to the Injured Tissue In Vivo.** To investigate whether IL-37-MSCs could migrate to the damaged intestine through the intravenous injection, intestine tissues were fixed by OCT to frozen section to detect the GFP expression. GFP expression was positive in the IL-37-MSC-treated and MSC-treated groups while the sham control group was negative, which meant that

infused IL-37-MSCs and MSCs could migrate to the injured tissue (Figure 1(e)).

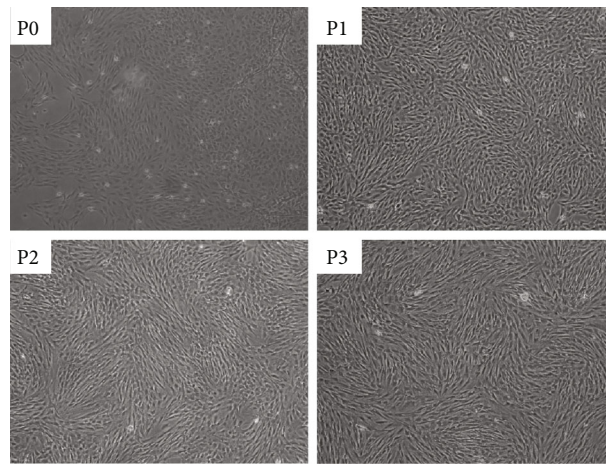
**3.3. IL-37-MSCs Significantly Ameliorated Pathological IRI Damage of the Intestine.** Chiu's score was used to assess the tissue damage. No obvious abnormal tissue changes were observed in the sham group (Figure 2(a)). However, intestinal injury in the untreated group was severe, which was characterized by villus damage, epithelial necrosis, subendothelial hemorrhage, and neutrophil infiltration. As expected, intestinal damage scores following IRI were significantly improved by the mere use of MSCs and rIL-37, furthermore improved by IL-37-MSC administration (IL-37-MSC treated vs. MSC treated,  $p$  < 0.01; IL-37-MSC treated vs. rIL-37 treated,  $p$  < 0.01, Figure 2(b)).

**3.4. IL-37-MSCs Improved Intestinal Barrier Function following Intestinal IRI.** To determine whether IL-37-MSCs could attenuate intestinal IRI, we measured the serum DAO and D-Lac, which represented the intestine barrier function as described above. As shown in Figure 3, it was found that DAO and D-Lac showed the highest levels in the untreated group, which reduced by different treatments. Compared with the MSCs- or rIL-37-treated group, IL-37-MSCs significantly decreased DAO and D-Lac levels in the serum (DAO level: IL-37-MSC treated vs. MSC treated,  $p$  < 0.01; IL-37-MSC treated vs. rIL-37 treated,  $p$  < 0.01, Figure 3(a); D-Lac level: IL-37-MSC treated vs. MSC treated,  $p$  < 0.05; IL-37-MSC treated vs. rIL-37 treated,  $p$  < 0.01, Figure 3(b)), which indicated that IL-37-MSCs could effectively improve intestine barrier function following intestinal IRI.

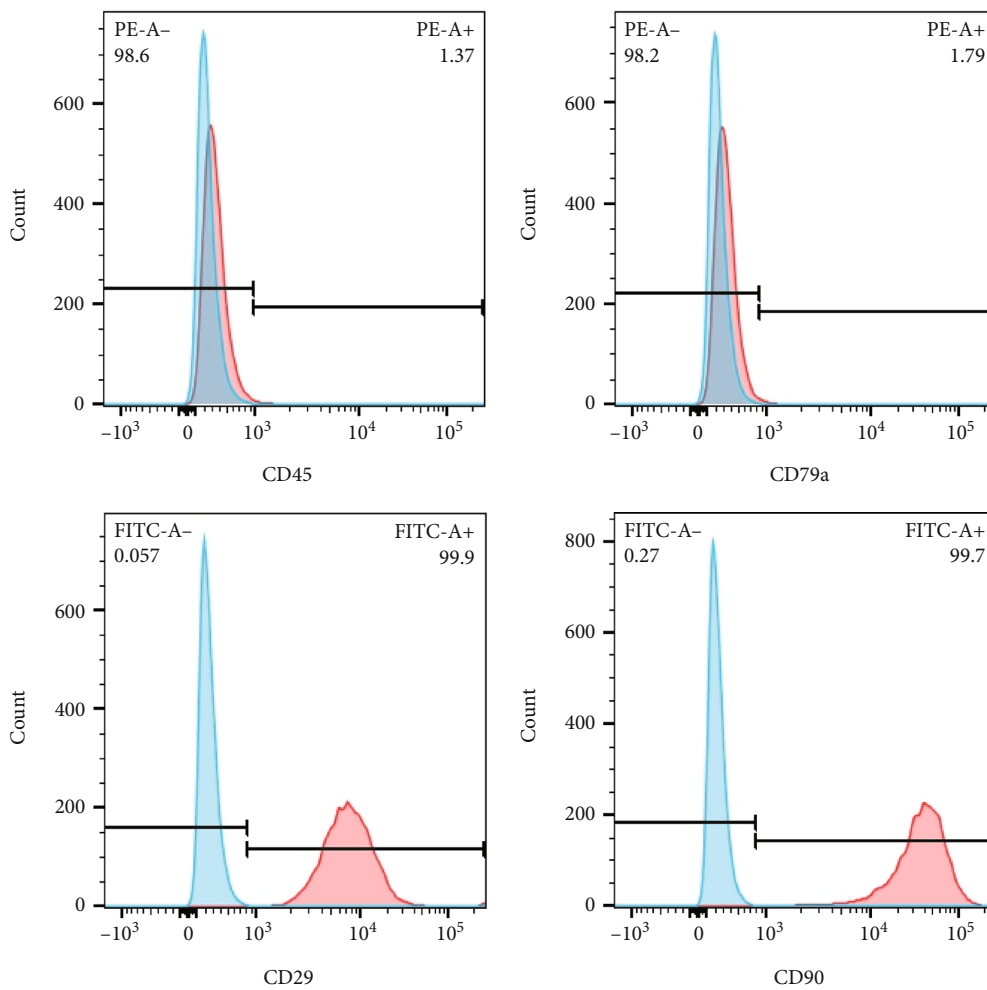
**3.5. IL-37-MSCs Decreased Local and Systemic Inflammation Cytokine IL-1 $\beta$ .** We used cytokine IL-1 $\beta$  level to evaluate local and systemic inflammation reactivity. Local and systemic cytokine IL-1 $\beta$  was significantly increased in the untreated IRI group (Figure 4). In addition, IL-37-MSC treatment significantly decreased local and systemic IL-1 $\beta$  level following IRI compared with MSCs and/or rIL-37 treatment (local IL-1 $\beta$  level: IL-37-MSC treated vs. MSC treated,  $p$  < 0.05; IL-37-MSC treated vs. rIL-37 treated,  $p$  < 0.001, Figure 4(a); systemic IL-1 $\beta$  level: IL-37-MSC treated vs. MSC treated,  $p$  < 0.05; IL-37-MSC treated vs. rIL-37 treated,  $p$  < 0.01, Figure 4(b)).

**3.6. Infusion of IL-37-MSCs Decreased the NLRP3 Inflammasome Activation and Downstream Cascade Reactions.** NLRP3 played an important role in the development of various diseases, and inhibiting NLRP3 activation could effectively attenuate intestinal IRI. In this study, to detect whether IL-37-MSCs could effectively inhibit NLRP3 inflammasome activation, we performed western blot to detect NLRP3 and its downstream cascade reactions. As shown in Figure 5(a), NLRP3 synthesis in the IL-37-MSC-treated group was significantly lower than that in the MSC-treated and/or rIL-37-treated groups (IL-37-MSC treated vs. MSC treated,  $p$  < 0.01; IL-37-MSC treated vs. rIL-37 treated,  $p$  < 0.01). Cleaved caspase-1 proteins in each group were in accordance with NLRP3 synthesis; compared with sole MSC or rIL-37 treatment, IL-37-MSCs markedly





(a)



(b)

FIGURE 1: Continued.



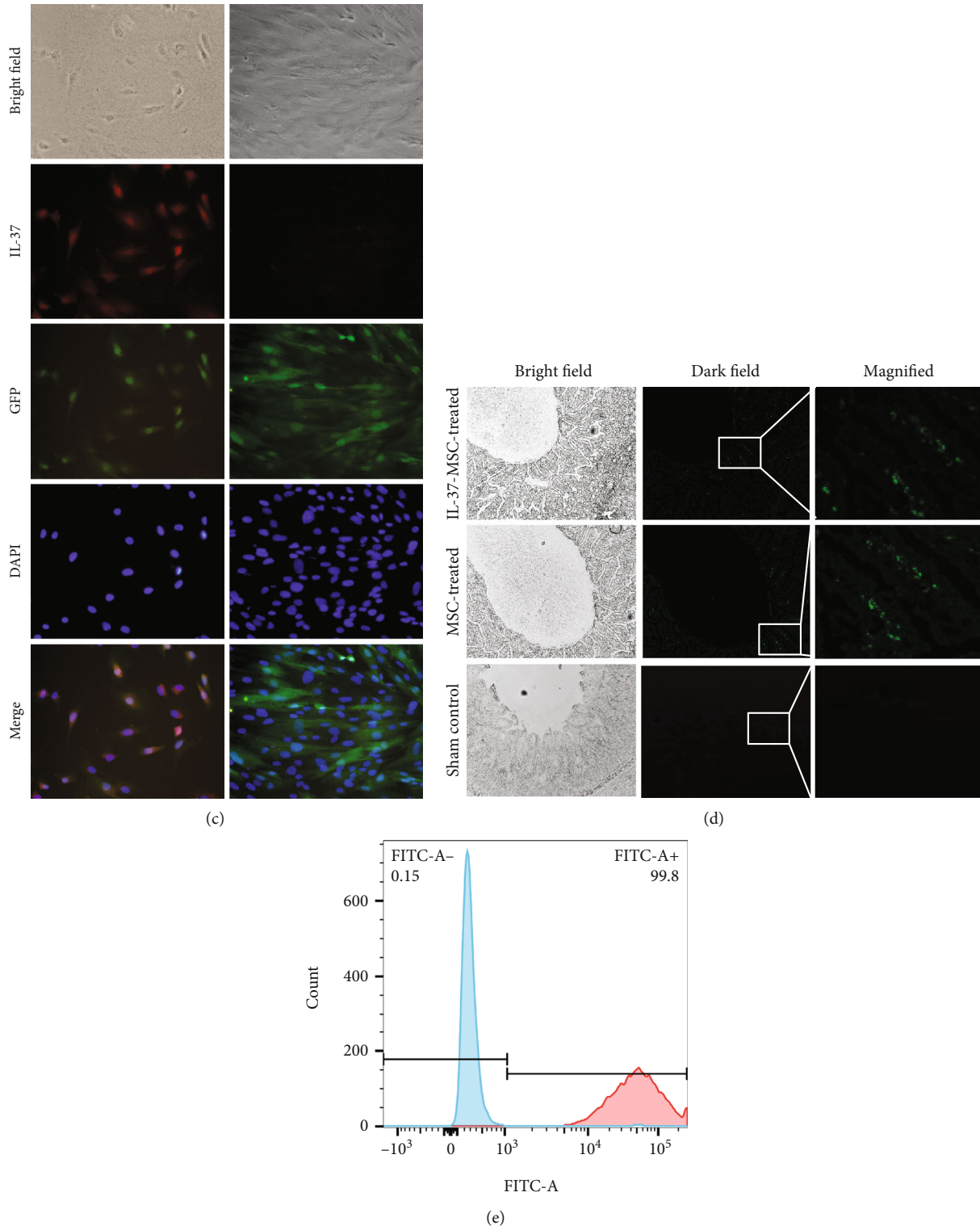


FIGURE 1: IL-37-MSCs and MSCs could migrate to the injured tissue. The morphology of MSCs. (a) Passages 0, 1, 2, and 3 of MSCs. (b) FACS analysis of MSC surface marker, surface expressions of CD29, CD45, CD79a, and CD90 were detected. (c) The IL-37 and GFP proteins were detected in IL-37-MSCs and MSCs. (d) IL-37-MSC GFP-positive rate was calculated; positive rate was above 99.8% which met our needs. (e) IL-37-MSC-treated and MSC-treated intestine exhibited significant GFP fluorescence while the sham group did not, which suggested that IL-37-MSCs and MSCs could migrate to the injured tissue.

decreased cleaved caspase-1 protein (IL-37-MSC treated vs. MSC treated,  $p < 0.001$ ; IL-37-MSC treated vs. rIL-37 treated,  $p < 0.001$ , Figure 5(b)). As a result, mature form processing

of IL-1 $\beta$  and IL-18 in tissues was also in accordance with NLRP3 synthesis; IL-1 $\beta$  and IL-18 proteins in the IL-37-MSC-treated group were lower than those in the MSC-

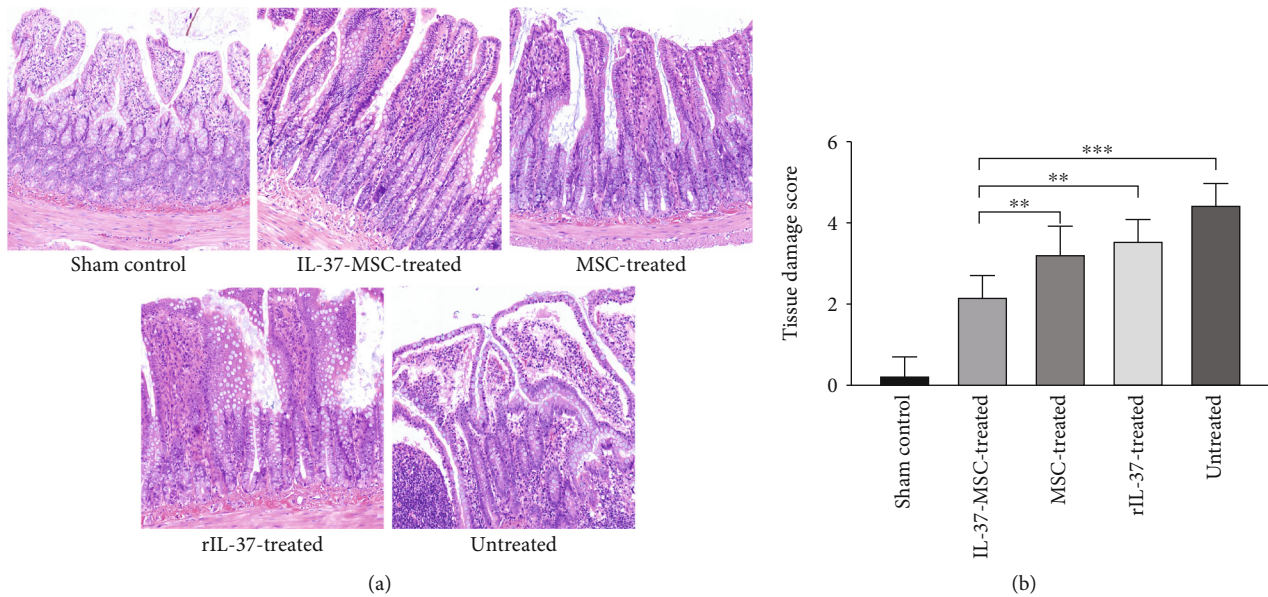


FIGURE 2: IL-37-MSCs significantly ameliorated pathological intestine damage following IRI. Microscopic findings illustrated the architecture of the ileum by 72 hours after reperfusion; the damage score was assessed according to Chiu's score. (a) Compared with the sham group, the untreated group demonstrated severe damage such as inflammatory cell infiltration, hemorrhage, and ulcer. However, as shown in (b), the IL-37-MSC-treated IRI group showed more significant therapeutic effects compared with the MSC-treated and rIL-37-treated groups. The data suggested that IL-37-MSCs provide a better protective role in intestinal IRI. Data shown were representative, and the  $p$  value was determined by one-way ANOVA followed by the LSD test. \* $p < 0.05$ , \*\* $p < 0.01$ , and \*\*\* $p < 0.001$ .

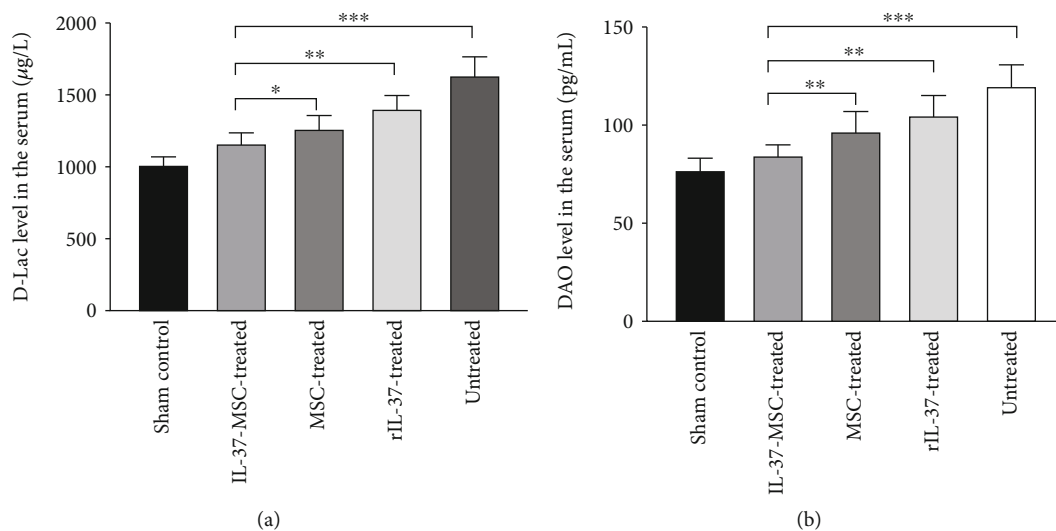


FIGURE 3: IL-37-MSCs could effectively improve intestinal barrier function following IRI. DAO and D-Lac were used to assess the gut barrier function. Serum samples were collected from the sham, IL-37-MSC-treated, MSC-treated, rIL-37-treated, and untreated IRI groups. In comparison with the MSC-treated and rIL-37-treated IRI groups, IL-37-MSCs significantly reduced serum levels of DAO and D-Lac, which meant IL-37-MSCs remarkably improved gut barrier function. Data shown were representative, and the  $p$  value was determined by one-way ANOVA followed by the LSD test. \* $p < 0.05$ , \*\* $p < 0.01$ , and \*\*\* $p < 0.001$ .

treated or rIL-37-treated group (IL-1 $\beta$  protein: IL-37-MSC treated vs. MSC treated,  $p < 0.001$ ; IL-37-MSC treated vs. rIL-37 treated,  $p < 0.001$ , Figure 5(c); IL-18 protein: IL-37-MSC treated vs. MSC treated,  $p < 0.001$ ; IL-37-MSC treated vs. rIL-37 treated,  $p < 0.001$ , Figure 5(d)).

### 3.7. IL-37-MSC Treatment Decreased Local mRNA Expression for TNF- $\alpha$ and IL-6. Proinflammatory cytokines

count in the intestinal IRI. Hence, decreasing these proinflammatory cytokine expressions may contribute to alleviate tissue injury. As shown in Figure 6, the TNF- $\alpha$  and IL-6 mRNA expressions in the IL-37-MSC-treated group were obviously lower than those in the MSC-treated or rIL-37-treated IRI groups (TNF- $\alpha$  mRNA expression: IL-37-MSC treated vs. MSC treated,  $p < 0.05$ ; IL-37-MSC treated vs. rIL-37 treated,  $p < 0.01$ , Figure 6(a); IL-6 mRNA expression:

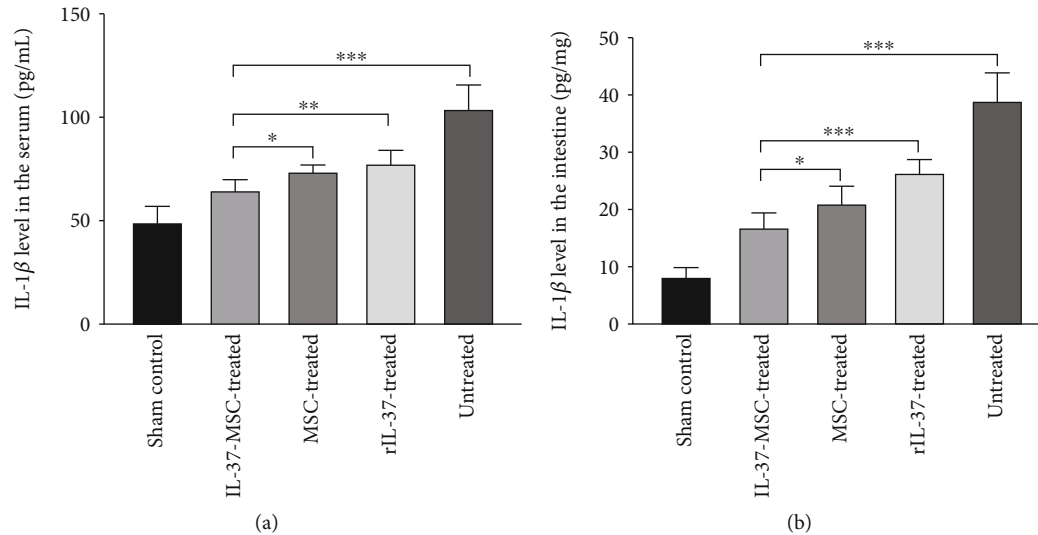


FIGURE 4: IL-37-MSCs could significantly decrease local and systemic inflammation activity. Local and systemic inflammation activity was assessed by IL-1 $\beta$  level in the local tissue and serum. Compared with MSC and rIL-37 treatment, IL-37-MSCs significantly alleviate the local and systemic inflammation activity. The  $p$  value was determined by one-way ANOVA followed by the LSD test. \* $p$  < 0.05, \*\* $p$  < 0.01, and \*\*\* $p$  < 0.001.

IL-37-MSC treated vs. MSC treated,  $p$  < 0.05; IL-37-MSC treated vs. rIL-37 treated,  $p$  < 0.01, Figure 6(b)).

#### 4. Discussion

Our study, which investigated the therapeutic effects of IL-37-MSC treatment on inhibiting intestinal IRI, provided several preclinical implications of IL-37 and gene-modified MSCs. First, as compared with the sham control group, tissue damage scores (H&E assessment) were remarkably enhanced in animals with IRI. As expected, the parameter was significantly suppressed in animals with IRI after MSC or rIL-37 treatment and further notably decreased following IL-37-MSC transplantation therapy. Second, intestinal barrier function as measured by DAO and D-Lac was preserved in a manner consistent with tissue damage scores in all groups. Third, not only local but also systemic inflammatory cytokine IL-1 $\beta$  level was markedly attenuated in all treatment groups following IRI. Then, the NLRP3-mediated proinflammatory signaling pathway was found to be upregulated in the untreated IRI group, which was significantly suppressed following MSC, rIL-37, and IL-37-MSC treatments, suggesting the multifactorial nature of underlying mechanisms involved in intestinal IRI, for which IL-37-MSCs demonstrated much more powerful effects than MSCs or rIL-37 alone in attenuation of intestinal IRI.

The intestinal tract was one of the organs that were highly sensitive to ischemia. In addition, intestinal IRI usually leads to systemic inflammatory responses (SIRs) and multiple organ dysfunction syndromes (MODs), which is one of the highest morbidity and mortality diseases in the clinic [3]. Various inflammatory cells are involved in the whole process of disease, such as mucosal cells, macrophages, neutrophils, and endothelial cells, which are responsible for the release of different cytokines, chemokines, and free radicals follow-

ing intestinal IRI. Therefore, we believe that the mechanism of ischemia reperfusion injury is closely related to the release of ROS after ischemia or hypoxia [7]. Excessive ROS activated NLRP3 inflammasome and eventually led to the excessive release of proinflammatory cytokines IL-1 $\beta$  and IL-18 [7]. The dysregulation of NLRP3 inflammasome could cause excessive inflammation and play a pivotal role in many human diseases. Previous studies have demonstrated that NLRP3 inflammasome is involved in ischemia reperfusion injury in several organs such as the heart, liver, and kidney. Interestingly, little has been reported about the role of NLRP3 in intestinal ischemia reperfusion injury until Wang et al. identified that NLRP3 actually count in intestinal IRI [30]. Several studies suggested that targeting inhibiting NLRP3 inflammasome activation could alleviate ischemia reperfusion injury occurring in different organs [7, 12, 13, 31, 32]. Therefore, inhibition of NLRP3 activation is incredibly effective at treating intestinal IRI.

A broad base of research supports cell therapy strategies to be a strongly effective way in the treatment of different diseases [16, 18, 33, 34]. MSCs act as adult stem/stromal cells that could differentiate into specific tissues cells induced by local microenvironment when they were damaged and could secrete various cytokines. Previous studies have demonstrated that MSCs, especially those adipose derived, possess anti-inflammatory and immunomodulatory functions. Intriguingly, MSCs and IL-37 both could inhibit NLRP3 inflammasome activation, but research has suggested different mechanisms were involved. MSCs have been noted for ischemia reperfusion injury, and good results have been obtained, which could decrease NLRP3 activation via clearing excessive ROS as reported [18]. However, as described above, IL-37 plays an important anti-inflammatory and immunomodulatory capacity in a variety of inflammatory and autoimmune diseases. In addition, IL-37 *in vivo* could

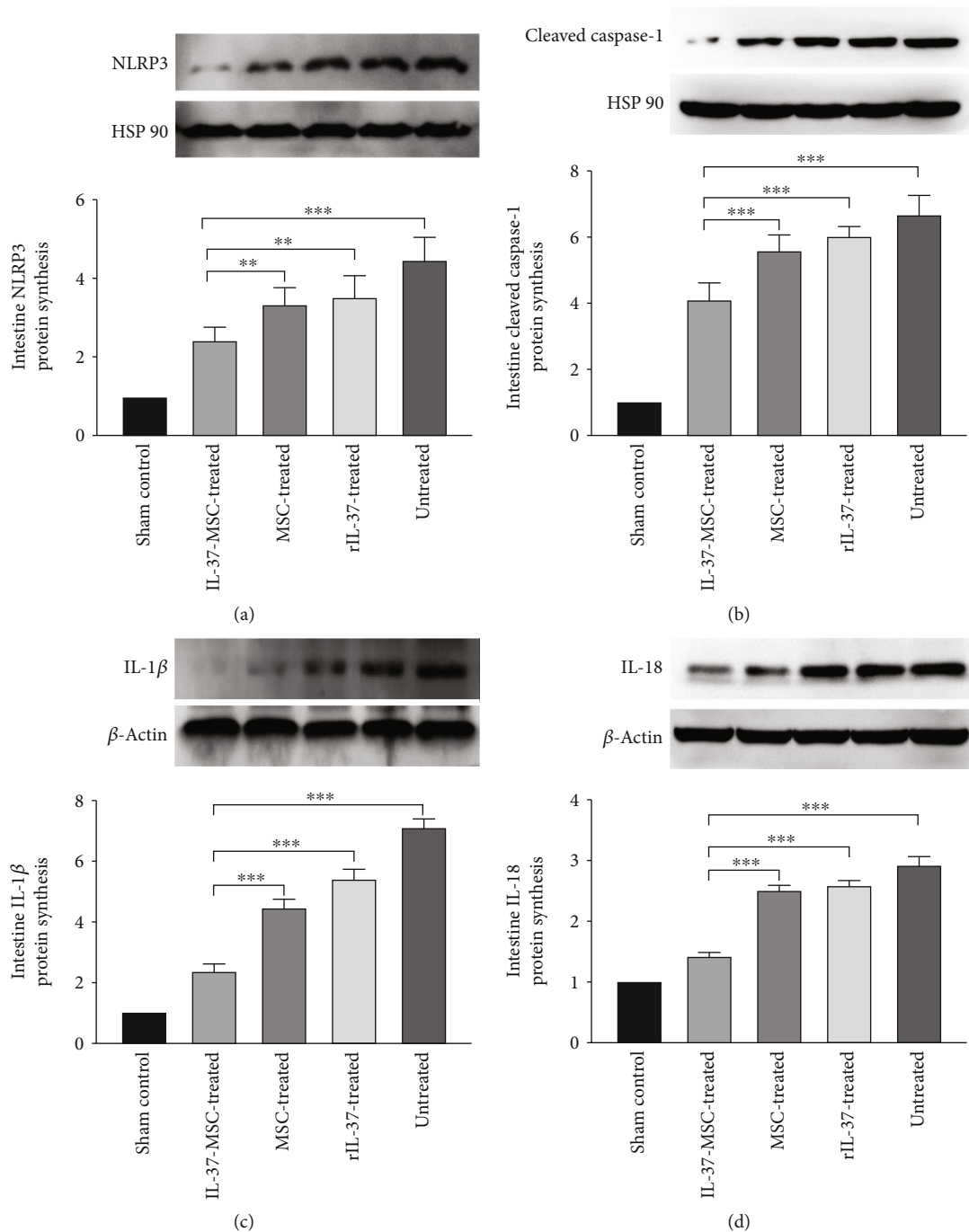


FIGURE 5: IL-37-MSC treatment decreased NLRP3 and downstream cascade protein synthesis. (a) Compared with MSC and IL-37 treatment, IL-37-MSCs significantly decreased the NLRP3 activation. In parallel with NLRP3 synthesis, cleaved caspase-1, IL-1 $\beta$ , and IL-18 proteins were significantly decreased following IL-37-MSC treatment compared with MSC and/or rIL-37 treatments (b–d), which suggested that IL-37-MSCs could inhibit the NLRP3-mediated signaling pathway. Data shown were representative, and the  $p$  value was determined by one-way ANOVA followed by the LSD test. \* $p < 0.05$ , \*\* $p < 0.01$ , and \*\*\* $p < 0.001$ .

inhibit NLRP3 activation also in colitis- and LPS-induced disease [19, 22, 35–37]. In a recent study, Rudloff et al. reported that IL-37 significantly suppresses inflammasome activity *in vivo* to ameliorate inflammasome-driven diseases, which could corroborate our study results to some extent [38].

However, either mesenchymal stromal cells or IL-37 showed limited roles to relieve intestinal IRI [25, 26, 39].

Thus, it was very important to find a way to enhance the effects of MSCs. During the past decades, remarkable progresses have been made in the area of gene-engineered MSC-based therapy. Based on these points, we utilized MSCs as a vehicle to drive IL-37 and further release IL-37 *in vivo* (the result is demonstrated in the supplementary figure (available here) that IL-37 expression in the serum in the IL-37-MSC-treated group was higher than that in the MSC-



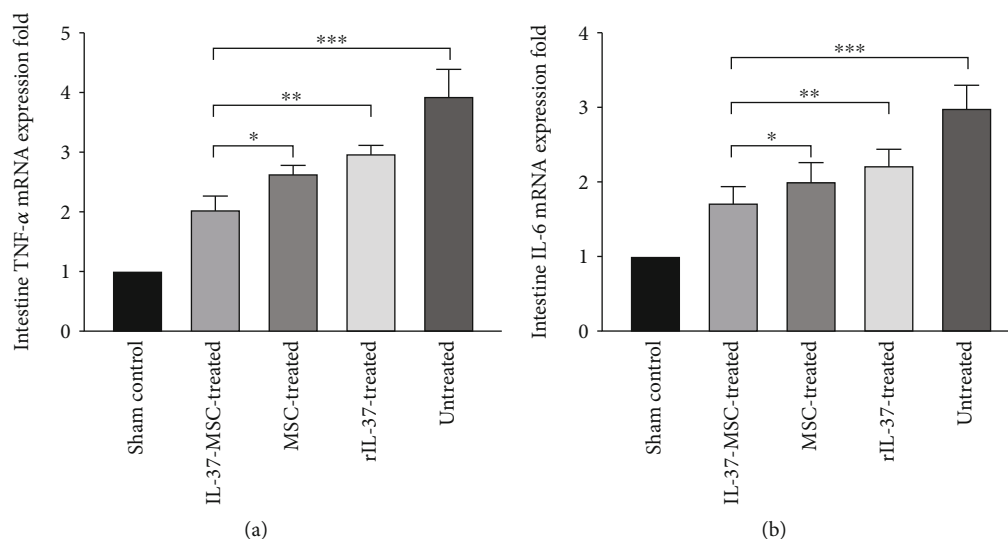


FIGURE 6: IL-37-MSC transplantation decreased IL-6 and TNF- $\alpha$  mRNA expression. IL-1 $\beta$  and IL-18 are key proinflammatory cytokines, and as their downstream proinflammatory molecules, IL-6 and TNF- $\alpha$  play a pivotal role in inflammatory reactivity. Intestine IL-6 and TNF- $\alpha$  mRNA expressions in the IL-37-MSC-treated group were significantly decreased compared with those in the MSC- and rIL-37-treated group. The  $p$  value was determined by one-way ANOVA followed by the LSD test. \* $p < 0.05$ , \*\* $p < 0.01$ , and \*\*\* $p < 0.001$ .

treated group) to help better inhibit NLRP3 inflammasome activation to alleviate damage, thereby enhancing the effects of MSCs in the intestinal IRI model.

This is the first study to demonstrate that IL-37 could play a protective role in the intestinal IRI and illustrated that IL-37 gene modification could enhance the therapeutic effects of MSCs in the ischemia reperfusion injury. However, many mechanisms are involved in the IL-37-MSC treatment in intestinal IRI, and more specific mechanisms remain to be explored.

## 5. Conclusion

In conclusion, IL-37 gene modification could enhance the therapeutic effects of MSCs. IL-37-MSCs improved intestine barrier function, improved injured tissue microenvironment, and inhibited the NLRP3-mediated signaling pathway, which exert a much better protective role in intestinal IRI than MSCs. NLRP3-related signaling pathways could be related to the process of IL-37-MSC-mediated protection. IL-37-MSC treatment acted as an effective tool to protect the intestine against IRI.

## Abbreviations

MSCs:	Mesenchymal stromal cells
rIL-37:	Recombinant interleukin 37
IL-37-MSCs:	Interleukin 37 gene-modified mesenchymal stromal/stem cells
IRI:	Ischemia reperfusion injury
SMA:	Superior mesenteric artery
NOD-like:	Nucleotide-binding oligomerization domain-like
NLRP3:	NOD-like receptor family, pyrin domain protein 3
FBS:	Fetal bovine serum

PBS:	Phosphate buffer saline
H&E:	Hematoxylin and eosin
DAO:	Diamine oxidase
D-Lac:	D-Lactate
IL-1 $\beta$ :	Interleukin 1 $\beta$
IL-18:	Interleukin 18.

## Data Availability

The dataset supporting the conclusions of this article is included within the article.

## Ethical Approval

All the experiments were performed according to the Chinese Council on Animal Care guidelines and the basis of protocols approved by the Animal Care and Use Committee of Tianjin Medical University (Tianjin, China) (IRB2019-YX-001).

## Conflicts of Interest

The authors declare that they have no conflict of interests.

## Authors' Contributions

Dejun Kong, Yonghao Hu, and Xiang Li are co-first authors on this paper. Dejun Kong designed and carried out the research, analyzed the data, and drafted the manuscript; Yonghao Hu and Xiang Li designed and carried out the research and polished the manuscript; Dingding Yu and Hongyue Li carried out the research; Yiming Zhao and Yafei Qin polished the manuscript; Baoren Zhang, Wang Jin, Bo Wang, Hongda Wang, and Guangming Li performed the research; H. Wang conceived the study, participated in research design and coordination, and helped to draft and

edit the manuscript. All authors read and approved the final manuscript.

## Acknowledgments

This work was supported by grants to H.W. from the National Natural Science Foundation of China (Nos. 81273257 and 81471584), the Tianjin Application Basis and Cutting-Edge Technology Research Grant (No. 14JCZDJC35700), the Li Jieshou Intestinal Barrier Research Special Fund (No. LJS\_201412), the Natural Science Foundation of Tianjin (No. 18JCZDJC35800), the Tianjin Medical University Talent Fund, and the Tianjin Research Innovation Project for Post-graduate Students to Dejun Kong (No. 2019YJSS184).

## Supplementary Materials

Supplementary figure: IL-37-MSc treatment increased IL-37 level in the serum. As shown in the supplementary figure, IL-37 level in the IL-37-MSc-treated group was higher than that in the MSc-treated group. The *p* value was determined by one-way ANOVA followed by the LSD test. \**p* < 0.05, \*\**p* < 0.01, and \*\*\**p* < 0.001. (*Supplementary Materials*)

## References

- [1] X. T. Yan, X. L. Cheng, X. H. He, W. Z. Zheng, Y. Xiao-Fang, and C. Hu, "The HO-1-expressing bone mesenchymal stem cells protects intestine from ischemia and reperfusion injury," *BMC Gastroenterology*, vol. 19, no. 1, p. 124, 2019.
- [2] C. Chassin, C. Hempel, S. Stockinger et al., "MicroRNA-146a-mediated downregulation of IRAK1 protects mouse and human small intestine against ischemia/reperfusion injury," *EMBO Molecular Medicine*, vol. 4, no. 12, pp. 1308–1319, 2012.
- [3] S. Acosta and M. Björck, "Modern treatment of acute mesenteric ischaemia," *The British Journal of Surgery*, vol. 101, no. 1, pp. e100–e108, 2014.
- [4] C. L. Chang, P. H. Sung, C. K. Sun et al., "Protective effect of melatonin-supported adipose-derived mesenchymal stem cells against small bowel ischemia-reperfusion injury in rat," *Journal of Pineal Research*, vol. 59, no. 2, pp. 206–220, 2015.
- [5] C. Hu, L. Zhao, D. Wu, and L. Li, "Modulating autophagy in mesenchymal stem cells effectively protects against hypoxia- or ischemia-induced injury," *Stem Cell Research & Therapy*, vol. 10, no. 1, p. 120, 2019.
- [6] A. R. Mridha, A. Wree, A. A. B. Robertson et al., "NLRP3 inflammasome blockade reduces liver inflammation and fibrosis in experimental NASH in mice," *Journal of Hepatology*, vol. 66, no. 5, pp. 1037–1046, 2017.
- [7] L. Minutoli, D. Puzzolo, M. Rinaldi et al., "ROS-mediated NLRP3 inflammasome activation in brain, heart, kidney, and testis ischemia/reperfusion injury," *Oxidative Medicine and Cellular Longevity*, vol. 2016, Article ID 2183026, 10 pages, 2016.
- [8] H. Guo, J. B. Callaway, and J. P.-Y. Ting, "Inflammasomes: mechanism of action, role in disease, and therapeutics," *Nature Medicine*, vol. 21, no. 7, pp. 677–687, 2015.
- [9] X. Liu, Z. Zhang, J. Ruan et al., "Inflammasome-activated gasdermin D causes pyroptosis by forming membrane pores," *Nature*, vol. 535, no. 7610, pp. 153–158, 2016.
- [10] P. Broz, "Immunology: caspase target drives pyroptosis," *Nature*, vol. 526, no. 7575, pp. 642–643, 2015.
- [11] J. Shi, Y. Zhao, K. Wang et al., "Cleavage of GSDMD by inflammatory caspases determines pyroptotic cell death," *Nature*, vol. 526, no. 7575, pp. 660–665, 2015.
- [12] Z. Qiu, S. Lei, B. Zhao et al., "NLRP3 inflammasome activation-mediated pyroptosis aggravates myocardial ischemia/reperfusion injury in diabetic rats," *Oxidative Medicine and Cellular Longevity*, vol. 2017, Article ID 9743280, 17 pages, 2017.
- [13] M. Ito, T. Shichita, M. Okada et al., "Bruton's tyrosine kinase is essential for NLRP3 inflammasome activation and contributes to ischaemic brain injury," *Nature Communications*, vol. 6, no. 1, p. 7360, 2015.
- [14] Y. Geng, D. Chen, J. Zhou et al., "Synergistic effects of electroacupuncture and mesenchymal stem cells on intestinal ischemia/reperfusion injury in rats," *Inflammation*, vol. 39, no. 4, pp. 1414–1420, 2016.
- [15] J. Li, W. Liu, and W. Yao, "Immortalized human bone marrow derived stromal cells in treatment of transient cerebral ischemia in rats," *Journal of Alzheimer's Disease*, vol. 69, no. 3, pp. 871–880, 2019.
- [16] Y. Wang, X. Chen, W. Cao, and Y. Shi, "Plasticity of mesenchymal stem cells in immunomodulation: pathological and therapeutic implications," *Nature Immunology*, vol. 15, no. 11, pp. 1009–1016, 2014.
- [17] P. Sun, J. Liu, W. Li et al., "Human endometrial regenerative cells attenuate renal ischemia reperfusion injury in mice," *Journal of Translational Medicine*, vol. 14, no. 1, p. 28, 2016.
- [18] D. Nakajima, Y. Watanabe, A. Ohsumi et al., "Mesenchymal stromal cell therapy during ex vivo lung perfusion ameliorates ischemia-reperfusion injury in lung transplantation," *The Journal of Heart and Lung Transplantation*, vol. 38, no. 11, pp. 1214–1223, 2019.
- [19] M. F. Nold, C. A. Nold-Petry, J. A. Zepp, B. E. Palmer, P. Büfler, and C. A. Dinarello, "IL-37 is a fundamental inhibitor of innate immunity," *Nature Immunology*, vol. 11, no. 11, pp. 1014–1022, 2010.
- [20] C. A. Nold-Petry, C. Y. Lo, I. Rudloff et al., "IL-37 requires the receptors IL-18R $\alpha$  and IL-1R8 (SIGIRR) to carry out its multifaceted anti-inflammatory program upon innate signal transduction," *Nature Immunology*, vol. 16, no. 4, pp. 354–365, 2015.
- [21] J. Banchereau, V. Pascual, and A. O'Garra, "From IL-2 to IL-37: the expanding spectrum of anti-inflammatory cytokines," *Nature Immunology*, vol. 13, no. 10, pp. 925–931, 2012.
- [22] P. Conti, A. Caraffa, F. Mastrangelo et al., "Critical role of inflammatory mast cell in fibrosis: potential therapeutic effect of IL-37," *Cell Proliferation*, vol. 51, no. 5, article e12475, 2018.
- [23] Y. Yang, Z. X. Zhang, D. Lian, A. Haig, R. N. Bhattacharjee, and A. M. Jevnikar, "IL-37 inhibits IL-18-induced tubular epithelial cell expression of pro-inflammatory cytokines and renal ischemia-reperfusion injury," *Kidney International*, vol. 87, no. 2, pp. 396–408, 2015.
- [24] B. Wu, K. Meng, Q. Ji et al., "Interleukin-37 ameliorates myocardial ischemia/reperfusion injury in mice," *Clinical and Experimental Immunology*, vol. 176, no. 3, pp. 438–451, 2014.
- [25] L. Huang, J. You, Y. Yao, and M. Xie, "Interleukin-13 gene modification enhances grafted mesenchymal stem cells survival after subretinal transplantation," *Cellular and Molecular Neurobiology*, vol. 40, no. 5, pp. 725–735, 2020.

- [26] N. Shomali, T. Gharibi, G. Vahedi et al., “Mesenchymal stem cells as carrier of the therapeutic agent in the gene therapy of blood disorders,” *Journal of Cellular Physiology*, vol. 235, no. 5, pp. 4120–4134, 2019.
- [27] L. M. Gonzalez, A. J. Moeser, and A. T. Blikslager, “Animal models of ischemia-reperfusion-induced intestinal injury: progress and promise for translational research,” *American Journal of Physiology. Gastrointestinal and Liver Physiology*, vol. 308, no. 2, pp. G63–G75, 2015.
- [28] C. H. Cheng, H. C. Lin, I. R. Lai, and H. S. Lai, “Ischemic post-conditioning attenuate reperfusion injury of small intestine,” *Transplantation*, vol. 95, no. 4, pp. 559–565, 2013.
- [29] C. Cosse, C. Sabbagh, S. Kamel, A. Galmiche, and J. M. Regimbeau, “Procalcitonin and intestinal ischemia: a review of the literature,” *World Journal of Gastroenterology*, vol. 20, no. 47, pp. 17773–17778, 2014.
- [30] Z. Wang, Z. Li, D. Feng et al., “Autophagy induction ameliorates inflammatory responses in intestinal ischemia-reperfusion through inhibiting NLRP3 inflammasome activation,” *Shock*, vol. 52, no. 3, pp. 387–395, 2019.
- [31] Y. Inoue, K. Shirasuna, H. Kimura et al., “NLRP3 regulates neutrophil functions and contributes to hepatic ischemia-reperfusion injury independently of inflammasomes,” *Journal of Immunology*, vol. 192, no. 9, pp. 4342–4351, 2014.
- [32] S. Nazir, I. Gadi, M. M. al-Dabet et al., “Cytoprotective activated protein C averts Nlrp3 inflammasome-induced ischemia-reperfusion injury via mTORC1 inhibition,” *Blood*, vol. 130, no. 24, pp. 2664–2677, 2017.
- [33] Z. Fazeli, A. Abedindo, M. D. Omrani, and S. M. H. Ghaderian, “Mesenchymal stem cells (MSCs) therapy for recovery of fertility: a systematic review,” *Stem Cell Reviews*, vol. 14, no. 1, pp. 1–12, 2018.
- [34] L. J. Green, H. Zhou, V. Padmanabhan, and A. Shikanov, “Adipose-derived stem cells promote survival, growth, and maturation of early-stage murine follicles,” *Stem Cell Research & Therapy*, vol. 10, no. 1, p. 102, 2019.
- [35] D. B. Ballak, J. A. van Diepen, A. R. Moschen et al., “IL-37 protects against obesity-induced inflammation and insulin resistance,” *Nature Communications*, vol. 5, no. 1, p. 4711, 2014.
- [36] P. Luo, C. Feng, C. Jiang et al., “IL-37b alleviates inflammation in the temporomandibular joint cartilage via IL-1R8 pathway,” *Cell Proliferation*, vol. 52, no. 6, article e12692, 2019.
- [37] Z. Yang, L. Kang, Y. Wang et al., “Role of IL-37 in cardiovascular disease inflammation,” *The Canadian Journal of Cardiology*, vol. 35, no. 7, pp. 923–930, 2019.
- [38] I. Rudloff, H. K. Ung, J. K. Dowling et al., “Parsing the IL-37-mediated suppression of inflammasome function,” *Cell*, vol. 9, no. 1, p. 178, 2020.
- [39] W. Q. Wang, K. Dong, L. Zhou et al., “IL-37b gene transfer enhances the therapeutic efficacy of mesenchymal stromal cells in DSS-induced colitis mice,” *Acta Pharmacologica Sinica*, vol. 36, no. 11, pp. 1377–1387, 2015.

## Research Article

# Patient-Centered Outcomes of Microfragmented Adipose Tissue Treatments of Knee Osteoarthritis: An Observational, Intention-to-Treat Study at Twelve Months

Nima Heidari<sup>1</sup>,<sup>ORCID</sup> Ali Noorani,<sup>1</sup> Mark Slevin,<sup>2</sup> Angela Cullen,<sup>1</sup> Laura Stark,<sup>1</sup> Stefano Olgiati,<sup>3</sup> Alberto Zerbi,<sup>4</sup> and Adrian Wilson<sup>1</sup>

<sup>1</sup>The Regenerative Clinic, 18-22 Queen Anne Street, London, UK

<sup>2</sup>Department of Life Sciences, Manchester Metropolitan University, UK

<sup>3</sup>Dept. of Morphology, Surgery and Experimental Medicine, Faculty of Medicine, University of Ferrara, 44121 Ferrara, Italy

<sup>4</sup>University of Milano, Dept. of Radiology, 20100 Milano, Italy

Correspondence should be addressed to Nima Heidari; [n.heidari@gmail.com](mailto:n.heidari@gmail.com)

Received 23 May 2020; Revised 13 July 2020; Accepted 16 July 2020; Published 4 August 2020

Academic Editor: Huseyin Sumer

Copyright © 2020 Nima Heidari et al. This is an open access article distributed under the Creative Commons Attribution License, which permits unrestricted use, distribution, and reproduction in any medium, provided the original work is properly cited.

**Introduction.** Microfragmented adipose tissue (MFAT) has been shown to benefit osteoarthritic patients by reducing pain and supporting tissue regeneration through a mesenchymal stem cell (MSC)-related paracrine mechanism. This observational study of 110 knees assessed patient-centered outcomes of pain, functionality, and quality of life, analyzing their variation at twelve months following one ultrasound-guided intra-articular injection of autologous MFAT for the treatment of knee osteoarthritis (KOA). **Method.** Inclusion criteria were as follows: VAS >50, and the presence of KOA as diagnosed on X-ray and MRI. Exclusion criteria included the following: recent injury (<3 months) of the symptomatic knee, intra-articular steroid injections performed within the last three months, and hyaluronic acid injections prior to this treatment. Changes in VAS, OKS, and EQ-5D were scored at baseline and twelve months following a single intra-articular injection of autologous MFAT. Score variation was analyzed utilizing a nonparametric paired samples Wilcoxon test. The statistical analysis is reproducible with Open Access statistical software R (version 4.0.0 or higher). The study was carried out with full patient consent, in a private practice setting. **Results.** Median VAS (pain) improved from 70 (IQR 20) to 30 (IQR 58) ( $p < 0.001$ ); median OKS (function) improved from 25 (IQR 11) to 33.5 (IQR 16) ( $p < 0.001$ ); and median EQ-5D (quality of life) improved from 0.62 (IQR 0.41) to 0.69 (IQR 0.28) ( $p < 0.001$ ). No adverse events were reported during the intraoperative, recovery, or postoperative periods. **Conclusions.** For patients with all grades of knee osteoarthritis who were treated with intra-articular injections of MFAT, statistically significant improvements in pain, function, and quality of life were reported. Although further research is warranted, the results are encouraging and suggest a positive role for intra-articular injection of MFAT as a treatment for knee osteoarthritis.

## 1. Introduction

Osteoarthritis (OA), the most prevalent form of arthritis, is characterized by chronic progressive degeneration and alteration of hyaline articular cartilage, subchondral bone, ligaments, capsule, synovium, and periarticular muscles [1]. The condition currently presents a substantial global socioeconomic burden and remains a leading cause of disability, particularly among the elderly population [2].

With an ageing population, this is a growing problem and is set to become the fourth leading cause of disability by the end of 2020 [3, 4]. In the UK, approximately one in seven people suffer with arthritis. This equates to ten million individuals. It is a complex and multifactorial disease involving genetic, environmental, and mechanical causes [5]. The disease can be classified into one of two groups depending upon its aetiology: primary (idiopathic or nontraumatic) and secondary (a result of trauma or mechanical malalignment) [6].



Advancements in regenerative medicine over the last decade have revealed the potential for mesenchymal stem cells (MSCs) to be used as a powerful therapeutic tool against tissue damage and degeneration [7–9]. Mesenchymal stem cells (MSCs), more recently termed Medicinal Signaling Cells [10], have shown promise as a standalone treatment for OA, or as an adjunct to traditional surgical correction of the mechanical environment. Since their discovery by Friedenstein in the late 1960s [11], extensive research has been implemented in an effort to exploit these cells for their true therapeutic potential.

The cells arise from pericytes that are found naturally occurring around the vasculature in various tissues throughout the body. Upon disruption of the stromal vascular fraction of tissue, a significant proportion of pericytes lift from the surface of the vessels and contribute to the tissue homeostatic response as the source of adipose-derived stem cells—MSCs [12, 13].

These MSCs respond by producing bioactive signaling molecules which act in a paracrine fashion to exhibit immunomodulatory, antimicrobial, angiogenic, and trophic/regenerative effects on tissue [5, 14]. This ultimately results in localized and tissue-specific change that encourages regeneration and healing [10].

Sources for MSCs include bone marrow, placenta, and dental pulp [15]. The use of such cells in biological therapy has always been hindered as they are challenging to obtain in large enough quantities to provide significant clinical benefit. Additionally, the extraction of such cells from bone marrow is a painful procedure, and a 1 ml sample provides only 0.01% of MSCs. Conversely, adipose tissue has been recognized as a reliable and potent source for MSCs. One MSC can be obtained per 100 adipose cells, in contrast to 1 MSC for every 100,000 bone marrow cells [16–18]. A promising feature of adipose-derived MSCs is in their localization as they represent 10–30% of normal body weight and produce a concentration of 5,000 cells per gram of tissue obtained [5, 19]. The use of adipose-derived MSCs is associated with minimal side effects arising and previous studies have shown no complications relating to malignancy or cancer [20]. It has also been suggested that these adipose-derived MSCs have multilineage potential and possess the same regenerative capacity as those derived from other tissues. Furthermore, the cells are not adversely influenced by the age of the patient; a factor that is very beneficial for an elderly population [21].

Given that arthritis is such a prevalent condition, especially among an ageing population [22], it is vital to identify the long-term efficacy of therapies that utilize the regenerative power of adipose-derived MSCs, and whether they can potentially prevent replacement surgery or delay it for as long as possible. Furthermore, it is important to identify whether treatment with adipose-derived MSCs, or as in this case, MFAT-containing MSCs (originating from the adipose blood vessels as pericytes, and that are released and primed during the extraction process through sheer stress and microfiltration of the fat) [23, 24] would be beneficial in providing an optimal biological environment for healing when used in conjunction with surgery [25]. Their use for the treatment of knee osteoarthritis (KOA) has produced very encouraging

results [26–28]. This case series aims to assess the response of our patient cohort over a one-year period following a routine single ultrasound-guided intra-articular injection of MFAT for all grades of KOA.

## 2. Method

The study was conducted in accordance with the principles of Good Clinical Practice (NIHR) and the General Medical Council (GMC) guidelines on research, patient consent to research and future publication, as well as adhering to and in accordance with the Declaration of Helsinki. The study was carried out in a private practice setting.

This observational, intention-to-treat study included the complete sample of 110 patients who agreed to be scored for pain (Visual Analogue Scale—VAS), function (Oxford Knee Score—OKS), and quality of life (EuroQol-5D—EQ-5D) at baseline regardless of subsequent changes to adherence or status during follow-up. All patients attended the private clinics of the authors (AW, NH) complaining of knee pain following a diagnosis of knee osteoarthritis.

Patients underwent clinical review and examination by an orthopaedic surgeon. The preoperative assessments included evaluation of imaging (X-ray in all cases and MRI in some) where the KOA was graded using the Kellgren & Lawrence (KL) grading system.

Inclusion criteria included VAS >50, no deformity greater than ten degrees of varus or valgus, and the presence of KOA as diagnosed on X-ray and/or MRI. Exclusion criteria included recent injury (<3 months) of the symptomatic knee, infectious joint disease, malignancy, pregnancy, anticoagulation or thrombocytopenia, coagulation disorder, and intra-articular steroid injections performed within the last three months. None of our patients had hyaluronic acid injections prior to this treatment.

The patients were informed of all possible options for treating their KOA including conservative means as well as injections of a number of substances including steroids, hyaluronic acid, platelet-rich plasma, and microfragmented adipose tissue. They also had surgical options detailed to them including osteotomy, partial and total knee replacement.

By study design, the paired samples have been selected and not randomized, so we could not assume a Gaussian distribution. For this reason, scores variation has been analyzed utilizing a nonparametric paired samples Wilcoxon test to assess statistically significant changes in the VAS, OKS, and EQ-5D scores before and after treatment at twelve months. For the same reason, summary statistics report median and interquartile ranges (IQR).

Summary statistics, statistical analysis, and statistical significance testing are reproducible with Open Access statistical software R (version 4.0.0 or higher; R function Wilcox test). Figures 1, 2, and 3 have been generated automatically from data by Open Access statistical software R (version 4.0.0 or higher; libraries ggpubr and Paired-Data); Table 1 summarizes the change in the median VAS, OKS, and EQ-5D scores at 12 months from baseline according to the OA grading. Data points are missing at random (12%) due to patients lost-to-follow-up; missing data have been

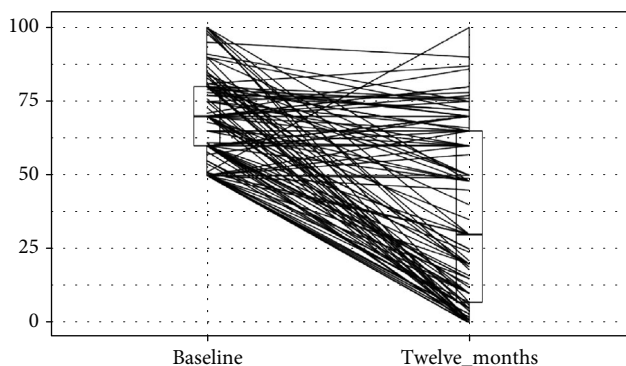


FIGURE 1: VAS scores at baseline and at twelve months follow-up. y-axis: Visual Analogue Scale (VAS) for pain value; boxplot showing L-estimators: maximum (100), minimum (50), median (70), and interquartile range (20); outliers plotted as individual points at baseline and maximum (100), minimum (0), median (30), and interquartile range (58); outliers plotted as individual points at 1 year follow-up. x-axis: Visual Analogue Scale (VAS) for pain at preoperative baseline and at twelve months follow-up. Connecting lines: heuristic visualization of single-patient trajectories of variation of Visual Analogue Scale (VAS) value for pain between preoperative baseline and twelve months follow-up; plotted with R (version 4.0.0 or higher; libraries ggpubr and PairedData). Source: Authors' Data and reproducible statistical analysis with Open Access statistical software R (version 4.0.0 or higher).

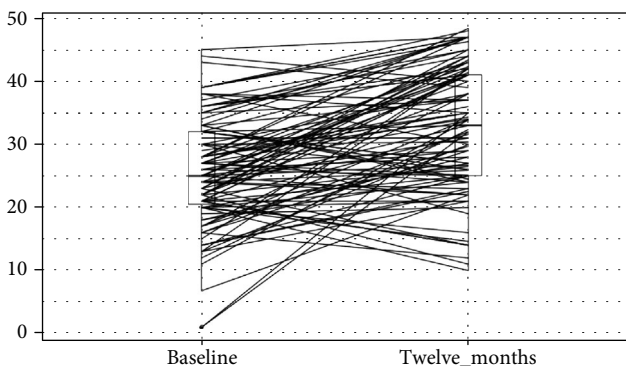


FIGURE 2: Oxford Knee Scores at baseline and at twelve months follow-up. y-axis: Oxford Knee Score (OKS) for function value; boxplot showing L-estimators: maximum (45), minimum (1), median (25), and interquartile range (11); outliers plotted as individual points at baseline and maximum (47), minimum (10), median (33), and interquartile range (16); outliers plotted as individual points at 1 year follow-up. x-axis: Oxford Knee Score (OKS) for function at preoperative baseline and at twelve months follow-up. Connecting lines: heuristic visualization of single-patient trajectories of variation of Oxford Knee Score (OKS) value for function between preoperative baseline and twelve months follow-up; plotted with R (version 4.0.0 or higher; libraries ggpubr and PairedData). Source: Authors' Data and reproducible statistical analysis with Open Access statistical software R (version 4.0.0 or higher).

estimated probabilistically with uncertainty (unbiased) using the statistical software package Amelia v1.7.6 or higher. The estimation procedure is replicable and repro-

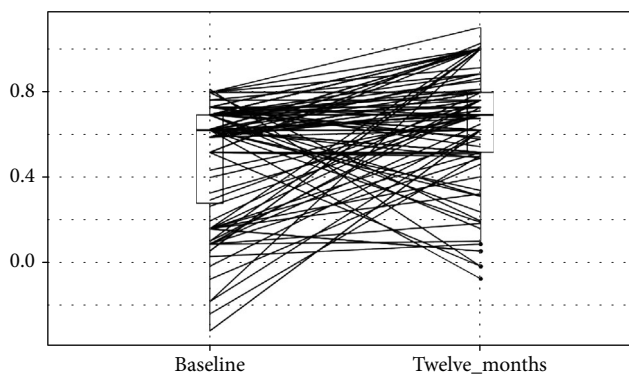


FIGURE 3: EQ-5D Scores at baseline and at twelve months follow-up. y-axis: EQ-5D for quality of life score value; boxplot showing L-estimators: maximum (0.812), minimum (-0.319), median (0.62), and interquartile range (0.41); outliers plotted as individual points at baseline and maximum (1), minimum (-0.074), median (0.69), and interquartile range (0.28); Outliers plotted as individual points at 1 year follow-up. x-axis: EQ-5D for quality of life score at preoperative baseline and at twelve months follow-up. Connecting lines: heuristic visualization of single-patient trajectories of variation of EQ-5D for quality of life score value for function between preoperative baseline and twelve months follow-up; plotted with R (version 4.0.0 or higher; libraries ggpubr and PairedData). Source: Authors' Data and reproducible statistical analysis with Open Access statistical software R (version 4.0.0 or higher).

TABLE 1: Variation of median VAS, OKS, and EQ-5D between baseline and 12 months follow-up grouped by OA Grade.

oa_grade	Count	VAS	OKS	EQ-5D
1	1	↑-48	↑2	↑0.2
2	12	↑-54	↑5.5	↑0.14
3	20	↑-28.5	↑3.5	0
4	68	↑-32.5	↑7	↑0.07
NA	9	↑-17	↑4	↓-0.03

Legend: variation of median VAS, OKS, and EQ-5D between baseline and twelve months follow-up has been grouped according to the grade of KOA. VAS improvement is a reduction in score plotted in green and arrow-up. All grades of OA show an improvement in pain as evidence by a reduction in the median VAS score. OKS also improved in all grades of OA with the most gains being made by those with the grade 4 group. EQ-5D improvement is an increase in score plotted in green and arrow-up, deterioration in red, and invariance in black. This shows a general trend in all severity of KOA towards improvement, but these data are not suitable for detailed subgroup analysis and statistical significance testing as grades 1 and 2 only represent 20% of the total group. Source: Authors' Data and reproducible statistical analysis with Open Access statistical software R (version 4.0.0 or higher).

ducible with Open Access statistical software R (4.0.0 or higher). The missingness map is visualized in Figure 4.

2.1. Patients. The series of 110 cases was comprised of 60 male and 50 female patients, with ages ranging from 42 to 94. Most of the patients had advanced KOA with 80% having a Kellgren-Lawrence (KL) grade of III or IV. 95 (96.4%) of the patients had idiopathic KOA, and 4 (3.6%) had posttraumatic KOA. (Table 2).

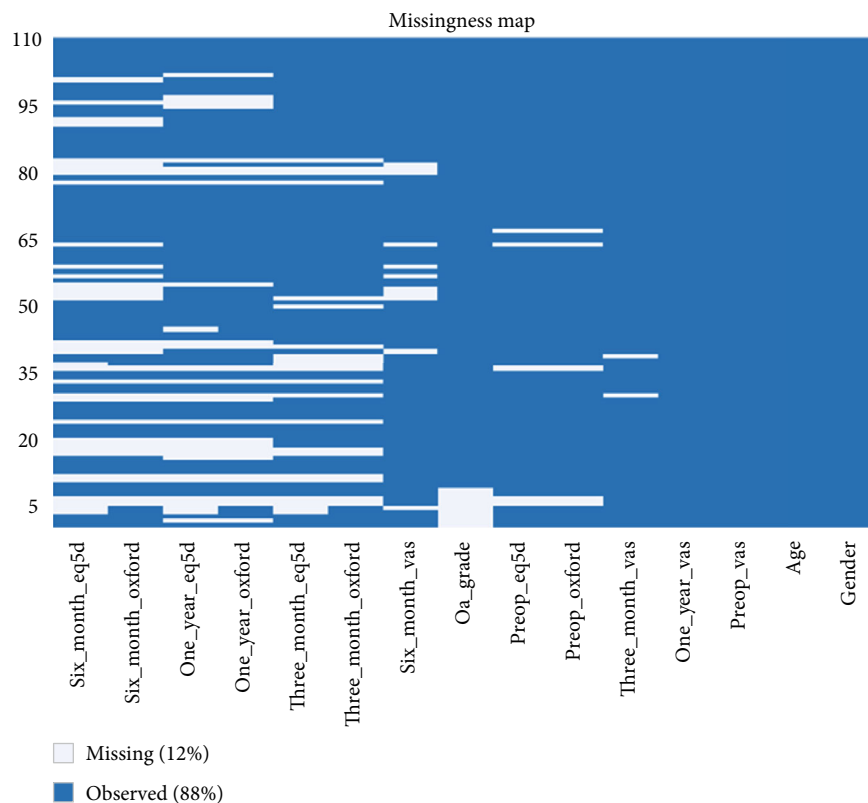


FIGURE 4: Missingness map. *x*-axis: outcome variables: gender, age, Visual Analogue Scale (VAS) for pain, Oxford Knee Score (OKS) for function, and EQ5D for quality of life at preoperative baseline and three, six, and twelve months follow-up. *y*-axis: data points missing at random (12%) due to patients lost-to-follow-up: missing data have been estimated probabilistically with uncertainty using the statistical software package Amelia v1.7.6 or higher. The estimation procedure is replicable and reproducible with Open Access statistical software R (4.0.0 or higher). The missingness map shows the missing data fields in our dataset. All patients have a preprocedure and 1 year VAS for pain as seen on the right-hand column of the plot. The left-hand column then the missing OKS and EQ5D.

One patient with posttraumatic OA had an injury as a child, and the other 3 had a combination of meniscal and ACL injuries that then lead to KOA.

**2.2. Source: Authors' Data.** Full and informed consent was undertaken for each part of the procedure including sedation, lipoaspiration, and image-guided intra-articular injection. All procedures were performed in an operating theatre as a day case, and patients were discharged approximately three hours following the completion of the procedure.

**2.3. Harvesting the Adipose Tissue.** The patient was placed under a sedation administered by an anaesthetist. A small incision was made to insert a 17G blunt cannula (connected to a luer-lock 60-cc syringe), and Klein sterile solution (containing saline, Lignocaine, and epinephrine) injected into the subcutaneous fat. Approximately, 150-200 ml of this solution was injected in 50 ml aliquots into the lower abdominal area. Adipose tissue (approximately 50 ml) was then harvested manually via a 13G blunt cannula (connected to a Vaclock 20 ml syringe), by a consultant plastic surgeon, experienced in this procedure. The area of fat harvest was tailored to the body habitus of each patient, (normally lower abdomen or flank areas) with the patient in a supine position.

An abdominal binder was then applied to the adipose tissue harvest site.

**2.4. Processing and Injecting the Lipoaspirate.** The lipoaspirate was processed using the Lipogems® system [29]. This is a disposable and single-use device. The lipoaspirate is introduced in a closed and aseptic manner into the low-pressure, full immersion, transparent plastic cylindrical container through stainless steel wire mesh. The device is prefilled with saline. Within the container, there are stainless steel ball bearings that work to mechanically fragment the fat, progressively reducing the size of the clusters of adipose tissue (from spheroidal clusters with a diameter of 1–3.5 mm to clusters of 0.2–0.8 mm) through mechanical agitation of the chamber much like a cocktail shaker. The chamber is flushed with saline to wash out impurities (e.g., oil, blood, and proinflammatory debris). The resulting product is then filtered through a 500-micron filter. This process takes approximately 20 minutes. A single 6-8 ml of this refined product was then injected directly into the knee joint under ultrasound guidance. This point of care device allows the procedure from lipoaspiration to the injection of the microfragmented fat to take place within the same sitting mitigating the need for any repeat visits from the patient.

TABLE 2: Patients' characteristics.

Characteristics	Number of patients (total = 110)	Percentage of patients (%)
Sex		
Male	60	54.5
Female	50	45.5
Age (years)		
Under 50	6	5.5
50-59	26	23.6
60-69	30	27.3
70-79	34	30.9
Over 80	14	12.7
Kellgren-Lawrence grade		
I	1	0.9
II	12	10.9
III	20	18.2
IV	68	61.8
Missing data	9	8.2
Aetiology of OA		
Idiopathic	106	96.4
Posttraumatic	4	3.6

**2.5. Postoperative Care.** All patients were provided with a pack which included analgesia (paracetamol and codeine), as well as a printed physiotherapy protocol. We advised our patients to avoid nonsteroidal anti-inflammatory drugs. Other nonpharmaceutical means of pain control such as rest and the use of warm and cold packs were advocated. Following discharge, outpatient physiotherapy sessions were scheduled for each patient. Patients were allowed to bear weight on their joint postprocedure; however, they were instructed to avoid any strenuous or high-impact activities for two weeks. Chemical thromboprophylaxis was not prescribed.

**2.6. Multiple Outcome Measurements.** Outcomes were measured using the Visual Analogue Scale (VAS) for pain, the Oxford Knee Score (OKS) for function, and the EQ5D for quality of life. All patients completed these questionnaires before treatment, and at three months, six months, and one year following treatment. Our analysis in this report includes the 12 months data.

VAS [30] is a validated measurement system that allows participants to measure their pain intensity along a continuous scale of values that otherwise cannot clearly be measured. Participants are presented with a horizontal line that is anchored by two extremes, between 0 and 100 (0 = no pain, 100 = worst pain), and are asked to place a point along the VAS line at the point that would represent their current level of pain.

OKS [31] comprised of 12 questions that were scored 0-4 with 0 being severe and 4 being none, covering pain and function of the knee. The best outcome is a score of 48, and the worst score possible is 0.

EuroQol-5 Dimension [32] is a standardized instrument developed by the EuroQol Group in order to measure the

health-related quality of life in a wide range of medical conditions. Five dimensions are measured in the respondent: mobility, self-care, usual activity, pain, and anxiety/depression. Scores were given between 1 and -1; this was recorded down with 1 being associated with a better quality of life whilst -1 the opposite.

### 3. Results

**3.1. Summary Results.** Median VAS (pain) improved from 70 (IQR 20) at baseline to 30 (IQR 58) at twelve months ( $p < 0.001$ ); median OKS (function) improved from 25 (IQR 11) to 33.5 (IQR 16) ( $p < 0.001$ ); and median EQ-5D (quality of life) improved from 0.62 (IQR 0.41) to 0.69 (IQR 0.28) ( $p < 0.001$ ). No adverse events were reported during the intraoperative, recovery, or postoperative periods.

Summary results are presented in Table 3 and Figures 1, 2, and 3. Figure 5 shows the study flow diagram with the data collection points of the study and attrition rate for collected scores. The missingness map (Figure 4) presents where scores have not been provided by the patients.

In Table 1, the variation of median VAS, OKS, and EQ-5D between baseline and twelve months follow-up has been grouped according to the grade of KOA. This shows a general trend in all severity of KOA towards improvement, but these data are not suitable for detailed subgroup analysis and statistical significance testing as grades 1 and 2 only represented 20% of the total sample.

### 4. Discussion

We report here the results of treating degenerative arthritis of the knee with autologous microfragmented adipose tissue. We found that 81% of our patients experienced a reduction in their pain and a concomitant improvement in their function with a single injection of MFAT. Median VAS, OKS, and EQ-5D between baseline and twelve months follow-up improved for all grades of KOA (Table 1). This shows a general trend in all severity of KOA towards improvement, but these data are not suitable for detailed subgroup analysis and statistical significance testing as grades 1 and 2 only represent 20% of the total sample size. The risks of this procedure are low and the possibility of reverting to more interventional approaches in those who do not improve remains. Of note is that higher grades of arthritis (KL grades III and IV) demonstrated an improvement in pain and function.

Knee OA is a debilitating condition that affects a significant proportion of the population in all nationalities. Current solutions include the correction of deformities to preserve the knee or otherwise joint sacrificing procedures such as total or partial replacement. These surgical options carry risk, and many individuals seek nonsurgical solutions and are not willing to consider surgery until these have been exhausted.

To this end, a growing number of clinicians are using biologics such as Platelet Rich Plasma and cell-based therapies to control pain in arthritis and delay the need for surgical intervention. Among these therapies being investigated is the use of microfragmented adipose tissue. A search



TABLE 3: Summary results.

Parameter	Assessment	Median score	IQR score	Nonparametric paired samples Wilcoxon test $p$ value
VAS	Pre-op	70	20	$p < 0.001$
	1 year	30	58	
OKS	Pre-op	25	11	$p < 0.001$
	1 year	33	16	
EQ-5D	Pre-op	0.62	0.41	$p < 0.001$
	1 year	0.69	0.28	

Summary of the results showing the median values and Interquartile range (IQR) of Visual Analogue Scale for pain (VAS), Oxford Knee Score (OKS), and EuroQuol 5D (EQ-5D) at baseline and at 1 year follow-up. A statistically significant improvement in all parameters is demonstrated with  $p < 0.001$ .

Source: Authors' Data and reproducible statistical analysis with Open Access statistical software R (version 4.0.0 or higher).

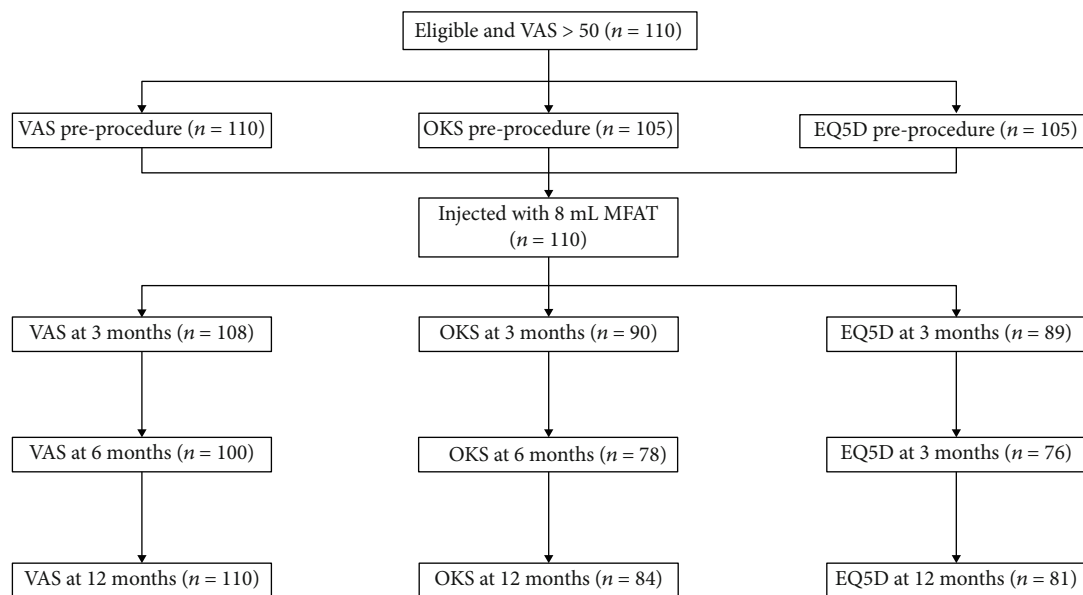


FIGURE 5: Study flow diagram depicts the touch points including the preprocedure assessment, injection of the knee, and subsequent follow-up and attrition in the collection of outcomes.

of clinicaltrials.gov revealed a number of ongoing studies assessing the effects of microfragmented adipose tissue for KOA.

In our study, we noted a very low number of adverse events and complications with pain at the harvest and injections sites. This experience is mirrored in the literature with a prospective study of 1524 patients, many with significant medical comorbidities, who received stromal vascular fraction procedures. At long term follow-up (22 to 64 months), 98% reported no adverse events and 0.72% reported a new cancer diagnosis [33]. In a systematic review and meta-analysis of 36 clinical trials of both autologous and allogeneic mesenchymal stem cells harvested from several tissue sources, there was no evidence of increased acute toxicity, organ system complications, infection, death, or malignancy [34].

More recently a number of clinical studies have demonstrated the safety and efficacy of microfragmented fat for the treatment of KOA. Russo et al. [35] reported on 30 patients who were treated with microfragmented fat as an

adjuvant for the surgical treatment of diffuse degenerative chondral lesions, with a follow-up of three years. 22 required no further treatment, and no adverse events were reported. They also noted that the improvements in Tegner-Lysholm Knee, VAS, IKDC-subjective, and total KOOS scores observed at one year were maintained at the three-year mark.

Panni et al. [27] reported similar results with 52 patients with early KOA, who received arthroscopic debridement followed by injection of microfragmented fat. At final follow-up, 96.2% of patients expressed satisfaction and reported good or excellent improvements in function and/or pain. Hudetz et al. [26] conducted a study where 20 patients with KOA were treated with a single intra-articular injection of microfragmented fat. He noted that 17 (85%) showed a substantial pattern of KOOS and WOMAC improvement, significant in all accounts.

**4.1. Study Limitations.** Our experience has mirrored that of many other colleagues regarding the use of MFAT in KOA. This treatment offers a minimally invasive and nonsurgical

method for the treatment of KOA. The main limitation of this study is the absence of a control group in our sample. This self-selected group did not want to have major surgery when they came to our clinic and were treated with an ultrasound-guided single injection of MFAT. We included all grades of arthritis but excluded those with deformity greater than ten degrees. It can be argued that this represents a heterogeneous group of disease. Combining the age range of our cohort (42 to 94) as well as the severity of their conditions (KL grade I-IV) makes for many variables and thus makes subgroup analysis difficult. However, this is a pragmatic representation of our clinical practice, and the highly statistically significant improvement of pain, function, and quality of life cannot be ignored.

The missingness map and study flow diagrams show an attrition rate of 12% in our data collection. Responder fatigue is a well-documented phenomenon and may introduce bias [36].

## 5. Conclusions

The benefit of this treatment to the individual is in the mitigation of complications and the associated recovery from surgical intervention. The aim of any intervention is the reduction in pain and improvement in function with a resultant betterment of quality of life. The hope is that this will then be reflected in the overall healthcare costs at a population level. Despite the limitations detailed above, our study represents an incremental step in defining the place for biologic treatments in degenerative joint disease. These findings are mirrored in a number of other studies [26–28]. What remains unclear is whether true restoration of the cartilage occurs or indeed if this is necessary for the clinical effects seen.

The authors caution that the retrospective nature of the study and the small number of patients make it impossible to draw definitive conclusions. The findings need to be validated with a randomized controlled trial, conducted over a longer period to check for long-term outcomes, to establish more clearly the stage of the disease best suited for treatment with biologics in order to maximize patient-centered efficacy.

## Data Availability

All data is available upon request

## Conflicts of Interest

S.O. has received in the past and is likely to receive in the future private and public funding for predictive computational medicine, predictive clinical trials, and predictive modeling in the field of regenerative medicine. The other authors declare no conflict of interest.

## Authors' Contributions

Conceptualization was conceived by N.H. and A.N.; methodology was designed by N.H.; software was worked by A.C. and S.O.; formal analysis was worked by N.H., A.C., and

S.O.; investigation was performed by N.H., A.W., A.N., and A.C.; data curation was gathered by A.C.; L.S. and N.H. wrote the original draft preparation; N.H., L.S., S.O., A.Z., M.S., and A.C. reviewed and edited the writing; visualization was conceptualized by N.H., L.S., and S.O.; supervision was performed N.H., A.N., and A.W.; project administration was prepared by N.H.; resources were collected by A.N.

## Acknowledgments

The Research team at The Regenerative Clinic for their hard work and diligence at collecting patient's questionnaires. All the staff at The Regenerative Clinic.

## References

- [1] H. Behzad, "Knee osteoarthritis prevalence, risk factors, pathogenesis and features: part I," *Caspian Journal of Internal Medicine*, vol. 2, no. 2, pp. 205–212, 2011.
- [2] S. Safiri, A. Kolahi, E. Smith et al., "Global, regional and national burden of osteoarthritis 1990–2017: a systematic analysis of the Global Burden of Disease Study 2017," *Annals of the Rheumatic Diseases*, vol. 79, no. 6, pp. 819–828, 2020.
- [3] A. Mobasheri and M. Batt, "An update on the pathophysiology of osteoarthritis," *Annals of Physical and Rehabilitation Medicine*, vol. 59, no. 5–6, pp. 333–339, 2016.
- [4] A. Stolzing, E. Jones, D. McGonagle, and A. Scutt, "Age-related changes in human bone marrow-derived mesenchymal stem cells: consequences for cell therapies," *Mechanisms of Ageing and Development*, vol. 129, no. 3, pp. 163–173, 2008.
- [5] P. Sarzi-Puttini, M. A. Cimmino, R. Scarpa et al., "Osteoarthritis: an overview of the disease and its treatment strategies," *Seminars in Arthritis and Rheumatism*, vol. 35, no. 1, pp. 1–10, 2005.
- [6] M. Blagojevic, C. Jinks, A. Jeffery, and K. P. Jordan, "Risk factors for onset of osteoarthritis of the knee in older adults: a systematic review and meta-analysis," *Osteoarthritis and Cartilage*, vol. 18, no. 1, pp. 24–33, 2010.
- [7] J. Chahla, C. S. Dean, G. Moatshe, C. Pascual-garrido, R. Serra Cruz, and R. F. Laprade, "Concentrated Bone Marrow Aspirate for the Treatment of Chondral Injuries and Osteoarthritis of the Knee: A Systematic Review of Outcomes," *Orthopaedic Journal of Sports Medicine*, vol. 4, no. 1, article 232596711562548, 2016.
- [8] C. A. Herberts, M. S. G. Kwa, and H. P. H. Hermsen, "Risk factors in the development of stem cell therapy," *Journal of Translational Medicine*, vol. 9, no. 1, 2011.
- [9] J. Burke, M. Hunter, R. Kolhe, C. Isales, M. Hamrick, and S. Fulzele, "Therapeutic potential of mesenchymal stem cell based therapy for osteoarthritis," *Clinical and Translational Medicine*, vol. 5, no. 1, p. 27, 2016.
- [10] A. I. Caplan, "Mesenchymal Stem Cells: Time to Change the Name!," *STEM CELLS Translational Medicine*, vol. 6, no. 6, pp. 1445–1451, 2017.
- [11] A. J. Friedenstein, "Osteogenic stem cells in the bone marrow," *Bone and Mineral Research*, vol. 7, pp. 243–272, 1990.
- [12] L. E. B. de Souza, T. M. Malta, S. K. Haddad, and D. T. Covas, "Mesenchymal stem cells and pericytes: to what extent are they related?," *Stem Cells and Development*, vol. 25, no. 24, pp. 1843–1852, 2016.

- [13] J. Zhang, C. Du, W. Guo et al., "Adipose tissue-derived pericytes for cartilage tissue engineering," *Current Stem Cell Research & Therapy*, vol. 12, no. 6, pp. 513–521, 2017.
- [14] F. G. Uselli, R. D'Ambrosi, C. Maccario, C. Indino, L. Manzi, and N. Maffulli, "Adipose-derived stem cells in orthopaedic pathologies," *British Medical Bulletin*, vol. 124, pp. 31–54, 2017.
- [15] T. Saito and S. Tanaka, "Molecular mechanisms underlying osteoarthritis development: notch and NF- $\kappa$ B," *Arthritis Research & Therapy*, vol. 19, no. 1, p. 94, 2017.
- [16] M. F. Pittenger, "Multilineage potential of adult human mesenchymal stem cells," *Science*, vol. 284, no. 5411, pp. 5143–5147, 1999.
- [17] F. Buttgeriet, G.-R. Burmester, and J. W. J. Bijlsma, "Non-surgical management of knee osteoarthritis: where are we now and where do we need to go?," *RMD Open*, vol. 1, no. 1, article e000027, 2015.
- [18] D. J. Hunter and S. Bierma-Zeinstra, "Osteoarthritis," *The Lancet*, vol. 393, no. 10182, pp. 1745–1759, 2019.
- [19] S. M. Watt, F. Gullo, M. van der Garde et al., "The angiogenic properties of mesenchymal stem/stromal cells and their therapeutic potential," *British Medical Bulletin*, vol. 108, no. 1, pp. 25–53, 2013.
- [20] R. D'Ambrosi, C. Indino, C. Maccario, L. Manzi, and F. G. Uselli, "Autologous Microfractured and purified adipose tissue for arthroscopic management of osteochondral lesions of the talus," *Journal of Visualized Experiments*, vol. 131, no. 131, 2018.
- [21] F. Berenbaum, "Osteoarthritis as an inflammatory disease (osteoarthritis is not osteoarthrosis!)," *Osteoarthritis and Cartilage*, vol. 21, no. 1, pp. 16–21, 2013.
- [22] M. Cross, E. Smith, D. Hoy et al., "The global burden of hip and knee osteoarthritis: estimates from the Global Burden of Disease 2010 study," *Annals of the Rheumatic Diseases*, vol. 73, no. 7, pp. 1323–1330, 2014.
- [23] T. A. Ahmed, W. G. Shousha, S. M. Abdo, I. K. Mohamed, and N. El-Badri, "Human adipose-derived pericytes: biological characterization and reprogramming into induced pluripotent stem cells," *Cellular Physiology and Biochemistry*, vol. 54, no. 2, pp. 271–286, 2020.
- [24] C. Tremolada, V. Colombo, and C. Ventura, "Adipose tissue and mesenchymal stem cells: state of the art and Lipogems® technology development," *Current Stem Cell Reports*, vol. 2, no. 3, pp. 304–312, 2016.
- [25] M. B. Murphy, K. Moncivais, and A. I. Caplan, "Mesenchymal stem cells: environmentally responsive therapeutics for regenerative medicine," *Experimental & Molecular Medicine*, vol. 45, no. 11, pp. e54–e54, 2013.
- [26] D. Hudetz, I. Boric, E. Rod et al., "Early results of intra-articular micro-fragmented lipoaspirate treatment in patients with late stages knee osteoarthritis: a prospective study," *Croatian Medical Journal*, vol. 60, no. 3, pp. 227–236, 2019.
- [27] A. Schiavone Panni, M. Vasso, A. Braile et al., "Preliminary results of autologous adipose-derived stem cells in early knee osteoarthritis: identification of a subpopulation with greater response," *International Orthopaedics*, vol. 43, no. 1, pp. 7–13, 2019.
- [28] J. Panchal, G. Malanga, and M. Sheinkop, "Safety and Efficacy of Percutaneous Injection of Lipogems Micro-Fractured Adipose Tissue for Osteoarthritic Knees," *American Journal of Orthopedics*, vol. 47, no. 11, 2018.
- [29] F. Bianchi, M. Maioli, E. Leonardi et al., "A new nonenzymatic method and device to obtain a fat tissue derivative highly enriched in pericyte-like elements by mild mechanical forces from human lipoaspirates," *Cell Transplantation*, vol. 22, no. 11, pp. 2063–2077, 2013.
- [30] M. Haefeli and A. Elfering, "Pain assessment," *European Spine Journal*, vol. 15, no. S1, pp. S17–S24, 2006.
- [31] J. Dawson, R. Fitzpatrick, D. Murray, and A. Carr, "Questionnaire on the perceptions of patients about total knee replacement," *The Journal of Bone and Joint Surgery. British*, vol. 80-B, no. 1, pp. 63–69, 1998.
- [32] EuroQol Group (1990-12-01), "EuroQol - a new facility for the measurement of health-related quality of life," *Health Policy*, vol. 16, no. 3, pp. 199–208, 1990.
- [33] M. Berman and E. Lander, "A prospective safety study of autologous adipose-derived stromal vascular fraction using a specialized surgical processing system," *The American Journal of Cosmetic Surgery*, vol. 34, no. 3, pp. 129–142, 2017.
- [34] M. M. Lalu, L. McIntyre, C. Pugliese et al., "Safety of cell therapy with mesenchymal stromal cells (SafeCell): A systematic review and meta-analysis of clinical trials," *PLoS ONE*, vol. 7, no. 10, article e47559, 2012.
- [35] A. Russo, D. Screpis, S. L. Di Donato, S. Bonetti, G. Piovan, and C. Zorzi, "Autologous micro-fragmented adipose tissue for the treatment of diffuse degenerative knee osteoarthritis: an update at 3 year follow-up," *Journal of Experimental Orthopaedics*, vol. 5, no. 1, p. 52, 2018.
- [36] A. M. Wood, I. R. White, and S. G. Thompson, "Are missing outcome data adequately handled? A review of published randomized controlled trials in major medical journals," *Clinical Trials: Journal of the Society for Clinical Trials*, vol. 1, no. 4, pp. 368–376, 2016.

## Review Article

# Functions of Circular RNAs in Regulating Adipogenesis of Mesenchymal Stem Cells

Fanglin Wang,<sup>1</sup> Xiang Li,<sup>2</sup> Zhiyuan Li,<sup>1</sup> Shoushuai Wang,<sup>1</sup> and Jun Fan <sup>1</sup>

<sup>1</sup>Department of Tissue Engineering, School of Fundamental Science, China Medical University, Shenyang, Liaoning 110122, China

<sup>2</sup>Department of Cell Biology, Key Laboratory of Cell Biology, Ministry of Public Health, And Key Laboratory of Medical Cell Biology, Ministry of Education, China Medical University, Shenyang, Liaoning 110122, China

Correspondence should be addressed to Jun Fan; [jfan@cmu.edu.cn](mailto:jfan@cmu.edu.cn)

Received 26 March 2020; Revised 7 July 2020; Accepted 8 July 2020; Published 1 August 2020

Academic Editor: Huseyin Sumer

Copyright © 2020 Fanglin Wang et al. This is an open access article distributed under the Creative Commons Attribution License, which permits unrestricted use, distribution, and reproduction in any medium, provided the original work is properly cited.

The mesenchymal stem cells (MSCs) are known as highly plastic stem cells and can differentiate into specialized tissues such as adipose tissue, osseous tissue, muscle tissue, and nervous tissue. The differentiation of mesenchymal stem cells is very important in regenerative medicine. Their differentiation process is regulated by signaling pathways of epigenetic, transcriptional, and posttranscriptional levels. Circular RNA (circRNA), a class of noncoding RNAs generated from protein-coding genes, plays a pivotal regulatory role in many biological processes. Accumulated studies have demonstrated that several circRNAs participate in the cell differentiation process of mesenchymal stem cells *in vitro* and *in vivo*. In the current review, characteristics and functions of circRNAs in stem cell differentiation will be discussed. The mechanism and key role of circRNAs in regulating mesenchymal stem cell differentiation, especially adipogenesis, will be reviewed and discussed. Understanding the roles of these circRNAs will present us with a more comprehensive signal path network of modulating stem cell differentiation and help us discover potential biomarkers and therapeutic targets in clinic.

## 1. Introduction

Circular RNAs are a new and intriguing class of noncoding RNA, produced from precursor mRNA (pre-mRNA), single-stranded, and covalently closed. circRNAs have been discovered for more than 40 years [1], once were described as the by-products of aberrant splicing with functional proteins [2–4]. This cognition has been changed in recent years, with the development of high-throughput sequencing technology and novel bioinformatics algorithms [5]. Thus, backspliced junctions of circRNAs can be reliably identified, through short-read paired-end RNA sequencing (RNA-seq) technology [6, 7]. By sequencing nonpolyadenylated transcriptomes, researchers find that circRNAs are generally expressed in eukaryotes. Their expression has characteristics of cell type-specific and tissue-specific [5, 8]. Although the functions of thousands of described circRNAs remain unknown, accumulated studies have already shown that circRNAs can participate

in cellular activities, embryonic development, neural development, and the development of a variety of human diseases [9, 10]. With the regulatory role of circRNAs, the researchers try to find out the potential functions of circRNAs in cell differentiation of mesenchymal stem cells.

The mesenchymal stem cells can be isolated from adult tissues, including bone marrow, adipose tissue, and umbilical cord, and other sources [11]. MSCs are multipotent stromal cells with low immunogenic potential that can differentiate into a variety of unique mesenchymal cell types, such as osteoblasts, chondrocytes, and adipocytes. With the development of regenerative medicine, MSCs have been widely applied in effective cell-based therapy for tissue regeneration and repair [12–14].

This review is aimed at presenting and discussing the mechanism on how circRNAs affect adipogenic differentiation of MSCs based on existing literature. Moreover, we propose to summarize the signal path network and figure out the direction to be studied.



## 2. Adipogenic Differentiation of MSCs

Mesenchymal stem cells are a heterogeneous population of multipotent elements resident in tissues such as bone marrow, muscle, and adipose tissue, which are primarily involved in developmental and regeneration processes [15]. MSCs participate in the repair/remodeling of many tissues. They have an ability termed “plasticity” in which they differentiate into specific cell-matured phenotypes under defined conditions [16]. The control of stem cell fate has been primarily attributed to the regulation of genetic and molecular mediators which are critical determinants for the lineage decision of stem cells. Though complex signaling pathways that drive commitment and differentiation, MSCs can differentiate into the osteogenic, chondrogenic, adipogenic, or myogenic lineage.

Adipogenesis is one of the significant differentiation directions of mesenchymal stem cells, which can be regulated by transcription factors [17]. In this process, MSCs restrict their fate to the adipogenic lineage, accumulate nutrients, and become triglyceride-filled mature adipocytes. This process can be divided into two steps. In the first step, ADSCs restrict themselves to the adipocyte lineage without any morphological changes, forming a preadipocyte (commitment step). Following this commitment is the terminal differentiation step, during which specified preadipocytes undergo growth arrest, accumulating lipids and forming functional, insulin-responsive mature adipocytes [18].

**2.1. Commitment Step.** At the launch stage of adipogenesis, the expression of c-Jun and c-Fos in ADSCs is increased [19]. c-Fos binds to the AP-2 promoter and modulates AP-2 expression [20]. At this moment, binding of AP-2 $\alpha$  to CCAAT/enhancer-binding protein (C/EBP)  $\alpha$  represses its activity to avoid C/EBP $\alpha$  preventing preadipocytes from entering mitotic clonal expansion. The signal transducers and activators of transcription (STAT) family, especially STAT 5A and 5B, are highly expressed in this stage [21]. The induction of STAT 5A/5B in preadipocytes is accompanied by the ectopic expression of C/EBP $\beta$  and  $\delta$  and is also coordinately regulated with the peroxisome proliferator-activated receptors (PPAR)  $\gamma$  [22]. After 2-6 hours of induction, the expression of c-Jun, c-Fos, etc. disappeared. In this early lineage commitment process, Wnt/ $\beta$ -catenin functions as a critical initiator, suppresses the induction of adipogenesis, and regulates the cell cycle [23, 24]. Reports have shown that Wnt10b appears to have an activating role in commitment and maintains preadipocytes in an undifferentiated state through inhibition of C/EBP- $\alpha$  and PPAR $\gamma$  [25, 26].

Following a delay of about 16–20 hours after induction, preadipocytes synchronously reenter DNA synthesis prophase of the cell cycle [27] and undergo several rounds of mitotic clonal expansion. Along with preadipocytes entering into S phase and mitotic clonal expanding, C/EBP $\beta$  gains its DNA-binding activity. C/EBP $\beta$  is phosphorylated twice sequentially, leading to the acquisition of DNA-binding function [28]. After 18–24 hours, the C/EBP $\alpha$  and PPAR $\gamma$  genes are transcriptionally activated by C/EBP $\beta$  through C/EBP regulatory elements in their proximal promoters

[29]. PPAR $\gamma$ 2 and C/EBP $\alpha$  coordinately transactivate a large group of genes that produce the adipocyte phenotype. They constituted the most important signal path of adipogenic differentiation, C/EBP $\beta$ + $\delta$ -PPAR $\gamma$ -C/EBP $\alpha$  [30].

**2.2. Terminal Differentiation Step.** Preadipocytes have entered the growth inhibition phase; then, the cells immediately return to the cell cycle and enter the asexual amplification stage. While the transcriptional activity of C/EBP $\beta$ / $\delta$  is enhanced by STAT 5A/5B, C/EBP $\alpha$  is increasingly expressed and achieved the highest concentration in the time of induction for 4 d. [22, 31]. The cells then exit the cell cycle losing their fibroblastic morphology and start accumulating triglyceride in the cytoplasm with the appearance and metabolic features of adipocytes [32]. Lipid accumulation drives the expression of the adipocyte fatty acid-binding protein, AP2, and mediates PPAR $\gamma$  expression. The insulin-sensitive transporter GLUT4 also expressed increasingly, promoting the triglyceride accumulation [18]. In the terminal differentiation, the canonical Wnt signaling pathway can also regulate adipogenesis by attenuating the expression of Wnt10b [25]. Wnt family members can also activate noncanonical pathway antagonizing the canonical pathway [32]. Through Wnt5b, the noncanonical pathway inhibits adipogenesis by decreasing the transcriptional activity of PPAR $\gamma$  and regulates insulin sensitivity of the differentiating adipocytes [33, 34]. Then activated phosphoinositide 3-kinase (PI3K)/serine/threonine protein kinases B (Akt) signaling in mesenchymal cells drives and maintains the adipogenesis around 7-28 d after induction [35]. With such complex factors regulated, adipogenic precursor cells complete triglyceride accumulation after a few days of induction, showing typical adipocyte morphology.

## 3. Characteristics and Functions of circRNA

circRNAs are generated from pre-mRNAs; most of them are arising from exons. By using the standard splice signals, two-step mechanism, and spliceosome machinery, the 3' tail of one exon is joined to the 5' head of an upstream exon; pre-mRNAs compose into a covalently closed and circular configuration [6, 36, 37]; besides, some circRNAs can also arise from introns [38]. The formation of circRNAs depends on the RNA-editing enzyme ADAR1 and can be facilitated by *cis*-regulatory elements and *trans*-acting factors [36, 39–42]. According to types of circularization, circRNAs can be classified into exonic circRNAs and intronic circRNAs. They are distinct and independent varieties in a generation. In recent years, researchers focus on clarifying the functions of circRNAs, which are involved in the regulation of multiple biological processes.

**3.1. miRNA Sponge.** circRNAs are usually considered one class of noncoding RNA, which mainly function as efficient microRNA (miRNA) sponge, which is involved with miRNA inhibition with regulatory potential [9, 43, 44]. Indeed, this phenomenon has been widely reported, circRNA overexpression could alleviate apoptosis and promote anabolism through the miRNA pathway [45, 46]. This route is generally

considered endogenous RNA (ceRNA) and constitutes a regulatory network across the transcriptome [47, 48]. In the regulation of MSC differentiation, sponging function of circRNA has been extensively investigated. However, only a few of circRNAs were showed to serve as miRNA sponge [49, 50]. They may play a part in other functions. In addition, some of the circRNAs do not display binding sites for miRNA; future efforts should be done to elucidate the mechanisms on improving circRNAs to expose their binding sites to the corresponding miRNAs.

**3.2. Sponging Protein.** There is still a large class of circRNAs with many protein binding sites, which are essential for strong and direct interaction between protein and circRNAs. Target protein can impact circularization rates of circRNA, and circRNA could then sponge out the excess protein by binding to it [51, 52]. circRNAs function as protein sponge and are less found in regulating MSC differentiation. This function is more directly related to protein-protein interaction, which means they are significant for MSC differentiation [53].

**3.3. Protein-Coding Function.** circRNAs are generally considered “noncoding” RNAs; in fact, they also serve as templates for protein translation. A few publications provide initial evidence that circRNAs contain an open reading frame and can encode polypeptides and even a protein isoform in a splicing-dependent/cap-independent manner [10, 49, 54]. A protein-coding function of circRNAs is recently discovered; it not only corrects the wrong perception but also provides a new research area.

**3.4. Other Functions.** circRNAs can be linked to exon skipping and affect the splicing of their linear mRNA counterparts [55]. Nuclear retained circular RNAs regulate transcription of their parental genes and splicing of their linear cognates [56]. A mount of circRNA-derived pseudogenes has been identified by retrieving noncolinear backsplicing junction sequences, which demonstrates that circRNAs are resources for the derivation of pseudogenes [57]. circRNA can also act as a protein subunit associated with the holoenzyme in metabolic adaptation, assembles and stabilizes the holoenzyme complex, and maintains basal activity [58].

Based on the above studies, it enlightens us that it is necessary for exploring how circRNAs regulate MSC differentiation. Additionally, epigenetic modifications can also occur in RNA, called the epitranscriptome, which refers to stable and heritable changes in gene expression that do not alter the RNA sequence. N6-Methyladenosine (m6A) is always found to occur in the consensus sequence identified as RRACH (R = G or A; H = A, C, or U) and promote the translation of the circRNAs [59]. It is the most abundant epigenetic modification in eukaryotes and plays a significant role in autophagy and adipogenesis regulation [60]. If we combine with epigenetic modification, researches about regulating functions of circRNA in MSCs may come to a new stage.

## 4. circRNA and Regulation of MSC Differentiation

circRNAs are the key regulators of gene expression and protein functions in epigenetic regulation. As previously mentioned, the differentiation of MSC is a highly controlled process, which is regulated by both proteins and noncoding RNAs. Due to their functions in regulating epigenetic and molecular biological processes, recent research suggests that circRNAs play a considerable role in cell fate decisions of MSC differentiation [10]. Current studies demonstrate that the majority of circRNAs participate in the process of adipogenesis, myogenesis, and osteogenesis of MSCs [61, 62].

**4.1. Adipogenesis and Osteogenesis of MSCs.** Osteogenesis is thought to be most closely related to adipogenesis in the differentiation of MSCs. There is a balance between adipogenic and osteogenic differentiation processes. circRNAs regulate adipogenesis and osteogenesis by, respectively, affecting a variety of signaling pathways, but in the end, they will converge at several major transcription factors that are shared in differentiation including PPAR $\gamma$  and WNT [63, 64].

Cerebellar degeneration-related protein 1 transcript (CDR1as), also known as circular RNA sponge for miR-7 (ciRS-7), was reported to be involved in the osteogenesis [61, 65]. CDR1as can inhibit osteogenesis and promotes adipogenesis by inhibition of miR-7 via targeting GDF5 through the MAPK signaling pathway in bone mesenchymal stem cells (BMSCs) [66]. Beyond that, many circRNAs can regulate the proliferation and osteogenesis of MSCs through sponging some specific miRNAs which are similar to their effect on adipogenesis and other differentiation [67–69].

**4.2. Myogenesis and Neuronal Differentiation.** circRNAs are also abundant in skeletal muscle tissue, and their expression levels can regulate muscle development, ageing, and differentiation. As described above, CDR1as is involved in various directions of differentiation in MSC. In skeletal muscle satellite cells (SMSCs), it subsequently activates myogenesis through sponging miR-7 [70, 71]. Several circRNAs also work in the same way by sponging miRNAs to promote or repress the myogenic differentiation of MSCs, such as circHIPK3 and circ-FoxO3 [72–74]. Other than that, circRNAs have been identified to be differentially expressed in different differentiation stages of neural stem cells (NSCs). It is likely that some specific circRNAs resulted in the corresponding expression of mRNA and involved in neuronal differentiation [75].

These shreds of evidence suggest that circRNAs play a significant role in regulating MSC differentiation. The current review is aimed at highlighting the regulation of adipogenic differentiation of MSCs by circRNAs.

## 5. circRNAs Regulate Adipogenesis

The pathways of circRNAs regulating osteogenesis and myogenesis are closely related to adipogenic differentiation. Even certain circRNAs play a multiplicative role that antagonizes among these directions of differentiation. Therefore,

TABLE 1: Circular RNAs regulate adipogenic differentiation.

circRNA	miRNA or protein	Target gene(s)	Cell	Related process	Reference
Hsa_circ_0001946 (CDR1as)	miR-7-5p	Wnt5b	BMSCs	↑Adipogenesis ↓Osteogenesis	[61]
Hsa_circ_0095570 (circH19)	PTBP1	SREBP1	hADSCs	↓Adipogenesis	[53]
CircFOXP1	miR-17-3p and miR-127-5p	Wnt5b and Wnt3a	BMSCs	↑Adipogenesis	[76]
circRNA 2: 27713879 27755789 and circRNA 2: 240822115 240867796	miR-328 miR-23a-5p and miR-326	C/EBP $\alpha$ TGF- $\beta$	MC3T3-E1	↓Adipogenesis ↑Osteogenesis	[77, 78]
circRNA-11897	miR-27a and miR-27b	PPAR $\gamma$	Adipocytes	↑Adipogenesis	[79]
circRNA-26852	miR-874 miR-486	PPAR $\alpha$ FOXO1	Adipocytes	↑Adipogenesis	[79]
CiRS-133	miR-133	PRDM16	Preadipocytes	↑WAT browning	[80]
circRNA-0046366	miR-34a	PDGFR $\alpha$	Adipocytes	↑Hepatocellular steatosis	[81, 82]
CircSAMD4A	miR-138-5p	EZH2	Preadipocytes	↑Adipogenesis	[83]

circRNA regulating cell differentiation of MSC is an exchange network that each differentiation direction is closely related. It suggests that the perspective of adipogenesis will contribute to understanding the landscape of the cell differentiation network of mesenchymal stem cells. The research methods of circRNAs regulating osteogenesis and myogenesis can also be used in the study on circRNA regulating network of adipogenesis. It is efficient for gene chip technology and bioinformation analysis to be used to preliminary screen. Combined with molecular biology experiment, the pathway of circRNA regulating adipogenesis could be basically verified. According to the regulatory network of circRNAs in adipogenesis, researchers can explore more directions of MSCs in clinical transformation.

Recent studies have demonstrated a few circRNAs acting as a miRNA sponge to regulate adipogenic differentiation, while other circRNAs can also compete with proteins that participate in the regulation of adipogenesis. Therefore, we emphasized the regulatory network of circRNAs in regulating adipogenesis (Table 1).

**5.1. CDR1as-miR-7-5p-WNT5B.** Confronting research discovers that circRNA, hsa\_circ\_0001946 (CDR1as), may play a crucial role in adipogenic/osteogenic differentiation process via CDR1as-miR-7-5p-WNT5B axis in BMSCs [61]. CDR1as has been reported to affect the expression of target genes and plays an important role in the pathogenesis via adsorbing miR-7-5p [84–86]. miR-7-5p can be sponged by CDR1as [66] and target WNT5B-3'UTR [61]. Experiments show that the upregulation of CDR1as will promote the expression of WNT5B via competitively harboring miR-7-5p. WNT5B, a member of the WNT family, can inhibit  $\beta$ -catenin in the WNT/ $\beta$ -catenin signaling pathway [87, 88]. Downregulation of  $\beta$ -catenin can promote the expression of PPAR $\gamma$ , which promotes adipogenic differentiation and inhibits osteogenic differentiation in BMSCs [61]. In 3T3-L1 preadipocytes, low expression of  $\beta$ -catenin can also pro-

mote adipogenic differentiation and inhibit osteoclast differentiation by inducing the expression of PPAR $\gamma$  [89, 90]. However, further studies will be needed to demonstrate the effects of circRNAs on BMSC adipogenic differentiation in vivo.

**5.2. CircH19-PTBP1.** Hsa\_circ\_0095570 derived from H19 pre-RNA, also called circH19, has putative binding sites with RNA-binding protein polypyrimidine tract-binding protein 1 (PTBP1) [53]. PTBP1, also known as hnRNP I, belongs to a subfamily of heterogeneous nuclear ribonucleoproteins (hnRNPs), which moves rapidly between the nucleus and cytoplasm as a shuttling protein [91]. On the asexual amplification stage, a basic helix-loop-helix transcription factor is expressed in adipocytes during adipogenesis and determination, called sterol-regulatory element-binding protein 1 (SREBP1, ADD1). One of its isoforms, SREBP-1c, contributes to the generation of PPAR $\gamma$  ligands and promotes energy mobilization with phosphorylation by MAPK [92, 93]. A previous study demonstrated that PTBP1 played an important role in the cleavage of SREBP1 precursor and translocation of nSREBP1 protein [94]. circH19 might interact with PTBP1 to block the function of PTBP1, resulting in the inhibition of SREBP1 precursor cleavage. To sum up, hsa\_circH19 suppresses PTBP1 and decreases the cleavage of the SREBP1 precursor, thus inhibiting the translocation of nSREBP1 to the nucleus. The inhibition of circH19 can promote the transcription of lipid-related genes, leading to lipid accumulation in hADSCs [53]. In other words, circH19 can function as an inhibitor of PTBP1 and prevents hADSCs from transforming into adipocytes with enhanced ability to absorb lipids. This is the first time to demonstrate that circRNA regulates MSC adipogenesis by sponging protein. High levels of hsa\_circH19 is an independent risk factor for metabolic syndrome. So, the expression of hsa\_circH19 might be related with lipid metabolism in adipose tissue from patients of metabolic syndrome.



**5.3. *CircFOXP1-miR-17-3p/miR127-5p.*** CircFOXP1 originates from the forkhead box (FOX) P1 gene, which is related to the maintenance of BMSC identity and regulation of differentiation. CircFOXP1 acts as an essential gatekeeper of BMSC identity, which can promote proliferation and differentiation by target sponging miR-17-3p and miR-127-5p [76]. The combined action of miR-17-3p and miR-127-5p may regulate growth, survival, and balance between undifferentiated and differentiated MSCs through epidermal growth factor receptor (EGFR) and noncanonical Wnt signaling [76, 95–97]. In BMSCs, elevated levels of circFOXP1 can preserve the BMSC multipotent state by sponging multiple miRNAs, sustain noncanonical via Wnt5b, and consequently inhibit the canonical Wnt pathway via Wnt3a [76]. This functional interaction is fundamental to inhibit miRNA activity and avoid interference of signaling cascades associated with stemness and differentiation. CircFOXP1 should be regarded as a regulator of sustaining mesenchymal stem cell identity and the capacity of MSCs to differentiate into the adipocytic lineage [76]. Knockdown circFOXP1 in MSCs will inhibit adipogenic differentiation and decrease accumulation of intracellular lipid droplets.

**5.4. *circRNA 2: 27713879|27755789 and circRNA 2: 240822115|240867796.*** Estrogen receptor (ER)  $\beta$  is structurally and functionally related to isoforms of ER. Its expression is increased during osteoblast differentiation [98]. It was shown that ER $\beta$  was capable of upregulating the expression levels of osteogenesis-related markers and inducing the osteogenic differentiation of MC3T3-E1 [77]. Recently, the experiment demonstrates that ER $\beta$  may regulate the expression levels of miR-328, miR-23a-5p, and miR-326 via circRNA 2: 27713879|27755789 and circRNA 2: 240822115|240867796 and consequently impact on the balance between osteogenic differentiation and adipogenic differentiation. In their experiment, circRNA 2: 27713879|27755789 and circRNA 2: 240822115|240867796 were identified to target miR-328 [78], while miR-328 can upregulate the expression of C/EBP $\alpha$  to inhibit cell proliferation and is involved in the dynamic balance between osteogenesis and adipogenesis [78]. circRNA 2: 27713879|27755789 and circRNA 2: 240822115|240867796 can also target miR-23a-5p and miR-326 as miRNA sponge by regulating the TGF- $\beta$  signaling pathway and serve as an inhibitor of adipogenic differentiation [78, 99, 100]. The above study shows that circRNAs can work together and affect several kinds of miRNA to achieve its regulating potential. This discovery is very helpful for contributing the circRNA regulating network in MSC differentiation.

**5.5. *circRNA-11897-miR-27a/miR-27b-PPAR $\gamma$ .*** miR-27 is an antiadipogenic microRNA partly by targeting prohibitin (PHB) and impairing mitochondrial function. Ectopic expression of miR-27a or miR-27b impaired mitochondrial biogenesis, structural integrity, and complex I activity accompanied by excessive reactive oxygen species production [101]. miR-27a can accelerate the hydrolysis of triglyceride and suppress adipocyte differentiation by repressing the expression of PPAR $\gamma$  [102]. Via identification and character-

ization of circRNAs, researchers find that circRNA-11897 can bind miR-27a and miR-27b [79]. By sponging miR-27a and miR-27b, circRNA-11897 regulates adipogenic differentiation and lipid metabolism of adipocyte in the subcutaneous adipose tissue [79]. Besides, the target genes of circRNA-11897 are also enriched in biological processes, which are related to lipid metabolisms such as fatty acid biosynthetic process, MAPK cascade reaction, extracellular-regulated protein kinase (ERK)1 and ERK2 cascade reaction, and cell proliferation [79]. In the early stage of adipogenic differentiation, the activated ERK signaling pathway can induce the expression of C/EBP and PPAR $\gamma$  and induce adipogenic differentiation of 3T3-L1 preadipocytes [103]. In a later stage, ERK1/2 is phosphorylated, and PPAR $\gamma$  is inactivated. Thus, preadipocyte differentiation is inhibited [104].

**5.6. *circRNA-26852-miR874-PPAR $\alpha$  and circRNA-26852-miR486-FOXO1.*** miR-874 and miR-486 are the target genes of circRNA-26852, which are enriched in biological processes of adipocyte in the subcutaneous adipose tissue. These miRNAs are related to fat deposition and lipid metabolism, such as regulation of triglyceride catabolic process, negative regulation of lipid storage, and phosphatidic acid biosynthetic process [79]. miR-874 can regulate lipid metabolism, glycerophospholipid metabolism, adipocyte differentiation, and glucose metabolism by inhibiting the expression of PPAR pathway-related genes, PPAR $\alpha$  [105, 106]. miR-486 can inhibit the transcription factor FOXO1 and plays a role in insulin functioning and triglyceride metabolism. Therefore, circRNA-26852 working as competing for endogenous RNAs of miR-874 and miR-486 may participate in adipogenic differentiation and lipid metabolism. The pathway enrichment analysis shows that the target genes of circRNA-26852 are enriched in the PPAR signaling pathway and transforming growth factor- $\beta$  (TGF $\beta$ ) signaling pathway. Through these two signaling pathways, circRNA-26852 regulates the transformation of mesenchymal stem cells into adipocytes [79]. In this research, it shows us a possibility of circRNA working in two directions simultaneously. It is going to be a new perspective in our future research.

**5.7. *CiRS-133-miR-133-RDM16.*** Exosomes play a key role in mediating signaling transduction between neighboring or distant cells by delivering microRNAs, proteins, lncRNAs, circRNAs, and DNAs [107]. A recent study has indicated that circRNA is enriched and stable in exosomes [108]. One exosome delivered circRNA, hsa\_circ\_0010522 (also named ciRS-133), can suppress specific adipose miR-133 levels in preadipocytes by adsorptive action [80]. PR domain containing 16 (PRDM16), a zinc finger transcription factor controlling a brown fat/skeletal muscle switch, has been proposed to be a bidirectional cell fate switch. It promotes brown adipose tissue (BAT) differentiation while inhibits myogenesis in myoblasts [109, 110]. Loss of PRDM16 function results in myogenic differentiation of preadipocytes isolated from BAT, while the gain of PRDM16 function leads to the genesis of BAT in myoblasts [111]. PRDM16 has also been found to be a determining factor of beige adipocytes in subcutaneous white adipose tissue (WAT) and promote browning of



WAT in gastric tumors [111, 112]. Previous studies have confirmed that miR-133 is the upstream regulator of PRDM16, and the miR-133/PRDM16 axis controls the formation of BAT and is linked to energy balance [7, 113]. By activating PRDM16 and suppressing miR-133, ciRS-133 activates uncoupling protein 1 (UCP1) and promotes the differentiation of preadipocytes into brown-like cells. Therefore, by targeting the miR-133/PRDM16 pathway, circulating exosomal ciRS-133 may be a common regulator that promotes white adipose browning of preadipocyte in WAT [80].

**5.8. *circRNA-0046366-miR-34a-PDGFR $\alpha$* .** Studies reveal that circRNA-0046366 inhibits hepatocellular steatosis by normalizing PPAR signaling. Besides, circRNA-0046366 can antagonize the activity of miR-34a via meiotic recombination- (MRE-) based complementation [81]. miR-34a will inhibit adipogenesis by targeting PDGFR $\alpha$  [82]. By sponging miR-34a, circRNA-0046366 is associated with triglyceride metabolism at both transcriptional and translational levels. Consequently, circRNA-0046366 promotes the adipogenic differentiation through activating the ERK signaling pathway [81, 82].

**5.9. *CircSAMD4A-miR-138-5p-EZH2*.** Experiments indicate that circSAMD4A also named hsa\_circ\_0004846 regulate preadipocyte differentiation by sponging miR-138-5p. Previously, miR-138-5p has been reported targeting various proteins associated with adipogenesis in MSCs [114]. Binding to miR-138-5p, CircSAMD4A can increase the expression of EZH2 which has two downstream targets Wnt10b and Wnt1. Thus, circSAMD4A can induce adipocyte differentiation via the canonical Wnt signaling pathway [83]. It suggests that circSAMD4A can serve as a potential prognostic marker or treatment target for the therapy of tumors or metabolic diseases.

## 6. Potential circRNA Regulatory Path

As described above, circRNAs can sponge miRNA or protein to play the regulation role in adipogenesis. In general, circRNAs participate in adipogenic differentiation by modulating PPAR or Wnt pathway. Besides those targeted factors as mentioned above, there are still potential targets that may be regulated by circRNAs.

**6.1. *CircPVT1-miR-125-PPAR $\alpha$  and PPAR $\gamma$* .** CircPVT1, also known as circ6, is generated from exon 2 of the PVT1 gene. It is located on chromosome 8q2. As a homologous gene of the long noncoding RNA PVT1 (human genome GRCh38/hg38), this circRNA plays a critical role in regulating human physiological and pathological functions. CircPVT1 is a senescence-associated circRNA showing markedly reduced levels in senescent fibroblasts [115]. By sponging the miR-125 family, CircPVT1 exhibits elevated levels in dividing cells and promotes cell proliferation [116]. The physiological functions of circPVT1 in gastric cancer cells include cell proliferation, cell apoptosis, and stem cell self-renewal [117]. On the launch signal of adipogenesis, c-Fos can bind to circPVT1 at its promoter region and promote the direct interaction between circPVT1 and miR-125 [116]. Studies have suggested that

miR-125 can enhance the proliferation and differentiation of ADSCs [99]. The expression of miR-125 is significantly changed at day 8 after adipogenic induction. It can dramatically reduce the mRNA expression of adipogenic markers C/EBP $\alpha$ , PPAR $\gamma$ , FABP4, fatty acid synthase (FASN), lipoprotein lipase (LPL), aP2, and estrogen-related receptor  $\alpha$  (ERR $\alpha$ ) [118]. Furthermore, miR-125 can inhibit the differentiation of preadipocytes by directly targeting KLF13 and affect the fatty acid composition in adipocytes by regulating elongase of very-long-chain fatty acids 6 (ELOVL6) [119]. In summary, circPVT1 may be a potential regulatory factor of adipogenesis, which simultaneously upregulates PPAR $\alpha$  and PPAR $\gamma$  by affecting miR-125.

**6.2. *Circ-0004194*.** Circ-0004194 expressed in a variety of human tissues is also called Circ $\beta$ -catenin. It can be translated into a novel 370-amino acid  $\beta$ -catenin isoform that was termed " $\beta$ -catenin-370aa." As the linear  $\beta$ -catenin mRNA transcript, circ $\beta$ -catenin uses the same start codon but its translation is terminated at a new stop codon created by circularization. A recent study demonstrates that this novel isoform can stabilize full-length  $\beta$ -catenin by antagonizing GSK3 $\beta$ -induced  $\beta$ -catenin phosphorylation and degradation. Thus circ $\beta$ -catenin potentiates the activation of the Wnt/ $\beta$ -catenin pathway in liver cancer [49]. Perhaps, circ $\beta$ -catenin can play the same role in adipogenesis, even in cell differentiation of MSCs. Protein coding by circRNA plays a significant role in adipogenesis but rare of them has been discovered. There is still a blank area waiting for exploration, especially in the regulation of MSC differentiation.

**6.3. *CircCDK13-miR-135b-5p-PI3K/AKT and JAK/STAT*.** CircCDK13 (hsa\_circ\_0001699), a novel circRNA transcribed from the human CDK13 gene, is closely related to cell senescence and regulation of cell cycle [120]. CircCDK13 may upregulate the relevant gene expression of the signaling pathway through sponge miR-135b-5p. Therefore, circCDK13 can inhibit the PI3K/AKT pathway and JAK/STAT signaling pathway which is a very critical regulatory machinery for cellular development and proliferation in liver cancer [121].

Beyond that, by repressing miR-9, circSMAD2 impedes the activation of STAT3 and MEK/ERK pathways in migration and epithelial-mesenchymal transition [122]. CircRNA-0044073 promotes the proliferation of cells by sponging miR-107 and activating the JAK/STAT signaling pathway [123]. There are still many factors that regulate adipogenesis which may be the targets of circRNAs, such as miR-143 [124], miR-130 [125], miR-145 [126], miR-181a [127], and let-7 [128].

## 7. Conclusion

Recent studies demonstrate that a large number of endogenous circRNAs have a major functional role in stem cell fate decision-making processes such as adipogenic differentiation. Therefore, we concluded the previous work into a primary molecular network on the regulation role of the circRNAs in adipogenesis of MSCs (Figure 1). The findings from circRNA investigations during adipogenesis suggest

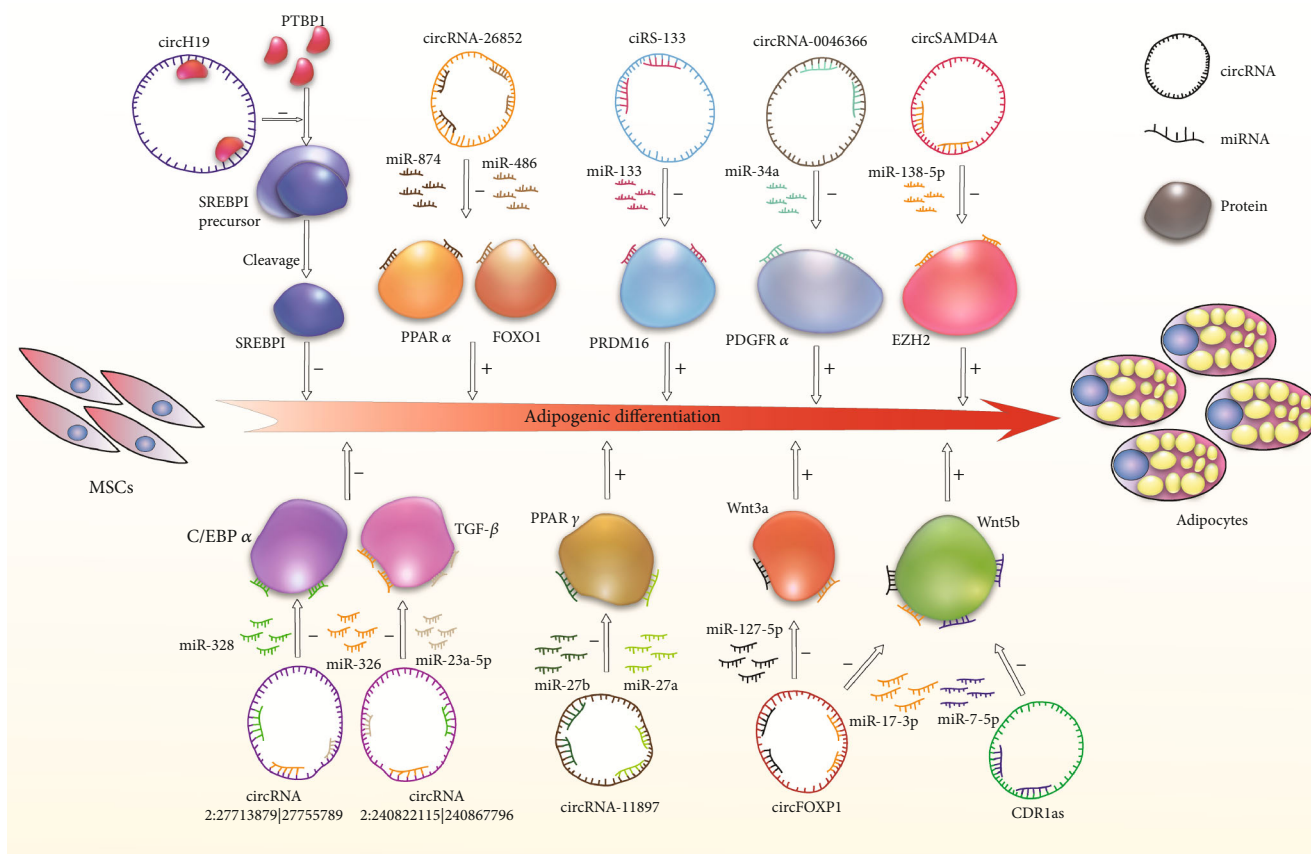


FIGURE 1: Circular RNAs regulate adipogenic differentiation.

the potential application of circRNAs or target miRNAs to treat lipid metabolism, bone diseases, and metabolic disorders. The molecular mechanism of circFOXPI in MSCs has been deeply discussed. It should be regarded as an essential gatekeeper of pivotal stem cell molecular networks and controlled MSC identification. With this being fundamental, circRNAs regulating cell differentiation can sum into a network which is helpful for clinical transformation. Exosomes are secreted by many different types of cells, which regulate cellular function by enabling cell-to-cell transfer of biologically active molecule, such as miRNA and circRNA. CiRS-133 in exosomes is closely linked with the browning of white adipose tissue by activating PRDM16 and suppressing miR-133. It not only provides a potential target for therapy but also lightens us with a possibility that exosomes serve as a messenger to deliver circRNAs into cells for clinical treatment.

While circRNAs are an epigenetic regulator, their potential role in modulating differentiation of MSCs is infinite. Current studies on circRNAs in MSCs' adipogenesis concentrate on the regulation of triglyceride accumulation. However, the study on circRNA regulating the commitment step of adipogenesis is still a blank field. The modes of circRNA regulating adipogenesis in existing reports are also unitary. Previous experiments mainly focused on circRNAs' function as sponge; the other functions should be explored in future study. To further elucidate the mechanisms of circRNAs on

adipogenesis in stem cells, future work should be conducted to expose their binding sites to the corresponding miRNAs.

The functions of circRNAs in regulating adipogenesis have a considerable reference value in the epigenetic regulation of cell differentiation. Future investigation on circRNAs has great potential usefulness and clinical transformation.

**Conflicts of Interest**

The authors declare that there is no conflict of interest regarding the publication of this paper.

**Authors' Contributions**

Fanglin Wang and Xiang Li contributed equally to this work, and should be considered co-first author.

**Acknowledgments**

This work was supported by Liaoning Revitalization Talents Program (no. XLYC1907124) and the National Natural Science Foundation of China (no. 81571919).

**References**

[1] M. T. Hsu and M. Coca-Prados, "Electron microscopic evidence for the circular form of RNA in the cytoplasm of

- eukaryotic cells,” *Nature*, vol. 280, no. 5720, pp. 339–340, 1979.
- [2] C. Cocquerelle, B. Mascrez, D. Héтуin, and B. Bailleul, “Mis-splicing yields circular RNA molecules,” *The FASEB Journal*, vol. 7, no. 1, pp. 155–160, 1993.
  - [3] Z. Pasman, M. D. Been, and M. A. Garcia-Blanco, “Exon circularization in mammalian nuclear extracts,” *RNA*, vol. 2, no. 6, pp. 603–610, 1996.
  - [4] S. Braun, H. Domdey, and K. Wiebauer, “Inverse splicing of a discontinuous pre-mRNA intron generates a circular exon in a HeLa cell nuclear extract,” *Nucleic Acids Research*, vol. 24, no. 21, pp. 4152–4157, 1996.
  - [5] J. Salzman, R. E. Chen, M. N. Olsen, P. L. Wang, and P. O. Brown, “Correction: Cell-type specific features of circular RNA expression,” *PLoS Genetics*, vol. 9, no. 12, 2013.
  - [6] W. R. Jeck and N. E. Sharpless, “Detecting and characterizing circular RNAs,” *Nature Biotechnology*, vol. 32, no. 5, pp. 453–461, 2014.
  - [7] W. R. Jeck, J. A. Sorrentino, K. Wang et al., “Circular RNAs are abundant, conserved, and associated with ALU repeats,” *RNA*, vol. 19, no. 2, pp. 141–157, 2013.
  - [8] A. Rybak-Wolf, C. Stottmeister, P. Glažar et al., “Circular RNAs in the mammalian brain are highly abundant, conserved, and dynamically expressed,” *Molecular Cell*, vol. 58, no. 5, pp. 870–885, 2015.
  - [9] I. F. Hall, M. Climent, M. Quintavalle et al., “Circ\_Lrp6, a circular RNA enriched in vascular smooth muscle cells, acts as a sponge regulating miRNA-145 function,” *Circulation Research*, vol. 124, no. 4, pp. 498–510, 2019.
  - [10] I. Legnini, G. di Timoteo, F. Rossi et al., “Circ-ZNF609 is a circular RNA that can be translated and functions in myogenesis,” *Molecular Cell*, vol. 66, no. 1, pp. 22–37.e9, 2017, e9.
  - [11] L. da Silva Meirelles, “Mesenchymal stem cells reside in virtually all post-natal organs and tissues,” *Journal of Cell Science*, vol. 119, no. 11, pp. 2204–2213, 2006.
  - [12] M. Packer, “The alchemist’s nightmare: might mesenchymal stem cells that are recruited to repair the injured heart be transformed into fibroblasts rather than cardiomyocytes?,” *Circulation*, vol. 137, no. 19, pp. 2068–2073, 2018.
  - [13] J. Bartolucci, F. J. Verdugo, P. L. González et al., “Safety and efficacy of the intravenous infusion of umbilical cord mesenchymal stem cells in patients with heart failure: a phase 1/2 randomized controlled trial (RIMECARD trial [Randomized Clinical Trial of Intravenous Infusion Umbilical Cord Mesenchymal Stem Cells on Cardiopathy]),” *Circulation Research*, vol. 121, no. 10, pp. 1192–1204, 2017.
  - [14] T. T. Tran and C. R. Kahn, “Transplantation of adipose tissue and stem cells: role in metabolism and disease,” *Nature Reviews Endocrinology*, vol. 6, no. 4, pp. 195–213, 2010.
  - [15] I. R. Suhito, Y. Han, J. Min, H. Son, and T. H. Kim, “In situ label-free monitoring of human adipose-derived mesenchymal stem cell differentiation into multiple lineages,” *Biomaterials*, vol. 154, pp. 223–233, 2018.
  - [16] P. Bianco, M. Riminucci, S. Gronthos, and P. G. Robey, “Bone marrow stromal stem cells: nature, biology, and potential applications,” *Stem Cells*, vol. 19, no. 3, pp. 180–192, 2001.
  - [17] P. M. de Sá, A. J. Richard, H. Hang, and J. M. Stephens, “Transcriptional regulation of adipogenesis,” *Comprehensive Physiology*, vol. 7, no. 2, pp. 635–674, 2017.
  - [18] A. L. Ghaben and P. E. Scherer, “Adipogenesis and metabolic health,” *Nature Reviews. Molecular Cell Biology*, vol. 20, no. 4, pp. 242–258, 2019.
  - [19] J. M. Stephens, M. Butts, R. Stone, P. H. Pekala, and D. A. Bernlohr, “Regulation of transcription factor mRNA accumulation during 3T3-L1 preadipocyte differentiation by antagonists of adipogenesis,” *Molecular and Cellular Biochemistry*, vol. 123, no. 1–2, pp. 63–71, 1993.
  - [20] R. J. Distel, H. S. Ro, B. S. Rosen, D. L. Groves, and B. M. Spiegelman, “Nucleoprotein complexes that regulate gene expression in adipocyte differentiation: direct participation of c-*\_fos\_*,” *Cell*, vol. 49, no. 6, pp. 835–844, 1987.
  - [21] J. B. Harp, D. Franklin, A. A. Vanderpuije, and J. M. Gimble, “Differential expression of signal transducers and activators of transcription during human adipogenesis,” *Biochemical and Biophysical Research Communications*, vol. 281, no. 4, pp. 907–912, 2001.
  - [22] M. Kawai, N. Namba, S. Mushiaki et al., “Growth hormone stimulates adipogenesis of 3T3-L1 cells through activation of the Stat5A/5B-PPAR $\gamma$  pathway,” *Journal of Molecular Endocrinology*, vol. 38, no. 1, pp. 19–34, 2007.
  - [23] G. Donati, V. Proserpio, B. M. Lichtenberger et al., “Epidermal Wnt/beta-catenin signaling regulates adipocyte differentiation via secretion of adipogenic factors,” *Proceedings of the National Academy of Sciences of the United States of America*, vol. 111, no. 15, pp. E1501–E1509, 2014.
  - [24] M. Chen, P. Lu, Q. Ma et al., “CTNBN1/ $\beta$ -catenin dysfunction contributes to adiposity by regulating the cross-talk of mature adipocytes and preadipocytes,” *Science Advances*, vol. 6, no. 2, p. eaax9605, 2020.
  - [25] M. Laudes, “Role of WNT signalling in the determination of human mesenchymal stem cells into preadipocytes,” *Journal of Molecular Endocrinology*, vol. 46, no. 2, pp. R65–R72, 2011.
  - [26] R. R. Bowers and M. D. Lane, “Wnt signaling and adipocyte lineage commitment,” *Cell Cycle*, vol. 7, no. 9, pp. 1191–1196, 2014.
  - [27] L. A. Davis and N. I. Zur Nieden, “Mesodermal fate decisions of a stem cell: the Wnt switch,” *Cellular and Molecular Life Sciences*, vol. 65, no. 17, pp. 2658–2674, 2008.
  - [28] Q. Q. Tang, M. Gronborg, H. Huang et al., “Sequential phosphorylation of CCAAT enhancer-binding protein  $\beta$  by MAPK and glycogen synthase kinase 3 $\beta$  is required for adipogenesis,” *Proceedings of the National Academy of Sciences of the United States of America*, vol. 102, no. 28, pp. 9766–9771, 2005.
  - [29] S. L. Clarke, C. E. Robinson, and J. M. Gimble, “CAAT/Enhancer Binding Proteins Directly Modulate Transcription from the Peroxisome Proliferator- Activated Receptor  $\gamma$ 2 Promoter,” *Biochemical and Biophysical Research Communications*, vol. 240, no. 1, pp. 99–103, 1997.
  - [30] U. A. White and J. M. Stephens, “Transcriptional factors that promote formation of white adipose tissue,” *Molecular and Cellular Endocrinology*, vol. 318, no. 1–2, pp. 10–14, 2010.
  - [31] Y. Liu, Y. D. Zhang, L. Guo et al., “Protein inhibitor of activated STAT 1 (PIAS1) is identified as the SUMO E3 ligase of CCAAT/enhancer-binding protein  $\beta$  (C/EBP $\beta$ ) during adipogenesis,” *Molecular and Cellular Biology*, vol. 33, no. 22, pp. 4606–4617, 2013.
  - [32] Q. Q. Tang and M. D. Lane, “Adipogenesis: from stem cell to adipocyte,” *Annual Review of Biochemistry*, vol. 81, no. 1, pp. 715–736, 2012.



- [33] C. Christodoulides, C. Lagathu, J. K. Sethi, and A. Vidal-Puig, "Adipogenesis and WNT signalling," *Trends in Endocrinology and Metabolism*, vol. 20, no. 1, pp. 16–24, 2009.
- [34] L. Michalik, B. Desvergne, and W. Wahli, "Peroxisome-proliferator-activated receptors and cancers: complex stories," *Nature Reviews. Cancer*, vol. 4, no. 1, pp. 61–70, 2004.
- [35] C. Song, Y. Huang, Z. Yang et al., "RNA-Seq analysis identifies differentially expressed genes in subcutaneous adipose tissue in Qaidamford cattle, cattle-yak, and Angus cattle," *Animals*, vol. 9, no. 12, p. 1077, 2019.
- [36] S. Starke, I. Jost, O. Rossbach et al., "Exon circularization requires canonical splice signals," *Cell Reports*, vol. 10, no. 1, pp. 103–111, 2015.
- [37] X. O. Zhang, H. B. Wang, Y. Zhang, X. Lu, L. L. Chen, and L. Yang, "Complementary sequence-mediated exon circularization," *Cell*, vol. 159, no. 1, pp. 134–147, 2014.
- [38] Y. Zhang, X. O. Zhang, T. Chen et al., "Circular intronic long noncoding RNAs," *Molecular Cell*, vol. 51, no. 6, pp. 792–806, 2013.
- [39] A. Ivanov, S. Memczak, E. Wyler et al., "Analysis of intron sequences reveals hallmarks of circular RNA biogenesis in animals," *Cell Reports*, vol. 10, no. 2, pp. 170–177, 2015.
- [40] M. C. Kramer, D. Liang, D. C. Tatomer et al., "Combinatorial control of Drosophila circular RNA expression by intronic repeats, hnRNPs, and SR proteins," *Genes & Development*, vol. 29, no. 20, pp. 2168–2182, 2015.
- [41] X. O. Zhang, R. Dong, Y. Zhang et al., "Diverse alternative back-splicing and alternative splicing landscape of circular RNAs," *Genome Research*, vol. 26, no. 9, pp. 1277–1287, 2016.
- [42] S. J. Conn, K. A. Pillman, J. Toubia et al., "The RNA binding protein quaking regulates formation of circRNAs," *Cell*, vol. 160, no. 6, pp. 1125–1134, 2015.
- [43] D. Han, J. Li, H. Wang et al., "Circular RNA circMTO1 acts as the sponge of microRNA-9 to suppress hepatocellular carcinoma progression," *Hepatology*, vol. 66, no. 4, pp. 1151–1164, 2017.
- [44] Y. Zhang, L. Du, Y. Bai et al., "CircDYM ameliorates depressive-like behavior by targeting miR-9 to regulate microglial activation via HSP90 ubiquitination," *Molecular Psychiatry*, vol. 25, no. 6, pp. 1175–1190, 2020.
- [45] S. Shen, Y. Wu, J. Chen et al., "CircSERPINE2 protects against osteoarthritis by targeting miR-1271 and ETS-related gene," *Annals of the Rheumatic Diseases*, vol. 78, no. 6, pp. 826–836, 2019.
- [46] Q. Li, X. Pan, D. Zhu, Z. Deng, R. Jiang, and X. Wang, "Circular RNA MAT2B promotes glycolysis and malignancy of hepatocellular carcinoma through the miR-338-3p/PKM2 Axis under hypoxic stress," *Hepatology*, vol. 70, no. 4, pp. 1298–1316, 2019.
- [47] L. Salmena, L. Poliseno, Y. Tay, L. Kats, and P. P. Pandolfi, "A ceRNA Hypothesis: The Rosetta Stone of a Hidden RNA Language?," *Cell*, vol. 146, no. 3, pp. 353–358, 2011.
- [48] Z. Cheng, C. Yu, S. Cui et al., "c\_ircTP63\_ functions as a ceRNA to promote lung squamous cell carcinoma progression by upregulating FOXM1," *Nature Communications*, vol. 10, no. 1, p. 3200, 2019.
- [49] W. C. Liang, C. W. Wong, P. P. Liang et al., "Translation of the circular RNA circ $\beta$ -catenin promotes liver cancer cell growth through activation of the Wnt pathway," *Genome Biology*, vol. 20, no. 1, p. 84, 2019.
- [50] A. Guria, K. Velayudha Vimala Kumar, N. Srikakulam et al., "Circular RNA profiling by Illumina sequencing via template-dependent multiple displacement amplification," *BioMed Research International*, vol. 2019, Article ID 2756516, 12 pages, 2019.
- [51] R. Ashwal-Fluss, M. Meyer, N. R. Pamudurti et al., "circRNA biogenesis competes with pre-mRNA splicing," *Molecular Cell*, vol. 56, no. 1, pp. 55–66, 2014.
- [52] W. W. Du, W. Yang, Y. Chen et al., "Foxo3 circular RNA promotes cardiac senescence by modulating multiple factors associated with stress and senescence responses," *European Heart Journal*, vol. 38, no. 18, pp. ehw001–eh1412, 2016.
- [53] Y. Zhu, W. Gui, X. Lin, and H. Li, "Knock-down of circular RNA H19 induces human adipose-derived stem cells adipogenic differentiation via a mechanism involving the polypyrimidine tract-binding protein 1," *Experimental Cell Research*, vol. 387, no. 2, p. 111753, 2020.
- [54] N. R. Pamudurti, O. Bartok, M. Jens et al., "Translation of CircRNAs," *Molecular Cell*, vol. 66, no. 1, pp. 9–21.e7, 2017, e7.
- [55] S. Kelly, C. Greenman, P. R. Cook, and A. Papantonis, "Exon skipping is correlated with exon circularization," *Journal of Molecular Biology*, vol. 427, no. 15, pp. 2414–2417, 2015.
- [56] Z. Li, C. Huang, C. Bao et al., "Exon-intron circular RNAs regulate transcription in the nucleus," *Nature Structural & Molecular Biology*, vol. 22, no. 3, pp. 256–264, 2015.
- [57] R. Dong, X. O. Zhang, Y. Zhang, X. K. Ma, L. L. Chen, and L. Yang, "CircRNA-derived pseudogenes," *Cell Research*, vol. 26, no. 6, pp. 747–750, 2016.
- [58] Q. Li, Y. Wang, S. Wu et al., "CircACCC1 regulates assembly and activation of AMPK complex under metabolic stress," *Cell Metabolism*, vol. 30, no. 1, pp. 157–173.e7, 2019.
- [59] S. Meng, H. Zhou, Z. Feng, Z. Xu, Y. Tang, and M. Wu, "Epigenetics in neurodevelopment: emerging role of circular RNA," *Frontiers in Cellular Neuroscience*, vol. 13, p. 327, 2019.
- [60] X. Wang, R. Wu, Y. Liu et al., "m6A mRNA methylation controls autophagy and adipogenesis by targeting Atg5 and Atg7," *Autophagy*, vol. 16, no. 7, pp. 1221–1235, 2020.
- [61] G. Chen, Q. Wang, Z. Li et al., "Circular RNA CDR1as promotes adipogenic and suppresses osteogenic differentiation of BMSCs in steroid-induced osteonecrosis of the femoral head," *Bone*, vol. 133, p. 115258, 2020.
- [62] Y. Wang, M. L. Li, Y. H. Wang et al., "A Zfp609 circular RNA regulates myoblast differentiation by sponging miR-194-5p," *International Journal of Biological Macromolecules*, vol. 121, pp. 1308–1313, 2019.
- [63] Z. Yuan, Q. Li, S. Luo et al., "PPAR $\gamma$  and Wnt signaling in adipogenic and osteogenic differentiation of mesenchymal stem cells," *Current Stem Cell Research & Therapy*, vol. 11, no. 3, pp. 216–225, 2016.
- [64] I. Takada, A. P. Kouzmenko, and S. Kato, "Wnt and PPAR $\gamma$  signaling in osteoblastogenesis and adipogenesis," *Nature Reviews Rheumatology*, vol. 5, no. 8, pp. 442–447, 2009.
- [65] Y. Zheng, X. Li, Y. Huang, L. Jia, and W. Li, "The circular RNA landscape of periodontal ligament stem cells during osteogenesis," *Journal of Periodontology*, vol. 88, no. 9, pp. 906–914, 2017.
- [66] N. Chen, G. Zhao, X. Yan et al., "A novel FLI1 exonic circular RNA promotes metastasis in breast cancer by coordinately



- regulating TET1 and DNMT1,” *Genome Biology*, vol. 19, no. 1, p. 218, 2018.
- [67] M. Zhang, L. Jia, and Y. Zheng, “circRNA expression profiles in human bone marrow stem cells undergoing osteoblast differentiation,” *Stem Cell Reviews and Reports*, vol. 15, no. 1, pp. 126–138, 2019.
- [68] S. Xiang, Z. Li, and X. Weng, “Changed cellular functions and aberrantly expressed miRNAs and circRNAs in bone marrow stem cells in osteonecrosis of the femoral head,” *International Journal of Molecular Medicine*, vol. 45, no. 3, pp. 805–815, 2020.
- [69] Z. Ouyang, T. Tan, X. Zhang et al., “CircRNA hsa\_circ\_0074834 promotes the osteogenesis-angiogenesis coupling process in bone mesenchymal stem cells (BMSCs) by acting as a ceRNA for miR-942-5p,” *Cell Death & Disease*, vol. 10, no. 12, p. 932, 2019.
- [70] L. Li, Y. Chen, L. Nie et al., “MyoD-induced circular RNA CDR1as promotes myogenic differentiation of skeletal muscle satellite cells,” *Biochim Biophys Acta Gene Regul Mech*, vol. 1862, no. 8, pp. 807–821, 2019.
- [71] B. Kyei, L. Li, L. Yang, S. Zhan, and H. Zhang, “CDR1as/miRNAs-related regulatory mechanisms in muscle development and diseases,” *Gene*, vol. 730, p. 144315, 2020.
- [72] B. Chen, J. Yu, L. Guo et al., “Circular RNA circHIPK3 promotes the proliferation and differentiation of chicken myoblast cells by sponging miR-30a-3p,” *Cells*, vol. 8, no. 2, p. 177, 2019.
- [73] X. Li, C. Li, Z. Liu et al., “Circular RNA circ-FoxO3 inhibits myoblast cells differentiation,” *Cell*, vol. 8, no. 6, p. 616, 2019.
- [74] R. Chen, T. Jiang, S. Lei et al., “Expression of circular RNAs during C2C12 myoblast differentiation and prediction of coding potential based on the number of open reading frames and N6-methyladenosine motifs,” *Cell Cycle*, vol. 17, no. 14, pp. 1832–1845, 2018.
- [75] Q. Yang, J. Wu, J. Zhao et al., “Circular RNA expression profiles during the differentiation of mouse neural stem cells,” *BMC Systems Biology*, vol. 12, Suppl 8, p. 128, 2018.
- [76] A. Cherubini, M. Barilani, R. L. Rossi et al., “FOXP1 circular RNA sustains mesenchymal stem cell identity via microRNA inhibition,” *Nucleic Acids Research*, vol. 47, no. 10, pp. 5325–5340, 2019.
- [77] X. Yin, X. Wang, X. Hu, Y. Chen, K. Zeng, and H. Zhang, “ER $\beta$  induces the differentiation of cultured osteoblasts by both Wnt/ $\beta$ -catenin signaling pathway and estrogen signaling pathways,” *Experimental Cell Research*, vol. 335, no. 1, pp. 107–114, 2015.
- [78] X. Li, B. Peng, X. Zhu et al., “Changes in related circular RNAs following ER $\beta$  knockdown and the relationship to rBMSC osteogenesis,” *Biochemical and Biophysical Research Communications*, vol. 493, no. 1, pp. 100–107, 2017.
- [79] A. Li, W. Huang, X. Zhang, L. Xie, and X. Miao, “Identification and characterization of CircRNAs of two pig breeds as a new biomarker in metabolism-related diseases,” *Cellular Physiology and Biochemistry*, vol. 47, no. 6, pp. 2458–2470, 2018.
- [80] H. Zhang, L. Zhu, M. Bai et al., “Exosomal circRNA derived from gastric tumor promotes white adipose browning by targeting the miR-133/PRDM16 pathway,” *International Journal of Cancer*, vol. 144, no. 10, pp. 2501–2515, 2019.
- [81] X. Y. Guo, F. Sun, J. N. Chen, Y. Q. Wang, Q. Pan, and J. G. Fan, “circRNA\_0046366 inhibits hepatocellular steatosis by normalization of PPAR signaling,” *World Journal of Gastroenterology*, vol. 24, no. 3, pp. 323–337, 2018.
- [82] Y. M. Sun, J. Qin, S. G. Liu et al., “PDGFR $\alpha$  regulated by miR-34a and FoxO1 promotes adipogenesis in porcine intramuscular preadipocytes through Erk signaling pathway,” *International Journal of Molecular Sciences*, vol. 18, no. 11, p. 2424, 2017.
- [83] Y. Liu, H. Liu, Y. Li et al., “Circular RNA SAMD4A controls adipogenesis in obesity through the miR-138-5p/EZH2 axis,” *Theranostics*, vol. 10, no. 10, pp. 4705–4719, 2020.
- [84] B. Kleaveland, C. Y. Shi, J. Stefano, and D. P. Bartel, “A network of noncoding regulatory RNAs acts in the mammalian brain,” *Cell*, vol. 174, no. 2, pp. 350–362.e17, 2018, e17.
- [85] R. C. Li, S. Ke, F. K. Meng et al., “CiRS-7 promotes growth and metastasis of esophageal squamous cell carcinoma via regulation of miR-7/HOXB13,” *Cell Death & Disease*, vol. 9, no. 8, p. 838, 2018.
- [86] Z. Liu, Y. Ran, C. Tao, S. Li, J. Chen, and E. Yang, “Detection of circular RNA expression and related quantitative trait loci in the human dorsolateral prefrontal cortex,” *Genome Biology*, vol. 20, no. 1, p. 99, 2019.
- [87] H. K. Choi, H. Yuan, F. Fang et al., “Tsc1 regulates the balance between osteoblast and adipocyte differentiation through autophagy/Notch1/ $\beta$ -catenin cascade,” *Journal of Bone and Mineral Research*, vol. 33, no. 11, pp. 2021–2034, 2018.
- [88] M. M. Weivoda, M. Ruan, C. M. Hachfeld et al., “Wnt signaling inhibits osteoclast differentiation by activating canonical and noncanonical cAMP/PKA pathways,” *Journal of Bone and Mineral Research*, vol. 34, no. 8, pp. 1546–1548, 2019.
- [89] A. Kanazawa, S. Tsukada, M. Kamiyama, T. Yanagimoto, M. Nakajima, and S. Maeda, “\_Wnt5b\_ partially inhibits canonical Wnt/ $\beta$ -catenin signaling pathway and promotes adipogenesis in 3T3-L1 preadipocytes,” *Biochemical and Biophysical Research Communications*, vol. 330, no. 2, pp. 505–510, 2005.
- [90] F. H. J. van Tienen, H. Laeremans, C. J. H. van der Kallen, and H. J. M. Smeets, “\_Wnt5b\_ stimulates adipogenesis by activating \_PPAR  $\gamma$ \_ and inhibiting the  $\beta$ -catenin dependent Wnt signaling pathway together with \_Wnt5a\_,” *Biochemical and Biophysical Research Communications*, vol. 387, no. 1, pp. 207–211, 2009.
- [91] E. Monzón-Casanova, M. Screen, M. D. Díaz-Muñoz et al., “The RNA-binding protein PTBP1 is necessary for B cell selection in germinal centers,” *Nature Immunology*, vol. 19, no. 3, pp. 267–278, 2018.
- [92] D. Eberlé, B. Hegarty, P. Bossard, P. Ferré, and F. Foufelle, “SREBP transcription factors: master regulators of lipid homeostasis,” *Biochimie*, vol. 86, no. 11, pp. 839–848, 2004.
- [93] M. M. Aagaard, R. Siersbaek, and S. Mandrup, “Molecular basis for gene-specific transactivation by nuclear receptors,” *Biochimica et Biophysica Acta*, vol. 1812, no. 8, pp. 824–835, 2011.
- [94] C. Liu, Z. Yang, J. Wu et al., “Long noncoding RNA H19 interacts with polypyrimidine tract-binding protein 1 to reprogram hepatic lipid homeostasis,” *Hepatology*, vol. 67, no. 5, pp. 1768–1783, 2018.
- [95] S. Yu, Q. Geng, J. Ma et al., “Heparin-binding EGF-like growth factor and miR-1192 exert opposite effect on

- Runx2-induced osteogenic differentiation," *Cell Death & Disease*, vol. 4, no. 10, p. e868, 2013.
- [96] S. C. Dickinson, C. A. Sutton, K. Brady et al., "The Wnt5a receptor, receptor tyrosine kinase-like orphan receptor 2, is a predictive cell surface marker of human mesenchymal stem cells with an enhanced capacity for chondrogenic differentiation," *Stem Cells*, vol. 35, no. 11, pp. 2280–2291, 2017.
- [97] R. Bilkovski, D. M. Schulte, F. Oberhauser et al., "Role of WNT-5a in the determination of human mesenchymal stem cells into preadipocytes," *The Journal of Biological Chemistry*, vol. 285, no. 9, pp. 6170–6178, 2010.
- [98] A. B. Khalid and S. A. Krum, "Estrogen receptors alpha and beta in bone," *Bone*, vol. 87, pp. 130–135, 2016.
- [99] Y. F. Tang, Y. Zhang, X. Y. Li, C. Li, W. Tian, and L. Liu, "Expression of miR-31, miR-125b-5p, and miR-326 in the adipogenic differentiation process of adipose-derived stem cells," *OMICS*, vol. 13, no. 4, pp. 331–336, 2009.
- [100] L. Guan, X. Hu, L. Liu et al., "bta-miR-23a involves in adipogenesis of progenitor cells derived from fetal bovine skeletal muscle," *Scientific Reports*, vol. 7, no. 1, 2017.
- [101] T. Kang, W. Lu, W. Xu et al., "MicroRNA-27 (miR-27) targets prohibitin and impairs adipocyte differentiation and mitochondrial function in human adipose-derived stem cells," *The Journal of Biological Chemistry*, vol. 288, no. 48, pp. 34394–34402, 2013.
- [102] T. Wang, M. Li, J. Guan et al., "MicroRNAs miR-27a and miR-143 regulate porcine adipocyte lipid metabolism," *International Journal of Molecular Sciences*, vol. 12, no. 11, pp. 7950–7959, 2011.
- [103] D. Prusty, B. H. Park, K. E. Davis, and S. R. Farmer, "Activation of MEK/ERK signaling promotes adipogenesis by enhancing peroxisome proliferator-activated receptor gamma (PPARgamma) and C/EBPalpha gene expression during the differentiation of 3T3-L1 preadipocytes," *The Journal of Biological Chemistry*, vol. 277, no. 48, pp. 46226–46232, 2002.
- [104] Y. Xing, F. Yan, Y. Liu, Y. Liu, and Y. Zhao, "Matrine inhibits 3T3-L1 preadipocyte differentiation associated with suppression of ERK1/2 phosphorylation," *Biochemical and Biophysical Research Communications*, vol. 396, no. 3, pp. 691–695, 2010.
- [105] Y. Guo, X. Zhang, W. Huang, and X. Miao, "Identification and characterization of differentially expressed miRNAs in subcutaneous adipose between Wagyu and Holstein cattle," *Scientific Reports*, vol. 7, no. 1, 2017.
- [106] X. Zhang, J. Guo, Y. Zhou, and G. Wu, "The roles of bone morphogenetic proteins and their signaling in the osteogenesis of adipose-derived stem cells," *Tissue Engineering. Part B, Reviews*, vol. 20, no. 1, pp. 84–92, 2014.
- [107] C. Thery, L. Zitvogel, and S. Amigorena, "Exosomes: composition, biogenesis and function," *Nature Reviews. Immunology*, vol. 2, no. 8, pp. 569–579, 2002.
- [108] Y. Li, Q. Zheng, C. Bao et al., "Circular RNA is enriched and stable in exosomes: a promising biomarker for cancer diagnosis," *Cell Research*, vol. 25, no. 8, pp. 981–984, 2015.
- [109] P. Seale, B. Bjork, W. Yang et al., "PRDM16 controls a brown fat/skeletal muscle switch," *Nature*, vol. 454, no. 7207, pp. 961–967, 2008.
- [110] P. Seale, S. Kajimura, W. Yang et al., "Transcriptional control of brown fat determination by PRDM16," *Cell Metabolism*, vol. 6, no. 1, pp. 38–54, 2007.
- [111] P. Seale, H. M. Conroe, J. Estall et al., "Prdm16 determines the thermogenic program of subcutaneous white adipose tissue in mice," *The Journal of Clinical Investigation*, vol. 121, no. 1, pp. 96–105, 2011.
- [112] H. Ding, S. Zheng, D. Garcia-Ruiz et al., "Fasting induces a subcutaneous-to-visceral fat switch mediated by microRNA-149-3p and suppression of PRDM16," *Nature Communications*, vol. 7, no. 1, 2016.
- [113] H. Yin, A. Pasut, V. D. Soleimani et al., "MicroRNA-133 controls brown adipose determination in skeletal muscle satellite cells by targeting Prdm16," *Cell Metabolism*, vol. 17, no. 2, pp. 210–224, 2013.
- [114] Z. Yang, C. Bian, H. Zhou et al., "MicroRNA hsa-miR-138 inhibits adipogenic differentiation of human adipose tissue-derived mesenchymal stem cells through adenovirus EID-1," *Stem Cells and Development*, vol. 20, no. 2, pp. 259–267, 2011.
- [115] A. C. Panda, I. Grammatikakis, K. M. Kim et al., "Identification of senescence-associated circular RNAs (SAC-RNAs) reveals senescence suppressor CircPVT1," *Nucleic Acids Research*, vol. 45, no. 7, pp. 4021–4035, 2017.
- [116] X. Li, Z. Zhang, H. Jiang et al., "Circular RNA circPVT1 promotes proliferation and invasion through sponging miR-125b and activating E2F2 signaling in non-small cell lung cancer," *Cellular Physiology and Biochemistry*, vol. 51, no. 5, pp. 2324–2340, 2018.
- [117] J. Chen, Y. Li, Q. Zheng et al., "Circular RNA profile identifies circPVT1 as a proliferative factor and prognostic marker in gastric cancer," *Cancer Letters*, vol. 388, pp. 208–219, 2017.
- [118] H. L. Ji, C. C. Song, Y. F. Li et al., "miR-125a inhibits porcine preadipocytes differentiation by targeting ERRA," *Molecular and Cellular Biochemistry*, vol. 395, no. 1–2, pp. 155–165, 2014.
- [119] J. Du, Y. Xu, P. Zhang et al., "MicroRNA-125a-5p affects adipocytes proliferation, differentiation and fatty acid composition of porcine intramuscular fat," *International Journal of Molecular Sciences*, vol. 19, no. 2, p. 501, 2018.
- [120] A. K. Greifengberg, D. Hönig, K. Pilarova et al., "Structural and functional analysis of the Cdk13/Cyclin K complex," *Cell Reports*, vol. 14, no. 2, pp. 320–331, 2016.
- [121] Q. Lin, Y. B. Ling, J. W. Chen et al., "Circular RNA circCDK13 suppresses cell proliferation, migration and invasion by modulating the JAK/STAT and PI3K/AKT pathways in liver cancer," *International Journal of Oncology*, vol. 53, no. 1, pp. 246–256, 2018.
- [122] N. Han, L. Ding, X. Wei, L. Fan, and L. Yu, "circSMAD2 governs migration and epithelial-mesenchymal transition by inhibiting microRNA-9," *Journal of Cellular Biochemistry*, 2019.
- [123] L. Shen, Y. Hu, J. Lou et al., "CircRNA-0044073 is upregulated in atherosclerosis and increases the proliferation and invasion of cells by targeting miR-107," *Molecular Medicine Reports*, vol. 19, no. 5, pp. 3923–3932, 2019.
- [124] H. Li, Z. Zhang, X. Zhou, Z. Y. Wang, G. L. Wang, and Z. Y. Han, "Effects of microRNA-143 in the differentiation and proliferation of bovine intramuscular preadipocytes," *Molecular Biology Reports*, vol. 38, no. 7, pp. 4273–4280, 2011.
- [125] E. K. Lee, M. J. Lee, K. Abdelmohsen et al., "miR-130 suppresses adipogenesis by inhibiting peroxisome proliferator-activated receptor gamma expression," *Molecular and Cellular Biology*, vol. 31, no. 4, pp. 626–638, 2011.

- [126] S. Lorente-Cebrián, N. Mejhert, A. Kulyté et al., “MicroRNAs regulate human adipocyte lipolysis: effects of miR-145 are linked to TNF- $\alpha$ ,” *PLoS One*, vol. 9, no. 1, article e86800, 2014.
- [127] H. Li, X. Chen, L. Guan et al., “MiRNA-181a regulates adipogenesis by targeting tumor necrosis factor- $\alpha$  (TNF- $\alpha$ ) in the porcine model,” *PLoS One*, vol. 8, no. 10, article e71568, 2013.
- [128] T. Sun, M. Fu, A. L. Bookout, S. A. Kliewer, and D. J. Mangelsdorf, “MicroRNA let-7 regulates 3T3-L1 adipogenesis,” *Molecular Endocrinology*, vol. 23, no. 6, pp. 925–931, 2009.

## Review Article

# Immunomodulatory Properties of Stem Cells in Periodontitis: Current Status and Future Prospective

Mengyuan Wang,<sup>1</sup> Jiang Xie,<sup>2</sup> Cong Wang,<sup>1</sup> Dingping Zhong,<sup>2</sup> Liang Xie<sup>ID</sup>,<sup>3</sup>  
and Hongzhi Fang<sup>ID</sup><sup>1</sup>

<sup>1</sup>Department of Stomatology, The Third People's Hospital of Chengdu, The Affiliated Hospital of Southwest Jiaotong University, Chengdu, China 610000

<sup>2</sup>The Third People's Hospital of Chengdu, The Affiliated Hospital of Southwest Jiaotong University, Chengdu, China 610000

<sup>3</sup>State Key Laboratory of Oral Diseases, National Clinical Research Center for Oral Diseases, West China Hospital of Stomatology, Sichuan University, Chengdu, China 610041

Correspondence should be addressed to Liang Xie; [lxie@scu.edu.cn](mailto:lxie@scu.edu.cn) and Hongzhi Fang; [1127958575@qq.com](mailto:1127958575@qq.com)

Received 19 March 2020; Revised 2 May 2020; Accepted 8 May 2020; Published 8 July 2020

Academic Editor: Sangho Roh

Copyright © 2020 Mengyuan Wang et al. This is an open access article distributed under the Creative Commons Attribution License, which permits unrestricted use, distribution, and reproduction in any medium, provided the original work is properly cited.

Periodontitis is the sixth-most prevalent chronic inflammatory disease and gradually devastates tooth-supporting tissue. The complexity of periodontal tissue and the local inflammatory microenvironment poses great challenges to tissue repair. Recently, stem cells have been considered a promising strategy to treat tissue damage and inflammation because of their remarkable properties, including stemness, proliferation, migration, multilineage differentiation, and immunomodulation. Several varieties of stem cells can potentially be applied to periodontal regeneration, including dental mesenchymal stem cells (DMSCs), nonodontogenic stem cells, and induced pluripotent stem cells (iPSCs). In particular, these stem cells possess extensive immunoregulatory capacities. In periodontitis, these cells can exert anti-inflammatory effects and regenerate the periodontium. Stem cells derived from infected tissue possess typical stem cell characteristics with lower immunogenicity and immunosuppression. Several studies have demonstrated that these cells can also regenerate the periodontium. Furthermore, the interaction of stem cells with the surrounding infected microenvironment is critical to periodontal tissue repair. Though the immunomodulatory capabilities of stem cells are not entirely clarified, they show promise for therapeutic application in periodontitis. Here, we summarize the potential of stem cells for periodontium regeneration in periodontitis and focus on their characteristics and immunomodulatory properties as well as challenges and perspectives.

## 1. Background

Periodontitis is a chronic inflammatory condition that gradually devastates tooth-supporting tissue, which is comprised of the periodontal ligament (PDL), gingiva, and alveolar bone. The severe form of periodontitis, which impacts 743 million around the world, is the sixth-most prevalent chronic disease [1, 2]. Periodontitis is not only the main reason for tooth loss in adults but is also related to a variety of chronic diseases (i.e., diabetes, obesity, osteoporosis, arthritis, depression, cardiovascular disease, and Alzheimer's disease) [3–5].

Conventional therapies focus on utilizing natural and synthetic materials to fill defects of periodontal tissue, but these substitutes do not result in the actual restoration of

the original physical structure and function of the tissue [6]. Due to the complexity of periodontal tissue, it is still a challenge to regenerate the periodontium. Tissue engineering approaches for regenerative dentistry consist of stem cells in the oral cavity, cytoskeleton, and growth factors. Stem cells exhibit highly promising therapeutic potential in periodontal regeneration owing to their self-renewal property and the plasticity of their potential to differentiate [7]. DMSCs, nonodontogenic stem cells, and iPSCs can be applied to periodontal tissue regeneration. Given the remarkable properties and versatility of stem cells, they are considered to be an efficient approach to regenerate periodontal tissue [8–10]. In addition, stem cells play a crucial role in immunosuppressive and anti-inflammatory functions [11]. In periodontitis, stem



cells can be delivered to a site of infection and function as critical players to control inflammation and the immune response, achieving a regenerative process [12].

Here, we briefly summarize the potential of stem cells for periodontium regeneration, mainly focusing on their characteristics and immunomodulatory properties as well as the challenges and perspectives for their application.

## 2. Pathological Mechanism of Periodontitis

Uncovering the mechanisms of inflammatory responses in periodontitis will facilitate the application of stem cells to treat this disease [13]. Periodontal tissue homeostasis is dependent on the balance between host immune defenses and microbial attacks [14]. Once the dysbiotic microbial community subverts a susceptible host, an inflammatory response is generated [15]. This process is mediated by the immune system of the host, which triggers the breakdown of tooth-supporting structures, resulting in the initiation of periodontitis (Figure 1).

### 2.1. Microbial Dysbiosis: The Causative Agent of Periodontitis.

The dysbiotic microbial community consists of anaerobic bacterial genera, including *Proteobacteria*, *Firmicutes*, *Spirochaetes*, *Synergistetes*, and *Bacteroidetes* [16]. The subgingival microenvironment affords opportunities for the microbial community due to the enrichment of inflammatory mediators. The dysbiotic microbial community subverts host immune responses by enhancing their nutrient acquisition and evasion strategies in the inflammatory milieu. The dysbiotic oral microbiota display synergistic interactions that can cause reciprocal proteomic and transcriptomic responses to reinforce nutrient acquisition [17, 18]. The dysbiotic oral microbiota procure nutrients from destructive inflammatory tissue, including heme-containing composites and degraded collagen peptides [19]. These periodontal bacteria can improve their fitness by regulating the communication with the host immune response. For example, these bacteria escape neutrophil-mediated assault and protect themselves from complement. As a result, periodontal tissue breakdown is increased by neutrophil-mediated responses due to the inability of the neutrophil to control the dysbiotic microbial attack [20].

**2.2. Host Susceptibility to Periodontitis.** Host susceptibility to periodontitis not only governs the transition from microbial synergy to dysbiosis but also determines the development of inflammation and the progression of irreversible tissue destruction [21, 22]. The progression and severity of periodontitis rely on host-related factors, including immunoregulatory dysregulation, immunodeficiencies, systemic diseases related to periodontitis (such as diabetes, cardiovascular disease, obesity, osteoporosis, arthritis, depression, and Alzheimer's disease), risk factors affecting the host's immune system (such as smoking, stress, ageing, and microbial factors), and regenerative responses [23, 24]. Defects or dysregulation of the host immune response leads to an inability to suppress dysbiotic microbial communities and the resultant pathogenesis. The susceptible host immune response is

subverted by dysbiotic microbiota, leading to the formation of a self-perpetuating pathogenic cycle [15].

**2.3. Immune Response in Periodontitis.** Once periodontitis is triggered by dysbiotic microbiota, the immune response in periodontitis changes from acute inflammation into the chronic condition and leads to the breakdown of the periodontium [25] (Figure 1).

Dysbiotic microbiota can reinforce their own tolerance to host immune responses by interacting with neutrophils and complement [14]. Neutrophils congregate in the gingival sulcus, while T cells, B cells, and monocytes are recruited. Neutrophils release elastase to degrade membrane proteins in some bacteria, which causes the breakdown of elastin and type IV collagen in the PDL and therefore disintegrates its attachment to the cementum and alveolar bone, leading to the formation of a periodontal pocket [26]. Neutrophils also secrete cytotoxic substances and degradative enzymes (i.e., reactive oxygen species and matrix metalloproteinases) that result in the inflammatory destruction of tissue [27]. In addition, neutrophils release the receptor activator of nuclear factor kappa-B ligand (RANKL), which is necessary for osteoclastogenesis and periodontal bone resorption [28]. Another major source of RANKL is via secretion from B cells and T cells in inflammatory lesions [29]. Specifically, neutrophils mediate the chemotactic recruitment of interleukin-(IL-) 17-mediated T helper 17 (Th17) cells through the expression of chemokine ligand (CCL) 2 and CCL20. Meanwhile, chemokine receptor (CCR) 2 and CCR6 are secreted by Th17 cells [30, 31]. Th17 cells are a subset of T cells that promote osteoclastogenesis and act as effective helpers of B cells [32]. The progression of periodontitis is characterized by inflammatory infiltration with large numbers of B cells and plasma cells accompanied by the increasing expression of immune complexes and complement fragments [33]. Specifically, B cells induce the conductive destruction of periodontal tissue which is due to matrix metalloproteinases and inflammatory cytokines secreted by B cells [34].

Macrophages remodel connective tissue by balancing matrix metalloproteinases and their tissue inhibitors. Macrophages also regulate bone homeostasis by mediating osteoblasts and osteoclasts. Moreover, this capacity of polymorphonuclear leukocytes and monocytes is achieved by the secretion of cytokines, including tumor necrosis factor  $\alpha$  (TNF- $\alpha$ ), adhesion molecules, IL-1 $\beta$ , and IL-6. These factors induce these cells to adhere to the endothelium and to increase the permeability of gingival capillaries and alveolar bone resorption [13, 35].

## 3. Characteristics, Immunological Properties, and Periodontal Regeneration Potential of Stem Cells

In this section, we review the characteristics as well as the immunological properties of stem cells, including DMSCs, nonodontogenic stem cells, and iPSCs. Specifically, we present stem cells as having potential efficacy for regenerating compromised tissues.

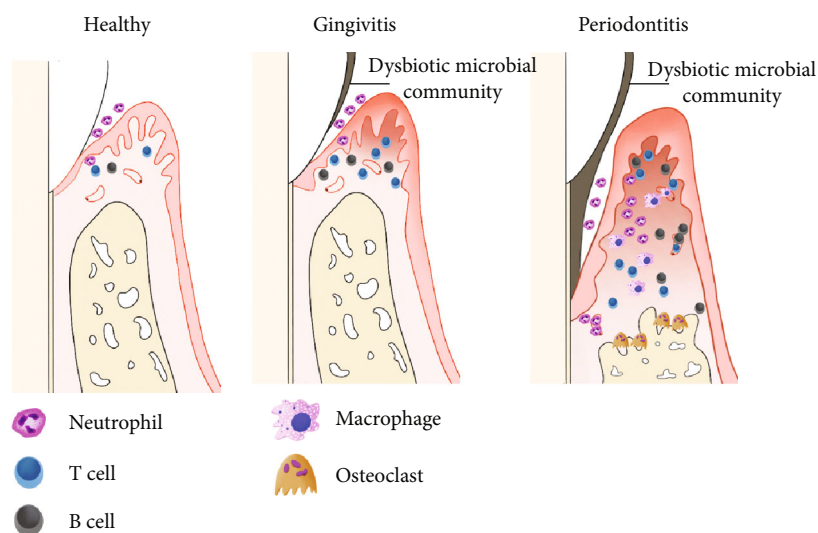


FIGURE 1: The pathological mechanism of periodontitis. Periodontal tissue homeostasis is dependent on the balance between the host immune defenses and microbial attacks. Once dysbiotic microbial communities subvert a susceptible host, the inflammatory dialog would be generated. Thus, dysbiotic microbiota act as a pathobiont which overactivate the inflammatory response, then trigger periodontal tissue breakdown associated with innate and adaptive immunoregulation, potentially resulting in resorption of supporting alveolar bone, even tooth loss and systemic complications.

**3.1. DMSCs.** DMSCs are composed of periodontal ligament stem cells (PDLSCs), dental follicle stem cells (DFSCs), dental pulp-derived stem cells (DPSCs), stem cells from apical papilla (SCAPs), stem cells from exfoliated deciduous teeth (SHEDs), gingival mesenchymal stem cells (GMSCs), and dental socket-derived stem cells (DSSCs) [36, 37] (Figure 2). DMSCs are multipotent stem cells with a self-renewal ability as well as multiple lineage differentiation potentials [38]. More importantly, DMSCs mediate the activity of various immune cells. The immunomodulatory potential of DMSCs mainly relies on inflammatory factors secreted by immune cells.

**3.1.1. PDLSCs.** The PDL is a connective tissue that connects the tooth root to the surrounding alveolar bone. The PDL originates from the dental follicle and plays a critical role in sustaining tooth homeostasis and providing nutrition. PDLSCs were first derived and identified from adult third molars [39]. PDLSCs have the potential to generate PDLs, alveolar bone, cementum, blood vessels, and peripheral nerves [40]. In addition, these cells also have a self-renewal capacity and high proliferative potential [41]. PDLSCs expressed various types of MSC-related cluster of differentiation (CD) markers, including CD73, CD90, and CD105, and lack expression of hematopoietic markers, such as CD14, CD19, CD34, CD40, CD45, CD80, and CD86 [42–44]. Human PDLSCs also express antigens such as TRA-1-60, TRA-1-81, sex-determining region Y-box (Sox) 2, alkaline phosphatase (ALP), stage-specific embryonic antigen-(SSEA-) 1, SSEA-3, SSEA-4, and reduced expression 1 [6, 45].

Recently, PDLSCs were deemed to be a promising potential cell source for the repair of periodontal defects following periodontitis on account of their immunomodulatory properties (Figure 3). Activated human peripheral blood mononuclear cells (PBMCs) generate interferon- (IFN-)  $\gamma$ ,

which induces PDLSCs to secrete some soluble factors (i.e., transforming growth factor- (TGF-)  $\beta$ , indoleamine 2,3-dioxygenase-1 (IDO-1), and hepatocyte growth factor (HGF)) that, in turn, partially decrease the proliferation of PBMCs [46]. Upregulated proliferation and downregulated apoptosis of neutrophils constitute another innate immune response mediated by PDLSCs [47]. PDLSCs also greatly inhibit T cell proliferation by reducing the secretion of major histocompatibility complex glycoprotein1b (GP1b) and prostaglandin E2 (PGE2) from dendritic cells (DCs) [48]. Additionally, PDLSCs improve the activity and proliferation of anti-inflammatory Treg cells and suppress proinflammatory Th1/Th2/Th17 cells [49]. In addition to these cells, the mechanism of immunosuppression is mediated by PDLSCs through the inhibition of B cell proliferation, migration, and differentiation. These properties of PDLSCs are achieved via stimulating the expression of programmed cell death protein 1 (PD-1) and its ligand (PD-L1) [50]. PDLSCs enhance the polarization of the anti-inflammatory phenotype (M2 phenotype) by stimulating Arginase- (Arg-) 1, CD163, and IL-10 and inhibiting TNF- $\alpha$  [47].

Currently, both the animal experiments and clinical trials demonstrate that PDLSCs can regenerate periodontal defects. Studies have reported that delivery of PDLSCs to periodontal defects in rat models improves periodontal regeneration by generating PDLs, cementum-like tissue, and new bone without inflammation [51]. More importantly, PDLSCs achieve periodontal regeneration without adverse effects. In a miniature swine periodontitis model, transplantation of an allogeneic PDLSC sheet achieved the regeneration of the periodontium and cured periodontitis through immunosuppressive effects and low immunogenicity [52]. A clinical study exhibited that autologous PDLSC transplantation possessed the advantages of stability and effectiveness during the long-term follow-up of patients with periodontitis,

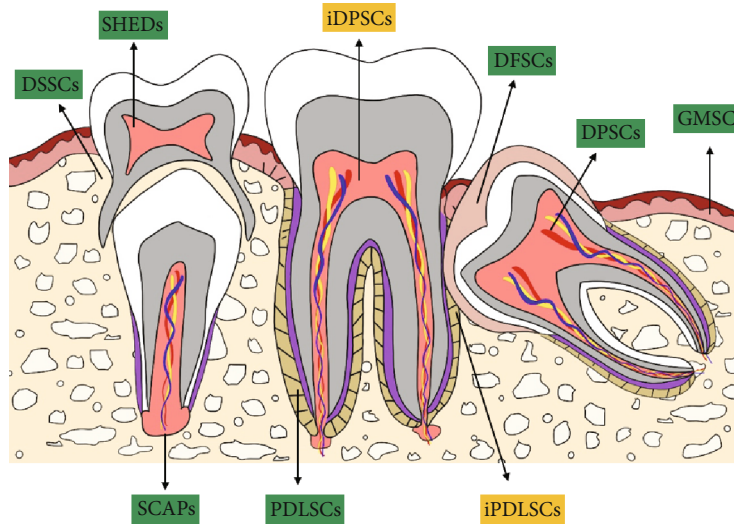


FIGURE 2: The different populations of dental mesenchymal stem cells and their distribution. PDLSCs: periodontal ligament stem cells; DFSCs: dental follicle stem cells; DPSCs: dental pulp-derived stem cells; SCAPs: stem cells from apical papilla; SHEDs: stem cells from exfoliated deciduous teeth; GMSCs: gingival mesenchymal stem cells; DSSCs: dental socket-derived stem cells; iPDLSCs: PDLSCs derived from infected tissue; iDPSCs: DPSCs derived from infected tissue.

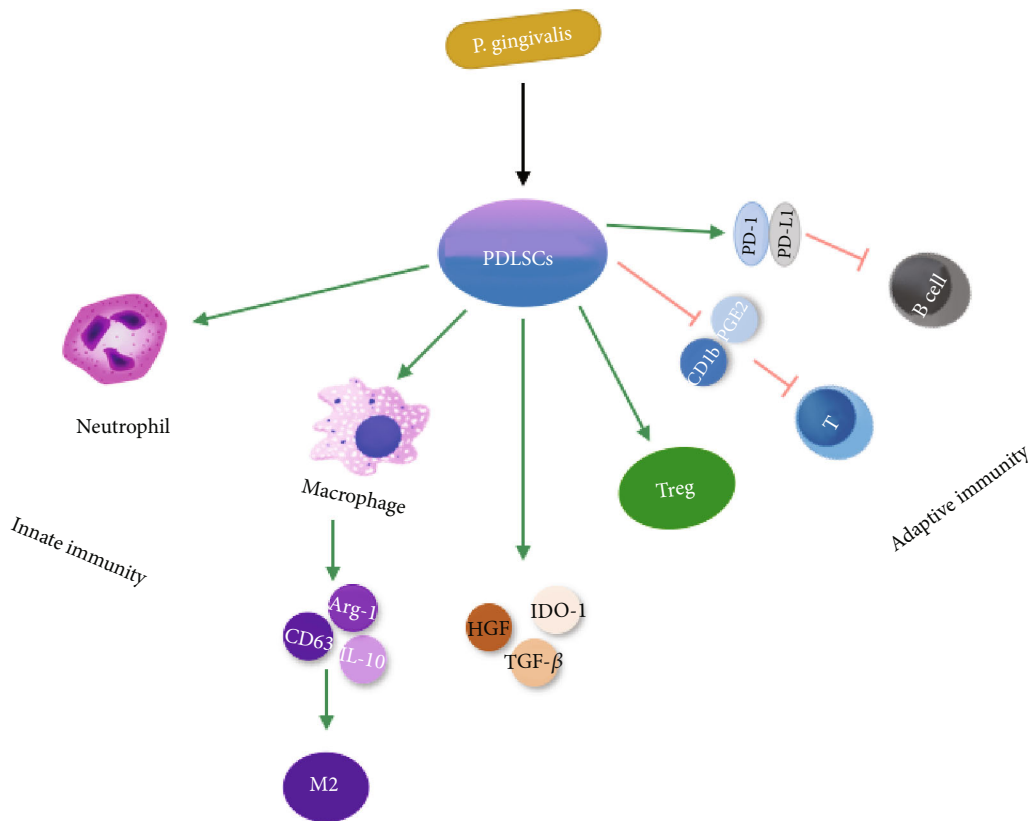


FIGURE 3: The immunological properties of PDLSCs linked with innate and adaptive immunity. PDLSCs possess immunoregulatory and anti-inflammatory capacities via both innate and adaptive immune responses.

suggesting that PDLSCs may be an innovative approach to treat periodontitis [46].

3.1.2. *DFSCs*. DFSCs are responsible for periodontium formation by migrating around the tooth germ and differentiating into

PDLs, osteoblasts, and cementoblasts [53]. Surface markers of DFSCs contain CD13, CD44, CD73, CD105, CD56, CD271, human leukocyte antigen- (HLA-) ABC, STRO-1, and NOTCH-1. Among them, STRO-1 and CD44 are common surface markers that are used to identify DFSCs [54].

The immunosuppressive properties of DFSCs are dependent on TLRs. In periodontitis, *P. gingivalis* and *F. nucleatum*s activate the expression of TLR2 and TLR4 on the membrane of DFSCs and then trigger DFSCs to inhibit the proliferation of peripheral blood mononuclear cells (PBMCs) [55]. Moreover, DFSCs can upregulate the secretion of the anti-inflammatory cytokine IL-10 and simultaneously downregulate the levels of the proinflammatory cytokines IL-4, IL-8, and IFN- $\gamma$ , thereby damaging bacterial adherence and internalization [56]. DFSCs exert anti-inflammatory effects and suppress bone degradation by mediating the phagocytic activity, chemotaxis, and NET formation of neutrophils and inducing macrophage polarization into the M2 phenotype [57].

Several animal experiments have proven that DFSCs possess the capacity to repair periodontal defects. In a canine model of periodontal defects, the potential of DFSCs to repair periodontal defects was proven via implantation of autologous DFSCs into defects, inducing the generation of new PDLs, alveolar bone, and cementum [36]. In another study, ectopic transplantation of DFSCs from human-impacted third molars into nude mice generated the cementum-PDL complex [58].

**3.1.3. DPSCs.** DPSCs were the first characterized mesenchymal stem cells derived from the dental pulp in 2002. These cells possess the potential to differentiate into osteogenic, adipogenic, chondrogenic, and neural cells and show high expression of surface markers of MSCs [59].

DPSCs possess the ability to mediate both innate and adaptive immune responses by interacting with T cells, B cells, macrophages, and natural killer (NK) cells [60]. DPSCs exert anti-inflammatory and immunosuppressive effects by suppressing the proliferation of activated T cells as well as triggering apoptotic programmed cell death [61]. DPSCs also inhibit immunoglobulin production of B cells and IL-17 by increasing the secretion of IFN- $\gamma$  [62]. The inhibitory effect of DPSCs on the proliferation of PBMCs is achieved by generating TGF and stimulating the mitogen-activated protein kinase (MAPK) signaling pathway [63]. DPSCs exert an anti-inflammatory function in two ways. On the one hand, DPSCs inhibit macrophages from secreting TNF- $\alpha$  by an IDO-dependent pathway. On the other hand, DPSCs initiate macrophage M2 polarization [64]. Induction of DPSC differentiation enhances the inhibitory effects of DPSCs on NK cell-mediated lysis and cytotoxicity.

In fact, Park and colleagues showed that DPSCs hardly repaired periodontal defects on account of their limited capacity to form a cementum-like structure, while PDLSCs regenerated the periodontium with new bone, cementum, and Sharpey's fibers [36]. As the function of DPSCs on pulp repair, there is little research about immunomodulatory properties of DPSCs in PDL tissue. Consequently, the present evidence indicates that DPSCs may not be an appropriate source for periodontal tissue engineering.

**3.1.4. SCAPs.** SCAPs were first isolated from human apical papilla tissue of immature permanent teeth in 2006 [65]. Similar to other MSCs, SCAPs show a self-renewal capacity, high proliferative potential, and low immunogenicity as well

as multilineage differentiation. STRO-1, CD24, and CD146 are widely expressed in SCAPs and are considered to be surface markers of SCAPs [66]. SCAPs can inhibit T cell proliferation by a mechanism independent of apoptosis [67]. It has also been reported that transplanting SCAPs into a periodontitis site significantly ameliorates the periodontitis parameters of periodontal tissue 12 weeks after transplantation [68]. All of these results suggest SCAPs may be a promising cell source for repairing the periodontium in regenerative dentistry.

**3.1.5. SHEDs.** SHEDs were first characterized and isolated from the human dental pulp of exfoliated deciduous teeth by Miura. SHEDs show the ability to regenerate bone and dentin-like tissue, with a high osteoinductive ability and proliferation rate [62].

SHEDs show immunomodulatory characteristics via mediating T cell activation, maturation, and differentiation. Moreover, downregulation of Th17 cells and upregulation of regulatory T cells (Tregs) are additional immunosuppressive effects of SHEDs [69]. Furthermore, SHEDs can suppress DCs from secreting the inflammatory cytokines IL-2, IFN- $\gamma$ , and TNF- $\alpha$  and can facilitate DCs to generate the anti-inflammatory factor IL-10 [70]. SHEDs induce polarization of bone marrow-derived macrophages towards M2 polarization, which contributes to the regeneration of the periodontium and anti-inflammatory effects in periodontal tissues [71].

In an experimental periodontitis model, delivery of SHEDs into periodontal tissues led to a reduction of cytokine expression, osteoclast differentiation, and gum bleeding as well as promoted the formation of new attachments of PDL and alveolar bone. These results suggest that SHEDs contribute to the improvement of periodontal regeneration and the decrease of periodontal tissue inflammation [72].

**3.1.6. GMSCs.** The epithelium and connective tissue make up the human gingiva, which is considered to be an essential constituent of the periodontium that exerts remarkable effects on periodontal regeneration and immunity and is notable for its wound healing properties without scarring. GMSCs were derived and identified from the lamina propria of gingival tissue in 2009 [73]. Based on their remarkable self-renewal, multilineage differentiation, and regenerative abilities, GMSCs are expected to be a suitable cell source in periodontal tissue engineering.

Recently, the easy accessibility and prominent immunomodulatory properties of GMSCs have led to more attention on the use of cellular therapy [74]. GMSC-induced immunomodulation represents a promising perspective in therapy of periodontal tissue inflammation via interaction with inflammatory cells and cytokines [74]. GMSCs communicate with the inflammatory environment through the expression of TLRs 1, 2, 3, 4, 5, 6, 7, and 10, which affect the immunomodulatory properties of GMSCs [75]. Human GMSCs show the capacity to facilitate the polarization of macrophages to the M2 phenotype; meanwhile, they inhibit the activation of M1 macrophages by producing PGE2, IL-6, and IL-10 [76]. Furthermore, GMSCs significantly reduce the activation and



maturation of DCs by a PGE2-related mechanism that suppresses the antigen presentation ability of DCs and weakens the inflammatory response [77]. Human GMSCs also reduce the proliferation and differentiation of Th1/Th2/Th17 cells. GMSCs have an inhibitory function on PHA-dependent T cell proliferation and activation by upregulating immunosuppressive factors, such as IDO and IL-10 [78].

A study reported that GMSCs mixed with an IL-1RA-hydrogel synthetic extracellular matrix, when delivered into a periodontitis model, led to an obvious improvement of regenerating PDLs, cementum, and alveolar bone [74]. In a dog model, the transplantation of GFP-labelled GMSCs into furcation defects obviously improved the regeneration of damaged periodontal tissues [79].

**3.1.7. DSSCs.** Recent studies have shown that dental sockets can be a potential source for periodontal regeneration. DSSCs have the potential to form colonies and can differentiate into osteoblasts, adipocytes, and chondrocytes [80]. Compared with BMSCs, colony formation, proliferation, and motility of DSSCs are stronger. DSSCs can positively express surface markers of stem cells, such as CD44, CD90, and CD271, and lack expression of hematopoietic markers, such as CD34 and CD45 [81].

Nakajima et al. reported that the transplantation of autologous DSSCs mixed with  $\beta$ -TCP/PGA into one-wall periodontal defects regenerated a new periodontium with PDL-like and cementum-like tissues and alveolar bone [80]. There are few studies on DSSCs, so more preclinical investigations are required to clarify the roles of DSSCs in tissue regeneration and immune regulation.

**3.2. Nonodontogenic Stem Cells.** Nonodontogenic stem cells are composed of bone marrow stromal stem cells (BMSCs) and adipose tissue-derived stem cells (ASCs).

**3.2.1. BMSCs.** BMSCs can differentiate into osteoblasts, chondrocytes, adipocytes, and muscle cells [82]. BMSCs are sorted by surface markers of octamer-binding transcription factor (Oct)-4, CD73, CD90, CD105, CD146, STRO-1, and Nanog and do not express HLA-DR, CD14, CD34, or CD45. BMSCs have the potential to regenerate periodontal defects by generating alveolar bone, Sharpey's fibers, and cementum [83]. BMSCs migrate into PDLs, alveolar bone, blood vessels, and cementum and differentiate into osteoblasts and fibroblasts after local or systematic transplantation [84].

Aside from regenerating destroyed tissues in periodontitis, BMSCs also play a crucial role in anti-inflammation and immunosuppressive function [85]. BMSCs mediate the survival and proliferation of T lymphocytes for the regulation of immunomodulation [86]. BMSCs inhibit inflammatory cytokines, including IL-1 and TNF- $\alpha$ , which indicates that the use of BMSCs for the treatment of chronic periodontitis might be feasible [85]. In a clinical study, the combined use of autologous BMSCs and platelet-rich plasma to treat periodontal defects shows obvious tissue regeneration effects [87]. Although a significant improvement in periodontal parameters has been observed, more clinical research is needed to reveal the function of BMSCs and their ability to

regulate inflammation and immunity to better target them for the treatment of periodontitis.

**3.2.2. ASCs.** The characteristics of ASCs are similar to those of BMSCs, such as expression of the markers STRO-1, CD29, CD44, CD71, CD90, and CD105 and the lack of expression of hematopoietic cell markers CD31, CD34, and CD45 [88]. ASCs can differentiate into osteoblast, adipocytes, chondrocytes, myogenic, and neurogenic cells. Compared to BMSCs, ASCs are superior because of their easier harvesting process and because of their fewer notable donor site complications [89]. More importantly, ASCs mixed with cytokines TNF- $\alpha$ , IFN- $\gamma$ , and IL-6 promote the expression of immune suppressive factors, including GBP4 and IL-1RA [90].

Preclinical studies have demonstrated that ASCs are potential candidate cells for the regeneration of periodontal destruction. ASCs can secrete growth factors, such as insulin-like growth factor binding protein-6, which facilitates the differentiation of ASCs into the periodontium [91]. Allogeneic ASCs were transplanted in a microminipig model of periodontal tissue defects and led to the generation of new PDL-like fibers, alveolar bone, and the cementum in defect sites [90].

**3.3. Induced Pluripotent Stem Cells (iPSCs).** The formation of iPSCs can be achieved by reprogramming somatic cells with the transcriptional markers Oct4, Sox2, Krüppel-like factor 4, and Myc [92]. iPSCs express special pluripotent markers, including TRA160, TRA180, MSC-heat shock protein 90, CD73, CD90, CD105, CD146, and CD106 [93]. iPSCs are pluripotent stem cells with the potential to generate iPSC-derived MSCs (iPSC-MSCs) and to differentiate into multilineage cells [94]. As a promising candidate, iPSCs not only have the potential to regenerate bone, cartilage, brain, heart, and liver tissue but also can be applied for inflammatory tissue regeneration in periodontitis [95]. Stem cells from dental tissue, including PDLs, buccal mucosa fibroblasts, gingival, apical papilla, and the dental pulp, have advantages for the generation of iPSCs [96].

Moreover, iPSC-MSCs can inhibit Th1/Th2/Th17 cells and upregulate the expression of Treg cells, suppressing the production of leukocytes and alveolar bone resorption [97, 98]. iPSCs are a potential cell source for the clinical prevention and treatment of periodontitis. Duan et al. showed that transplantation of iPSCs to a scaffold with enamel-derived factors significantly increased PDL, alveolar bone, and cementum formation in a mouse periodontal defect model compared with iPSC-empty groups [99]. Another study reported that iPSCs could inhibit inflammation and decrease alveolar bone resorption in a rat model of periodontitis. In addition, Hynes et al. stated that iPSC-MSCs could repair periodontal tissue defects and control inflammation while lessening alveolar bone destruction [100].

## 4. Interaction of Stem Cells with the Inflammatory Milieu of the Periodontium

What happens to the stem cells in periodontitis and how they interact with periodontal inflammation are crucial for the

application of stem cells into periodontal regeneration [101]. For instance, the interaction of stem cells and immune cells in the inflammatory milieu may be completely different from that in a healthy state with altered regenerative processes and immunomodulatory properties [102]. Thus, it is essential to understand the properties of stem cells derived from inflammatory tissue as well as the inflammatory responses and immunomodulation properties of stem cells in an inflamed microenvironment.

**4.1. Stem Cells from Inflammatory Tissue.** Inflamed stem cells exhibit characteristics including maintenance of stemness, formation of colonies, a higher proliferation rate, multilineage differentiation potential, and lower immunogenicity and immunosuppression [102].

In this section, we introduce the properties and immunoregulation of DMSCs in inflammatory periodontal sites. Among stem cells, DMSCs derived from infected tissue possess the significant advantages of being easily accessible and having fewer ethical complications [103]. Compared with other DMSCs, PDLSCs are considered to be an ideal cell source for periodontal regeneration [104], but there are still problems with obtaining enough PDLSCs from healthy donor sources. PDLSCs derived from inflamed periodontal sites are considered inflammatory periodontal ligament stem cells (iPDLSCs). Compared to PDLSCs, iPDLSCs have higher proliferative and migratory capacities. However, iPDLSCs exhibit lower osteogenic differentiation because of alterations of the osteogenesis-related signaling pathway, such as the Wnt/ $\beta$ -catenin, noncanonical Wnt/ $\text{Ca}^{2+}$ , p38-MAPK, and NF- $\kappa$ B signaling pathways [105, 106]. More importantly, iPDLSCs also have reduced immunosuppressive properties and less efficiently suppress T cell proliferation, PBMC proliferation, and Th17 differentiation in contrast to cells from healthy tissue [107]. High levels of IFN- $\gamma$ , TNF- $\alpha$ , IL-2, and IDO and low expression of IL-10 are also characteristic of iPDLSCs [108]. A study reporting on the transplantation of collagen sponges combined with iPDLSCs isolated from inflamed human periodontal tissue into immunodeficient nude rats led to the formation of new PDL-like tissue, bone, and collagen fibers. Although complete regeneration was not achieved, the repair effect of iPDLSCs on periodontal defects was similar to that of PDLSCs from healthy periodontal tissues [51]. Compared with normal DPSCs, DPSCs derived from infected tissue (iDPSCs) show similar surface marker expression, proliferation properties, and multilineage differentiation potential [109, 110]. DPSCs derived from infected human tissue were layered onto  $\beta$ -tricalcium phosphate and grafted into periodontal defects in the root furcation. The outcome revealed new formation of alveolar bone [111]. These results have important implications for achieving periodontium regeneration with DMSCs obtained from inflammatory tissues in the future [112]. It may be a promising strategy to cultivate or even genetically modify DMSCs obtained from infected tissue, avoiding the destruction of the healthy periodontium while implanting DMSCs into inflamed periodontium tissue to achieve regeneration [113, 114].

However, there are still various issues that should be taken into account before translational application. For

example, the source of inflamed stem cells, the inflammatory status, and the experimental design are confounding variables that will affect the quality and quantity of stem cells [115]. Furthermore, the inclusion criteria as well as the procedure for the isolation and transplantation of the inflamed stem cells should be established and standardized to further explore and verify the long-term effects of inflamed stem cells via *in vivo* and *in vitro* experiments [57, 116, 117].

**4.2. Effect of the Infected Microenvironment on Stem Cells.**

The interaction of stem cells with the surrounding infected microenvironment could affect the mechanism of periodontal tissue repair and the regeneration outcome [102]. Transplantation of stem cells into periodontal defects is usually performed in an inflamed periodontal milieu, and the immunomodulatory capacity of stem cells is determined by diverse inflammatory cytokines. Therefore, understanding the effect of inflammatory cytokines on stem cells is critical to optimize and implement stem cell-mediated clinical approaches [118, 119].

Various inflammatory cytokines can specifically mediate the immunomodulatory activity of stem cells [120]. Among various inflammatory mediators, TNF- $\alpha$ , IL-1 $\beta$ , IL-6, and IFN- $\gamma$  are the most effective proinflammatory cytokines during periodontitis [121]. The proinflammatory cytokines TNF- $\alpha$ , IL-1 $\alpha$ , IL-1 $\beta$ , and IFN- $\gamma$  exert critical effects by mitigating the immunosuppressive capacities of stem cells [122]. Low levels of IFN- $\gamma$  improve antigen-presenting functions of stem cells and thus reduce their lysis. In contrast, high levels would reverse their antigen-presenting functions and show the opposite effect [123, 124].

Several studies have demonstrated the effects of an infected microenvironment on DMSCs. For example, *P. gingivalis*-LPS significantly enhanced cellular proliferation of DMSCs [125]. In addition, coculturing PDLSCs with IL-1 $\beta$ /TNF- $\alpha$  could enhance the proliferation rate of PDLSCs [126]. The surface markers of DMSCs, such as PDLSCs and GMSCs, do not change within the IL-1 $\beta$ /TNF- $\alpha$ -inflamed microenvironment. However, the effect may be compromised or may even lead to stem cell apoptosis when the IL-1 $\beta$ /TNF- $\alpha$  stimulus surpasses a certain level. The differentiation potential of DMSCs could be mediated by proinflammatory cytokines and microbial pathogens [127]. Specifically, *P. gingivalis*-LPS and *E.coli*-LPS inhibit PDLSCs' osteoblastic differentiation [125, 128]. IL-1 $\beta$ /TNF- $\alpha$  are responsible for reducing the osteogenesis of PDLSCs by stimulating the canonical Wnt/ $\beta$ -catenin pathway and inhibiting the noncanonical Wnt/ $\text{Ca}^{2+}$  pathway in the local periodontal milieu [106].

Other stem cells also exert important effects on the infected microenvironment. An increasing number of studies have shown that IFN- $\gamma$  is required for BMSCs to exert their immunosuppressive effect on T lymphocyte proliferation. Additionally, both LPS and IFN- $\gamma$  can induce the secretion of functional IDO and IL-10 by BMSCs [129]. LPS-induced proliferation of PBMCs could be inhibited by BMSCs [73]. Transplantation of BMSCs into LPS-stimulated models could inhibit the production of inflammatory cytokines and ameliorate inflammatory tissue destruction [130]. The interaction of ASCs with the inflammatory microenvironment is necessary to achieve tissue regeneration. In response

TABLE 1: The characteristic of different stem cells could be potentially applied to periodontal regeneration.

Stem cell	Multipotent differentiation	Immunomodulatory properties	Clinical trails
<i>DMSCs</i>			
PDLSCs	Osteoblast, adipocytes, chondrocytes, cementoblast, and neurogenic cells	Inhibition of PBMCs, T cells, B cells, promotion of Treg cells, neutrophils, and M2 phenotype macrophage	NCT01357785 NCT01082822
DFSCs	Osteoblast, adipocytes, chondrocytes, cementoblast, neurogenic cells, cardiomyocyte, and dentin-like cell	Inhibition of PBMCs, promotion of Treg cells, neutrophils, and M2 phenotype macrophage	
DPSCs	Osteoblast, adipocytes, odontoblast, neurogenic cells, cardiomyocyte, and hepatocyte	Inhibition of PBMCs, T cells, B cells, and NK cells; promotion of Treg cells, neutrophils, and M2 phenotype macrophage	NCT03386877 NCT02523651
SCAPs	Osteoblast, adipocytes, odontoblast, neurogenic cells, and hepatocyte	Low immunogenicity; inhibition of T cells	
SHEDs	Osteoblast, adipocytes, chondrocytes, and neurogenic cells	Inhibition of Th17 cells; promotion of Treg cells and M2 phenotype macrophage	
GMSCs	Osteoblast, adipocytes, chondrocytes, and neurogenic cells	Inhibition of M1 macrophages, Th1/Th2/Th17 cells, and DCs; promotion of Treg cells and M2 phenotype macrophage	NCT03137979
DSSCs	Osteoblast, adipocytes, and chondrocytes	No report	
<i>Nonodontogenic stem cells</i>			
BMSCs	Osteoblast, adipocytes, and chondrocytes	Inhibition of T lymphocyte survival and proliferation; secretion of IL-1 and TNF- $\alpha$	NCT02449005
ASCs	Osteoblast, adipocytes, chondrocytes, myogenic cells, and neurogenic cells	Promotion of immune suppressive factors GBP4 and IL-1RA	NCT04270006
<i>iPSCs</i>			
iPSCs	Osteoblast, adipocytes, chondrocytes, myogenic cells, neurogenic cells, cementoblast, cardiomyocyte, and dentin-like cell	Inhibition of Th1/Th2/Th17 cells; promotion of Treg cells	

The clinical trial data have been extracted from <https://clinicaltrials.gov/>.

to inflammatory cytokines, ASCs facilitate the anti-inflammatory and immunosuppressive potential through the induction of polarization of macrophages to the M2 phenotype [131]. When stimulated with TNF- $\alpha$  and IFN- $\gamma$ , ASCs significantly increased their immunomodulatory capacities [132].

## 5. Conclusion, Future Clinical Application, and Challenges

To date, application of extracellular matrix scaffolds, bone grafts, and growth factors achieve only limited regeneration of intrabony defects [133]. In the past few years, developing data have indicated that stem cells have great potential in periodontitis due to the positive inflammatory-regenerative effects of these cells in the inflamed microenvironment [36, 134]. These stem cells have remarkable properties and versatility due to their stemness, proliferation, migration, and multilineage differentiation abilities and their immunosuppressive and anti-inflammatory functions in a local inflamed microenvironment [118, 135, 136].

The immunoregulatory effects of stem cells make them a promising therapy for periodontitis. Although several reports have indicated that the stem cells mentioned above can be delivered into infectious sites and function as critical players in the control of inflammation and the regulation of immune

responses to achieve regeneration in models of periodontitis, the immunomodulatory capabilities of these cells have not entirely been elucidated [137, 138]. Moreover, evidence of stem cell-mediated immunomodulation is limited both *in vitro* and *in vivo*. It is very complicated to recreate extremely polluted surroundings in animal models because human periodontal lesions are filled with granulation tissue, calculus, pathogenic biofilms, and plaque [139]. Furthermore, there are various differences in the mechanisms of stem cell-mediated immunomodulation between humans and animals [140]. The quality and quantity of stem cells can be modulated by numerous factors, including the sources of stem cells and the experimental design [141]. The inclusion of subjects and procedures for the isolation and transplantation of stem cells can influence the outcome of regeneration and immunomodulation.

Therefore, inclusion criteria as well as a standard procedure for the isolation and transplantation of the stem cells should be established to further explore the long-term effects of stem cells. Standard animal models of periodontitis should be constructed to mimic human periodontal lesions. Selection of suitable biomaterial scaffolds and the appropriate combination with growth factors for stem cells may improve their periodontal regeneration and immunosuppression functions. More importantly, preclinical studies and clinical trials are critical to understand the mechanism of stem cell-

mediated immunomodulation in the inflammatory milieu to pave the way for applying stem cells to periodontal tissue engineering (Table 1).

## Abbreviations

DMSCs:	Dental mesenchymal stem cells
iPSCs:	Induced pluripotent stem cells
iDMSCs:	DMSCs derived from infected tissue
PDL:	Periodontal ligament
TLRs:	Toll-like receptors
RANKL:	Receptor activator of nuclear factor kappa-B ligand
IL:	Interleukin
Th17:	T helper 17
CCL:	Chemokine ligand
CCR:	Chemokine receptor
TNF- $\alpha$ :	Tumor necrosis factor $\alpha$
PDLSCs:	Periodontal ligament stem cells
DFSCs:	Dental follicle stem cells
DPSCs:	Dental pulp-derived stem cells
SCAPs:	Stem cells from apical papilla
SHED:	Stem cells from exfoliated deciduous teeth
GMSCs:	Gingival mesenchymal stem cells
DSSCs:	Dental socket-derived stem cells
Sox:	Sex-determining region Y-box
ALP:	Alkaline phosphatase
SSEA:	Stage-specific embryonic antigen
CD:	Cluster of differentiation
PGE2:	Prostaglandin E2
PBMCs:	Peripheral blood mononuclear cells
IFN:	Interferon
TGF- $\beta$ :	Transforming growth factor- $\beta$
IDO-1:	Indoleamine 2,3-dioxygenase-1
HGF:	Hepatocyte growth factor
PD-1:	Programmed cell death protein 1
PD-L1:	Programmed cell death protein ligand 1
Arg:	Arginase
HLA:	Human leukocyte antigen
NK cells:	Natural killer cells
MAPK:	Mitogen-activated protein kinase
Tregs:	Regulatory T cells
DCs:	Dendritic cells
BMSCs:	Bone marrow stromal stem cells
ASCs:	Adipose tissue-derived stem cells
Oct:	Octamer-binding transcription factor
HLA:	Human leukocyte antigen
iPDLSCs:	Inflammatory periodontal ligament stem cells.

## Data Availability

The human clinical trials data included in this review are available at <https://clinicaltrials.gov/>.

## Disclosure

The authors state that this manuscript includes original unpublished work.

## Conflicts of Interest

The authors declare no conflicts of interest.

## Authors' Contributions

All authors have made substantial, direct, and intellectual contributions to the work. At the same time, all authors participated in designing the study and drafting and writing the manuscript as well as approving it for submission.

## Acknowledgments

This work was supported by grants from the National Natural Science Foundation of China (NSFC, 81600842) and Science Foundation of Health Commission of Sichuan Province (17PJ547).

## References

- [1] N. J. Kassebaum, E. Bernabé, M. Dahiya, B. Bhandari, C. J. L. Murray, and W. Marcenes, "Global burden of severe periodontitis in 1990-2010: a systematic review and meta-regression," *Journal of Dental Research*, vol. 93, no. 11, pp. 1045–1053, 2014.
- [2] M. A. Peres, B. Daly, C. C. Guarnizo-Herreño, H. Benzian, and R. G. Watt, "Oral diseases: a global public health challenge – authors' reply," *The Lancet*, vol. 395, no. 10219, pp. 186–187, 2020.
- [3] R. J. Genco and T. E. Van Dyke, "Reducing the risk of CVD in patients with periodontitis," *Nature Reviews Cardiology*, vol. 7, no. 9, pp. 479–480, 2010.
- [4] G. Hajishengallis, "Periodontitis: from microbial immune subversion to systemic inflammation," *Nature Reviews Immunology*, vol. 15, no. 1, pp. 30–44, 2015.
- [5] E. Lalla and P. N. Papapanou, "Diabetes mellitus and periodontitis: a tale of two common interrelated diseases," *Nature Reviews Endocrinology*, vol. 7, no. 12, pp. 738–748, 2011.
- [6] W. Zhu and M. Liang, "Periodontal ligament stem cells: current status, concerns, and future prospects," *Stem Cells International*, vol. 2015, Article ID 972313, 11 pages, 2015.
- [7] P. Bianco, P. G. Robey, I. Saggio, and M. Riminucci, "Mesenchymal stem cells in human bone marrow (skeletal stem cells): a critical discussion of their nature, identity, and significance in incurable skeletal disease," *Human Gene Therapy*, vol. 21, no. 9, pp. 1057–1066, 2010.
- [8] E. P. Chalisserry, S. Y. Nam, S. H. Park, and S. Anil, "Therapeutic potential of dental stem cells," *Journal of Tissue Engineering*, vol. 8, Article ID 2041731417702531, 2016.
- [9] Y. C. Guo, M. Y. Wang, S. W. Zhang et al., "Ubiquitin-specific protease USP34 controls osteogenic differentiation and bone formation by regulating BMP2 signaling," *The EMBO Journal*, vol. 37, no. 20, 2018.
- [10] W. Liu, L. Zhou, C. Zhou et al., "GDF11 decreases bone mass by stimulating osteoclastogenesis and inhibiting osteoblast differentiation," *Nature Communications*, vol. 7, no. 1, article 12794, 2016.
- [11] B. Hernández-Monjaraz, E. Santiago-Osorio, A. Monroy-García, E. Ledesma-Martínez, and V. Mendoza-Núñez, "Mesenchymal stem cells of dental origin for inducing tissue



- regeneration in periodontitis: a mini-review," *International Journal of Molecular Sciences*, vol. 19, no. 4, p. 944, 2018.
- [12] X. Fu, L. Jin, P. Ma, Z. Fan, and S. Wang, "Allogeneic stem cells from deciduous teeth in treatment for periodontitis in miniature swine," *Journal of Periodontology*, vol. 85, no. 6, pp. 845–851, 2014.
- [13] P. J. Ford, J. Gamonal, and G. J. Seymour, "Immunological differences and similarities between chronic periodontitis and aggressive periodontitis," *Periodontology 2000*, vol. 53, no. 1, pp. 111–123, 2010.
- [14] K. Barth, D. G. Remick, and C. A. Genco, "Disruption of immune regulation by microbial pathogens and resulting chronic inflammation," *Journal of Cellular Physiology*, vol. 228, no. 7, pp. 1413–1422, 2013.
- [15] G. Hajishengallis, "Immunomicrobial pathogenesis of periodontitis: keystones, pathobionts, and host response," *Trends in Immunology*, vol. 35, no. 1, pp. 3–11, 2014.
- [16] Z. L. Deng, S. P. Szafranski, M. Jarek, S. Bhujju, and I. Wagner-Döbler, "Dysbiosis in chronic periodontitis: key microbial players and interactions with the human host," *Scientific Reports*, vol. 7, no. 1, article 3703, 2017.
- [17] A. Mira, A. Simon-Soro, and M. A. Curtis, "Role of microbial communities in the pathogenesis of periodontal diseases and caries," *Journal of Clinical Periodontology*, vol. 44, Supplement 18, pp. S23–S38, 2017.
- [18] F. A. Roberts and R. P. Darveau, "Microbial protection and virulence in periodontal tissue as a function of polymicrobial communities: symbiosis and dysbiosis," *Periodontology 2000*, vol. 69, no. 1, pp. 18–27, 2015.
- [19] D. Baraniya, M. Naginyte, T. Chen et al., "Modeling normal and dysbiotic subgingival microbiomes: effect of nutrients," *Journal of Dental Research*, vol. 99, no. 6, pp. 695–702, 2020.
- [20] D. K. Gaudilliere, A. Culos, K. Djebali et al., "Systemic immunologic consequences of chronic periodontitis," *Journal of Dental Research*, vol. 98, no. 9, pp. 985–993, 2019.
- [21] K. S. Kornman, "Contemporary approaches for identifying individual risk for periodontitis," *Periodontology 2000*, vol. 78, no. 1, pp. 12–29, 2018.
- [22] M. L. Laine, W. Crielaard, and B. G. Loos, "Genetic susceptibility to periodontitis," *Periodontology 2000*, vol. 58, no. 1, pp. 37–68, 2012.
- [23] A. Stabholz, W. A. Soskolne, and L. Shapira, "Genetic and environmental risk factors for chronic periodontitis and aggressive periodontitis," *Periodontology 2000*, vol. 53, no. 1, pp. 138–153, 2010.
- [24] M. A. Reynolds, "Modifiable risk factors in periodontitis: at the intersection of aging and disease," *Periodontology 2000*, vol. 64, no. 1, pp. 7–19, 2014.
- [25] G. Nussbaum and L. Shapira, "How has neutrophil research improved our understanding of periodontal pathogenesis?," *Journal of Clinical Periodontology*, vol. 38, Supplement 11, pp. 49–59, 2011.
- [26] H. Alfakry, E. Malle, C. N. Koyani, P. J. Pussinen, and T. Sorsa, "Neutrophil proteolytic activation cascades: a possible mechanistic link between chronic periodontitis and coronary heart disease," *Innate Immunity*, vol. 22, no. 1, pp. 85–99, 2015.
- [27] A. Mantovani, M. A. Cassatella, C. Costantini, and S. Jaillon, "Neutrophils in the activation and regulation of innate and adaptive immunity," *Nature Reviews Immunology*, vol. 11, no. 8, pp. 519–531, 2011.
- [28] A. Chakravarti, M. A. Raquil, P. Tessier, and P. E. Poubelle, "Surface RANKL of Toll-like receptor 4-stimulated human neutrophils activates osteoclastic bone resorption," *Blood*, vol. 114, no. 8, pp. 1633–1644, 2009.
- [29] M. Kajiya, G. Giro, M. A. Taubman, X. Han, M. P. A. Mayer, and T. Kawai, "Role of periodontal pathogenic bacteria in RANKL-mediated bone destruction in periodontal disease," *Journal of Oral Microbiology*, vol. 2, no. 1, 2010.
- [30] M. Pelletier, L. Maggi, A. Micheletti et al., "Evidence for a cross-talk between human neutrophils and Th17 cells," *Blood*, vol. 115, no. 2, pp. 335–343, 2010.
- [31] P. Miossec and J. K. Kolls, "Targeting IL-17 and T<sub>H</sub>17 cells in chronic inflammation," *Nature Reviews Drug Discovery*, vol. 11, no. 10, pp. 763–776, 2012.
- [32] D. T. Graves, T. Oates, and G. P. Garlet, "Review of osteoimmunology and the host response in endodontic and periodontal lesions," *Journal of Oral Microbiology*, vol. 3, no. 1, 2011.
- [33] S. Kurgan and A. Kantarci, "Molecular basis for immunohistochemical and inflammatory changes during progression of gingivitis to periodontitis," *Periodontology 2000*, vol. 76, no. 1, pp. 51–67, 2018.
- [34] T. Berglundh, M. Donati, and N. Zitzmann, "B cells in periodontitis: friends or enemies?," *Periodontology 2000*, vol. 45, no. 1, pp. 51–66, 2007.
- [35] J. Meyle and I. Chapple, "Molecular aspects of the pathogenesis of periodontitis," *Periodontology 2000*, vol. 69, no. 1, pp. 7–17, 2015.
- [36] J. Y. Park, S. H. Jeon, and P. H. Choung, "Efficacy of periodontal stem cell transplantation in the treatment of advanced periodontitis," *Cell Transplantation*, vol. 20, no. 2, pp. 271–286, 2011.
- [37] C.-Y. C. Huang, D. Pelaez, J. D. Bendala, F. Garcia-Godoy, and H. S. Cheung, "Plasticity of stem cells derived from adult periodontal ligament," *Regenerative Medicine*, vol. 4, no. 6, pp. 809–821, 2009.
- [38] M. Wang, Q. Yuan, and L. Xie, "Mesenchymal stem cell-based immunomodulation: properties and clinical application," *Stem Cells International*, vol. 2018, Article ID 3057624, 12 pages, 2018.
- [39] B. M. Seo, M. Miura, S. Gronthos et al., "Investigation of multipotent postnatal stem cells from human periodontal ligament," *The Lancet*, vol. 364, no. 9429, pp. 149–155, 2004.
- [40] A. Tomokiyo, S. Yoshida, S. Hamano, D. Hasegawa, H. Sugii, and H. Maeda, "Detection, characterization, and clinical application of mesenchymal stem cells in periodontal ligament tissue," *Stem Cells International*, vol. 2018, Article ID 5450768, 9 pages, 2018.
- [41] C. Martínez, P. C. Smith, J. P. Rodriguez, and V. Palma, "Sonic hedgehog stimulates proliferation of human periodontal ligament stem cells," *Journal of Dental Research*, vol. 90, no. 4, pp. 483–488, 2011.
- [42] N. Kawanabe, S. Murata, K. Murakami et al., "Isolation of multipotent stem cells in human periodontal ligament using stage-specific embryonic antigen-4," *Differentiation*, vol. 79, no. 2, pp. 74–83, 2010.
- [43] K. Iwasaki, M. Komaki, N. Yokoyama et al., "Periodontal ligament stem cells possess the characteristics of pericytes," *Journal of Periodontology*, vol. 84, no. 10, pp. 1425–1433, 2013.

- [44] L. Wang, H. Shen, W. Zheng et al., "Characterization of stem cells from alveolar periodontal ligament," *Tissue Engineering Part A*, vol. 17, no. 7-8, pp. 1015–1026, 2011.
- [45] J. Xiong, D. Menicanin, P. S. Zilm, V. Marino, P. M. Bartold, and S. Gronthos, "Investigation of the cell surface proteome of human periodontal ligament stem cells," *Stem Cells International*, vol. 2016, Article ID 1947157, 13 pages, 2016.
- [46] O. Andrukhov, J. S. A. Hong, O. Andrukhova, A. Blufstein, A. Moritz, and X. Rausch-Fan, "Response of human periodontal ligament stem cells to IFN- $\gamma$  and TLR-agonists," *Scientific Reports*, vol. 7, no. 1, p. 12856, 2017.
- [47] J. Liu, B. Chen, J. Bao, Y. Zhang, L. Lei, and F. Yan, "Macrophage polarization in periodontal ligament stem cells enhanced periodontal regeneration," *Stem Cell Research & Therapy*, vol. 10, no. 1, p. 320, 2019.
- [48] C. Shin, M. Kim, J. A. Han et al., "Human periodontal ligament stem cells suppress T-cell proliferation via down-regulation of non-classical major histocompatibility complex-like glycoprotein CD1b on dendritic cells," *Journal of Periodontal Research*, vol. 52, no. 1, pp. 135–146, 2017.
- [49] J. Ng, K. Hynes, G. White et al., "Immunomodulatory properties of induced pluripotent stem cell-derived mesenchymal cells," *Journal of Cellular Biochemistry*, vol. 117, no. 12, pp. 2844–2853, 2016.
- [50] O. Liu, J. Xu, G. Ding et al., "Periodontal ligament stem cells regulate B lymphocyte function via programmed cell death protein 1," *Stem Cells*, vol. 31, no. 7, pp. 1371–1382, 2013.
- [51] J. Qiu, X. Wang, H. Zhou et al., "Enhancement of periodontal tissue regeneration by conditioned media from gingiva-derived or periodontal ligament-derived mesenchymal stem cells: a comparative study in rats," *Stem Cell Research & Therapy*, vol. 11, no. 1, p. 42, 2020.
- [52] G. Ding, Y. Liu, W. Wang et al., "Allogeneic periodontal ligament stem cell therapy for periodontitis in swine," *Stem Cells*, vol. 28, no. 10, pp. 1829–1838, 2010.
- [53] H. Yang, J. Li, Y. Hu et al., "Treated dentin matrix particles combined with dental follicle cell sheet stimulate periodontal regeneration," *Dental Materials*, vol. 35, no. 9, pp. 1238–1253, 2019.
- [54] T. Zhou, J. Pan, P. Wu et al., "Dental follicle cells: roles in development and beyond," *Stem Cells International*, vol. 2019, Article ID 9159605, 17 pages, 2019.
- [55] J. Liu, L. Wang, W. Liu, Q. Li, Z. Jin, and Y. Jin, "Dental follicle cells rescue the regenerative capacity of periodontal ligament stem cells in an inflammatory microenvironment," *PLoS One*, vol. 9, no. 10, article e108752, 2014.
- [56] K. Chatzivasileiou, C. A. Lux, G. Steinhoff, and H. Lang, "Dental follicle progenitor cells responses to *Porphyromonas gingivalis* LPS," *Journal of Cellular and Molecular Medicine*, vol. 17, no. 6, pp. 766–773, 2013.
- [57] X. Chen, B. Yang, J. Tian et al., "Dental follicle stem cells ameliorate lipopolysaccharide-induced inflammation by secreting TGF- $\beta$ 3 and TSP-1 to elicit macrophage M2 polarization," *Cellular Physiology and Biochemistry*, vol. 51, no. 5, pp. 2290–2308, 2018.
- [58] W. Guo, L. Chen, K. Gong, B. Ding, Y. Duan, and Y. Jin, "Heterogeneous dental follicle cells and the regeneration of complex periodontal tissues," *Tissue Engineering Part A*, vol. 18, no. 5-6, pp. 459–470, 2012.
- [59] T. L. Fernandes, J. P. Cortez de SantAnna, I. Frisene et al., "Systematic review of human dental pulp stem cells for cartilage regeneration," *Tissue Engineering Part B, Reviews*, vol. 26, no. 1, pp. 1–12, 2020.
- [60] L. Ji, L. Bao, Z. Gu et al., "Comparison of immunomodulatory properties of exosomes derived from bone marrow mesenchymal stem cells and dental pulp stem cells," *Immunologic Research*, vol. 67, no. 4-5, pp. 432–442, 2019.
- [61] A. T. Özdemir, R. B. Özgül Özdemir, C. Kırmaz et al., "The paracrine immunomodulatory interactions between the human dental pulp derived mesenchymal stem cells and CD4 T cell subsets," *Cellular Immunology*, vol. 310, pp. 108–115, 2016.
- [62] M. Maioli, V. Basoli, S. Santaniello et al., "Osteogenesis from dental pulp derived stem cells: a novel conditioned medium including melatonin within a mixture of hyaluronic, butyric, and retinoic acids," *Stem Cells International*, vol. 2016, Article ID 2056416, 8 pages, 2016.
- [63] S. Tomic, J. Djokic, S. Vasilijic et al., "Immunomodulatory properties of mesenchymal stem cells derived from dental pulp and dental follicle are susceptible to activation by toll-like receptor agonists," *Stem Cells and Development*, vol. 20, no. 4, pp. 695–708, 2011.
- [64] S. Lee, Q. Z. Zhang, B. Karabucak, and A. D. le, "DPSCs from inflamed pulp modulate macrophage function via the TNF- $\alpha$ /IDO axis," *Journal of Dental Research*, vol. 95, no. 11, pp. 1274–1281, 2016.
- [65] W. Sonoyama, Y. Liu, T. Yamaza et al., "Characterization of the apical papilla and its residing stem cells from human immature permanent teeth: a pilot study," *Journal of Endodontia*, vol. 34, no. 2, pp. 166–171, 2008.
- [66] J. Kang, W. Fan, Q. Deng, H. He, and F. Huang, "Stem cells from the apical papilla: a promising source for stem cell-based therapy," *BioMed Research International*, vol. 2019, Article ID 6104738, 8 pages, 2019.
- [67] G. Ding, Y. Liu, Y. An et al., "Suppression of T cell proliferation by root apical papilla stem cells in vitro," *Cells, Tissues, Organs*, vol. 191, no. 5, pp. 357–364, 2010.
- [68] G. Li, N. Han, X. Zhang et al., "Local injection of allogeneic stem cells from apical papilla enhanced periodontal tissue regeneration in minipig model of periodontitis," *BioMed Research International*, vol. 2018, Article ID 3960798, 8 pages, 2018.
- [69] S. Yildirim, N. Zibandeh, D. Genc, E. M. Ozcan, K. Goker, and T. Akkoc, "The comparison of the immunologic properties of stem cells isolated from human exfoliated deciduous teeth, dental pulp, and dental follicles," *Stem Cells International*, vol. 2016, Article ID 4682875, 15 pages, 2016.
- [70] F. de Sá Silva, R. N. Ramos, D. C. de Almeida et al., "Mesenchymal stem cells derived from human exfoliated deciduous teeth (SHEDs) induce immune modulatory profile in monocyte-derived dendritic cells," *PLoS One*, vol. 9, no. 5, article e98050, 2014.
- [71] Z. Li, C. M. Jiang, S. An et al., "Immunomodulatory properties of dental tissue-derived mesenchymal stem cells," *Oral Diseases*, vol. 20, no. 1, pp. 25–34, 2014.
- [72] X. Gao, Z. Shen, M. Guan et al., "Immunomodulatory role of stem cells from human exfoliated deciduous teeth on periodontal regeneration," *Tissue Engineering. Part A*, vol. 24, no. 17-18, pp. 1341–1353, 2018.
- [73] Q. Zhang, S. Shi, Y. Liu et al., "Mesenchymal stem cells derived from human gingiva are capable of immunomodulatory functions and ameliorate inflammation-related tissue

- destruction in experimental colitis,” *Journal of Immunology*, vol. 183, no. 12, pp. 7787–7798, 2009.
- [74] K. M. Fawzy El-Sayed and C. E. Dorfer, “Gingival mesenchymal stem/progenitor cells: a unique tissue engineering gem,” *Stem Cells International*, vol. 2016, Article ID 7154327, 16 pages, 2016.
- [75] K. Fawzy-El-Sayed, M. Mekhemar, S. Adam-Klages, D. Kabelitz, and C. Dorfer, “TLR expression profile of human gingival margin-derived stem progenitor cells,” *Medicina Oral, Patología Oral y Cirugía Bucal*, vol. 21, no. 1, pp. e30–e38, 2016.
- [76] Q. Z. Zhang, A. L. Nguyen, W. H. Yu, and A. D. le, “Human oral mucosa and gingiva: a unique reservoir for mesenchymal stem cells,” *Journal of Dental Research*, vol. 91, no. 11, pp. 1011–1018, 2012.
- [77] W. R. Su, Q. Z. Zhang, S. H. Shi, A. L. Nguyen, and A. D. le, “Human gingiva-derived mesenchymal stromal cells attenuate contact hypersensitivity via prostaglandin E2-dependent mechanisms,” *Stem Cells*, vol. 29, no. 11, pp. 1849–1860, 2011.
- [78] C. M. Jiang, J. Liu, J. Y. Zhao et al., “Effects of hypoxia on the immunomodulatory properties of human gingiva-derived mesenchymal stem cells,” *Journal of Dental Research*, vol. 94, no. 1, pp. 69–77, 2014.
- [79] X. Yu, S. Ge, S. Chen et al., “Human gingiva-derived mesenchymal stromal cells contribute to periodontal regeneration in beagle dogs,” *Cells, Tissues, Organs*, vol. 198, no. 6, pp. 428–437, 2014.
- [80] R. Nakajima, M. Ono, E. S. Hara et al., “Mesenchymal stem/progenitor cell isolation from tooth extraction sockets,” *Journal of Dental Research*, vol. 93, no. 11, pp. 1133–1140, 2014.
- [81] J. Luo, J. Xu, J. Cai, L. Wang, Q. Sun, and P. Yang, “The in vitro and in vivo osteogenic capability of the extraction socket-derived early healing tissue,” *Journal of Periodontology*, vol. 87, no. 9, pp. 1057–1066, 2016.
- [82] N. Baryawno, D. Przybylski, M. S. Kowalczyk et al., “A cellular taxonomy of the bone marrow stroma in homeostasis and leukemia,” *Cell*, vol. 177, no. 7, pp. 1915–1932.e16, 2019, e16.
- [83] M. Paknejad, M. B. Eslaminejad, B. Ghaedi et al., “Isolation and assessment of mesenchymal stem cells derived from bone marrow: histologic and histomorphometric study in a canine periodontal defect,” *The Journal of Oral Implantology*, vol. 41, no. 3, pp. 284–291, 2015.
- [84] N. Hasegawa, H. Kawaguchi, A. Hirachi et al., “Behavior of transplanted bone marrow-derived mesenchymal stem cells in periodontal defects,” *Journal of Periodontology*, vol. 77, no. 6, pp. 1003–1007, 2006.
- [85] J. Du, Z. Shan, P. Ma, S. Wang, and Z. Fan, “Allogeneic bone marrow mesenchymal stem cell transplantation for periodontal regeneration,” *Journal of Dental Research*, vol. 93, no. 2, pp. 183–188, 2013.
- [86] L. Xiao, Y. Zhou, L. Zhu et al., “SPHK1-S1PR1-RANKL axis regulates the interactions between macrophages and BMSCs in inflammatory bone loss,” *Journal of Bone and Mineral Research*, vol. 33, no. 6, pp. 1090–1104, 2018.
- [87] Y. Yamada, S. Nakamura, K. Ito et al., “Injectable bone tissue engineering using expanded mesenchymal stem cells,” *Stem Cells*, vol. 31, no. 3, pp. 572–580, 2013.
- [88] L. Xu, Y. Liu, Y. Sun et al., “Tissue source determines the differentiation potentials of mesenchymal stem cells: a comparative study of human mesenchymal stem cells from bone marrow and adipose tissue,” *Stem Cell Research & Therapy*, vol. 8, no. 1, p. 275, 2017.
- [89] G. T. Huang, S. Gronthos, and S. Shi, “Mesenchymal stem cells derived from dental tissues vs. those from other sources: their biology and role in regenerative medicine,” *Journal of Dental Research*, vol. 88, no. 9, pp. 792–806, 2009.
- [90] V. S. Venkataiah, K. Handa, M. M. Njuguna et al., “Periodontal regeneration by allogeneic transplantation of adipose tissue derived multi-lineage progenitor stem cells in vivo,” *Scientific Reports*, vol. 9, no. 1, p. 921, 2019.
- [91] K. Sawada, M. Takedachi, S. Yamamoto et al., “Trophic factors from adipose tissue-derived multi-lineage progenitor cells promote cytodifferentiation of periodontal ligament cells,” *Biochemical and Biophysical Research Communications*, vol. 464, no. 1, pp. 299–305, 2015.
- [92] K. Takahashi and S. Yamanaka, “Induction of pluripotent stem cells from mouse embryonic and adult fibroblast cultures by defined factors,” *Cell*, vol. 126, no. 4, pp. 663–676, 2006.
- [93] H. Yang, R. M. Aprecio, X. Zhou et al., “Therapeutic effect of TSG-6 engineered iPSC-derived MSCs on experimental periodontitis in rats: a pilot study,” *PLoS One*, vol. 9, no. 6, article e100285, 2014.
- [94] K. Hynes, D. Menichanin, R. Bright et al., “Induced pluripotent stem cells: a new frontier for stem cells in dentistry,” *Journal of Dental Research*, vol. 94, no. 11, pp. 1508–1515, 2015.
- [95] A. Revilla, C. González, A. Iriondo et al., “Current advances in the generation of human iPSCs: implications in cell-based regenerative medicine,” *Journal of Tissue Engineering and Regenerative Medicine*, vol. 10, no. 11, pp. 893–907, 2016.
- [96] N. Malhotra, “Induced pluripotent stem (iPS) cells in dentistry: a review,” *International Journal of Stem Cells*, vol. 9, no. 2, pp. 176–185, 2016.
- [97] K. Hynes, R. Bright, V. Marino et al., “Potential of iPSC-derived mesenchymal stromal cells for treating periodontal disease,” *Stem Cells International*, vol. 2018, Article ID 2601945, 12 pages, 2018.
- [98] P. P. Cheng, X. C. Liu, P. F. Ma et al., “iPSC-MSCs combined with low-dose rapamycin induced islet allograft tolerance through suppressing Th1 and enhancing regulatory T-cell differentiation,” *Stem Cells and Development*, vol. 24, no. 15, pp. 1793–1804, 2015.
- [99] X. Duan, Q. Tu, J. Zhang et al., “Application of induced pluripotent stem (iPS) cells in periodontal tissue regeneration,” *Journal of Cellular Physiology*, vol. 226, no. 1, pp. 150–157, 2011.
- [100] K. Hynes, D. Menicanin, J. Han et al., “Mesenchymal stem cells from iPSCs facilitate periodontal regeneration,” *Journal of Dental Research*, vol. 92, no. 9, pp. 833–839, 2013.
- [101] K. M. Fawzy El-Sayed, M. Elahmady, Z. Adawi et al., “The periodontal stem/progenitor cell inflammatory-regenerative cross talk: a new perspective,” *Journal of Periodontal Research*, vol. 54, no. 2, pp. 81–94, 2018.
- [102] C. Zheng, J. Chen, S. Liu, and Y. Jin, “Stem cell-based bone and dental regeneration: a view of microenvironmental modulation,” *International Journal of Oral Science*, vol. 11, no. 3, p. 23, 2019.
- [103] S. Guo, J. Kang, B. Ji et al., “Periodontal-derived mesenchymal cell sheets promote periodontal regeneration in



- inflammatory microenvironment,” *Tissue Engineering Part A*, vol. 23, no. 13-14, pp. 585–596, 2017.
- [104] Q. Zhai, Z. Dong, W. Wang, B. Li, and Y. Jin, “Dental stem cell and dental tissue regeneration,” *Frontiers in Medicine*, vol. 13, no. 2, pp. 152–159, 2019.
- [105] H. N. Tang, Y. Xia, Y. Yu, R. X. Wu, L. N. Gao, and F. M. Chen, “Stem cells derived from “inflamed” and healthy periodontal ligament tissues and their sheet functionalities: a patient-matched comparison,” *Journal of Clinical Periodontology*, vol. 43, no. 1, pp. 72–84, 2016.
- [106] N. Liu, S. Shi, M. Deng et al., “High levels of  $\beta$ -catenin signaling reduce osteogenic differentiation of stem cells in inflammatory microenvironments through inhibition of the noncanonical Wnt pathway,” *Journal of Bone and Mineral Research*, vol. 26, no. 9, pp. 2082–2095, 2011.
- [107] D. Liu, J. Xu, O. Liu et al., “Mesenchymal stem cells derived from inflamed periodontal ligaments exhibit impaired immunomodulation,” *Journal of Clinical Periodontology*, vol. 39, no. 12, pp. 1174–1182, 2012.
- [108] C. Li, X. Wang, J. Tan, T. Wang, and Q. Wang, “The immunomodulatory properties of periodontal ligament stem cells isolated from inflamed periodontal granulation,” *Cells, Tissues, Organs*, vol. 199, no. 4, pp. 256–265, 2015.
- [109] D. J. Alongi, T. Yamaza, Y. Song et al., “Stem/progenitor cells from inflamed human dental pulp retain tissue regeneration potential,” *Regenerative Medicine*, vol. 5, no. 4, pp. 617–631, 2010.
- [110] A. Attar, M. B. Eslaminejad, M. S. Tavangar et al., “Dental pulp polyps contain stem cells comparable to the normal dental pulps,” *Journal of Clinical and Experimental Dentistry*, vol. 6, no. 1, pp. e53–e59, 2014.
- [111] Y. Li, X. Nan, T. Y. Zhong, T. Li, and A. Li, “Treatment of periodontal bone defects with stem cells from inflammatory dental pulp tissues in miniature swine,” *Tissue Engineering and Regenerative Medicine*, vol. 16, no. 2, pp. 191–200, 2019.
- [112] Y. D. Cho, K. H. Kim, H. M. Ryoo, Y. M. Lee, Y. Ku, and Y. J. Seol, “Recent advances of useful cell sources in the periodontal regeneration,” *Current Stem Cell Research & Therapy*, vol. 14, no. 1, pp. 3–8, 2019.
- [113] K. H. Chien, Y. L. Chang, M. L. Wang et al., “Promoting induced pluripotent stem cell-driven biomineralization and periodontal regeneration in rats with maxillary-molar defects using injectable BMP-6 hydrogel,” *Scientific Reports*, vol. 8, no. 1, p. 114, 2018.
- [114] Y. Tang, L. Liu, P. Wang, D. Chen, Z. Wu, and C. Tang, “Periostin promotes migration and osteogenic differentiation of human periodontal ligament mesenchymal stem cells via the Jun amino-terminal kinases (JNK) pathway under inflammatory conditions,” *Cell Proliferation*, vol. 50, no. 6, article e12369, 2017.
- [115] O. Andrukhov, C. Behm, A. Blufstein, and X. Rausch-Fan, “Immunomodulatory properties of dental tissue-derived mesenchymal stem cells: implication in disease and tissue regeneration,” *World Journal of Stem Cells*, vol. 11, no. 9, pp. 604–617, 2019.
- [116] S. Onizuka and T. Iwata, “Application of periodontal ligament-derived multipotent mesenchymal stromal cell sheets for periodontal regeneration,” *International Journal of Molecular Sciences*, vol. 20, no. 11, article 2796, 2019.
- [117] J. C. Park, J. M. Kim, I. H. Jung et al., “Isolation and characterization of human periodontal ligament (PDL) stem cells (PDLSCs) from the inflamed PDL tissue: in vitro and in vivo evaluations,” *Journal of Clinical Periodontology*, vol. 38, no. 8, pp. 721–731, 2011.
- [118] Y. Zhou, L. Zheng, X. Zhou, J. Li, and X. Xu, “Dental mesenchymal stem cells in inflamed microenvironment: potentials and challenges for regeneration,” *Current Stem Cell Research & Therapy*, vol. 10, no. 5, pp. 412–421, 2015.
- [119] L. Hu, Y. Liu, and S. Wang, “Stem cell-based tooth and periodontal regeneration,” *Oral Diseases*, vol. 24, no. 5, pp. 696–705, 2018.
- [120] A. F. Stadler, P. D. M. Angst, R. M. Arce, S. C. Gomes, R. V. Oppermann, and C. Susin, “Gingival crevicular fluid levels of cytokines/chemokines in chronic periodontitis: a meta-analysis,” *Journal of Clinical Periodontology*, vol. 43, no. 9, pp. 727–745, 2016.
- [121] X. Y. Zheng, C. Y. Mao, H. Qiao et al., “Plumbagin suppresses chronic periodontitis in rats via down-regulation of TNF- $\alpha$ , IL-1 $\beta$  and IL-6 expression,” *Acta Pharmacologica Sinica*, vol. 38, no. 8, pp. 1150–1160, 2017.
- [122] D. Whiting, W. O. Chung, J. D. Johnson, and A. Paranjpe, “Characterization of the cellular responses of dental mesenchymal stem cells to the immune system,” *Journal of Endodontia*, vol. 44, no. 7, pp. 1126–1131, 2018.
- [123] J. L. Chan, K. C. Tang, A. P. Patel et al., “Antigen-presenting property of mesenchymal stem cells occurs during a narrow window at low levels of interferon-gamma,” *Blood*, vol. 107, no. 12, pp. 4817–4824, 2006.
- [124] W. K. Chan, A. S. Y. Lau, J. C. B. Li, H. K. W. Law, Y. L. Lau, and G. C. F. Chan, “MHC expression kinetics and immunogenicity of mesenchymal stromal cells after short-term IFN- $\gamma$  challenge,” *Experimental Hematology*, vol. 36, no. 11, pp. 1545–1555, 2008.
- [125] H. Kato, Y. Taguchi, K. Tominaga, M. Umeda, and A. Tanaka, “Porphyromonas gingivalis LPS inhibits osteoblastic differentiation and promotes pro-inflammatory cytokine production in human periodontal ligament stem cells,” *Archives of Oral Biology*, vol. 59, no. 2, pp. 167–175, 2014.
- [126] Y. Liu, L. Wang, T. Kikuri et al., “Mesenchymal stem cell-based tissue regeneration is governed by recipient T lymphocytes via IFN- $\gamma$  and TNF- $\alpha$ ,” *Nature Medicine*, vol. 17, no. 12, pp. 1594–1601, 2011.
- [127] H. Yang, L. N. Gao, Y. An et al., “Comparison of mesenchymal stem cells derived from gingival tissue and periodontal ligament in different incubation conditions,” *Biomaterials*, vol. 34, no. 29, pp. 7033–7047, 2013.
- [128] T. Kukulj, D. Trivanović, I. O. Djordjević et al., “Lipopolysaccharide can modify differentiation and immunomodulatory potential of periodontal ligament stem cells via ERK1,2 signaling,” *Journal of Cellular Physiology*, vol. 233, no. 1, pp. 447–462, 2018.
- [129] A. Lawitschka, L. Ball, and C. Peters, “Nonpharmacologic treatment of chronic graft-versus-host disease in children and adolescents,” *Biology of Blood and Marrow Transplantation*, vol. 18, no. 1, pp. S74–S81, 2012.
- [130] Z. H. Zhang, W. Zhu, H. Z. Ren et al., “Mesenchymal stem cells increase expression of heme oxygenase-1 leading to anti-inflammatory activity in treatment of acute liver failure,” *Stem Cell Research & Therapy*, vol. 8, no. 1, p. 70, 2017.
- [131] P. Anderson, L. Souza-Moreira, M. Morell et al., “Adipose-derived mesenchymal stromal cells induce immunomodulatory



- macrophages which protect from experimental colitis and sepsis,” *Gut*, vol. 62, no. 8, pp. 1131–1141, 2013.
- [132] R. Domenis, A. Cifù, S. Quaglia et al., “Pro inflammatory stimuli enhance the immunosuppressive functions of adipose mesenchymal stem cells-derived exosomes,” *Scientific Reports*, vol. 8, no. 1, article 13325, 2018.
- [133] N. Donos, E. Calciolari, N. Brusselaers, M. Goldoni, N. Bostanci, and G. N. Belibasakis, “The adjunctive use of host modulators in non-surgical periodontal therapy. A systematic review of randomized, placebo-controlled clinical studies,” *Journal of Clinical Periodontology*, 2019.
- [134] S. A. Tassi, N. Z. Sergio, M. Y. O. Misawa, and C. C. Villar, “Efficacy of stem cells on periodontal regeneration: systematic review of pre-clinical studies,” *Journal of Periodontal Research*, vol. 52, no. 5, pp. 793–812, 2017.
- [135] Y. Wu, L. Xie, M. Wang et al., “Mettl3-mediated m<sup>6</sup>A RNA methylation regulates the fate of bone marrow mesenchymal stem cells and osteoporosis,” *Nature Communications*, vol. 9, no. 1, article 4772, 2018.
- [136] P. Bindal, T. S. Ramasamy, N. H. A. Kasim, N. Gnanasegaran, and W. L. Chai, “Immune responses of human dental pulp stem cells in lipopolysaccharide-induced microenvironment,” *Cell Biology International*, vol. 42, no. 7, pp. 832–840, 2018.
- [137] J. H. Kim, C. H. Jo, H. R. Kim, and Y. I. Hwang, “Comparison of immunological characteristics of mesenchymal stem cells from the periodontal ligament, umbilical cord, and adipose tissue,” *Stem Cells International*, vol. 2018, Article ID 8429042, 12 pages, 2018.
- [138] G. Sriram, V. P. Natu, I. Islam et al., “Innate immune response of human embryonic stem cell-derived fibroblasts and mesenchymal stem cells to periodontopathogens,” *Stem Cells International*, vol. 2016, Article ID 8905365, 15 pages, 2016.
- [139] L. Fiorillo, G. Cervino, A. Herford et al., “Interferon crevicular fluid profile and correlation with periodontal disease and wound healing: a systemic review of recent data,” *International Journal of Molecular Sciences*, vol. 19, no. 7, article 1908, 2018.
- [140] T. Vigo, C. Procaccini, G. Ferrara et al., “IFN- $\gamma$  orchestrates mesenchymal stem cell plasticity through the signal transducer and activator of transcription 1 and 3 and mammalian target of rapamycin pathways,” *The Journal of Allergy and Clinical Immunology*, vol. 139, no. 5, pp. 1667–1676, 2017.
- [141] M. Kibschull, S. J. Lye, S. T. Okino, and H. Sarras, “Quantitative large scale gene expression profiling from human stem cell culture micro samples using multiplex pre-amplification,” *Systems Biology in Reproductive Medicine*, vol. 62, no. 1, pp. 84–91, 2015.

## Research Article

# Cerebrospinal Fluid Pulsation Stress Promotes the Angiogenesis of Tissue-Engineered Laminae

Linli Li,<sup>1</sup> Yiqun He,<sup>1</sup> Han Tang,<sup>1</sup> Wei Mao,<sup>1</sup> Haofei Ni,<sup>1</sup> Feizhou Lyu <sup>1,2</sup> and Youhai Dong <sup>1</sup>

<sup>1</sup>Department of Orthopedics, Shanghai Fifth People's Hospital, Fudan University, China

<sup>2</sup>Department of Orthopedics, Huashan Hospital, Fudan University, China

Correspondence should be addressed to Feizhou Lyu; spinefeizhou@163.com and Youhai Dong; youhaidong1964@163.com

Received 2 March 2020; Revised 11 May 2020; Accepted 17 May 2020; Published 2 July 2020

Academic Editor: Huseyin Sumer

Copyright © 2020 Linli Li et al. This is an open access article distributed under the Creative Commons Attribution License, which permits unrestricted use, distribution, and reproduction in any medium, provided the original work is properly cited.

**Background.** Angiogenesis is a prerequisite step to achieve the success of bone regeneration by tissue engineering technology. Previous studies have shown the role of cerebrospinal fluid pulsation (CSFP) stress in the reconstruction of tissue-engineered laminae. In this study, we investigated the role of CSFP stress in the angiogenesis of tissue-engineered laminae. **Methods.** For the *in vitro* study, a CSFP bioreactor was used to investigate the impact of CSFP stress on the osteogenic mesenchymal stem cells (MSCs). For the *in vivo* study, forty-eight New Zealand rabbits were randomly divided into the CSFP group and the Non-CSFP group. Tissue-engineered laminae (TEL) was made by hydroxyapatite-collagen I scaffold and osteogenic MSCs and then implanted into the lamina defect in the two groups. The angiogenic and osteogenic abilities of newborn laminae were examined with histological staining, qRT-PCR, and radiological analysis. **Results.** The *in vitro* study showed that CSFP stress could promote the vascular endothelial growth factor A (VEGF-A) expression levels of osteogenic MSCs. In the animal study, the expression levels of angiogenic markers in the CSFP group were higher than those in the Non-CSFP group; moreover, in the CSFP group, their expression levels on the dura mater surface, which are closer to the CSFP stress stimulation, were also higher than those on the paraspinal muscle surface. The expression levels of osteogenic markers in the CSFP group were also higher than those in the Non-CSFP group. **Conclusion.** CSFP stress could promote the angiogenic ability of osteogenic MSCs and thus promote the angiogenesis of tissue-engineered laminae. The pretreatment of osteogenic MSC with a CSFP bioreactor may have important implications for vertebral lamina reconstruction with a tissue engineering technique.

## 1. Background

Tissue engineering techniques have been successfully used to repair the vertebral lamina defect. The reconstructed artificial laminae can reconstruct the posterior column structure of the spine, effectively reducing the occurrence of epidural scar tissue, nerve root adhesion, and spinal degradation [1, 2].

Previous studies have investigated the effect of biological and mechanical factors on the formation of the artificial vertebral laminae. The result revealed that the biological factors released from the bone end could initiate the early onset osteogenesis of the artificial laminae, and the mechanical stimulation of cerebrospinal fluid pulsation (CSFP) stress could promote the osteogenesis and remodeling of the artificial laminae [3, 4].

When bone defects are repaired using tissue engineering technology, angiogenesis is a prerequisite step to achieve the success of bone regeneration [5]. Many strategies have been used to enhance vascularization of tissue-engineered bone, such as a specific scaffold design, the addition of stem cells or angiogenic factors, *in vitro* prevascularization of tissue-engineered bone, and *in vivo* prevascularization [6–13]. Mesenchymal stem cells (MSCs) are among the most promising stem cell types for vascular tissue engineering and have been widely used among all the above-mentioned strategies [6, 7, 9], because MSCs not only can transdifferentiate into all cell lineages of three germ layers including blood vessel cells arising from mesodermal tissue but also can secrete a series of angiogenic factors, such as vascular endothelial growth factor (VEGF), Monocyte Chemoattractant

Protein 1 (MCP-1), Interleukin (IL-6), exosomes, and miRNAs [6, 7]. The expression levels of VEGF-A also elevated during MSC osteogenesis [14]. Previous studies have shown that mechanical stimulations, especially the fluid shear stress and cyclic strain, could induce MSCs towards vascular differentiation and MSCs to express angiogenic factors [7]. But few studies are investigating the role of pulsation stress, especially the CSFP stress, on the angiogenic abilities of MSCs.

CSFP is a continuous pulsation stress caused by heartbeat and respiration, and it changes with cardiac and respiratory rhythms [15]. In rabbits, the spinal dura mater pumped like a blood vessel with cerebrospinal fluid flowing inside, creating the cerebrospinal fluid pulsation stress. And the previous study confirmed that the CSFP stress at the lumbar vertebrae ranged from 10 to 20 mm water pressure, with a frequency of 3-4 Hz [3]. Therefore, we made a speculation that the CSFP stress could promote the angiogenic factor expressions of MSCs and then promote the angiogenesis of tissue-engineered laminae (Figure 1(a)).

Thus, in this study, we aimed to investigate the role of CSFP stress on the angiogenic ability of tissue-engineered laminae (TEL) constructed by osteogenic MSCs and hydroxyapatite-collagen I scaffold. For the *in vitro* study, we used the CSFP bioreactor to investigate the impact of CSFP stress on the osteogenic Wharton jelly mesenchymal stem cells (MSCs). For the *in vivo* study, we implanted TEL into the lamina defect site in both CSFP and Non-CSFP groups. Then, the angiogenic and osteogenic abilities of newborn laminae were examined with histological staining, qRT-PCR, and radiological analysis for up to 12 weeks postimplantation.

## 2. Materials and Methods

**2.1. Intervention of Osteogenic MSCs in the CSFP Bioreactor.** The MSCs we used in this study were isolated from rabbit umbilical cord Wharton's jelly. The isolation, culture, and osteogenic differentiation of MSCs were described in the previous article [3]. After 14 days of culture in the osteogenic medium (containing 10 nM dexamethasone, 10 mM  $\beta$ -glycerophosphate sodium, 50 mg/ml ascorbic acid, and 10 nM 1,25-dihydroxy vitamin D<sub>3</sub>, Sigma-Aldrich, USA), the osteogenic WJ-MSCs were used for the following experiments.

Under the sterile condition, the PLGA scaffolds (Nuoqi, Chongqing, China) were cut to the size of 40 mm  $\times$  15 mm  $\times$  0.1 mm. The osteogenic MSCs were trypsinized and resuspended in media at a concentration of  $1 \times 10^6$ /ml. Then, 100  $\mu$ l cell suspension was pipetted on one side of each scaffold and cultured in Petri dishes in the incubator at 37°C under a 5% CO<sub>2</sub> atmosphere. After 2 hours, the osteogenic medium was added, and all constructs were placed in the osteogenic medium for 8 hours before being fixed in the bioreactor.

The setting condition of the CSFP bioreactor was as below: flow velocity, 6 cm/s; frequency, 3 Hz. For the CSFP +osteogenic MSC group, the constructs were fixed by the clip on the pulsation tube in the CSFP bioreactor. For the osteo-

genic MSC group, the constructs were fixed by the clip on the control tube in the CSFP bioreactor. And we used undifferentiated MSCs seeded on the PLGA scaffolds as the control group for qRT-PCR analysis. After 24 hours, the constructs were taken out for qRT-PCR analysis and immunofluorescence assay of VEGF-A (Figure 2).

**2.2. Tissue-Engineered Lamina Construction.** The protocol was approved by the Committee on the Ethics of Animal Experiments of Fudan University (No. 20150482A168). The hydroxyapatite-collagen I scaffold was bought from the Beijing Allgens Medical Science & Technology Co., Ltd. Under the sterile condition, the hydroxyapatite-collagen I scaffold was cut to the size of 10 mm  $\times$  8 mm  $\times$  1 mm. After 2 weeks of culture in osteogenic medium, osteo-differentiated MSCs were trypsinized and resuspended in media at a concentration of  $1 \times 10^6$ /ml. Then, 100  $\mu$ l cell suspension was pipetted on one side of each scaffold, and after 30 min, 100  $\mu$ l cell suspension was pipetted on the other side. All constructs were placed in the osteogenic medium for another week before implantation.

In order to observe the cell activity on the scaffold, the osteogenic MSCs in the scaffolds were stained with live/dead (Thermo Fisher, USA) and the nucleus was counterstained with DAPI (Southern Biotech, USA). And the constructs were observed under a confocal microscope (ZEISS).

**2.3. Construction of CSFP and Non-CSFP Rabbit Models.** Forty-eight 2-month-old male rabbits weighing  $2.25 \pm 0.25$  kg were randomly divided into the CSFP group ( $n = 24$ ) and the Non-CSFP group ( $n = 24$ ). The animals were anesthetized with pentobarbital sodium (1 ml/kg intraperitoneally). The surgical procedures of making rabbit models were described in below.

For rabbits in the CSFP group, we located the spinous process of fifth lumbar vertebrae by the anatomical landmark and made a 3 cm longitudinal skin incision. The superficial fascia and paraspinal muscle were retracted to expose the spinous process, which was then removed to expose the native laminae. At last, a bone defect measuring 10 mm  $\times$  8 mm was created on the native laminae by a rongeur to expose the dura. The removal of native laminae left two flesh cancellous bone ends measuring 10 mm  $\times$  2 mm. The TEL was fixed in the bone defect (Figure 1(b)).

For rabbits in the Non-CSFP group, we removed the paraspinal muscle with a detacher to expose the spinous process and laminae and then removed the spinous process by a rongeur. By removing the spinous process, a cancellous bone end measuring 10 mm  $\times$  4 mm was created, similar to that of the CSFP group (10 mm  $\times$  2 mm  $\times$  2), while preserving the dura surface cortex of laminae. The TEL was fixed onto the lamina defect site (Figure 1(c)).

**2.4. Immunofluorescence Assay.** For the MSC-PLGA constructs, the constructs were fixed with 3% paraformaldehyde in PBS for 10 min. Nonspecific binding was then reduced by incubating cells with 5% BSA (Gibco, USA) for 30 min. VEGF-A was then labeled with its specific primary antibody (Abcam; cat. no. ab1316; 5  $\mu$ g/ml) for 12 hours at 4°C. Cells

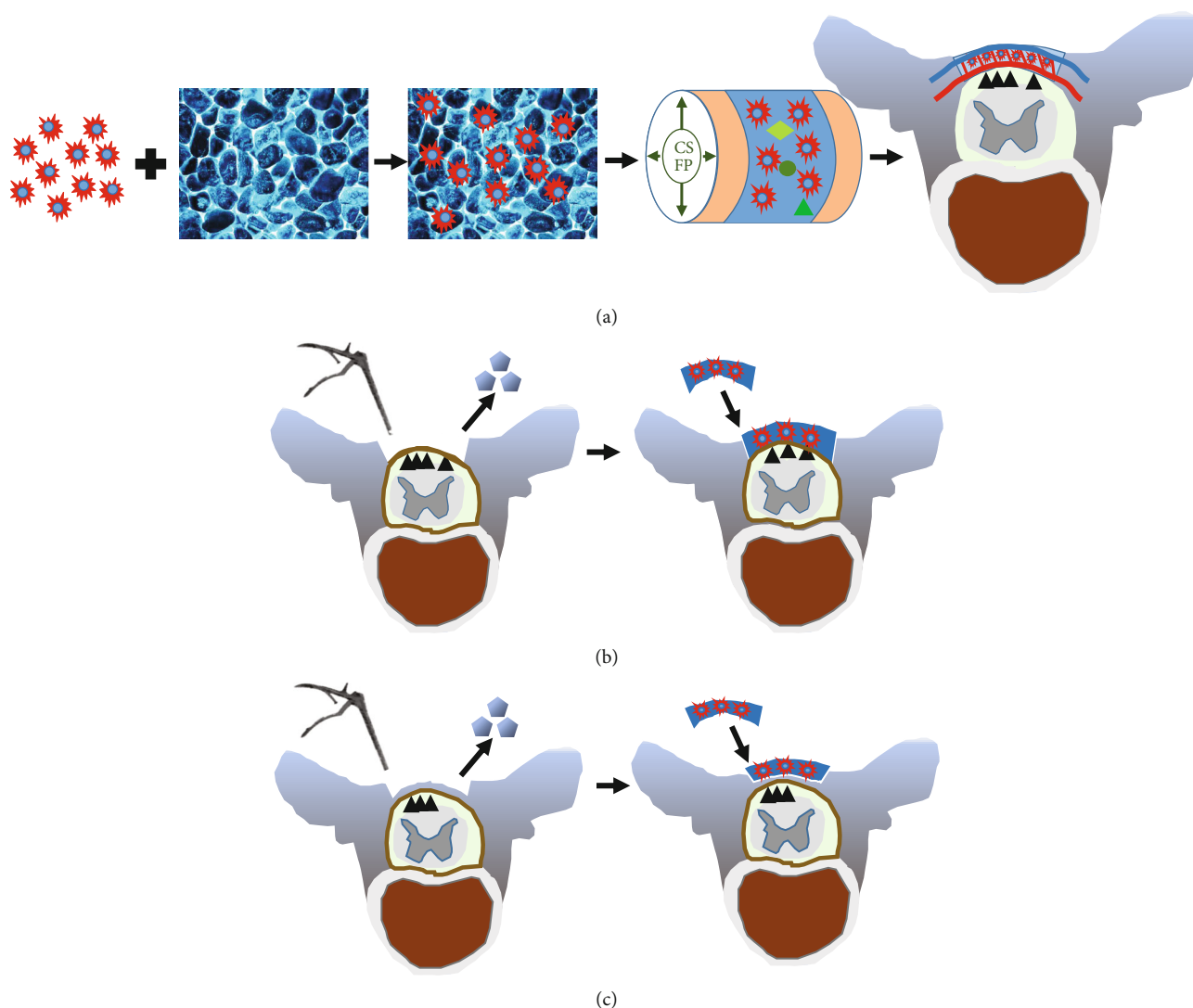


FIGURE 1: (a) Schematic illustration of the effects of CSFP stress on the angiogenesis of tissue-engineered laminae. (b) The diagrammatic sketch of the CSFP animal model. The native laminae were removed by rongeur, and then, the TEL was implanted into the laminae defect. (c) The diagrammatic sketch of the Non-CSFP animal model. The outer cortex of the native laminae was removed by rongeur, and then, the tissue-engineered laminae (TEL) was implanted onto the inner cortex.

were then washed with PBS and incubated with rabbit anti-mouse horseradish peroxidase-conjugated secondary antibodies (Jackson ImmunoResearch Laboratories, Inc. USA; dilution, 1:100) for 1 hour and DAPI Fluoromount G (Southern Biotech, USA) for 5 min. Each sample was then imaged using a fluorescence inversion microscope system (Leica, Germany) with dual excitations.

**2.5. Micro-CT (Computed Tomography) Examination.** The tissue specimens were harvested in the 2<sup>nd</sup>, 4<sup>th</sup>, 8<sup>th</sup>, and 12<sup>th</sup> weeks after implantation and were immediately fixed in freshly prepared 4% (*w/v*) paraformaldehyde. The osteogenesis of specimens was examined using micro-CT at the Shanghai Public Health Clinical Center. The 3D model was reconstructed manually using the GEHC MieroView2.0+ABA software. The threshold was set at 1000 for all the samples,

except the sample of the Non-CSFP group at the 2<sup>nd</sup> week (threshold = 500).

**2.6. Histological Staining.** After the micro-CT examination, the tissue specimens were decalcified with 10% ethylenediaminetetraacetic acid for 4 weeks. Tissue sections with 6  $\mu\text{m}$  thickness were cut on a microtome and mounted onto glass slides. The sections were processed for routine histological analysis by hematoxylin-eosin (HE) staining and immunohistochemistry (IHC) staining.

**2.7. IHC Staining.** After baking for 2 h at 60°C, the sections were dewaxed with xylenes and then rehydrated through a series of graded ethanol to distilled water. Endogenous peroxidase activity was blocked with 0.3% hydrogen peroxide for 30 min at 37°C. For antigen retrieval, the sections were submerged in sodium citrate buffer (pH 6.0) for 10 min and



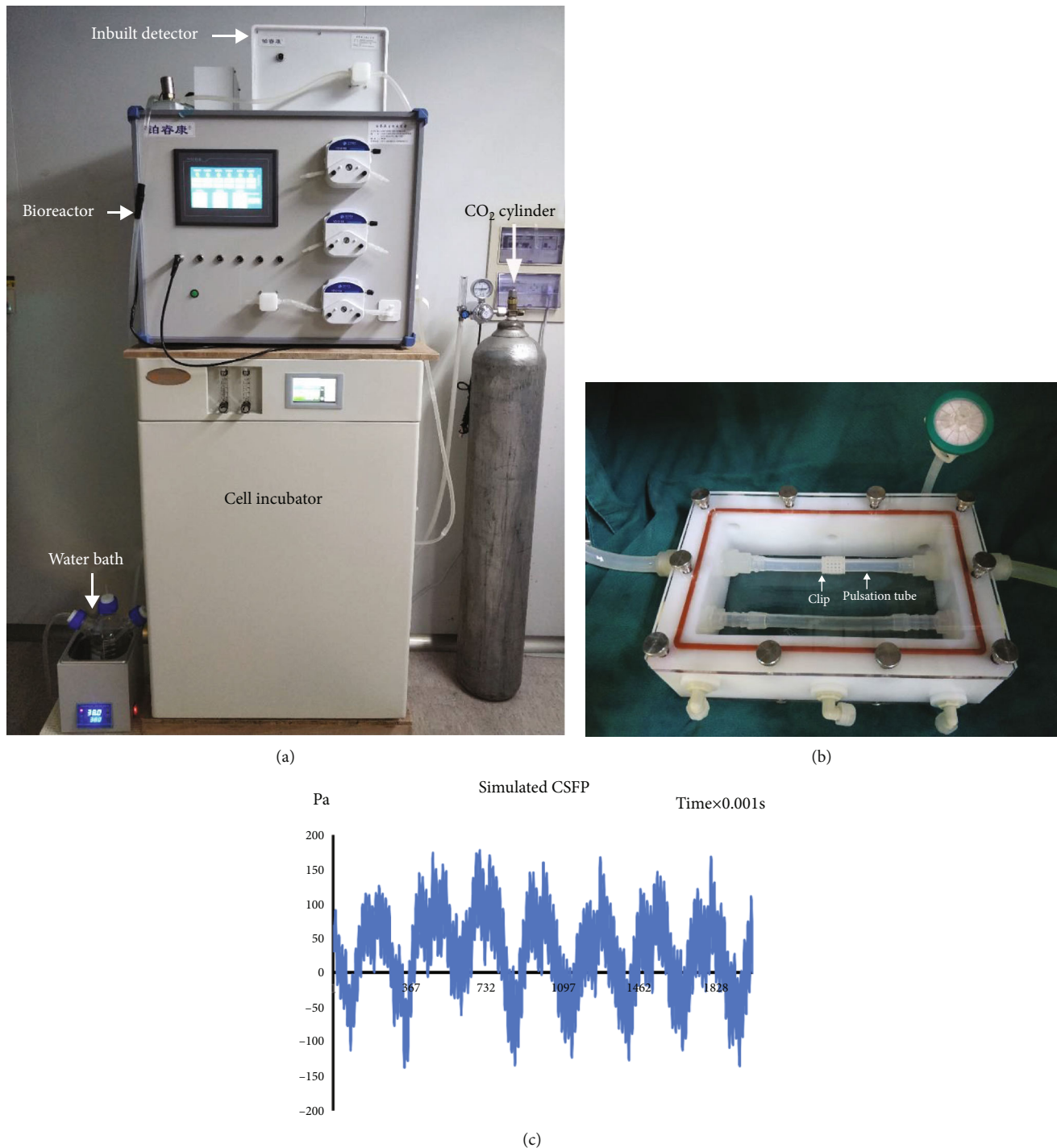


FIGURE 2: Cerebrospinal fluid pulsation bioreactor system. (a) The modules of the bioreactor system. (b) The response chamber, which was placed in the cell incubator, and the cell sheets were placed between the clip and the pulsation tube. (c) The simulated waves of CSFP stress by the bioreactor system.

then incubated with normal goat serum for 30 min at 37°C to reduce the nonspecific binding. The mouse anti-PECAM1 (Invitrogen; cat. no. MA5-13188), anti-bFGF (Abbiotec, cat. no. 250559), and anti-BMP2 (Abcam, cat. no. ab6285) were applied at the dilution of 1:50 overnight at 4°C and followed by incubation with horseradish peroxidase- (HRP-) conjugated secondary antibodies (Changdao, China). After rinsing, staining was performed with DAB and counterstained

with hematoxylin to display the nucleus. Each slide was imaged using the inversion microscope system (Leica, Germany). The images were analyzed by the software of Image J.

For immunofluorescence assay, the processing of the slides was the same as the above. PECAM1 was then labeled with its specific primary antibody (Servicebio; cat. no. GB13063; dilution, 1:50) for 12 hours at 4°C. Then, the sections were washed with PBS and incubated with donkey

anti-rabbit horseradish peroxidase-conjugated secondary antibodies (Servicebio; cat. no. GB21404; dilution, 1:300) for 1 hour and DAPI (Servicebio; cat. no. G1012) for 10 min. The slides were sealed with antifluorescence quenching sealant. Each slide was imaged using a fluorescence inversion microscope system (Leica, Germany) with dual excitations.

**2.8. Quantitative Real-Time PCR.** For MSC-PLGA constructs, the total RNA was extracted from the constructs using TRIzol® Reagent (Life Technologies, USA). All RNA samples were then treated with RNase-free DNase I (Qiagen, Valencia, CA) to digest the genomic DNA. Aliquots of 500 ng total RNA were reverse transcribed to cDNA using the PrimeScript™ RT Master Mix (TaKaRa, Japan). Quantitative real-time PCR (qRT-PCR) was performed using a 7900 Real-Time PCR System (Applied Biosystems) with the Power SYBR Green PCR Master Mix (Applied Biosystems, Warrington, UK). The relative gene expression was calculated using the following equation:  $\Delta Ct = Ct(VEGF-A) - Ct(CTB)$ ;  $\Delta\Delta Ct = \Delta Ct(\text{CSFP+osteogenic MSCs/osteogenic MSCs}) - \Delta Ct(\text{undifferentiated MSCs})$ ; fold change =  $2^{-\Delta\Delta Ct}$ .

For the animal study, tissue specimens were harvested in the 2<sup>nd</sup>, 4<sup>th</sup>, 8<sup>th</sup>, and 12<sup>th</sup> weeks after implantation and immediately immersed in the TRIzol® Reagent (Life Technologies, USA). Native laminae were also harvested in the 0<sup>th</sup> week as the normal laminae. The tissue specimens were then grounded until there was no obvious tissue residual. Total RNA was extracted from the grounded tissue using TRIzol® Reagent. The following procedures were the same as mentioned above. The relative gene expression was calculated using the following equation:  $\Delta Ct = Ct(\text{test genes}) - Ct(CTB)$ ;  $\Delta\Delta Ct = \Delta Ct(\text{artificial laminae}) - \Delta Ct(\text{normal laminae})$ ; fold change =  $2^{-\Delta\Delta Ct}$ .

The gene-specific primers used for *PECAM-1*, *VEGF-A*, *OCG-3*, *Osterix*, and *ACTB* are listed in Table 1.

**2.9. Statistical Analysis.** Each experiment was repeated three times. Statistical analyses were performed using SPSS version 19.0 for Windows. One-way analysis of variance (ANOVA) was used to confirm comparisons of the variables. Significance was identified as a *p* value of less than 0.05. \* represents *p* values < 0.05.

### 3. Results

**3.1. CSFP Bioreactor.** The *VEGF-A* mRNA expression level in the CSFP+osteogenic MSC group was significantly higher than that in the osteogenic MSC group and the undifferentiated group. The IF staining of *VEGF-A* also showed that the CSFP+osteogenic MSC group had higher *VEGF-A* expression (Figure 3).

**3.2. TEL Construction.** The live/dead staining showed that almost all the osteogenic MSCs survived 7 days after implantation into hydroxyapatite-collagen I scaffold, and the cells tightly adhered to the trabeculae structure of the scaffold. The scaffold has blue autofluorescence (Figure 4).

**3.3. Micro-CT Examination.** In the CSFP group, the artificial laminae grew gradually from the two sides of bone ends to

the middle, and the bone defect narrowed correspondingly. In the 12<sup>th</sup> week, the artificial laminae on dural surface realized symphysis, with a similar arch and smoothness with the native laminae, while the artificial laminae on the paraspinal muscle surface had not realized symphysis (Figures 5(a)–5(d)).

In the Non-CSFP group, the ectopic artificial laminae grew from the paraspinal muscle side towards the native laminae side. From the 2<sup>nd</sup> week to the 12<sup>th</sup> week, the number of bone trabeculae on the paraspinal muscle surface of the artificial ectopic laminae increased gradually, while there was little trabecula formation on the native laminae side (Figures 5(e)–5(h)).

**3.4. HE Staining.** In the CSFP group, the artificial laminae grew from the two sides of the bone ends to the middle. The bone growth rate on the dural surface was higher than that on the paraspinal muscle surface. In the 8<sup>th</sup> week, the lamina defect was less than 200  $\mu\text{m}$ ; the trabecula amount of the artificial laminae on the dural surface was higher than that on the paraspinal muscle surface (Figure 6(b)). In the 12<sup>th</sup> week, the laminae on the dural surface were completely developed, showing similar trabecula structure and curvature to the native laminae; however, the artificial laminae on the paraspinal muscle surface were still undergoing osteogenesis (Figures 6(c), 6(g), and 6(h)).

In the Non-CSFP group, the artificial ectopic laminae grew from the paraspinal muscle side towards the native laminae side. The trabecula density and amount of the artificial ectopic laminae on the paraspinal muscle surface were higher than those on the native laminae side. From 4 weeks to 12 weeks, the number of trabeculae increased, but the arrangement of the trabecular bone was always disorganized (Figures 6(d)–6(f)). Besides, the osteogenesis process resembled endochondral ossification (Figure 6(d)).

**3.5. Angiogenesis.** The angiogenesis of the two groups was analyzed through the protein expression levels of *PECAM-1* and bFGF and the mRNA expression levels of *PECAM-1* and *VEGF-A*. They showed similar expression trends.

IHC staining showed that the expression levels of *PECAM-1* in the CSFP group increased from the 2<sup>nd</sup> week to the 8<sup>th</sup> week and then decreased from the 12<sup>th</sup> week, while the expression levels of *PECAM-1* in the Non-CSFP group increased slowly from the 2<sup>nd</sup> week to the 12<sup>th</sup> week, and the protein expression levels of *PECAM-1* in the CSFP group were significantly higher than those in the Non-CSFP group in the 2<sup>nd</sup>, 4<sup>th</sup>, and 8<sup>th</sup> weeks (*p* < 0.05) (Figures 7(a)–7(g)).

The protein expression levels of bFGF in the CSFP group increased from the 2<sup>nd</sup> week to the 8<sup>th</sup> week and then decreased from the 12<sup>th</sup> week, while the expression levels of bFGF in the Non-CSFP group increased from the 2<sup>nd</sup> week to the 12<sup>th</sup> week; the expression levels of bFGF in the CSFP group were significantly higher than those in the Non-CSFP group in the 2<sup>nd</sup> and 4<sup>th</sup> weeks (*p* < 0.05). (Figures 8(a)–8(e)).

The mRNA expression trends of *PECAM-1* and *VEGF-A* were consistent with the protein expression trends of *PECAM-1* and bFGF, and the mRNA expression levels of

TABLE 1: Sequences of oligonucleotide primers used for quantitative real-time qRT-PCR.

Genes	Forward primer (5'-3')	Reverse primer (5'-3')
OSTERIX	GCA CGA AGA AGC CAT ACT C	TGA CAG AAG CCC ATT GGT
OCG3	CGG CTA CAC CAT TGG GAT GT	GCG GGA TCG ACA ATA GGG TT
VEGFA	TAA ACC CCA CGA AGT GGT GA	TGA CGT TGA ACT CCT CGG TG
PECAM1	AGA AGT GGA AGT GTC CTC GGT G	GAG CCT TCC GTC CTA GAG TAT CTG
ACTB	CCC GAC AGC CAG GTC ATC	GTT GAA GGT GGT CTC GTG G

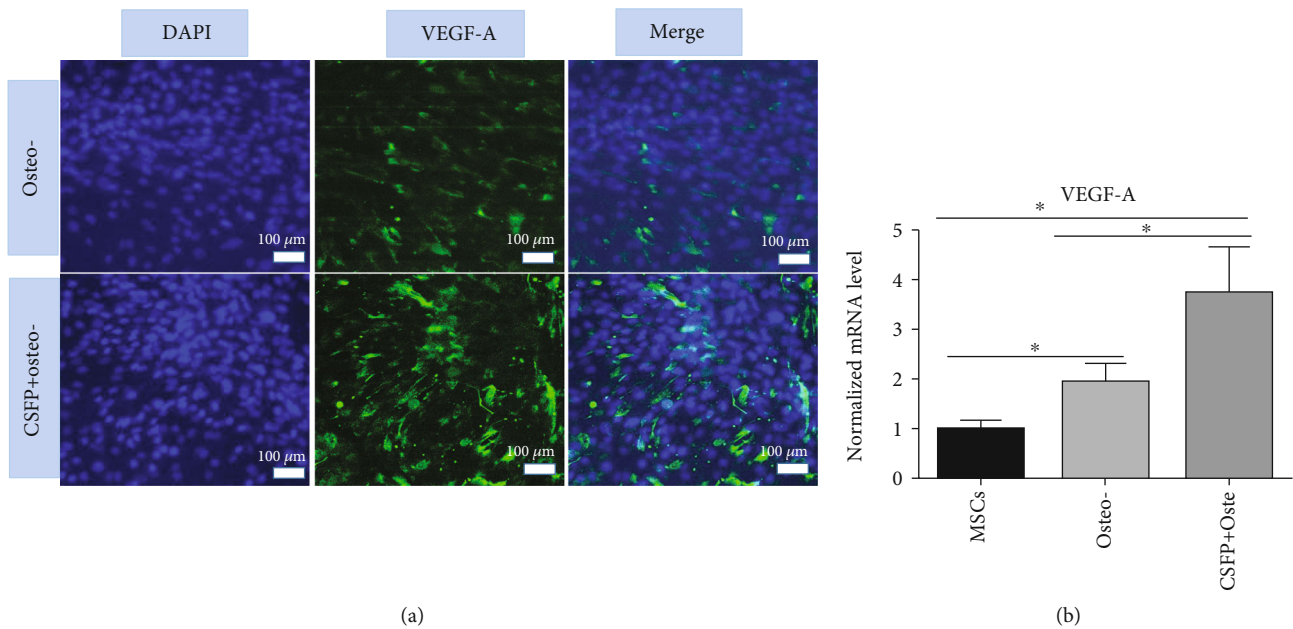


FIGURE 3: The VEGF-A expression of osteogenic WJ-MSCs with/without CSFP stimulation in the CSFP bioreactor system. (a) IF staining showed the CSFP+osteogenic WJ-MSC group had higher VEGF-A expression levels. (b) QRT-PCR assay showed the CSFP+osteogenic WJ-MSC group had higher VEGF-A mRNA expression levels.

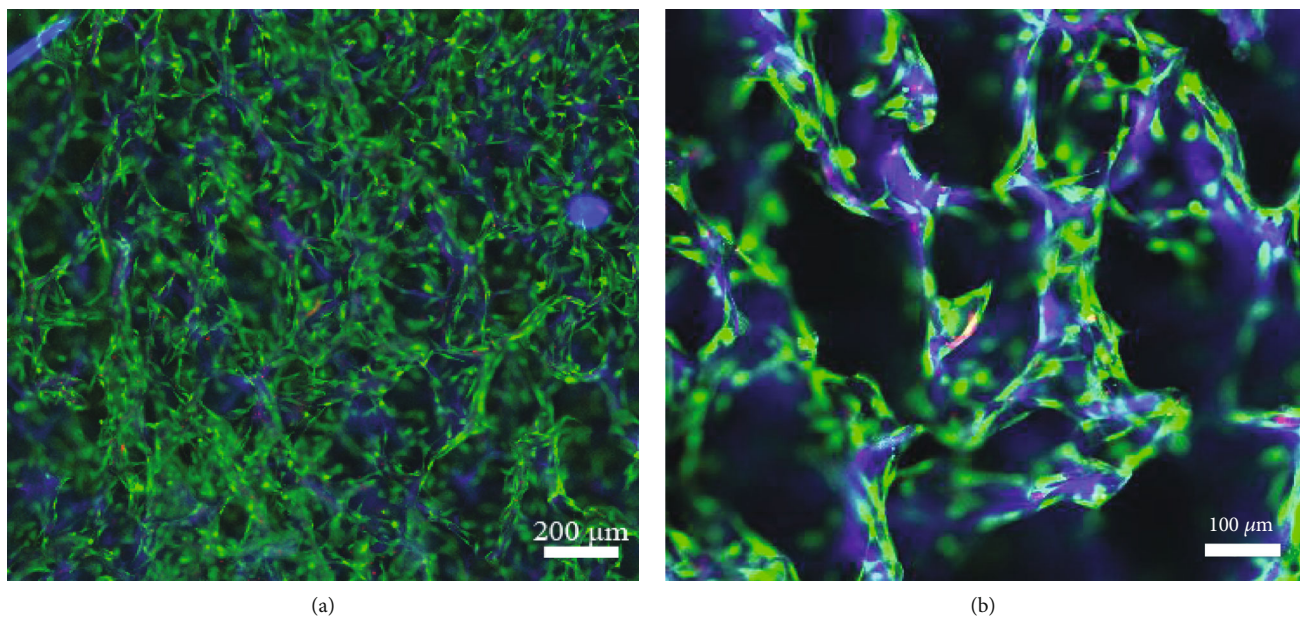


FIGURE 4: The live/dead staining of the TEL made by osteogenic and hydroxyapatite-collagen I scaffold. The scaffold had blue autofluorescence.



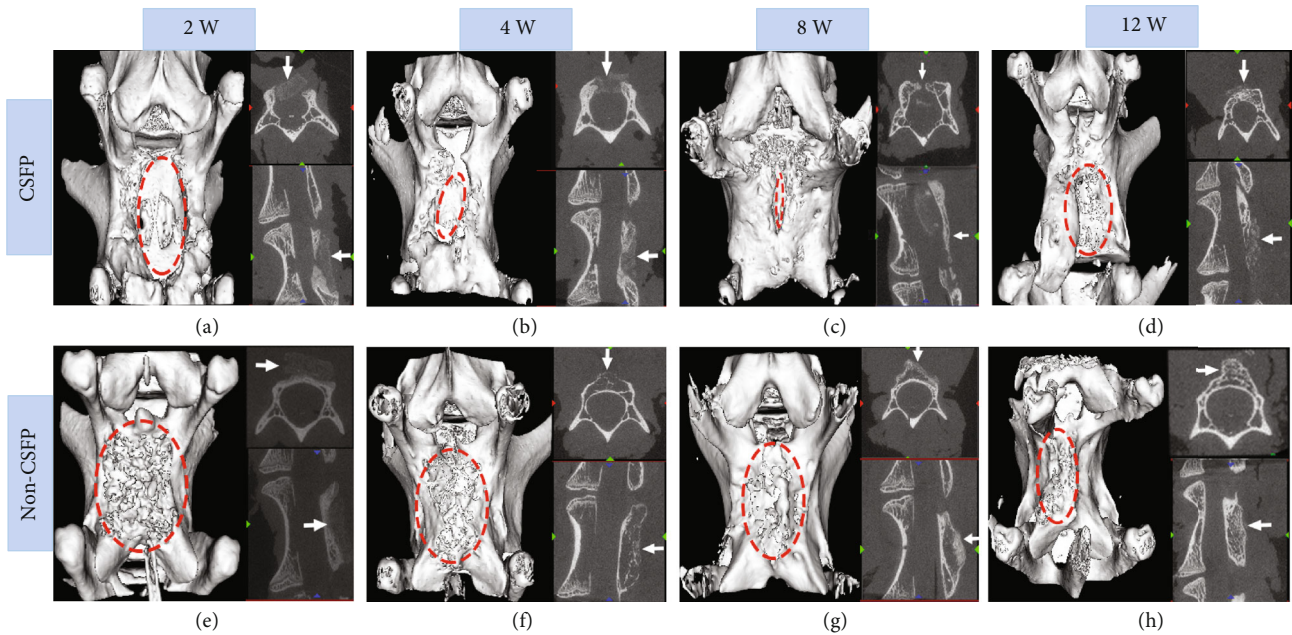


FIGURE 5: The 3D reconstruction pictures of the newborn laminae in the CSFP and Non-CSFP groups at the 2<sup>nd</sup>, 4<sup>th</sup>, 8<sup>th</sup>, and 12<sup>th</sup> weeks. The dashed red oval in images (a), (b), and (c) showed the laminae defect, and the dashed red oval in other images showed the observation area.

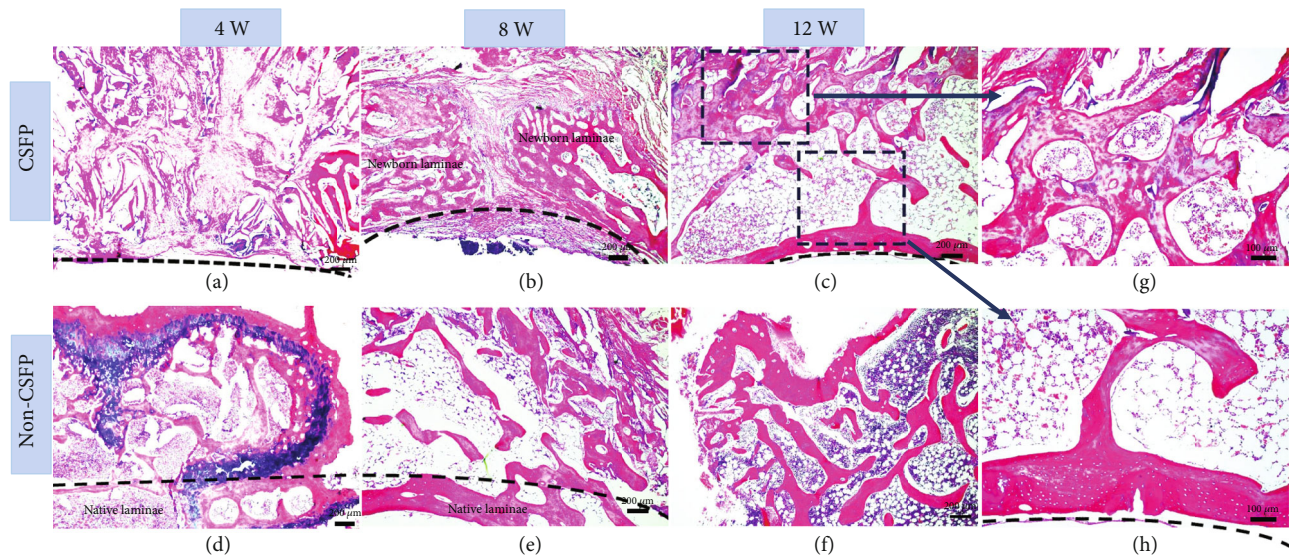


FIGURE 6: (a–f) Representative images of HE staining of newborn laminae in the CSFP group and the Non-CSFP group at the 4<sup>th</sup>, 8<sup>th</sup>, and 12<sup>th</sup> weeks. (g) The paraspinous surface of the newborn laminae in the 12<sup>th</sup> week. (h) The dural surface of the newborn laminae in the 12<sup>th</sup> week. The dashed line in images (a), (b), (c), and (h) showed the vertebral canal. The dashed line in images (d) and (e) showed the outer cortex of native laminae.

*PECAM-1* and *VFGF-A* in the CSFP group were significantly higher than those in the Non-CSFP group in the 2<sup>nd</sup>, 4<sup>th</sup>, and 8<sup>th</sup> weeks ( $p < 0.05$ ) (Figures 7(h) and 8(f)).

Moreover, in the CSFP group, the protein expression levels of bFGF on the dural surface were higher than those on the paraspinous muscle surface in the 8<sup>th</sup> week (Figure 8(a)). In the 12<sup>th</sup> week, the undeveloped artificial laminae on the paraspinous muscle surface showed higher

expression levels of *PECAM-1* than the developed artificial laminae on the dural surface (Figures 7(b), 7(e), and 7(f)).

Immunofluorescence staining showed, in the CSFP group, an abundance of organized small vessels in the artificial laminae in the 8<sup>th</sup> week, and the vessels became more developed in the 12<sup>th</sup> week. In the Non-CSFP group, few vessels formed near the native laminae side in the ectopic artificial laminae in the 8<sup>th</sup> week, and many small vessels



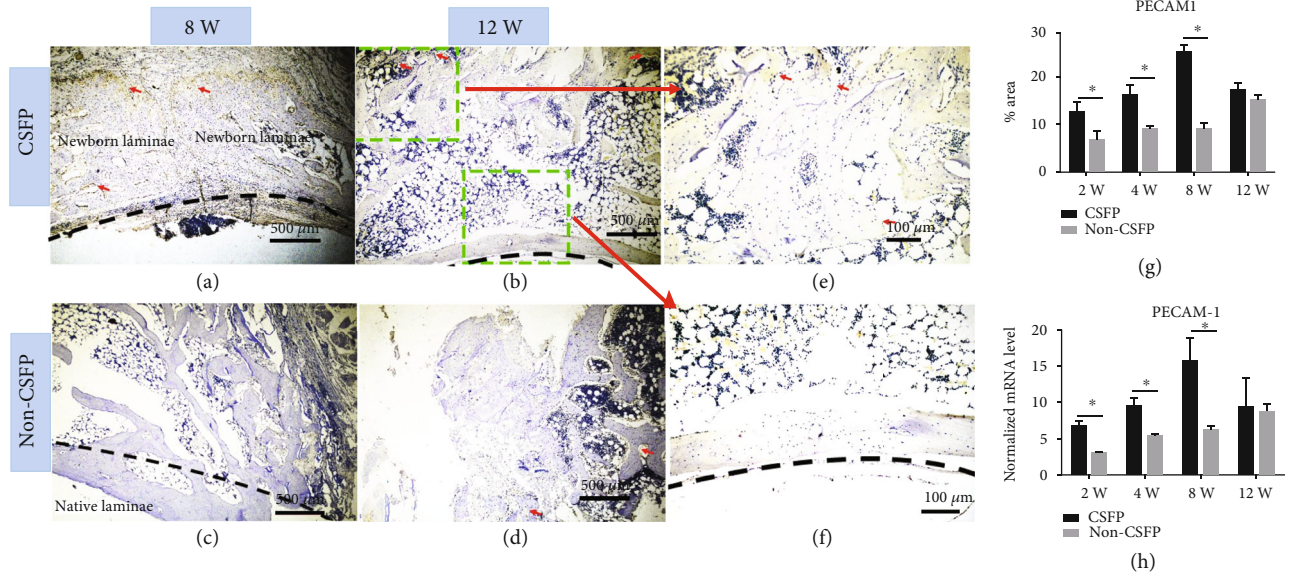


FIGURE 7: (a–d) Representative images of PECAM1 IHC staining of newborn laminae in the CSFP group and the Non-CSFP group at the 4<sup>th</sup> and 8<sup>th</sup> weeks. (e) The PECAM1 IHC staining of the paraspinal surface of the newborn laminae in the 12<sup>th</sup> week. (f) The PECAM1 IHC staining of the dural surface of the newborn laminae in the 12<sup>th</sup> week. (g) Quantification of PECAM1 expression by IHC staining. (h) QRT-PCR analysis of PECAM1 expressions. The red arrow showed positive staining. The dashed line in images (a), (b), and (f) showed the vertebral canal. The dashed line in images (c) showed the outer cortex of native laminae.

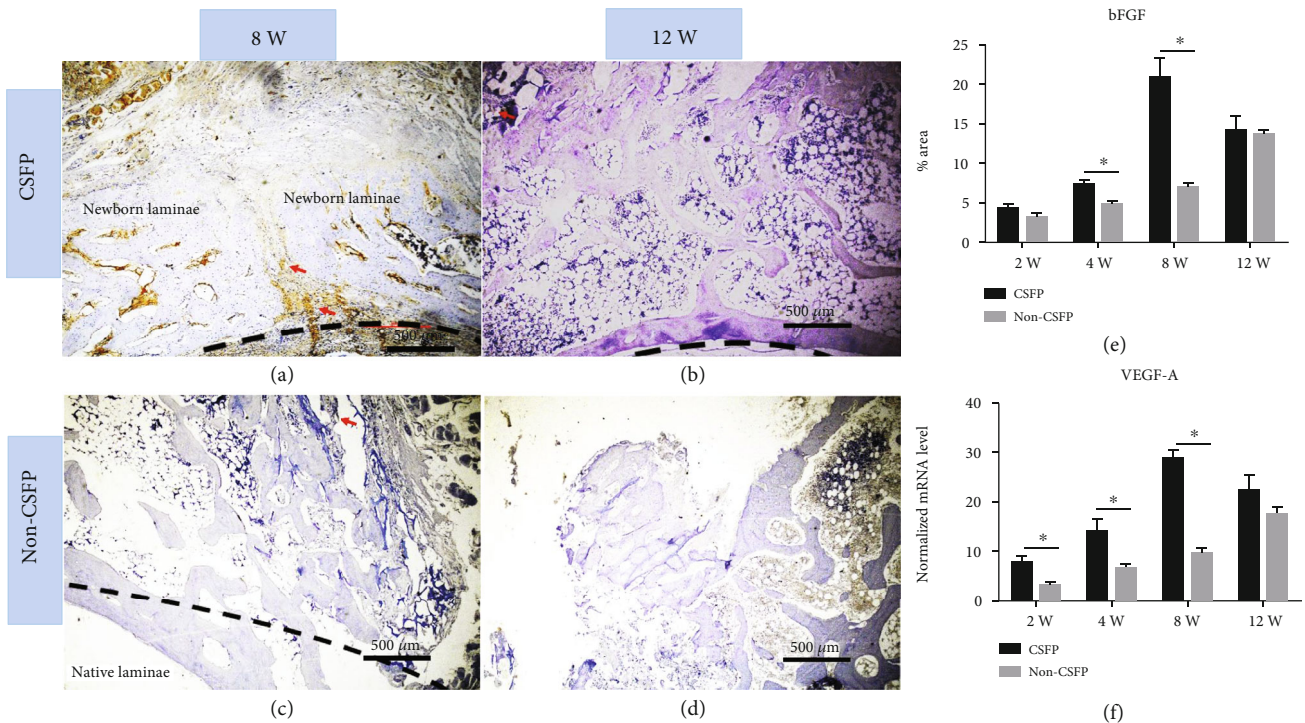


FIGURE 8: (a–d) Representative images of bFGF IHC staining of newborn laminae in the CSFP group and the Non-CSFP group in the 8<sup>th</sup> and 12<sup>th</sup> weeks. (e) Quantification of bFGF expression by IHC staining. (f) QRT-PCR analysis of *VEGF-A* expressions. The red arrow showed positive staining. The dashed line in images (a) and (b) showed the vertebral canal. The dashed line in images (c) showed the outer cortex of native laminae.

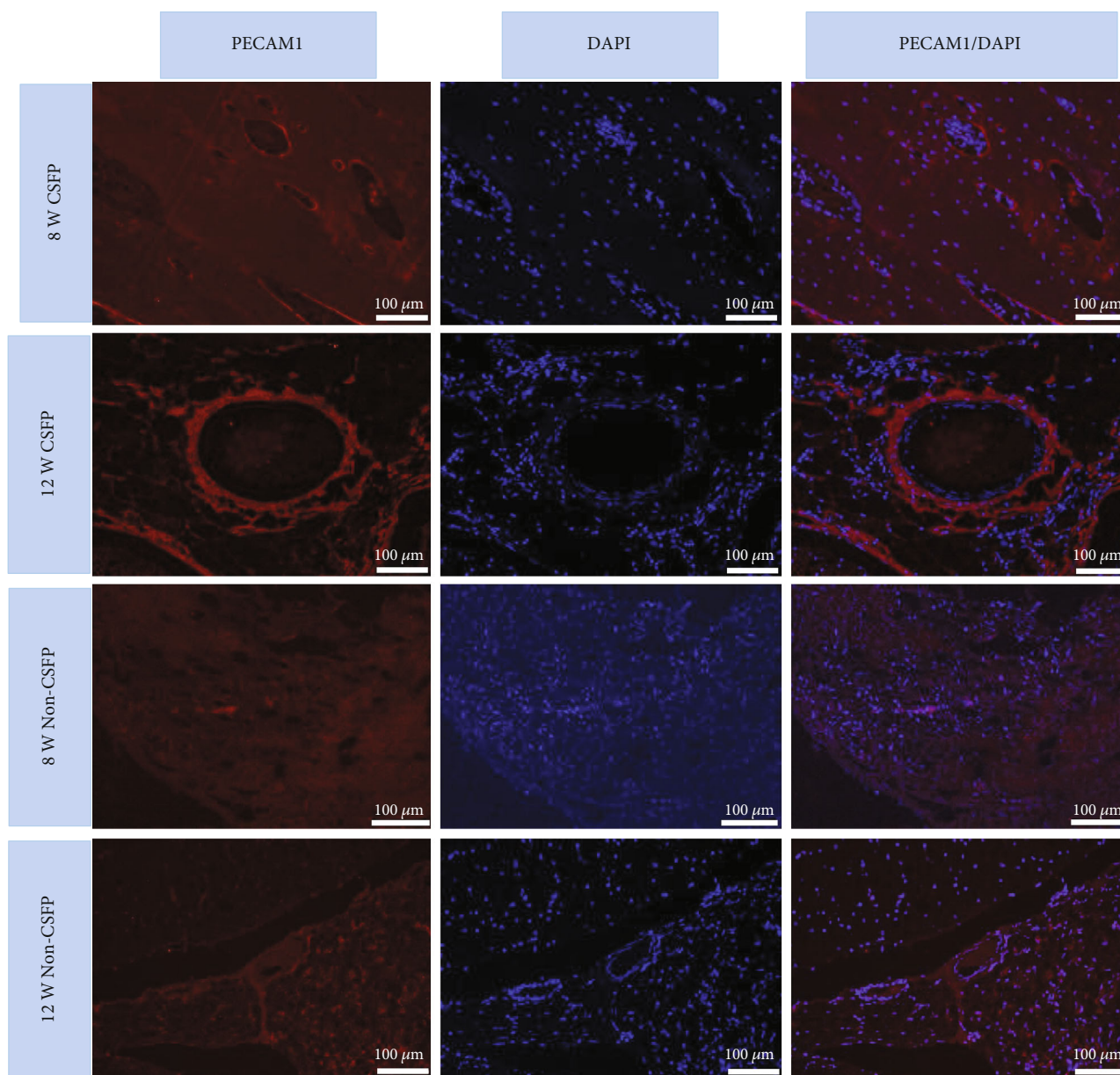


FIGURE 9: Immunofluorescence staining of PECAM1 of the newborn laminae in the CSFP group in the 8<sup>th</sup> and 12<sup>th</sup> weeks.

formed near the paraspinal surface side in the ectopic artificial laminae at the 12<sup>th</sup> week (Figure 9).

**3.6. Osteogenesis.** The osteogenesis of the two groups was analyzed through the protein or mRNA expression levels of the osteogenic markers of BMP-2, Osterix, and OCG-3.

IHC staining showed that the expression levels of BMP-2 in the CSFP group increased from the 2<sup>nd</sup> week to the 8<sup>th</sup> week and decreased in the 12<sup>th</sup> week, while its expression levels in the Non-CSFP group increased slowly from the 2<sup>nd</sup> week to the 12<sup>th</sup> week, and the expression levels of BMP-2 in the CSFP group were significantly higher than those in the Non-CSFP group in the 2<sup>nd</sup>, 4<sup>th</sup>, and 8<sup>th</sup> weeks ( $p < 0.05$ ) (Figures 10(a)–10(f) and 10(i)).

The mRNA expression of the *Osterix* increased from the 2<sup>nd</sup> week to the 12<sup>th</sup> week, and the mRNA expression levels of the *Osterix* in the CSFP group were significantly higher than those in the Non-CSFP group in the 2<sup>nd</sup>, 4<sup>th</sup>, and 8<sup>th</sup> weeks ( $p < 0.05$ ) (Figure 10(j)). The mRNA expression levels of *OCG-3* in the CSFP group increased from the 2<sup>nd</sup> week to the 12<sup>th</sup> week in both groups; the mRNA expression levels of *OCG-3* in the CSFP group were significantly higher than those in the Non-CSFP group in the 8<sup>th</sup> and 12<sup>th</sup> weeks ( $p < 0.05$ ) (Figure 10(k)).

Moreover, in the CSFP group, the protein expression levels of BMP-2 on the dural surface were higher than those on the paraspinal muscle surface in the 8<sup>th</sup> week (Figure 10(b)). In the 12<sup>th</sup> week, the undeveloped artificial



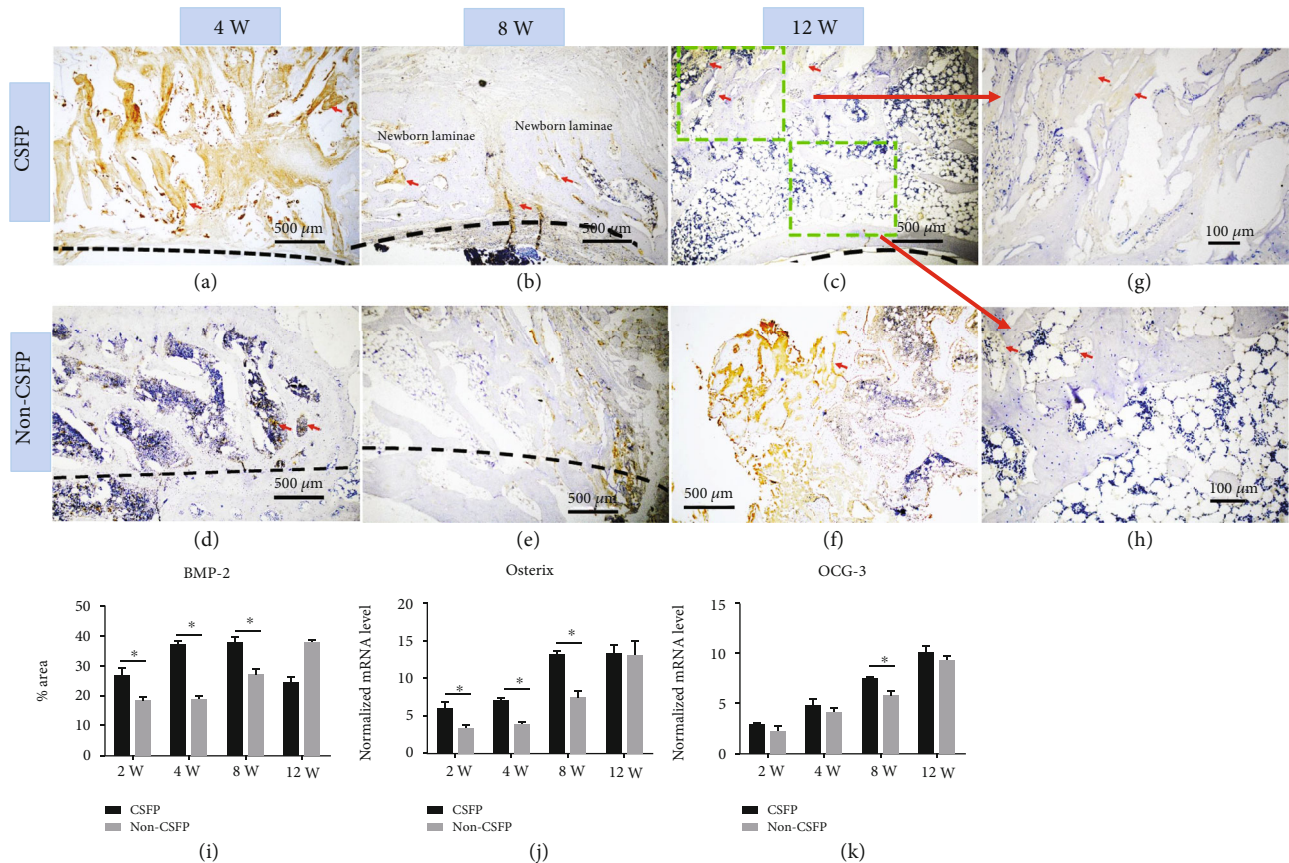


FIGURE 10: (a–c) Representative images of BMP-2 IHC staining of newborn laminae in the CSFP group and the Non-CSFP group in the 4<sup>th</sup>, 8<sup>th</sup>, and 12<sup>th</sup> weeks. (g) The BMP-2 IHC staining of the paraspinal surface of the newborn laminae in the 12<sup>th</sup> week. (h) The BMP-2 IHC staining of the dural surface of the newborn laminae in the 12<sup>th</sup> week. (i) Quantification of BMP-2 expression by IHC staining. QRT-PCR analysis of *Osterix* (j) and *ODG-3* (k) expressions. The red arrow showed positive staining. The dashed line in images (a), (b), and (c) showed the vertebral canal. The dashed line in images (d) and (e) showed the outer cortex of native laminae.

laminae on the paraspinal muscle surface showed higher expression levels of BMP-2 than the developed artificial laminae on the dural surface (Figures 10(c), 10(g), and 10(h)).

#### 4. Discussion

MSCs are among the most promising stem cell types for vascular tissue engineering, which can provide both seed cells and favorable cytokines for blood vessel formation [6]. Firstly, MSCs can be differentiated into several vascular cell phenotypes, including endothelial cells and smooth muscle cells. Secondly, MSCs can also secrete various angiogenic cytokines, such as VEGF, MCP-1, IL-6, and exosomes, which can promote the proliferation and migration of endothelial cells. The *in vivo* microenvironment of MSCs not only contains biochemical factors but also exerts biomechanical forces, which could influence their angiogenic ability [7]. In this study, we investigated the role of CSFP, a specific pulsation force, in the angiogenic ability of tissue-engineered laminae made by osteogenic MSCs and hydroxyapatite-collagen I scaffold.

The effect of shear stress or cyclic strain on different types of MSCs has been studied previously. For example, bone-marrow-derived MSCs from many species can differentiate

into endothelial-like cells when they are stimulated through physiological shear stress or cyclic strain conditions [16–18]. Shear stress can induce MSCs to release VEGF-A, HGF, bFGF, and IGF-1 [19]. Besides, shear stress can also induce MSCs to release exosomes, which may serve as an essential mediator of angiogenesis by transferring genetic materials and angiogenic molecules [7]. In this study, we used the CSFP bioreactor to simulate rabbit CSFP and stimulate the osteogenic MSCs, finding that the CSFP could promote the expression of angiogenic factors of osteogenic MSCs. The animal study also found that the CSFP group expressed more angiogenic factors than the Non-CSFP group; moreover, in the CSFP group, the dural surface (closer to the mechanical stimulation of CSFP) of the newborn laminae also expressed more angiogenic factors than the paraspinal muscle surface at the 8<sup>th</sup> week. These results showed that CSFP stress could promote the angiogenic activities of MSCs and the angiogenesis of the newborn laminae.

A previous study has shown that CSFP could promote the osteogenesis of newborn laminae [4]. In this study, we also determined several osteogenic markers, and the CSFP group also showed higher BMP-2, Osterix, and OCG-3 expressions than those of the Non-CSFP group. The lamina symphysis of the dural surface, which was closer to the mechanical

stimulation of CSFP, preceded that of the paraspinal muscle surface. Thus, we made clear once again that CSFP stress could promote the osteogenesis, but whether the effect is direct or as a result of better vascularization is still unknown. The formation of blood vessels and bone is not isolated processes, and they are tightly coupled by a special vessel subtype (type H vessel), which highly expresses CD31 (PECAM-1) and Emcn [20]. Type H endothelial cells could regulate angiogenesis and osteogenesis through the Notch signaling pathway [21]. Further research efforts are thus required to explore the relationship between angiogenesis and osteogenesis. In this study, we also found that the protein expression levels of BMP-2 decreased in the 12<sup>th</sup> week, while the mRNA expression levels of Osterix and OCG-3 still increased. In the 12<sup>th</sup> week, the artificial laminae on dural surface realized symphysis, and there was a little expression of BMP-2 in this area; the BMP-2 mostly expressed on the paraspinal muscle surface, which still underwent bone formation; thus, the BMP-2 expression levels decreased compared to the 8<sup>th</sup> week. The discrepancy between protein expression and mRNA expression is also commonly seen [22]. Moreover, from the 12<sup>th</sup> week, the artificial laminae began the remodeling process, and bone resorption outweighs bone formation [3]. These might explain for the decrease of BMP-2 expression levels in the CSFP group.

There is a limitation in this study due to the different biomaterials used for *in vivo* and *in vitro* studies. In the previous studies [3, 4], we have successfully used microporous hydroxyapatite-collagen I scaffold to reconstruct the artificial laminae, so we continued to use it for the *in vivo* study. However, the bioreactor study requires the use of membrane biomaterials with elastic modulus, which could respond to the simulated CSFP stress. Besides, MSCs had to attach to the surface of the membrane in monolayer to ensure the consistency of CSFP stress on the cells. Microporous hydroxyapatite-collagen I scaffolds did not meet these requirements, so we chose the PLGA membrane with elastic modulus for the *in vitro* study.

## 5. Conclusion

In conclusion, CSFP stress could promote the angiogenic ability of osteogenic MSCs and thus promote the angiogenesis and osteogenesis of tissue-engineered laminae. The pretreatment of osteogenic MSC with the CSFP bioreactor may have important implications for vertebral lamina reconstruction with a tissue engineering technique.

## Data Availability

The datasets used during the current study are available from the corresponding author on reasonable request.

## Conflicts of Interest

The authors declare that there are no conflicts of interest regarding the publication of this paper.

## Acknowledgments

The study was supported by the National Natural Science Foundation of China (81672179).

## References

- [1] Y. Dong, X. Chen, and Y. Hong, "Tissue-Engineered Bone Formation *In Vivo* for Artificial Laminae of the Vertebral Arch Using  $\beta$ -Tricalcium Phosphate Bioceramics Seeded With Mesenchymal Stem Cells," *Spine*, vol. 38, no. 21, pp. E1300–E1306, 2013.
- [2] Y. Dong, X. Chen, M. Wang, and Y. Hong, "Construction of Artificial Laminae of the Vertebral Arch Using Bone Marrow Mesenchymal Stem Cells Transplanted in Collagen Sponge," *Spine*, vol. 37, no. 8, pp. 648–653, 2012.
- [3] L. Li, Y. He, X. Chen, and Y. Dong, "The role of continuous cerebrospinal fluid pulsation stress in the remodeling of artificial vertebral laminae: a comparison experiment," *Tissue Engineering. Part A*, vol. 25, no. 3-4, pp. 203–213, 2019.
- [4] L. Li, X. Chen, Y. He, and Y. Dong, "Biological and mechanical factors promote the osteogenesis of rabbit artificial vertebral laminae: a comparison study," *Tissue Engineering. Part A*, vol. 24, no. 13-14, pp. 1082–1090, 2018.
- [5] K.-K. Sivaraj and R.-H. Adams, "Blood vessel formation and function in bone," *Development*, vol. 143, no. 15, pp. 2706–2715, 2016.
- [6] H. Tao, Z. Han, Z. C. Han, and Z. Li, "Proangiogenic Features of Mesenchymal Stem Cells and Their Therapeutic Applications," *Stem Cells International*, vol. 2016, 11 pages, 2016.
- [7] P. Dan, E. Velot, V. Decot, and P. Menu, "The role of mechanical stimuli in the vascular differentiation of mesenchymal stem cells," *Journal of Cell Science*, vol. 128, no. 14, pp. 2415–2422, 2015.
- [8] U. Helmrich, N. Di Maggio, S. Güven et al., "Osteogenic graft vascularization and bone resorption by VEGF-expressing human mesenchymal progenitors," *Biomaterials*, vol. 34, no. 21, pp. 5025–5035, 2013.
- [9] F. Geiger, H. Lorenz, W. Xu et al., "VEGF producing bone marrow stromal cells (BMSC) enhance vascularization and resorption of a natural coral bone substitute," *Bone*, vol. 41, no. 4, pp. 516–522, 2007.
- [10] H. Wang, H. Cheng, X. Tang et al., "The synergistic effect of bone forming peptide-1 and endothelial progenitor cells to promote vascularization of tissue engineered bone," *Journal of Biomedical Materials Research. Part A*, vol. 106, no. 4, pp. 1008–1021, 2018.
- [11] K. Nakano, K. Murata, S. Omokawa et al., "Promotion of osteogenesis and angiogenesis in vascularized tissue-engineered bone using osteogenic matrix cell sheets," *Plastic and Reconstructive Surgery*, vol. 137, no. 5, pp. 1476–1484, 2016.
- [12] Á. E. Mercado-Pagán, A. M. Stahl, Y. Shanjani, and Y. Yang, "Vascularization in bone tissue engineering constructs," *Annals of Biomedical Engineering*, vol. 43, no. 3, pp. 718–729, 2015.
- [13] J.-R. Garcia and A.-J. Garcia, "Biomaterial-mediated strategies targeting vascularization for bone repair," *Drug Delivery and Translational Research*, vol. 6, no. 2, pp. 77–95, 2016.
- [14] H. Mayer, H. Bertram, W. Lindenmaier, T. Korff, H. Weber, and H. Weich, "Vascular endothelial growth factor (VEGF-A) expression in human mesenchymal stem cells: autocrine and paracrine role on osteoblastic and endothelial



- differentiation,” *Journal of Cellular Biochemistry*, vol. 95, no. 4, pp. 827–839, 2005.
- [15] K.-C. Bradley, “Cerebrospinal fluid pressure,” *Journal of Neurology, Neurosurgery, and Psychiatry*, vol. 33, no. 3, pp. 387–397, 1970.
- [16] N.-F. Huang and S. Li, “Mesenchymal stem cells for vascular regeneration,” *Regenerative Medicine*, vol. 3, no. 6, pp. 877–892, 2008.
- [17] D.-H. Kim, S.-J. Heo, S.-H. Kim, J. W. Shin, S. H. Park, and J. W. Shin, “Shear stress magnitude is critical in regulating the differentiation of mesenchymal stem cells even with endothelial growth medium,” *Biotechnology Letters*, vol. 33, no. 12, pp. 2351–2359, 2011.
- [18] T.-M. Maul, D.-W. Chew, A. Nieponice, and D. A. Vorp, “Mechanical stimuli differentially control stem cell behavior: morphology, proliferation, and differentiation,” *Biomechanics and Modeling in Mechanobiology*, vol. 10, no. 6, pp. 939–953, 2011.
- [19] P. Zhang, J. Baxter, K. Vinod, T. N. Tulenko, and P. J. di Muzio, “Endothelial differentiation of amniotic fluid-derived stem cells: synergism of biochemical and shear force stimuli,” *Stem Cells and Development*, vol. 18, no. 9, pp. 1299–1308, 2009.
- [20] A.-P. Kusumbe, S.-K. Ramasamy, and R.-H. Adams, “Coupling of angiogenesis and osteogenesis by a specific vessel subtype in bone,” *Nature*, vol. 507, no. 7492, pp. 323–328, 2014.
- [21] S.-K. Ramasamy, A.-P. Kusumbe, L. Wang, and R. H. Adams, “Endothelial notch activity promotes angiogenesis and osteogenesis in bone,” *Nature*, vol. 507, no. 7492, pp. 376–380, 2014.
- [22] Y. Guo, P. Xiao, S. Lei et al., “How is mRNA expression predictive for protein expression? A correlation study on human circulating monocytes,” *Acta Biochimica et Biophysica Sinica*, vol. 40, no. 5, pp. 426–436, 2008.

## Research Article

# Retinoic Acid Signal Negatively Regulates Osteo/Odontogenic Differentiation of Dental Pulp Stem Cells

Jiangyi Wang <sup>1,2</sup>, Guoqing Li,<sup>2</sup> Lei Hu,<sup>2,3</sup> Fei Yan,<sup>4</sup> Bin Zhao,<sup>2</sup> Xiaoshan Wu,<sup>5</sup> Chunmei Zhang,<sup>2</sup> Jinsong Wang,<sup>2,6</sup> Juan Du <sup>1</sup> and Songlin Wang <sup>2,6</sup>

<sup>1</sup>Laboratory of Molecular Signaling and Stem Cell Therapy, Beijing Key Laboratory of Tooth Regeneration and Function Reconstruction, Capital Medical University School of Stomatology, Beijing, China

<sup>2</sup>Molecular Laboratory for Gene Therapy and Tooth Regeneration, Beijing Key Laboratory of Tooth Regeneration and Function Reconstruction, Capital Medical University School of Stomatology, Beijing, China

<sup>3</sup>Department of Prosthodontics, Capital Medical University School of Stomatology, Beijing, China

<sup>4</sup>Xiangya Stomatological Hospital and School of Stomatology, Central South University, Changsha, Hunan, China

<sup>5</sup>Department of Oral and Maxillofacial Surgery, Xiangya Hospital, Central South University, Changsha, China

<sup>6</sup>Department of Biochemistry and Molecular Biology, Capital Medical University School of Basic Medical Sciences, Beijing, China

Correspondence should be addressed to Juan Du; [juandug@ccmu.edu.cn](mailto:juandug@ccmu.edu.cn) and Songlin Wang; [slwang@ccmu.edu.cn](mailto:slwang@ccmu.edu.cn)

Received 21 February 2020; Accepted 6 March 2020; Published 27 June 2020

Guest Editor: Sangho Roh

Copyright © 2020 Jiangyi Wang et al. This is an open access article distributed under the Creative Commons Attribution License, which permits unrestricted use, distribution, and reproduction in any medium, provided the original work is properly cited.

Retinoic acid (RA) signal is involved in tooth development and osteogenic differentiation of mesenchymal stem cells (MSCs). Dental pulp stem cells (DPSCs) are one of the useful MSCs in tissue regeneration. However, the function of RA in osteo/odontogenic differentiation of DPSCs remains unclear. Here, we investigated the expression pattern of RA in miniature pig tooth germ and intervened in the RA signal during osteo/odontogenic differentiation of human DPSCs. Deciduous canine (DC) germs of miniature pigs were observed morphologically, and the expression patterns of RA were studied by *in situ* hybridization (ISH). Human DPSCs were isolated and cultured in osteogenic induction medium with or without RA or BMS 493, an inverse agonist of the pan-retinoic acid receptors (pan-RARs). Alkaline phosphatase (ALP) activity assays, alizarin red staining, quantitative calcium analysis, CCK8 assay, osteogenesis-related gene expression, and *in vivo* transplantation were conducted to determine the osteo/odontogenic differentiation potential and proliferation potential of DPSCs. We found that the expression of *RARβ* and *CRABP2* decreased during crown calcification of DCs of miniature pigs. Activation of RA signal *in vitro* inhibited ALP activities and mineralization of human DPSCs and decreased the mRNA expression of *ALP*, *osteocalcin*, *osteopontin*, and a transcription factor, *osterix*. With BMS 493 treatment, the results were opposite. Interference in RA signal decreased the proliferation of DPSCs. *In vivo* transplantation experiments suggested that osteo/odontogenic differentiation potential of DPSCs was enhanced by inverting RA signal. Our results demonstrated that downregulation of RA signal promoted osteo/odontogenic differentiation of DPSCs and indicated a potential target pathway to improve tissue regeneration.

## 1. Introduction

Retinoic acid (RA), the main active derivative of vitamin A, found in embryos and adult vertebrates [1], is essential for embryonic development [2–4] and, like several other molecules, continues to play vital roles after the development is completed [5]. RA signaling is activated when RA binds to cellular retinoic acid-binding protein (CRABP), which translocates RA from the cytoplasm into the nucleus. In the

nucleus, heterodimers of nuclear retinoic acid receptors (RARs) and retinoid X receptors (RXRs) recognize RA and regulate transcription by association with retinoic acid response elements (RAREs) in the promoter regions of DNA [6]. Previous studies have shown the dynamic expression patterns of RA-relative signaling molecules in developing tooth [3, 7–9] and reported that RA signals regulated the initiation and formation of dentition at early stages of development [10–12]. An excess amount of RA has negative

effects on the maintenance of stem cell niche and enamel formation [13, 14]. RA signaling is also involved in bone metabolism and osteoblast differentiation [15–17]. Interactions have been reported between RA and several molecules from osteo/odontogenic-related pathways, like bone morphogenic protein (BMP) [18], fibroblast growth factor (FGF) [13], and members of the Wnt signaling pathway [16, 19]. However, to the best of our knowledge, the direct role of RA in dentin mineralization and odontoblast differentiation is not yet reported.

As mesenchymal stem cells (MSCs) have key roles in tissue engineering, their sources and the regulation of their differentiation mechanisms in tissue regeneration are active areas of research. Dental pulp stem cells (DPSCs) have been isolated from an adult dental pulp and are characterized by their high proliferation rate, self-renewal capability, and their potential to differentiate into osteoblasts, odontoblasts, adipocytes, etc. [20]. Currently, DPSCs are widely studied as potential seed cells in regeneration for dentin pulp-like complex and periodontal tissue and bone [21–24]. Our previous studies [25–27] have identified the role of DPSCs in functional root and periodontal regeneration. Our recent research observed that, compared to other mesenchymal stem cells, DPSCs have superior resistance to cellular senescence in culture and under an inflammatory environment [28]. All these observations suggested that DPSCs can be a promising source of MSCs for tooth regeneration. Improvement in the differentiation efficacy of DPSCs can greatly facilitate their utility in tissue regeneration.

In this study, we used deciduous canines (DCs) of miniature pigs between late bell stage and calcification stage to study the expression pattern of RA in the dental papilla (DP) during crown calcification. Using human DPSCs, we investigated if RA had the presumed effects in osteo/odontogenic differentiation of human DPSCs. Our results revealed the negative effect of RA, both in crown calcification and in osteo/odontogenic differentiation of DPSCs, and we successfully improved the regeneration of bone-like tissue by inverting the RA signal, a novel method to promote the bone/dentin regeneration.

## 2. Materials and Methods

**2.1. Animals.** Pregnant miniature pigs were obtained from the Animal Science Institute of Chinese Agriculture University. The gestation age was calculated from the day of insemination. Pregnancy was verified through B-type ultrasonography. All procedures acquired approval from the Animal Care Use Committee of Capital Medical University (Beijing, China) (Permit Number: AEEI-2016-063). Pregnant pigs were anesthetized and sacrificed as previously described [29]. The DCs were harvested on embryonic day 50 (E50) and embryonic day 60 (E60).

**2.2. In Situ Hybridization (ISH).** RNA probe synthesis and nonradioactive *in situ* hybridization were carried out as described previously [30, 31]. The primers used for reverse transcriptase polymerase chain reaction (RT-PCR) are listed in Table 1. Briefly, total RNA was extracted from

TABLE 1: Primer sequences used in the RT-PCR.

Gene symbol	Primer sequences (5' -3')
RAR $\alpha$ -sense	CTAAACGTCTGCCAGGCTTC
RAR $\alpha$ -antisense	CGGGATGCATGAAATGGCTG
CRABP2-sense	CCCAACTTCTCTGGCAACTGG
CRABP2-antisense	TCTAGAAGGAAGGGTAGGGGAG

TABLE 2: Primer sequences used in the real-time PCR.

Gene symbol	Primer sequences (5' -3')
GAPDH-F	GGAGCGAGATCCCTCCAAAAT
GAPDH-R	GGCTGTTGTCATACTTCTCATGG
ALP-F	GACCTCCTCGGAAGACACTC
ALP-R	TGAAGGGCTTCTTGTCTGTG
OPN-F	CGCAGACCTGACATCCAGTA
OPN-R	GTGGGTTTCAGCACTCTGGT
OCN-F	TCACACTCCTCGCCCTATTG
OCN-R	GGTCTCTTCACTACCTCGC
OSX-F	CCCACCTCAGGCTATGCTAA
OSX-R	GCCTTGTACCAGGAGCCATA

DC tooth germs from miniature pigs on E50-60. After RT-PCR, the DNA bands of interest were extracted and their DNA sequences were determined. Digoxigenin-(DIG-) labeled RNA probes were synthesized with DIG-UTP and T7 RNA polymerase (10881767001; Roche, Switzerland) and DIG RNA labeling mix solution (11277073910; Roche). For the staining process, slides were deparaffinized and rehydrated completely and then digested with 1  $\mu$ g/mL proteinase K for 30 min at 37°C. After refixation with 4% paraformaldehyde- (PFA-) PBS, the sections were dehydrated in 25, 50, 75, and 100% ethanol successively before air-drying for 1 hour. Hybridization was performed overnight with diluted probes in an RNase-free incubator at 70°C. In the next day, the sections were rinsed for 3 to 4 hours and incubated with antibodies (alkaline phosphatase-conjugated anti-digoxigenin, Fab fragments) (11093274910; Roche) overnight. Signal detection was performed with the NBT/BCIP substrate (S3771; Promega, Madison, WI).

**2.3. Cell Cultures.** Human tooth tissues were obtained from impacted third molars, under approved guidelines set by the Beijing Stomatological Hospital, Capital Medical University. All procedures were performed with informed consent from patients. The isolation and culture of DPSCs were performed as reported previously [32]. DPSCs at passages 3 to 5 were used in the following experiments. DPSCs were cultured for 3-14 days in osteogenic induction medium containing 100  $\mu$ M of ascorbic acid, 2 mM of  $\beta$ -glycerophosphate, 1.8 mM of  $\text{KH}_2\text{PO}_4$ , and 10 nM of dexamethasone. In the experimental groups, to activate the RA signal, RA (Sigma-Aldrich, Santa Louis, USA) was used and, to inhibit RA signal, BMS 493 (Tocris, Cat. No. 3509), an inverse agonist of

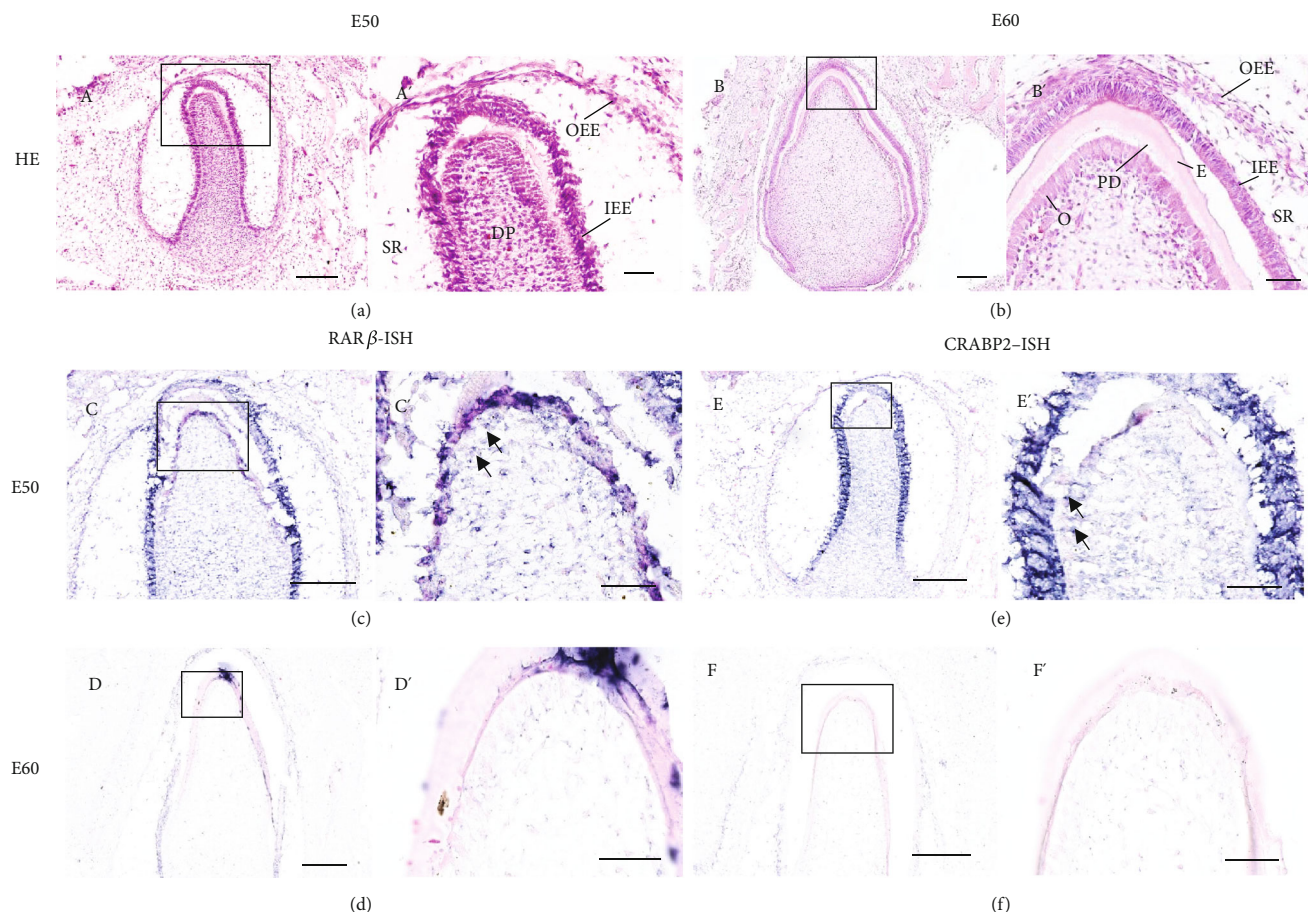


FIGURE 1: Morphological changes and mRNA expression changes of *RARβ* and *CRABP2* in the DP during crown calcification of DC of miniature pig. (A, A') In HE staining of DC on E50, tooth germ develops into bell stage; (A') exhibits the enlarged image of the boxed region in (A). The enamel organ (EO) forms and surrounds the dental papilla (DP) which is located next to the inner enamel epithelium (IEE). (B, B') In HE staining of DC on E60, tooth germ develops into calcification stage; (B') exhibits the enlarged image of the boxed region in (B). The elongated odontoblasts (O) appear at the frontier of the DP. The predentin (PD) and enamel are secreted between the DP and EO. The outer enamel epithelium (OEE) and stellate reticulum (SR) can be identified on E50 and E60. The expression patterns of *RARβ* and *CRABP2* in DP are studied by in situ hybridization (ISH); the boxed regions in (C–F) are enlarged in (C'–F'). Expression levels of *RARβ* and *CRABP2* are largely decreased in DP from E50 to E60. Scale bars represent 200  $\mu\text{m}$  (A–F) and 50  $\mu\text{m}$  (A'–F').

pan-RARs, was used. For each experiment, RA and BMS 493 stock solutions were initially diluted in DMSO and then in culture medium for  $10^{-7}$  M,  $10^{-6}$  M, and  $10^{-5}$  M according to a previous literature [13, 19, 33].

**2.4. Alkaline Phosphatase (ALP) Assay and Alizarin Red Staining.** After osteogenic induction for 7 days, ALP activity assay was performed using an ALP activity kit following the instruction from the manufacturer's protocol (Sigma-Aldrich). Signal strength was normalized based on protein concentration. After 14 days of induction, mineralization was detected. The cultured DPSCs were fixed with 70% ethanol and stained in 2% Alizarin red (Sigma-Aldrich). To calculate their calcium contents, the above samples were destained with 10% cetylpyridinium chloride before measuring their absorbance at 562 nm on a multiplate reader. Their calcium contents were derived from a standard calcium curve, constructed using calcium dilutions of the same solu-

tion. In each group, the final calcium level was normalized to total protein concentration in duplicate plates.

**2.5. Cell Proliferation Assay.** To analyze the effects of RA signal intervention on DPSC proliferation, cell proliferation assay was performed in 96-well plates using cell counting kit-8 (CCK8; Dojindo, Tokyo, Japan). After osteogenic induction for 1, 2, 3, 4, and 5 days, 10% CCK8 reagent was added to each well and incubated at 37°C for 2 h before measuring the optical density (OD) values of the samples at 450 nm on a microplate reader. Cell proliferation capacities were represented by the OD values.

**2.6. RNA Isolation, RT-PCR, and Real-Time RT-PCR.** Total RNA was extracted from DPSCs using TRIzol reagent (Invitrogen). Using 2  $\mu\text{g}$  of RNA, cDNA was synthesized with random hexamers or oligo (dT) and reverse transcriptase according to the manufacturer's protocol (Invitrogen). Real-time RT-PCR reactions were carried out using the QuantiTect



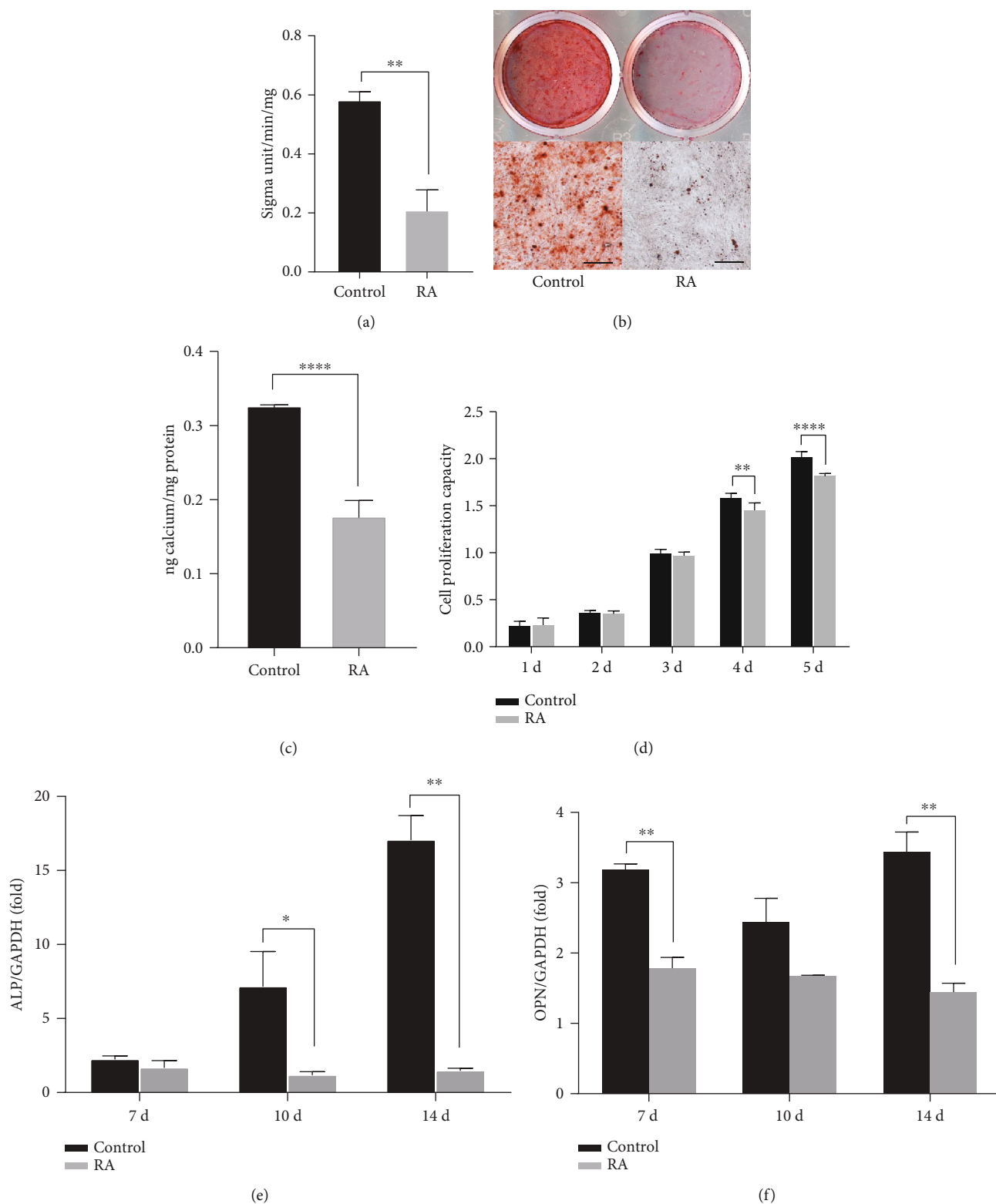


FIGURE 2: Continued.

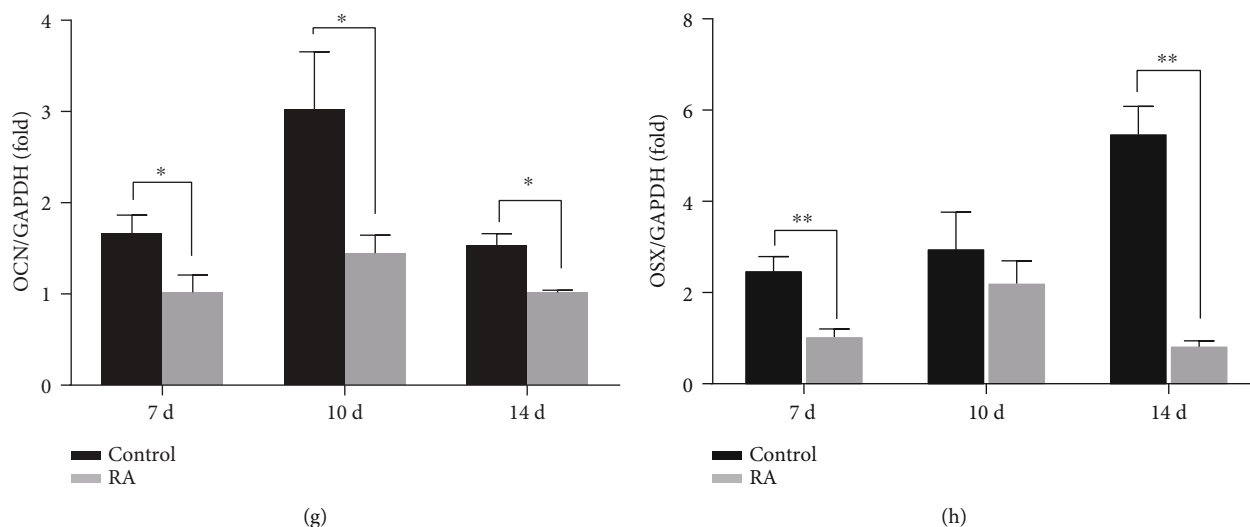


FIGURE 2: RA inhibits osteo/odontogenic differentiation and proliferation of human DPSCs. (a) ALP activity assay results show RA inhibits ALP activities in human DPSCs after osteogenic induction for 7 days. Alizarin red staining (b) and quantitative calcium measurement (c) results show RA reduces osteogenic differentiation of human DPSCs after osteogenic induction for 14 days. Calcium nodules are observed under a microscope and displayed below (b). (d) CCK8 assays exhibit significant induction in the proliferation of DPSCs by RA after 4-day induction. Real-time RT-PCR results show RA downregulates the expressions of osteogenesis-related markers ALP (e), OPN (f), OCN (g), and transcription factor OSX (h) in human DPSCs. GAPDH is applied as the internal control. Student's *t*-test is performed to calculate statistical significance. All error bars mean the SD ( $n = 3$ ). \* $P < 0.05$ , \*\* $P < 0.01$ , and \*\*\*\* $P < 0.0001$ . Scale bars represent 200  $\mu\text{m}$  (b).

SYBR Green PCR kit (Qiagen, Hilden, Germany) and an iCycleriQ Multi-color Real-time RT-PCR Detection System. The primers used for the specific genes are shown in Table 2.

**2.7. Transplantation in Nude Mice.** The present study was performed in accordance with an approved protocol. Eight-week-old female BALB/c nude mice were maintained with free access to water and regular food. Human DPSCs were cultured at the presence or absence of BMS 493 for 3 days before combining with 40 mg of hydroxyapatite/tricalcium phosphate (HA/TCP) ceramic particles. The mixture was then transplanted subcutaneously on the dorsal side of the nude mice. After 8 weeks, the transplants were harvested and fixed with 10% formalin for 48 h and decalcified in buffered 10% EDTA (pH 8.0) for a month prior to embedding in paraffin wax and sectioning.

**2.8. Histological Analyses.** Sections were stained with hematoxylin and eosin (HE) to detect morphological changes in the DP of DC from miniature pigs and new bone formation in transplants. Masson's trichrome staining was applied to evaluate the collagen fibril deposits. Image-Pro Plus 6.0 (Media Cybernetics, Rockville, MD) was used for qualitative measurement of mineralization.

**2.9. Immunohistochemistry Staining.** Immunohistochemistry staining was carried out as previously described [34]. Briefly, sections were deparaffinized, hydrated, and immersed in 10%  $\text{H}_2\text{O}_2$  for 10 min to quench the endogenous peroxidase. They were incubated with a primary antibody at 4°C overnight. The primary antibodies used here included those against dentin sialophosphoprotein (DSPP) (Cat. No. ab216892, Abcam, Cambridge, UK), osteocalcin (OCN) (Cat. No.

ab13418, Abcam, Cambridge, UK), and collagen type I (COL-1) (Cat No. NB600-408, Novus Biological Centennial, USA). In the next day, the sections were washed and incubated in secondary antibody at room temperature. DAB staining was performed with DAB Substrate Kit (Cell Signaling, Danvers, MA, USA) and counterstaining with HE. Image-Pro Plus 6.0 (Media Cybernetics, Rockville, MD) was used for the qualitative measurement of mineralization.

**2.10. Statistical Analysis.** All statistical calculations were carried out using SPSS 13.0 statistical software. Student's *t*-test was performed to determine the statistical significance.  $P$  value  $\leq 0.05$  was considered to be significant.

### 3. Results

**3.1. RA Signaling Decreases during Crown Calcification of Deciduous Canine from Miniature Pig.** First, we used the DCs from miniature pigs as a model for crown calcification in tooth development. HE staining showed that the enamel of DCs became obvious on E50 (Figures 1(A) and 1(A')), but in DP, the elongated odontoblasts with secreted predentin did not appear until E60 (Figures 1(B) and 1(B')). As a result, we designate the development stages of DCs of miniature pigs on E50 and E60 as late bell and calcification stages, respectively. To investigate the role of RA signaling during crown calcification, we studied the RNA expression patterns of *RA receptors*  $\alpha$  (*RAR $\alpha$* ) and  $\beta$  (*RAR $\beta$* ) and *cellular retinoic acid-binding proteins 1 and 2* (*CRABP1* and *CRABP2*) in DCs from E50 to E60. We found that *RAR $\alpha$*  was not expressed in the whole tooth germ of DCs from E50 to E60 and *CRABP1* expression showed little difference between the two stages (data not shown), while the mRNA expressions of *RAR $\beta$*

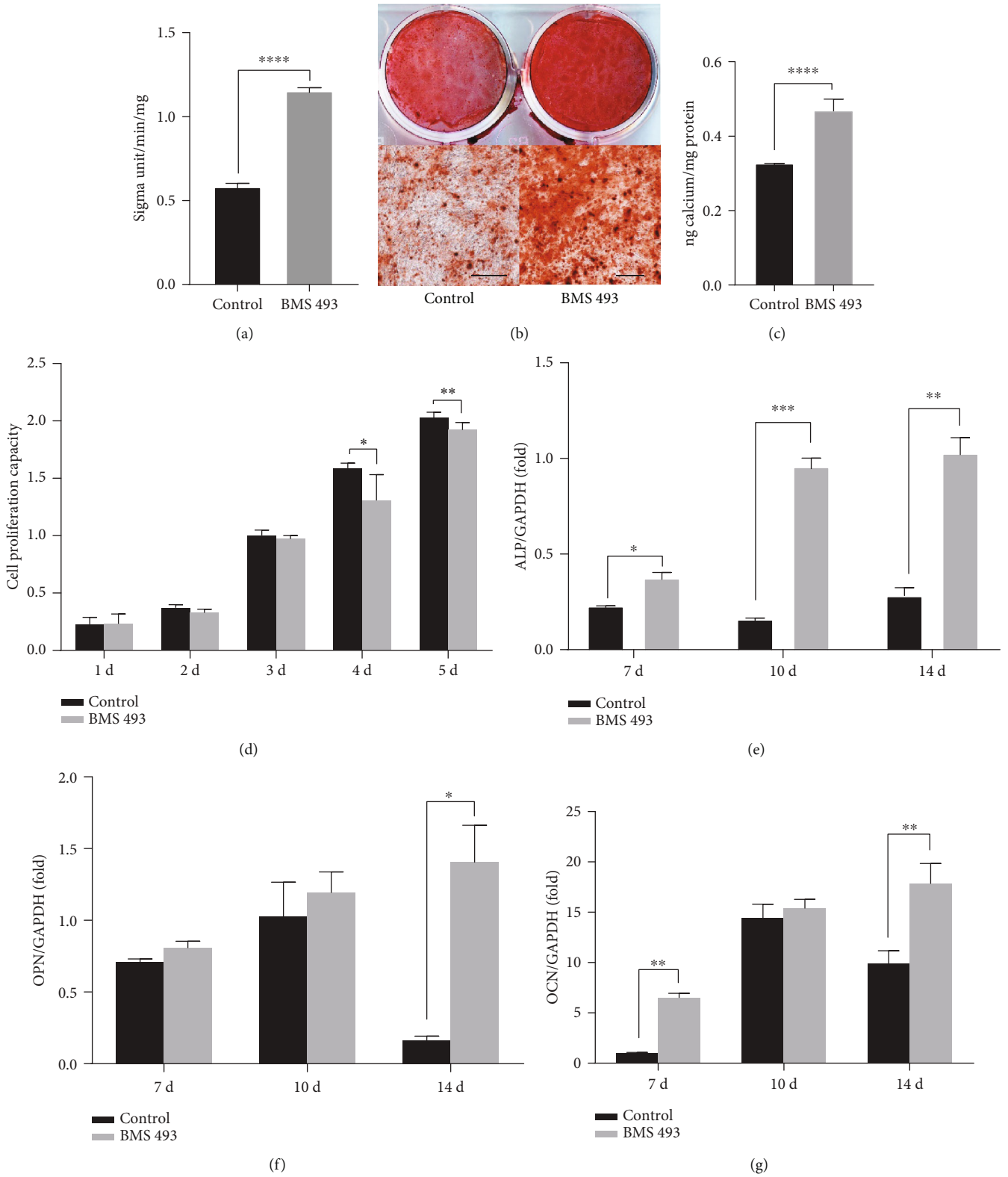


FIGURE 3: Continued.

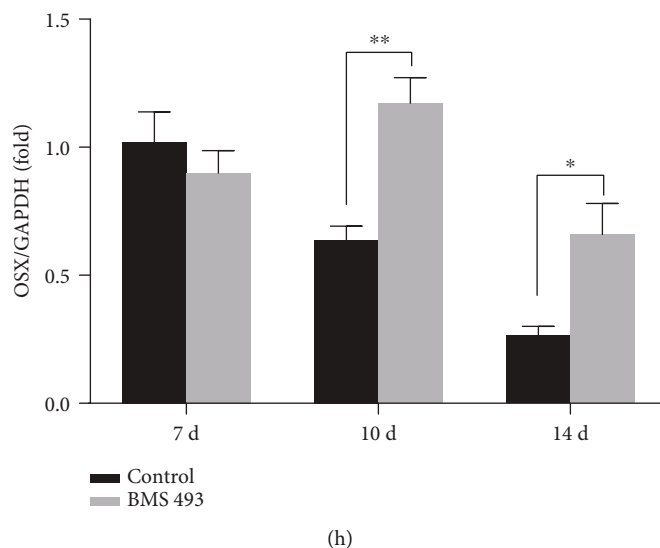


FIGURE 3: BMS 493 enhances osteo/odontogenic differentiation and inhibits proliferation of human DPSCs. (a) ALP activity assay results exhibit enhanced ALP activities in human DPSCs by BMS 493 after osteogenic induction for 7 days. Alizarin red staining (b) and quantitative calcium measurement (c) results show more mineralization nodules in human DPSCs by BMS 493 after osteogenic induction for 14 days. Calcium nodules are observed under a microscope and displayed below (b). (d) CCK8 assays show the proliferation of DPSCs is largely suppressed by BMS 493 after 4-day induction. Real-time RT-PCR results show BMS 493 upregulates the expressions of osteogenesis-related markers ALP (e), OPN (f), OCN (g), and transcription factor OSX (h) in human DPSCs. GAPDH is applied as the internal control. Student's *t*-test is performed to calculate statistical significance. All error bars mean the SD ( $n = 3$ ). \* $P < 0.05$ , \*\* $P < 0.01$ , \*\*\* $P < 0.001$ , and \*\*\*\* $P < 0.0001$ . Scale bars represent  $200 \mu\text{m}$  (b).

(Figures 1(C), 1(C'), 1(D), and 1(D')) and *CRABP2* (Figures 1(E), 1(E'), 1(F), and 1(F')) were prominent at E50 in mesenchymal cells and significantly decreased at E60. Considering the simultaneous decrease of *RAR $\beta$*  and *CRABP2* can downregulate the activation of RA signal, we suggest that RA signal plays a negative role in crown calcification and odontoblast differentiation.

**3.2. RA Inhibits Osteogenic Differentiation and Cell Proliferation of DPSCs In Vitro.** DPSCs are dental stem cells isolated from the dental pulp, which is derived from the dental papilla, the mesenchymal compartment, during development. Based on our above finding, we raise a hypothesis that osteogenic potential of DPSCs could be controlled by RA signal, in addition to its involvement in mineralization of dentin during tooth development. To confirm this, DPSCs were cultured in osteogenic medium with or without RA supplement. First, ALP activity, an early marker for osteogenic differentiation, was analyzed. Experimental groups were treated with  $10^{-7}$  M,  $10^{-6}$  M, and  $10^{-5}$  M of RA, based on a previous literature [13, 19]. In DPSCs, ALP activity decreased on day 7 in the above experimental groups. We chose the minimum effective concentration of  $10^{-7}$  M (Figure 2(a)) for further experiments. After 14 days of culture, DPSCs treated with RA showed fewer mineralization nodules (Figure 2(b)) and quantitative measurements revealed lower concentrations of calcium (Figure 2(c)) than in the control group. Proliferation of DPSCs decreased by RA after 4 days of induction, as seen in CCK8 assay (Figure 2(d)). Real-time RT-PCR was performed to evaluate the expression levels of osteogenic genes including *ALP*, *osteocalcin* (*OCN*), *osteopontin* (*OPN*), and a related transcription

factor *osterix* (*OSX*). Compared with the control group, there was significant reduction in the expression of the osteogenic markers (*ALP*, *OCN*, and *OPN*) and *OSX* in RA-treated DPSCs on days 3, 7, 10, and 14 (Figures 2(e)–2(h)). These results show that RA inhibits osteogenic differentiation and proliferation of DPSCs *in vitro*.

**3.3. BMS 493 Promotes Osteogenic Differentiation and Inhibits Proliferation of DPSCs In Vitro.** To confirm further the role of RA signal in osteogenic differentiation of DPSCs,  $10^{-7}$  M,  $10^{-6}$  M, and  $10^{-5}$  M of BMS 493, an inverse agonist of pan-RARs, were added in the culture medium to modulate the RA signal in DPSCs. With the addition of  $10^{-7}$  M BMS 493, ALP activity increased after 7 days of culture (Figure 3(a)), and more mineralization nodules (Figure 3(b)) and higher concentrations of calcium (Figure 3(c)) were seen. Proliferation of DPSCs decreased in the group treated with  $10^{-7}$  M BMS (Figure 3(d)). Next, we studied the expression of osteogenic genes by semiquantitative RT-PCR. During the 14-day long osteogenic induction, the expression of *ALP*, *OCN*, *OPN*, and *OSX* enhanced significantly in BMS 493-treated DPSCs, compared to the control group (Figures 3(e)–3(h)). Taken together, these results indicate that BMS 493 promotes osteogenic differentiation and inhibits the proliferation of DPSCs *in vitro*.

**3.4. BMS 493 Promotes Osteogenic Differentiation of DPSCs In Vivo.** To test whether the RA signal affects osteogenesis *in vivo*, human DPSCs were treated with or without BMS 493 for 3 days before mixing them with HA/TCP ceramic particles and transplanting subcutaneously into nude mice. After eight weeks, the transplanted tissues were retrieved



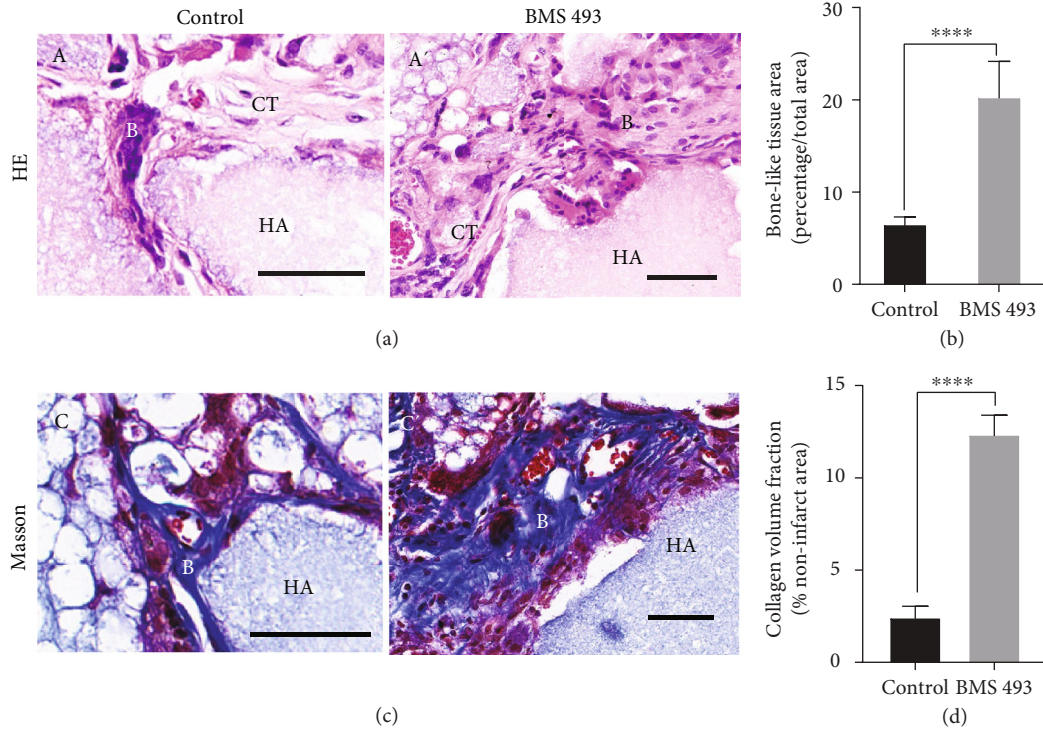


FIGURE 4: Blocking RA signal enhances the bone-like tissue formation and collagen fibril deposits from human DPSCs *in vivo*. Human DPSCs cultured at the presence or absence of BMS 493 were transplanted subcutaneously into immunodeficient BALB/c nude mice, and the transplants were harvested after 8 weeks. (A, A') HE staining of the transplants exhibits improved bone-like tissue formation by BMS 493 treatment. (C, C') Masson's trichrome staining exhibits more collagen fibril deposits by BMS 493 treatment. Qualitative measurements are used to evaluate bone-like tissue area (B) and collagen volume fraction (D). Scale bars represent  $20\ \mu\text{m}$  (A, A', C, C'). All error bars mean the SD ( $n = 5$ ). \*\*\*\*  $P < 0.0001$ . B: bone-like tissue; CT: connective tissue; HA: hydroxyapatite/tricalcium carrier.

and decalcified. HE staining showed the formation of more bone-like tissue in BMS 493-treated DPSCs than in the control groups (Figures 4(A) and 4(A')). In Masson's trichrome staining, collagen fibrils are stained blue, in contrast to a red background of cells and other structure. Here, it exhibited larger areas of blue, indicating more fibrous tissue formation, which is an early stage in bone formation, in BMS 493-treated DPSCs, compared to controls (Figures 4(C) and 4(C')). Qualitative measurements revealed more newly formed bone tissues (Figure 4(B)) and collagen fibrous tissues (Figure 4(D)) in BMS 493-treated groups than in control groups. Further, IHC was performed to evaluate the osteo/odontogenic marker expressions. Expression levels of DSPP, OCN, and COL-1 were significantly higher in the BMS 493-treated group than in the control (Figures 5(a), 5(b), 5(d), 5(e), 5(g), and 5(h)). Qualitative measurements confirmed the relative differences in the expression of DSPP, OCN, and COL-1 between the BMS 493 group and control group (Figures 5(c), 5(f), and 5(i)). Taken together, these results show that the bone/dentin regenerative potential of DPSCs can be enhanced substantially by inverting RA signal *in vivo*.

#### 4. Discussion

Retinoic acid is an early signal in embryonic development and has a crucial role in the early stage of tooth development

[10–12]. Studies have shown the participation of RAR signals in postnatal bone metabolism [35]. A negative role of RA and RAR was reported in osteogenesis and bone mineralization [16, 19, 36]. In murine tooth development,  $RAR\beta$  expression is initiated during bell stage and is seen in odontoblasts [37]. The expression of CRABP2 is seen in dental mesenchymal cells and decreases during dentin development in mouse [38]. CRABP2 knockdown enhances odontoblastic differentiation of human DPSCs. It is downregulated during osteogenic differentiation from myogenic progenitor cells and negatively regulates osteogenic differentiation [39]. Miniature pigs are similar to humans in their mandibular anatomy and diphyodont dentition [40]. In the present study, the simultaneous decrease in the expression of  $RAR\beta$  and CRABP2 in dental mesenchymal cells of miniature pigs during tooth development indicated the negative role of RA signal in odontogenic differentiation and dentin mineralization.

In recent years, DPSCs are proved to be a promising choice in dentin and bone regeneration. The ability to manipulate the stem cells accurately to a desired cell lineage remains a much pursued goal of research [41]. Given the negative role of RA in mineralization, we propose that blocking RA signal may be an effective method for dentin regeneration from DPSCs. Knocking down the CRABP2 in DPSCs through transfection with lentivirus promoted the odontogenic differentiation of DPSCs *in vitro* [38]. However, procedural difficulties and safety issues are the

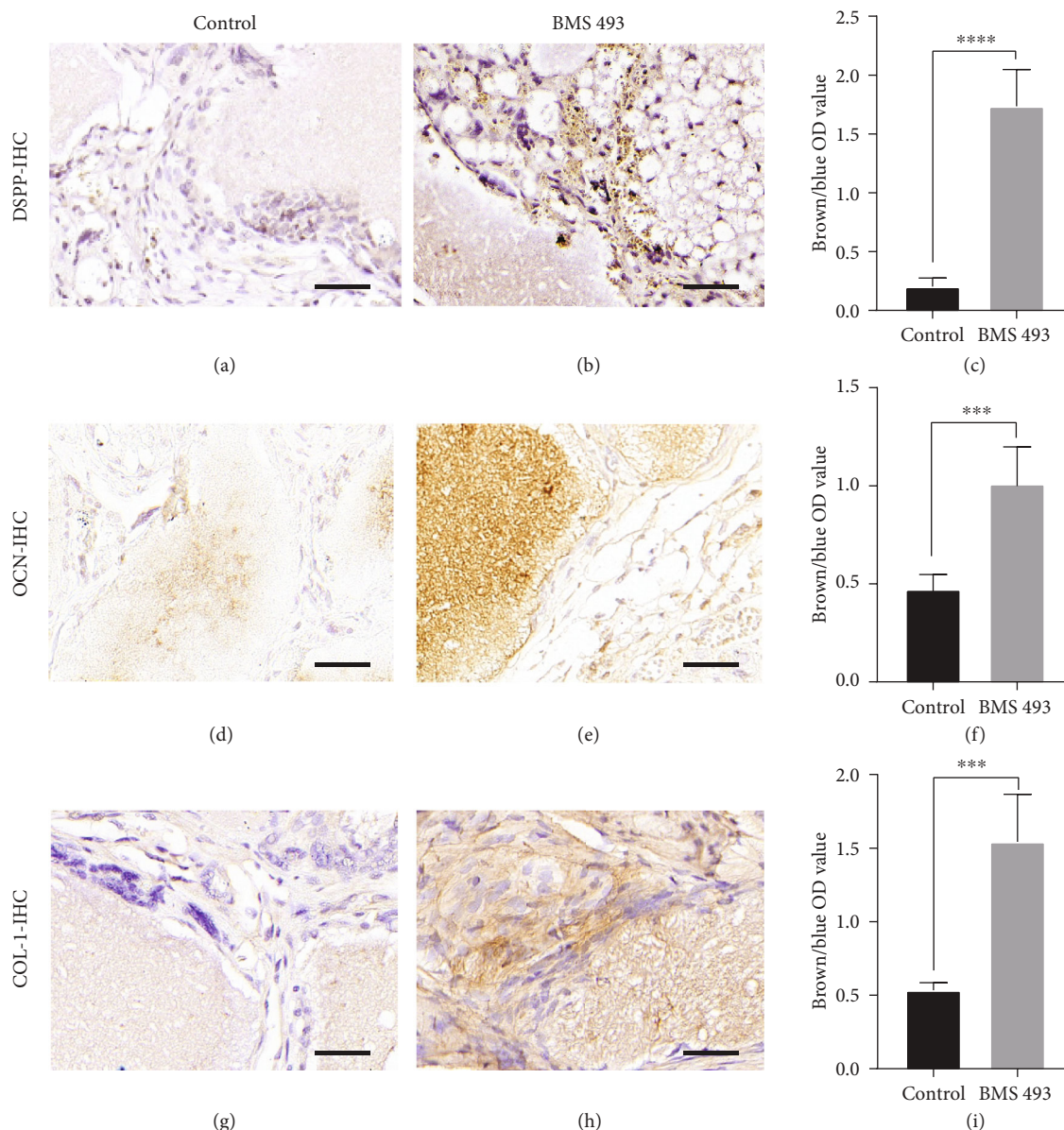


FIGURE 5: Blocking RA signal enhances the expression of osteo/odontogenic related factors from human DPSCs in vivo. Immunohistochemical (IHC) staining reveals expression levels of DSPP (a, b), OCN (d, e), and COL-1 (g, h). Qualitative measurements of IHC staining show expressions of DSPP (c), OCN (f), and COL-1 (i) are enhanced significantly by BMS 493 treatment. All error bars mean the SD ( $n = 5$ ). \*\*\* $P < 0.001$  and \*\*\*\* $P < 0.0001$ .

roadblocks in the clinical application of lentivirus transfection. In this scenario, inverting the RA signal by BMS 493 is a new method to improve the osteo/odontogenic differentiation of DPSCs in tissue regeneration, both *in vitro* and *in vivo*. The present results showed that BMS 493 enhanced the osteo/odontogenic differentiation potential in DPSCs *in vitro* and enhanced the regeneration of bone-like tissue *in vivo*. Although previous studies have shown the RA signal had a significant role in regulating the proliferation of different cell types [42, 43], interesting results were investigated in our work that the proliferation of human DPSCs was decreased whenever activating or blocking RA signal after 4 days of culture, which suggests that the proliferation of DPSCs may be independent from

RA signaling and the osteogenic induction may influence the cell proliferation.

Different stages of the osteo/odontogenic differentiation of MSCs are characterized by several markers. ALP participates in bone mineralization and is an early osteogenic differentiation marker [44, 45], while OPN and OCN are specific matrix proteins associated with bone metabolism and remodeling and are late osteoblastic differentiation markers in MSCs [45, 46]. During osteogenic induction *in vitro*, we studied the expression of ALP, OPN, and OCN by real-time RT-PCR. Their synchronous decrease due to RA treatment indicated the negative effect of RA in osteogenesis of DPSCs in both early and late differentiation periods. OSX is a key transcription factor specifically expressed in developing

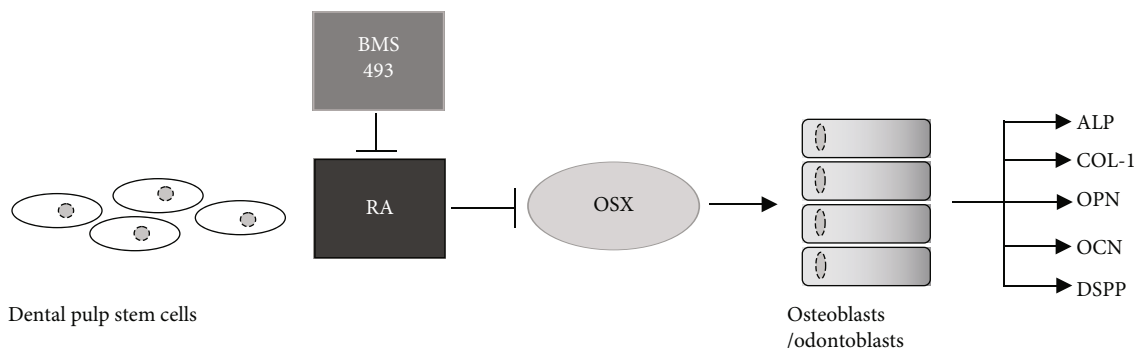


FIGURE 6: The schematic diagram of the effect of RA on DPSCs. Activation of RA inhibits osteo/odontogenic differentiation of DPSCs and the expression levels of osteo/odontogenic related factors ALP, COL-1, OPN, OCN, and DSPP by downregulating the expression of OSX.

bones [47] and enhances the osteogenic differentiation potential of stem cells [48, 49]. In mouse tooth development, OSX was reported to be highly expressed in osteogenic mesenchyme and odontoblasts, and its overexpression in mouse odontoblast-like cells resulted in enhanced transcription of an odontogenic marker, *DSPP* [50]. By real-time RT-PCR, we detected the downregulation of *OSX* due to RA and its enhancement due to BMS 493. These results suggested a role for *OSX* in regulating RA signal in osteogenic differentiation of DPSCs (Figure 6). Future research needs to explore the role of RA and related signals during osteo/odontogenic differentiation and focus on the specific mechanisms of action of RA on *OSX*. *DSPP* is an odontogenic marker widely expressed in mature odontoblasts and dentin [51, 52]. *COL-1* is a major component of mineralized tissues, and reports support its potential to improve the survival and expression of osteogenic and chondrogenic phenotypes in MSCs *in vivo* [53]. The present research proved that treatment with BMS 493 improved the expression of *DSPP*, *COL-1*, and *OCN* as well as enhanced the mineralization of DPSCs *in vivo*.

In contrast, some studies have suggested a positive role for the RA pathway in osteogenic differentiation of MSCs [54–56] and dental pulp cells [57–59]. However, their *in vitro* induction time was mostly shorter than 7 days while osteogenesis is a long and dynamic process. In addition, a long-term *in vitro* culture of stem cells from periodontal ligaments and pulp of human exfoliated deciduous teeth showed improved osteogenic differentiation by RA [60]. Different culture conditions, varied induction time, and different cell types may explain this discrepancy. In any case, the specific mechanisms of RA signal in osteo/odontogenic differentiation remain to be delineated.

## 5. Conclusion

This study indicated that the RA signaling pathway was involved in dental crown calcification and demonstrated that activation of RA signal decreased the osteogenic differentiation potential of DPSCs and blocking RA signal enhanced it *in vitro* and *in vivo*. The modulation of RA signaling has potential for improving the tissue regeneration and explains the mechanisms of osteogenesis and odontogenesis. The rela-

tionship between RA and its downstream signals needs to be studied in greater details to understand this process better.

## Data Availability

All the data used to support the findings of this study are available from the corresponding author upon request.

## Conflicts of Interest

The authors declare no competing interests in the article.

## Acknowledgments

This work was supported by the National Natural Science Foundation of China (NSFC 81570940 and 81873706 to JD); the Discipline Construction Fund from the Beijing Stomatological Hospital, School of Stomatology, Capital Medical University (19-09-02 to JD); Chinese Academy of Medical Sciences Research Unit (No. 2019RU020); and Capital Medical University, Beijing Municipality Government grants, to SW (Beijing Scholar Program—PXM2018\_014226\_000021).

## Supplementary Materials

Supplementary Figure 1: Intervention in RA signal with different concentrations of RA and BMS 493 *in vitro* alters the ALP activities differentially (A, B). (*Supplementary Materials*)

## References

- [1] G. C. Vilhais-Neto and O. Pourquié, “Retinoic acid,” *Current Biology*, vol. 18, no. 5, pp. R191–R192, 2008.
- [2] S. H. Lee, K. K. Fu, J. N. Hui, and J. M. Richman, “Noggin and retinoic acid transform the identity of avian facial prominences,” *Nature*, vol. 414, no. 6866, pp. 909–912, 2001.
- [3] K. Niederreither, V. Fraulob, J. M. Garnier, P. Chambon, and P. Dollé, “Differential expression of retinoic acid-synthesizing (RALDH) enzymes during fetal development and organ differentiation in the mouse,” *Mechanisms of Development*, vol. 110, no. 1-2, pp. 165–171, 2002.
- [4] D. Summerbell and M. Maden, “Retinoic acid, a developmental signalling molecule,” *Trends in Neurosciences*, vol. 13, no. 4, pp. 142–147, 1990.



- [5] M. Maden, "Retinoic acid in the development, regeneration and maintenance of the nervous system," *Nature Reviews. Neuroscience*, vol. 8, no. 10, pp. 755–765, 2007.
- [6] J. Marill, N. Idres, C. Capron, E. Nguyen, and G. Chabot, "Retinoic acid metabolism and mechanism of action: a review," *Current Drug Metabolism*, vol. 4, no. 1, pp. 1–10, 2003.
- [7] J. E. Kronmiller and C. S. Beeman, "Spatial distribution of endogenous retinoids in the murine embryonic mandible," *Archives of Oral Biology*, vol. 39, no. 12, pp. 1071–1078, 1994.
- [8] E. Ruberte, P. Dolle, A. Krust, A. Zelent, G. Morriss-Kay, and P. Chambon, "Specific spatial and temporal distribution of retinoic acid receptor gamma transcripts during mouse embryogenesis," *Development*, vol. 108, no. 2, pp. 213–222, 1990.
- [9] B. K. B. Berkovitz, M. Maden, P. McCaffery, and A. W. Barrett, "The distribution of retinaldehyde dehydrogenase-2 in rat and human orodental tissues," *Archives of Oral Biology*, vol. 46, no. 12, pp. 1099–1104, 2001.
- [10] Y. Gibert, L. Bernard, M. Debiais-Thibaud et al., "Formation of oral and pharyngeal dentition in teleosts depends on differential recruitment of retinoic acid signaling," *The FASEB Journal*, vol. 24, no. 9, pp. 3298–3309, 2010.
- [11] Y. Gibert, E. Samarut, M. K. Ellis, W. R. Jackman, and V. Laudet, "The first formed tooth serves as a signalling centre to induce the formation of the dental row in zebrafish," *Proceedings of the Royal Society B: Biological Sciences*, vol. 286, no. 1904, article 20190401, 2019.
- [12] P. Seritrukul, E. Samarut, T. T. Lama, Y. Gibert, V. Laudet, and W. R. Jackman, "Retinoic acid expands the evolutionarily reduced dentition of zebrafish," *The FASEB Journal*, vol. 26, no. 12, pp. 5014–5024, 2012.
- [13] J. Xi, S. He, C. Wei et al., "Negative effects of retinoic acid on stem cell niche of mouse incisor," *Stem Cell Research*, vol. 17, no. 3, pp. 489–497, 2016.
- [14] S. Morkmued, V. Laugel-Haushalter, E. Mathieu et al., "Retinoic acid excess impairs amelogenesis inducing enamel defects," *Frontiers in Physiology*, vol. 7, p. 673, 2017.
- [15] N. Blum and G. Begemann, "Osteoblast de- and redifferentiation are controlled by a dynamic response to retinoic acid during zebrafish fin regeneration," *Development*, vol. 142, no. 17, pp. 2894–2903, 2015.
- [16] A. C. Green, P. Kocovski, T. Jovic et al., "Retinoic acid receptor signalling directly regulates osteoblast and adipocyte differentiation from mesenchymal progenitor cells," *Experimental Cell Research*, vol. 350, no. 1, pp. 284–297, 2017.
- [17] J. Skillington, L. Choy, and R. Derynck, "Bone morphogenetic protein and retinoic acid signaling cooperate to induce osteoblast differentiation of preadipocytes," *The Journal of Cell Biology*, vol. 159, no. 1, pp. 135–146, 2002.
- [18] Y. Shao, Q. Z. Chen, Y. H. Zeng et al., "All-trans retinoic acid shifts rosiglitazone-induced adipogenic differentiation to osteogenic differentiation in mouse embryonic fibroblasts," *International Journal of Molecular Medicine*, vol. 38, no. 6, pp. 1693–1702, 2016.
- [19] L. A. Roa, M. Bloemen, C. E. L. Carels, F. A. D. T. G. Wagener, and J. W. von den Hoff, "Retinoic acid disrupts osteogenesis in pre-osteoblasts by down-regulating WNT signaling," *The International Journal of Biochemistry & Cell Biology*, vol. 116, article 105597, 2019.
- [20] S. Gronthos, M. Mankani, J. Brahim, P. G. Robey, and S. Shi, "Postnatal human dental pulp stem cells (DPSCs) *in vitro* and *in vivo*," *Proceedings of the National Academy of Sciences*, vol. 97, no. 25, pp. 13625–13630, 2000.
- [21] L. Hu, Z. Gao, J. Xu et al., "Decellularized swine dental pulp as a bioscaffold for pulp regeneration," *BioMed Research International*, vol. 2017, Article ID 9342714, 9 pages, 2017.
- [22] Y. Fujii, Y. Kawase-Koga, H. Hojo et al., "Bone regeneration by human dental pulp stem cells using a helioxanthin derivative and cell-sheet technology," *Stem Cell Research & Therapy*, vol. 9, no. 1, p. 24, 2018.
- [23] M. Tatullo, M. Marrelli, K. M. Shakesheff, and L. J. White, "Dental pulp stem cells: function, isolation and applications in regenerative medicine," *Journal of Tissue Engineering and Regenerative Medicine*, vol. 9, no. 11, pp. 1205–1216, 2015.
- [24] A. Bakopoulou and I. About, "Stem cells of dental origin: current research trends and key milestones towards clinical application," *Stem Cells International*, vol. 2016, Article ID 4209891, 20 pages, 2016.
- [25] Y. Cao, Z. Liu, Y. Xie et al., "Adenovirus-mediated transfer of hepatocyte growth factor gene to human dental pulp stem cells under good manufacturing practice improves their potential for periodontal regeneration in swine," *Stem Cell Research & Therapy*, vol. 6, no. 1, p. 249, 2015.
- [26] F. Wei, T. Song, G. Ding et al., "Functional tooth restoration by allogeneic mesenchymal stem cell-based bio-root regeneration in swine," *Stem Cells and Development*, vol. 22, no. 12, pp. 1752–1762, 2013.
- [27] J. Hu, Y. Cao, Y. Xie et al., "Periodontal regeneration in swine after cell injection and cell sheet transplantation of human dental pulp stem cells following good manufacturing practice," *Stem Cell Research & Therapy*, vol. 7, no. 1, p. 130, 2016.
- [28] L. Ma, J. Hu, Y. Cao et al., "Maintained properties of aged dental pulp stem cells for superior periodontal tissue regeneration," *Aging and Disease*, vol. 10, no. 4, pp. 793–806, 2019.
- [29] A. Li, T. Song, F. Wang et al., "MicroRNAome and expression profile of developing tooth germ in miniature pigs," *PLoS One*, vol. 7, no. 12, article e52256, 2012.
- [30] F. Wang, Y. Li, X. Wu et al., "Transcriptome analysis of coding and long non-coding RNAs highlights the regulatory network of cascade initiation of permanent molars in miniature pigs," *BMC Genomics*, vol. 18, no. 1, p. 148, 2017.
- [31] X. Wu, J. Hu, G. Li et al., "Biomechanical stress regulates mammalian tooth replacement via the integrin  $\beta$ 1-RUNX2-Wnt pathway," *The EMBO Journal*, vol. 39, no. 3, article e102374, 2020.
- [32] L. Hu, B. Zhao, Z. Gao et al., "Regeneration characteristics of different dental derived stem cell sheets," *Journal of Oral Rehabilitation*, pp. 1–7, 2019.
- [33] T. M. Abashev, M. A. Metzler, D. M. Wright, and L. L. Sandell, "Retinoic acid signaling regulates Krt5 and Krt14 independently of stem cell markers in submandibular salivary gland epithelium," *Developmental dynamics: an official publication of the American Association of Anatomists*, vol. 246, no. 2, pp. 135–147, 2017.
- [34] G. Li, N. Han, H. Yang et al., "Homeobox C10 inhibits the osteogenic differentiation potential of mesenchymal stem cells," *Connective Tissue Research*, vol. 59, no. 3, pp. 201–211, 2018.
- [35] A. C. Green, T. J. Martin, and L. E. Purton, "The role of vitamin A and retinoic acid receptor signaling in post-natal



- maintenance of bone," *The Journal of Steroid Biochemistry and Molecular Biology*, vol. 155, Part A, pp. 135–146, 2016.
- [36] T. Lind, A. Sundqvist, L. Hu et al., "Vitamin a is a negative regulator of osteoblast mineralization," *PLoS One*, vol. 8, no. 12, article e82388, 2013.
- [37] A. Bloch-Zupan, D. Décimo, M. Loriot, M. P. Mark, and J. V. Ruch, "Expression of nuclear retinoic acid receptors during mouse odontogenesis," *Differentiation*, vol. 57, no. 3, pp. 195–203, 1994.
- [38] Y. Yan, S. Qi, S.-q. Gong, G. Shang, and Y. Zhao, "Effect of CRABP2 on the proliferation and odontoblastic differentiation of hDPSCs," *Brazilian Oral Research*, vol. 31, article e112, 2017.
- [39] R. Wang, Q. Yang, W. Xiao, R. Si, F. Sun, and Q. Pan, "Cellular retinoic acid binding protein 2 inhibits osteogenic differentiation by modulating LIMK1 in C2C12 cells," *Development, Growth & Differentiation*, vol. 57, no. 8, pp. 581–589, 2015.
- [40] S. Wang, Y. Liu, D. Fang, and S. Shi, "The miniature pig: a useful large animal model for dental and orofacial research," *Oral Diseases*, vol. 13, no. 6, pp. 530–537, 2007.
- [41] D. Hughes and B. Song, "Dental and nondental stem cell based regeneration of the craniofacial region: a tissue based approach," *Stem Cells International*, vol. 2016, Article ID 8307195, 20 pages, 2016.
- [42] J. Zhang, B. Deng, X. Jiang et al., "All-trans-retinoic acid suppresses neointimal hyperplasia and inhibits vascular smooth muscle cell proliferation and migration via activation of AMPK signaling pathway," *Frontiers in Pharmacology*, vol. 10, p. 485, 2019.
- [43] S. Mishra, K. K. Kelly, N. L. Rumian, and J. A. Siegenthaler, "Retinoic acid is required for neural stem and progenitor cell proliferation in the adult hippocampus," *Stem Cell Reports*, vol. 10, no. 6, pp. 1705–1720, 2018.
- [44] L. Hesse, K. A. Johnson, H. C. Anderson et al., "Tissue-nonspecific alkaline phosphatase and plasma cell membrane glycoprotein-1 are central antagonistic regulators of bone mineralization," *Proceedings of the National Academy of Sciences*, vol. 99, no. 14, pp. 9445–9449, 2002.
- [45] I. Mortada and R. Mortada, "Dental pulp stem cells and osteogenesis: an update," *Cytotechnology*, vol. 70, no. 5, pp. 1479–1486, 2018.
- [46] C. De Fusco, A. Messina, V. Monda et al., "Osteopontin: relation between adipose tissue and bone homeostasis," *Stem Cells International*, vol. 2017, Article ID 4045238, 6 pages, 2017.
- [47] K. Nakashima, X. Zhou, G. Kunkel et al., "The novel zinc finger-containing transcription factor osterix is required for osteoblast differentiation and bone formation," *Cell*, vol. 108, no. 1, pp. 17–29, 2002.
- [48] W. Y. Baek, M. A. Lee, J. W. Jung et al., "Positive regulation of adult bone formation by osteoblast-specific transcription factor osterix," *Journal of Bone and Mineral Research*, vol. 24, no. 6, pp. 1055–1065, 2009.
- [49] T. Komori, "Regulation of osteoblast differentiation by transcription factors," *Journal of Cellular Biochemistry*, vol. 99, no. 5, pp. 1233–1239, 2006.
- [50] S. Chen, J. Gluhak-Heinrich, Y. H. Wang et al., "Runx2, osx, and dspp in tooth development," *Journal of Dental Research*, vol. 88, no. 10, pp. 904–909, 2009.
- [51] H. Ritchie, "The functional significance of dentin sialoprotein-phosphoryn and dentin sialoprotein," *International Journal of Oral Science*, vol. 10, no. 4, p. 31, 2018.
- [52] Q. Zhu, M. P. Gibson, Q. Liu et al., "Proteolytic processing of dentin sialoprophosphoprotein (DSPP) is essential to dentinogenesis," *The Journal of Biological Chemistry*, vol. 287, no. 36, pp. 30426–30435, 2012.
- [53] M. Alonso, S. Claros, J. Becerra, and J. A. Andrades, "The effect of type I collagen on osteochondrogenic differentiation in adipose-derived stromal cells *in vivo*," *Cytotherapy*, vol. 10, no. 6, pp. 597–610, 2008.
- [54] T. Karakida, R. Yui, T. Suzuki, M. Fukae, and S. Oida, "Retinoic acid receptor  $\gamma$ -dependent signaling cooperates with BMP2 to induce osteoblastic differentiation of C2C12 cells," *Connective Tissue Research*, vol. 52, no. 5, pp. 365–372, 2011.
- [55] Z. Weng, C. Wang, C. Zhang et al., "All-trans retinoic acid promotes osteogenic differentiation and bone consolidation in a rat distraction osteogenesis model," *Calcified Tissue International*, vol. 104, no. 3, pp. 320–330, 2019.
- [56] A. C. C. Cruz, F. T. G. d. S. Cardozo, R. d. S. Magini, and C. M. O. Simões, "Retinoic acid increases the effect of bone morphogenetic protein type 2 on osteogenic differentiation of human adipose-derived stem cells," *Journal of Applied Oral Science*, vol. 27, 2019.
- [57] M. Ohishi, M. Horibe, D. Ikedo et al., "Effect of retinoic acid on osteopontin expression in rat clonal dental pulp cells," *Journal of Endodontics*, vol. 25, no. 10, pp. 683–685, 1999.
- [58] S. M. San Miguel, M. Goseki-Sone, E. Sugiyama, H. Watanabe, M. Yanagishita, and I. Ishikawa, "Tissue-nonspecific alkaline phosphatase mRNA expression and alkaline phosphatase activity following application of retinoic acid in cultured human dental pulp cells," *Archives of Oral Biology*, vol. 44, no. 10, pp. 861–869, 1999.
- [59] S. Thaweboon, B. Thaweboon, S. Choonharuangdej, P. Chunhabundit, and P. Suppakpatana, "Induction of type I collagen and osteocalcin in human dental pulp cells by retinoic acid," *Southeast Asian Journal of Tropical Medicine and Public Health*, vol. 36, no. 4, pp. 1066–1069, 2005.
- [60] K. Chadipiralla, J. M. Yochim, B. Bahuleyan et al., "Osteogenic differentiation of stem cells derived from human periodontal ligaments and pulp of human exfoliated deciduous teeth," *Cell and Tissue Research*, vol. 340, no. 2, pp. 323–333, 2010.